

**SOLAR ENERGY IN  
CONSTRUCTION: AN ASSESSMENT  
OF SOLAR WALL THERMAL  
PERFORMANCE IN EUROPE**

**ROY WORMALD**

**A thesis submitted in partial  
fulfilment of the requirements  
of Liverpool John Moores  
University for the degree of  
Doctor of Philosophy**

**March 1998**

LIVERPOOL JOHN MOORES UNIVERSITY  
Aldham Roberts L.R.C.  
TEL 0151 231 3701/3634

# CONTENTS

	<i>Page</i>
Abstract	
<b>CHAPTER ONE - THE IMPACT OF RISING ENERGY DEMAND</b>	<b>1</b>
1.1 Resources	2
1.2 The greenhouse effect	10
1.3 Lessons from past climatic change	15
<b>CHAPTER TWO - SOLAR ENERGY: THEORETICAL CONSIDERATIONS</b>	<b>25</b>
2.1 The solar constant	26
2.2 The spectral distribution of solar radiation	26
2.3 Heat transfer in solar walls	31
2.4 Solar radiation: transmission and absorption	42
2.5 Solar collectors	51
2.6 Passive solar design	60
<b>CHAPTER THREE - THE POULTON LANCELYN SCHOOL</b>	<b>68</b>
3.1 Introduction	69
3.2 Construction details	69
3.3 Instrumentation	76
3.4 Commissioning of the monitoring installation at Poulton Lancelyn	85
3.5 Treatment of results	85
3.6 Contribution of the solar wall to a classroom's energy requirement	100
3.7 The thermal performance of the solar wall	107
3.8 Errors involved in the measurement of temperature and energy production from a solar wall	120

<b>CHAPTER FOUR - DEVELOPMENT OF A USER FRIENDLY COMPUTER PROGRAM FOR THE ASSESSMENT OF THE PERFORMANCE OF THE POULTON LANCELYN SOLAR WALL</b>	<b>123</b>
4.1 Modular programs	124
4.2 System specific simulation programs	125
4.3 Dynamic thermal modelling of the Poulton Lancelyn solar wall	127
4.4 Development of the computer model	137
4.5 Program description	148
4.6 Errors and accuracy produced when using finite difference equations	156
<b>CHAPTER FIVE - ASSESSMENT OF SOLAR WALL PERFORMANCE</b>	<b>162</b>
5.1 Use of the computer simulation program for the Poulton Lancelyn school	163
5.2 Validation by modelling solar walls	183
5.3 Economic assessment	188
5.4 Conclusions	196
<b>CHAPTER SIX - TRANSPARENT INSULATION</b>	<b>197</b>
6.1 Introduction	198
6.2 Transparent insulation in practice	206
6.3 Performance of model solar walls	215
6.4 The potential for solar walls providing solar heat in Europe	230
6.5 The simulation of solar wall behaviour in European locations	236
6.6 Estimation of the length of a heating season	250
<b>CHAPTER SEVEN - CONCLUSION: FUTURE PROSPECTS FOR SOLAR ENERGY IN CONSTRUCTION</b>	<b>264</b>
7.1 Future prospects	265
7.2 The world photovoltaic market	267

<b>7.3</b>	<b>The market for transparently insulated walls</b>	<b>271</b>
<b>7.4</b>	<b>Conclusion</b>	<b>271</b>
	<b>REFERENCES</b>	<b>274</b>
	<b>APPENDICES</b>	<b>284</b>
<i>Appendix 1</i>	Economic assessment methods	
<i>Appendix 2</i>	The temperature control unit	
<i>Appendix 3</i>	Computer program codes used in solar wall performance simulation	
<b>3.1</b>	The Poulton Lancelyn solar wall program of solar wall temperatures	
<b>3.2</b>	Subroutine to print hourly values	
<b>3.3</b>	Subroutine to plot hourly values of solar wall temperatures	
<b>3.4</b>	Subroutine to plot the daily change in solar wall temperatures	
<b>3.5</b>	Subroutine to determine the daily heat output from the Poulton Lancelyn solar wall	
<b>3.6</b>	Subroutine to determine the monthly energy output	
<b>3.7</b>	Block data input for the solar wall program	
<b>3.8</b>	A simplified finite difference solar wall program for PC's	
<b>3.9</b>	Simplified program: subroutine for total energy production from different types of solar wall	
<b>3.10</b>	Simplified program: subroutine for daily heat production from different types of solar walls	
<b>3.11</b>	Simplified program: subroutine to plot daily change of surface and cavity temperatures	
<b>3.12</b>	Simplified program: Manchester radiation and temperature data	



- 3.13** Simplified program: Plymouth radiation and temperature data
- 3.14** Simplified program: London radiation and temperature data
- 3.15** Simplified program: Lerwick radiation and temperature data
- 3.16** Simplified program: Aberdeen radiation and temperature data
- 3.17** A simplified steady state solar wall program to calculate energy savings and economic benefits for different types of solar walls at various European locations
- 3.18** Program to evaluate the length of heating season at various locations in Europe
- 3.19** Program to determine the angles of incidence of radiation falling on a south facing solar wall

**Appendix 4** Sol-air temperature

## **Abstract**

This thesis presents an account of the monitoring and simulation of the performance of solar walls, with an essay into the prediction of their energy production, their efficiency, and their economy in different parts of Europe.

A three dimensional finite difference program has been written to simulate the behaviour of mass solar walls in any climate using hourly values of meteorological data. Results from monitoring the performance of a low energy school (with solar wall) at Poulton Lancelyn, Wirral, were used for program validation. This program was used to optimise UK design. To confirm the performance of this optimised design, an instrumented, rooftop exposure site was established at Clarence Street using suitably exposed model solar walls. NPV/K and simple payback were used as economic criteria.

South facing single glazed model solar walls were clad with transparent insulation material (TIM). The energy produced and temperatures during stagnation were measured and the computer simulation program modified. Results indicate the great potential of transparent insulation technology in cold climates.

A steady state program has been developed for the rapid assessment of solar wall performance at locations in Europe between 40°N and 60°N. Three types of solar wall have been compared: a single glazed unventilated Trombe wall and similar single glazed and double glazed Trombe walls with added transparent insulation. Single glazed Trombe walls are shown to be unsuitable for use in Northern Europe, but transparently insulated solar walls work with high efficiency wherever there is sufficient solar insolation. Their performance in terms of energy production, efficiency, and simple payback times are shown to be well suited for use at high latitudes, but are only quasi economic at present.

In the short term, energy resource depletion is not a problem. In the long term the use of transparent insulation to produce solar walls for use in environmentally benign buildings seems a promising technology.

# **CHAPTER ONE - THE IMPACT OF RISING ENERGY DEMAND**

**LIVERPOOL JOHN MOORES UNIVERSITY**  
Aldham Roberts L.R.C.  
TEL 0151 231 3701/3634



## 1.1 RESOURCES

At the beginning of the *Green History of the World* by Ponting <sup>1</sup>, there is an Easter Island analogy that conveys forebodings as to the possible future of man or woman kind in contemporary society. Although now deforested, the island was not always so. An elaborate social and ceremonial life had once been sustained based on a cult of stone statue construction. This necessitated the felling of large quantities of trees to provide a flexible track of rollers for statue transportation. Prodigious soil erosion ensued and that quite complex society collapsed, after one thousand years of flourishing existence.

Incredibly, even as the timber resource was quite clearly in rapid decline, competition between clans to build more and more statues (and so deplete the forest remnants even more quickly) intensified. Demand for prestige and the statues that provided it, remained unabated even in extremis. Societal collapse was sudden, the population's decline rapid.

The whole earth, Ponting declares, like Easter Island, is a similar closed system, where humans endeavour to, and have succeeded in, growing more and more food, tapping more and more resources, producing and sustaining an ever more complex society. As technical sophistication grew, so energy sources changed from wood gathering, coal burning, oil combustion, to the fission of nuclear fuel. Attitudes to energy resource exploitation however have remained unchanged. Resources were, and are, deemed to be almost inexhaustible, as if vast rivers of oil were eternally flowing, and that the earth was composed of infinitely deep chasms of coal. An exponential growth in energy consumption ensued (see <sup>2,3,4</sup> and **Fig 1.1**), fuelling a similar growth in population (**Fig 1.2a** and **Fig 1.2b**), sustained by a much increased production of food (**Fig 1.3**).



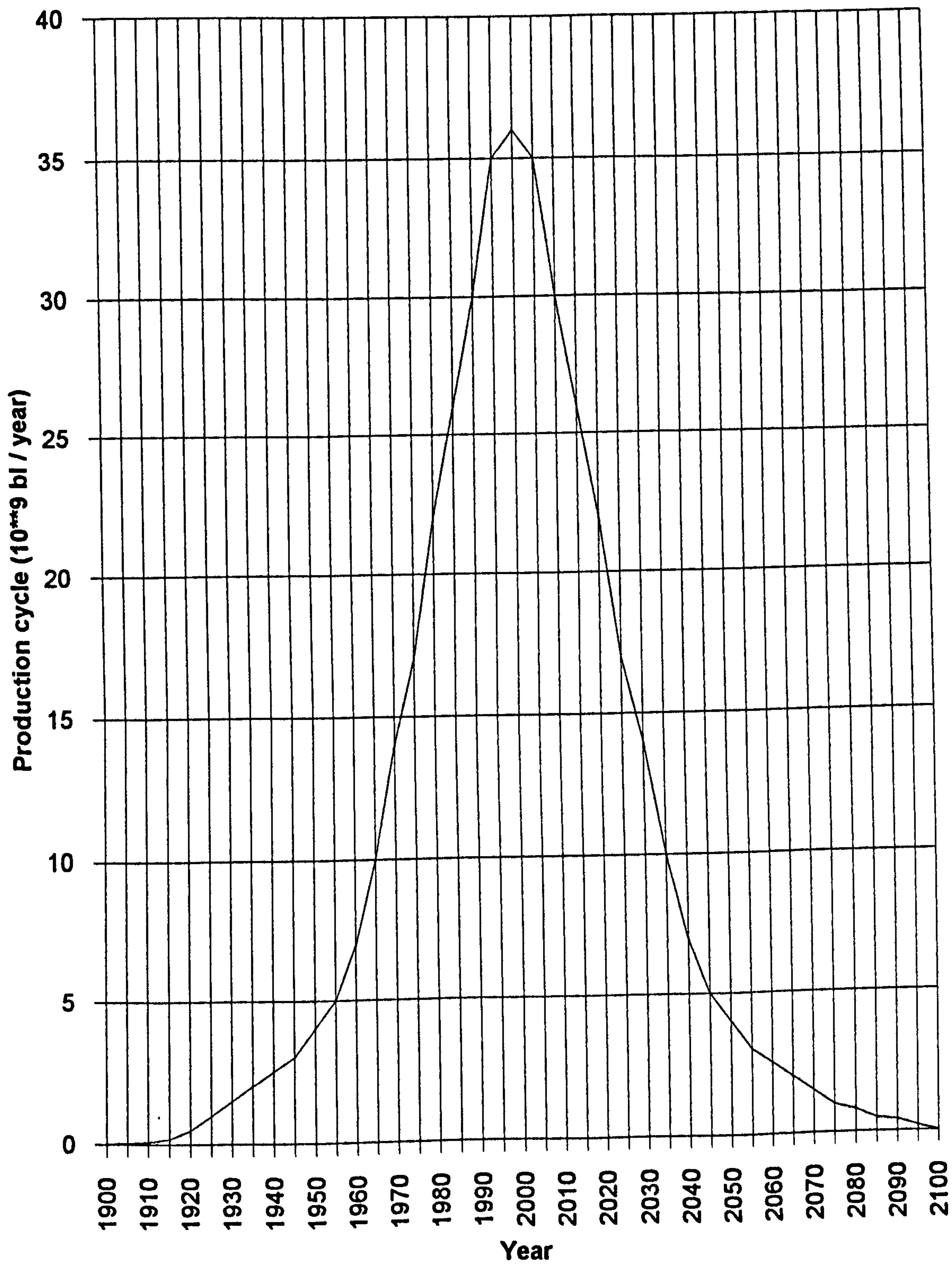


**Fig. 1.1 Cycle of world oil production.**  
**Ryman estimate:  $Q(\infty) = 2100$  billion barrels.**

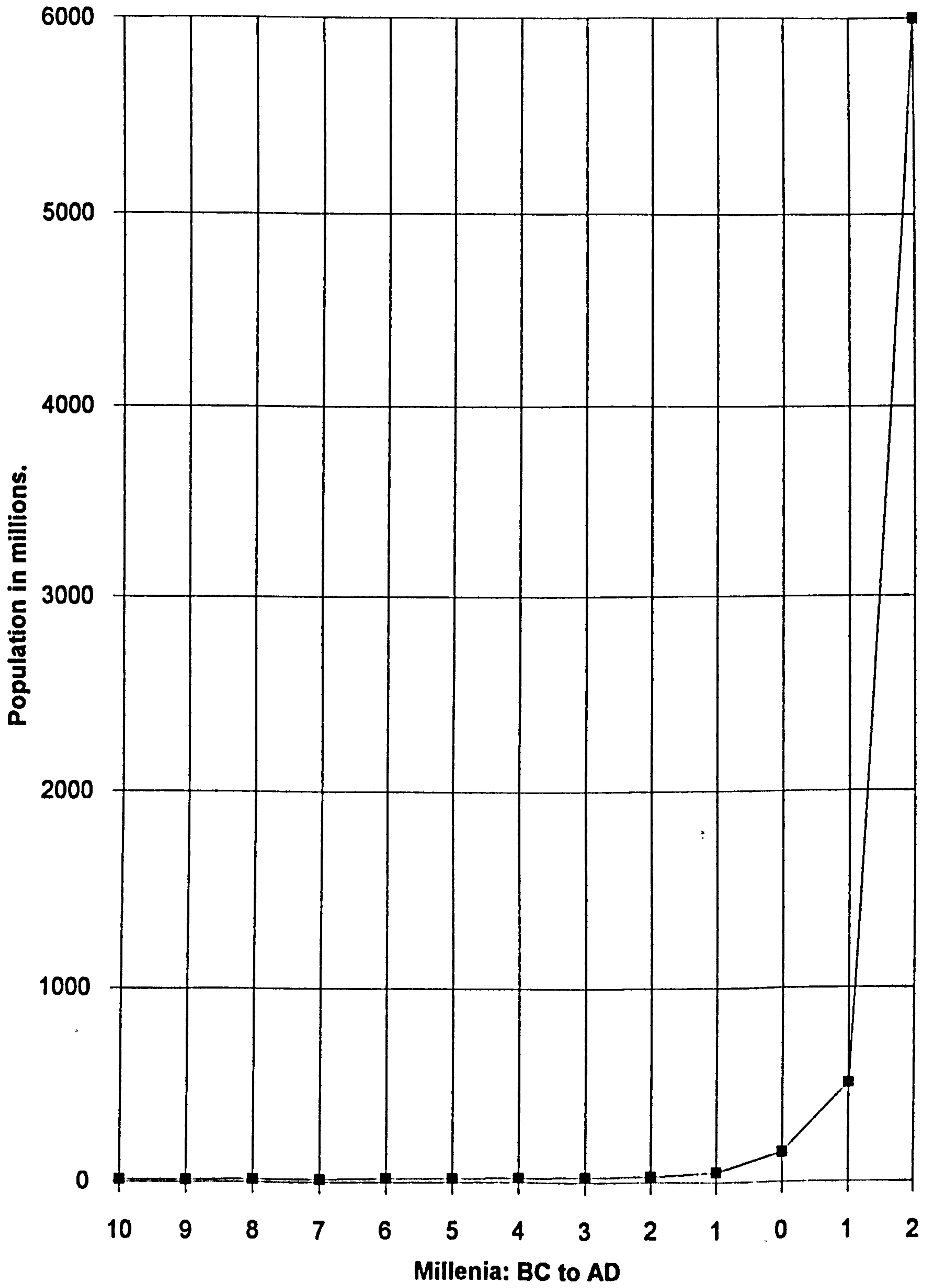


Fig. 1.2(a) World population growth: 10,000 BC-2000 AD.

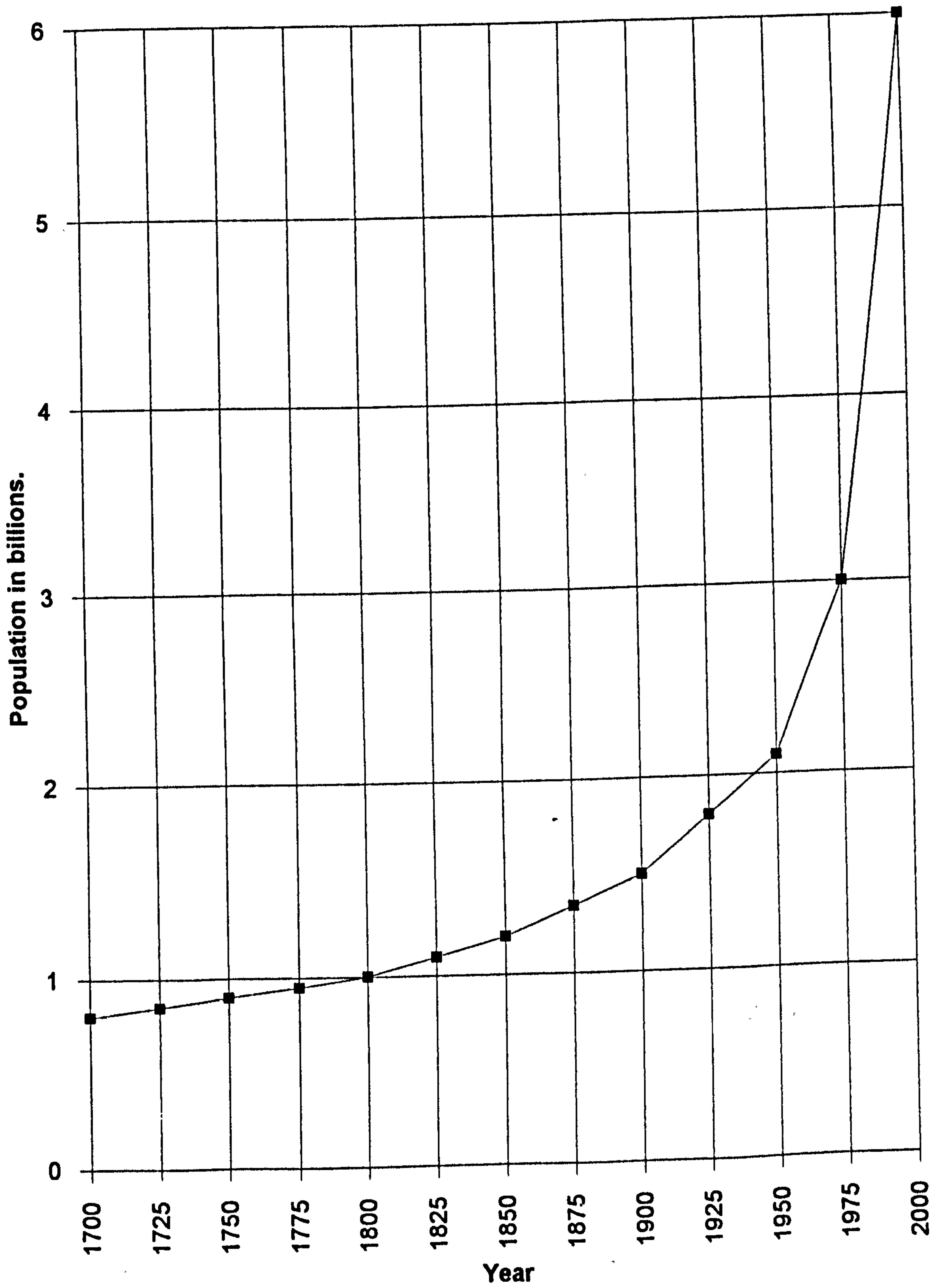
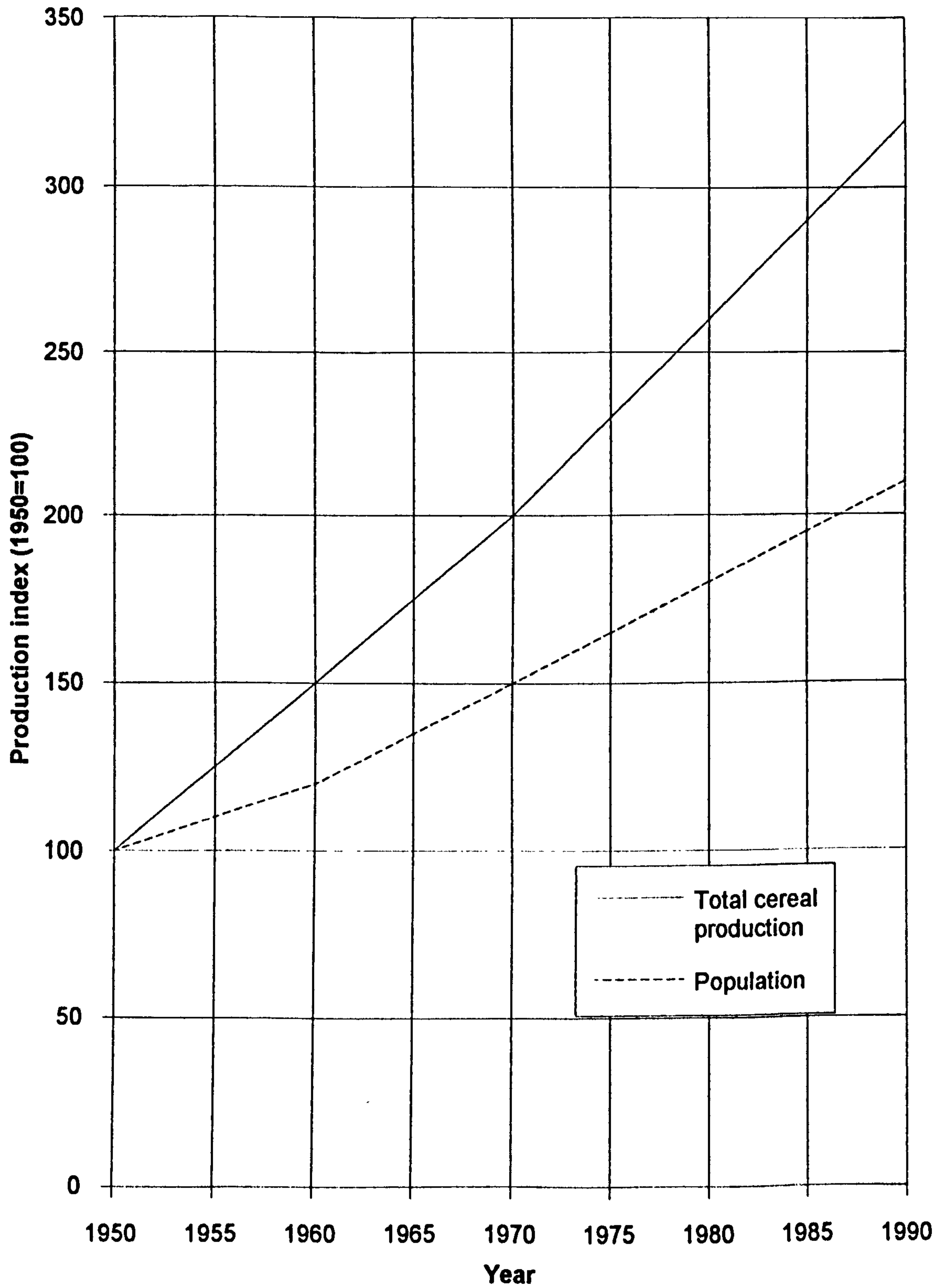


Fig. 1.2(b) World population growth: 1700-2000 AD.



**Fig. 1.3 World grain production 1950-1990.**



In the 1970's, a cartel of oil producers, the Organisation of Petroleum Exporting Countries, increased their prices and produced a world economic crisis. This did not endure, for the value of the voluminous investments of the oil states in the industrialised West suffered too. The crisis provoked concern and debate about energy resource lifetimes at high depletion rates (several hundred years for coal, perhaps 50 years for oil). Images of an Easter Island syndrome were evoked, and the adequacy of resources to sustain the living standard of future global populations was questioned (see <sup>5</sup> and Fig 1.3).

In the short term (a few human lifespans) energy resource depletion is not a problem, in the medium term (1000 years) it is. This epoch of massive fossil fuel consumption must be regarded as abnormal, transitory and ephemeral (see Fig 1.4). The historical pattern is of low levels of energy usage and slow rates of change. Quite the opposite to the contemporary frenetic delirium pervading our present consumption patterns. Re-entry into a more sustainable lifestyle requires a complete revision of the pattern of our economic and social thinking, now apparently based on the false assumption that contemporary growth rates can be sustained for ever.

Virtual exhaustion of the world's easily utilizable fossil fuel resources could produce a traumatic cultural and population decline to the level of primitive existence. One solution would be to develop a long lasting and reliable energy source, of appropriate magnitude, to sustain our highly energy dependant culture. Such a criterion would appear to be a sine qua non for the survival of civilisation as we know it.

The examples of Windscale, Three Mile Island and Chernobyl, plus the dangers and difficulties of radioactive waste disposal, seem to negate the increased use of nuclear

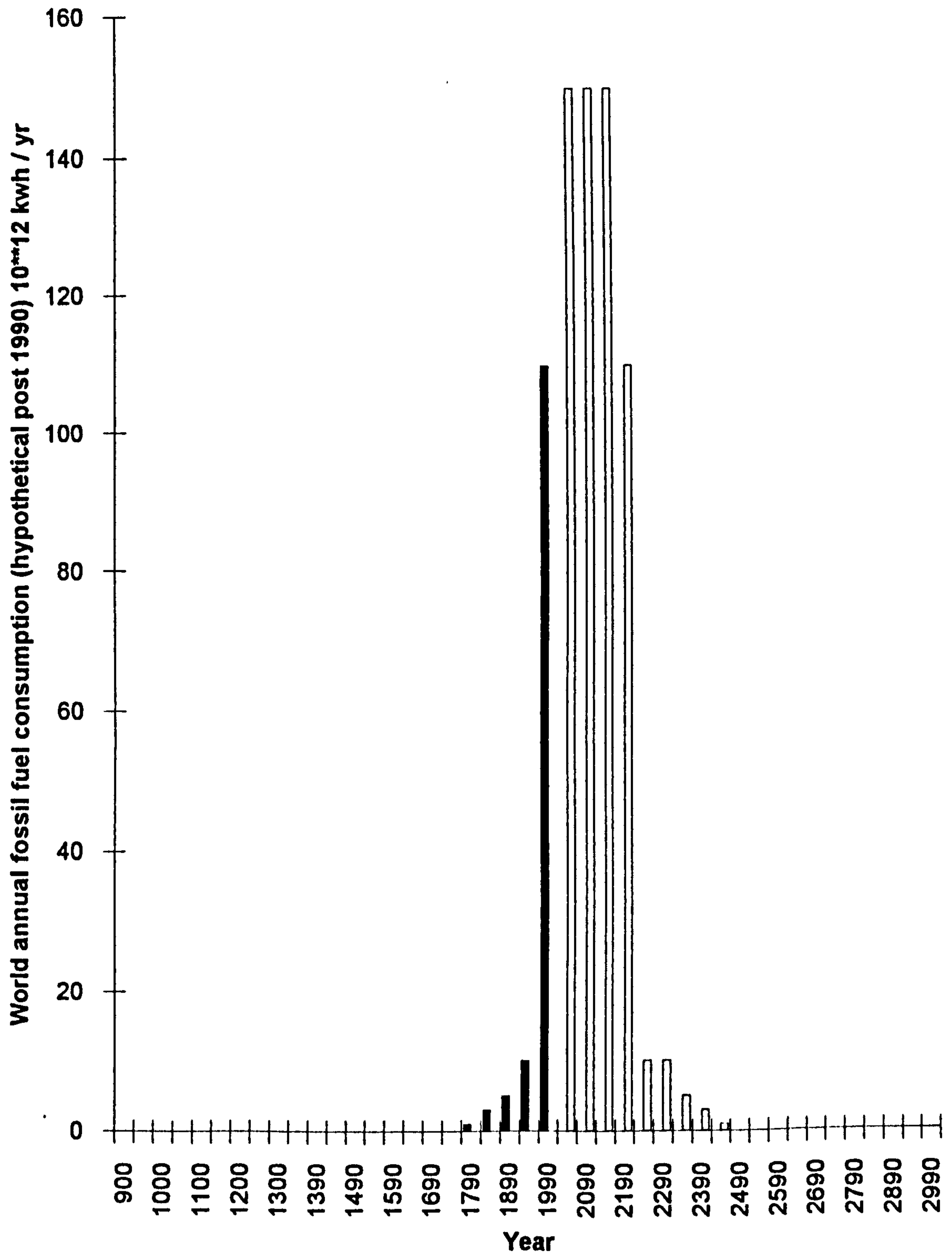


**Fig. 1.4 The epoch of exploitation of fossil fuels in historical perspective.**

fuels as the potential savior of civilisation. This leaves solar energy, direct solar radiation or one of its many manifestations (wind, hydro, wave, biomass), as the viable candidate for use as a long lasting energy source. It is pollution free and can be relied on to preserve (approximately) its present rate of production for the rest of the sojourn of Homo Sapiens on this planet.

The proposition that “population increases as the means of subsistence increases, unless prevented by powerful checks”, was a basic tenet of T.R.Malthus’s *An essay on the principle of population as it affects the future improvement of mankind* in 1798<sup>6</sup>.

Consensus opinion to date has been that massive and cheap energy inputs, in addition to technological expertise, are sufficient to remove all checks and to resolve all problems of scarcity. Nevertheless, populations of other species have rarely reached full potential before other limiting factors appeared. For example: the reproductive inhibition produced by endocrine stress induced by overcrowding.

Unfortunately we are changing our environment. Soil, water and air are being grossly and perhaps irreversibly polluted. There is the possibility of climatic change induced by air pollution that would seriously endanger the soils capacity to sustain high levels of food production. Since these are now so necessary to sustain inflated human populations, we are forewarned of a potential Malthusian check to our present ceaseless and prolific expansion.



## 1.2 THE GREENHOUSE EFFECT<sup>7 & 8</sup>

The immediate problems facing the earth are not connected with the scarcity of fossil fuel resources but with their present abundance. One major concern is based on the fact that man's use of fossil fuels represents a net input to the heat budget of the earth's atmospheric system and has the potential to significantly alter our climate.

The scientific argument says that the only way to radiate this extra heat to space is for the earth to increase its surface temperature<sup>9, 10 & 11</sup>. According to the Stefan Boltzmann radiation law the annual energy input  $E$  to a body (which must equal the energy output when equilibrium prevails) is related to surface temperature  $T$  by the equation:

$$E = \sigma AT^4 \quad (1.1)$$

where:

$\sigma$  = Stefan-Boltzmann constant.

$A$  = Radiating surface area.

The power output ( $E_e$ ) radiated from the earth of radius  $R$ , emittance  $\epsilon = 1$  and surface temperature  $T_e$  will therefore be:

$$E_e = 4\pi R^2 \sigma T_e^4 \quad (1.2)$$

If the extraterrestrial solar irradiance (the solar constant) is  $G_0$ , and the proportion of the irradiance reflected back to space (the albedo) is  $\rho_0$ , then the power received by the earth from the sun ( $E_s$ ) is:

$$E_s = \pi R^2 (1 - \rho_0) G_0 \quad (1.3)$$



Since power output must equal power input solving 1.2 and 1.3 for  $T_e$  gives a value of approximately 250K, that is  $-23^\circ\text{C}$  for the surface temperature of the earth.

The “black body theory” is not exactly correct when applied to the earth with its skin of air and water above its surface. Significant amounts of heat radiated from the earth’s surface are absorbed by atmospheric gases, with a resulting rise in their temperature and thus of the air. The gases mainly responsible for this “greenhouse effect” are carbon dioxide and water vapour. There are others present in smaller quantities (see *Table 1.1*). Generically they are known as radiative forcing agents, methane being 30 times, nitrous oxide 150 times and the chlorofluorocarbons 100000 times more potent than carbon dioxide itself. As a result the earth’s surface temperature is higher, due to both pre-industrial and it is thought post-industrial concentrations of carbon dioxide in the atmosphere. The elevation has been to an average value of about  $14^\circ\text{C}$ , the present approximate surface temperature of the earth. The increase in carbon dioxide emissions in world regions from 1950 to 1985 is illustrated in **Fig 1.5(a)** and **1.5(b)**.

Differentiating the Stefan Boltzmann equation can lead to a relationship between the change in energy input and the change in surface temperature that would be observed:

$$\frac{dE}{E} = 4 \frac{dT}{T} \quad (1.4)$$

If fossil fuel energy combustion were to be increased to a value of  $10^{16}$  kWh/annum, which is 1% of the present solar input of  $10^{18}$  kWh/annum, present surface temperatures would increase by  $0.7^\circ\text{C}$  without taking into consideration the greenhouse effect. This alone would melt the polar ice caps. Fortunately current fuel heat inputs are considerably smaller at just .01% of solar input, around  $10^{14}$  kWh/annum.

The greenhouse effect however could increase global surface temperatures much more than would fossil fuel heat inputs alone. The inevitable emissions of carbon dioxide and

Table 1.1 The principal greenhouse gases.

Gas	Principal source	Current concentration	Contribution to global warming
Carbon Dioxide (CO <sub>2</sub> )	Fossil fuel combustion Deforestation	350 ppmv	55%
Chlorofluorocarbons (CFC's)	Refrigerants	.28 ppbv	24%
Methane (CH <sub>4</sub> )	Rice paddies Enteric fermentation Natural gas leaks	1.7 ppmv	15%
Nitrous oxide (N <sub>2</sub> O)	Fossil fuel combustion	0.3 ppmv	6%

ppmv = parts per million by volume

ppbv = parts per billion by volume

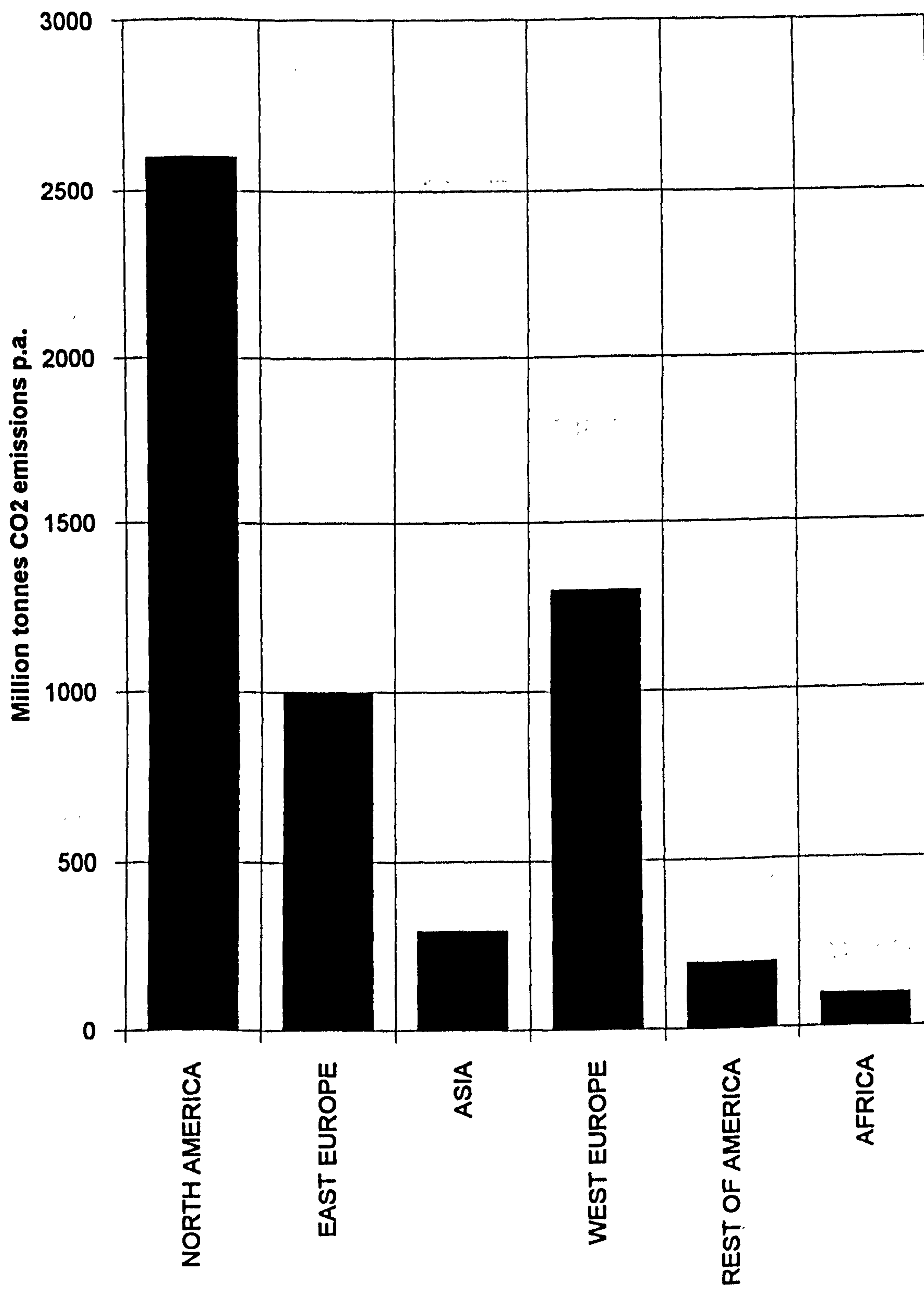


Fig. 1.5(a) CO2 emissions in world regions: 1950.

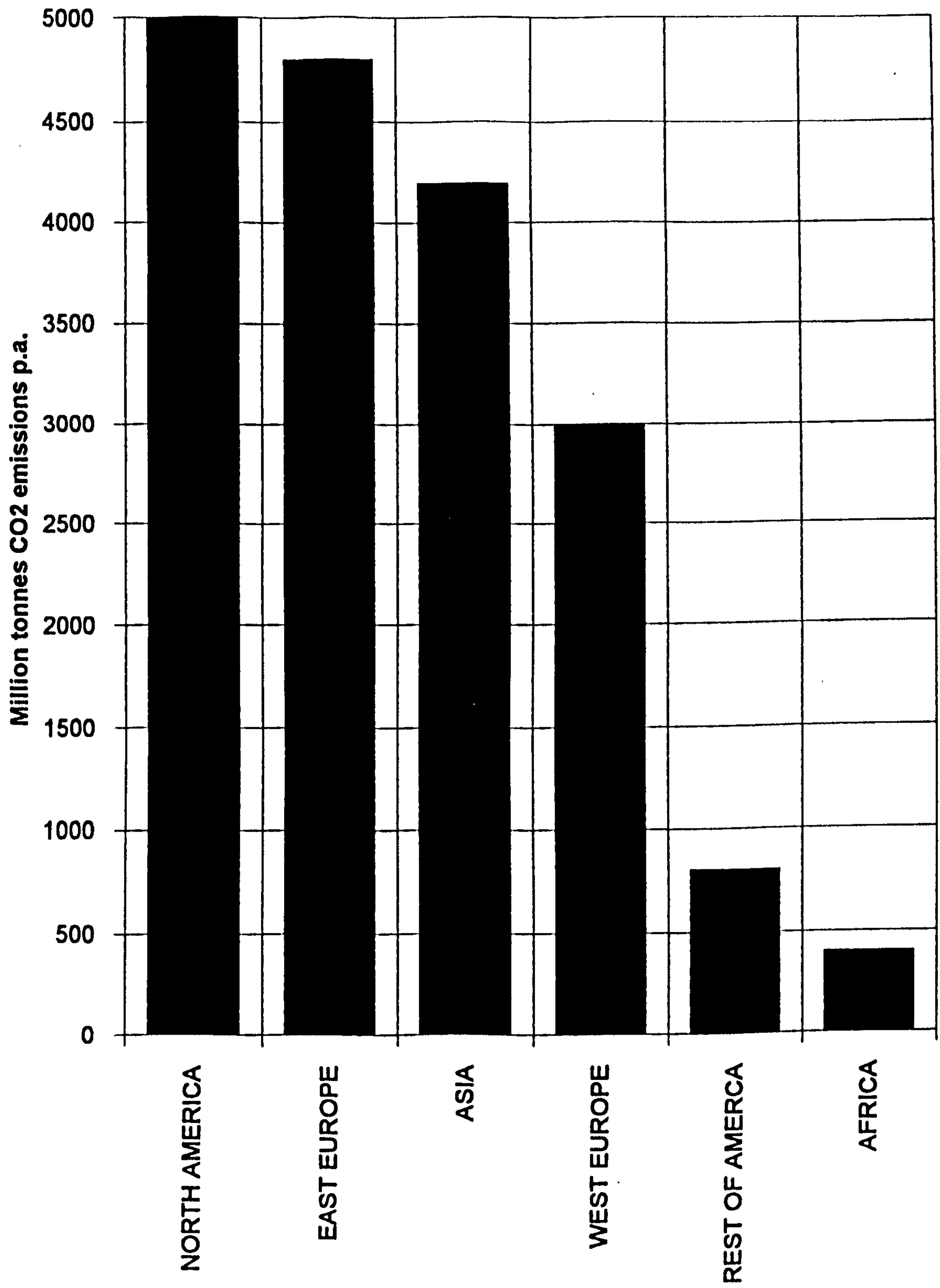


Fig. 1.5(b) CO2 emissions in world regions: 1985.



other warming agents have the potential to produce severe climatic disturbance, with local changes occurring long before global ones. For example the heat supplied by the burning of fossil fuels in London is equivalent to 20% of the solar input it receives. This extra input has raised the temperature in the middle of London over its surroundings by 10°C in winter and 5°C in summer.

### 1.3 LESSONS FROM PAST CLIMATIC CHANGE <sup>12</sup>

Ice core studies have shown that the carbon dioxide content of the atmosphere over the past 60,000 years has varied in proportion to the air temperature (see **Fig 1.6**). The match is not exact for there are other radiative forcing processes at work. These include changes in solar energy output, volcanic eruptions, sulphur dioxide pollution, and other natural variations caused by the constant redistribution of energy from and to the atmosphere, oceans, land and life. There is inexactitude and it is not yet possible to specify with certainty what the future climatic changes will be.

About 65 million years ago the earth's climate completed its change from the era of dinosaurs at a temperature of +15°C above the present, to a much colder climate (see **Fig 1.7**). The planet became covered with ice at the polar regions with temperatures some -5°C below the present. After that the climate stabilised. The stabilisation involved the cyclic growth and decay of ice sheets outside the polar regions over a period of 100,000 years. A regular rhythmic pattern developed of a warm interglacial period followed by a gradual return of the ice sheet <sup>13 & 14</sup>. Finally after 85,000 years there was an extraordinarily rapid termination of the glacial state back to the warmth of the interglacial. As the ice warmed up, dead plants and frozen methane under the ice were exposed and decomposed. Carbon dioxide levels in the atmosphere increased by 30%

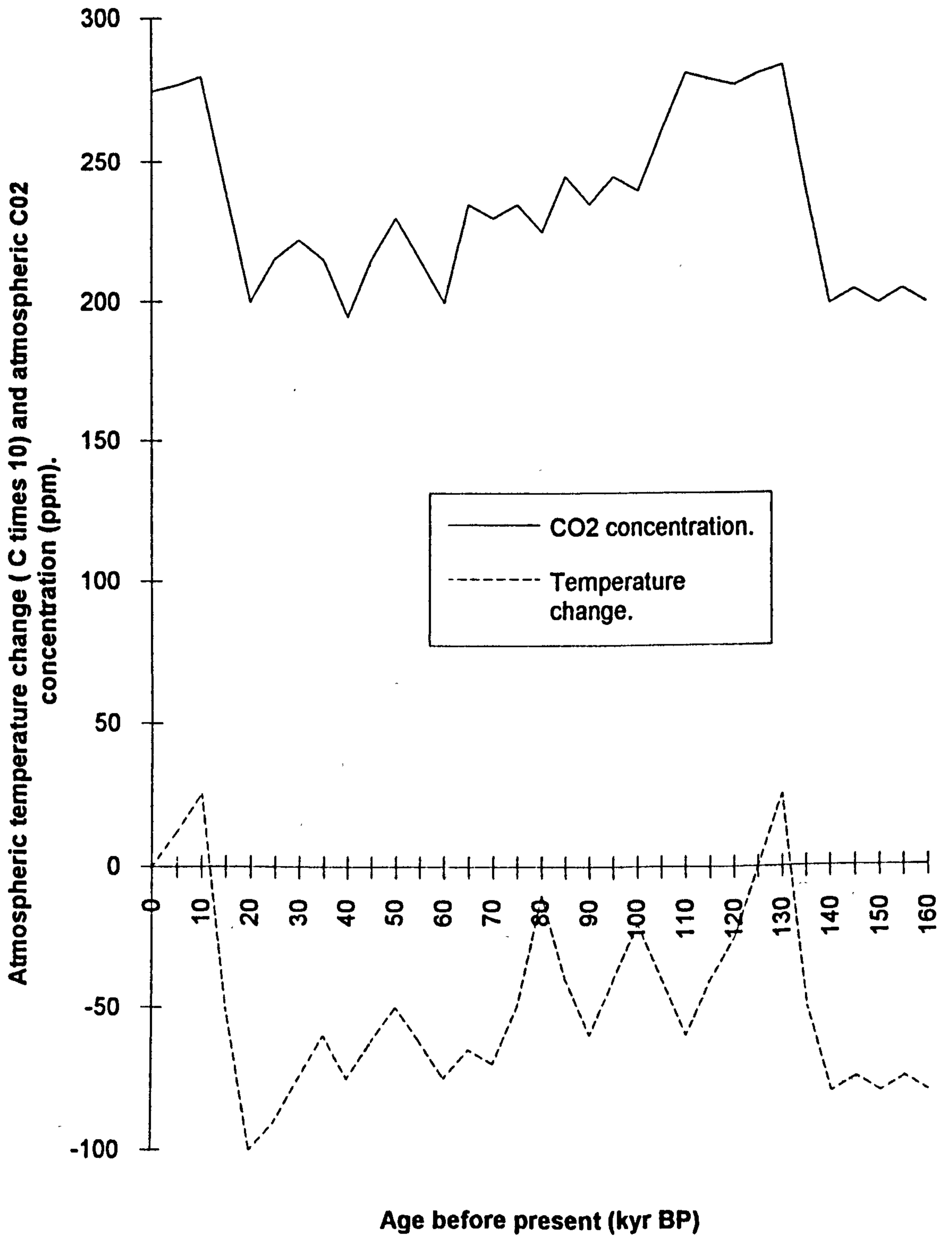


**Fig.1.6 Atmospheric temperature and CO2 concentrations in glacial and interglacial times (obtained from ice core studies).**

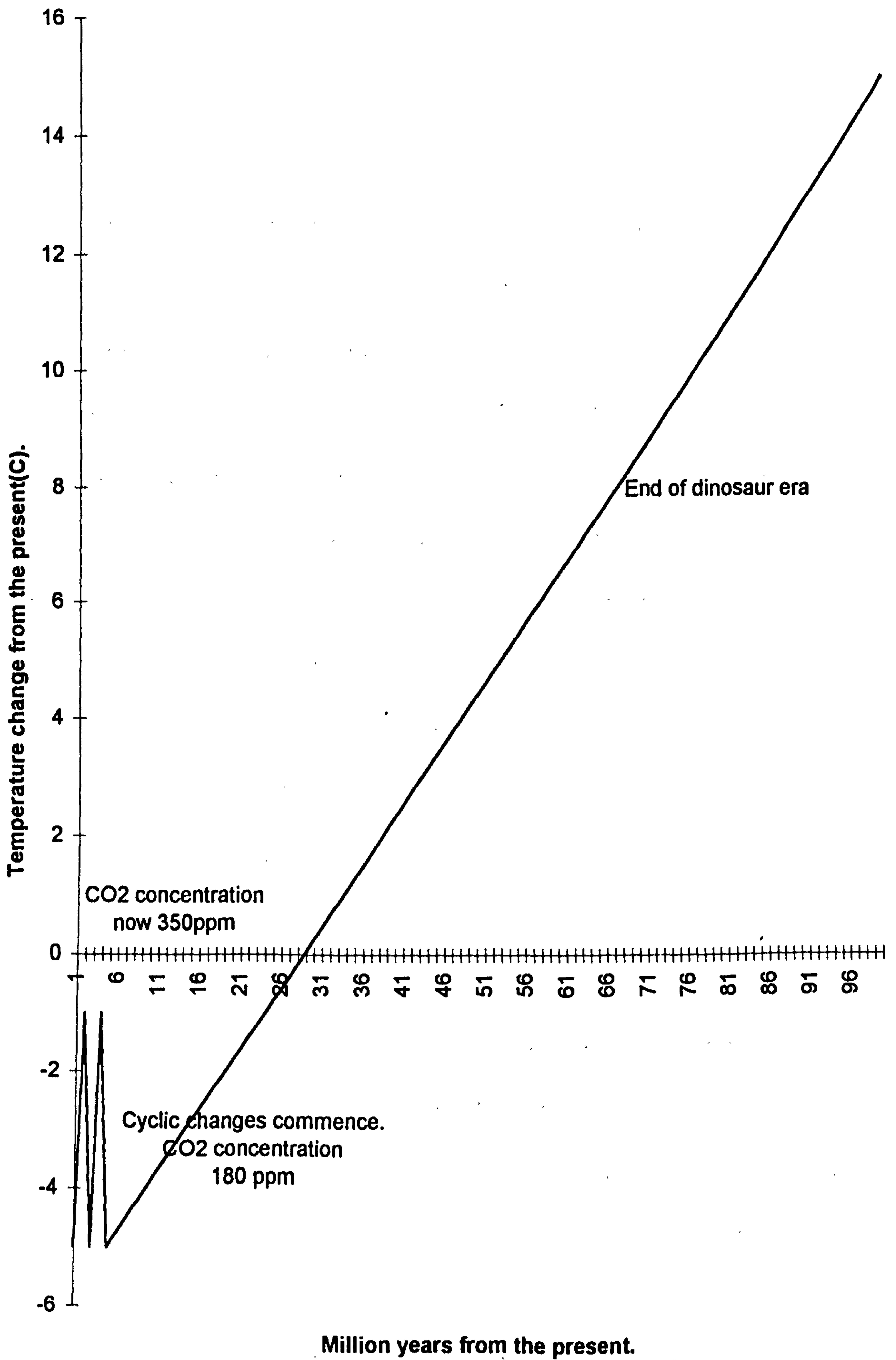


Fig. 1.7 Temperature changes through the ages.

and methane levels by 100%, thus enhancing the greenhouse effect and returning the earth to its previously warmer condition <sup>15</sup>.

This release of carbon dioxide and methane was beneficial to life forms such as Homo Sapiens since it extended the length of interglacial warmth. The actual rate of change of temperature was quite slow. As the world warmed up the temperature changed by just .001°C per annum. Hardwood forests were able successfully to move northwards to cooler zones. However the rate of release of greenhouse gases is now higher it would seem than ever before experienced in geological time. The Intergovernmental Panel for Climate Change (see Fig 1.7 and <sup>16</sup>) predicts that global warming could produce a 0.03°C temperature rise per annum over the next 100 years. The resultant climatic changes would be so rapid that they would exceed the capacity of natural communities such as forests to migrate. They would die out to be replaced by savannah, shrubland, and grassland. Successional species such as weeds and insect pests would proliferate. Soils would become drier, crop yields would be affected. Sea levels would rise.

A good illustration of the effect of contemporary warming is demonstrated at this moment in the Antarctic <sup>17</sup>. The Larsen ice shelf melted away in 1995. For the first time in recorded history James Ross Island, normally connected to the mainland by an ice shelf, can be sailed around. The Wordie ice shelf too has disintegrated. The whole of the West Antarctic ice sheet has now the potential to slide into the surrounding ocean raising sea levels. There is no immediate problem, it will take many years to happen. The concept is simply mentioned here to support the hypothesis that predicted greenhouse effects are beginning to occur.



It is not really an issue whether our climate has changed. It has. One sign is the variation in average global surface temperature since the middle of the last century (see Fig 1.8). Because instruments have changed during the period for which we have observations, there are formidable problems in reconstructing this variation. Nevertheless after taking these factors into account, it seems clear that the earth's surface has warmed up by a few tenths of a degree. A bigger issue is whether we can explain that warming. In particular, can we attribute any part of it to human activity?

Traditionally many climate scientists have hedged their bets, using the double negative that warming is "not inconsistent with the effects of human activity". The Intergovernmental Panel on Climate Change in 1995 went one step beyond "not inconsistent" to state that "the balance of evidence suggests a discernible human influence on global climate". However the computer simulations used have not been able to include every factor that influences such change and we may never be able to unambiguously identify the human influence on the climate over the past century. It does seem clear though, that on a global scale over the last century, the input of human induced factors that cause climate change have been substantial. Some of these, in particular the levels of carbon dioxide will continue to grow bigger in the coming decade.

The majority view of the panel is that we should be starting to encourage the use of the main routes to survival should the changes be as severe as predicted. These include: energy efficiency, increased use of renewable forms of energy, less greenhouse gas intensive agriculture, reduced deforestation, and reforestation. The panel thought that the adoption of energy efficient technologies by emerging nations would make it possible for them to achieve a level of amenities similar to Europe in the 1970's for their populations.

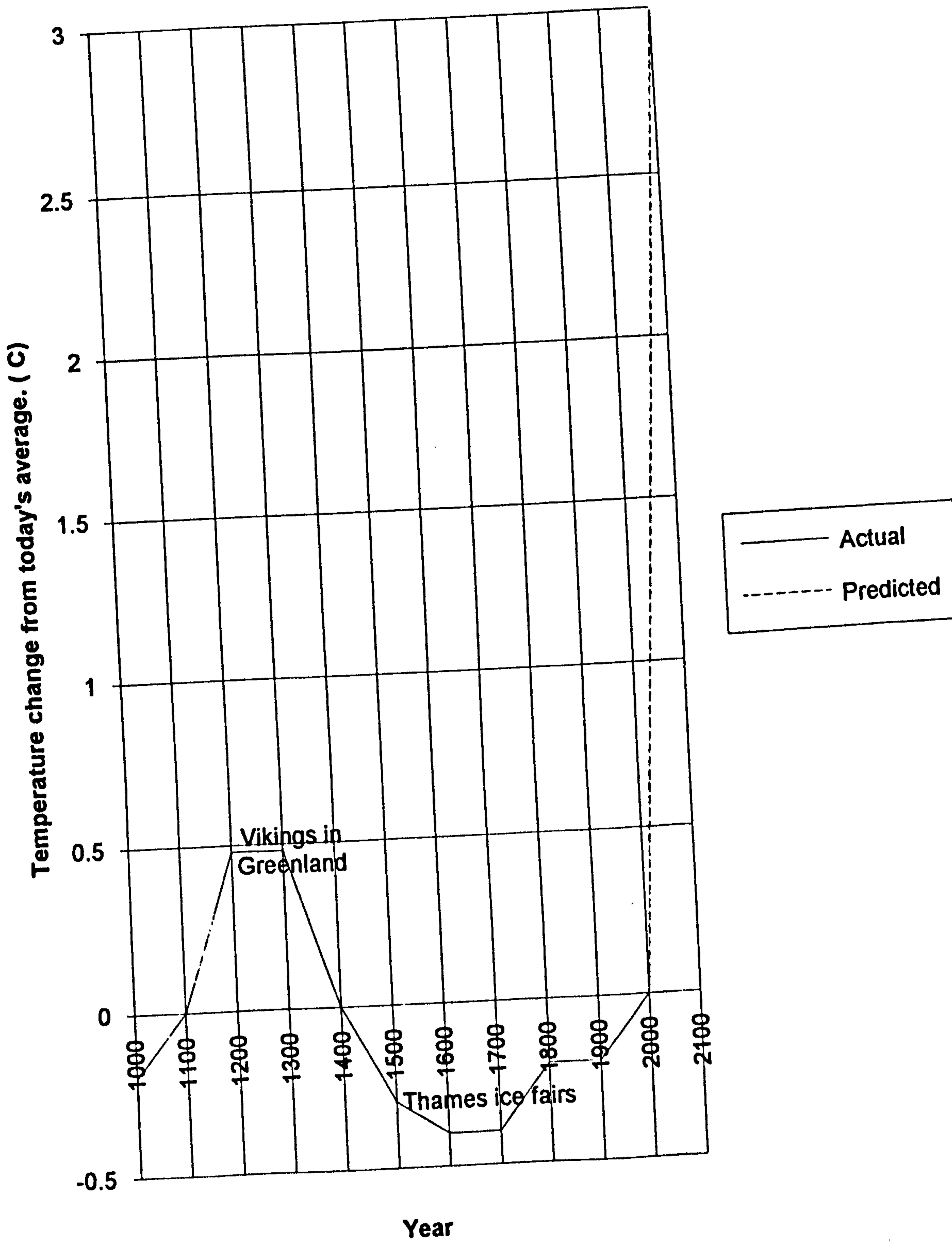


Fig. 1.8 Changes in average global surface temperatures 900-2100 AD.

LIVERPOOL JOHN MOORES UNIVERSITY  
Aldham Roberts L.R.C.  
TEL. 0151 231 3701/3634

Such a policy would minimise the use of energy intensive, polluting, technological routes towards the goal of increased standards of living.

What will actually happen? The view of the Shell Petroleum Company is that renewable energies must become cost effective with existing fossil fuel based technologies before their widespread application can occur. Shell's view is that even if significant improvements in the efficient use of energy are made, the growing world population will still require a much increased primary energy supply, and this will be met from diverse sources<sup>18</sup>. Fossil fuels will continue to be the main source, then as renewables become more cost competitive they will play an increasing role. Shell envisages the global demand for fossil fuels increasing some 40% by 2030, which is a business as usual policy (see Fig 1.9). By that time renewable energy should provide a significant amount of the total fuel usage: 40% is predicted. An absence of comment by Shell on the growth of greenhouse gas emissions, makes the view of the World Energy Council particularly pertinent. Their proposition is that: "Renewable energies can make a growing contribution to providing major alternatives to fossil fuels, but insufficient to prevent major increases in most global greenhouse gas emissions and their atmospheric concentration over the next few decades."<sup>19</sup>

The European Commission takes a more positive approach. They support the view that the only realistic long term solution to the energy- environment problem is offered by increased use of renewable energy. They agree that the main barrier to more widespread use of renewable energies is due to the low price of fossil fuels. The commission realise that fossil fuel prices will not remain low for ever, and feel that renewable energies should be developed now, in order to be ready to replace fossil fuel technologies in the not so distant future<sup>20</sup>.



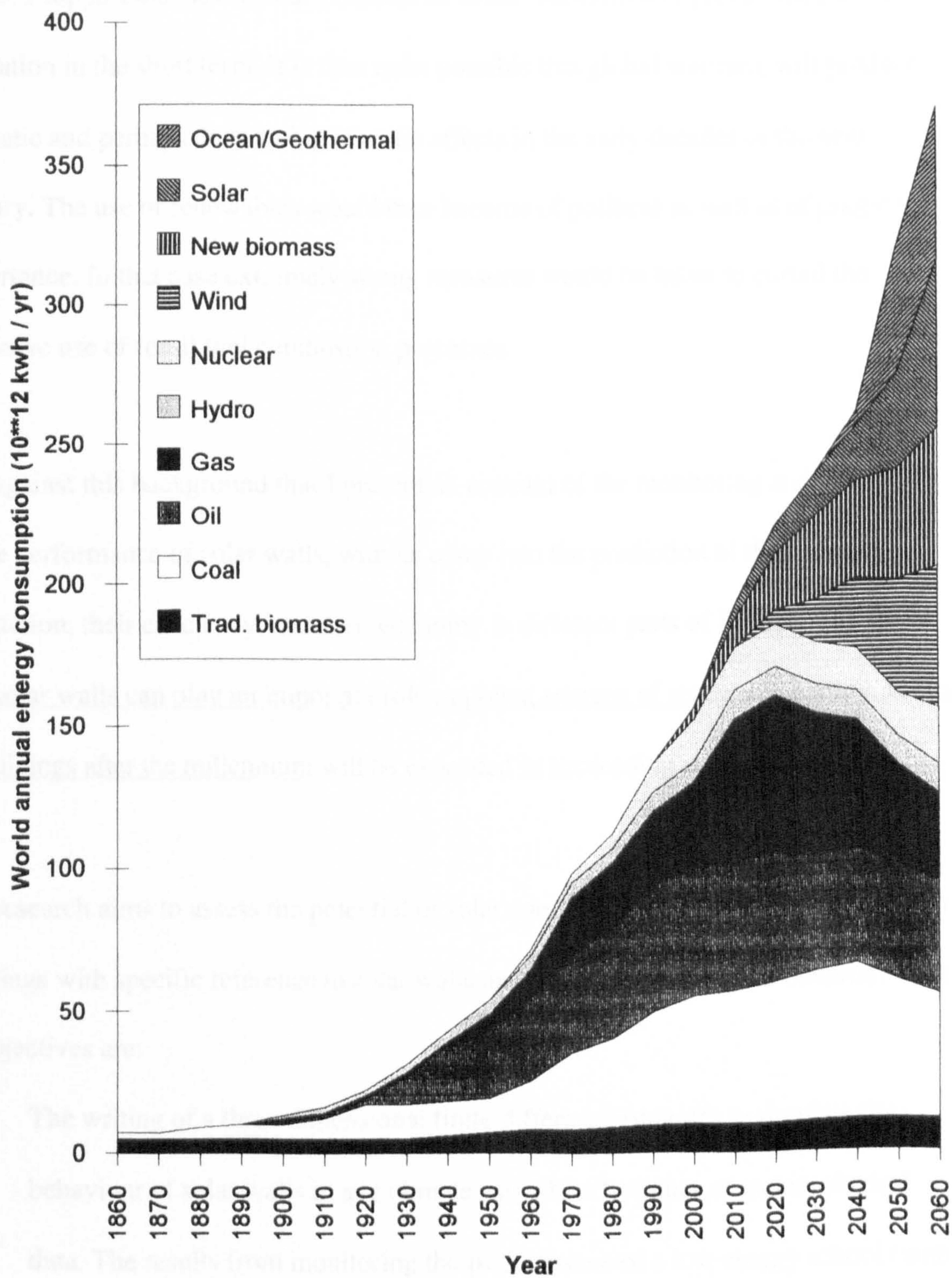


Fig. 1.9 Shell scenario for sustained growth using renewable energy sources.



These several views all support the importance of renewable energy for a sustainable future. I support the view that a “business as usual” scenario will prevail for energy utilisation in the short term. It is then quite possible that global warming will produce dramatic and perhaps devastating climatic effects in the early decades of the next century. The use of renewables would then become of political as well as of pragmatic importance. In that case extremely strong measures would be taken to curtail the excessive use of fossil fuel combustion processes.

It is against this background that I present an account of the monitoring and simulation of the performance of solar walls, with an essay into the prediction of their energy production, their efficiency, and their economy in different parts of Europe. The thesis: that solar walls can play an important role as potent sources of renewable energy, for use in buildings after the millennium will be expanded in succeeding chapters.

The research aims to assess the potential of solar energy for reducing energy demand in buildings with specific reference to solar walls and transparent insulation material. Thus its objectives are:

- (i) The writing of a three dimensional finite difference program to simulate the behaviour of solar walls in any climate using hourly values of meteorological data. The results from monitoring the performance of a low energy school (with solar wall) at Poulton Lancelyn, Wirral are to be used for program validation.
- (ii) Confirmation of optimised solar wall design using suitably exposed model solar walls.
- (iii) Assessment of the performance of transparent insulation material (TIM) using TIM clad model walls and modifications to the computer program.

- (iv) The development of a steady state program for the rapid assessment of solar wall performance in Western Europe.

# **CHAPTER TWO - SOLAR ENERGY: THEORETICAL CONSIDERATIONS**

## 2.1 THE SOLAR CONSTANT

The sun and its attendant planets, have physical properties that are well defined. The sun is a large ball of compressed gas, some 87,000 miles in diameter and 93 million miles away from earth. Inside, hydrogen gas atoms, fuse under intense pressure, protons change to neutrons, and new nuclei are born, via reactions such as:  $4\text{H}^1_1 \rightarrow \text{He}^2_4 + 2\text{e}^-$ . Extremely large amounts of energy are released, the core heating up to a temperature estimated to be 10 million °C, the surface to 6050 °C, and solar radiation results.

**Fig 2.1** represents the solar interior, the dense core of which generates 90% of the heat. Solar output is not constant, for dark areas (pores and sunspots) occur at times, producing variations in the emitted energy, and there is a long term diminution of the output of the sun<sup>21</sup>. For engineering purposes, at the present time, it is convenient to take the solar output as unvarying and equal in magnitude to the solar constant:  $G_{sc}$ . This is the extraterrestrial radiation received on unit area of surface, held perpendicular to its direction of propagation, the current value being  $1367 \pm 1 \text{ W/m}^2$ <sup>(22)</sup>. The solar constant is actually the value of the radiation received when the earth is at the equinoxes of its elliptical orbit. At other times the solar constant is modified to take such variation into account via the formula:

$$G_{ON} = G_{SC} \left( 1 + \frac{0.033 \cos 360N}{365} \right) \text{ W/m}^2. \quad (2.1)$$

## 2.2 THE SPECIAL DISTRIBUTION OF SOLAR RADIATION

*Table 2.1* indicates the accepted values of extraterrestrial solar irradiance for wavelengths between 250 nm and 2000 nm issued by the World Radiation Centre.

Extremely short wave components such as X-rays are quickly removed from the solar



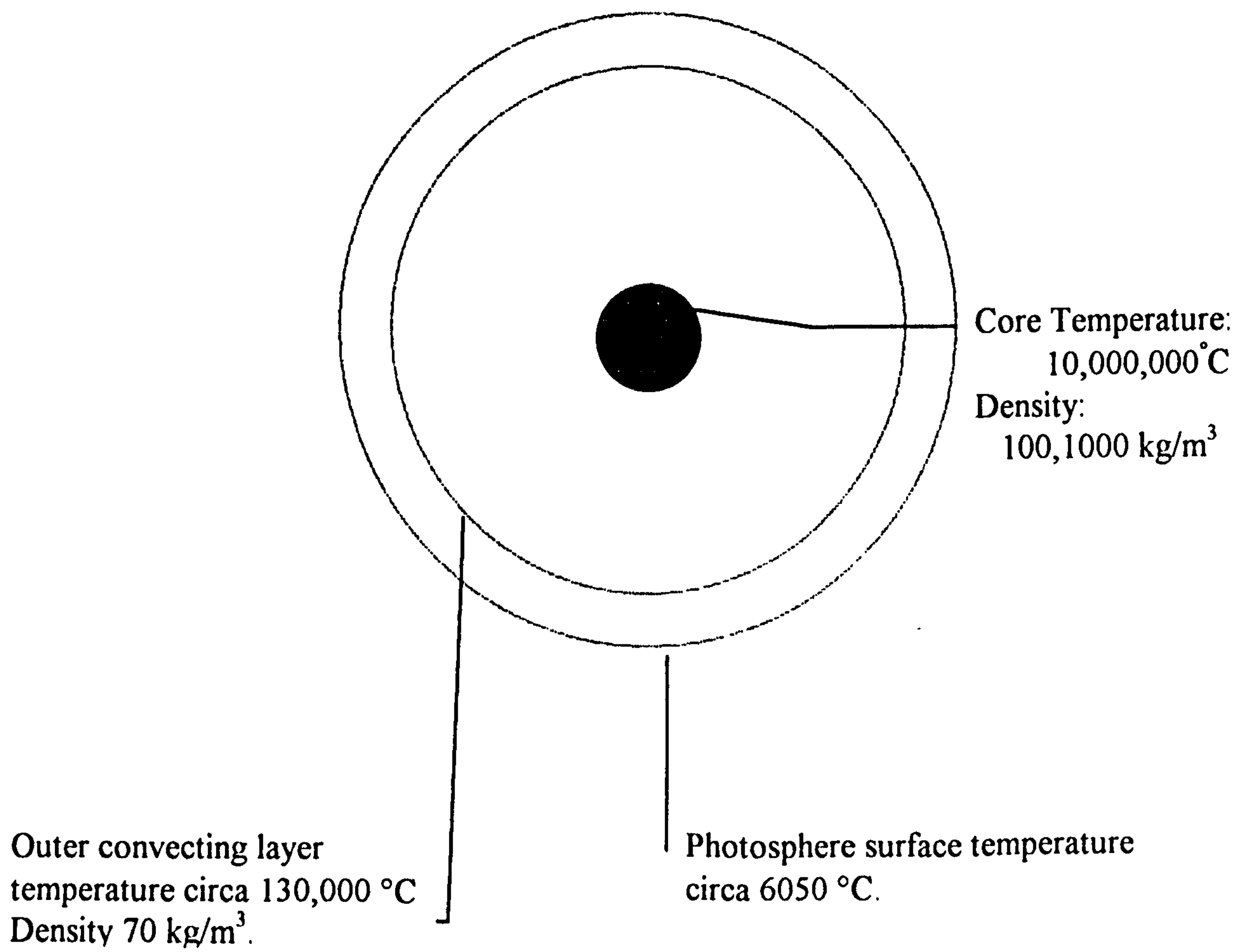


Fig. 2.1 Solar structure.

**Table 2.1 Extraterrestrial solar irradiance (the WRC spectrum) in increments of wavelength.**

Wavelength $\lambda$ $\mu\text{m}$	Solar irradiance $G_{\text{SC},\lambda}$ $\text{W}/\text{m}^2/\mu\text{m}$
.250	13.8
.300	542.3
.350	983
.400	1477
.450	1995
.500	1918
.550	1875
.600	1765
.700	1416.6
.800	1133.3
.900	911.9
1.0	756.5
1.1	591.1
1.2	505.6
1.3	429.5
1.4	354.7
1.5	296.6
1.6	241.7
1.8	169.0
2.0	100.7

radiation falling upon the earth by interaction with ionospheric gases in the outer layers of the atmosphere. Parts of another short wave component: ultra-violet radiation, manages to penetrate the atmosphere but fortunately its most energetic and damaging components (below 290nm) are removed by the ozone in the troposphere before they reach the earth's surface.

Solar radiation further attenuates as it passes through the troposphere (the lowest atmospheric layer) where it is scattered and absorbed by air molecules, water vapour, water droplets, and dust particles. The amount of this attenuation depends on the path length of the atmosphere traversed which is designated : the air mass. Air mass zero is extraterrestrial, air mass 1 that at the zenith, air mass 5 that near the horizon. The radiation that eventually reaches the earth's surface has small amounts of energy in the ultra-violet above 290 nm, a peak in the green-red region and substantial but diminishing amounts in the short wave infra-red. The solar spectral distribution is shown in *Table 2.1* and **Fig 2.2**, where the absorption produced by water vapour and carbon dioxide for longer wavelength radiation can be seen.

Often the only available solar data for a given European site covering long periods in the past is the historical record of daily sunshine hours, rather than the actual solar irradiance on a given plane. However once the sunshine hours of a locality are known, use of the solar constant and knowledge of how atmospheric attenuation affects the incoming radiation (using for example the Linke turbidity factor) will enable the beam and diffuse values for the solar radiation at that locality to be calculated. Such values for solar

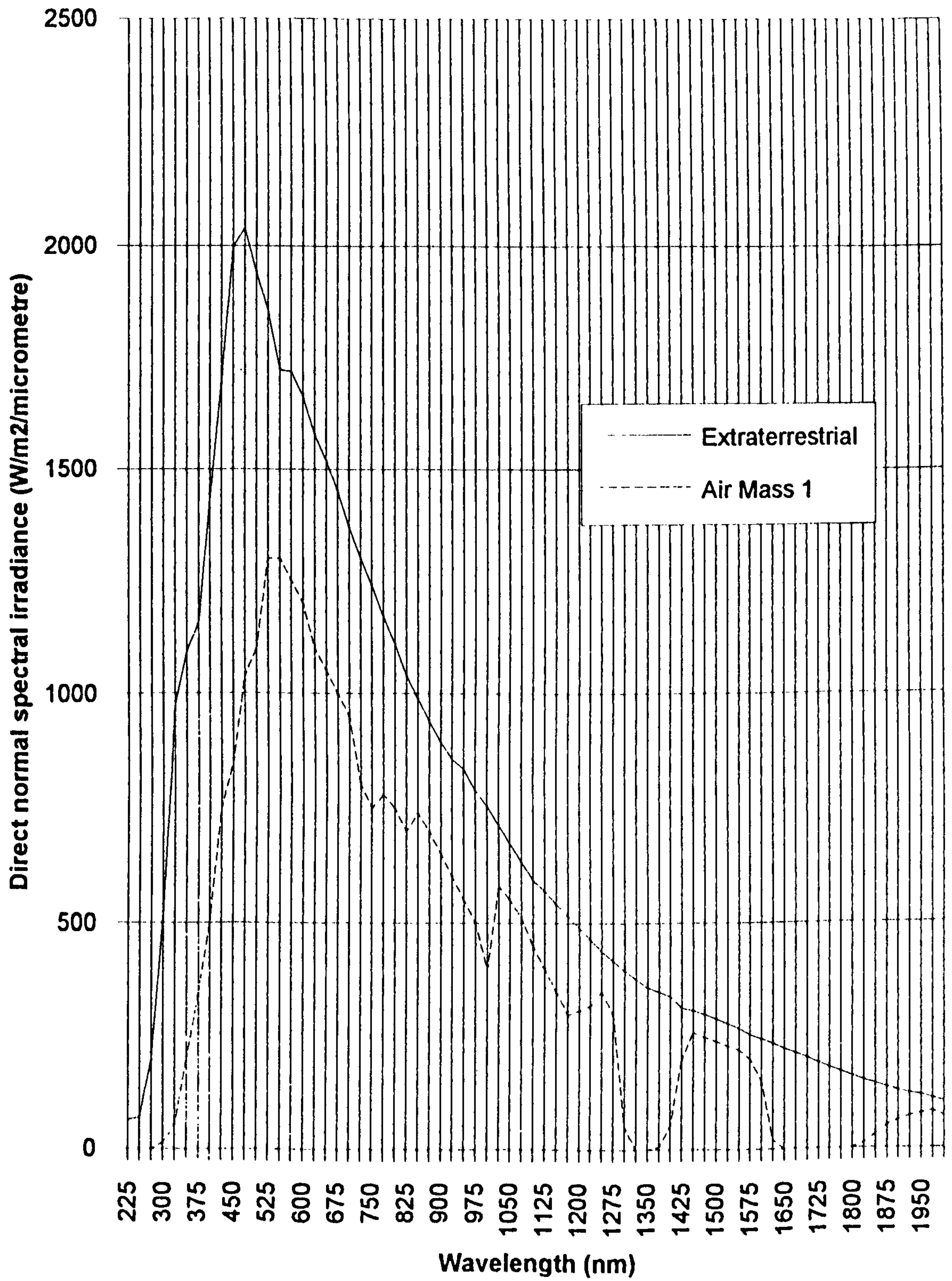


Fig. 2.2 Approximate spectral distribution of beam irradiance for air masses 0 and 1.



radiation falling on vertical surfaces facing south, averaged over all weather conditions, have been widely used in this work in addition to using actual measured data.

## 2.3 HEAT TRANSFER IN SOLAR WALLS

Before commencing the modelling of solar walls, it is appropriate to review the physics of the heat transfer process through them by radiation, convection and conduction in order that relevant algorithms may be selected.

### (1) Radiation

Radiation is electromagnetic energy propagated through space with the speed of light. It is emitted by bodies as their constituent electrons, excited to higher energy states by elevated temperatures, lose energy as the body cools. Such radiation is emitted over a wide range of frequency and wavelength (see *Table 2.2*), travelling with the speed of light  $c$ , wavelength  $\lambda$  and frequency  $\nu$  such that:

$$c = \lambda \nu \quad (2.2)$$

Energy associated with the radiation can be conceptualised by envisaging its transit through space in the form of particulate bundles of waves called photons of zero mass and charge, each with energy  $E$  determined by:

$$E = h\nu = \frac{hc}{\lambda} \quad (2.3)$$

where  $h = 6.6256 \times 10^{-34}$  Js is Planck's constant.

Table 2.2 The electromagnetic spectrum.

Radiation	Wavelength/m	Frequency/Hz	Particle energy/eV
Gamma	$10^{-12}$	$10^{21}$	$10^7$
			$10^5$
X Rays	$10^{-10}$	$10^{19}$	$10^3$
			$10^2$
Ultraviolet	$10^{-8}$	$10^{17}$	$10^2$
			$10^1$
Visible	$10^{-6}$	$10^{15}$	$10^1$
			$10^0$
Infrared	$10^{-4}$	$10^{13}$	$10^{-1}$
			$10^{-2}$
	$10^{-2}$	$10^{11}$	$10^{-3}$
	1	$10^9$	$10^{-4}$
			$10^{-5}$
	$10^2$	$10^8$	$10^{-6}$
Radiowaves	$10^2$	$10^8$	$10^{-6}$
			$10^{-7}$
	$10^4$	$10^6$	$10^{-7}$

Clearly low wavelength ultra-violet radiation has more energy associated with it than longer wavelength infra red radiation.

Planck also related the energy emitted at a given wavelength by an ideal absorber and emitter of radiation to its temperature  $T$  K. This energy, emitted by a blackbody (b), at a wavelength ( $\lambda$ ) is:

$$E_{b\lambda} = \frac{2\pi h C_0^2}{\lambda^5 (e^{hC_0/kT} - 1)} = \frac{C_1}{\lambda^5 (e^{C_2/\lambda T} - 1)} \quad (2.4)$$

where  $C_0 = 2.998 \times 10^8$  m/s is the speed of light in vacuum,  $k = 1.3805 \times 10^{-23}$  J/K,  $C_1 = 3.741 \times 10^{-16}$  m<sup>2</sup>W and  $C_2 = .014388$  mK

Plotting this energy distribution for temperatures of 6,000 K and 400 K gives the curves shown in **Fig 2.3**. A temperature of 6,000 K is approximately the surface temperature of the sun, and so the 6,000 K curve is an approximation of the distribution of solar radiation outside the earth's atmosphere.

For engineering purposes it is the total energy evolved from a heated body  $E_b$ , that is more pertinent. This energy is found by integration over all wavelengths to be:

$$E_b = \int_0^\infty E_{b\lambda} d\lambda = \sigma T^4 \quad (\text{W/m}^2) \quad (2.6)$$

where  $\sigma = 5.6697 \times 10^{-8}$  W/m<sup>2</sup>K<sup>4</sup> is the Stefan Boltzmann constant.

### Infra red radiation exchange between gray surfaces

Within a solar wall, radiation exchange occurs between parallel surfaces placed quite close to each other (see **Fig 2.4**). Such surfaces are defined as gray if their emitted radiation is independent of wavelength, but less than that of a blackbody. The fraction of

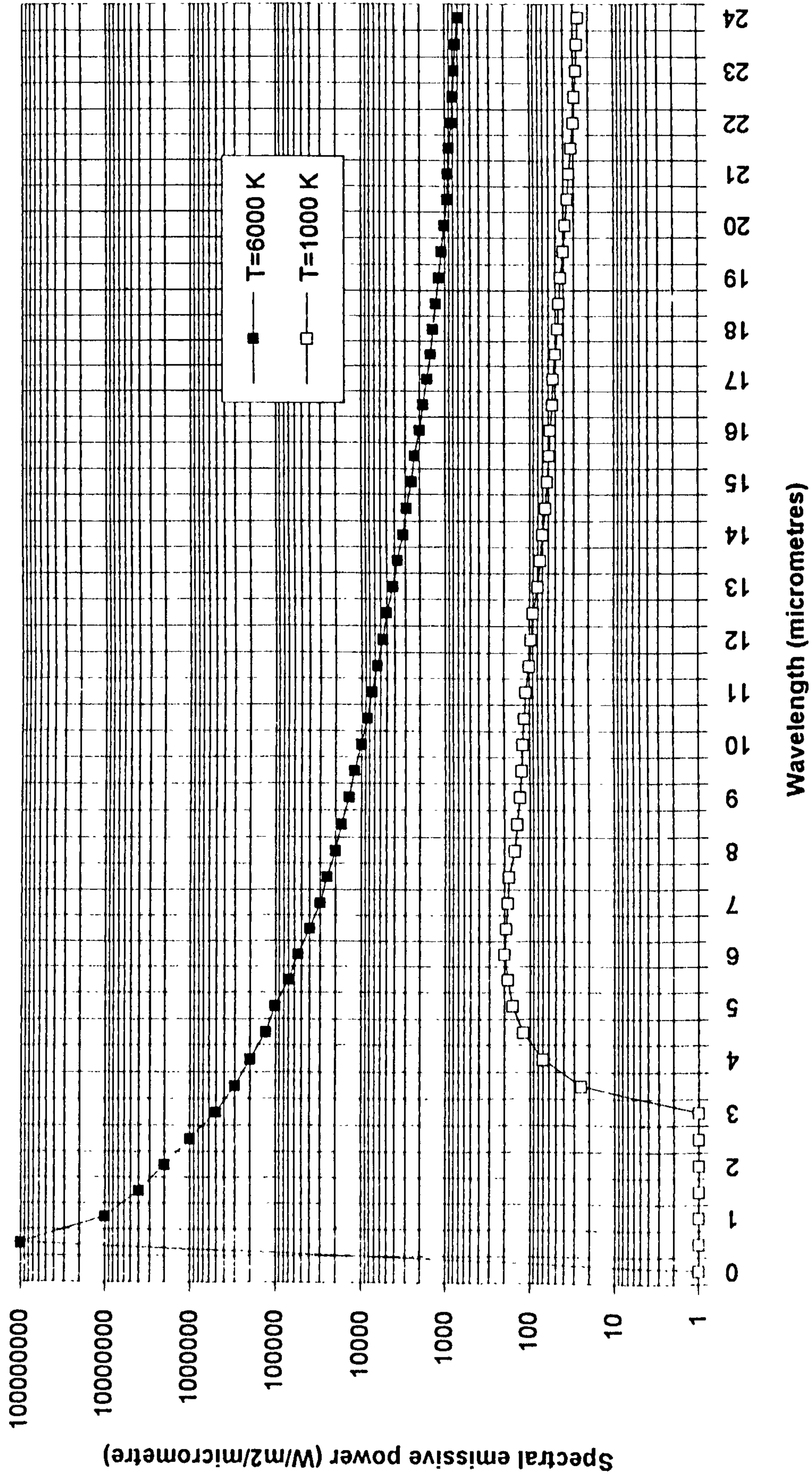


Fig.2.3 Approximate spectral distribution of blackbody radiation at two different temperatures.



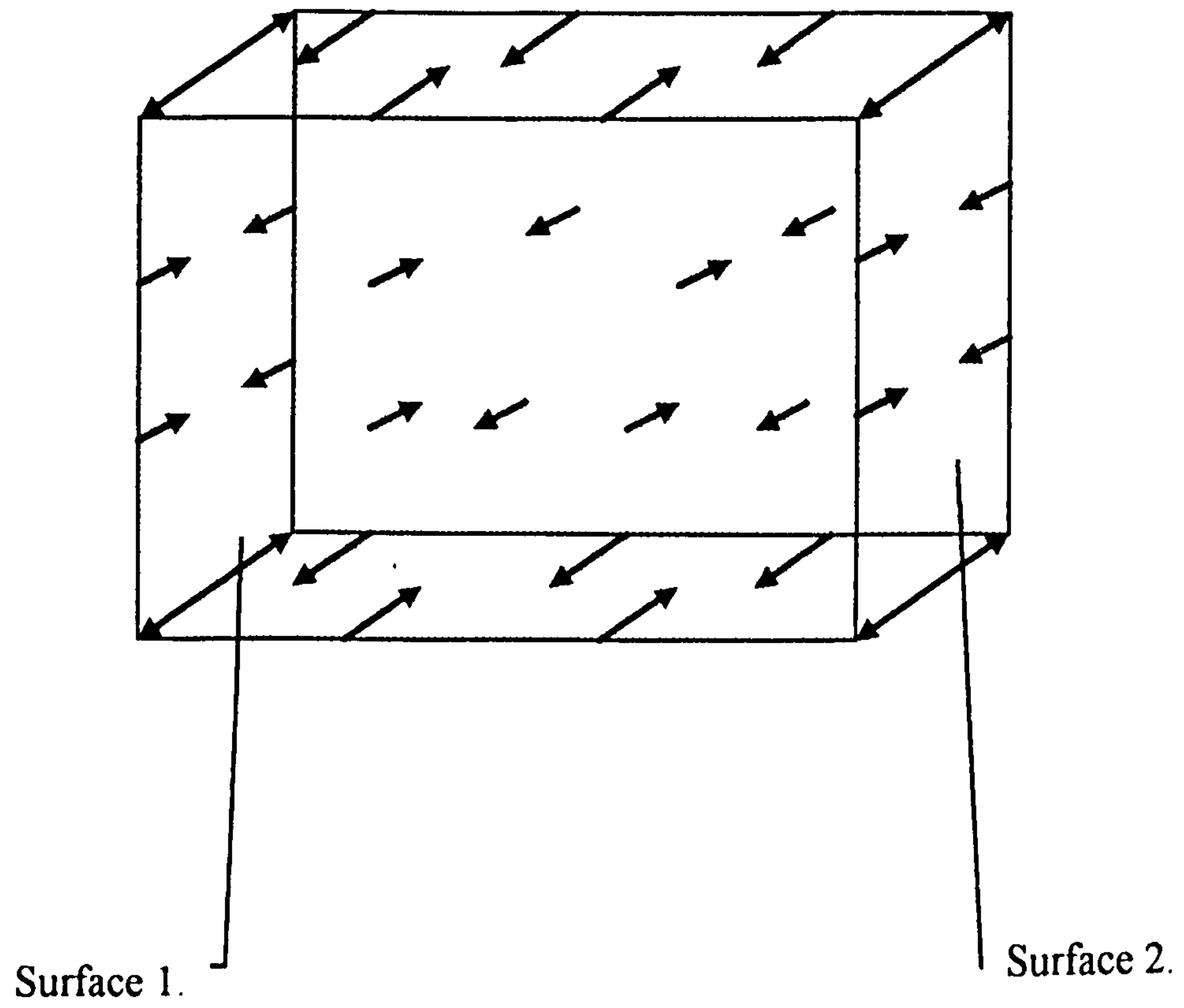


Fig. 2.4 Radiation exchange between parallel plates.

radiation emitted, compared to that emitted by a blackbody is the emissivity  $\epsilon$ . Applying (2.6) to two parallel diffuse surfaces at temperatures  $T_1$  and  $T_2$  and emissivities  $\epsilon_1$  and  $\epsilon_2$  radiating to each other, the net heat transfer  $Q$  between the two surfaces is:

$$Q = \frac{A\sigma((T_2)^4 - (T_1)^4)}{\frac{1}{\epsilon_1} + \frac{1}{\epsilon_2} - 1} \quad (2.7)$$

where  $A$  is the area of each surface.

This equation can be simplified to:

$$Q = \frac{A\sigma((T_2)^2 + (T_1)^2)(T_2 + T_1)(T_2 - T_1)}{\frac{1}{\epsilon_1} + \frac{1}{\epsilon_2} - 1} \quad (W) \quad (2.8)$$

and then to:

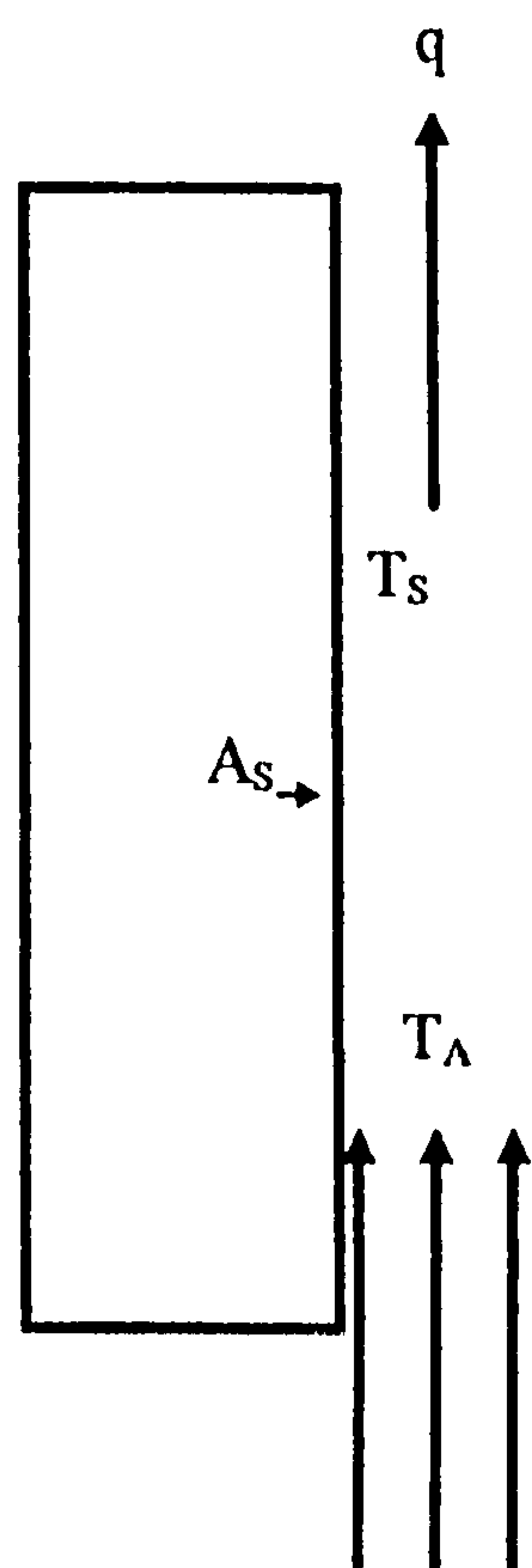
$$Q = Ah_r(T_2 - T_1) \quad (W) \quad (2.9)$$

Here  $h_r$  is a heat transfer coefficient for use when heat is lost or gained by radiation from emitting surfaces such as solar walls. Clearly radiant heat transfer between two surfaces is highly dependent on the temperature difference between them.

## (2) Convection

This process also plays an important part in the heat transfer between two flat parallel plates and between building surfaces (see **Fig 2.5**). Practically, convection heat transfer coefficients, designated  $h_c$ , are used to relate the heat transfer rate  $Q$  to the temperature differences between surfaces and the surrounding air via an equation of form:

$$Q = h_c A (T_s - T_a) \quad (W) \quad (2.10)$$



$q = h.A_s.(T_s - T_A) = \text{heat transfer rate (W)}$ .  
 $T_s = \text{surface temperature. } T_A = \text{air temperature.}$   
 $h = \text{convection heat transfer coefficient (W/m}^2\text{K)}$   
 $A_s = \text{surface area (m}^2\text{)}$

**Fig. 2.5 Heat transfer by convection at a vertical surface.**

Heat transfer at building surfaces is more complex than that between the small plates used for much of the published work on natural convection in air. Waters<sup>23</sup> has demonstrated that an equation for turbulent heat transfer:  $Nu = m'(Ra)^{1/3}$  can be used to obtain convection heat transfer coefficients suitable for applications in buildings. Nu is the Nusselt number, and Ra the Rayleigh number:

$Ra = g\beta\Delta TL^3 / (\nu\alpha)$ , where:

$g$	=	gravitational constant
$\beta$	=	volumetric coefficient of expansion
$\Delta T$	=	temperature difference between plates
$\nu$	=	kinematic viscosity
$\alpha$	=	thermal diffusivity
$L$	=	plate spacing

In the literature, Fischenden and Saunders<sup>24</sup>, give a value of  $m' = 0.12$ . The equations for calculating the convective heat transfer coefficients then become:

$$h_c = 1.44(\Delta T)^{1/3} \quad (\text{For vertical surfaces and turbulent flow})$$

$$h_c = 1.68(\Delta T)^{1/3} \quad (\text{For horizontal surfaces, heat flow up, turbulent flow})$$

$$h_c = 0.64(\Delta T/x)^{1/4} \quad (\text{For horizontal surfaces, heat flow down, laminar flow})$$

Here  $\Delta T$  is the temperature difference between the surfaces, and  $x$  = the average length of the side of a surface. Waters uses these equations for determining temperatures, heating and cooling loads in buildings.

For the relatively constant temperature differences observed in buildings these equations can be simplified. Danter<sup>25</sup> suggests using values of 3.0, 4.3, and 1.5 W/m<sup>2</sup> for vertical surfaces, horizontal surfaces with upward flow, and horizontal surfaces with downward flow of heat respectively. These convection heat transfer coefficient values, applying to natural convection in buildings, have been adopted by the CIBS<sup>26</sup> for internal use.

Externally, forced convection heat transfer coefficients are more appropriate:



$$h_c = 5.8 + 4.1v \quad (2.11)$$

where  $v$  = wind speed (m/s)

Practically, external exposure has been simplified to just three categories:

- sheltered with  $v = 1.0$  m/s.
- normal with  $v = 3.0$  m/s.
- severe with  $v = 9.0$  m/s.

These categories relate to lower exposed floors, the 4th to 8th floors and upper floors in urban areas. They, together with the simplified convection heat transfer coefficients have been used in the computer modelling undertaken here.

### (3) Conduction: steady state heat flow

The equation governing the flow of heat in an isotropic solid of constant thermal conductivity is:

$$\frac{\delta T}{\delta t} = \alpha \nabla^2 T + \frac{H(t)}{\rho c} \quad (2.12)$$

where:

$T$  = the temperature at any point in the solid  $k$  = thermal conductivity.

$\rho$  = density

$\alpha = k/\rho c$  = thermal diffusivity

$H(t)$  = the rate of heat generation per unit volume.

There is usually no heat generation within the material of a building and so  $H(t)$  may be set to zero. Equation 2.12 then becomes the Fourier equation. For steady state heat transfer,  $\delta T/\delta t = 0$ , and the equation reduces further to:

$$\nabla^2 T = 0. \quad (2.13)$$

For linear heat flow, equation 2.12 becomes:

$$\frac{\delta T}{\delta t} = \alpha \frac{\delta^2 T}{\delta x^2} \quad (2.14)$$

and equation 2.13 becomes:

$$\frac{dT}{dx} = \text{constant} = -\frac{q}{k} \quad (2.15)$$

where  $q$  is the heat flow per unit area. Since the simplest and most frequent case of conduction in buildings can often be considered as heat flow through a plane wall, equations 2.14 and 2.15 are the most used.

For steady state linear heat flow it is convenient to rearrange 2.15 to read:

$$q = -k \frac{dT}{dx} = -k \frac{T_2 - T_1}{l} = \frac{T_1 - T_2}{l/k} \quad (2.16)$$

where  $l$  is the thickness of the material.

The equation is analogous to Ohms law, the quantity  $l/k$  being called the thermal resistance. For a multilayer wall the heat flow is given by:

$$q = \frac{T_1 - T_2}{l_1/k_1} = \frac{T_2 - T_3}{l_2/k_2} = \frac{T_3 - T_4}{l_3/k_3} \quad (2.17)$$

whence:

$$q = \frac{T_1 - T_4}{(l_1/k_1 + l_2/k_2 + l_3/k_3)} \quad (2.18)$$

$T_1$  and  $T_4$  are the surface temperatures of layers 1 and 4 and  $T_2$  and  $T_3$  are the temperatures at the boundaries of the intermediate layers.

The resistance  $R$  of a composite wall is thus the sum of the individual resistance's of its component layers:

$$R = R_1 + R_2 + R_3 = l_1/k_1 + l_2/k_2 + l_3/k_3 \quad (2.19)$$

The convection and radiation exchange at each wall surface give rise to additional surface resistance's: the internal surface resistance  $R_{si}$  and the external surface resistance  $R_{so}$  which may be added to the wall resistance to give:

$$R = R_{si} + R_1 + R_2 + R_3 + R_{so} \quad (2.20)$$

The heat flow may then be calculated from the air temperatures  $T_{ai}$  and  $T_{ao}$ , inside and outside the wall. The common practice is to express the total resistance as a conductance, or 'U-value', so that heat flow may be then calculated using the equation:

$$q = U (T_{ai} - T_{ao}), \text{ where } U = 1/R \quad (2.21)$$

The U-values of many walls, floors and roofs are given in many text books, and guides<sup>26</sup>.

#### **(4) Conduction: the transient state<sup>27</sup>**

There are many difficulties in obtaining a solution of equation 2.14 for non-steady state linear heat flow. Solutions for a single homogeneous wall are available, but are much more difficult to obtain for a multi-layer wall. Most of the solutions given in text books are for idealised cases such as when:

- a step change in heat input occurs to one surface of the wall.
- a step change in temperature occurs at one surface.
- a periodic change of temperature occurs at one surface.

It is usually impossible to choose boundary conditions suitable for use with the text book solutions which correspond exactly with situations occurring in practice.

Many of the difficulties which arise in trying to produce an analytical solution of the equation governing non-steady state heat flow can be avoided by using numerical methods in which the derivatives of the heat conduction equation are replaced by finite difference ratios. A full description of finite difference methods and the way they have been applied in this study is given later.

#### **2.4 SOLAR RADIATION: TRANSMISSION AND ABSORPTION<sup>28</sup>**

The first step in modelling solar collector performance is to produce equations which determine the amount of radiation passing through transparent collector covers, together with the quantity absorbed at the collector absorbing surface.



This is best done by dividing the task into three parts:

- finding the transmittance through the glazing after reflection losses
- finding the transmittance through the glazing after absorption losses
- finding the proportion of radiation absorbed at the collector absorbing surface

### Solar transmittance after reflection $\tau_r$

Relevant equations for the reflection of radiation at glazing interfaces have been derived by Fresnel, which take into account the polarisation of solar radiation as it passes through transparent covers. The relevant equations for reflectance are:

$$r_{\perp} = \sin^2(\theta_2 - \theta_1) / \sin^2(\theta_2 + \theta_1) \quad (2.22)$$

$$r_{\parallel} = \tan^2(\theta_2 - \theta_1) / \tan^2(\theta_2 + \theta_1) \quad (2.23)$$

$$r = (r_{\perp} + r_{\parallel}) / 2 \quad (2.24)$$

For refraction by Snell's law:

$$n_2 / n_1 = \sin \theta_1 / \sin \theta_2 \quad (2.25)$$

where:

$\theta_1$  = angle of incidence

$\theta_2$  = angle of reflection

$n_1$  = refractive index, medium 1

$n_2$  = refractive index medium 2

$r_{\perp}$  = reflection of perpendicular component for unpolarised radiation

$r_{\parallel}$  = reflection of parallel component for unpolarised radiation

The total transmittance after reflection through a non absorbing cover is shown in Fig 2.6. For 1 cover and two polarised components, transmittance can be calculated from the equations:

$$\tau_{\perp} = (1-r_{\perp})^2 \cdot \sum_{N=0}^{N=\infty} r_{\perp}^{2N} = (1-r_{\perp})/(1+r_{\perp}) \quad (2.26)$$

$$\tau_{\parallel} = (1-r_{\parallel})^2 \cdot \sum_{N=0}^{N=\infty} r_{\parallel}^{2N} = (1-r_{\parallel})/(1+r_{\parallel}) \quad (2.27)$$

The overall transmittance, (the average of the two components) will then be:

$$t_r = (t_{\perp}+t_{\parallel})/2 = ((1-r_{\perp})/(1+r_{\perp}) + (1-r_{\parallel})/(1+r_{\parallel}))/2 \quad (2.28)$$

For N covers, extension of the above analysis gives:

$$t_{rN} = (1 + (1-r_{\perp})/(1 + (2N-1)r_{\perp}) + (1-r_{\parallel})/(1 + (2N-1)r_{\parallel}))/2 \quad (2.29)$$

Solar transmittance after absorption by the glazing:  $\tau_a$

As radiation passes through a partially transparent medium such as glazing, some of it is absorbed, as described by Bouguer's law:

$$\frac{dI}{dx} = -KI \quad (2.30)$$

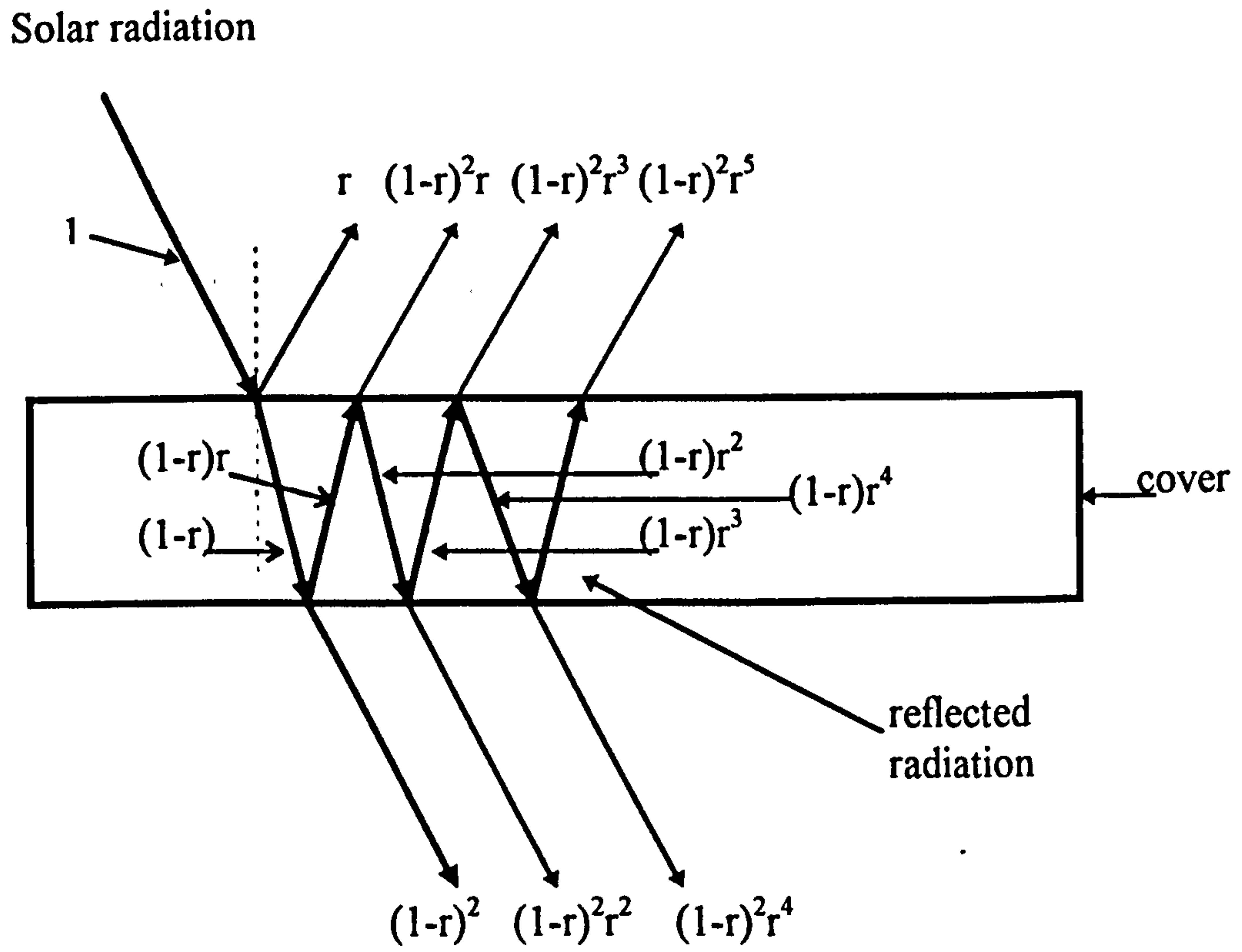
where:

I = the radiation intensity at a distance x in the medium

K = the extinction coefficient

On integrating:

$$\tau_a = \frac{I_{\text{transmitted}}}{I_{\text{incident}}} = \exp(-KL/\cos\theta_2) \quad (2.31)$$



$$\text{Overall transmittance} = (1-r)^2 \sum_{N=0}^{N=\infty} r^{2N}$$

Fig. 2.6 Transmission through one non absorbing cover.

where:

$L$  = thickness of glazing

Values of  $K = 4\text{m}^{-1}$  (for iron free glass) and  $L = .004\text{m}$  have been used in the determination of  $\tau_a$ .

The overall transmittance:  $\tau$

From these values of transmittance by absorption and reflection an overall value is determined from the approximate relation:

$$\tau \approx \tau_a \tau_r \quad (2.32)$$

where  $\tau_a$  and  $\tau_r$  are the transmittances for a system of  $N$  covers.  $L$  is taken as the total cover thickness when evaluating  $\tau_a$ .

Clearly, the transmittance is dependant on the angle of incidence of the beam radiation falling on a solar wall throughout a day. To enable transmittance values to be calculated, for use in the main solar wall simulation program, a preliminary computer program was written to calculate the angles of incidence for vertical south facing surfaces. For simplification, values for these angles occurring on a day at the middle of a month throughout the year were included as data in the main program. Algorithms used were obtained from Page<sup>29</sup>. The main algorithm for a south facing wall is:

$$\cos v = \cos \gamma \cdot \cos a_f$$

where:

$v$  = angle of incidence

$\gamma$  = solar altitude



$a_f$  = wall solar azimuth

The computer program code is given in *Appendix 3.19*

Transmittances may be calculated for each hourly angle of incidence throughout a day for use in the solar wall modelling process. Examples of the change in transmittance of iron free glass with angle of incidence, for systems of one and two covers, are shown in **Fig 2.7**.

#### Transmittance for diffuse radiation.

The preceding analysis applies to the beam component of solar. Radiation falling on a solar collector also includes that scattered from the sky and possibly reflected from the ground. Such radiation is diffuse and isotropic. Equivalent angles of beam radiation that give the same transmittance as such diffuse radiation when falling on sloped surfaces have been calculated (see **Fig 2.8**). The value for vertical walls has been used in the modelling process. In such a case diffuse radiation becomes equivalent to beam radiation arriving at an incidence angle of  $60^\circ$ .

#### The transmittance-absorptance product

After passing through a cover system, a fraction of the remaining solar radiation is absorbed into the generally opaque body of the solar collector. The fraction of the incident radiation absorbed is initially  $\tau\alpha$ , where  $\alpha$  is the absorptance of the absorber surface. After multiple reflections between the absorber and cover (see **Fig 2.9**), this fraction increases to:

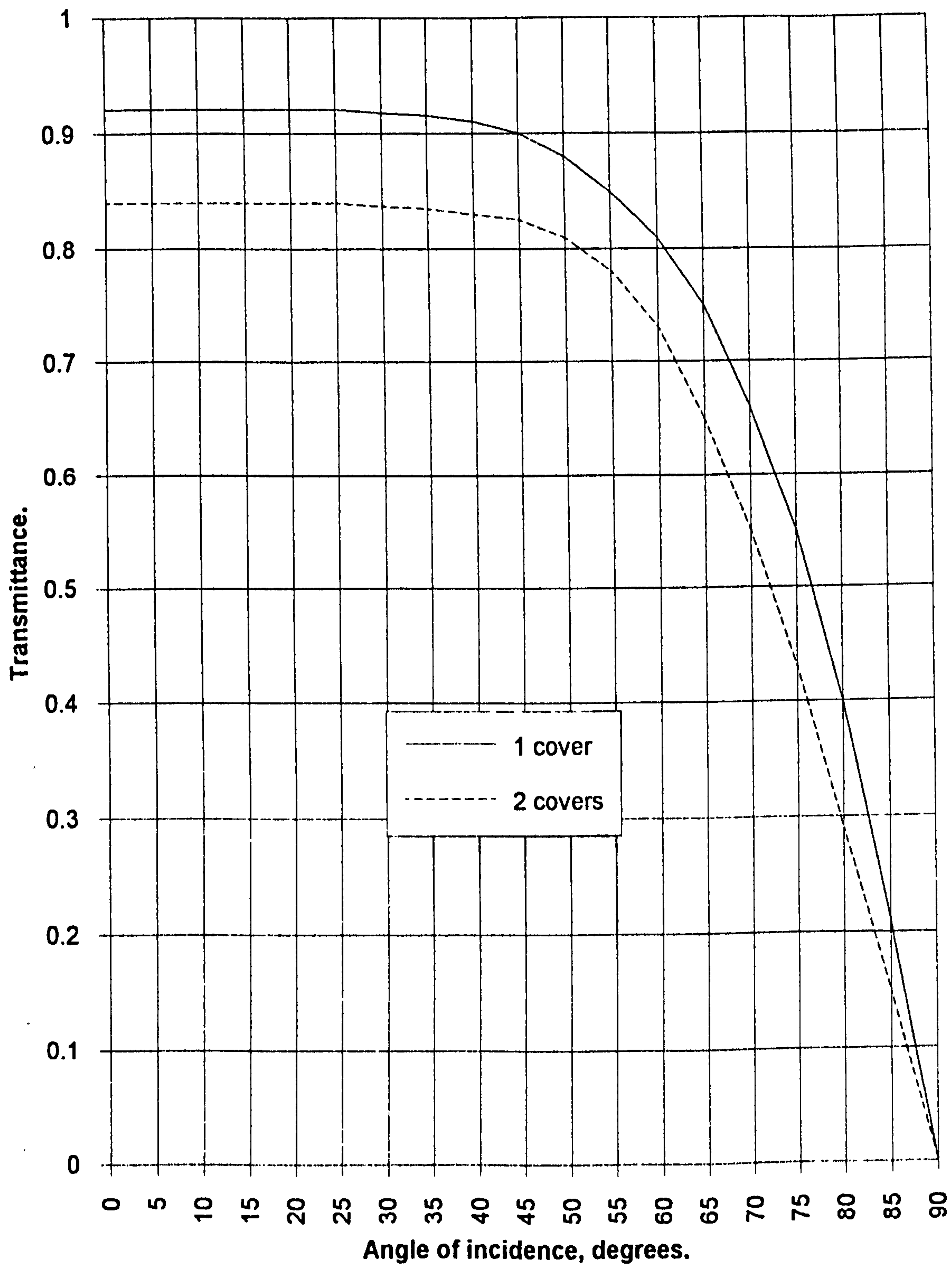
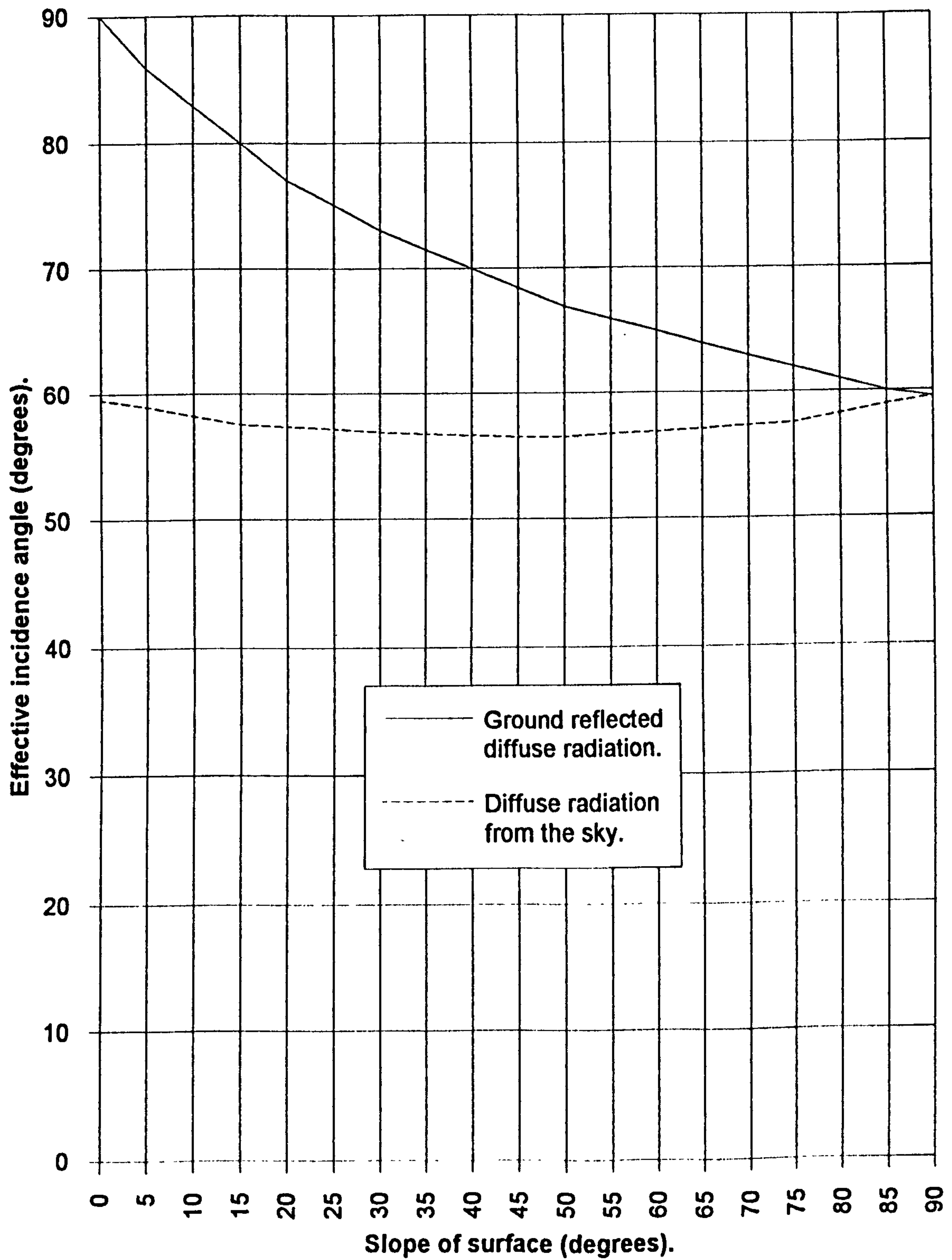


Fig. 2.7 Transmittance of 1 and 2 covers for iron free glass of refractive index 1.525.



**Fig.2.8 Effective incidence angle of isotropic diffuse radiation on sloped surfaces.**

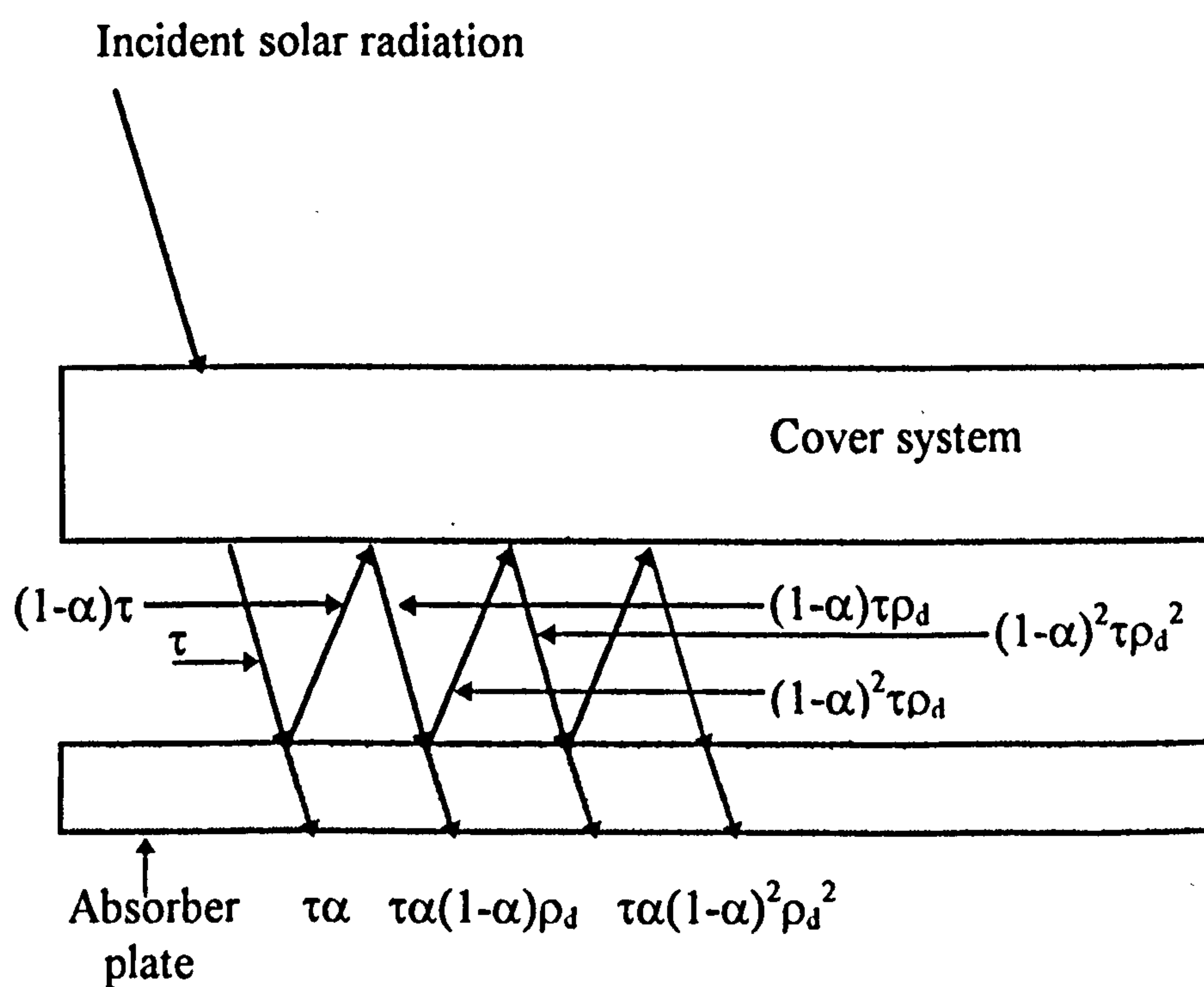


Fig. 2.9 Absorption of solar radiation by an absorber plate under a cover system.



$$(\tau\alpha) = \tau\alpha \cdot \sum_{n=0}^{n=\infty} ((1-\alpha)\rho_d)^n = \tau\alpha / (1 - (1-\alpha)\rho_d) \quad (2.34)$$

Here  $\rho_d = (1 - \tau_r)$  is the reflectance at the internal side of the cover system. For practical purposes, for use in the simulation program described later, such evaluation is unnecessary. It is more convenient to use the approximate relation:

$$(\tau\alpha) = 1.01\tau\alpha \quad (2.35)$$

### The angular dependence of the transmittance-absorptance product

The angular dependence of transmittance  $\tau$  has been discussed. Experimentally determined values of the dependence of solar absorptance on incidence angle, for flat, matt black or selectively coated surfaces, are shown in **Fig 2.10**. The values of  $(\tau\alpha)$  for use in solar wall and solar collector calculations, for single or double glazing over absorber surfaces, can then be found from the data quoted. Klein<sup>103</sup> has produced typical curves which illustrate the angular dependence of  $(\tau\alpha)$  (see **Fig 2.11**) for 1 or 2 covers of 2.5 mm thickness iron free glass. Similar data has been incorporated in the simulation program.

## 2.5 SOLAR COLLECTORS

These are heat exchangers which convert solar radiation into heat, so raising the temperature of a fluid such as air or water. They operate under conditions of low intensity, variable, incident solar radiation flux which at its highest, (without concentration) is of the order of 1100 W/m<sup>2</sup>. Even though they appear unpromising, flat plate collectors have shown themselves to be useful in delivering sufficient energy to

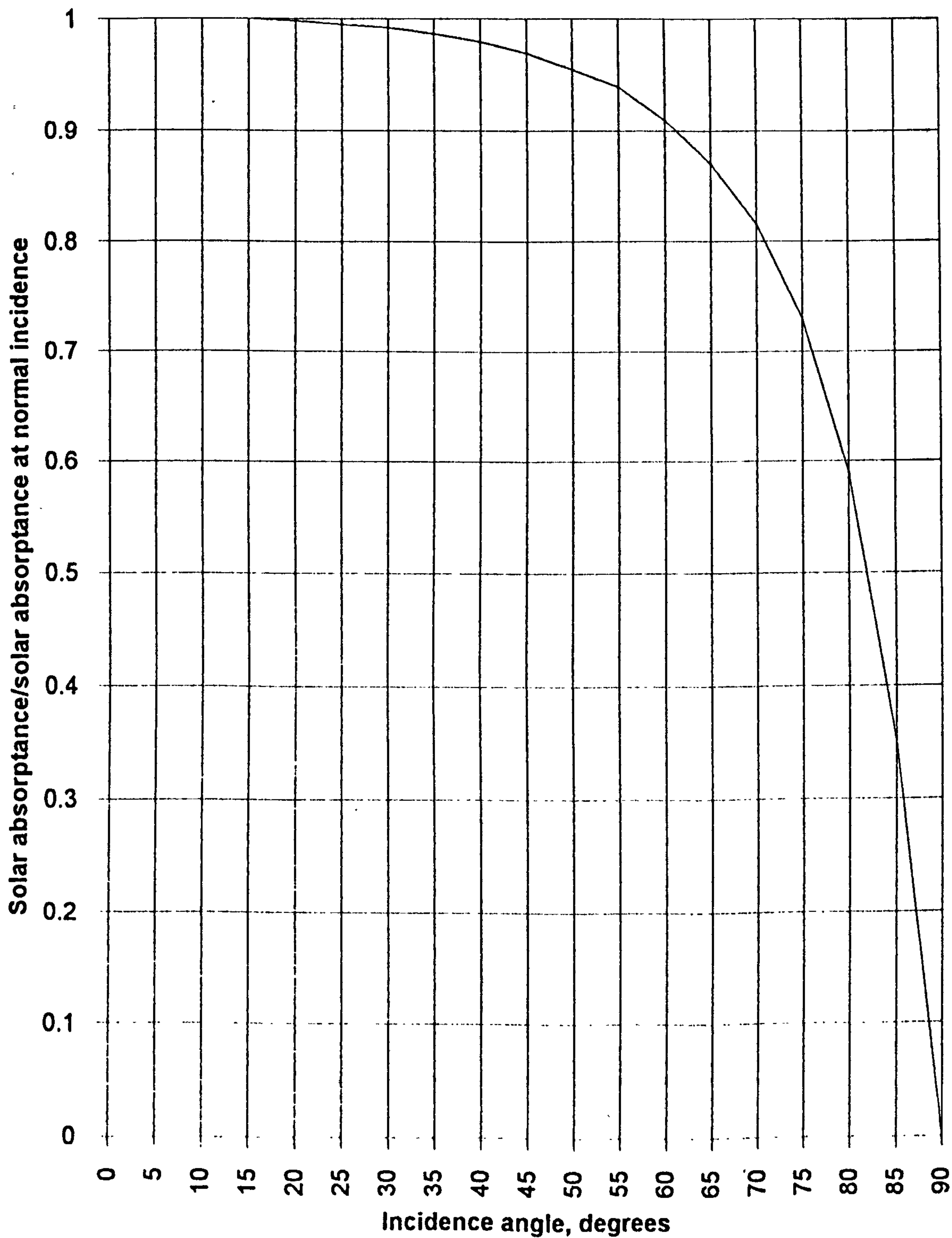
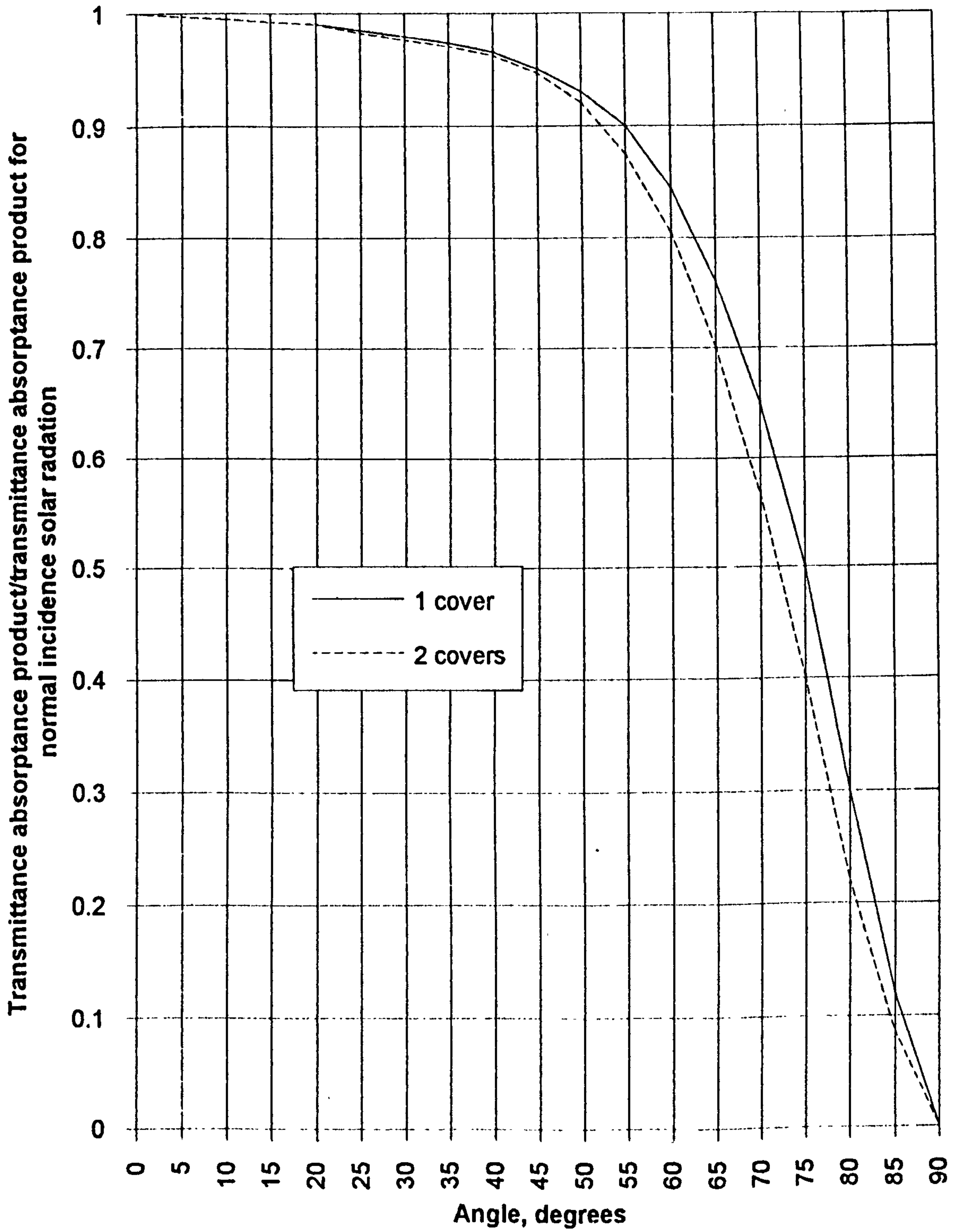


Fig.2.10 Ratio of solar absorptance to solar absorptance at normal incidence for a flat black surface. From Beckman et al. (1977).(30)



**Fig. 2.11 The angular dependence of the transmittance-absorptance product for 3mm thick iron free glass. Adopted from Klein (1979).(103)**

plate collectors have shown themselves to be useful in delivering sufficient energy to produce a modest elevation of fluid temperatures above the ambient. Their major application has been the heating of water and the interior of buildings. The walls of buildings for example, become solar collectors immediately some form of transparent insulation is applied.

### Basic energy balance equations

It is instructive to understand the operation of a typical solar collector. Its essential parts are depicted in Fig 2.12(a). The application of transparent materials such as glazing, immediately reduces convective and radiative losses from an absorber to the environment, as does the insulation to its sides and rear. The higher the thermal conductivity of the absorber, the more rapid the heat transfer will be to the fluid in a water or air heating collector. In the special case of a collector integrated into the wall of a building, back insulation is often dispensed with. Heat can then be efficiently transferred to the interior, after an appropriate time lag, depending on the thickness and thermal conductivity of the absorber wall material.

The steady state performance of a collector is then determined by the difference between:

- (i) the solar radiation absorbed by the collector per unit area of collector front surface:

$$S = (\tau\alpha)_{AV} \cdot I_T \quad (\text{W/m}^2) \quad (2.36)$$

- (ii) the thermal energy lost from the collector to the surroundings per unit area of front surface:

$$Q_{Lc}/A_c = U_{Lc} \cdot (T_{pm} - T_a) \quad (\text{W/m}^2) \quad (2.37)$$



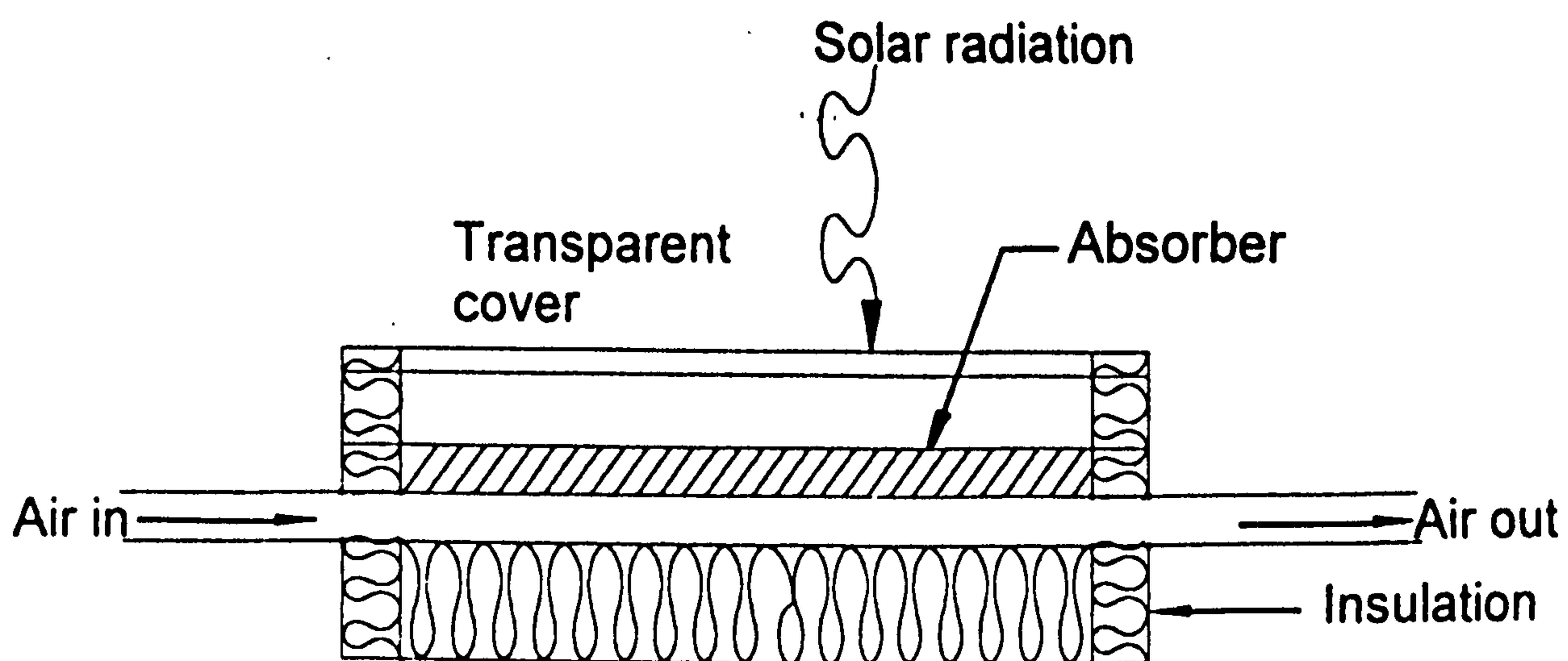


**Fig. 2.12(a) Cross section of a flat plate air heating collector.**

where:

$I_T$  = average solar irradiation over one hour on a tilted plane  $W/m^2$

$U_L$  = collector overall heat loss coefficient  $W/m^2 K$

$T_{pm}$  = absorber plate mean temperature  $K$

$T_a$  = external air temperature  $K$

$A_C$  = front surface area of collector  $m^2$

Then the useful energy output per unit area of collector surface is:

$$Q_U/A_C = (\tau\alpha)_{AV} \cdot I_T - U_L(T_{pm} - T_a) \quad (W/m^2) \quad (2.38)$$

Equation 2.38 is generally converted, for ease of use, to the form:

$$Q_U/A_C = (\tau\alpha)_{AV} \cdot I_T - U_L \cdot F_R \cdot (T_{fi} - T_a) \quad (W/m^2) \quad (2.39)$$

where:

$T_{fo}$  = fluid outlet temperature

$T_{fi}$  = fluid inlet temperature

$F_R$  = collector heat removal factor

If the energy is removed by the fluid flowing at  $m'$   $kg/m^3s$ , with specific heat  $c_p$ ,

then the heat removed is:

$$Q_U = m' \cdot c_p \cdot (t_{fo} - t_{fi}) \quad (2.40)$$

and:

$$F_R = \frac{m' c_p (t_{fo} - t_{fi})}{A_C (S - U_L (t_{fo} - t_{fi}))} \quad (2.41)$$

### The optimum spacing between the glazing and the absorber

It is relatively simple to calculate the thermal conductance between the absorber plate and the external environment. This conductance is known as the top loss coefficient.

When this conductance is plotted against the values of the spacing between the absorber and glazing, distinct minima are seen to occur at spacings of 10 mm and 50 mm.

Accordingly a spacing value of 50 mm was adopted for all the simulation and experimental work undertaken and reported here.

### The collector heat capacity

As the collector heats up, heat is stored in the absorber plate and the cover plate.

Assuming that the heat losses from the cover to the air are the same as from the plate to air, an overall effective collector heat capacity can be defined. Taking this into account the plate temperature and therefore the temporal performance of solar collectors<sup>31</sup> can be determined using an equation of the form:

$$\frac{S - U_L \cdot (T_P - T_a)}{S - U_L \cdot (T_{p\text{initial}} - T_a)} = \exp\left(\frac{-A_C U_L t}{(mc)_e}\right) \quad (2.42)$$

Such equations, will evaluate the absorber plate temperature  $T_P$  after a time  $t$ ,

where :

$(mc)_e$  = an effective collector heat capacity including that of cover and plate

$T_{p\text{initial}}$  = initial plate temperature K

Many measurements of the performance of high thermal conductivity, flat plate collectors, indicate that the use of simple steady energy balance equations give a very satisfactory representation of their behaviour<sup>32</sup>. This is certainly not the case for the irradiation of massive solar walls, with their large thermal capacity and low thermal conductivity. In this case, the rate of heat transfer to the interior is slow, and heat losses from the absorber become more important.

A complete analysis of collector behaviour should therefore include all the design parameters of the steady state model, plus an analysis of transient behaviour in which the thermal capacity of the solar collector is taken into account. Such is the approach of many thermal simulation programs such as TRNSYS<sup>33</sup> and is also the approach used here.

### The efficiency of energy production

The useful energy produced by a solar collector per unit area is:

$$\frac{Q_U}{A_C} = F_R \cdot (G_T \cdot (\tau\alpha) - U_L \cdot (T_{fo} - T_{fi})) \quad (2.43)$$

where:

$G_T$  = the solar irradiance falling on the collector at some given tilt angle ( $W/m^2$ )

In terms of fluid flow rate  $m'$  and fluid thermal capacity  $c_p$ , this quantity equates to:

$$\frac{Q_U}{A_C} = m' \cdot c_p \cdot (T_{fo} - T_{fi}) \quad (2.44)$$

Instantaneous collector efficiency  $\eta$  is defined as:

Rate of useful energy production  
Incident solar irradiance

which becomes:

$$\eta = \frac{Q_U}{A_C G_T} = \frac{m' \cdot c_p (T_{fo} - T_{fi})}{G_T} = \frac{F_R \cdot (\tau\alpha) - F_R \cdot U_L \cdot (T_{fo} - T_{fi})}{G_T} \quad (2.45)$$

Such equations form the basis of expression for results obtained from solar collector testing<sup>34</sup>. Plots with collector efficiency as ordinates, and  $(T_{fo} - T_{fi})/G_T$  as abscissae, then characterise a collector's performance. Typical graphs are drawn in Fig 2.12, a technique adopted later to illustrate a solar wall's performance.



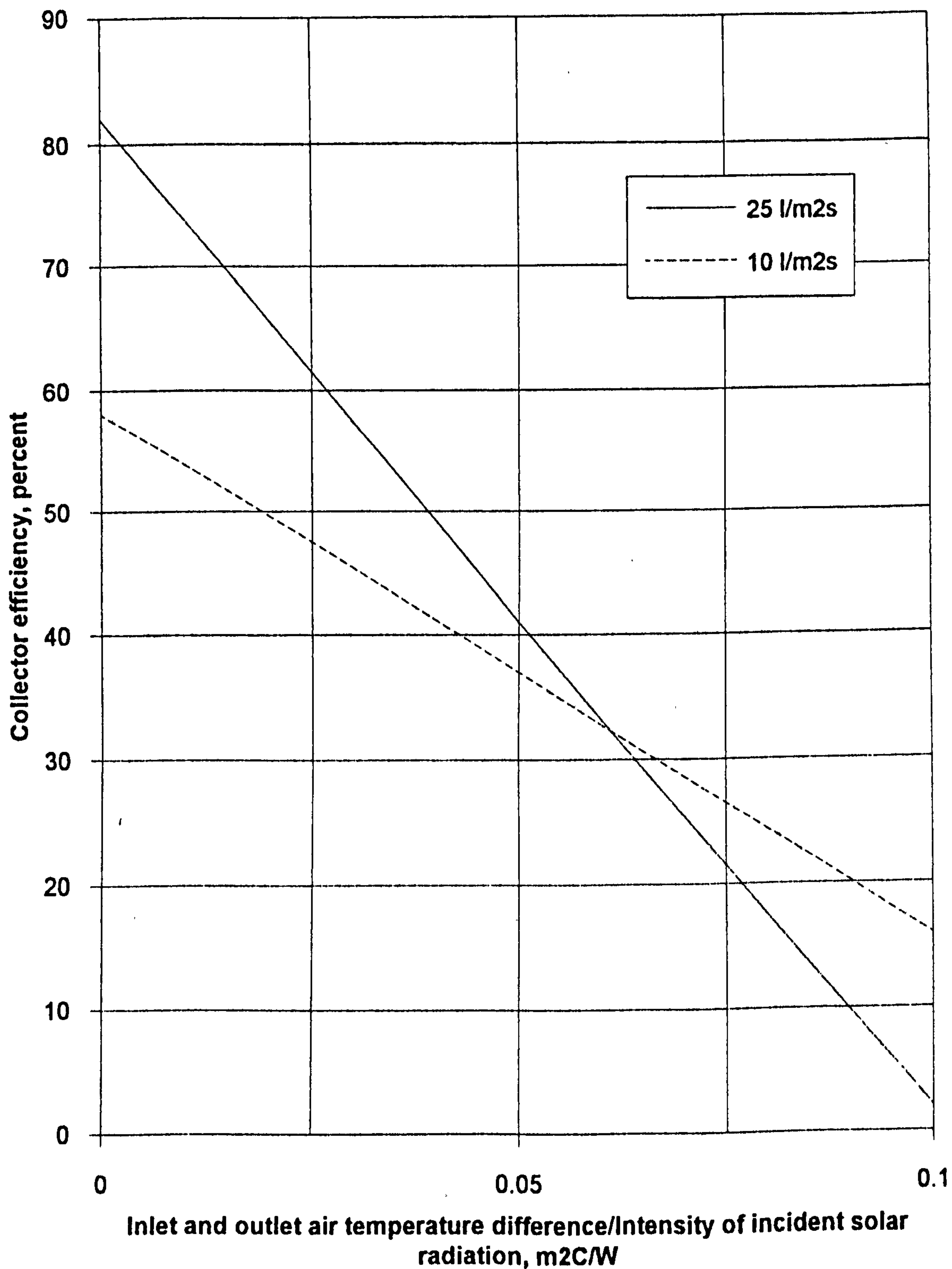


Fig. 2.12 Characteristic curves for solar air heaters at two air flow rates.

## 2.6 PASSIVE SOLAR DESIGN

Knowledge of the beneficial effects of sunlight are of ancient provenance.

Hippocrates practised sunlight therapy at the Health Temple on Kos. Heliotherapy for tuberculosis was an important treatment in Swiss Alpine sanatoria. In the 1920's and 1930's many schools and hospitals were oriented to accept sunlight to improve the health of pupils and patients alike<sup>35</sup>.

A report titled: *The orientation of buildings* gave the architect of 1933, guidance on sunlighting<sup>36</sup>. With the advent of antibiotics came the virtual demise of viral infection. Interest in the medical benefits of solar radiation declined. Later, with the construction of energy efficient buildings using low levels of natural light, where the purity of the air itself is in doubt, the health of occupants has become of concern<sup>37</sup>. Architects are returning to the theme that heating and lighting with sunshine and ventilating with fresh air confers positive physiological as well as psychological benefits on the habitants of passive solar buildings.

### The concept

If solar energy is allowed into a room unimpeded, the resulting energy input is called direct gain, and this principle is used for heating air in rooms and conservatories in passive buildings, with most of the fenestration facing south.

Too much glazing can create problems: glare and discomfort from direct sunshine plus overheating and damage to fabrics. Comfort criteria sets limits to the quantity of incident solar energy that can be used directly. To overcome such disadvantages solar

energy can be used in indirect, isolated gain systems. Their features have been classified by Norton<sup>38</sup> and are summarised in Fig 2.13.

In a vented Trombe-Michel wall, thermocirculation from the front allows some of the heat to pass directly into an adjacent room by convection from the front wall surface. Some 10 percent of the heat is transferred in this fashion, the rest being transferred later by conduction through the wall to the internal surface.

In an unvented Trombe wall, heat is transferred solely by conduction to the internal surface. If the heat then radiates and convects into the internal space it is labelled an indirect gain system. If the solar wall is thermally decoupled from the building by an insulating separating wall it is called an isolated gain system. Thermosyphoning air panels which use thin metal sheets as the collector plate and transfer heat rapidly by conduction to or from an interior, must necessarily be insulated by a separating wall to avoid excessive heat loss externally. They are examples of isolated gain systems. Their advantage is that because of the high thermal conductivity of the thin metal collector plates, an almost immediate convective heat input is produced. They are ideal for daytime heating in cool climates.

#### Trombe walls and thermosyphoning air panels.

Indirect systems are basically variations on the theme of the Trombe-Michel walls which were originally developed at Odeillo in the French Pyrenees for the heating of mountain chalets<sup>39</sup>. A combination of direct thermocirculation and delayed conduction through the wall provided a lengthy heating period throughout the

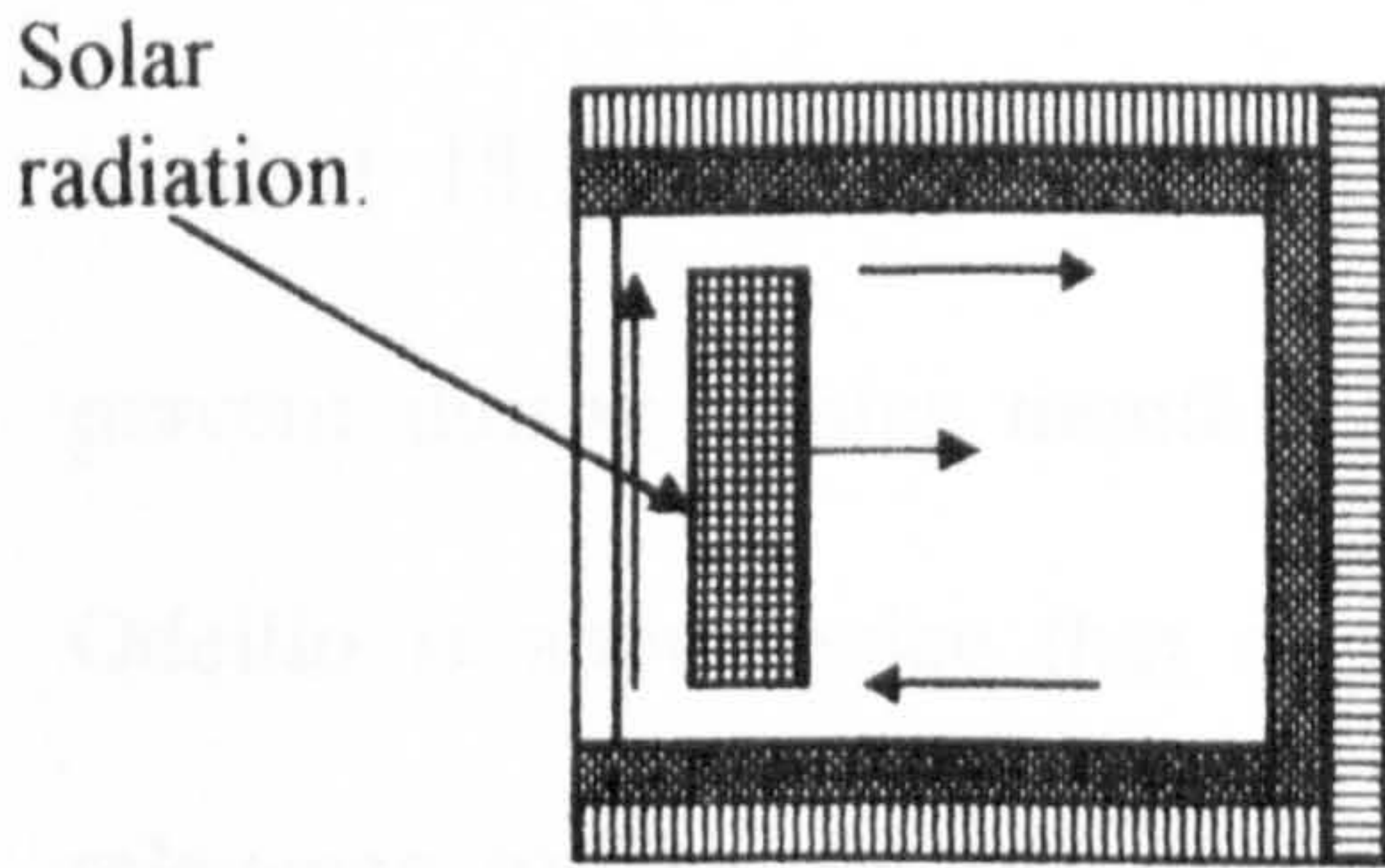


Solar wall system.

Description.

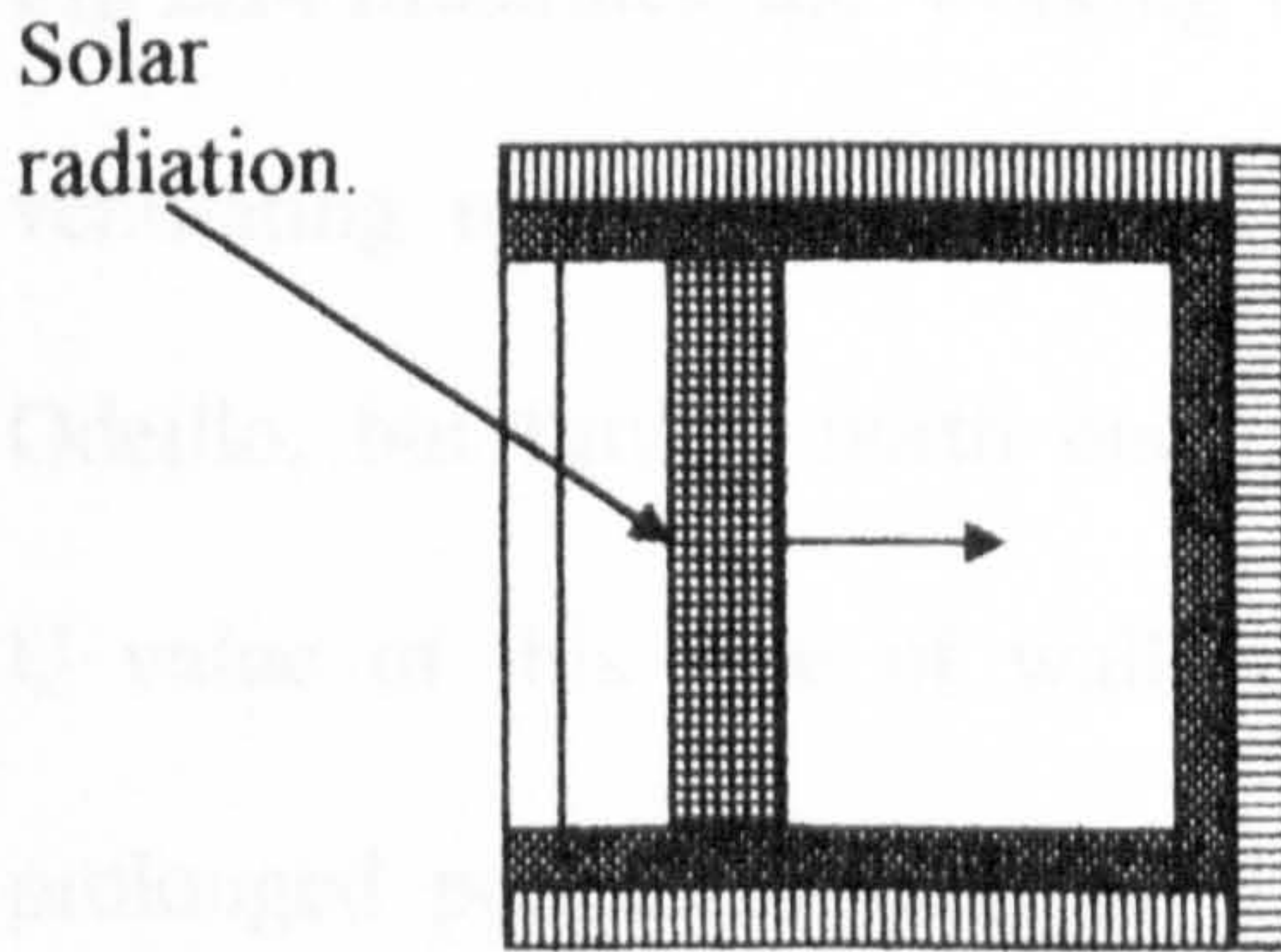
Heat transfer method.

Indirect gain.



Trombe-Michel wall.  
(uninsulated mass absorber)

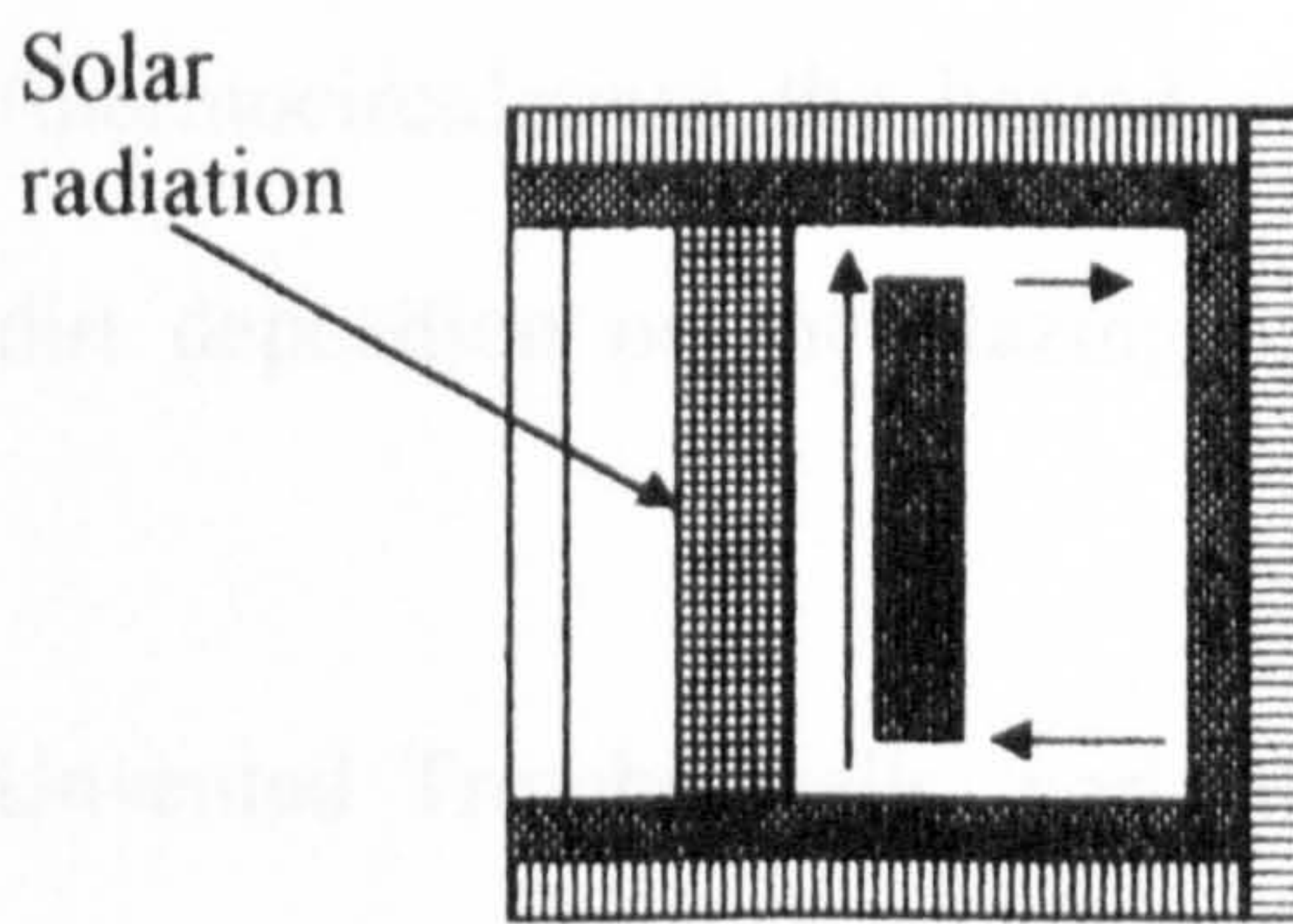
Conduction through the absorber, thermocirculation from the front surface.



Unvented mass wall.  
(uninsulated mass absorber)

Conduction through the absorber.

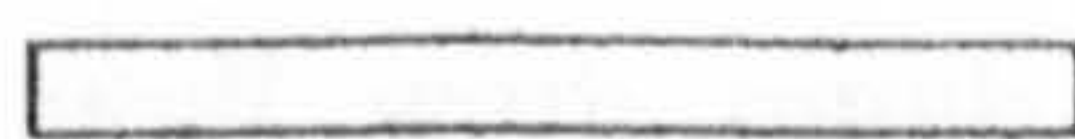
Isolated gain.



Unvented solar wall, with thermocirculation from an internal insulated cavity.

Conduction through the absorber, thermocirculation from internal cavity at rear of absorber.

(Thermosyphoning air collectors use thin metal absorbers).



Glazing or Transparent Insulation Material.



Absorber of brick, concrete, metal et al.



Structural material of building (eg brick).



Insulation material of room and solar wall.

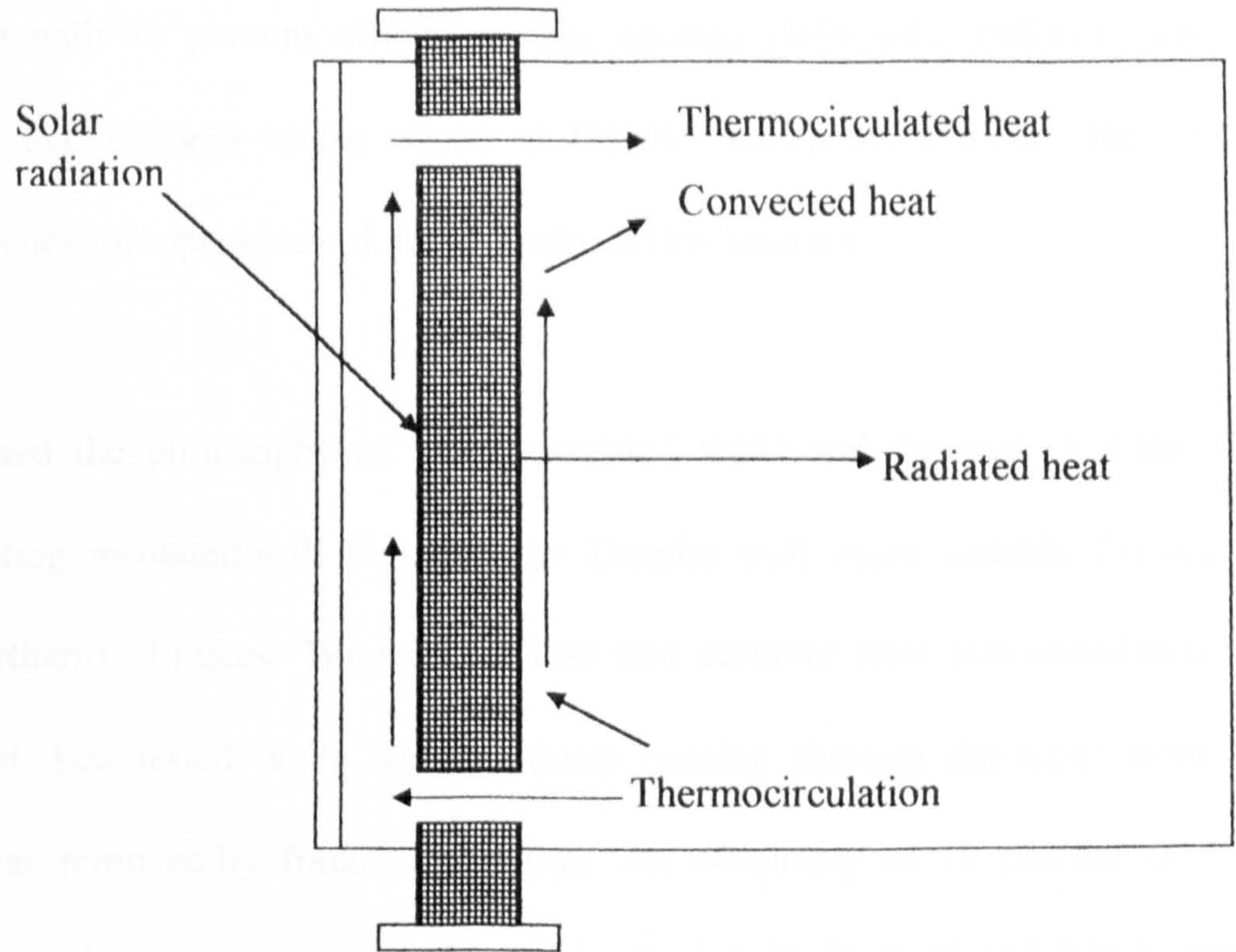
Fig. 2.13 Indirect and isolated gain solar wall systems.  
From Norton et al.(1990).(38)



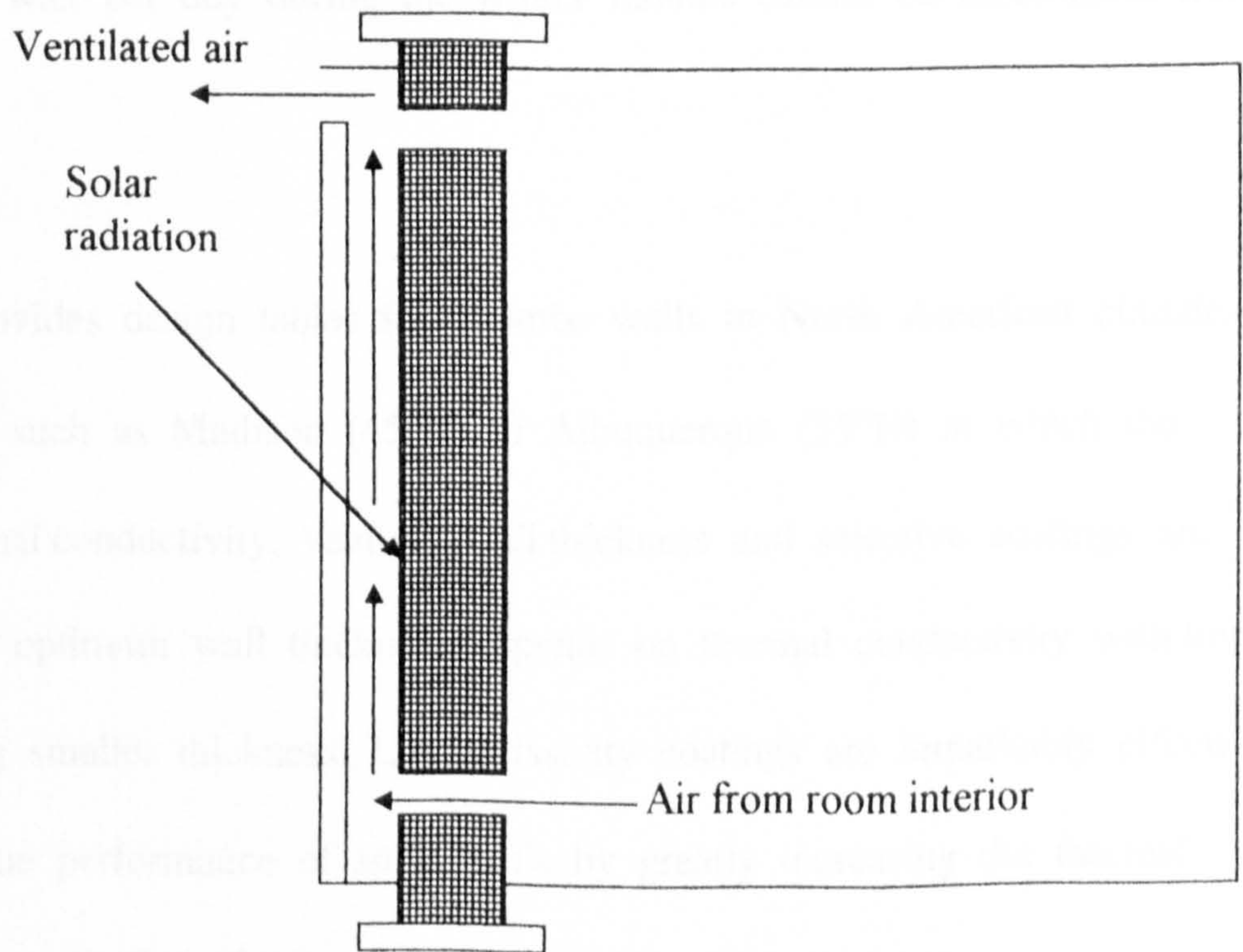
day. Such walls are easy to operate, easy to construct, and add little to the cost of a building since much of the structure is required whether designed as a Trombe wall or not. The efficiency with which heat is produced from the incident  $18.3\text{MJ/m}^2$  per day of solar radiation is quoted as 30 percent to 40 percent during winter months. Since the amount of solar radiation incident at Odeillo is about twice that in the UK during the winter, such results have little relevance to Trombe wall performance in northern latitudes.

**Fig 2.14** illustrates the working of the original Trombe wall in its heating and ventilating mode. Clearly, from the results quoted, this design works well at Odeillo, but further north one can conclude that it will not. The excessively high U value of this type of wall will produce too great a heat loss during the rather prolonged periods without sunshine at higher latitudes. For more acceptable performance, such walls should be better insulated, and for relatively maintenance free operation it is best to forgo the small advantage provided by venting (thermocirculating) the heated air from the front of the wall. Venting encourages dirt deposition on the glazing and increases the need for cleaning.

Unvented Trombe walls work almost as well as vented ones<sup>40</sup> according to Utzinger, who found that the auxiliary energy requirements of a building with a vented solar wall were much the same as for an unvented one. Balcomb et al<sup>41</sup>, provide more evidence and indicate that venting leads to a few per cent improvement relative to unvented walls. Ohanessian simulated the performance of an Odeillo type Trombe wall<sup>42</sup> in Melbourne at  $38^\circ\text{S}$ , using solar radiation data measured for 28 days in July and August. A Trombe wall of  $35\text{m}^2$  area was estimated to deliver 7 percent of the heating requirements of a solar house, the



Trombe wall in heating mode.



Trombe wall in ventilation mode.

Fig. 2.14 Working processes of Trombe-Michel solar walls.  
From Trombe (1979).(39)



wall operating with 11 percent efficiency. The average daily solar radiation was less than half that incident in the winter at Odeillo, which accounts for the much reduced efficiency of operation of these walls at this location.

Lee <sup>43</sup>, endorsed the philosophy of using unvented walls and decoupling them with a separating insulated wall to make the Trombe wall more suitable for use in cooler (northern) climates. Winter heat loss and summer heat gain would thus be greatly reduced. Lee tested walls with air ducts running through the mass from which heat was removed by forced circulation. An efficiency of 19 percent is quoted for December and January with simple glazing in front of and black paint on the surface of the wall. The average values for the insolation falling on the glazing of the wall per day during the winter months cannot be ascertained from his work.

Balcomb <sup>44</sup> provides design tables for Trombe walls in North American climates from locations such as Madison (45°N) to Albuquerque (35°N) in which the effects of thermal conductivity, venting, wall thickness and selective coatings are discussed. The optimum wall thickness depends on thermal conductivity with lower values dictating smaller thickness. Low emissivity coatings are remarkably effective in improving the performance of solar walls by greatly increasing the thermal insulation at front wall surfaces.

Isolated gain collectors such as thermosyphoning air panels were invented by Morse in 1881 <sup>45</sup>. They produce immediate heat by convection and since the collector is isolated from the heated space, heat losses during periods of no gain are low. They operate in the same manner as unvented, decoupled Trombe walls,

but the absorber is a metal such as aluminium or steel and not concrete or brick. Two schools in Essex have such thermosyphoning air panels, but only one, that at Nazeing has been monitored by Norton<sup>46</sup>. They perform satisfactorily, but these simple air heaters have far too long a payback period to be economic.

Francheshi reviewed the use of solar thermosyphoning air panels in the United States<sup>47</sup>. This was a prelude to a demonstration project in which thermosyphoning air panels were installed by Wimpey as a retrofit to existing houses<sup>48</sup>. It was concluded that the overall cost of a thermosyphoning system has to be reduced by a factor of two before the payback period becomes economic.

Two UK schools are known to have collector storage walls, one at St. Cleer, Cornwall<sup>49</sup>, and the other at Poulton Lancelyn, Wirral. Johnson<sup>50</sup>, describes the construction of the Trombe wall at the Poulton Lancelyn School, Wirral. It is unvented and decoupled from the building by an insulated separating wall, the air being removed from a cavity between the mass wall and separating wall by ducting and a fan.

Solar houses built at Bebington, Wirral incorporate simple Trombe walls, where vented air is ducted into the roof space for circulation to the interior, and conducted heat passes directly inside. For reasons previously discussed these walls should be, and were unsuccessful both energetically and in economic terms<sup>51</sup>.

Early constructions with Odeillo type or decoupled Trombe walls with rear insulation, were relatively unsuccessful in efficiency and economic terms, because the loss of heat from the front of the wall reduced their efficiency. Such walls have been superseded by the development of transparent insulation material, and



the effects of that material in greatly improving the efficiency and utility of Trombe walls will be reported later.

**CHAPTER THREE - THE POULTON  
LANCELYN SCHOOL**

### 3.1 INTRODUCTION

In 1961 the St. George's School was built in Wallasey, England<sup>52</sup>. Its south facade consisted of a large expanse of double glazing, with solar control blinds in a gap between them. Internally, thick concrete floors and brick walls acted as a heat store, behind a well insulated external facade (see Fig 3.1). The architect over-optimistically installed no conventional heating system. Temperatures fell too low in the depth of winter, and in compensation the tungsten filament lights in the classrooms were allowed to burn all night, to provide some supplementary heating. This practice upset the economic performance of the building. It became just as expensive to heat as all the other conventionally heated schools of a similar size in Wallasey, using oil fired boilers. In 1973 oil prices rose sharply, and the advantages of using renewable energy for heating under such conditions became apparent. The energy bills at St. George's School were now only 50% of those at other similar sized conventional schools in the area. This was before the era of cheap North Sea gas. This experience highlighted the economic advantage of passive solar heating in economies where fuels are expensive. It provided motivation for the design of other low energy consuming buildings in the Wirral area. One such building was the Poulton Lancelyn primary school.

### POULTON LANCELYN SCHOOL<sup>53</sup>

### 3.2 CONSTRUCTION DETAILS

The plan of the school site and classrooms is shown in Fig 3.2 and Fig 3.3. A plan of the wall is shown in Fig 3.4 and a section in Fig 3.5.

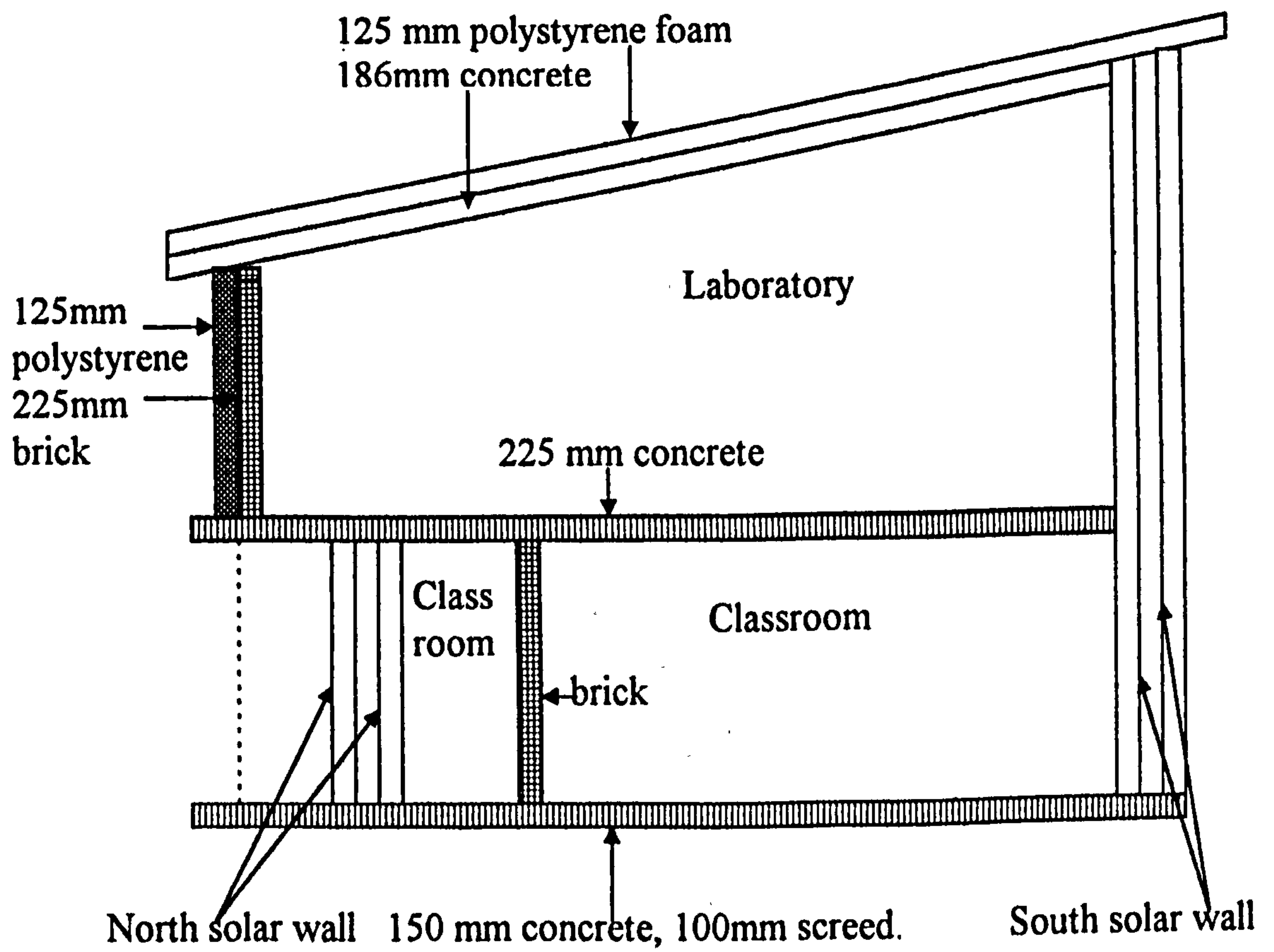


Fig. 3.1 St. George's school, Wallasey.



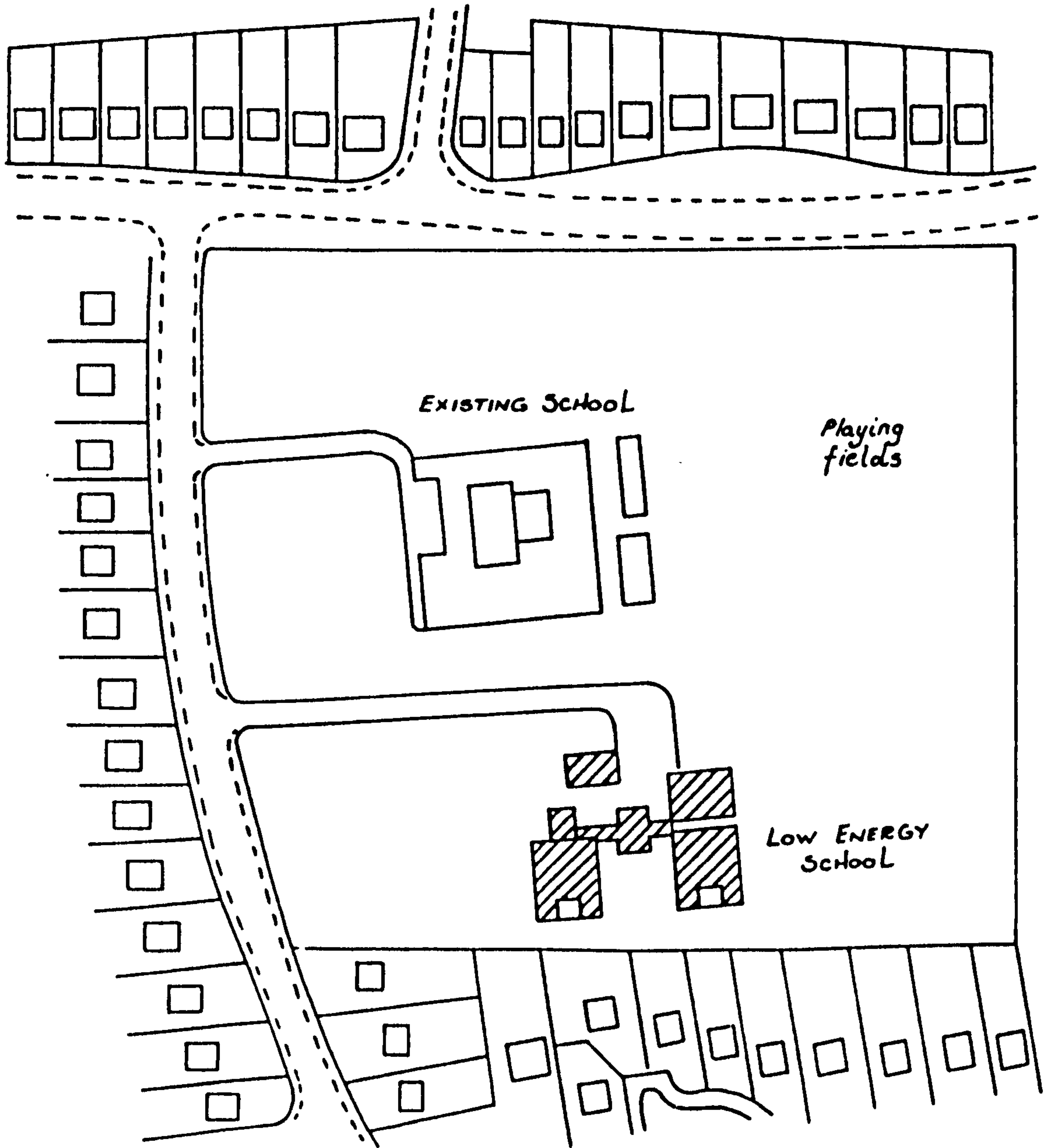
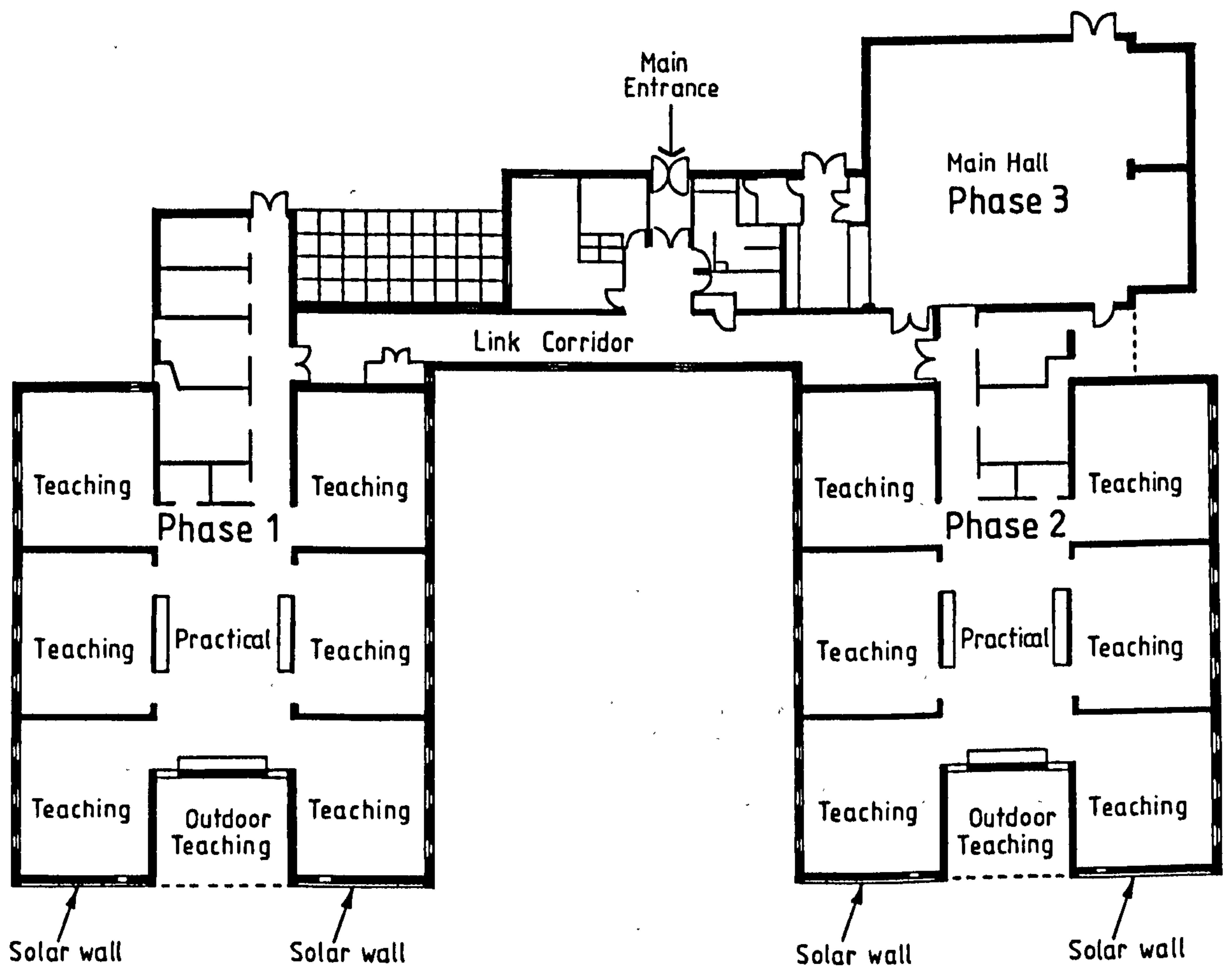


Fig. 3.2 Site of Poulton Lancelyn primary school (scale 1:1000)

LIVERPOOL JOHN MOORES UNIVERSITY  
Aldham Roberts L.R.C.  
TEL 0151 231 3701/3634



**Fig. 3.3 Plan of Poulton Lancelyn primary school.**

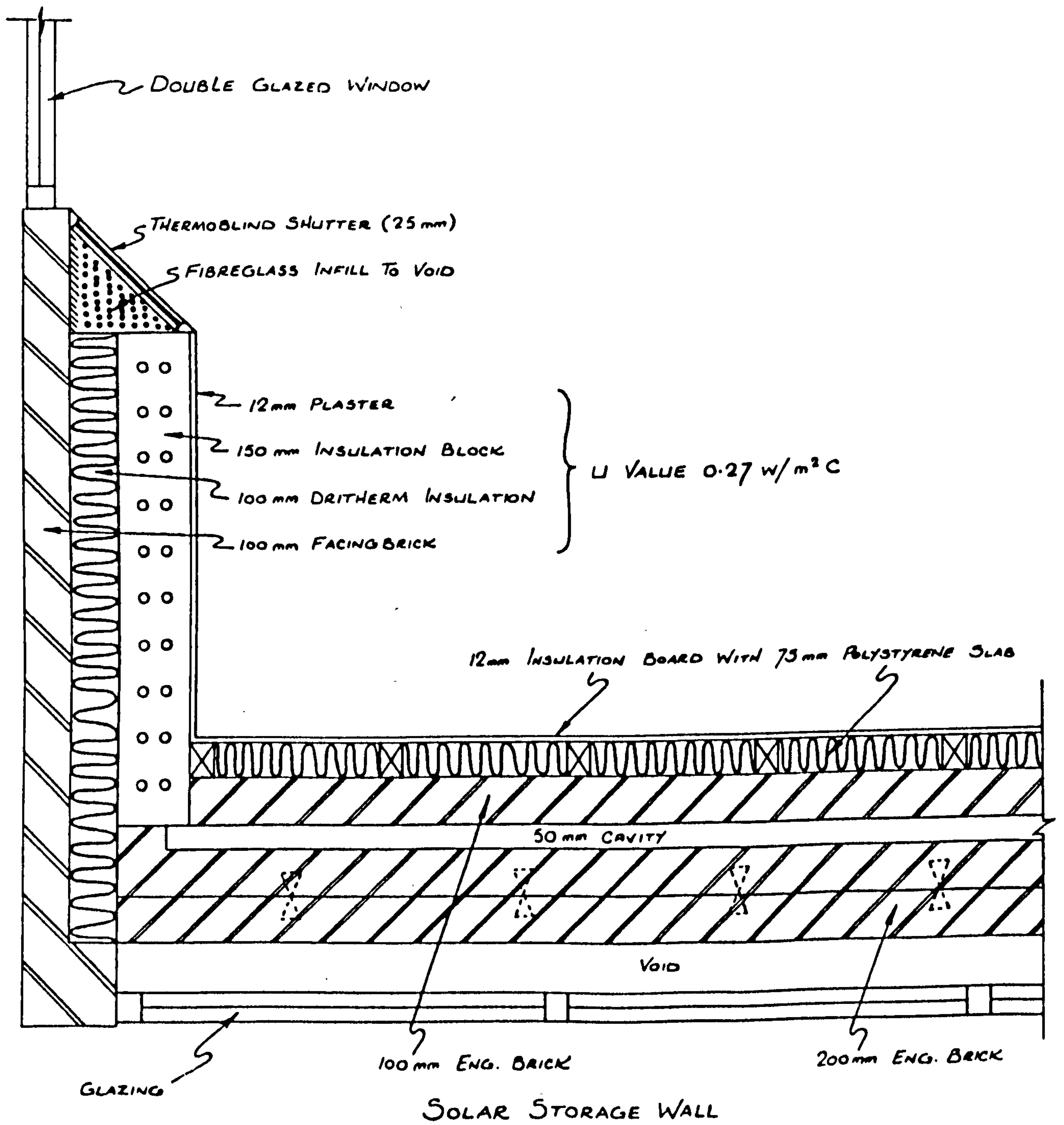


Fig. 3.4 Plan of solar wall at Poulton Lancelyn primary school.

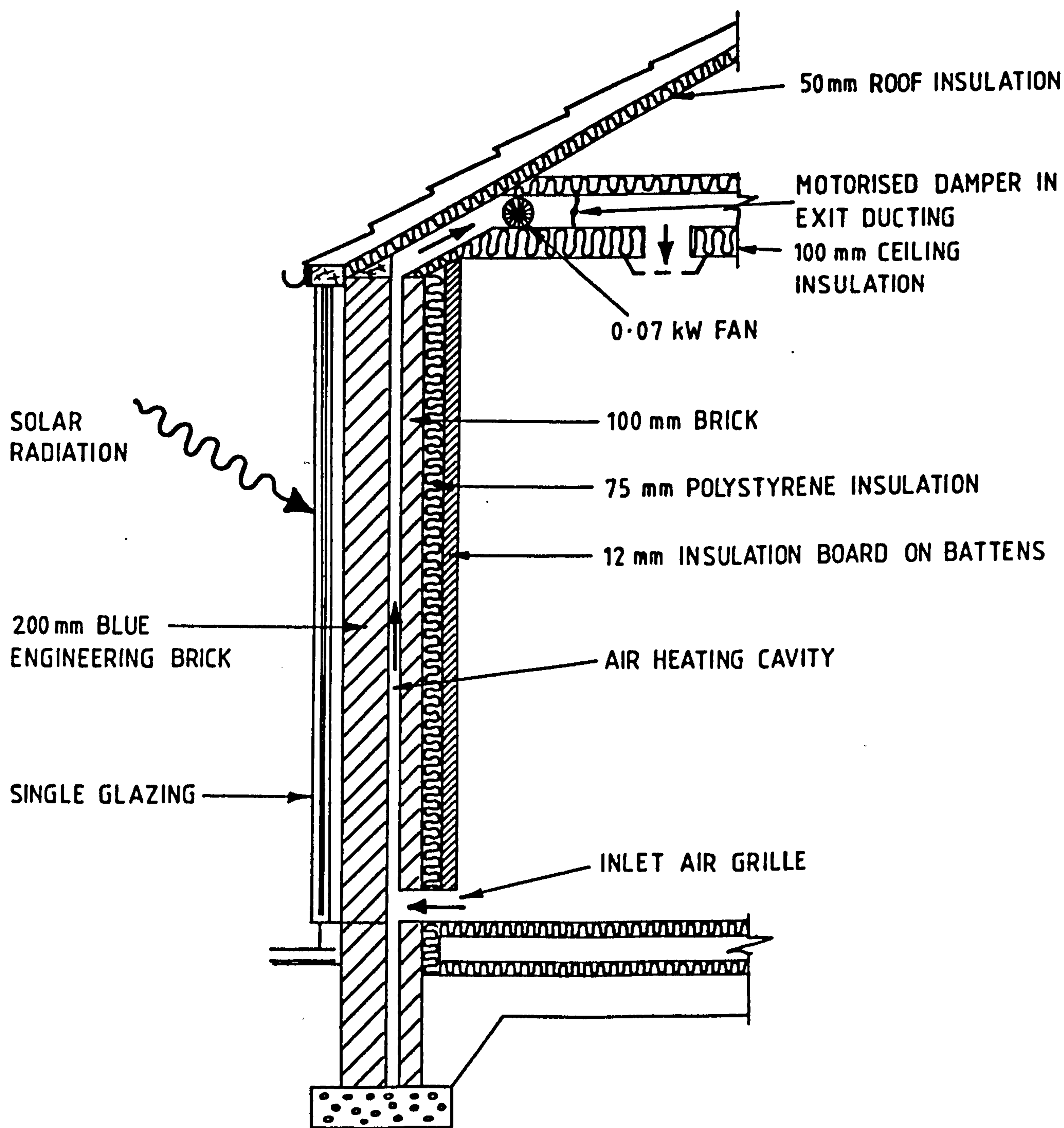


Fig. 3.5 Section of solar wall at Poulton Lancelyn.



The Poulton Lancelyn was designed as a low energy consuming building with exceptionally well insulated walls, roof and floor. The U-values are 0.28, 0.33 and 0.44 W/m<sup>2</sup>K respectively. The external walls consist of: a brick external leaf, insulated cavity and lightweight concrete block. The windows are double glazed without low emissivity coating (U=2.9 W/m<sup>2</sup>K). They cover about 25% of the eastern and western facades. Internal shutters reduce their night time U-value to 1.1 W/m<sup>2</sup>K. There are triple glazed roof lights in the practical area, and automatic lighting controls. Heating in the monitored part (phase 1), is by a gas fired boiler and air handling plant in the roof space. The heated air is transported to the classrooms through insulated ducting. Some of the heat in the exhaust air extracted from these rooms is recovered using a thermal wheel, and transferred to the incoming fresh air supply. About 25% of the external wall area faces south and about 80% of the south facing wall area is occupied by Trombe walls. They are three in number for each of two phases of the school. They are placed outside the thick thermal insulation, so that heat does not pass directly by conduction to the adjacent classrooms. Instead air from the classroom is drawn into the bottom of a cavity between the rear of the Trombe wall and the well insulated brick rear leaf. The air is then heated and passes out at the top of the wall into the ducting of the air handling system. For ease of maintenance, and to produce solar heat flow with a time delay the Trombe wall was unvented. There is no passage of heated air from the front, only the time delayed heat conducted through the brick front leaf is used. These solar walls are thus isolated passive components, delivering heat to the building interior whenever there is sufficient solar insolation, but possessing sufficient thermal insulation to prevent undue heat loss from the interior.

The front leaves of the Trombe walls are 200 mm thick and designed to deliver heat into their internal cavities with a time delay of about 3 hours. The heat is then stored for use later in the day.

Each solar wall is single glazed with a 50 mm cavity between the glazing and a 200 mm thick Staffordshire blue engineering brick, front leaf. Behind this solar absorber, lies another 50 mm cavity, followed by a rear leaf of 100 mm thick brick covered with plastered 75 mm thick polystyrene insulation. The walls are unvented. There is no thermocirculation from the glazed front cavities. Air to be heated, is drawn from an adjoining classroom, through a vent in the rear leaf near the floor. The air is heated in the rear cavity by heat conducted through the absorber. The heat is passed into the ducting at the top of the wall and back into the classroom, using a small fan and control damper. This fan is only activated and the damper opened, if the temperature of the air at the top of the wall exceeds that of the classroom air, provided that the air heating system is switched off and the classroom air is less than 20°C.

The idea was to use the stored heat in the Trombe wall to reduce the amount of energy used in preheating the school the next morning.

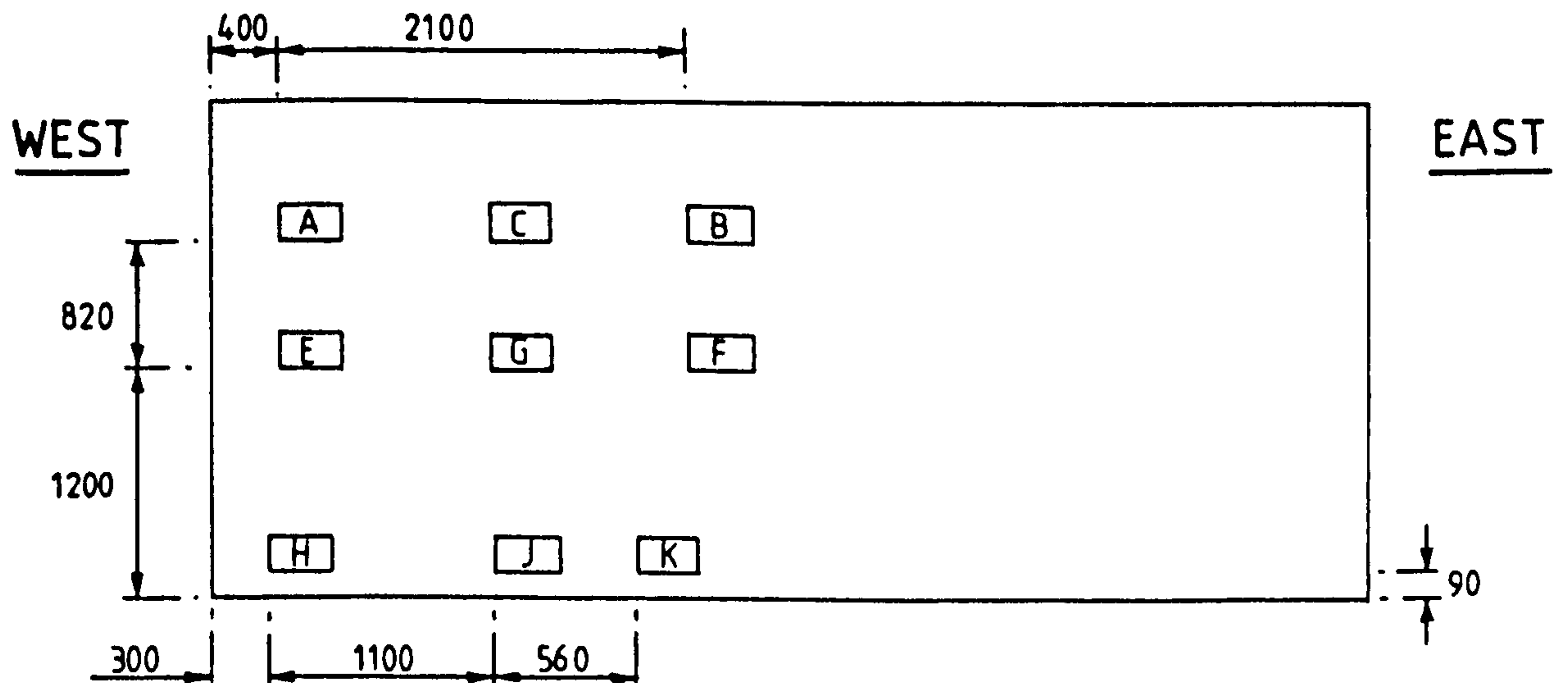
### **3.3 INSTRUMENTATION**

Several Pyrotenax, stainless steel sheathed copper-constantan thermocouples were installed in one of the Trombe walls during its construction; their positions are indicated in Fig 3.6. They were placed at the top and bottom of the internal cavity to measure the temperature of the incoming and outgoing air. Further

## (a) Section Viewing from South

A, B, C, E, F, G : THERMOCOUPLE POSITIONS IN SOLAR WALL

H, J, K : THERMOCOUPLE POSITIONS IN AIR INLETS



## (b) Section Viewing from East

POSITIONS OF THERMOCOUPLES AT EACH LOCATION (A, B, C, E, F, G)

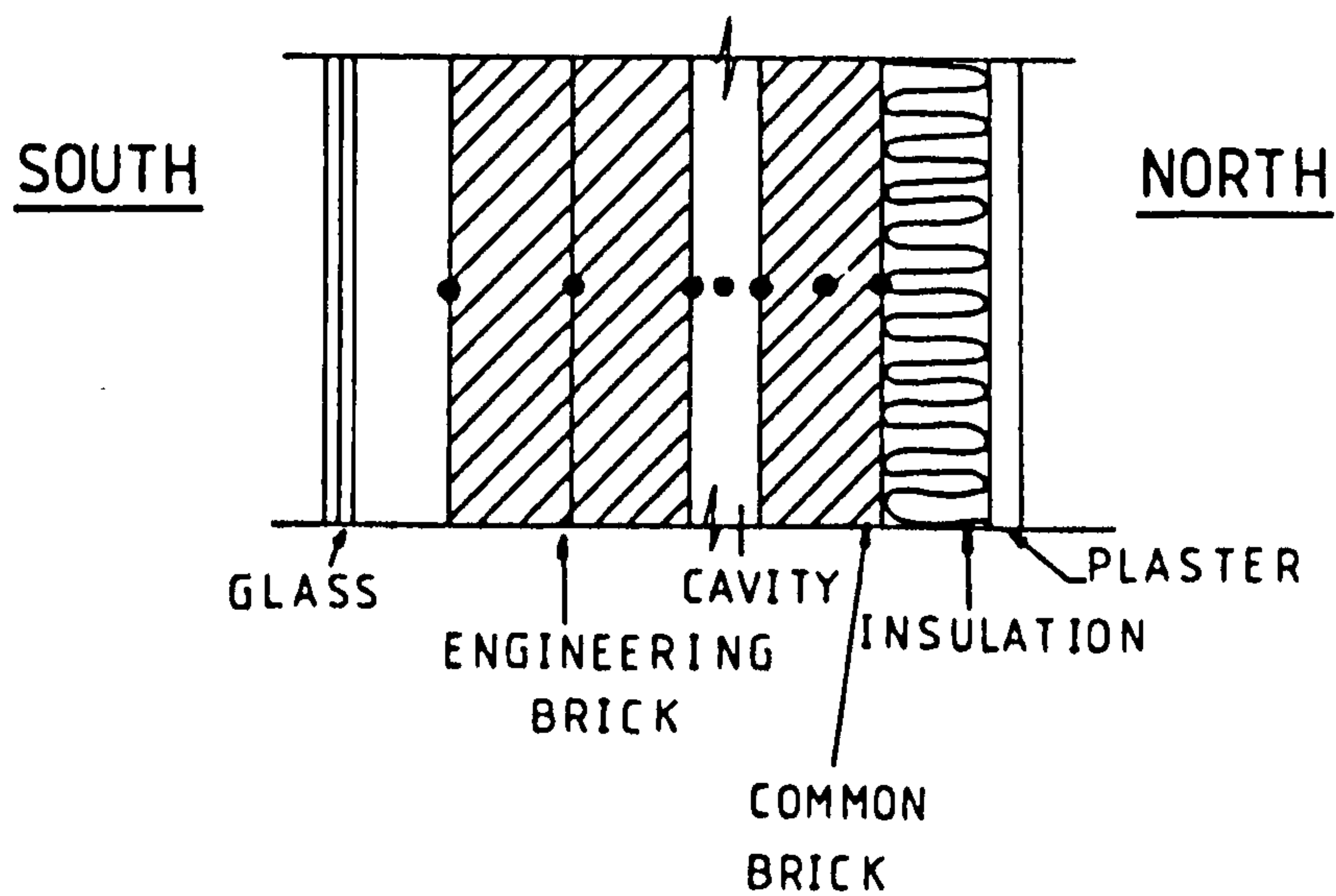


Fig. 3.6 Positions of temperature sensors in solar wall.

thermocouples were installed in the adjoining classroom at 0.5, 1.25 and 2.0 metres above floor level to measure the stratification of room air temperature. A further thermocouple in a Stevenson screen on the roof of the building, measured the local outside air temperature. Thermocouples were chosen in preference to platinum resistance thermometers (accurate to  $\pm 0.1^\circ\text{C}$ ) or thermistors for reasons of:

- cheapness since once embedded within a wall, they could not be recovered.
- several years experience of measuring temperatures with thermocouples.

For long term monitoring the accuracy of thermocouples ( $\pm 0.5^\circ\text{C}$ ), with outputs measured using digital voltmeters was felt to be acceptable for general building temperature measurement. The standard relation between millivolt output and temperature for thermocouples given in the appropriate British Standard<sup>54</sup>, was used in the determination of these temperatures.

A Kipp and Zonen CM5 solarimeter, consisting of 14 blackened manganin-constantan thermojunctions arranged in rectangular form, all enclosed in concentric glass hemispheres was installed. It was oriented to measure the solar radiation falling on the south facing surface of the Trombe wall. The solarimeter was surrounded by a white guard plate to prevent radiation from behind entering the glass hemispheres. It has a linear response to within 1%, a response time of 12 seconds and a temperature dependence of output of around 0.2% per  $^\circ\text{C}$ . This solarimeter was recalibrated by the Meteorological Office prior to use. The literature (55), cites  $\pm 5\%$  as the order of accuracy when measuring solar radiation with such an instrument. A Lintronic solarimeter, less accurate but cheaper, was also installed to backup the Kipp and Zonen readings. The calibration of the Kipp and Zonen solarimeter used to monitor the Trombe wall

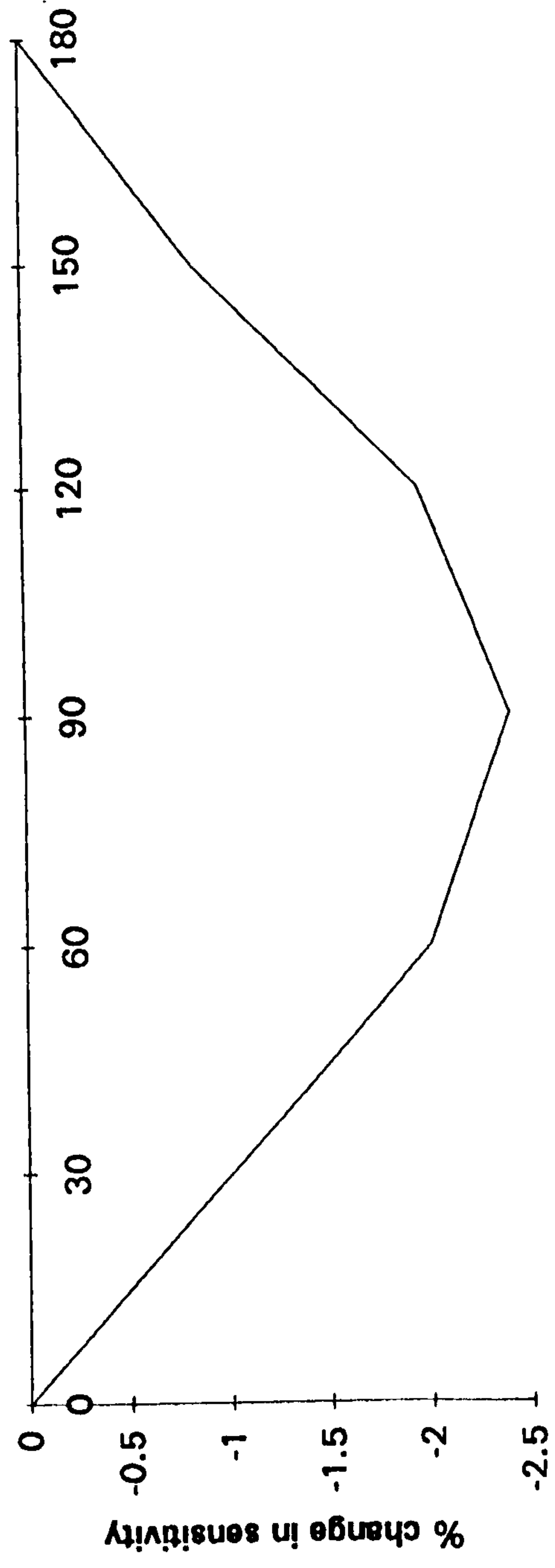


was 1.2 mV per  $\text{W/m}^2$ . The angular dependence of the CM5 solarimeter's output is shown in Fig 3.7.

For reference purposes the wind speed was also recorded using a cup anemometer made by Vector Instruments Limited. This produced a variable output voltage related to windspeed.

The determination of the flow of air through the Trombe wall, which would enable heat outputs to be determined, was difficult to measure, either continuously or directly. Accordingly it was decided to measure the air speed in the duct at the top of the Trombe wall using a thin film anemometer. This value could then be converted into the rate of air flow through the wall and ducting and then to the air speed in the wall cavity itself. The thin film anemometer gave an output of:  $x \text{ mV/ms}^{-1}$ . If  $y \text{ mV}$  was the output of the anemometer,  $A_d \text{ m}^2$  the duct cross section area and  $A_c \text{ m}^2$  the cavity cross section area, then the air flow rate equals:  $A_d(y/x) \text{ m}^3 \text{ s}^{-1}$ . The cavity air speed then became:  $(A_d/A_c)(y/x) \text{ ms}^{-1}$ .

An indication of how long the small solar wall fan circulated air through the cavity in one hour between data readings was made by measuring the on/off time of the fan in that time period. A mercury switch was activated by the damper in the ducting. The damper opens as soon as the fan starts operating, turning the switch on. The switch was connected to a small resistance, the value of which was measured every 15 seconds. With switch and fan on, 103.8 ohms was recorded. With switch and fan off, the resistance changed to 201.5 ohms (see Fig 3.8). The fraction of fan operating time in an hour, can then be determined from the formula:  $(201.5 - \text{average resistance measured in the hour}) / (201.5 - 103.8)$ .



Angle of inclination of solarimeter: horizontal = 0 (degrees)

Fig. 3.7 Variation in sensitivity with angle of inclination for a CM5 solarimeter

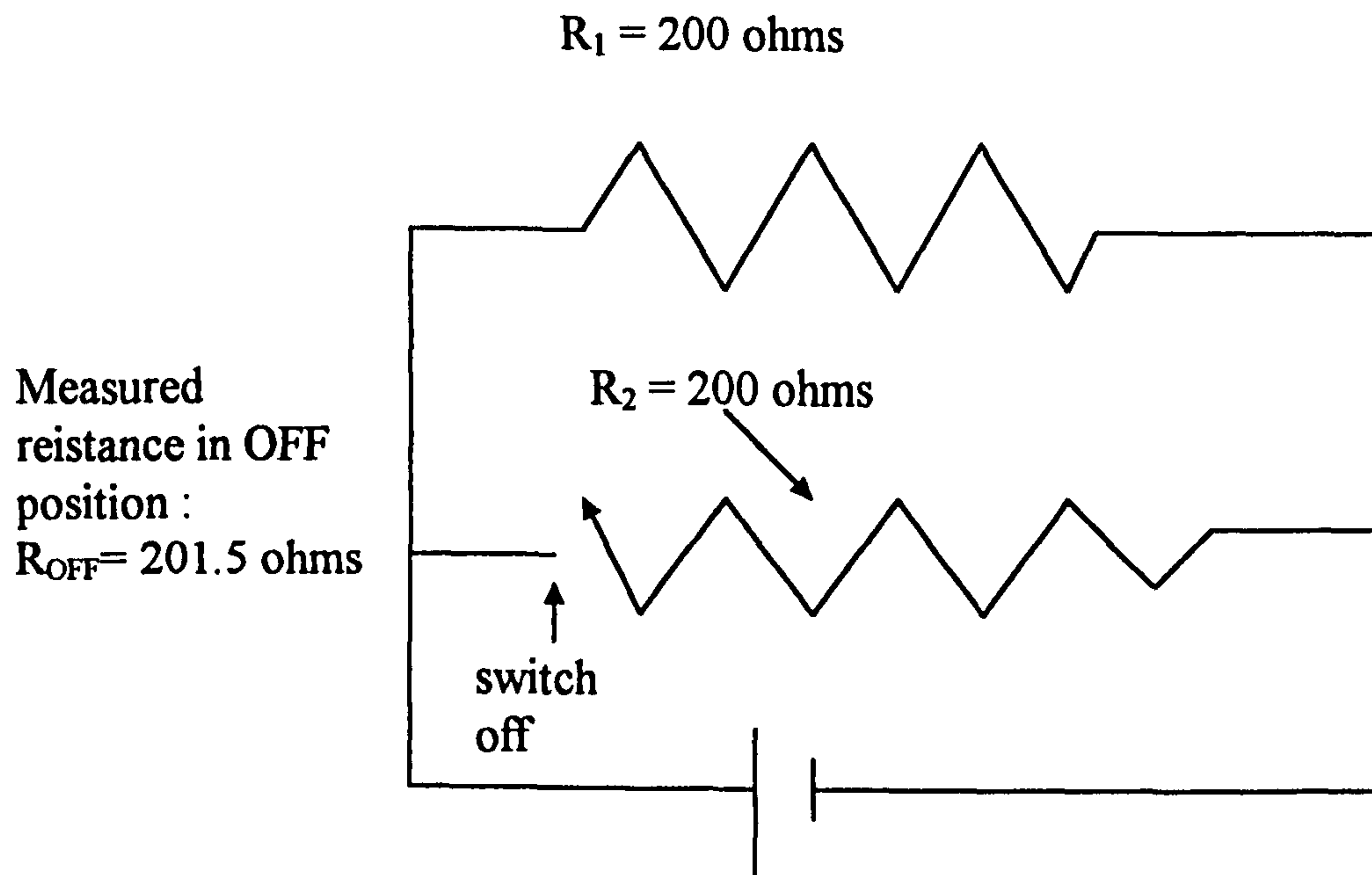


**Fig.3.8(a) Switch in off position with solar wall fan off and the ducting damper closed.**

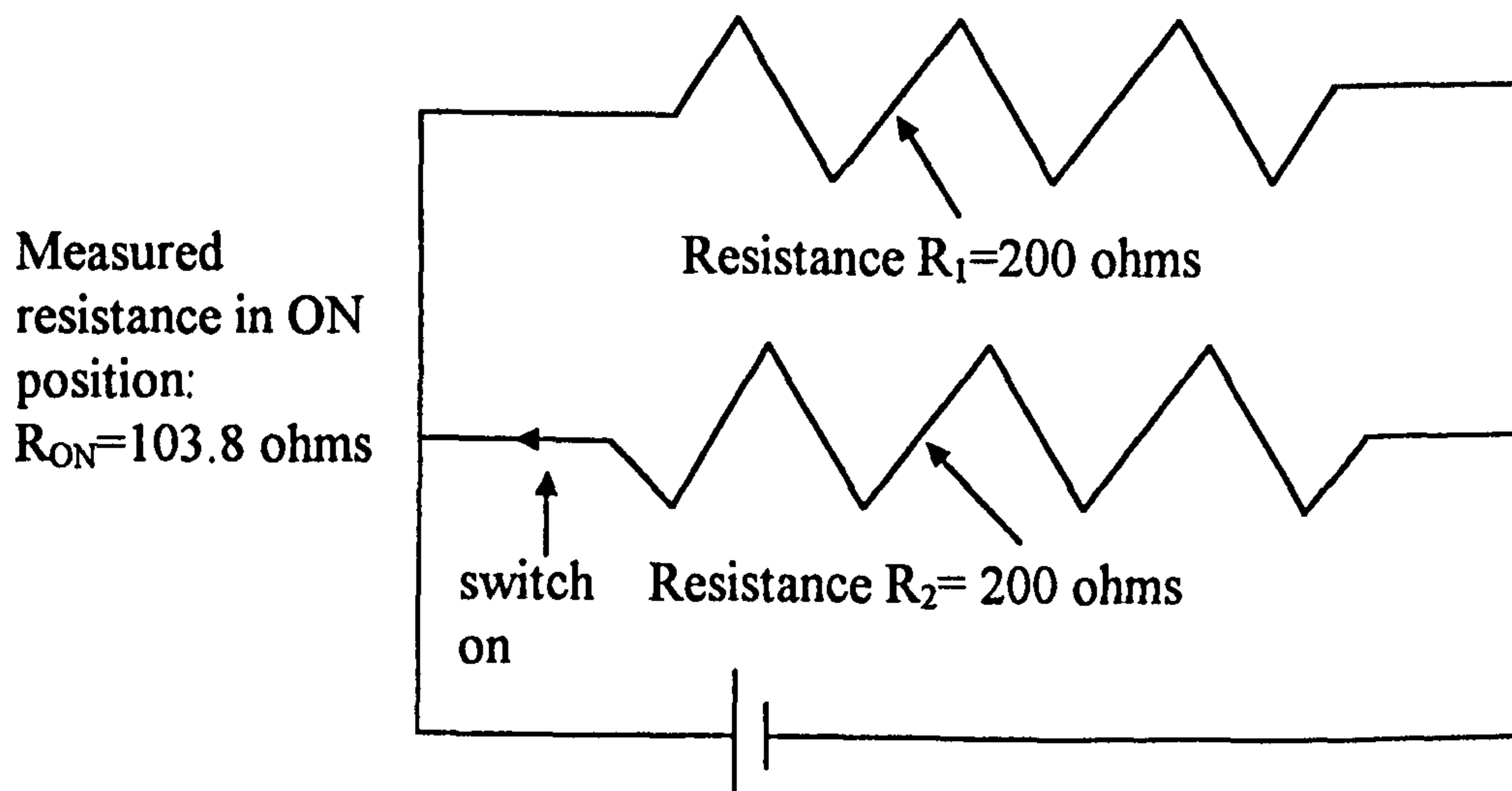


**Fig.3.8(b) Switch in on position with solar wall fan on and the ducting damper open**

The fraction of time the solar wall fan operates to deliver heat in one hour is given by:  
 $(201.5 - \text{average resistance measured in one hour}) / (201.5 - 103.8)$

**Fig. 3.8 Schematic diagram to show the operation of a mercury switch / resistance network which will indicate the fraction of time the solar wall operates in one hour**

All the sensors: thermocouples, solarimeters, anemometer and resistances were connected to Solartron 3530A data logger using 12 way screened coaxial cables running inside the roof space of the school. The Solartron, manufactured by the Schlumberger Instrumentation Group<sup>56</sup>, proved to be an extremely reliable instrument.

It uses dependable reed relays to monitor 20 channels continuously at 10 channels or more per second. Each channel can be separately programmed to read millivoltages, voltages and resistances. The millivolt readings can be converted directly to temperatures or to irradiance when thermocouples or solarimeters are used. Voltages can be converted to wind speed from an anemometer's readings and resistance to temperature from the output of a Platinum resistance thermometer.

The data logger was programmed to record data at hourly intervals, quite suitable for slowly changing parameters such as temperature. In the case of solar radiation and switch resistance, their mean value over an hour is required. Statistical processing is available on the Solartron, and when it was used for such cases the data logger was set to the maximum number of readings that could be made per hour. This was 255 readings, equivalent to 1 channel read every 14.1 seconds. For the accurate sampling of solar irradiation data this is an adequate time interval<sup>57</sup>.

To limit the error in temperature measurements using thermocouples an accurate 'Xeref' electronic reference cold junction was used. This instrument, using the



Peltier effect, kept the ice point controlled to within  $\pm .05^{\circ}\text{C}$ . This makes temperature measurement more accurate than if the cold junction sensors provided within the Solartron had been used. In that case the error in ice point determination would be  $\pm .6^{\circ}\text{C}$ . The Solartron itself is sensitive to  $\pm .001$  mV, the error in reading to 2 digits, again  $\pm .001$  mV. This implies an error in temperature measurement of  $\pm .002$  mV or  $\pm 0.25^{\circ}\text{C}$  due to the Solartron and thus  $\pm 0.3^{\circ}\text{C}$  for the temperature resulting from the combined use of the data logger and 'Xeref' cold junction.

The Apricot XI portable computer was used to transfer data from the in situ data logger to the laboratory for processing. The choice of computer was dictated by its compact size which with its handle facilitated its transportation to and from the school. At the school the computer was connected to a small vide screen and to the Solartron via its IEEE rear connection. A data transfer program had been written to output data from that recorded on a cartridge by the Solartron to the Apricot hard disk. The program first created a named file on the disk, then called the Solartron to transfer its output of one month's data recording from 20 logged channels. A serial file of parametric information was thus transferred to the computer. The computer was then taken back to the laboratory at the School of the Built Environment where the file was transferred to 3.5" floppy disks for storage.

To analyze the data further programs were written to convert the sequential data for each month monitored into tabular form. Directly recorded hourly values of solar radiation, wind speed, temperatures and resistance together with the

statistical averages of solar radiation and resistance over that period were then printed out. In addition the amount of heat produced from the air circulating through the rear of the Trombe wall was calculated for the periods of fan operation. The calculation was made from a knowledge of the fan operating time and the temperatures of the air entering and leaving the Trombe wall.

The ensemble of recorded data was thus converted into a compact form for printing. A whole years data, with measurements at hourly intervals, could be presented in a neat form that made subsequent interpretation of the results a relatively simple matter. Purchase of a 20 channel data logger was a conscious decision, to limit the mass of information that monitoring would bring. In the event, only about half of the data was used, the other channels duplicating the information, for use if trouble occurred with a specific sensor.

In addition to digital data logging, analogue recording of extra sensors was made, using a chart recorder. One of these sensors was a platinum resistance thermometer. It was placed near to a ceiling mounted air diffuser and measured the temperature of the air entering the adjacent classroom from the air handling system. This enabled the time at which the heating commenced and finished in the morning and evening to be determined, as a check on the digital recorded data on fan operating times.

To estimate the efficacy of the low energy consuming construction of the school and provide knowledge of what fraction of the energy consumption is provided by the solar wall, the electricity and gas meters were frequently read to record

the total fossil fuel energy consumed at Poulton Lancelyn during the monitoring period.

### **3.4 COMMISSIONING OF THE MONITORING INSTALLATION AT POULTON LANCELYN**

Measurements of temperatures, wind speed, irradiance and other parameters were taken over a three year period. During that time, faults were found which affected the solar wall's performance. The fan installed at the top of the duct that was responsible for conveying heat into a classroom did not work. There was considerable leakage of hot air from the join between the ducting and cavity top so that much of the solar heated air was initially wasted. There was insufficient thermal insulation over the ducting conveying the heated air to the adjoining classroom. The fan fault was due to incorrect wiring, but it took several months for the responsible electrical contractors to rectify it. The hot air leaks were cured using silicone sealant and the insulation was upgraded with thick layers of fibreglass. Data was collected during 1985 and 1986 so that the operation of the wall was investigated right through a complete heating season.

### **3.5 TREATMENT OF RESULTS**

*Tables 3.1 to 3.12* assemble together the daily record of some of the temperatures recorded from November 1985 to October 1986, together with the energy flows which were calculated as detailed below. The positions and nomenclature for the temperatures and energy values presented in these tables are given

in Fig 3.9. These energy flows were calculated using the equations given below for periods between hour H-1 and hour H. All variables used in the calculations were representative of their average values during each hourly period.

1) Energy produced by the solar wall from hour H-1 to hour H on day D

$$E_{D,H} = V.F_L.A_C.F.(T_C - T_{AI}) \text{ (Wh)} \quad (3.1)$$

2) Energy produced by the solar wall in one day

$$E_D = \sum_{D,H=7.00}^{D+1,H=7.00} E_{D,H}/1000 \text{ (kWh)} \quad (3.2)$$

The above equation evaluates the energy produced from irradiation falling on the solar wall during the whole of day D. This energy flows from the cavity when the fan and damper system begin to operate at 16:00 hours, day D, terminating at 7:00 hours, day D+1.

3) Solar energy incident on the mass wall, hour H-1 to Hour H, day D

$$S_{D,H} = I_{D,H}.A_W/1000 \text{ (kWh)} \quad (3.3)$$

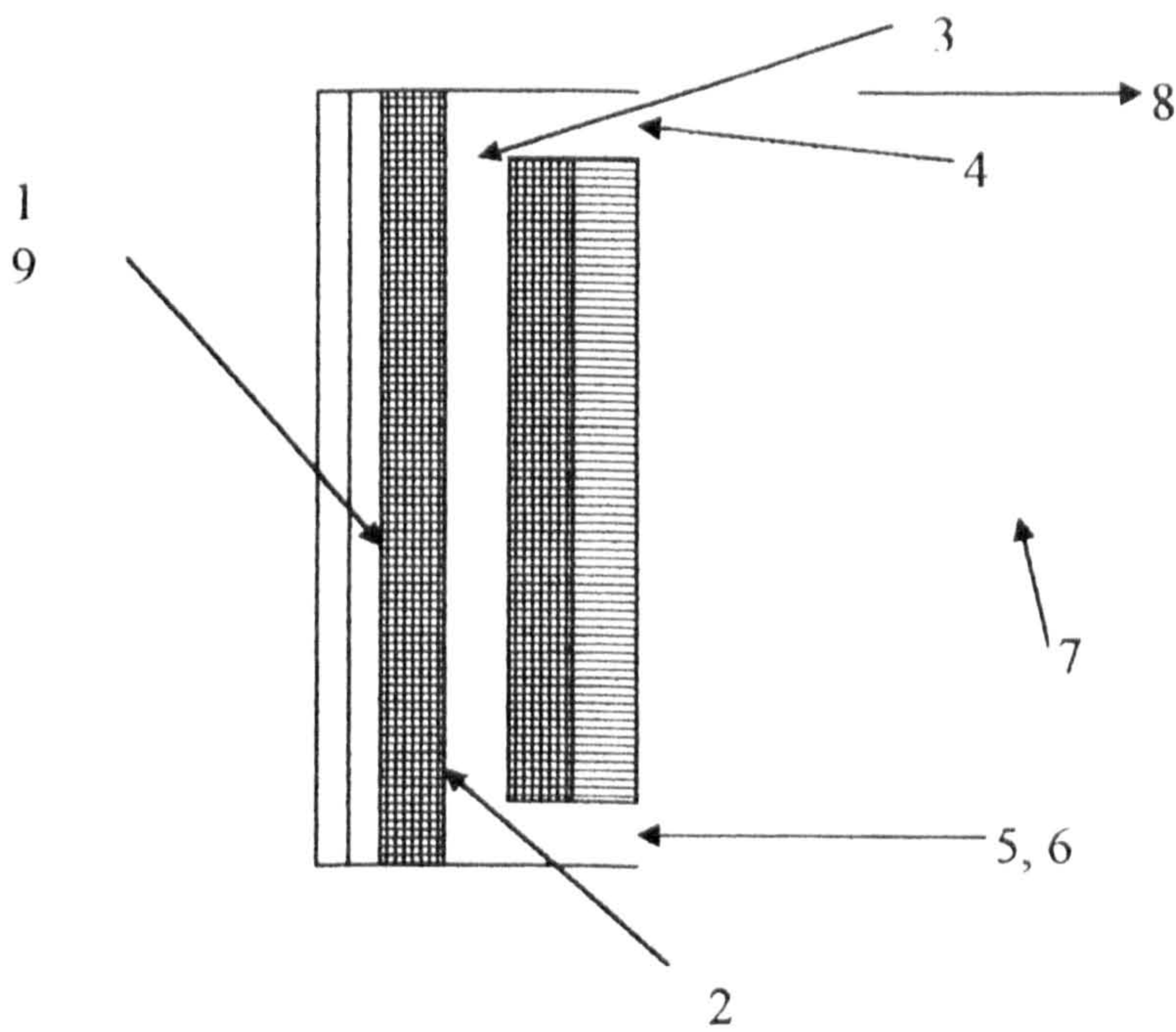
4) Solar energy incident on the mass wall, day D

$$S_D = \sum_{D,H=1.00}^{D,H=24.00} I_{D,H}.A_W/1000 \text{ (kWh)} \quad (3.4)$$

5) Efficiency of energy production, day D

$$EFF_D = (E_D/S_D).100 \text{ (%) } \quad (3.5)$$





1. Maximum daily temperature, front surface, outer leaf.
2. Maximum daily temperature, back surface, outer leaf.
3. Maximum daily temperature, cavity near top of solar wall.
4. Maximum daily temperature, air entering ducting at top of solar wall.
5. Maximum daily temperature, room air before entering solar wall.
6. Minimum daily temperature, room air before entering solar wall.
7. Average daily temperature, external air
8. Total energy produced by the solar wall in a day.
9. Total solar energy incident on the wall in a day.
10. Efficiency of energy production by the solar wall.

**Fig. 3.9** Diagram showing the positions and giving the nomenclature for the temperature and energy values presented in Tables 3.1 to 3.12.





**Poulton Lancelyn Solar Wall Data**  
**Table 3.2 December 1985**

DAY	M A X I M A					Minm	Aver	ENERGY FLOW		
	1	2	3	4	5	6	7	8*	9	10
	°C							kWh		%
1	11.6	11.5	13.0	22.7	12.2	11.4	12.8	-	1.0	-
2	12.9	12.9	17.7	34.5	17.9	11.6	12.8	-	0.8	-
3	23.7	17.5	19.3	34.5	17.4	13.5	13.3	-	40.2	-
4	16.1	16.7	18.4	30.7	18.3	14.1	10.2	-	1.4	-
5	13.0	14.7	16.8	32.7	18.4	13.8	7.2	-	1.9	-
6	12.2	12.6	17.5	34.6	19.0	13.3	7.2	-	6.1	-
7	19.0	14.2	15.3	18.4	13.6	12.0	7.3	-	34.4	-
8	17.7	13.3	14.0	22.7	12.5	11.7	4.1	-	22.3	-
9	10.7	12.1	15.3	35.3	17.8	11.7	1.6	-	6.0	-
10	8.1	10.2	16.3	35.0	19.3	11.7	2.6	-	0.8	-
11	15.4	12.5	17.3	35.0	17.8	12.1	5.4	-	26.7	-
12	11.2	11.9	17.2	35.0	18.0	12.6	7.6	-	3.5	-
13	14.9	13.9	17.2	34.0	17.2	13.1	11.6	-	7.6	-
14	14.6	14.0	16.4	15.1	13.9	12.9	12.0	-	4.9	-
15	15.8	14.3	14.5	14.2	13.0	12.5	12.5	-	8.9	-
16	14.8	14.1	17.3	34.4	18.1	12.5	10.5	-	11.3	-
17	13.3	13.8	17.4	33.7	17.8	13.3	11.1	-	1.3	-
18	20.5	15.9	17.6	28.4	19.4	13.3	4.6	-	11.3	-
19	13.5	14.5	17.3	34.4	19.1	13.6	8.2	-	7.7	-
20	12.7	13.3	16.8	33.7	19.5	13.7	10.5	-	2.1	-
21	14.5	13.9	16.2	15.8	14.6	13.3	11.2	-	2.7	-
22	13.7	13.3	14.3	12.3	13.1	11.7	6.2	-	9.3	-
23	12.2	11.6	14.1	35.6	16.3	11.5	6.5	-	9.5	-
24	9.3	10.9	14.3	34.8	16.0	11.6	3.5	-	1.3	-
25	10.0	9.6	13.5	34.7	15.7	11.4	4.1	-	8.2	-
26	9.6	9.4	12.7	34.6	15.5	10.9	4.2	-	6.0	-
27	13.2	9.8	12.4	32.9	15.1	9.6	2.1	-	22.3	-
28	15.4	9.6	11.1	21.8	10.7	8.8	4.3	-	44.8	-
29	15.7	10.0	12.0	24.0	11.2	9.1	4.8	-	43.7	-
30	7.3	8.5	12.7	32.6	14.0	9.3	3.1	-	7.1	-
31	9.5	8.7	13.9	34.2	14.9	9.3	5.0	-	12.2	-

**Poulton Lancelyn Solar Wall Data**  
**Table 3.3 January 1986**

DAY	M A X I M A					Minm	Aver	ENERGY FLOW		
	1	2	3	4	5			6	7	8*
	°C					kWh				
1	7.2	8.5	13.6	34.1	14.9	10.0	2.7	-	5.0	-
2	6.4	7.5	12.6	34.2	14.7	9.8	3.0	-	1.0	-
3	15.9	10.7	13.0	33.4	14.8	9.5	2.8	-	40.3	-
4	12.1	12.3	12.0	21.3	10.9	8.9	1.6	-	1.5	-
5	8.8	7.7	9.5	27.1	12.1	8.6	2.4	-	7.5	-
6	14.0	10.5	16.4	35.3	15.1	9.7	2.3	-	28.0	-
7	6.9	9.0	13.5	33.8	18.2	10.1	0.7	-	1.4	-
8	5.6	7.4	15.3	32.0	16.3	9.3	0.3	-	1.3	-
9	8.0	9.3	17.2	35.0	19.5	8.3	2.3	-	3.6	-
10	13.2	11.0	15.6	36.0	19.4	11.4	8.0	-	17.3	-
11	14.4	11.3	14.3	12.6	12.3	10.3	6.4	-	21.3	-
12	14.0	11.0	11.3	25.5	12.4	9.8	6.8	-	24.1	-
13	11.3	11.5	17.2	35.4	18.6	10.0	9.3	-	1.6	-
14	11.7	11.2	15.3	34.4	19.5	11.7	6.5	-	6.9	-
15	15.8	13.2	17.1	34.9	18.7	11.9	6.1	-	16.9	-
16	13.3	12.1	14.9	34.9	19.3	11.9		-	10.5	-
17	13.3	12.1	16.6	35.8	19.8	12.3	3.2	-	1.8	-
18	10.0	10.3	13.7	13.0	12.6	11.3	9.0	-	1.1	-
19	11.0	10.4	11.4	11.6	11.3	10.3	8.0	-	2.4	-
20	14.1	11.5	15.8	35.2	18.3	10.1	10.7	-	13.4	-
21	13.1	12.1	15.3	35.1	19.1	12.0	5.8	-	15.6	-
22	12.4	11.1	14.9	32.4	19.3		3.9	-	10.2	-
23	18.5	13.7	16.1	34.9	18.0	11.7	5.4	-	32.9	-
24	23.4	16.1	17.0	33.9	18.0	11.7	4.2	-	35.6	-
25	26.2	16.8	15.7	15.1	11.9	10.0	3.6	-	52.8	-
26	21.3	14.2	15.1	20.8	10.2	9.6	2.7	-	33.4	-
27	12.9	12.4	15.5	31.5	16.8	9.6	3.7	-	10.5	-
28	12.4	11.0	18.0	35.8	17.7	10.5	2.2	-	15.7	-
29	8.2	10.1	15.4	35.8	17.5	11.0	1.6	-	1.8	-
30	7.7	9.1	19.5	35.5	17.2	11.1	3.5	-	1.0	-
31	7.5	9.1	16.2	35.8	17.5	11.1	3.2	-	1.1	-





**Poulton Lancelyn Solar Wall Data**  
**Table 3.5 March 1986**

DAY	M A X I M A					Minm	Aver	ENERGY FLOW		
	1	2	3	4	5			6	7	8*
	°C							kWh		%
1	29.3	19.7	19.1	17.2	11.7	9.7	2.3	-	41.5	-
2	38.7	22.2	18.1	20.0	10.6	9.4	4.9	1.6	64.5	2.4
3	21.9	18.6	17.9	34.2	17.6	10.0	4.3	-	26.3	-
4	14.3	15.4	17.6	79.5	16.2	11.0	8.6	-	5.7	-
5	28.4	18.6	17.7	29.4	16.5	11.9	8.1	-	36.3	-
6	25.0	18.4	18.0	34.2	16.7	11.9	5.3	-	32.1	-
7	19.4	17.0	17.2	32.7	16.3	11.8	5.9	-	26.9	-
8	36.9	22.4	18.9	17.1	12.3	11.2	5.6	-	57.0	-
9	18.3	19.6	18.3	15.5	11.5	10.6	5.3	-	14.5	-
10	17.4	14.4	15.5	33.9	16.7	10.3	5.2	-	12.6	-
11	19.9	16.0	16.5	34.0	16.4	11.3	5.1	-	24.5	-
12	13.3	15.0	15.5	34.0	17.5	12.0	3.7	-	6.5	-
13	13.8	12.0	15.1	33.8	17.2	11.6	2.9	-	12.6	-
14	12.9	11.8	15.8	33.1	16.8	11.6	6.6	-	6.9	-
15	14.6	12.8	14.7	13.5	12.3	11.5	9.9	-	6.9	-
16	13.2	12.6	13.1	12.1	11.4	10.6	7.6	-	7.0	-
17	33.8	21.6	18.7	34.3	16.7	10.4	6.4	-	54.1	-
18	18.3	19.5	18.2	33.7	17.3	12.2	5.2	-	5.1	-
19	43.2	26.2	22.0	31.5	16.7	11.8	7.6	1.6	66.9	2.4
20	35.3	24.3	21.3	32.5	17.0	13.0	7.2	-	45.0	-
21	37.9	25.2	22.1	32.1	16.9	12.8	8.9	-	51.5	-
22	22.8	20.7	21.6	19.0	13.8	12.9	10.8	.1	17.9	.5
23	31.8	21.0	18.0	16.3	12.8	11.3	6.1	-	46.7	-
24										
25										
26	24.9	19.4	18.5	24.7	15.4	11.7		-	13.7	-
27	38.1	25.0	20.5	19.2	13.2	11.8	8.8	-	64.2	-
28	20.0	21.9	19.9	17.0	12.2	11.3	6.6	-	12.9	-
29	23.3	17.0	15.4	14.4	11.2	10.1	6.4	-	29.6	-
30	16.5	14.9	14.5	18.1	11.1	9.9	3.8	-	15.8	-
31	17.6	13.4	12.7	28.8	13.3	9.8	4.1	-	8.6	-

**Poulton Lancelyn Solar Wall Data**  
**Table 3.6 April 1986**

DAY	M A X I M A					Minm	Aver	ENERGY FLOW		
	1	2	3	4	5			6	7	8*
	°C							kWh		%
1	30.5	19.6	17.1	31.9	15.3	9.7	6.4	-	43.6	-
2	31.9	22.7	19.6	34.2	15.3	11.1	5.4	4.3	52.4	8.2
3	20.1	19.8	17.8	31.9	15.1	11.2	4.1	-	21.3	-
4	30.0	18.3	18.9	32.3	15.3	11.1	5.2	-	45.5	-
5	27.4	20.1	18.2	17.2	12.1	10.9	4.0	2.1	36.6	5.7
6	27.1	18.3	16.2	14.7	10.9	10.1	4.0	-	31.3	-
7	13.7	15.9	15.9	33.8	17.0	9.6	3.1	-	10.7	-
8	10.1	12.2	17.4	34.6	17.9	11.0	4.1	-	3.1	-
9	34.1	20.7	17.6	34.7	16.7	11.3	6.5	-	47.0	-
10	29.3	20.8	18.2	33.7	18.0	12.0	4.4	-	35.8	-
11	32.8	22.1	19.0	33.4	17.9	12.1	4.7	-	42.6	-
12	24.3	18.6	18.3	17.3	13.1	12.1	6.6	-	26.3	-
13	21.0	17.4	16.8	14.8	12.0	11.2	5.4	-	18.5	-
14	23.4	17.3	16.4	34.1	17.6	11.0	6.2	-	24.1	-
15	19.1	15.9	16.0	32.8	18.4	12.1	6.4	-	14.3	-
16	15.8	15.1	15.6	31.4	18.0	12.0	6.1	-	11.0	-
17	12.1	13.8	15.0	33.4	18.0	12.3	4.6	-	2.8	-
18	30.3	19.8	17.4	32.0	18.0	12.0	5.8	-	40.9	-
19	18.4	18.0	17.0	16.0	12.8	11.8	5.9	-	13.8	-
20	32.5	21.7	17.9	16.5	12.6	11.3	8.5	-	38.5	-
21										
22	31.4	22.7	19.9	20.9	15.6	13.1	8.2	-	4.2	-
23	29.4	21.5	19.8	29.5	18.2	13.4	8.1	-	24.1	-
24	25.6	20.0	19.4	28.4	17.9	13.8	7.6	-	14.9	-
25	30.2	22.1	19.8	29.2	17.8	13.6	8.1	.1	30.5	.3
26	31.3	22.2	19.7	20.3	14.2	13.0	7.8	4.0	30.0	13.0
27	40.2	26.4	21.6	21.3	14.0	12.3	7.8	6.2	55.2	11.2
28	22.5	23.2	20.7	29.6	17.7	13.1		-	8.0	-
29	33.8	23.2	20.1	31.6	17.5	13.3	8.5	-	43.6	-
30	21.0	21.5	19.7	30.4	18.0	14.1	9.9	-	14.0	-
31										

LIVERPOOL JOHN MOORES UNIVERSITY  
Aldham Roberts L.R.C.  
TEL 0151 231 3701/3634



**Poulton Lancelyn Solar Wall Data**  
**Table 3.7 May 1986**

DAY	M A X I M A					Minm	Aver	ENERGY FLOW		
	1	2	3	4	5	6	7	8*	9	10
	°C							kWh		%
1	40.7	27.7	23.5	27.3	19.2	14.2	13.0	4.3	55.8	7.3
2	30.3	25.4	23.1	25.3	19.6	15.5	13.2	4.6	24.7	18.0
3	25.6	23.1	21.5	20.1	16.1	14.3	10.2	0.2	14.5	1.2
4	26.4	20.4	19.4	17.3	14.3	13.4	9.7	-	23.4	-
5	27.1	20.6	18.9	28.9	15.7	13.5	10.2	-	21.2	-
6	29.5	22.2	20.1	28.0	18.5	13.9	10.3	-	25.2	-
7	25.8	21.2	19.8	24.9	18.9	14.6	9.9	-	20.1	-
8	24.4	20.2	19.4	26.3	16.2	14.6	9.5	-	20.8	-
9	19.3	19.2	18.6	25.8	18.6	14.2	13.2	-	9.6	-
10	18.3	17.7	17.9	16.9	14.9	13.8	12.8	-	7.0	-
11	21.6	18.2	17.0	16.6	13.8	13.3	11.6	-	17.1	-
12	25.6	20.8	19.1	20.2	16.3	13.7	11.4	-	3.6	-
13	30.5	23.3	20.9	29.2	18.5	14.3	10.8	-	34.3	-
14	24.7	21.9	20.6	30.2	19.3	14.9	8.8	-	22.5	-
15	35.3	24.9	21.2	33.3	18.4	14.6	8.7	-	43.8	-
16	24.7	22.0	22.2	32.1	19.3	14.8	11.0	-	33.7	-
17	22.0	23.4	21.9	19.8	15.8	14.5	11.6	-	7.1	-
18	27.5	21.1	19.1	19.8	15.2	14.1	13.0	-	26.1	-
19	31.1	24.2	21.8	30.5	19.5	14.5	13.9	-	31.7	-
20	22.5	23.2	21.6	20.9	18.8	15.4	13.8	-	10.4	-
21	28.3	22.0	20.1	22.5	18.8	15.4	10.6	-	27.3	-
22	31.3	23.7	21.2	31.5	19.4	15.0	11.3	-	28.9	-
23	35.4	26.4	23.0	25.0	19.5	15.6	12.3	-	40.1	-
24	32.2	24.8	22.0	22.0	16.2	15.3	14.6	-	28.1	-
25	32.9	24.5	21.9	22.7	15.6	14.8	14.1	-	28.8	-
26	35.7	26.7	23.1	22.9	16.0	14.9	13.0	4.1	42.3	9.6
27	26.9	24.4	22.1	19.4	15.5	14.7	10.9	1.7	28.1	6.0
28	34.8	24.6	20.9	21.0	15.3	13.8	9.7	5.8	42.1	13.8
29	30.2	22.8	19.9	19.8	14.9	13.8	10.4	6.2	33.6	18.4
30	27.7	22.2	19.9	20.6	14.7	13.7	11.5	1.3	27.8	4.7
31	21.0	20.9	19.5	17.8	14.5	13.8	10.9	-	11.0	-





**Poulton Lancelyn Solar Wall Data**  
**Table 3.9 July 1986**

DAY	M A X I M A					Minm	Aver	ENERGY FLOW		
	1	2	3	4	5			6	7	8*
	°C							kWh		Z
1	38.9	30.6	27.6	29.4	21.7	17.8	16.9	2.0	45.4	4.4
2	33.3	28.8	26.9	26.8	22.9	18.4	17.2	1.4	31.2	4.5
3	42.3	31.7	27.4	27.3	22.0	18.0	16.8	1.1	50.0	2.2
4	28.4	29.3	27.1	24.2	21.8	18.5	16.3	1.7	17.1	9.9
5	27.5	24.7	24.2	23.2	18.8	18.2	15.1	1.5	26.8	5.6
6	31.2	25.5	23.4	23.4	18.2	17.4	14.3	3.6	33.9	10.6
7	39.3	28.8	24.8	24.3	19.9	16.5	14.5	3.9	51.4	7.6
8	31.3	26.9	23.6	22.2	20.0	17.1	14.2	3.2	31.7	10.1
9	27.3	24.1	22.2	21.3	20.2	16.1	13.6	.2	25.5	7.8
10	29.1	24.5	22.8	22.6	20.5	16.6	14.9	2.1	32.3	6.5
11	28.4	24.6	23.3	25.1	21.3	16.7	16.3	-	22.1	-
12	31.1	25.6	23.8	26.8	18.8	17.6	16.6	3.1	31.0	10.0
13	28.6	24.9	23.2	23.8	18.9	17.5	17.3	11	22.8	48.2
14	25.2	23.8	23.1	23.8	21.4	18.1	18.3	-	14.8	-
15	34.2	27.6	25.6	29.3	22.8	18.5	21.2	.2	31.8	.6
16	35.4	29.0	27.0	29.0	22.4	18.1	15.4	1.4	10.7	13.1
17	30.9	27.7	26.6	24.4	20.6	17.7	14.4	-	30.1	-
18	29.0	24.8	20.8	23.1	18.8	17.9	14.3	4.3	29.4	14.6
19	26.8	23.6	22.4	23.4	18.0	17.3	15.1	.7	22.9	3.0
20	27.1	23.3	22.4	22.2	17.7	17.7	14.7	.2	23.3	.85
21	30.9	24.7	22.4	23.3	18.1	16.8	14.8	5.8	34.5	16.8
22	31.5	25.1	22.7	22.8	17.5	16.8	13.4	.7	33.3	2.1
23	28.2	23.9	22.4	20.4	16.9	16.2	12.5	-	29.4	-
24	32.0	24.6	22.4	23.8	16.8	15.8	14.8	-	31.5	-
25	30.3	24.3	22.3	22.3	17.1	16.3	15.0	-	31.0	-
26	35.2	26.5	23.6	24.3	17.6	16.4	15.9	2.4	40.0	60.0
27	28.6	25.0	23.2	23.3	17.2	16.5	16.9	3.3	26.0	12.7
28	23.5	23.6	22.6	20.8	17.2	16.7	16.5	-	9.9	-
29	32.7	24.7	22.1	22.1	17.0	16.3	14.9	.5	38.0	1.3
30	22.8	23.6	22.0	19.8	16.5	15.8	13.0	-	5.6	-
31	18.0	19.0	19.3	17.3	15.7	15.0	12.8	-	8.4	-

**Poulton Lancelyn Solar Wall Data**  
**Table 3.10 August 1986**

DAY	M A X I M A					Minm	Aver	ENERGY FLOW		
	1	2	3	4	5	6	7	8*	9	10
	°C							kWh		%
1	22.3	19.2	18.1	20.5	15.4	14.5	13.1	-	19.3	-
2	22.7	19.5	18.4	19.8	15.6	15.0	15.0	-	16.7	-
3	21.6	19.7	18.8	19.8	15.5	14.9	13.7	-	15.2	-
4	26.8	21.7	20.0	21.8	15.7	14.9	9.6	-	24.3	-
5	34.7	25.9	27.6	23.9	16.3	14.9	14.6	3.7	43.5	8.5
6	25.8	24.0	22.0	20.7	16.2	15.5	14.9	-	17.8	-
7	20.1	21.0	20.6	18.5	15.7	15.1	13.7	-	9.5	-
8	24.2	20.6	19.2	20.2	15.6	14.8	9.7	-	25.6	-
9	32.1	23.7	21.2	23.7	16.0	14.7	14.6	6.5	37.9	17.2
10	33.1	24.6	22.0	23.2	16.8	15.5	16.8	18.6	37.2	50.0
11	23.4	23.3	21.0	19.8	16.5	15.7	13.8	1.9	8.2	12.2
12	24.9	21.3	20.2	22.4	16.1	15.2	15.7	-	23.0	-
13	21.3	20.8	20.1	19.1	15.9	15.6	15.6	-	11.7	-
14	30.9	23.6	21.2	22.8	16.3	15.4	15.3	1.4	33.3	4.2
15	23.7	22.5	21.0	19.3	16.1	15.3	13.5	.1	15.4	.6
16	20.6	19.8	19.5	17.1	15.2	14.7	13.3	-	15.9	-
17	38.0	26.5	22.5	23.9	16.3	14.6	14.6	9.5	53.1	17.8
18	24.3	24.3	20.3	19.2	15.9	15.2	12.7	2.7	15.5	17.4
19	34.7	24.6	21.4	21.8	15.8	14.6	12.7	4.3	46.6	9.2
20	42.4	28.8	24.0	24.3	16.3	14.7	13.5	13.2	58.5	22.6
21	25.7	26.0	21.2	19.3	15.8	15.1	12.5	4.0	14.9	26.8
22	22.1	20.0	19.7	19.5	15.3	14.8	13.1	.2	16.0	1.3
23	20	19.5	20	20.7	15.3	14.4	13.4	.9	29.0	3.1
24	41.3	28.2	23.5	23.8	16.1	14.4	13.4	11.4	60.2	18.9
25	25.2	25.4	20.9	19.1	15.6	14.6	11.4	-	5.6	-
26	16.6	17.8	18.4	15.8	14.6	13.8	12.4	-	4.5	-
27	23.7	19.4	17.7	17.3	14.4	13.4	12.6	-	28.4	-
28	33.2	24.3	20.9	20.2	14.9	13.6	12.5	3.2	47.3	6.8
29	26.9	21.3	19.4	18.4	14.6	13.5	7.2	2.6	17.2	15.1
30	24.5	19.9	18.5	18.9	14.5	13.7	12.4	-	22.0	-
31	36.4	25.3	21.6	21.1	14.7	13.4	11.7	5.3	52.7	10.1







**Poulton Lancelyn Solar Wall Data**  
**Table 3.12 October 1986**

DAY	M A X I M A					Minm	Aver	ENERGY FLOW		
	1	2	3	4	5			6	7	8*
	°C					kWh			z	
1	21.4	21.8	21.2	20.2	19.0	15.8	11.8	-	14.9	-
2	32.7	23.6	21.6	20.7	18.7	15.7	12.9	-	49.4	-
3	34.3	24.6	22.7	24.5	19.2	25.7	11.4	7	51.3	13.6
4	33.5	24.3	21.8	21.4	16.3	15.5	13.3	12.0	50.5	23.7
5	27.4	22.3	20.9	21.1	15.9	15.3	14.9	3.6	26.0	13.8
6	30.3	23.5	22.2	23.1	18.6	15.6	16.1	.6	33.3	1.8
7	22.1	22.2	21.9	20.6	19.2	16.4	15.7	-	8.9	-
8	23.2	20.8	20.4	22.1	19.1	16.1	15.1	-	15.6	-
9	18.9	20.1	20.1	19.3	18.8	15.9	13.9	-	2.0	-
10	19.5	18.0	18.0	18.9	18.2	15.4	11.8	-	10.3	-
11	37.1	24.5	21.5	21.4	15.3	14.4	10.7	3.1	68.0	4.6
12	30.7	22.3	20.4	19.4	14.8	13.7	9.1	1.6	50.4	3.2
13	19.7	20.3	19.9	23.8	17.7	14.4	12.6	-	3.1	-
14	18.2	17.4	18.1	20.2	17.9	15.1	12.6	-	5.4	-
15	33.1	22.4	20.6	22.7	17.5	14.7	9.6	.5	60.4	.8
16	29.4	23.0	21.5	20.6	16.6	14.3	3.0	10.7	20.0	53.5
17	30.2	21.7	21.0	23.9	17.7	14.4	8.3	2	54.7	3.6
18	18.1	19.6	18.8	17.2	14.8	13.4	9.1	-	7.9	-
19	20.8	16.1	16.2	13.9	13.3	12.2	7.1	-	37.3	-
20	15.1	14.8	15.3	27.3	15.6	12.1	7.3	-	15.2	-
21	13.1	13.3	14.4	26.4	15.5	12.2	9.5	-	3.4	-
22	20.2	16.0	16.6	26.4	15.1	12.3	8.4	-	40.0	-
23	19.3	16.0	17.1	26.6	15.5	12.1	7.2	-	31.0	-
24	13.8	14.8	16.2	26.6	15.4	12.5	8.5	-	5.2	-
25	12.9	13.4	15.4	14.5	13.0	11.8	9.8	-	3.3	-
26	23.3	17.0	15.8	15.7	12.1	11.5	10.1	-	47.8	-
27	17.0	16.2	17.2	26.7	16.9	11.9	13.8	-	7.3	-
28	16.1	16.1	17.1	20.1	17.0	14.2	13.4	-	2.3	-
29	25.0	18.9	18.7	26.0	16.5	14.0	19.0	-	50.3	-
30	20.8	17.7	17.9	25.2	16.7	13.7	10.4	-	32.9	-
31	19.3	17.0	17.4	25.6	16.6	13.5	9.1	-	16.4	-

Nomenclature of variables measured between hours H-1 and H

$A_c$  wall cavity, cross section area ( $m^2$ )

$A_w$  solar wall, insulated surface area ( $m^2$ )

$F_L$  air speed in wall cavity ( $ms^{-1}$ )

$F$  fraction of time that wall fan operates in an hour

$V$  volumetric specific heat capacity of air ( $J/m^3 K$ )

$I_{D,H}$  hourly average value of irradiation on solar wall ( $W/m^2$ )

$T_c$  average air temperature at cavity top ( $^{\circ}C$ )

$T_{AI}$  average temperature of classroom air ( $^{\circ}C$ )

$T_{AO}$  average external air temperature ( $^{\circ}C$ )

### **3.6 CONTRIBUTION OF THE SOLAR WALL TO A CLASSROOM'S ENERGY REQUIREMENT**

The heat from the internal cavity passes to the adjacent classroom, thereby diminishing its energy needs. The energy consumption of the whole of phase 1 of the school ( $E$  kWh), was recorded for each month from the electricity and gas meters. The volume of one classroom is approximately  $1/9$  of the total volume of phase 1. There are three solar walls in phase 1 and 3 solar wall fans. Each fan consumes  $F$  kWh in a month. The non-renewable energy consumption (electricity and gas) of the classroom next to the solar wall is therefore:

$$(E-3.F)/9 + F = E/9 + 2.F/3 \quad (\text{kWh per month}) \quad (3.6)$$

A solar wall contribution to a classroom's energy requirement in a month would then be:

$$\text{Solar contribution} = \frac{\text{Energy from the solar wall}}{\text{Total energy used by the classroom}}$$

*Tables 3.13* and *3.14* show print outs obtained using a program written to collate each months' data from the data stored on the hard disk of the Apricot computer. This program was written in Basic. It processed the sequential output of 'compact' form data from the data logger, which had been stored on the Apricot computer's hard disk. The basic program took into consideration all possible markers that might precede the actual data during its processing.

The program produced daily tables of output, an example being shown in **Fig 3.10**.

Monthly data was extracted manually from the daily processed data. It was tabulated for each month of the period from November 1985 to October 1986.

*Tables 3.1* to *3.12*, show the maximum daily temperatures reached by the front and back surfaces of the mass wall, and the top of the internal cavity. They show too, the maximum and minimum temperatures of the room air before entering the wall and the average daily external air temperature. Values are given for the total solar irradiation incident on the wall, the heat energy produced and the computed efficiency of energy production from the mass wall ensemble.

These results are assembled in *Table 3.15*. This Table displays the energy produced, the efficiency of its production and the percentage contribution of solar heat to classroom energy demand. Measurement of the monthly energy demand of Phase 1 (E) and of the solar wall fans (F), allows the amount of non-renewable energy input into a classroom to be calculated (see *Table 3.16*). The energy used

Table 3.13 Output from data on Apricot computer hard disk for hours 0-11, July 24.

aug90 24 / 7

CH	HOUR	0	1	2	3	4	5
1	C	22.6	22.9	23.8	24.1	25.3	26.6
2	C	24.9	25.6	26.6	27.1	28.5	29.4
3	C	24.4	25.3	26.4	27.1	28.5	29.6
4	C	24.2	25.1	26.4	27.1	28.7	29.8
5	C	24	25	26.4	27.2	28.7	29.9
6	C	24.6	24.8	25.3	25.5	26.5	27.4
7	C	25.9	26.4	27.2	27.6	28.8	29.6
8	C	24.3	25.2	26.5	27.1	28.6	29.6
9	C	24.1	25.1	26.4	27.1	28.6	29.7
10	C	20.6	21.4	22.5	23.1	24.7	25.8
11	C	11.2	11	11.6	11.9	13.8	15.6
12	C	2.2	1.3	.1	1	2.9	4.1
13	W/M2	.9	.6	.9	1.1	7	44.4
14	C	22.2	22.8	23.8	24.2	25.6	26.6
15	M/S	.6	.6	.8	.7	1.8	1.1
16	W/M2	1.3	1.6	1.9	1.3	3.3	20.8
17	DHM	103.8	201.4	201.4	201.4	201.4	201.4
18	C	4.5	5.2	6.2	6.7	7.4	8.2
19	C	4.7	5.4	6.4	6.9	7.5	8.3
20	C	4.7	5.4	6.4	6.9	7.5	8.3
MEAN VALUES							
13	W/M2	.1	.6	.9	1	13.5	49
15	M/S	1.1	1	.9	.9	1	1.4
16	W/M2	1.6	1.5	1.5	1.3	7	23.2
17	DHM	164.8	157.9	189.6	201.4	201.4	198.6

aug90 24 / 7

CH	HOUR	6	7	8	9	10	11
1	C	27.8	28.7	29.3	29.8	30.1	30.1
2	C	29.9	29.8	29.3	28.5	27.1	25.4
3	C	30.1	29.9	29.6	28.6	27.5	25.6
4	C	30.4	30.4	29.9	29	27.5	25.6
5	C	30.5	30.6	30.1	29.2	27.7	25.6
6	C	28	28.4	28.7	29.4	29.9	32.2
7	C	30	29.8	29.3	28.4	27.2	25.7
8	C	30.2	30.1	29.7	28.7	27.4	25.5
9	C	30.3	30.3	29.8	28.8	27.4	25.4
10	C	26.4	26.6	26.5	26	25	23.3
11	C	17.8	21.6	22.8	27.6	26.8	25.5
12	C	5	5.3	4.9	4.1	2.5	.5
13	W/M2	66	86.6	149.6	251.9	341.6	412.5
14	C	27.1	24.9	26.8	27.4	27.1	26.3
15	M/S	2	2.6	1.5	.1	4	1.5
16	W/M2	32.3	46	144.7	224.1	343.3	400.1
17	DHM	201.4	201.4	201.3	201.3	201.2	201.1
18	C	8.5	8.2	7.4	6	4.2	2
19	C	8.600001	8.3	7.6	6.2	4.5	2.3
20	C	8.5	8.2	7.6	6.1	4.4	2.3
MEAN VALUES							
13	W/M2	71.6	96.3	167.7	271.9	357.9	422.6
15	M/S	1.5	1.6	1.5	2	1.9	1.8
16	W/M2	34.2	63.4	158.3	246.7	349.5	410.6
17	DHM	201.4	201.4	201.3	201.2	201.2	201.1



**Table 3.14 Output from data on Apricot computer hard disk for hours 12-23, 24 July.**

aug90 24 / 7

CH	HOUR	12	13	14	15	16	17
1	C	28.5	25.3	24.6	23.6	22.6	22.1
2	C	22.6	18.6	17.5	17.3	17.8	18.6
3	C	22.8	18.7	17.4	17.1	17.4	18.2
4	C	22.6	18.2	16.6	16	16.1	16.6
5	C	22.5	18	16.3	15.6	15.5	16
6	C	33.6	33.1	34	33.9	31.6	29.4
7	C	23.4	20	19.7	20.2	21.2	22.2
8	C	22.6	18.3	16.9	16.4	16.6	17.3
9	C	22.4	18	16.4	15.8	15.9	16.5
10	C	20.7	16.7	15.7	14.6	14.6	15.1
11	C	25.8	18.9	17	16.4	16.9	15.2
12	C	2.6	7.2	9	10	10.3	10.2
13	W/M2	446.7	459.2	411.5	313.8	210.7	102.1
14	C	24.3	20.8	19.5	19.5	20	20.2
15	M/S	3	3.6	2.1	2.2	3.8	1.6
16	W/M2	426	425.8	375	313.6	182.7	120.8
17	DHM	201.1	201	201	201	201	201
18	C	.4	3.2	4	4.3	3.9	3.1
19	C	.2	2.5	3	2.5	1.7	.8
20	C	0	2.7	3.4	3.1	2.5	1.6
		MEAN VALUES					
13	W/M2	450.6	449.9	398.5	303.9	194.5	91.1
15	M/S	1.9	2.2	2.5	2.1	2.1	1.7
16	W/M2	429.4	416.9	368.1	290	175	101.7
17	DHM	201.1	201	201	201	201	201

aug90 24 / 7

CH	HOUR	18	19	20	21	22	23
1	C	22.1	22.1	22.5	23.2	24.1	24.5
2	C	19.5	20.6	22.1	23.7	25.3	26.2
3	C	19	20	21.5	23	24.5	25.5
4	C	17.5	18.6	20.3	22.1	23.8	24.9
5	C	16.9	18	19.7	21.6	23.4	24.6
6	C	25	27.2	27	27.1	27.5	27.5
7	C	23	23.9	25	26.2	27.4	28
8	C	18.2	19.4	21	22.7	24.4	25.4
9	C	17.4	18.6	20.3	22.1	23.9	25.1
10	C	15.4	16	17.1	18.4	19.8	20.7
11	C	15.9	14.1	13.3	13.1	12.6	11.1
12	C	9.8	9	7.7	6	4.4	3.1
13	W/M2	44.5	17.5	1.9	1.4	2.8	3.6
14	C	20.4	20.5	21.1	22	23	23.5
15	M/S	1.8	1	1.5	.9	0	.1
16	W/M2	35.4	18.8	7.1	4.1	3.9	2.2
17	DHM	201	201.1	201.1	201.2	201.2	201.3
18	C	2.3	1.4	.2	1	2.3	3.1
19	C	.4	0	.7	1.8	2.9	3.6
20	C	1	.4	.4	1.6	2.7	3.4
		MEAN VALUES					
13	W/M2	37.2	16.3	2	.7	3.2	2.7
15	M/S	1.3	1	1.2	.7	.2	.1
16	W/M2	34.2	17.6	6.6	3.9	3.6	2.5
17	DHM	201	201.1	201.1	201.2	192.7	177.3

aug90 24 / 7  
TROMBE HEAT (KWH), IF 1 HOUR OPERATION.

HR	FAN HEAT (KWH)	HR	FAN HEAT (KWH)	HR	FAN HEAT (KWH)
0	ON .1931423	1	ON .2026612	2	ON 4.667349E-02
	ON 2.037462		ON 2.40041		ON .6534289
3	OFF 0	4	OFF 0	5	ON 7.369499E-03
	OFF 0		OFF 0		ON .1707267
6	OFF 0	7	OFF 0	8	OFF 0
	OFF 0		OFF 0		OFF 0
9	OFF 0	10	OFF 0	11	OFF 0
	OFF 0		OFF 0		OFF 0
12	OFF 0	13	OFF 0	14	OFF 0
	OFF 0		OFF 0		OFF 0
15	ON 1.535312E-02	16	ON 1.668373E-02	17	OFF 0
	ON 4.708291E-02		ON 5.005118E-02		OFF 0
18	OFF 0	19	OFF 0	20	OFF 0
	OFF 0		OFF 0		OFF 0
21	OFF 0	22	ON 8.843398E-02	23	ON .2088025
	OFF 0		ON .5785056		ON 1.518117

CH	AVERAGE	MAXIMA	MINIMA	MEASURE
1	25.25042	30.09	22.05	C
2	24.24459	29.89	17.3	C
3	24.05292	30.09	17.07	C
4	23.64417	30.41	15.96	C
5	23.46083	30.55	15.54	C
6	28.76417	34.04	24.6	C
7	25.66459	29.96	19.63	C
8	23.84	30.15	16.41	C
9	23.54667	30.29	15.75	C
10	20.69375	26.64	14.56	C
11	16.96833	27.57	10.95	C
12	5.138334	10.34	.1	C
13	6.841924E-03	.0223173	.0000299	W/M2
14	23.31667	27.39	19.46	C
15	.2576027	.63766	.0052762	M/S
16	1.568133E-03	426.0483	1.308328	W/M2
17	197.1475	201.409	103.842	DHM
18	4.320417	8.51	.22	C
19	4.021667	8.57	.02	C
20	4.122084	8.54	0	C
CH	AVERAGE	MAXIMA	MINIMA	MEASURE
13 M	6.892681E-03	.0218973	4.75E-06	W/M2
15	.2248159	.399011	9.479699E-03	M/S
16	1.574325E-03	429.44	.0000161	W/M2

Fig. 3. 10 Data from Apricot computer hard disk for 24 July 1990.

**Table 3.15 Energy produced and efficiency of operation of Poulton Lancelyn solar wall**

MONTH	INCIDENT SOLAR ENERGY	ENERGY FROM SOLAR WALL	NON RENEWABLE ENERGY USED BY ADJACENT CLASSROOM	EFFICIENCY OF ENERGY PRODUCTION	SOLAR WALL CONTRIBUTI TO CLASSRO ENERGY REQUIREMEN
	kWh	kWh	kWh	%	%
NOVEMBER	543	-	1087	-	-
DECEMBER	367	-	1292	-	-
JANUARY	418	-	1148	-	-
FEBRUARY	615	-	1150	-	-
MARCH	870	3.3	1141	.4	.3
APRIL	811	16.7	472	2.1	3.4
MAY	791	28.2	402	3.6	6.6
JUNE	908	74.4	256	8.2	22.5
JULY	872	57.7	172	6.6	25.1
AUGUST	826	89.5	58	10.8	60.7
SEPTEMBER	1137	134.0	514	11.8	20.7
OCTOBER	821	41.1	569	5.1	6.7
SEPTEMBER TO MAY	6373	223.3	7776	3.5	2.8
YEAR NOV - OCT	8979	445	8262	5.0	5.1

**Table 3.16 Non-renewable energy used by a classroom adjacent to the solar wall at Poulton Lancelyn.**

MONTH	ENERGY USED BY PHASE 1	ENERGY USED BY SOLAR WALL FAN	NON RENEWABLE ENERGY USED BY CLASSROOM ADJACENT TO SOLAR WALL
	E	F	
	kWh	kWh	kWh
NOVEMBER	9783	-	1087
DECEMBER	11628	-	1292
JANUARY	10332	-	1148
FEBRUARY	10350	-	1150
MARCH	10278	.2	1142
APRIL	4239	1.4	472
MAY	3600	2.4	402
JUNE	2277	4.5	256
JULY	1521	3.9	172
AUGUST	486	5.7	58
SEPTEMBER	4572	9.5	514
OCTOBER	5103	3.3	569
SEPTEMBER to MAY	69885	16.8	7776
YEAR NOV-OCT	74169	30.9	8262



by a solar wall fan was obtained from its power rating and the proportion of time the fan operated in the hours that it was switched on.

These results show that no heat energy at all emerges from the solar wall in November, December, January or February. In March and April too, the amount produced is extremely small. Only modest amounts of energy are produced during the remainder of the year. The efficiency of energy production for the whole year is just 5 percent. The solar contribution to a classroom's energy requirement is also circa 5 percent. The amounts of solar energy input into the wall, together with the energy output from the wall every month are plotted as a bar chart in **Fig 3.11**. They clearly show the extremely poor performance produced.

What are the reasons for this abysmal performance? Is the Trombe wall concept unsuited to application at northern latitudes? Resolution of such queries will be attempted later.

### **3.7 THE THERMAL PERFORMANCE OF THE SOLAR WALL**

Plots of the variation of temperatures of the wall surfaces, the internal cavity, the internal and external air were plotted in **Fig 3.12** to **Fig 3.17** for various days in 1985 and 1986. One plot shows the solar wall front surface (FF) temperatures warming up from 6°C to 34°C during a day in February, **Fig 3.15**. After a time lag due to the passage of heat through the dense brick, the solar wall back surface (BF) also warms up, from 9°C to 19°C. The internal air of the adjacent classroom was 18°C during the day. At 16.00 hours the school heating system

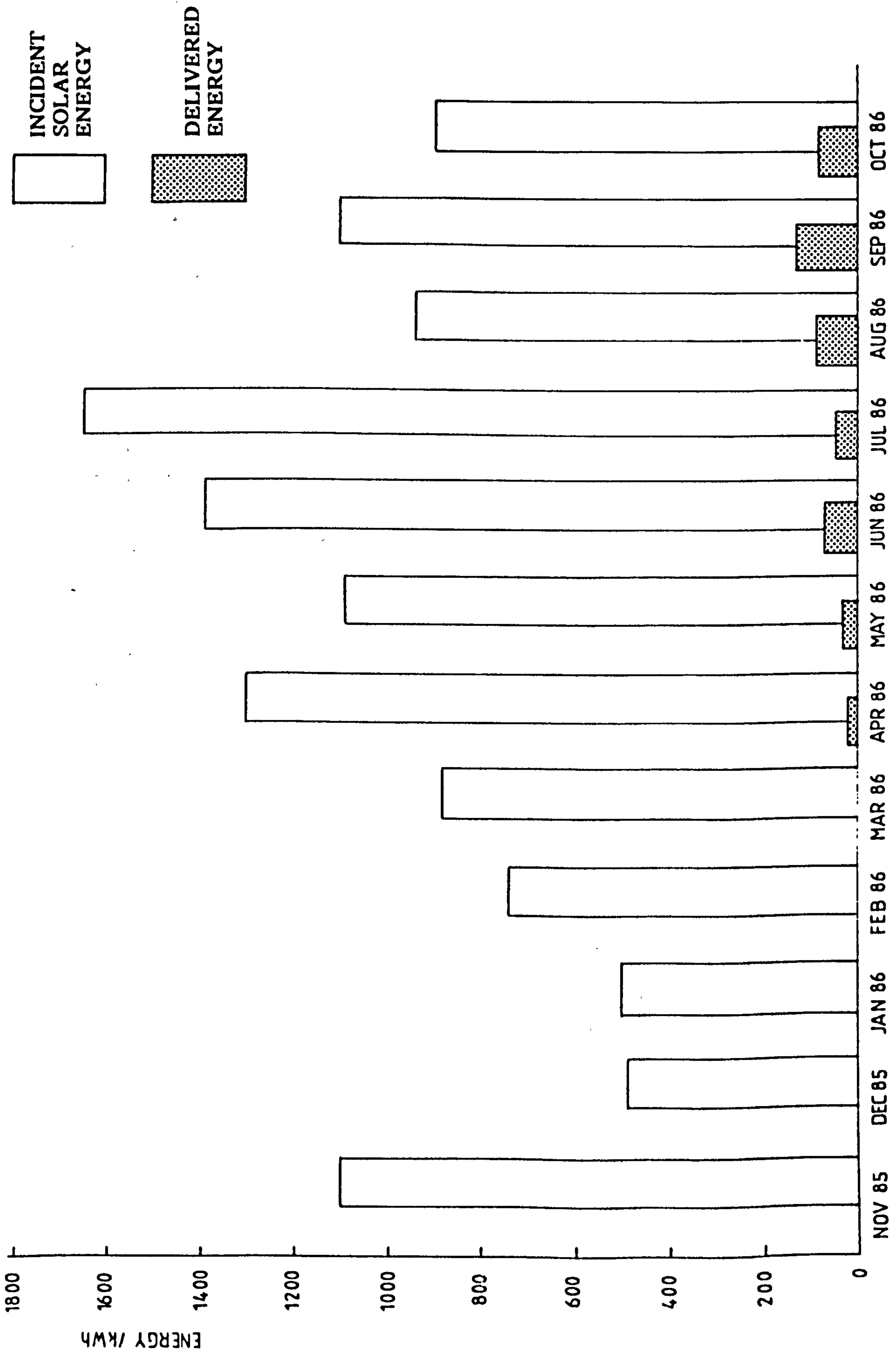


Fig. 3.11 Energy input and output to and from solar wall.

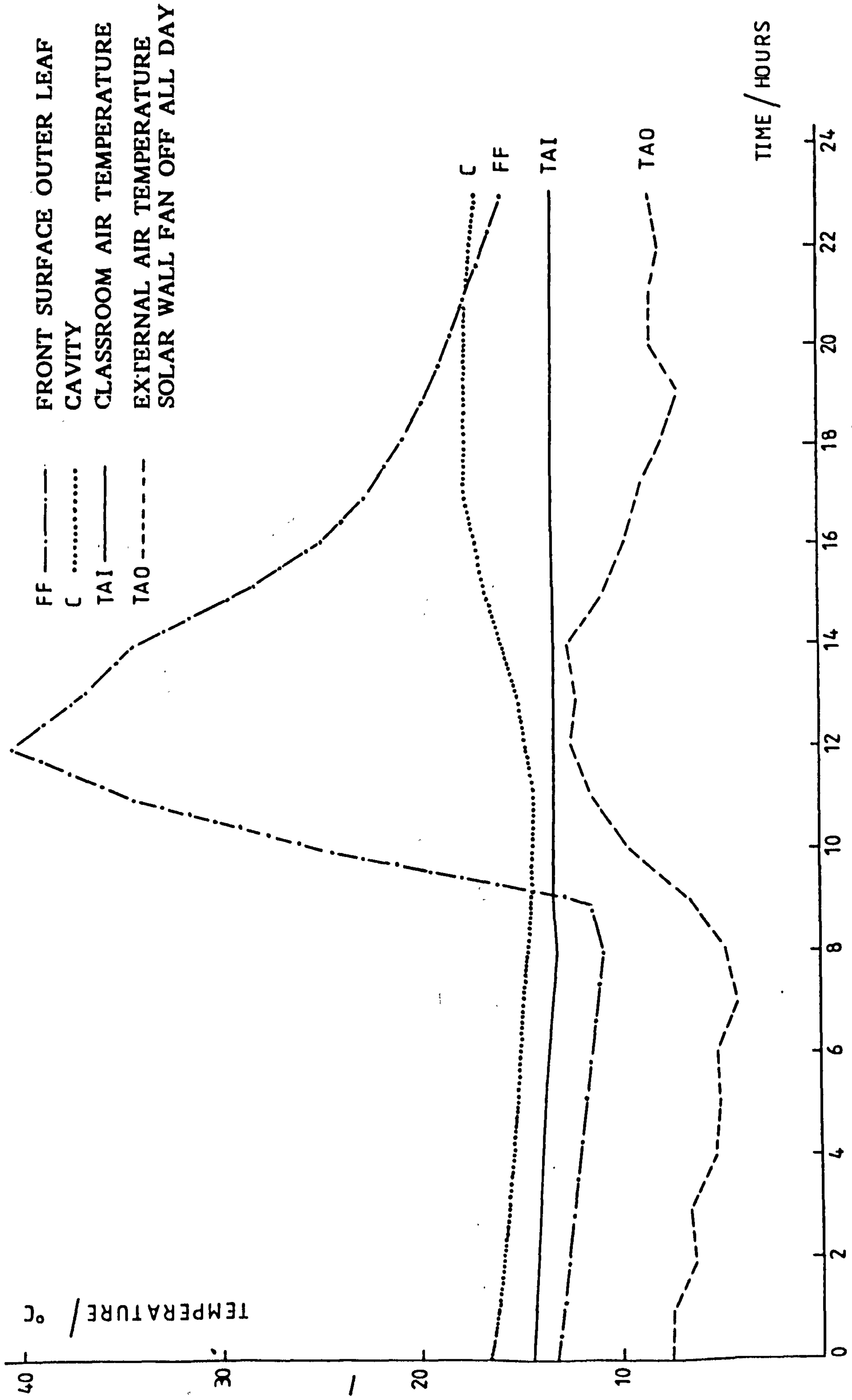


Fig. 3.12 Temperatures of front surface and cavity of solar wall, Saturday November 15 1986.

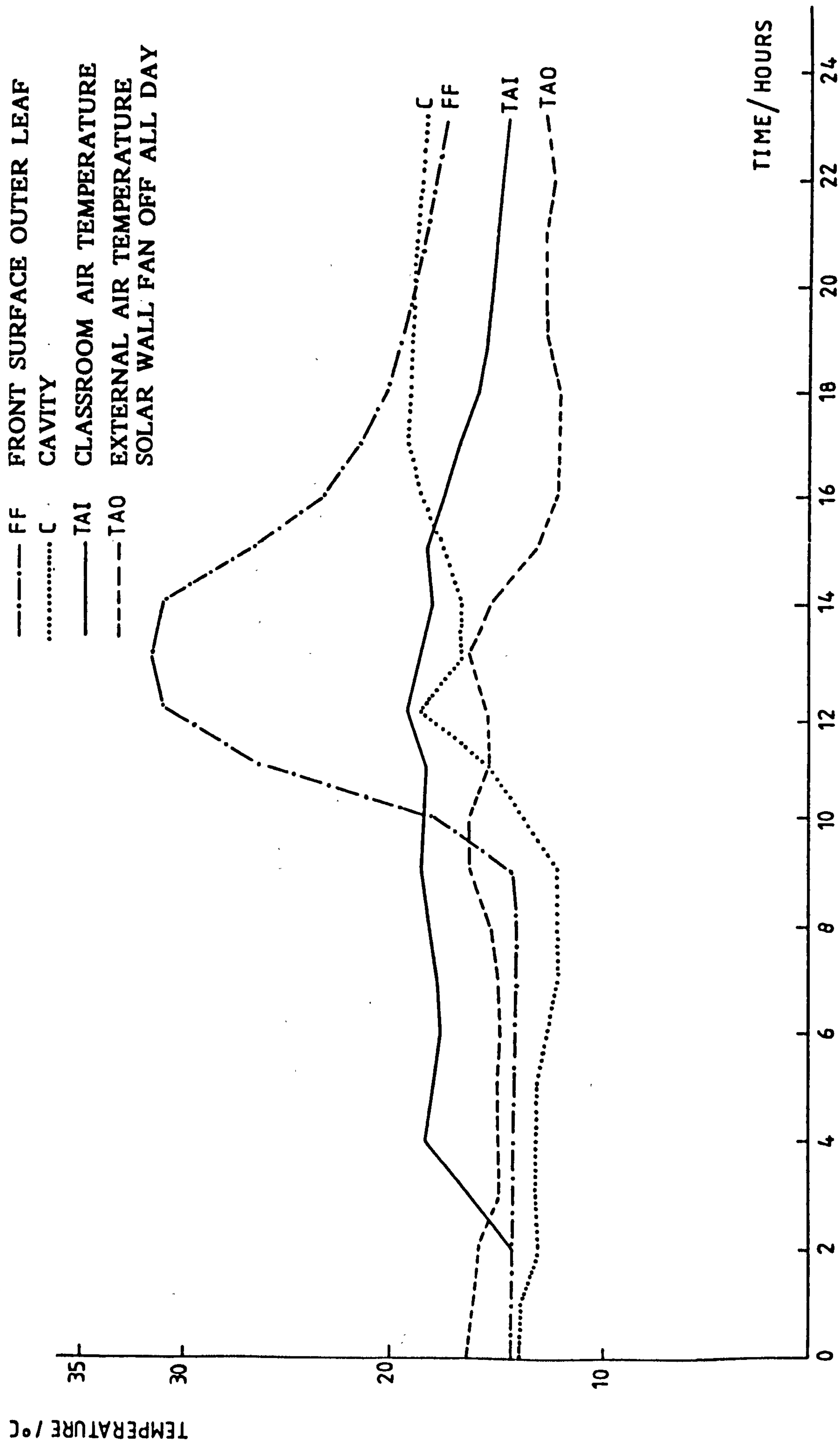


Fig. 3.13 Temperatures of front surface and cavity of solar wall, Tuesday December 3 1985.



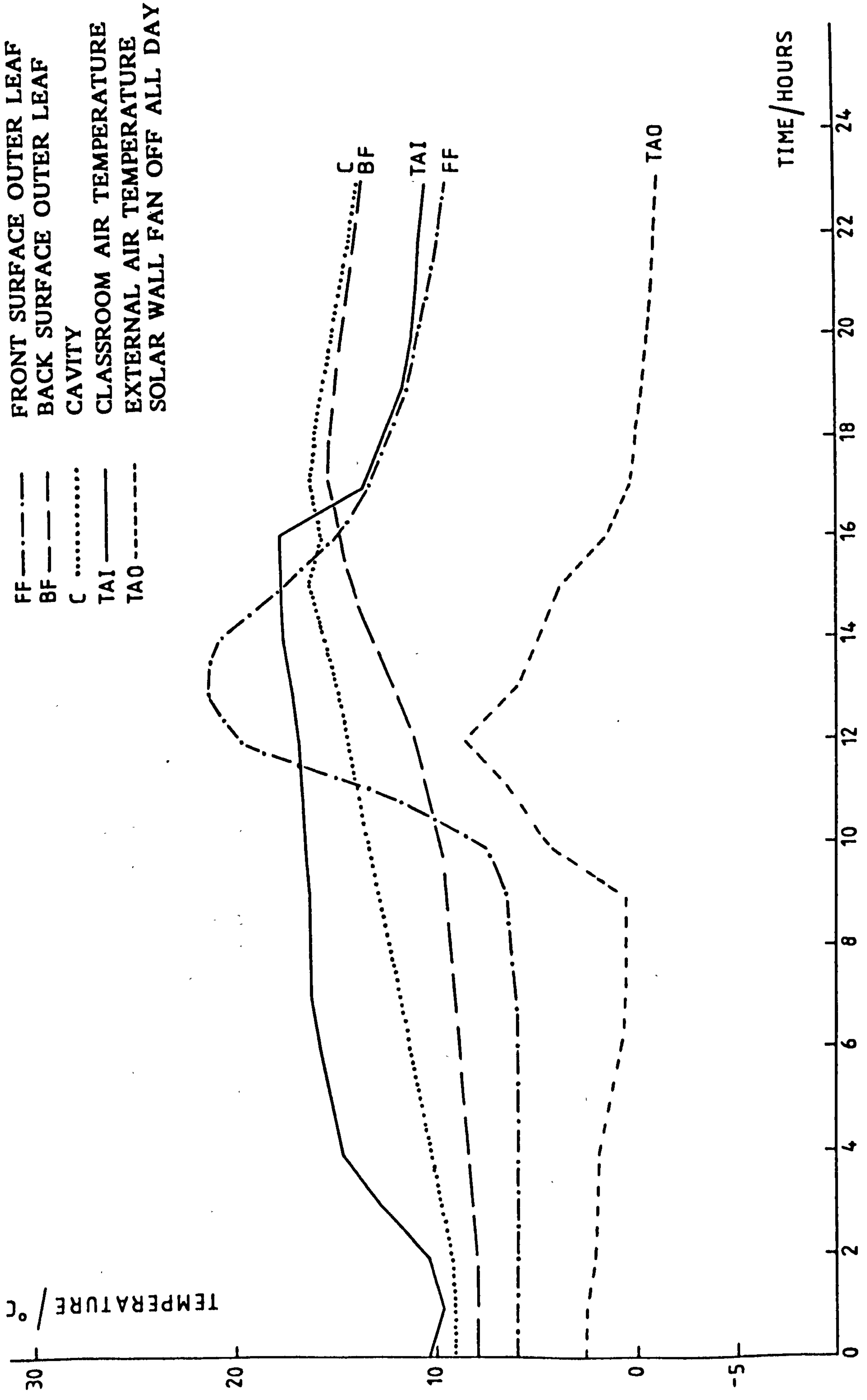


Fig. 3.14 Temperatures of surfaces and cavity of solar wall, Monday January 6 1986.

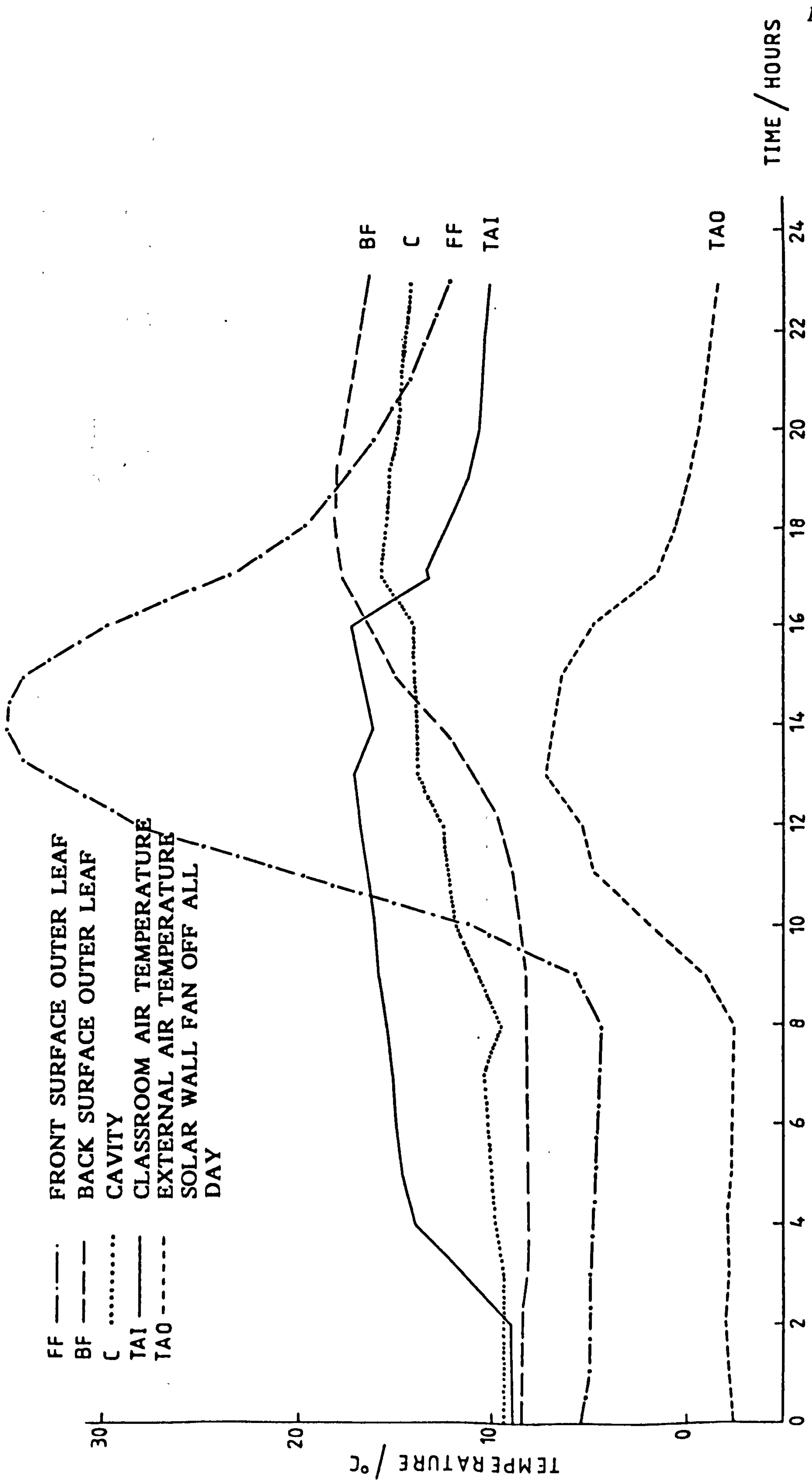


Fig. 3.15 Temperatures of surfaces and cavity of solar wall, Thursday 13 February 1986.

LIVERPOOL JOHN MOORES UNIVERSITY  
 Aldham Roberts L.R.C.  
 TEL 0151 231 3701/3634

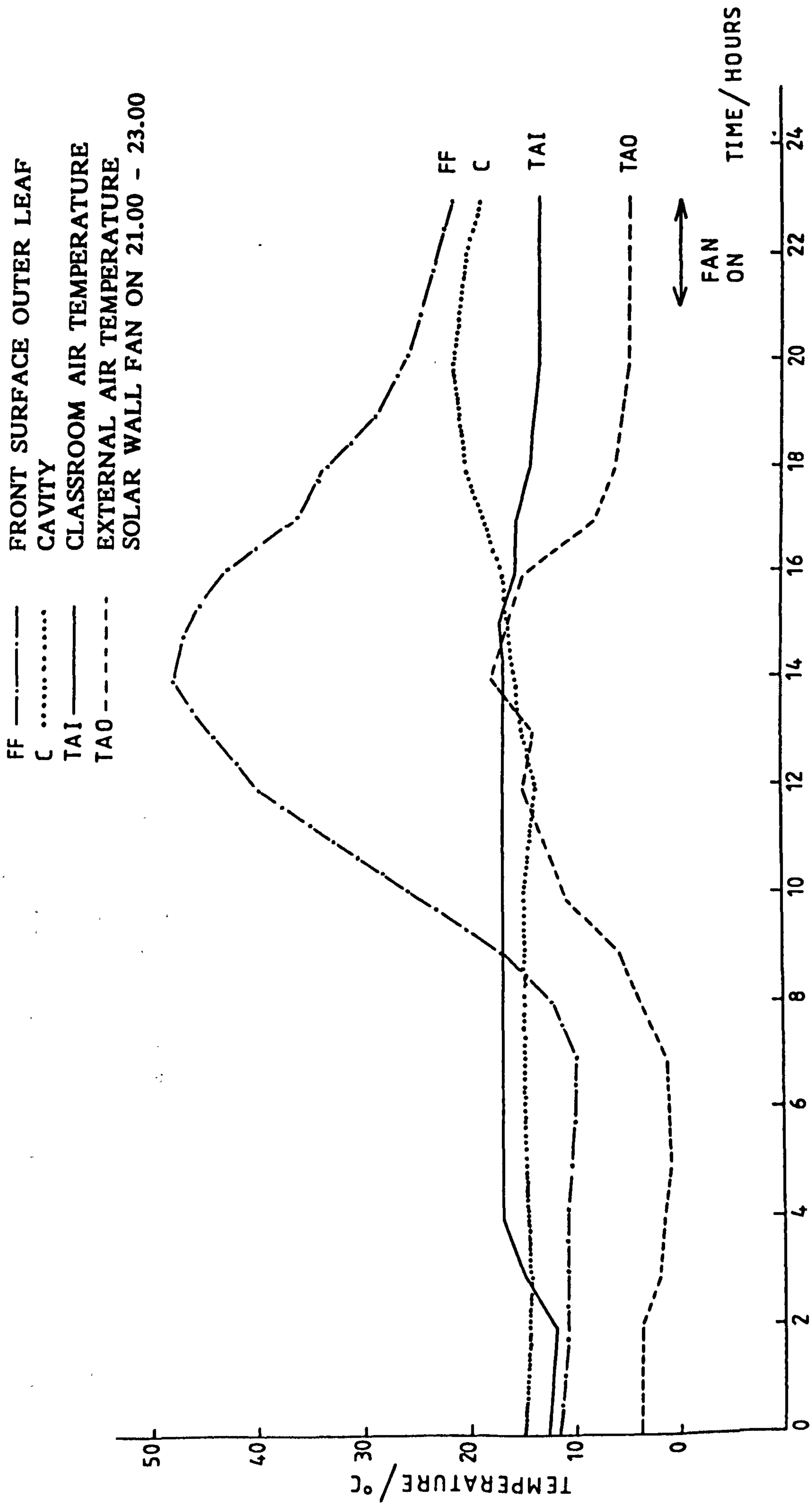


Fig. 3.16 Temperatures of front surface and cavity of solar wall, Wednesday 19 March 1986.

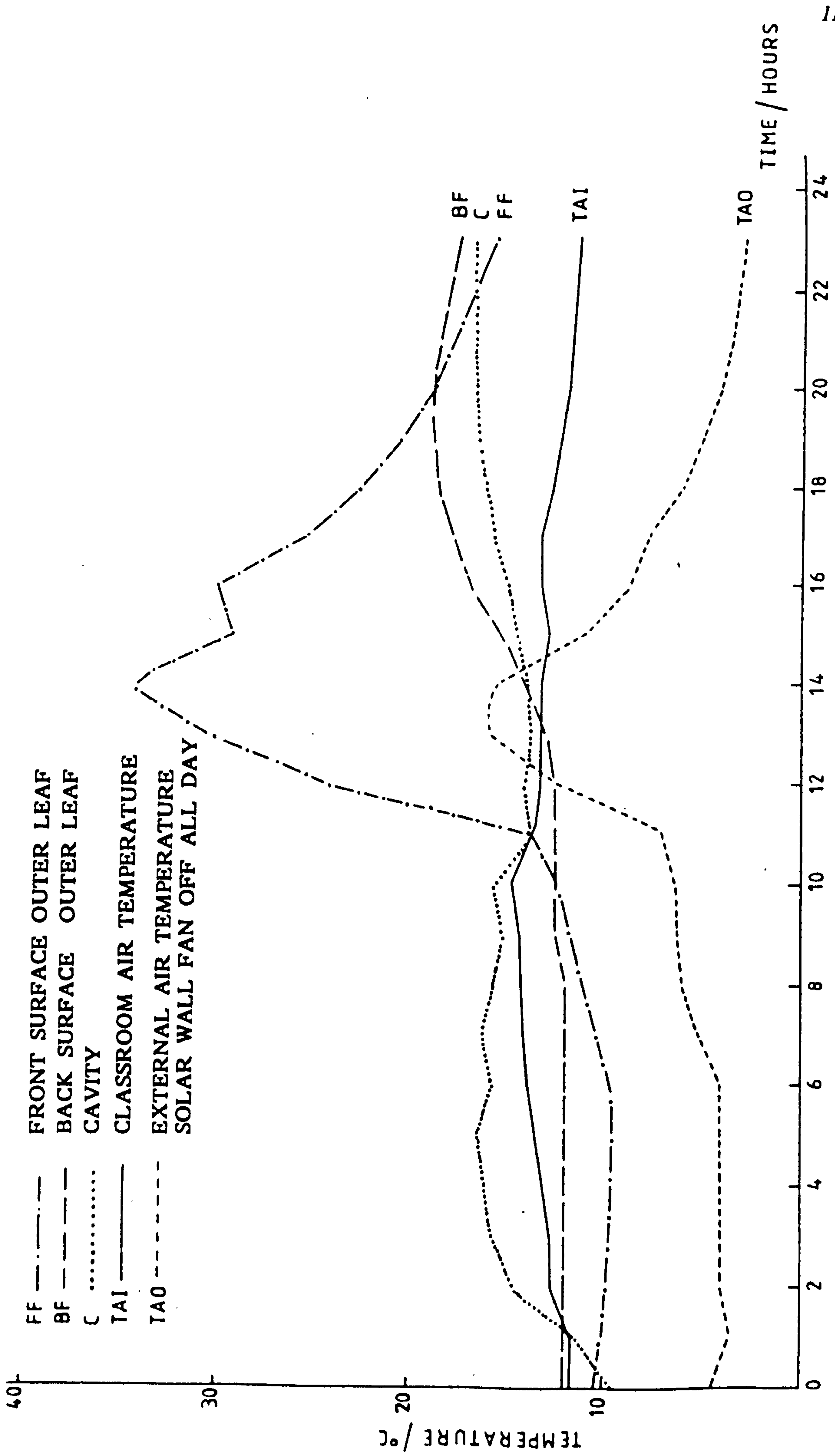


Fig. 3.17 Temperatures of front surface and cavity of solar wall, Tuesday April 1 1986.



switched off and the internal air temperature ( $T_{AI}$ ) fell. Energy should then have been delivered to the classroom, because of the difference in temperature between the cavity air and the interior. After establishment of equilibrium, the cavity air temperature and internal air temperature should then coincide. Monitored data showed that this was not so, and the fan had not operated. The graph also indicates that the Poulton Lancelyn heating system came on at around 3:00 a.m. and not at 7:00 a.m., which is the appropriate time to commence preheating.

This incident was clearly a regular occurrence. On Saturday, November 15, at 17:00 hours, the cavity air temperature was  $17.6^{\circ}\text{C}$ , the classroom air temperature  $14.1^{\circ}\text{C}$  (see Fig 3.12). Clearly, at this time, the fans should have delivered heat but did not. It was suspected that the solar wall cavity air temperature sensor (installed by the Wirral Borough Council contractors) was operating incorrectly. This sensor was responsible for starting the solar wall fan but was sited in one of the unmonitored solar walls to which access was not readily available. The contractors were contacted, but this fault remained unrectified during the period of monitoring. The too early start of the heating system was traced to an inappropriate use of the electronically controlled optimiser system. This will be referred to later.

As part of the monitoring system, continuous chart recordings, had been made of various temperatures at the classroom air inlet and at the top of the solar wall cavity. Fig 3.18 represents such a recording for Tuesday, January 14. It can be seen that as the heating system switches on (at the unreasonable hour of 2:30 a.m. and until it switches off at 16:00 hours) the temperature of the air at the

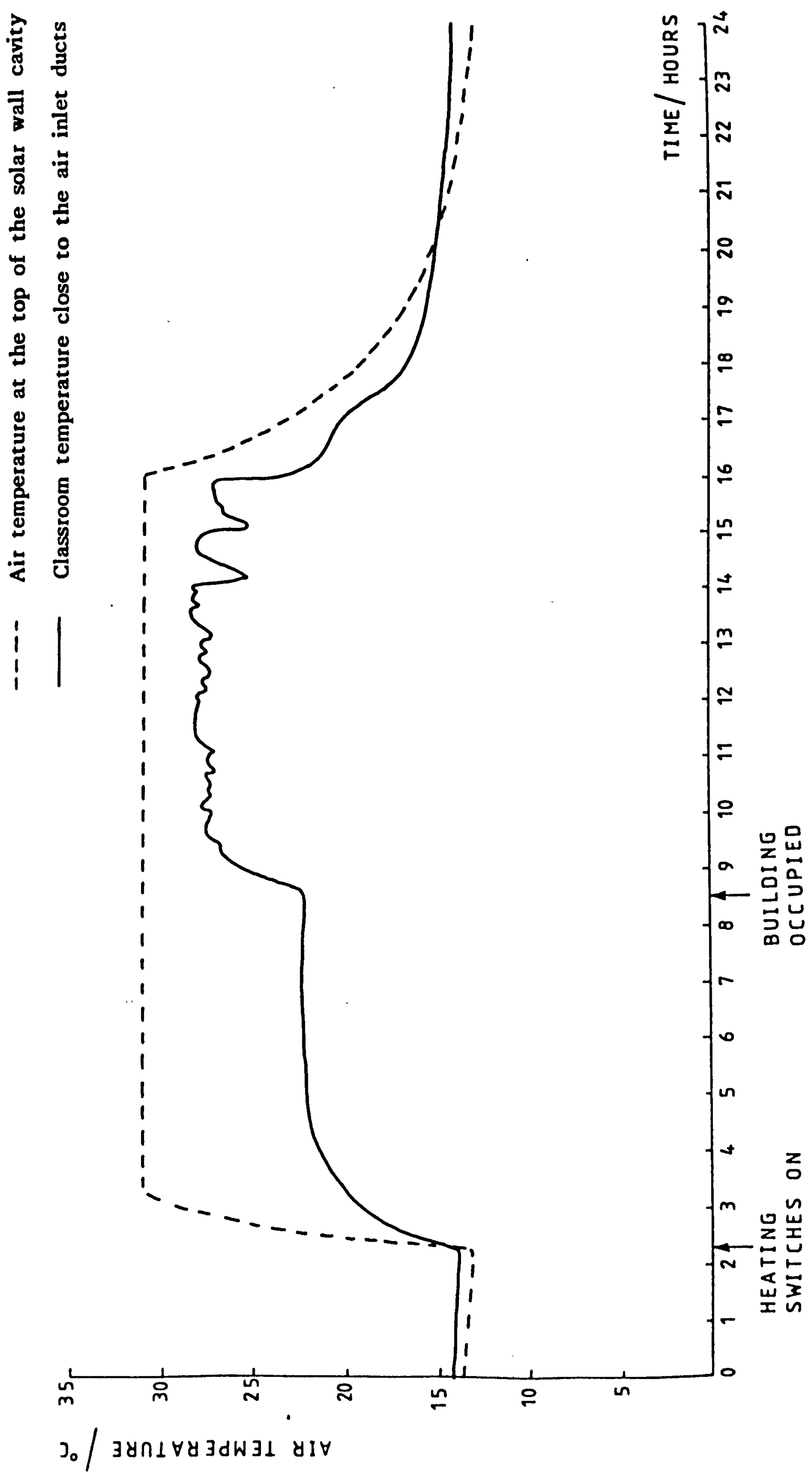


Fig. 3.18 Temperatures close to classroom air inlet duct and at the top of the solar wall cavity, Tuesday January 14 1986

cavity top rises to circa 32°C. The temperature of the classroom air close to the solar wall inlet duct rose from 22°C (unoccupied state) to 28°C (occupied condition). The high temperature at the top of the wall cavity implies that hot air from the gas fired heating system is leaking past the dampers, and heating the top portion of the solar wall rear cavity. This unnecessarily consumes energy. Fig 3.14 shows this happening on January 6, 1986 when the temperature of the cavity air starts to rise from circa 10°C at 2:00 a.m. to 14°C at 8:00 a.m. before any solar radiation had fallen on the wall at all.

Such observations imply that the connection of such a passive solar component, producing only small amounts of energy, to the main heating system of a building is an inappropriate and unwise procedure. It also shows that dampers are inefficient barriers to the passage of heat.

The performance of the Poulton Lancelyn solar walls is thus poorer than it should have been, due to a variety of factors that include:

- suspected inefficient sensing of cavity wall air and a not sufficiently precise operation of the solar wall fan
- ineffective optimiser operation leading to extraordinarily long pre-heat times
- use of a damper (an inefficient barrier to the reverse passage of heat through the solar wall from the gas fired air handling system)

In addition the solar wall temperature plots show that the cavity wall temperature simply does not get hot enough during the spring or winter to deliver very much

heat to the relatively warm, well insulated, classroom interior as it cools slowly at night.

Similar solar walls, with a 220 mm thick, brick front leaf, were constructed at Acorn Close in the Wirral by Merseyside Improved Housing Association and monitored by Pilkington Brothers PLC. These, double glazed Trombe walls are vented, and pass heat to internal rooms by thermocirculation and direct radiation from their internal wall surface. Each wall has 50 percent more exposed surface area than the Trombe walls at Poulton Lancelyn. Pilkingtons found that each Acorn Close solar wall contributed 19 percent to the annual energy requirements of a house, in comparison with the 5 percent solar wall contribution to each classroom at Poulton Lancelyn.

Comparison can be made with the hypothetical case where double glazing is installed at Poulton Lancelyn, excessive energy consumption due to premature preheating is reduced and the ratio of Trombe wall area to floor area of heated space is similar to that at Acorn Close. In this case it is estimated that the solar walls at Poulton Lancelyn would only contribute about 12 percent to a classroom's energy requirement. Direct use of solar energy as at Acorn Close rather than indirect as at Poulton Lancelyn (with its attendant greater heat loss during storage and duct transfer) is shown to be a more efficient way of using a low level heat source.

Even if slightly better performance of such Trombe wall systems is obtained, they are still not a practical, economic proposition. They are not cost effective. The



payback of such solar walls is of the order of 60 years. To increase their effectiveness and economic performance, their efficiency must also be increased.

This means, from a priori consideration:

- decreasing heat losses from the front surface of the solar wall
- decreasing heat lost by passage through the ducting
- increasing the amount of heat passing through the mass wall

The use of selective coatings, transparent insulation, no ducting, thinner walls and lower thermal capacity are some of the ways in which increased efficiency could be achieved.

In conclusion the poor performance of the Trombe walls at Poulton Lancelyn is attributed to:

1. Excessive energy consumption through the use of extraordinarily long preheat times
2. Incorrect setting of the cavity air temperature sensor, leading to insufficient operation of the solar wall fan
3. Poor thermal insulation at the front of the solar wall due to the use of single glazing only
4. The use of high thermal capacity brick at the rear of the wall instead of lower thermal capacity insulating material
5. A thickness of the single glazed mass solar wall, too great for the prevailing environmental conditions, so that the rear surface temperature of the wall never becomes too high.

### 3.8 ERRORS INVOLVED IN THE MEASUREMENT OF TEMPERATURE AND ENERGY PRODUCTION FROM A SOLAR WALL <sup>58</sup>

To measure the error involved in calculating energy production from solar walls, it is necessary to know the errors involved in measuring the temperatures (T) and flow rates (FL) of the air passing through it. These are the variables, which together with the volumetric specific heat of air, are used to calculate the energy produced from a solar wall via the formula:

$$E = V \cdot FL \cdot (T_C - T_{AI}) \quad (3.7)$$

Temperatures such as  $T_C$ , of the cavity and  $T_{AI}$  of the internal air, were measured using thermocouples, an ice reference point and a data logger.

The air speed (v) from the cavity was found using an Air Flow Developments AM 5000 digital anemometer. The flow rate (FL) in the cavity of the solar wall is a product of the measured air speed and the cavity cross section area ( $A_C$ ) given by:

$$FL = v \cdot A_C \quad (3.8)$$

The errors involved in such measurements and calculations are detailed below.

#### The error in air speed measurement

The accuracy of measuring air speed is given as +/- 5% by the manufacturers.

The fractional error in measuring an air speed of  $1 \text{ ms}^{-1}$ , inside the solar wall cavity is therefore:

$$\Delta v/v = .05/1 = .05 \quad (3.9)$$

The error in cavity cross section area measurement

The cavity cross section area is given by:  $A_C = L \cdot W$  where  $L$  is the length and  $W$  is the width of the cavity. Both can be measured to  $\pm .001$  m on architectural drawings.

This being so, the fractional error in the calculation of cross section area of the internal cavity is:

$$\begin{aligned} \Delta A_C / A_C &= \sqrt{((\Delta L / L)^2 + (\Delta W / W)^2)} & (3.10) \\ &= \sqrt{(.001/6.8)^2 + (.001/.05)^2} = .02 \end{aligned}$$

The error in the measurement of flow rate

The fractional error in flow rate measurement is:

$$\begin{aligned} \Delta FL / FL & & (3.11) \\ &= \sqrt{((\Delta v / v)^2 + (\Delta A_C / A_C)^2)} = \sqrt{(.05^2 + .02^2)} = \pm .054 \end{aligned}$$

The error in the measurement of the temperature differential of the inlet and outlet air from the cavity at the Poulton Lancelyn School

Millivolt outputs were recorded for each temperature using an ice point reference junction. The accuracy of this measurement on the data logger is given in the operating manual as:  $\pm (.005\% \text{ of reading} + 2 \text{ digits} + .001) \text{ mV}$ , for the 10 mV scale in use. The error is therefore circa  $\pm .011 \text{ mV}$ , for the range of temperatures measured. The output of a type T thermocouple is approximately .04 mV per °C. The error in temperature estimation is thus about  $\pm 0.28 \text{ }^\circ\text{C}$ .

The compounded error in the temperature differential between two such readings is greater, and estimated as  $\pm 0.4^\circ\text{C}$ :

$$\begin{aligned}\Delta(T_C - T_{AI}) &= \pm \sqrt{(T_C^2 + T_{AI}^2)} & (3.12) \\ &= \pm \sqrt{(0.28^2 + 0.28^2)} = \pm 0.4^\circ\text{C}\end{aligned}$$

The error in the calculation of the energy produced from the Poulton Lancelyn solar wall

The fractional error in the amounts of the energy produced from a solar wall may be calculated from equation 3.7 as:

$$\Delta E/E = \pm \sqrt{((\Delta FL/FL)^2 + (\Delta(T_C - T_{AI})/(T_C - T_{AI}))^2)} \quad (3.13)$$

giving (when there exists a differential temperature of only  $1^\circ\text{C}$ ):

$$\Delta E/E = \pm \sqrt{(0.054^2 + 0.4^2/1)} = \pm 0.4$$

This large error of  $\pm 40$  per cent is attributed to the error involved in the measurement of temperature differentials.

The error in the measurements of temperature differentials produced by model solar walls at Clarence Street

The necessity of installing single thermocouples in the Poulton solar wall during its construction was referred to previously. This was not the case for the model solar walls. There, thermopiles consisting of six thermocouples in series, were used to measure cavity air inlet and outlet temperatures. This meant that the measured output of the temperature sensors (in millivolts) is increased six times.

The accuracy of temperature differential measurement was accordingly much improved from an estimated  $\pm 0.28^\circ\text{C}$  at Poulton Lancelyn to a lower value of approximately  $\pm 0.05^\circ\text{C}$  at Clarence Street.



**CHAPTER FOUR - DEVELOPMENT  
OF A USER FRIENDLY COMPUTER  
PROGRAM FOR THE ASSESSMENT  
OF THE PERFORMANCE OF THE  
POULTON LANCELYN SOLAR WALL**

## 4.1 MODULAR PROGRAMS

The appropriate computational tool selected for use in a passive solar design will depend on the amount of information asked for in the initial brief. This could range from just the calculation of the annual energy consumption up to a demand for a simulation of the daily dynamic performance and energy balances of the building system. When a detailed simulation is required, every energy flow must be described by an appropriate differential or algebraic equation expressing its dynamic or steady state balance. The instructions of the system, with time dependent climatic conditions and auxiliary heat demand must be included too. The complexity of such a mathematical model necessitates the use of numerical methods to solve the resultant set of equations developed with their associated time varying input functions. Multi-dimensional models can be written (a 3 dimensional representation being developed in this work). When a computer program is written, the physical models used represent a compromise between the desire for technical simplification and satisfaction with the accuracy of the predictions produced. The computer model written for this work, for example, uses standard values of heat transfer coefficients and achieves an average error on the predictions of temperatures produced in the solar wall of just +1.4%, which is deemed highly satisfactory.

Such computer simulation programs for the design of solar systems can be purchased, and are often modular to make them universally applicable. Each modular program includes a variety of different components which can be joined together: data readers, data interpolation, radiation processors, integrators, weather data generators, multi-zone building, thermal storage, heat exchangers, hydronics controllers. Such programs enable the user to develop new system concepts and offer full flexibility to simulate a large variety of different solar

system types. Because the modules use the same simulation methodology and mathematical algorithms, the whole process of comparison of results between different systems tends to be more meaningful than the use of different programs from different sources. The main snag with modular programs lies with the demands on the user. They are not in the least "user friendly". They need expertise for their operation, and are quite unsuitable for the general practitioner. They are, in fact, research and development tools, and are often used as standard references when developing other simpler and much easier to use, simulation models.

Three such, well known, modular simulation programs are:

1. TRNSYS (a transient system simulation program developed at the Solar Energy Laboratory, University of Wisconsin) <sup>59</sup>.
2. SERI-RES (developed at the Solar Energy Research Institute, Colorado) <sup>60</sup>.
3. ESP (developed at Strathclyde University, Glasgow) <sup>61</sup>.

Of these the most widely used by American and European research workers in the solar energy field is TRNSYS. It is known to be accurate, and runs on IBM-PC compatible microcomputers, unlike ESP, which to date requires an expensive and dedicated computer of its own. In addition a module has been written to simulate the performance of collector-storage walls and of walls fronted by transparent insulation material.

## 4.2 SYSTEM SPECIFIC SIMULATION PROGRAMS

For general use, it is better to use a computer program specially written to model a specific type of solar system. Such a model can be termed: "A system specific simulation program".

This model will be completely fixed by the solar programmer who will be responsible for the physical simplifications introduced, and to the degree of detail with which the system is represented. The program will be written so that the solar system component sizes and properties which constitute the set of user defined input parameters can easily be varied. This "second level" type of computer program is often used to optimize the performance of systems, and to yield detailed energy balances on a daily or monthly basis. In comparison with modular programs, system specific programs have significantly reduced computation times, and are much easier to use. The user no longer has to build up a detailed system representation from elementary system components. This task will already have been performed by the simulation model designers, and no expertise in system modelling will be required of the user of such a specific model at all. This will be in complete contrast to the problems that beset an aspiring user of TRNSYS, SERI-RES or ESP, for these programs are quite difficult to use, requiring mental agility and experience to select and incorporate the elementary component models from a module library into a running program.

The mode of operation of the Poulton Lancelyn unvented thermal storage wall is different from that of an unvented wall which could be simulated by TRNSYS in that the use of the conducted heat through the wall is delayed until required by the attached insulation damper and ducting system. It was decided in view of the above discussion that there would be considerable advantages in writing a dedicated system specific program to simulate its performance, in view of both the more accurate modelling possible, and the simplicity of its operation when used to optimise performance. Accordingly, a finite difference computer simulation program was developed as a specific tool to simulate the performance of matt black painted, of selectively coated, and later, of TIM faced unvented collector-storage walls.



The use of the resultant system specific simulation program enabled a whole variety of different parameters (emissivities, absorptivities, wall thicknesses, TIM thicknesses, glazing types, air flow rates) to be varied with ease, using hourly solar radiation and external temperature values for any climate for which appropriate meteorological data was available, from a variety of different locations, as dynamically varying input values. The simplicity of the program's operation allowed over 1000 runs to be processed relatively quickly. If TRNSYS et al had been used, computation times would have increased by a factor of 5 to 10 and therefore be dauntingly long. Experience with the system specific simulation program written to model the Poulton Lancelyn solar wall, described later, confirmed the consensus that such programs are the computational tools best fitted to the needs of daily practice in solar system design.

### 4.3 DYNAMIC THERMAL MODELLING OF THE POULTON LANCELYN SOLAR WALL

#### Theory

A program was written to model the performance of the Poulton Lancelyn solar wall in three dimensions, initially for use on a mainframe computer, then later modified to run on any IBM compatible PC. This model provided the basis for subsequent amendments to simulate the performance of solar walls incorporating selective coatings or transparent insulation.

The three dimensional differential equation governing the flow of heat conduction in such a system is:

$$k \left( \frac{\delta^2 T}{\delta x^2} + \frac{\delta^2 T}{\delta y^2} + \frac{\delta^2 T}{\delta z^2} \right) + q = \rho c \frac{\delta T}{\delta t} \quad (\text{W/m}^3) \quad (4.1)$$

where:

$x, y, z$	=	space coordinates (m)
$t$	=	time (s)
$T$	=	temperature ( $^{\circ}\text{C}$ )
$k$	=	thermal conductivity (W/mk)
$\rho$	=	density of solid ( $\text{kg/m}^3$ )
$c$	=	specific heat of solid (J/kgK)
$q$	=	rate of heat generation per unit volume ( $\text{W/m}^3$ )

This equation can be cast in a finite difference form suitable for the evaluation of temperatures at nodal points. A set of such equations for an array of nodal points in a solar wall will approximate to the exact solution of the original partial differential equations governing the overall heat flow. Different forms of these equations for the evaluation of temperature at space coordinate  $x$ , time  $t$  and time step  $\Delta t$ , for one dimensional heat conduction are:

$$1. \quad T(x, t + \Delta t) = T(x, t) + R(T(x + \Delta x, t) - 2.T(x, t) + T(x - \Delta x, t)) \quad (4.2)$$

where  $R = \alpha \Delta t / \Delta x^2$  and  $\alpha = k / \rho c$ , the thermal diffusivity.

Equation (4.2) relating temperature at the next time ( $t + \Delta t$ ) to the present temperature, is known as the Euler or explicit finite difference equation.

$$2. \quad T(x, t + \Delta t) = T(x, t) + R(T(x + \Delta x, t + \Delta t) - 2.T(x, t + \Delta t) + T(x - \Delta x, t + \Delta t)) \quad (4.3)$$

Equation (4.3) evaluating temperatures at the next time step ( $t + \Delta t$ ) from future temperatures at time ( $t + \Delta t$ ), is known as the implicit finite difference equation.

$$3. \quad T(x, t + \Delta t) = T(x, t) + R/2.(T(x + \Delta x, t + \Delta t) - 2.T(x, t + \Delta t) + T(x - \Delta x, t + \Delta t) + T(x + \Delta x, t) - 2.T(x, t) + T(x - \Delta x, t)) \quad (4.4)$$

Equation (4.4), the Crank-Nicolson equation is essentially an average of the previously cited finite difference equations.

$$4. \quad T(x,t + \Delta t) = T(x,t)\exp(-R,M(x,t)) \quad (4.5)$$

$$\text{where } M(x,t) = (2.T(x,t) - T(x + \Delta x,t) - T(x, t + \Delta t))/T(x,t) \quad (4.6)$$

The relative accuracy and stability of these methods for predicting temperature distributions and hence energy yields through and from a solar wall can be conveniently studied by converting all the different equations into a common form showing the future temperature of a single node in terms of its present temperature:

$$T(x,t + \Delta t) = \Lambda T(x,t) \quad (4.7)$$

where  $\Lambda$  has the following values:

Euler explicit equation:  $\Lambda = 1 - 2.R$

Pure implicit equation:  $\Lambda = 1 / (1 + 2.R)$

Crank-Nicolson equation:  $\Lambda = (1 - R) / (1 + R)$

Bhattacharya equation:  $\Lambda = \exp(-2.R)$

Values of  $\Lambda$  are shown in *Table 4.1* and **Fig 4.1** for various values of  $R$ .

Myers<sup>62</sup> has given the exact solution for the single node heat transfer model, and it proves to be identical to the exponential difference equation of Bhattacharya<sup>63</sup>.

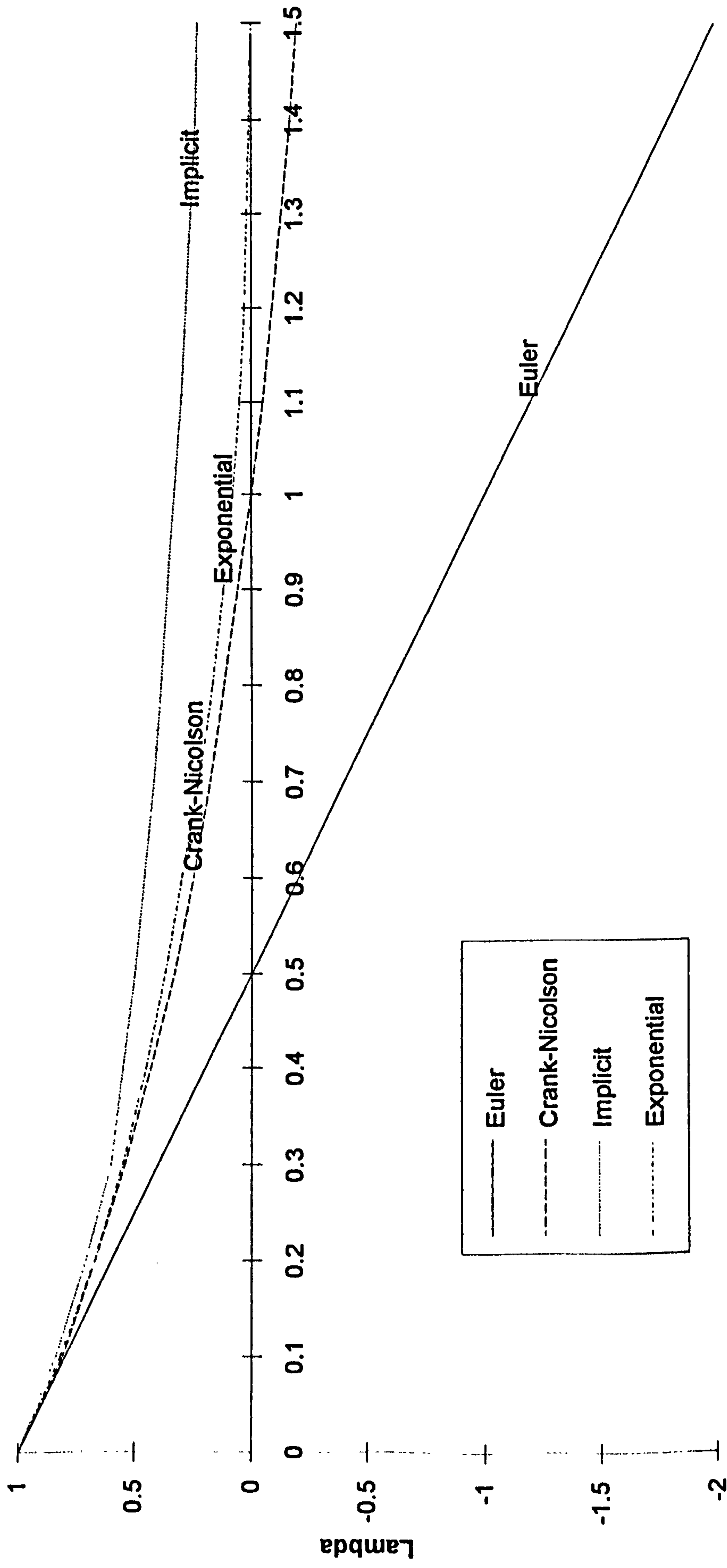
Bhattacharya states that his equation will predict results with an accuracy comparable with or better than that obtainable by other methods when applied to multi nodal models simulating heat transfer processes. *Table 4.1* and **Fig 4.1** show that the four methods produce identical results with very small time steps. Between  $R = 0.5$  and  $R = 1.0$  both the exponential and the Crank-Nicolson method give almost exact values for temperature. The Euler (explicit) method, although initially more accurate than the implicit method, becomes increasingly inaccurate above  $R = 0.2$ .

**Table 4.1 Values of  $\Lambda$  for different values of R and for different finite difference equations**

<b>R</b>	<b>EULER</b>	<b>CRANK</b>	<b>IMPLICIT</b>	<b>EXPONENTIAL</b>
<b>.01</b>	<b>.98</b>	<b>.98</b>	<b>.98</b>	<b>.98</b>
<b>.05</b>	<b>.90</b>	<b>.90</b>	<b>.91</b>	<b>.90</b>
<b>.1</b>	<b>.80</b>	<b>.81</b>	<b>.84</b>	<b>.82</b>
<b>.2</b>	<b>.60</b>	<b>.67</b>	<b>.71</b>	<b>.67</b>
<b>.3</b>	<b>.40</b>	<b>.54</b>	<b>.60</b>	<b>.55</b>
<b>.4</b>	<b>.20</b>	<b>.43</b>	<b>.56</b>	<b>.45</b>
<b>.5</b>	<b>0.0</b>	<b>.33</b>	<b>.50</b>	<b>.37</b>



Fig.4.1 Lambda versus R for various finite different equations



R

Above that value the implicit method is more accurate than the explicit. The implicit method is generally less accurate than the Crank-Nicolson but always steady. Explicit solutions oscillate above  $R = 0.5$ , the Crank-Nicolson above  $R = 1.0$ , when they should not be used.

Which of these methods is the most suitable for building heat transfer simulation? A typical value for the diffusivity ( $\alpha$ ) of a building material for use in the application of finite difference equations to building heat transfer problems would be  $10^{-6} \text{ m}^2/\text{s}$ .

Internodal distances ( $\Delta x$ ) between the nodes at which temperatures are to be determined in a building structure would be of the order of: 50 mm, 75 mm or 100 mm, and if the time increment used ( $\Delta t$ ) between each evaluation was 1 hour, then  $R$  would become 1.4, 0.64 and 0.36 respectively. The use of the explicit form is thus excluded when hourly time intervals are used (for oscillations in successive temperature estimations would then be produced). The use of hourly time intervals is generally the norm in building heat transfer simulation, this being the minimum interval at which meteorological data is generally available. It seems that three of the cited methods: the implicit, the Crank-Nicolson, the Bhattacharya, can all be used to solve the partial differential heat conduction equations associated with building heat transfer. An investigation of the errors produced in the evaluation of temperature distributions in, and the energy production from, solar walls using these methods will be reported later.

In the simulations reported here, the pure implicit formulation was used, since the solutions are always steady, allowing even small internodal distances to be used in the simulation equations.

## The finite difference approximation and use of a nodal network for one dimensional heat flow in a solid

The equation governing the transient flow of heat in a solid is represented by equation (4.1). A simple way of using this equation has been referred to: its replacement by a finite difference equation which need only be satisfied at certain nodal points within the solid.

Let Fig 4.2 represent a slice through a solid, with nodal points at a, b and c, each a distance  $\delta x$  apart. Let the current temperatures of a, b and c, be:  $T(x,t)$ ,  $T(x-\delta x, t)$  and  $T(x+\delta x, t)$  respectively. The future temperature of node a will be represented by:  $T(x, t+\delta t)$ . The corresponding resistance network for one dimensional heat flow is then depicted in Fig 4.3.

The one dimensional heat conduction equation is:

$$k \frac{\delta^2 T}{\delta x^2} + q = \rho c \frac{\delta T}{\delta t} \quad (4.8)$$

Expanding:

$$\frac{k}{\delta x^2} [T(x-\delta x, t) - T(x, t) - T(x, t) + T(x+\delta x, t)] + q = \rho c \frac{[T(x, t+\delta t) - T(x, t)]}{\delta t} \quad (4.9)$$

Or representing:

$T^1_a = T(x, t+\delta t)$  = future temperature at node a

$T_a = T(x, t)$  = present temperature at node a

$T_b = T(x-\delta x, t)$  = present temperature at node b

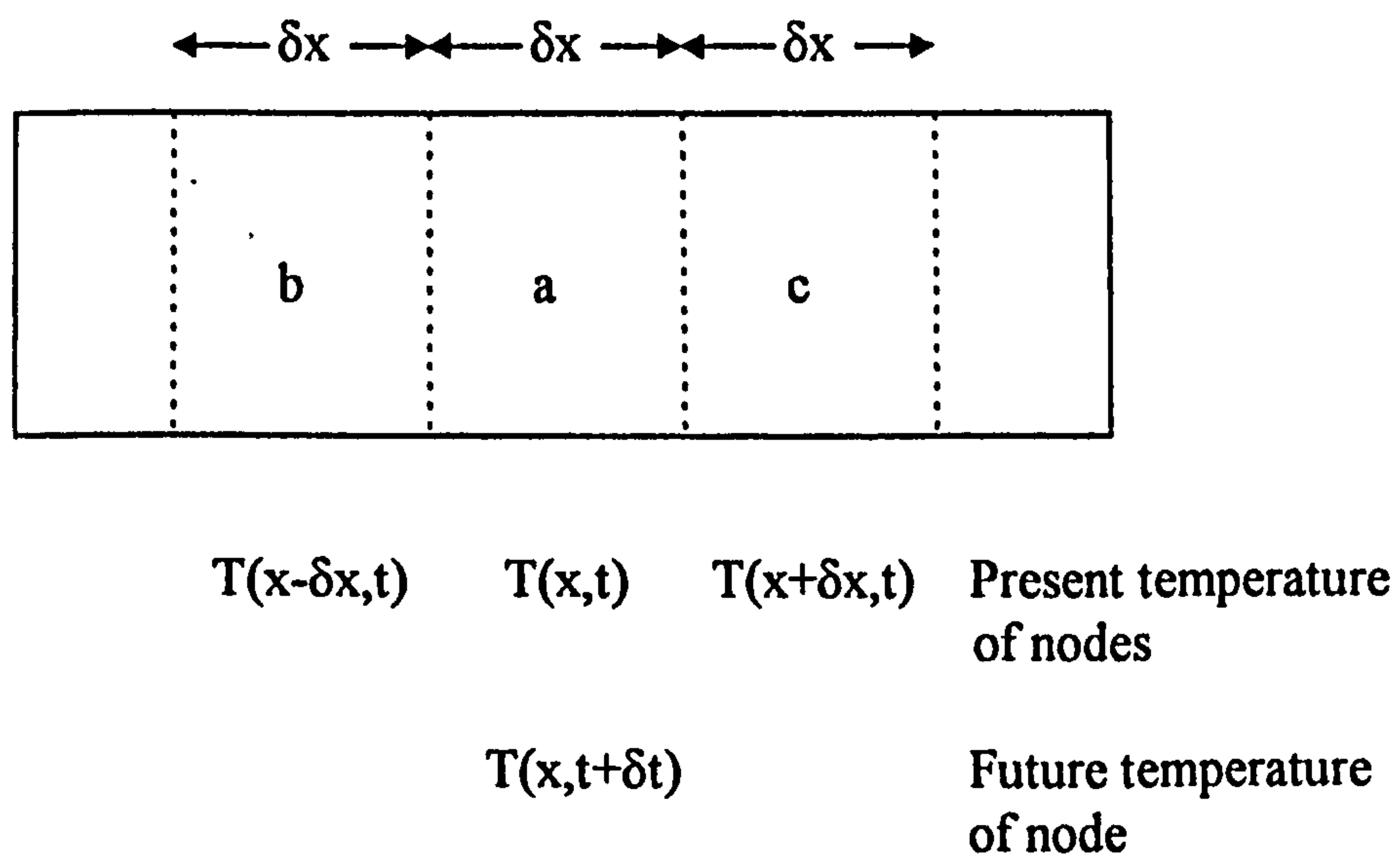


**Fig. 4.2 Nodes in one dimensional heat flow**

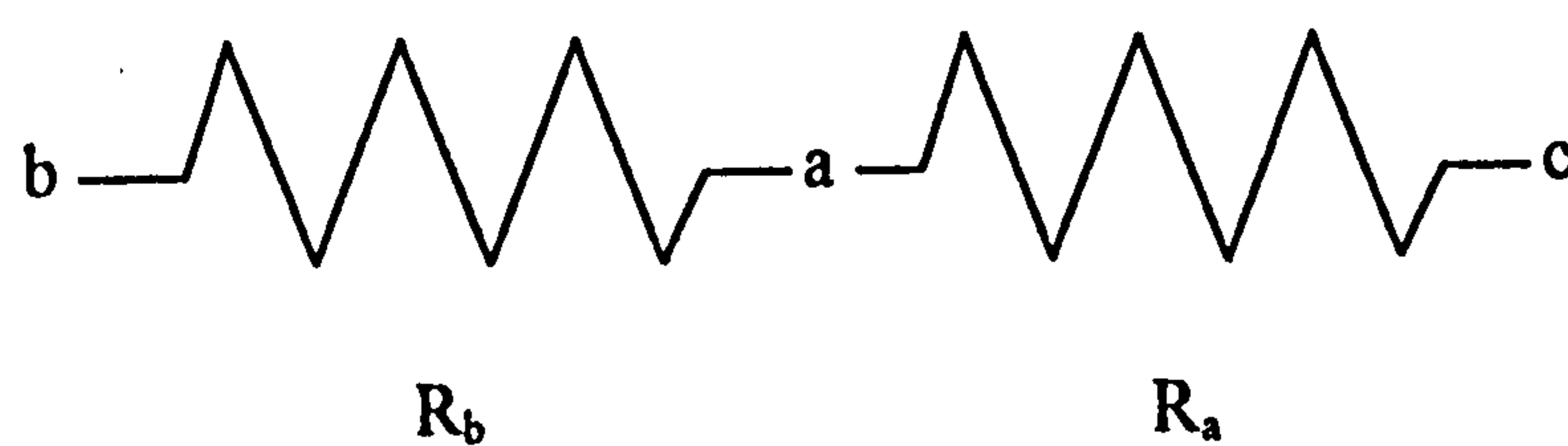


**Fig. 4.3 Nodal thermal resistance network**



$T_c = T(x + \delta x, t) =$  present temperature at node c

then it follows that:

$$\frac{k}{\delta x^2} [T_b - 2T_a + T_c] + q = \frac{\rho c}{\delta t} (T_a^1 - T_a) \quad (4.10)$$

Thermal resistance is defined as  $l/k$  where  $l$  is the distance traversed by the heat flow.

Thus, in this instance the thermal resistance between nodes b and a:  $R_b = \delta x/k$ . Similarly

$R_a = \delta x/k$  and:

$$\frac{T_b - T_a}{R_b \delta x} + \frac{T_c - T_a}{R_a \delta x} + q = \frac{\rho c}{\delta t} (T_a^1 - T_a) \quad (\text{W/m}^3) \quad (4.11)$$

$$\frac{T_b - T_a}{R_b} + \frac{T_c - T_a}{R_a} + q \delta x = \frac{\rho c \delta x}{\delta t} (T_a^1 - T_a) \quad (4.12)$$

$$\frac{T_b - T_a}{R_b/A} + \frac{T_c - T_a}{R_a/A} + q A \delta x = \frac{\rho c A \delta x}{\delta t} (T_a^1 - T_a) \quad (\text{W}) \quad (4.13)$$

where  $A$  represents the cross section area ( $\text{m}^2$ ) of the solid through which heat is flowing, and,  $A \delta x$  is the volume of solid (in  $\text{m}^3$ ) between nodes.

Thus  $C = \rho c A \delta x$  is the thermal capacity of a node (since  $\delta x$  is also the distance between the divisions between nodes) and  $Q = q A \delta x$  (W) is the actual energy that may be generated at a node.

Thus:

$$\frac{(T_b - T_a)}{R_b/A} + \frac{(T_c - T_a)}{R_a/A} + Q = \frac{C}{\delta t} (T_a^1 - T_a) \quad (\text{W}) \quad (4.14)$$

Equation (4.14) represents the heat balance about node a, it permits the use of unequal node spacings, it can be extended to three dimensional heat flow. The left hand side

denotes energy flowing into node a, the right hand side the heat stored in the material surrounding the node.

If solar irradiance :  $G, (W/m^2)$  is incident upon node a, for a time interval  $\Delta t$  seconds, then  $Q = GA$  and the heat balance becomes:

$$\frac{(T_b - T_a)}{R_b/A} + \frac{(T_c - T_a)}{R_c/A} + GA = \frac{C}{\Delta t} (T_a^1 - T_a) \quad (W) \quad (4.15)$$

As written, these equations evaluate the future temperature of nodal point a;  $(T_a^1)$  after time interval  $\Delta t$ , in terms of the present temperatures of nodal points a, b, c:  $(T_a, T_b, T_c)$  and represent therefore the explicit formulation in which forward finite difference equations have been used to produce the equation. In similar fashion the future temperature of node a:  $(T_a^1)$  can be found using the future temperatures of nodes b and c:  $(T_b^1, T_c^1)$  in conjunction with the present temperature of node a:  $(T_a)$  from the equation:

$$\frac{(T_b^1 - T_a^1)}{R_b/A} + \frac{(T_c^1 - T_a^1)}{R_c/A} + Q = \frac{C}{\Delta t} (T_a^1 - T_a) \quad (4.16)$$

This is the implicit formulation, which as previously stated, is more suitable for use in simulating building heat transfer problems using large time steps. This method was therefore applied to a three dimensional nodal network, to model the heat transfer through the south facing thermal storage wall at Poulton Lancelyn. To gain experience in writing such a large program a small 7 node one dimensional model was written first (in FORTRAN). This was later extended to three dimensions using 175 nodal points, arranged throughout the wall (see *Appendix 3.1*). Originally written to run on a DEC mainframe computer, the program was rewritten for use on IBM-PC compatible microcomputers using just 45 nodal points (see *Appendix 3.8*). The set of heat balance

equations, evolved for steady state heat transfer between the nodal points during each time period, was solved using Gauss-Siedel iteration.

#### 4.4 DEVELOPMENT OF THE COMPUTER MODEL

##### Introduction

The wall was conceptually divided up into sections by a series of nodal points arranged in three dimensions throughout the wall. Initially 7 nodes (labelled I) were introduced along the length of the wall defined as the X direction, 9 nodes (labelled J) were placed across the width of the wall (the Y direction) and 7 nodes (labelled K) were inserted upon the height of the wall (the Z direction). Figs 4.4, 4.5 and 4.6 show the way in which these nodal points are distributed through the wall, each being linked by a thermal resistance and each internal node being associated with a thermal capacity. Nodes at the front surface of the mass wall receive energy input from transmitted solar radiation, nodes in the centre of the internal cavity lose energy by the flow of ventilating air. Fig 4.7 shows the general environment of an internal node and the arrangement of thermal resistances  $X(I,J,K)$  etc which arrive at and emerge from the central node (I,J,K). It also indicates the capacitance  $C(I,J,K)$  of the node and the energy input  $Q(I,J,K)$  at the node itself. The symbols used to designate thermal resistance and thermal capacity, plus the formulae for their calculation are also shown in *Table 4.2*.

When an interface between two materials or between a solid material and air, occurs, then the internodal thermal or solid resistance is the sum of the resistance of the materials involved. When the internodal line runs along an interface the thermal

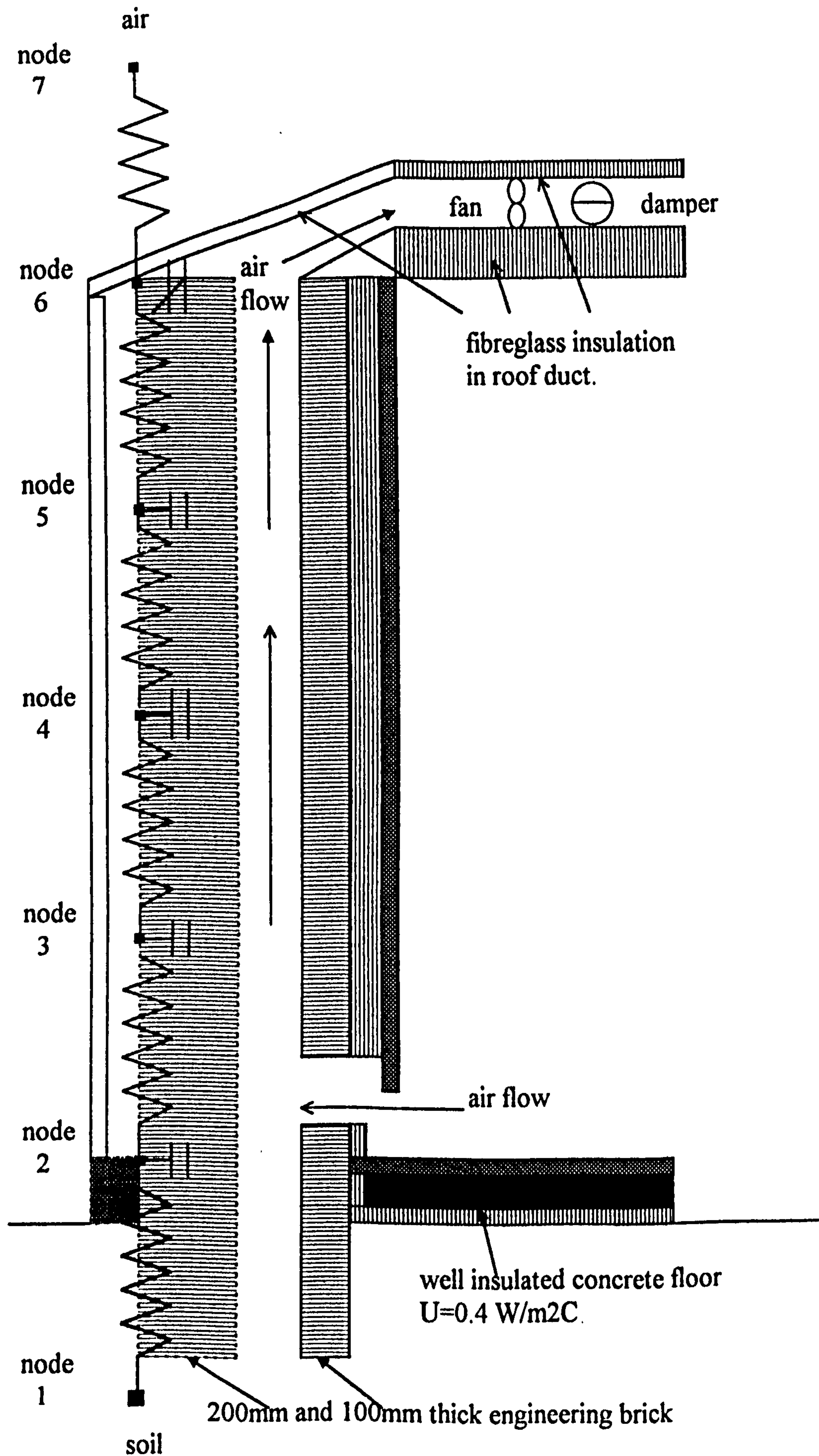


Fig. 4.4 K nodal points in the Z direction along a vertical face of the solar wall. The value of K is given alongside each node.



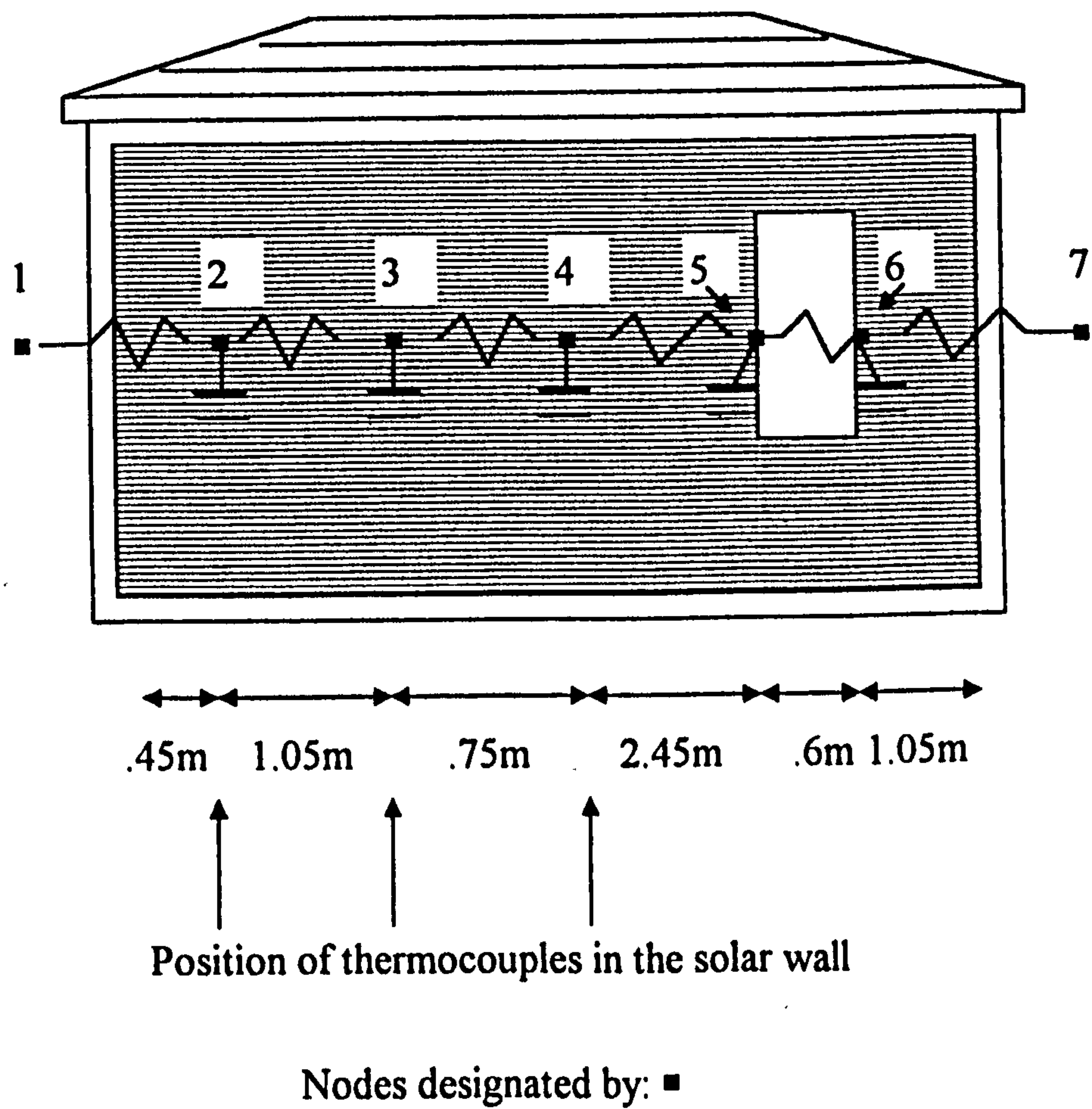
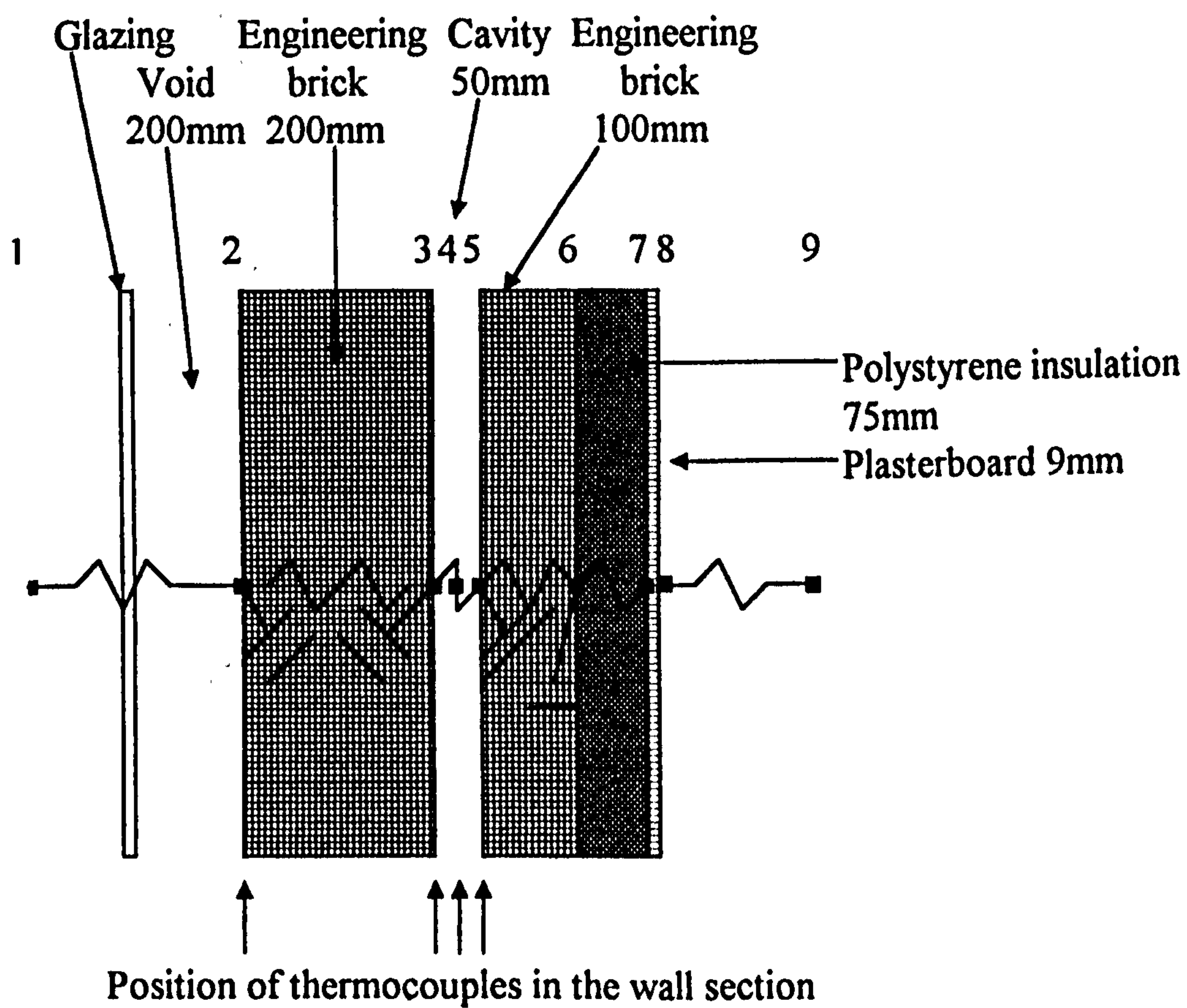
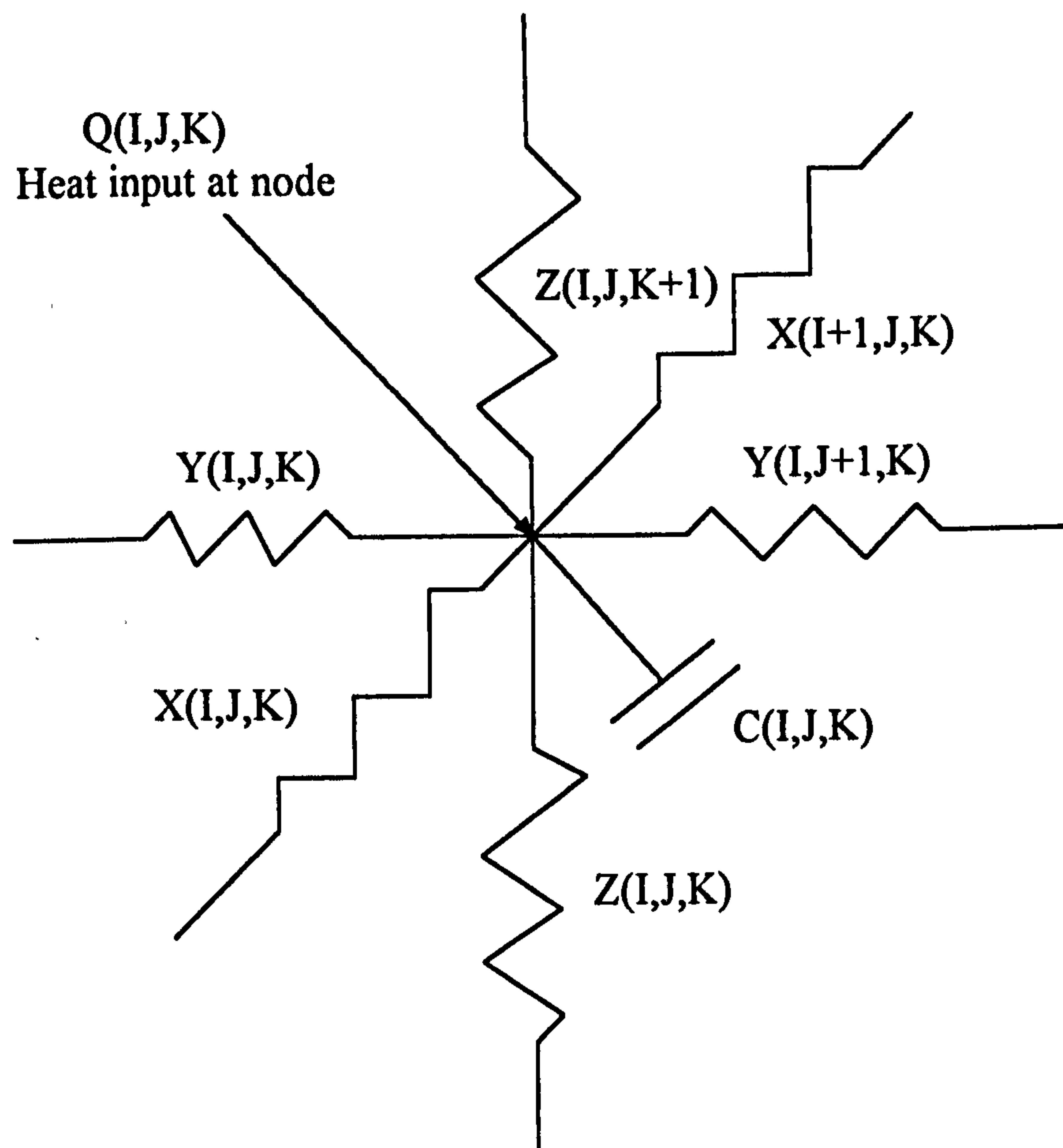


Fig. 4.5 I nodal points in the X direction along the south facing solar wall, at  $J=2$  and  $K=4$ . The value of I is given above each node.



Nodes designated by: ■

Fig. 4.6 J nodal points in the Y direction through a section of the storage wall.  
The value of J is given above each node.



$X(I,J,K)$ ,  $Y(I,J,K)$ ,  $Z(I,J,K)$  denote inter nodal thermal resistances.  
 $C(I,J,K)$  denotes nodal thermal capacity.  
 $Q(I,J,K)$  is the energy generation term.

**Fig.4.7 The nodal environment of an I,J,K node in the X,Y,Z directions**

**Table 4.2 Designation of the thermal capacity and thermal resistances between nodes and nodal points in the finite difference computer program**

Nodal and internodal designation	Thermal resistance	Thermal capacity	Method of calculation
I,J,K		C(I,J,K)	$\rho cV$
between I-1,J,K and I,J,K	X(I,J,K)		L(X)/K(X)
between I,J-1,K and I,J,K	Y(I,J,K)		L(Y)/K(Y)
between I,J,K-1 and I,J,K	Z(I,J,K)		L(Z)/K(Z)
between I,J,K and I+1,J,K	X(I+1,J,K)		L(X)/K(X)
between I,J,K and I,J+1,K	Y(I,J+1,K)		L(Y)/K(Y)
between I,J,K and I,J,K+1	Z(I,J,K+1)		L(Z)/K(Z)

$\rho$  = density of nodal material ( $\text{kg/m}^3$ )

$c$  = specific heat of nodal material ( $\text{J/kgK}$ )

$V$  = volume of material associated with node ( $\text{m}^3$ )

L(X),L(Y),L(Z) = distances between nodes in a specified direction (m)

K(X),K(Y),K(Z) = the thermal conductivity of internodal material in a specified direction ( $\text{W/mK}$ )



resistance used is the average of the thermal resistances on either side. When a node occurs at an interface between materials the thermal capacity is the sum of that of the materials on either side. The thermal capacity of air, being small, is ignored. **Fig 4.8** shows how the volume of material associated with a node (I,J,K), used in computing thermal capacity, is obtained. **Fig. 4.9** shows in similar fashion, how the area associated with a node, used in calculating heat flow into the node, is obtained.

Application of such principles, enabled numerical values to be allocated to all the 288 resistances and 175 capacities required by the initial model. Chapman<sup>64</sup> was consulted when dealing with problems which arose in assigning such values. Thermal conductivity data, air and cavity resistances etc were obtained, from manufacturers data or the CIBS Guide<sup>26</sup>.

### **Energy generation at nodes**

Solar irradiance falls upon the solar wall front surface after transmission through glazing and is absorbed. There is a resulting heat input at nodal points  $J=2$ , the heat inputs produced are designated:  $Q(I,2,K)$ . Heat conducted through the mass wall is subsequently removed by forced convection in the wall cavity. Heat, in this solar wall design is extracted from the internal cavity at nodal points designated  $J=4$ , the amount extracted is represented by  $Q(I,4,K)$ . The formulae used for the calculation of these quantities are shown in *Table 4.3*.

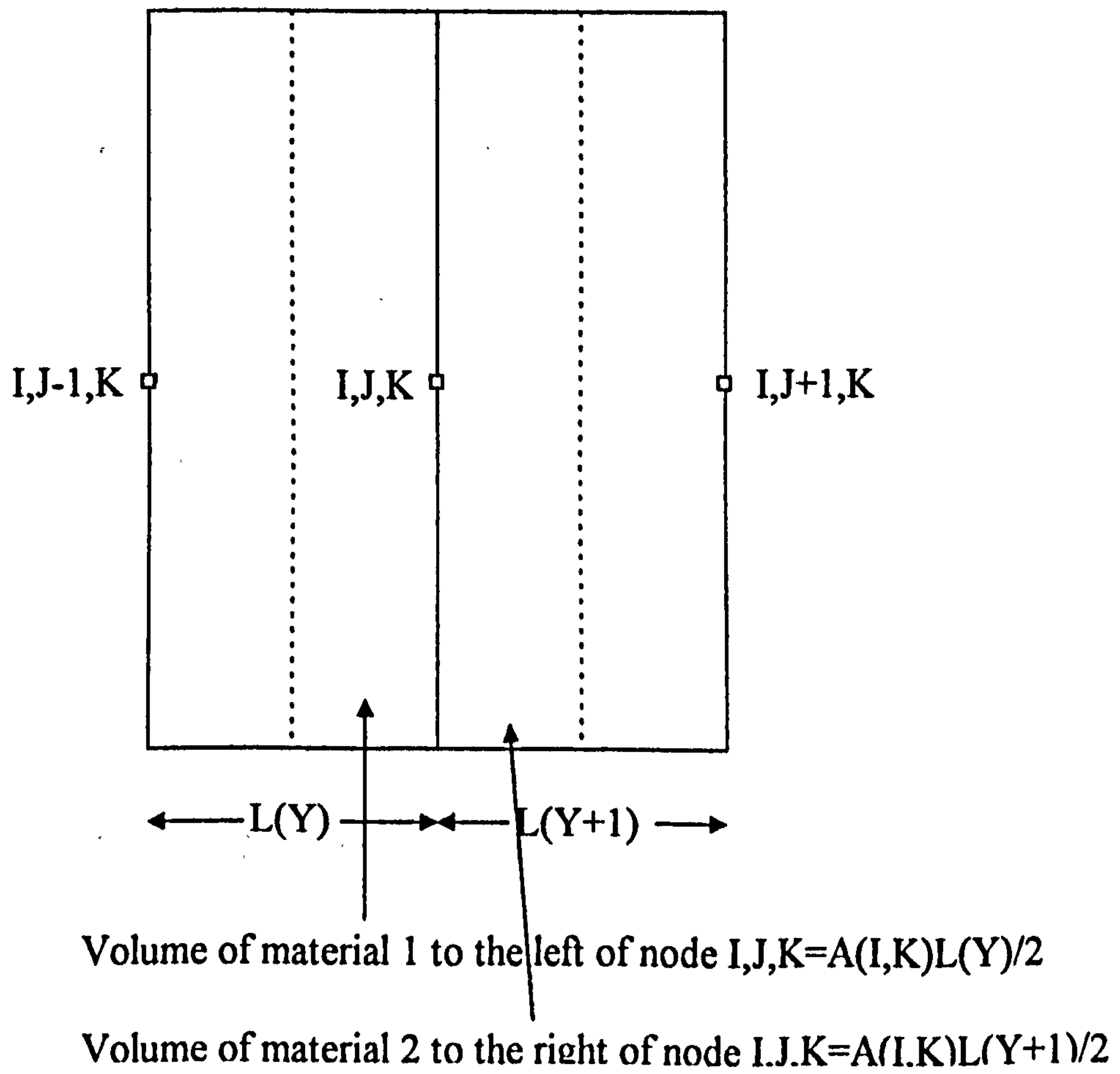
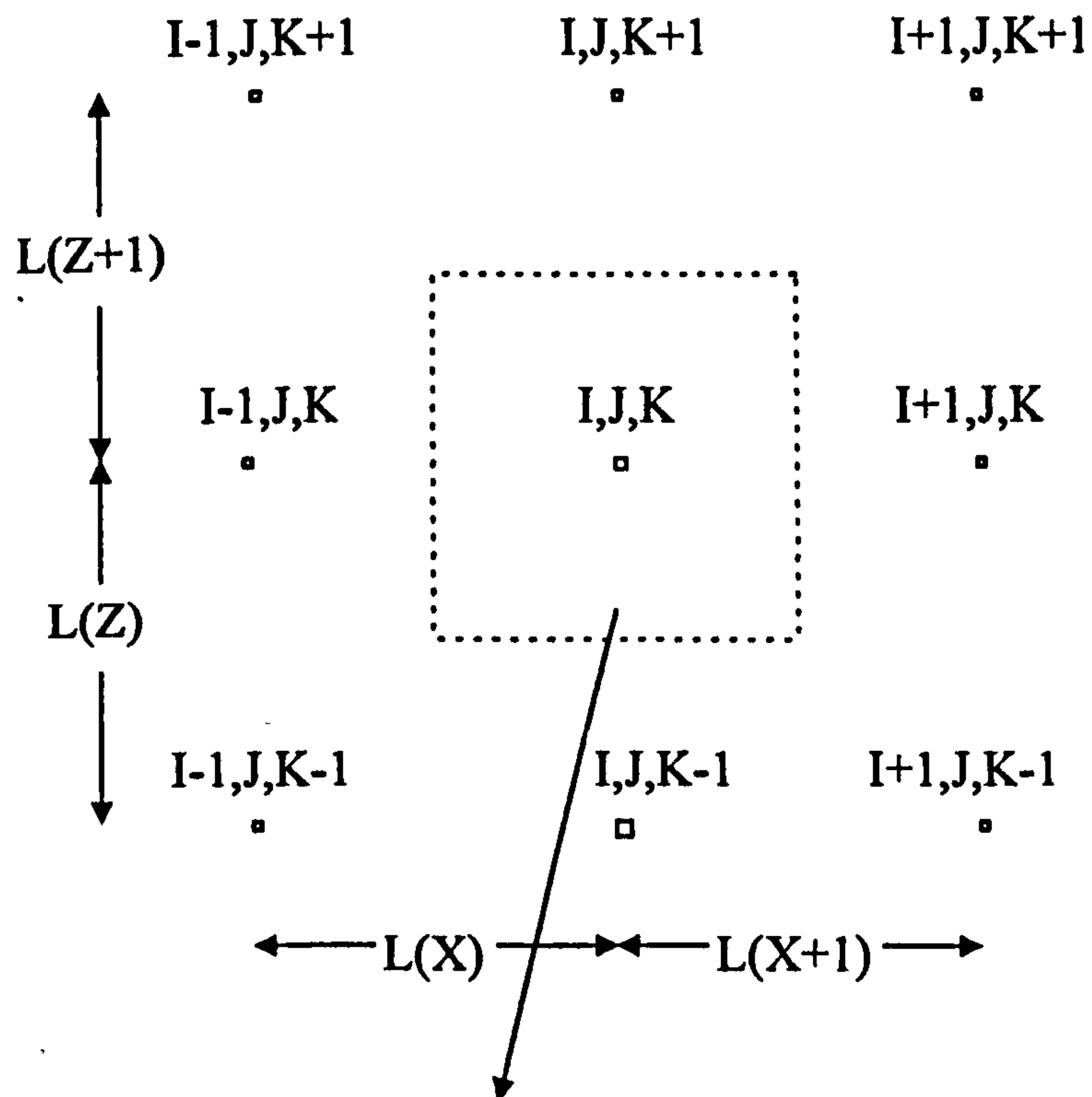


**Fig. 4.8** The volume of material associated with node  $I,J,K$ .



Area associated with node  $I,J,K$  along an XZ surface:

$$A(I,K) = \frac{(L(X) + L(X+1)) \cdot (L(Z) + L(Z+1))}{2}$$

**Fig.4.9** The area associated with node  $I,J,K$  used in the calculation of heat flows.

Table 4.3 - Formulae for the computation of energy flows

Node	Function	Energy symbol	Computational formulae
I,2,K	solar input	$Q(I,J,K)$	$\alpha \cdot TR(M,H) \cdot G(M,D,H) \cdot A(I,K) \cdot 0.95$
I,4,K	heat removal by cavity air, except K=2	$-Q(I,4,K)$	$1200 \cdot AF \cdot A \cdot (F(I,4,K) - F(I,4,K-1))$
I,4,2	heat removal at inlet node 2	$-Q(I,4,2)$	$1200 \cdot AF \cdot A \cdot (F(I,4,2) - T_I(D,H+1))$
$TR(M,H)$	=	glazing transmittance (month M, hour H).	
$\alpha$	=	absorptance of wall surface to solar radiation.	
$G(M,D,H)$	=	average hourly solar irradiance on wall surface (month: M, day: D, hour: H). ( $W/m^2$ ).	
0.95	=	reduction factor applied to solar radiation accounting for glazing bars.	
1200	=	volumetric specific heat of air ( $J/m^3K$ ).	
AF	=	air flow rate in cavity (m/s).	
A	=	cross section area of cavity (in the XY direction) ( $m^2$ ).	
$F(I,4,K)$	=	future temperature of node I,4,K ( $^{\circ}C$ ).	
$T(I,4,K)$	=	present temperature of node I,4,K ( $^{\circ}C$ ).	
$T_I(D,H+1)$	=	future temperature of internal room air ( $^{\circ}C$ ).	
$A(J,K)$	=	area of surface around an I node through which heat transfer occurs ( $m^2$ )	
$A(I,K)$	=	area of surface around a J node through which heat transfer occurs ( $m^2$ )	
$A(I,J)$	=	area of surface around a K node through which heat transfer occurs ( $m^2$ )	



The energy balance at a node I,J,K may then be written:

$$\frac{C(I,J,K).(F(I,J,K) - T(I,J,K))}{TM} =$$

$$A(I,K) \cdot \frac{(F(I,J-1,K) - F(I,J,K))}{Y(I,J,K)} + \frac{(F(I,J+1,K) - F(I,J,K))}{Y(I,J+1,K)} +$$

$$A(J,K) \cdot \frac{(F(I-1,J,K) - F(I,J,K))}{X(I,J,K)} + \frac{(F(I+1,J,K) - F(I,J,K))}{X(I+1,J,K)} +$$

$$A(I,J) \cdot \frac{(F(I,J,K-1) - F(I,J,K))}{Z(I,J,K)} + \frac{(F(I,J,K+1) - F(I,J,K))}{Z(I,J,K+1)} + Q(I,J,K)$$

where TM is the time increment in seconds.

To solve the equation, it was rearranged so that F(I,J,K), the future temperature of a node, was equated to the other parameters. Then if I is varied from 2 to 6, J from 2 to 8 and K from 2 to 6, 175 separate equations are generated, and then solved using Gauss-Siedel iteration.

At the commencement of iteration, the present temperature of every node is known from monitored data or steady state calculation. The future temperatures of all external nodes are similarly known, the future temperatures of internal nodes are not, and are assigned an assumed value. As each equation is solved, the assumed temperatures are changed to the newly computed values, until after successive computations they differ by no more than 0.1°C.

After each time increment (of 1 hour), the future temperatures are reassigned to become the prevailing temperature. As this process repeats, the temperature of every node in the wall can be computed over the whole period for which monitored or other input data is available.

## Energy obtained from the internal cavity

Solar irradiance absorbed at the front surface of the mass wall passes by conduction and convection to the central cavity. Heat from this cavity is conveyed into the internal room using a small fan. The amount of energy transferred is shown in *Table 4.4*.

### 4.5 PROGRAM DESCRIPTION

The program was written in Fortran. Constants such as wall thicknesses, thermal conductivities and thermal capacities are inserted into DATA statements. Variables such as the hourly values of internal and external air temperature, and the solar irradiance on a south facing vertical wall are placed in Block Data statements. Glazing transmittance values were calculated for each daylight hour for a day in the middle of a month (via a specially written program solfactor) and placed at the end of the main program (please see *Appendix 3.7*).

The values of the internal and external air temperatures for the present and future hour are assigned to the relevant nodes of the computer model at the start of a run. Nodes placed (conceptually) 1.2m below ground, were assigned a temperature of 10°C, at which depth a constant value prevails all year<sup>64</sup>.

Overshadowing of the top of the mass wall surface by its architrave was accounted for, when calculating the areas around the nodes at the front wall surface.

Removal of heat from the cavity was only allowed (as in practice) between 16.00 and 07.00 hours, if the temperature at the cavity top exceeds the air temperature of the room

**Table 4.4 Energy production from the internal cavity.**

Node at top of internal cavity	Energy production	Computational formula used
I,4,6	$Q(H+1)$	$1200.A.AF.(\sum_{I=2}^{I=6} F(I,4,6) - TI(D,H+1))$

$I=6$

$\frac{\sum_{I=2}^{I=6} F(I,4,6)}{5} = \text{Average future temperature at the cavity top}$

next to the wall. During operation, the program will calculate the temperatures of each nodal point in the wall, together with the energy produced by the wall at time intervals of 1 hour. Subroutines were incorporated to allow selection of the output required. These subroutines are labelled 1. Hourprint 2. Hourplot 3. Dayplot 4. Heat and 5. Energy

### Subroutine functions

#### *1. Hourprint*

To print hourly nodal temperatures, at selected heights, in a horizontal slice through the wall (see *Appendix 3.2*).

#### *2. Hourplot*

Plots the hourly temperature distribution, at selected heights, through a wall section at position  $I=2$ . Thermocouples were installed at this position, to check on computational accuracy (see *Appendix 3.3*).

#### *3. Dayplot*

Plots the temperature change at  $I=3$ ,  $K=5$ , near the top of the mass wall, at three points in the section:

- At the front surface :  $J=2$ .
- At the rear surface:  $J=3$ .
- In the ventilated cavity:  $J=4$ .

(see *Appendix 3.4*)



#### 4. Heat

The hourly energy production by the wall is computed, then summed to provide the daily energy delivered (see *Appendix 3.5*).

Finally, the daily efficiency of energy production is determined as:

$$\text{Efficiency} = \frac{\text{Daily energy production}}{\text{Solar irradiation per day}}$$

#### 5. Energy

This calculates:

- The average daily irradiation, over the period of the computations.
- The solar irradiation received in the above period.
- The heat energy produced in the period.
- The average efficiency of energy production in the period.

(see *Appendix 3.6*).

#### Examples of the output

**Fig 4.10** shows the temperature distribution in July, for node 1=2 near to one side and at the top of the solar wall. Initially, the temperature is less than 15°C outside the wall insulation and internally the temperature is constant at 18°C. From 9:00 am onwards, solar radiation falling on the front surface of the wall elevates its temperature. This temperature peaks at 33°C in the early afternoon and subsequently, the internal surface of the mass wall rises too at 12:00 am, peaking at 25°C in the early evening. Operation of the solar wall fan at 16:00 then reduces the internal cavity temperature, as heat transfers to the interior. **Fig 4.11** shows the change in temperature of the front and rear

INPUT INTERNAL ROOM TEMPERATURE  
 \*18.  
 INPUT THICKNESS OF FRONT LEAF OF WALL.  
 \*.1  
 ENTER 1=NO,2=SINGLE,3=DOUBLE GLAZING,4=SG+NIGHT INSULATION,5=DG+NIGHT INSULATION  
 \*3  
 INPUT AIR FLOW RATE IN CAVITY  
 \*2.5  
 INITIAL TEMPERATURES FOR ITERATION  
 AIRIN AIR-PL PL-INS INS-BK BK-CAV CAV CAU-BK BK-CAV CAVITY AIROUT  
 18.0 17.9 17.9 16.8 15.3 15.3 15.2 15.2 15.1 15.0  
 DAY= 1  
 INPUT 1=HOURPRINT,2=HOURPLOT,3=ROTH,4=DAYPLOT,5=DAILY HEAT,6=MONTHLY ENERGY  
 \*2  
 ARE YOU AT A GIGI,WITH PRINTER? 1=YES,0=NO  
 \*0  
 INPUT 1,2,3,4,5,6,7 FOR H PLOT POSITIONS,TERMINATE WITH0(2=BOTTON,6=TOP OF TROMBE WALL)  
 \*5  
 \*0  
 K=5

TEMPERATURE DISTRIBUTION THROUGH TROMBE WALL AT I=2  
 0 5 10 15 20 25 30 35 40 45 50 55 60 65  
 \*\*\*\*\*  
 1 \* \* \* \* \*  
 2 \* \* \* \* \*  
 3 \* \* \* \* \*  
 4 \* \* \* \* \*  
 5 \* \* \* \* \*  
 6 \* \* \* \* \*  
 7 \* \* \* \* \*  
 8 \* \* \* \* \*  
 9 \* \* \* \* \*  
 HOUR 1

K=5  
 TEMPERATURE DISTRIBUTION THROUGH TROMBE WALL AT I=2  
 0 5 10 15 20 25 30 35 40 45 50 55 60 65  
 \*\*\*\*\*  
 1 \* \* \* \* \*  
 2 \* \* \* \* \*  
 3 \* \* \* \* \*  
 4 \* \* \* \* \*  
 5 \* \* \* \* \*  
 6 \* \* \* \* \*  
 7 \* \* \* \* \*  
 8 \* \* \* \* \*  
 9 \* \* \* \* \*  
 HOUR 2

K=5  
 TEMPERATURE DISTRIBUTION THROUGH TROMBE WALL AT I=2  
 0 5 10 15 20 25 30 35 40 45 50 55 60 65  
 \*\*\*\*\*  
 1 \* \* \* \* \*  
 2 \* \* \* \* \*  
 3 \* \* \* \* \*  
 4 \* \* \* \* \*  
 5 \* \* \* \* \*  
 6 \* \* \* \* \*  
 7 \* \* \* \* \*  
 8 \* \* \* \* \*  
 9 \* \* \* \* \*  
 HOUR 3

K=5  
 TEMPERATURE DISTRIBUTION THROUGH TROMBE WALL AT I=2  
 0 5 10 15 20 25 30 35 40 45 50 55 60 65  
 \*\*\*\*\*  
 1 \* \* \* \* \*  
 2 \* \* \* \* \*  
 3 \* \* \* \* \*  
 4 \* \* \* \* \*  
 5 \* \* \* \* \*  
 6 \* \* \* \* \*  
 7 \* \* \* \* \*  
 8 \* \* \* \* \*  
 9 \* \* \* \* \*  
 HOUR 4

K=5  
 TEMPERATURE DISTRIBUTION THROUGH TROMBE WALL AT I=2  
 0 5 10 15 20 25 30 35 40 45 50 55 60 65  
 \*\*\*\*\*  
 1 \* \* \* \* \*  
 2 \* \* \* \* \*  
 3 \* \* \* \* \*  
 4 \* \* \* \* \*  
 5 \* \* \* \* \*  
 6 \* \* \* \* \*  
 7 \* \* \* \* \*  
 8 \* \* \* \* \*  
 9 \* \* \* \* \*  
 HOUR 5

K=5  
 TEMPERATURE DISTRIBUTION THROUGH TROMBE WALL AT I=2  
 0 5 10 15 20 25 30 35 40 45 50 55 60 65

Fig. 4.10 Computer program output showing temperature distribution in July for node I=2 near to one side and towards the top of the solar wall.

K=5  
 TEMPERATURE DISTRIBUTION THROUGH TROMBE WALL AT I=2  
 0 5 10 15 20 25 30 35 40 45 50 55 60 65  
 \*\*\*\*\*  
 1 \* \* \* \* \*  
 2 \* \* \* \* \*  
 3 \* \* \* \* \*  
 4 \* \* \* \* \*  
 5 \* \* \* \* \*  
 6 \* \* \* \* \*  
 7 \* \* \* \* \*  
 8 \* \* \* \* \*  
 9 \* \* \* \* \*

HOUP 8

K=5  
 TEMPERATURE DISTRIBUTION THROUGH TROMBE WALL AT I=2  
 0 5 10 15 20 25 30 35 40 45 50 55 60 65  
 \*\*\*\*\*  
 1 \* \* \* \* \*  
 2 \* \* \* \* \*  
 3 \* \* \* \* \*  
 4 \* \* \* \* \*  
 5 \* \* \* \* \*  
 6 \* \* \* \* \*  
 7 \* \* \* \* \*  
 8 \* \* \* \* \*  
 9 \* \* \* \* \*

HOUP 9

K=5  
 TEMPERATURE DISTRIBUTION THROUGH TROMBE WALL AT I=2  
 0 5 10 15 20 25 30 35 40 45 50 55 60 65  
 \*\*\*\*\*  
 1 \* \* \* \* \*  
 2 \* \* \* \* \*  
 3 \* \* \* \* \*  
 4 \* \* \* \* \*  
 5 \* \* \* \* \*  
 6 \* \* \* \* \*  
 7 \* \* \* \* \*  
 8 \* \* \* \* \*  
 9 \* \* \* \* \*

HOUP 10

K=5  
 TEMPERATURE DISTRIBUTION THROUGH TROMBE WALL AT J=2  
 0 5 10 15 20 25 30 35 40 45 50 55 60 65  
 \*\*\*\*\*  
 1 \* \* \* \* \*  
 2 \* \* \* \* \*  
 3 \* \* \* \* \*  
 4 \* \* \* \* \*  
 5 \* \* \* \* \*  
 6 \* \* \* \* \*  
 7 \* \* \* \* \*  
 8 \* \* \* \* \*  
 9 \* \* \* \* \*

HOUP 11

K=5  
 TEMPERATURE DISTRIBUTION THROUGH TROMBE WALL AT I=2  
 0 5 10 15 20 25 30 35 40 45 50 55 60 65  
 \*\*\*\*\*  
 1 \* \* \* \* \*  
 2 \* \* \* \* \*  
 3 \* \* \* \* \*  
 4 \* \* \* \* \*  
 5 \* \* \* \* \*  
 6 \* \* \* \* \*  
 7 \* \* \* \* \*  
 8 \* \* \* \* \*  
 9 \* \* \* \* \*

HOUP 12

K=5  
 TEMPERATURE DISTRIBUTION THROUGH TROMBE WALL AT I=2  
 0 5 10 15 20 25 30 35 40 45 50 55 60 65  
 \*\*\*\*\*  
 1 \* \* \* \* \*  
 2 \* \* \* \* \*  
 3 \* \* \* \* \*  
 4 \* \* \* \* \*  
 5 \* \* \* \* \*  
 6 \* \* \* \* \*  
 7 \* \* \* \* \*  
 8 \* \* \* \* \*  
 9 \* \* \* \* \*

HOUP 13

K=5  
 TEMPERATURE DISTRIBUTION THROUGH TROMBE WALL AT J=2  
 0 5 10 15 20 25 30 35 40 45 50 55 60 65  
 \*\*\*\*\*  
 1 \* \* \* \* \*  
 2 \* \* \* \* \*  
 3 \* \* \* \* \*  
 4 \* \* \* \* \*  
 5 \* \* \* \* \*  
 6 \* \* \* \* \*  
 7 \* \* \* \* \*  
 8 \* \* \* \* \*  
 9 \* \* \* \* \*

HOUP 14

TEMPERATURE DISTRIBUTION THROUGH TROMBE WALL AT I=2

	0	5	10	15	20	25	30	35	40	45	50	55	60	65
1	*				*									*
2	*							*						*
3	*					*								*
4	*					*								*
5	*					*								*
6	*				*									*
7	*			*										*
8	*			*										*
9	*			*										*

HOUR 15

K=5

TEMPERATURE DISTRIBUTION THROUGH TROMBE WALL AT I=2

	0	5	10	15	20	25	30	35	40	45	50	55	60	65
1	*				*									*
2	*							*						*
3	*					*								*
4	*					*								*
5	*					*								*
6	*				*									*
7	*			*										*
8	*			*										*
9	*			*										*

HOUR 16

K=5

TEMPERATURE DISTRIBUTION THROUGH TROMBE WALL AT I=2

	0	5	10	15	20	25	30	35	40	45	50	55	60	65
1	*				*									*
2	*							*						*
3	*					*								*
4	*					*								*
5	*					*								*
6	*				*									*
7	*			*										*
8	*			*										*
9	*			*										*

HOUR 17

K=5

TEMPERATURE DISTRIBUTION THROUGH TROMBE WALL AT I=2

	0	5	10	15	20	25	30	35	40	45	50	55	60	65
1	*				*									*
2	*							*						*
3	*					*								*
4	*				*									*
5	*				*									*
6	*				*									*
7	*			*										*
8	*			*										*
9	*			*										*

HOUR 18

K=5

TEMPERATURE DISTRIBUTION THROUGH TROMBE WALL AT I=2

	0	5	10	15	20	25	30	35	40	45	50	55	60	65
1	*				*									*
2	*							*						*
3	*					*								*
4	*				*									*
5	*				*									*
6	*				*									*
7	*			*										*
8	*			*										*
9	*			*										*

HOUR 19

K=5

TEMPERATURE DISTRIBUTION THROUGH TROMBE WALL AT I=2

	0	5	10	15	20	25	30	35	40	45	50	55	60	65
1	*				*									*
2	*							*						*
3	*					*								*
4	*				*									*
5	*				*									*
6	*				*									*
7	*			*										*
8	*			*										*
9	*			*										*

HOUR 20

K=5

TEMPERATURE DISTRIBUTION THROUGH TROMBE WALL AT I=2

	0	5	10	15	20	25	30	35	40	45	50	55	60	65
1	*				*									*
2	*							*						*
3	*					*								*
4	*				*									*
5	*				*									*
6	*				*									*
7	*			*										*
8	*			*										*
9	*			*										*

HOUR 21



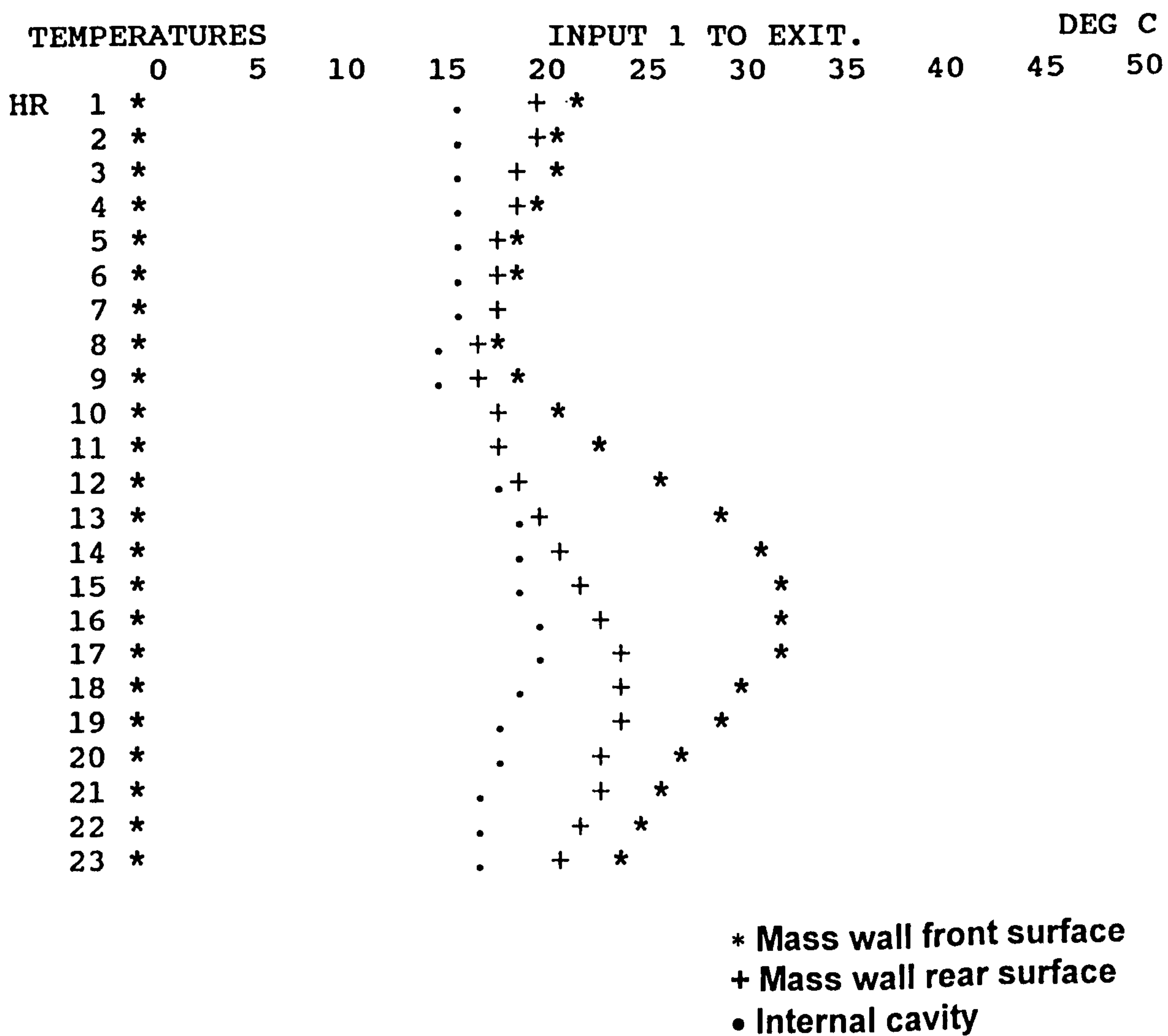


Fig. 4.11 Computer output showing temperature of inside and outside surfaces of the solar wall versus time in hours at  $l=2$  and  $K=5$ .

mass wall surface and the internal cavity over 24 hours. **Fig 4.11** also shows the drop in temperature of the internal cavity at 16:00, when heat transfer commences and the wall fan starts to operate.

The accuracy of these temperature and energy values that result from the use of finite difference approximations is important and is the topic of the next section.

#### **4.6 ERRORS AND ACCURACY PRODUCED WHEN USING FINITE DIFFERENCE EQUATIONS**

The computer program used to simulate the performance of the Poulton Lancelyn school was written using the implicit finite difference equation formulation. It seemed appropriate to compare the accuracy with which three other formulations: the Euler explicit, the Crank-Nicolson and the Bhattacharya exponential method could also evaluate temperatures within and energy production from solar walls. A shorter 1 dimensional program was used for this task, and the four different variants of the finite difference equations included within it. Hourly monitored values of the internal and external temperatures and the solar irradiation on a vertical plane for one particular day were used as input data. The computed temperature of the front wall surface and rear wall surface were output for all four different formulations. These results compared with the actual values monitored are shown in *Table 4.5* and graphed in **Fig 4.12**. Percentage errors are shown in *Table 4.6*. The Euler explicit, the Crank-Nicolson and the Bhattacharya methods, are shown to be the most accurate in representing these temperatures. The Euler explicit formulation however, is best not used. It is unstable at the high values of  $R = \alpha\Delta t/\rho c\Delta x^2$  that occur in building studies. Use of the implicit

**Table 4.5 Temperatures computed using four different finite difference methods: (the explicit, the Crank-Nicolson, Bhattacharya, implicit), compared to actual values.**

Hour	Wall surface temperatures										air temperature	
	Measured		Explicit		Crank-Nicolson		Bhattacharya		Implicit		outside	inside
	Front	Rear	Front	Rear	Front	Rear	Front	Rear	Front	Rear		
0	22.5	23	22.5	23	22.5	23	22.5	23	22.5	23	11.5	16.2
2	20	22.5	20.8	22.1	20.8	22.1	20.8	22.1	20.9	22.1	11.5	16.2
4	18.7	22	19.5	21.3	19.5	21.3	19.5	21.3	19.7	21.4	11.5	16.5
6	17.5	21	18.5	20.6	18.5	20.6	8.5	20.6	18.7	20.7	11.3	18
8	18.5	20	18.2	20.1	18.2	20.1	18.2	20.1	18.2	20.2	11.5	18.5
10	23	20	23.5	20.2	23.5	20.2	23.5	20.2	23.3	20.4	13	18.5
12	32.5	21	33.8	21.7	34	21.7	33.8	21.7	33.2	22.1	14.7	18
14	39	23	38.8	24.2	38.9	24.3	38.8	24.2	38.1	24.4	14.5	19
16	38	26.2	39	26.4	39.1	26.4	39	26.4	38.6	26.3	13.5	19
18	35	27.5	35.2	27.6	35.2	27.6	35.2	27.6	35.1	27.3	12.7	18
20	30	27.5	30.3	27.3	30.2	27.2	30.3	27.3	30.5	27	12.5	17.5
22	27.5	25.3	26.8	26	26.7	25.8	26.8	26	27.1	25.9	11	16.5
24	24	25.1	24.1	24.6	23.8	24.6	24.1	24.6	24.3	24.6	10.2	16





**Table 4.6 Percentage errors involved in the estimation of the surface temperature of solar wall using different finite difference formulations.**

Hour	Percentage error in estimating the rear wall surface temperature.			
	Explicit	Crank-Nicolson	Bhattacharya	Implicit
2	-2.8	-2.8	-2.8	-2.8
4	-2.6	-2.6	-2.6	-2.2
6	-1.9	-1.9	-1.9	-1.4
8	0.5	0.5	0.5	1
10	1	1	1	2
12	3.3	3.3	3.3	4.8
14	5.2	5.6	5.2	6
16	0.8	0.8	0.8	0.4
18	0.4	0.4	0.4	-0.8
20	-0.7	-1	-1	-1.8
22	2.8	2	2	2.4
24	-2.8	-2	-2	-2

formulation is in this case only slightly less accurate than using the other formulations. Errors produced when estimating energy production from solar walls from 16.00 - 24.00 for the implicit method have been estimated and are shown in *Table 4.7*. They are dependant on the errors in cavity air temperature which are closely related to those of the rear face of the mass wall. The maximum error is seen to be  $\pm 6\%$ . The implicit method is accurate enough for this study, but since the Crank-Nicolson (or Bhattacharya) are rather more accurate, the use of such finite difference methods is preferred, a conclusion in agreement with that of Waters <sup>65</sup>.

**Table 4.7 Percentage errors involved in the estimation of energy production from solar walls for one typical day using the implicit method.**

Hour	Percentage error
16	1
18	-2
20	-5
22	6
24	-6

# **CHAPTER FIVE - ASSESSMENT OF SOLAR WALL PERFORMANCE**



## 5.1 USE OF THE COMPUTER SIMULATION PROGRAM FOR POULTON LANCELYN SCHOOL <sup>66</sup>

I have described the development of a computer program to simulate the performance of the Poulton Lancelyn solar wall, and shown that the results of simulating the temperatures of the faces of the mass wall closely parallel monitored values. This program was thus validated in its ability to reproduce monitored hourly changes of temperature in a solar wall.

The amounts of energy delivered by the solar wall have been evaluated. Energy production calculations were made for the period when the school heating system is switched off, from 16.00 in the afternoon until the theoretical commencement of preheating at 06.00 the next day. The Poulton Lancelyn solar wall was not working correctly. Its operational faults have already been described. The computed values for energy production will as a result be greater than the measured values. In addition, there are errors involved in the computation of energy production from the Poulton Lancelyn solar wall through the use of temperature differentials obtained from the outputs of two single thermocouples. These can be of the order of 6 per cent (see *Table 4.7*). In spite of this, the results obtained will be quite suitable for use when making decisions as to whether such walls constitute a worthwhile means of reducing the energy consumption of buildings.

The main purpose of writing this computer program was to permit the study of the effects of varying major parameters which affect the performance of solar walls. These effects include: cavity air speed, wall thickness, glazing type and the use of low

emissivity coatings. In the study, solar walls have generally been treated as solar panels tested for consecutive 24 hour periods.

### Environmental parameters used in the computer simulation

From each months weather data, a day of high solar irradiation was selected. Hourly values of irradiation and external air temperature were stored in a data file and then input into the program. This input was repeated to simulate successive days of the same alternating weather until energy production per day reached a steady value. The energy produced depends on the temperature of the air entering the solar wall to be heated. In the simulation, this temperature was kept constant at 10°C, 15°C or 18°C.

### Theory

An ordinary (metal plate) solar collector under conditions of constant irradiation (steady state conditions) will experience no effect from its thermal capacity, and the following equation will hold for its efficiency  $\eta$ :

$$\eta = \frac{F_R(\tau\alpha - U_L(T_C - T_{AO}))}{I} \quad (5.1)$$

For a solar wall with considerable mass to be heated, where the irradiation is not constant, it is best to consider a whole days energy output when evaluating its efficiency.

If repeated use of the same solar input is used, with the input rising and falling by the same amount each day, the influence of thermal capacity upon performance will be negated. The wall will gain and lose successively, the same amounts of heat. The daily efficiency  $\eta_{DAY}$ , for such a solar input, may then be assessed by the following equation, analogous to the preceding one:

$$\eta_{\text{DAY}} = F_R \left( \tau\alpha - \frac{24 \cdot U_L (\bar{T}_C - \bar{T}_{AO})}{H} \right) = F_R \left( \tau\alpha - \frac{24 \cdot U_L \cdot \Delta\bar{T}}{H} \right) \quad (5.2)$$

Plots of efficiency of solar walls versus  $\Delta\bar{T}/H$  thus should be and are, straight lines.

### Nomenclature

$U_L$  Overall heat loss coefficient  $\text{W/m}^2\text{K}$

$F_R$  Collector heat removal factor

$\tau\alpha$  Transmittance-absorptance product

$I$  Solar irradiation on collector surface  $\text{W/m}^2$

$H$  Daily solar irradiation  $\text{Wh/m}^2$

$T_{AO}$  External air temperature  $^{\circ}\text{C}$

$\bar{T}_{AO}$  Average daily external air temperature  $^{\circ}\text{C}$

$T_C$  Cavity air temperature  $^{\circ}\text{C}$

$\bar{T}_C$  Average daily cavity air temperature  $^{\circ}\text{C}$

$\Delta\bar{T}$  Average daily cavity/external air temperature differential:  $(\bar{T}_C - \bar{T}_{AO})$   $^{\circ}\text{C}$

### The effect of cavity air speed

In Fig 5.1 the efficiencies of a single glazed, 100 mm thick, selectively coated wall are computed, using March weather data, an inlet temperature of  $10^{\circ}\text{C}$ , and varying air speeds through the internal cavity. Efficiency is seen to rise with air speed until a maximum is reached above  $1.0 \text{ ms}^{-1}$ . An efficiency of 33% from a cavity air speed of  $0.5 \text{ ms}^{-1}$  (as used at Poulton Lancelyn) is close to the optimum efficiency of 35% at air speeds above  $1.0 \text{ ms}^{-1}$ . The latter value will be used in future simulations.

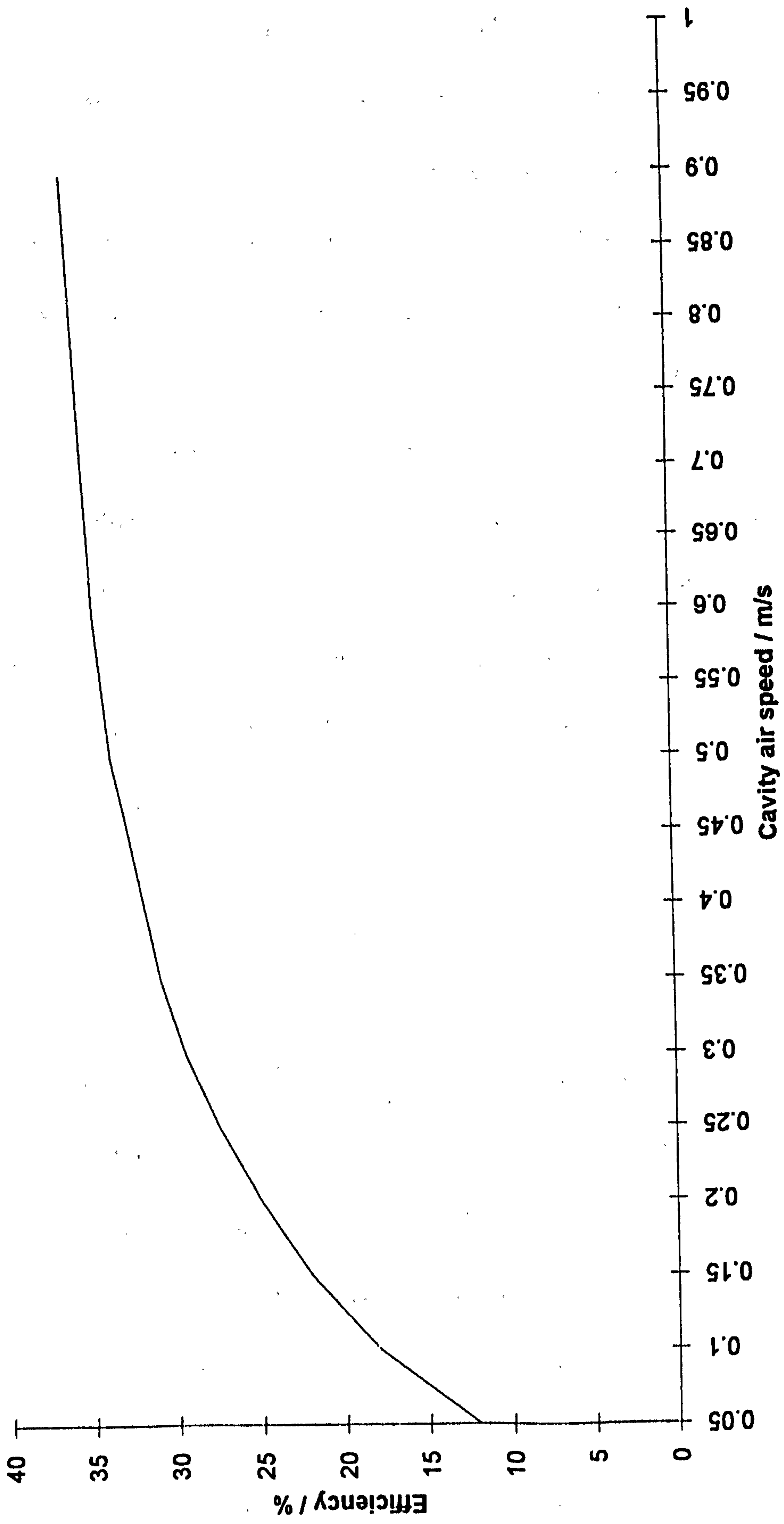


**Fig 5.1 Effect of cavity air speed on the efficiency of a selectively coated solar wall in March.**



### The effect of solar wall thickness

Simulations were performed using March weather data, cavity air speeds of  $1.0 \text{ ms}^{-1}$ , inlet air temperatures of  $10^\circ\text{C}$ ,  $15^\circ$  and  $18^\circ\text{C}$  for single glazed non selectively coated solar walls of varying thicknesses. Efficiencies rise as solar wall thickness decreases (see **Fig 5.2** and *Table 5.1*). A limit to this increase is reached, dictated by increased heat losses produced by a rise in temperature of the solar wall as its thermal capacity decreases. In practice reduced thickness between the front surface and internal cavity of a solar wall, can be achieved using a single 100 mm brick front leaf, or by using perforated blocks. Lee <sup>43</sup> used the latter approach. In his work, internal slots positioned inside a 75 mm thick concrete block of a single glazed solar wall, approached its external surface to within less than 50 mm. Lee measured an efficiency for this solar wall construction of 18.7% during March, for air inlet temperatures of about  $19^\circ\text{C}$ . This is roughly what would be expected from the data cited in *Table 5.1*.

### The effect of double glazing or selective coatings

Simulations were performed for several types of solar wall, all with 50 mm cavities, and rear leaves of aerated concrete plus polystyrene insulation. The construction of the solar walls fronting the internal cavity are:

- S1        Single glazed, 100 mm outer leaf, engineering brick.
- S2        Single glazed, 200 mm outer leaf, engineering brick.
- D1        Double glazed, 100 mm outer leaf, engineering brick.
- D2        Double glazed, 200 mm outer leaf, engineering brick.
- LED1    Low emissivity double glazed, 100 mm outer leaf, engineering brick.

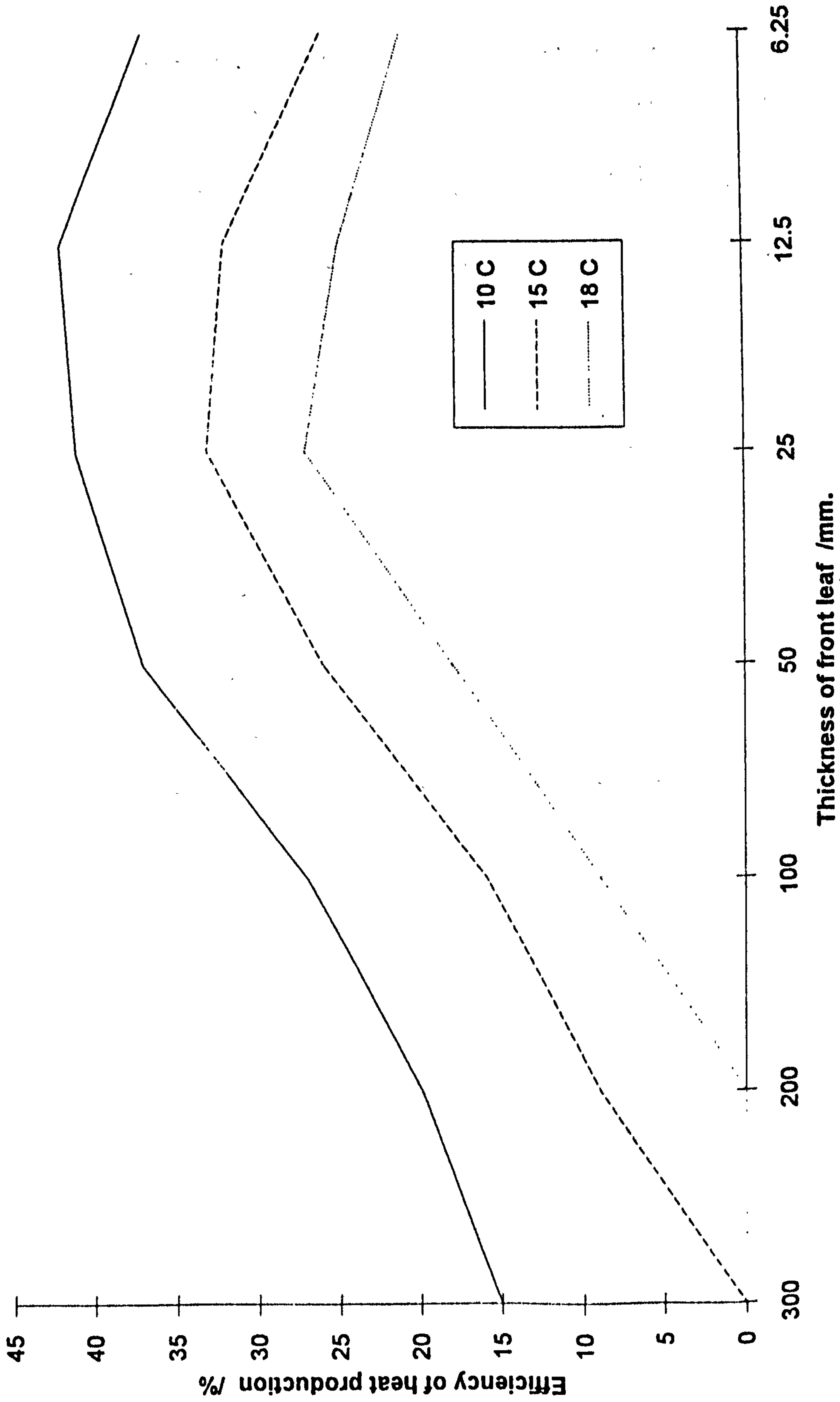


**Fig 5.2 Computed efficiencies, using March weather data, for a single glazed brick wall of varying thickness at air inlet temperatures of 10 C, 15 C and 18 C.**

**Table 5.1 Computed efficiencies using March weather data, for a single glazed brick solar wall of varying thickness, at air inlet temperatures: 10C, 15C, and 18C.**

Thickness of front leaf mm	Efficiencies at air inlet temperatures of: 10 C, 15 C, 18 C.		
	10 C	15 C	18 C
300	15	0	0
200	20	9	0
100	27	16	9
50	37	26	18
25	41	33	27
12.5	42	32	25
6.25	37	26	21

LED2 Low emissivity double glazed, 200 mm outer leaf, engineering brick.

SC1 Single glazed, selectively coated, 100 mm outer leaf, engineering brick.

Type S2, closely resembles the solar walls at Poulton Lancelyn. Figs 5.3 to 5.11 plot the efficiency  $\eta$ , versus  $\overline{\Delta T}/H$  for these different types of solar wall, using one day of high irradiation for each of the heating season months (September to May). The efficiencies produced, at cavity air inlet temperatures of 10°C and 15°C are indicated on the graphs. Values of efficiencies for the various wall types are collated in *Table 5.2*.

These graphs and tables indicate that the Poulton Lancelyn type solar wall is the least efficient of the solar wall variants investigated. In December and January, such a solar wall will produce no energy at all when using air at 15°C, and works at only 8% efficiency when the air is at 10°C. Its performance is thus unspectacular and pedestrian, throughout the year. Van Wieringens comments<sup>67</sup>, that such walls are most unsuitable for use in northern climates is most appropriate, and quite justified.

Selectively coated walls show significant improvement. The Maxorb foil coating the front brick surface enhances absorptivity and reduces emissivity to quite low values, thereby increasing solar gain and reducing radiative heat losses. During the winter the single glazed 100 mm thick selectively coated wall, SC1, averages 18% efficiency at 15°C air inlet temperature, and 32% at 10°C. In contrast, Poulton Lancelyn type solar walls: S2, give a mere 3% efficiency at 15°C and 13% efficiency at 10°C over the same period. Over a whole heating season from September to May, a selectively coated wall produces average efficiencies of 25% at 15°C air inlet temperature, and 35% at 10°C air inlet temperature, in complete contrast to the much poorer performance of a Poulton



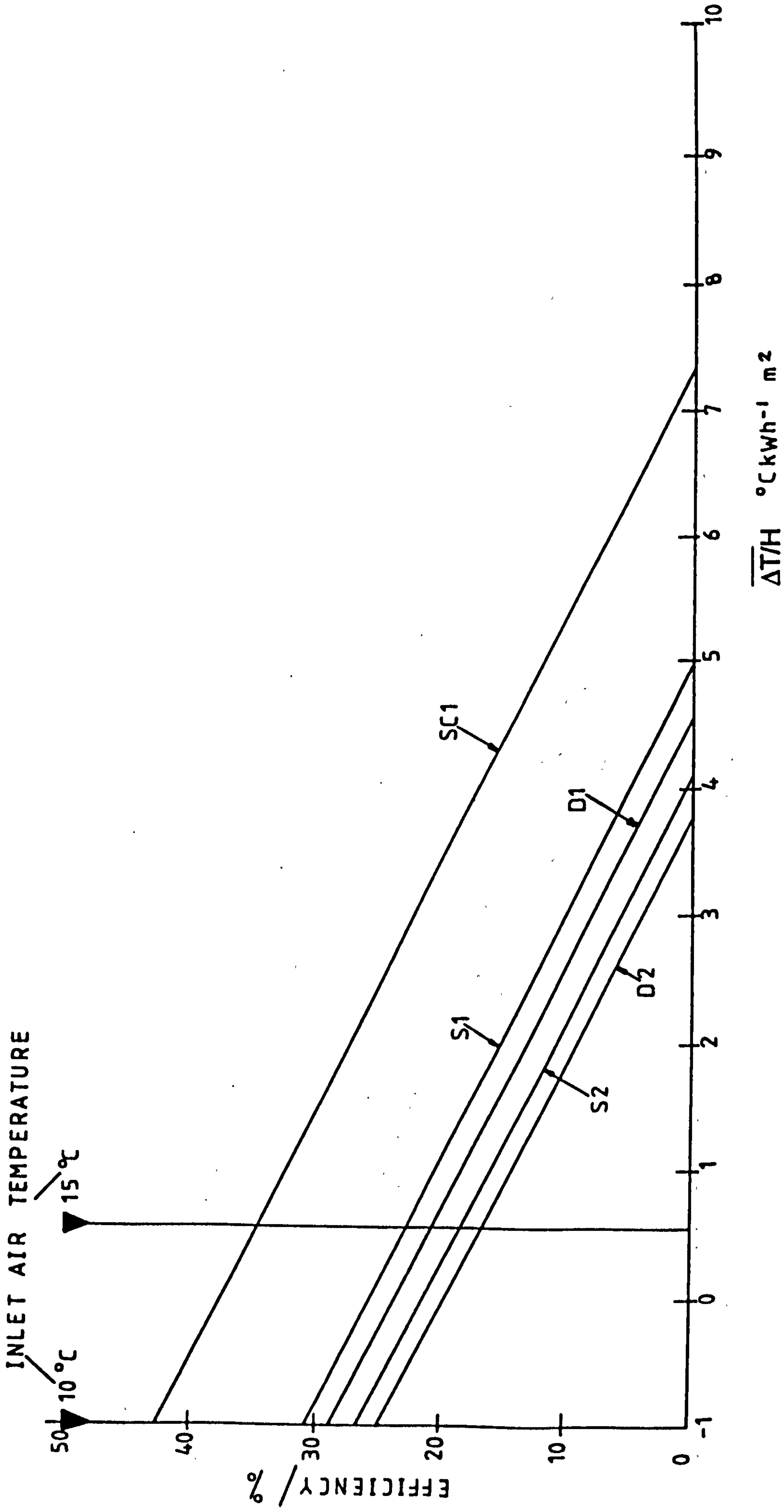


Fig. 5.3 Variation in efficiency of solar walls using September 1986 weather data.

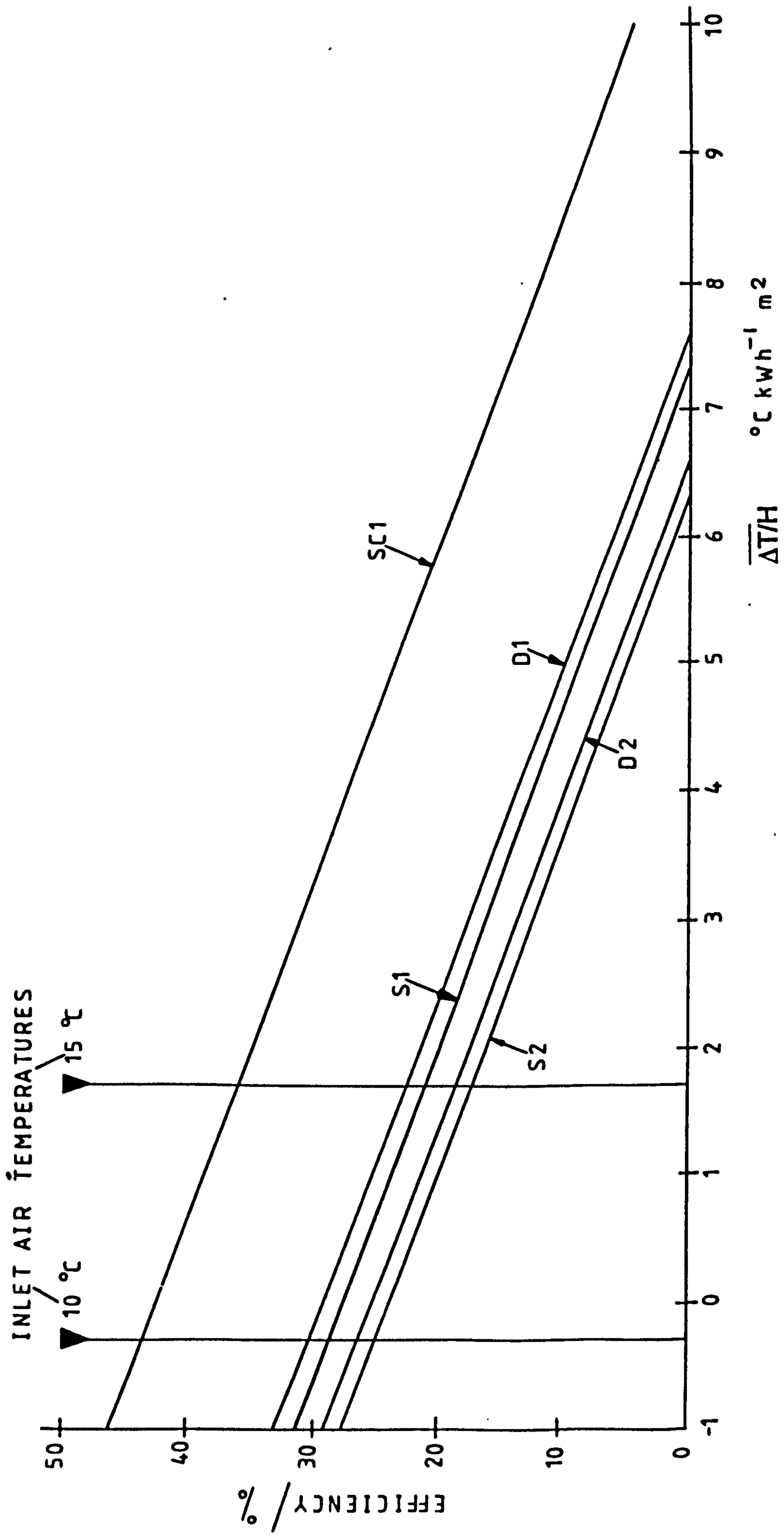


Fig. 5.4 Variation in efficiency of solar walls using October 1986 weather data.

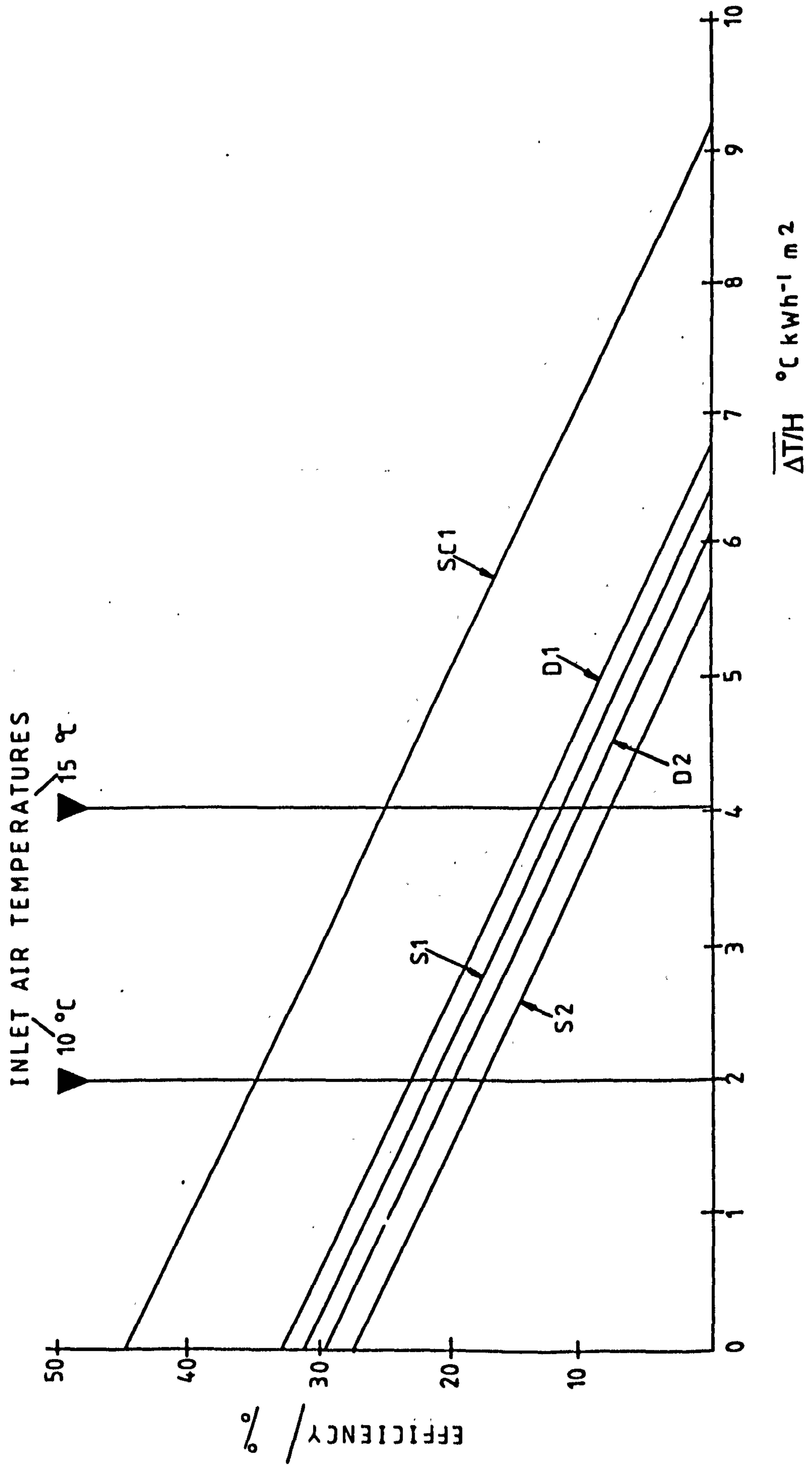


Fig. 5.5 Variation in efficiency of solar walls using November 1986 weather data.

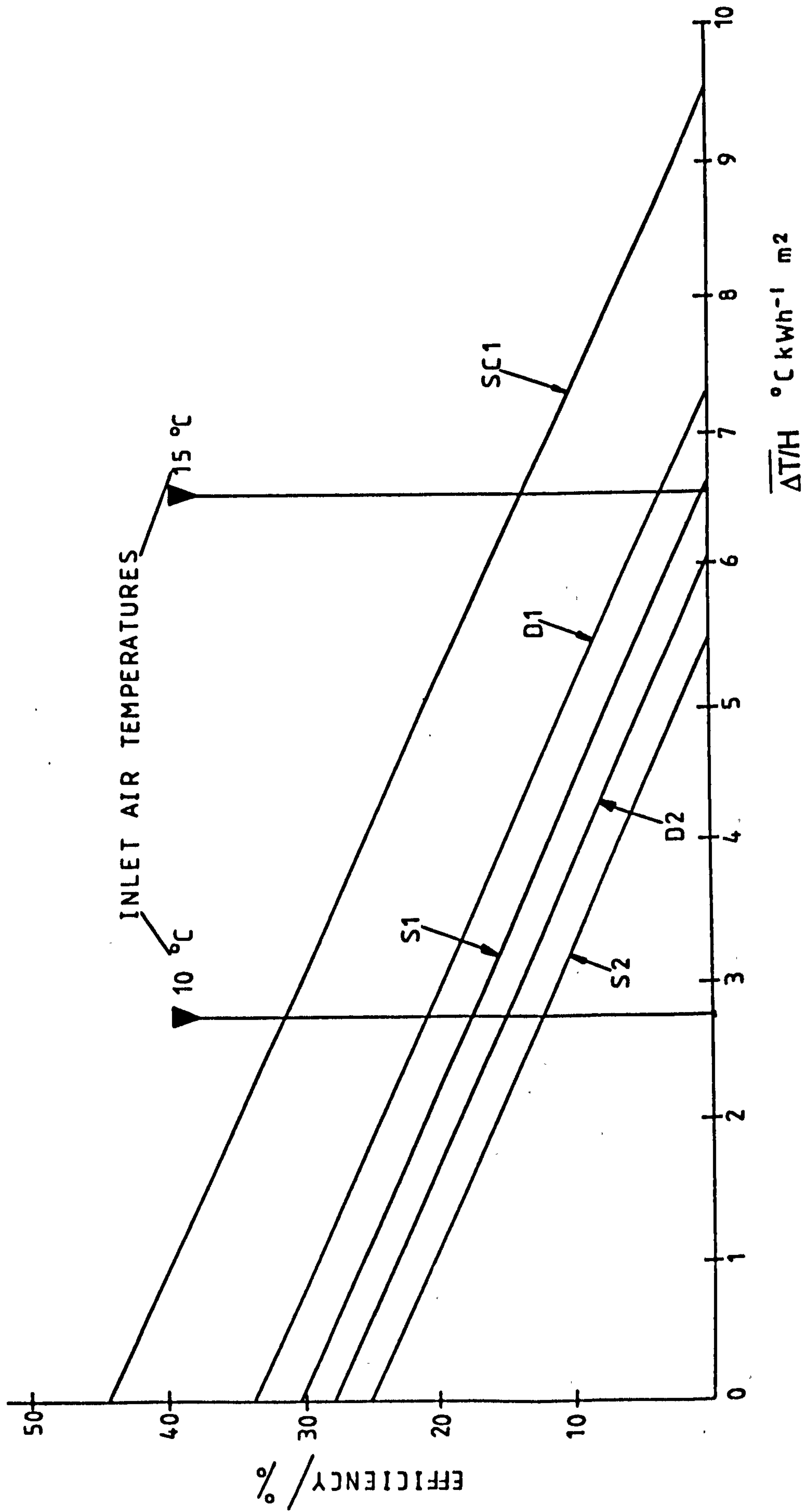


Fig. 5.6 Variation in efficiency of solar walls using December 1986 weather data.



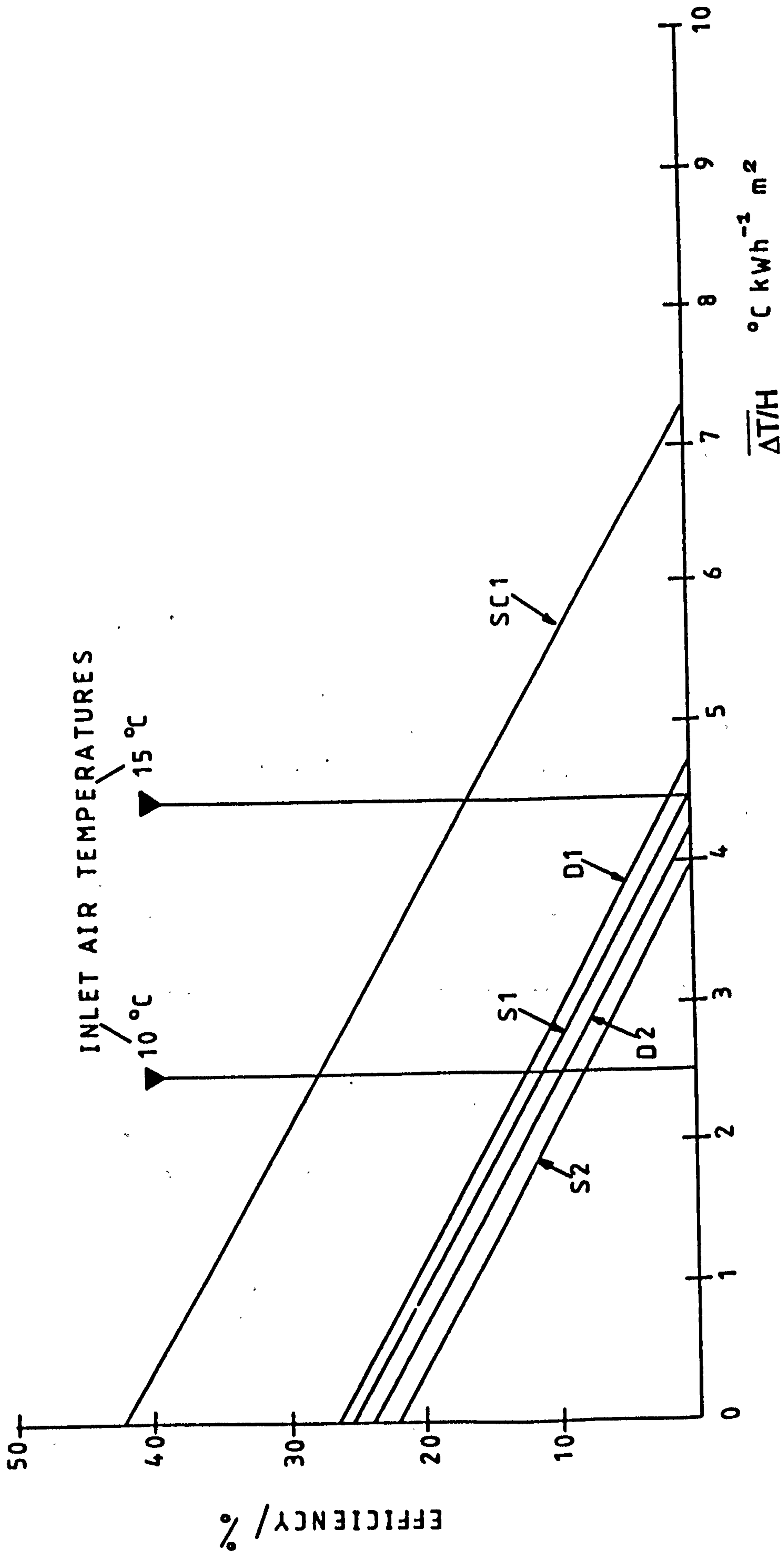


Fig. 5.7 Variation in efficiency of solar walls using January 1986 weather data.

LIVERPOOL JOHN MOORES UNIVERSITY  
 Alchem Roberts L.R.C.  
 TEL 0151 231 3701/3634

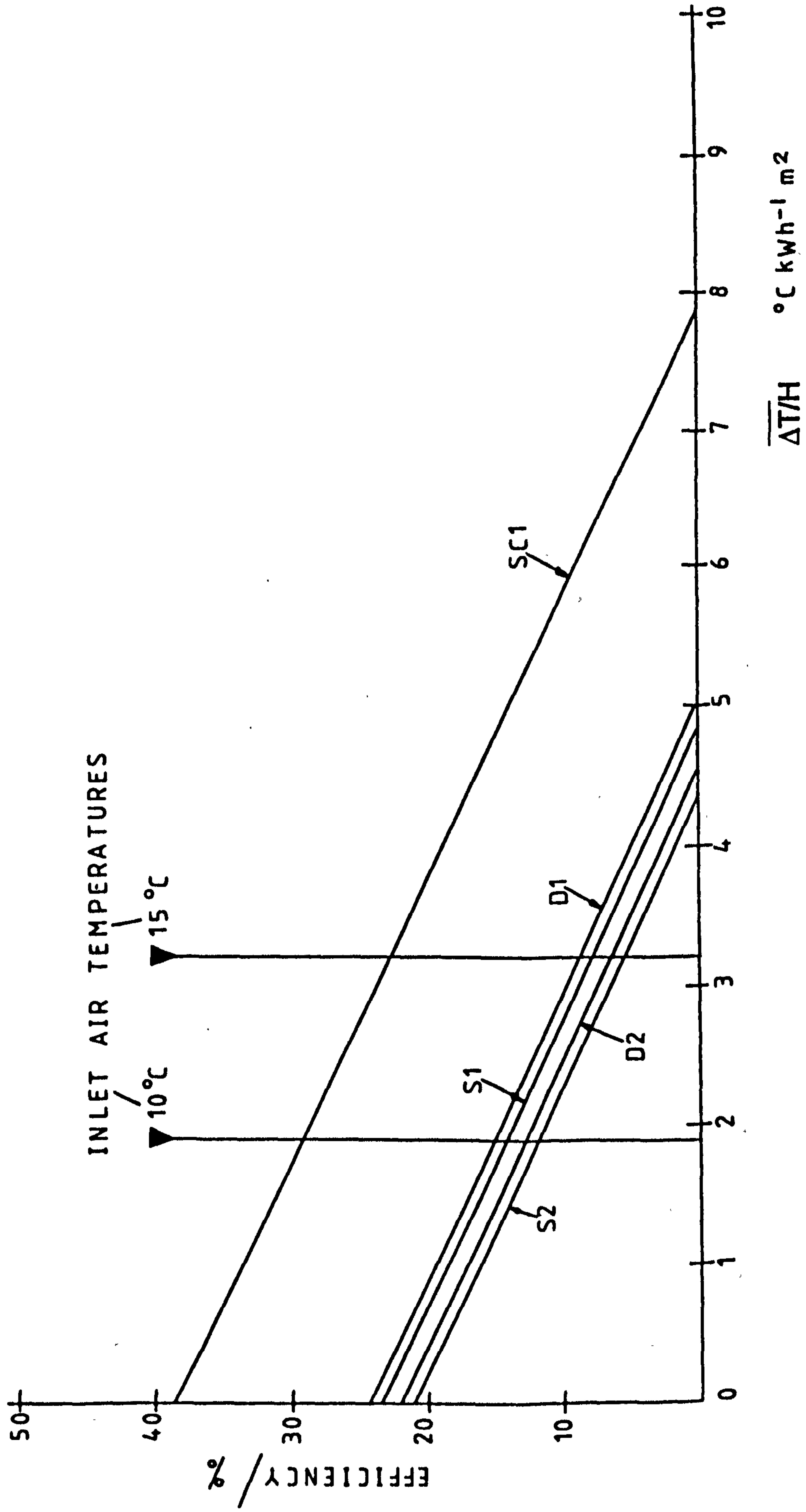


Fig. 5.8 Variation in efficiency of solar walls using February 1986 weather data.

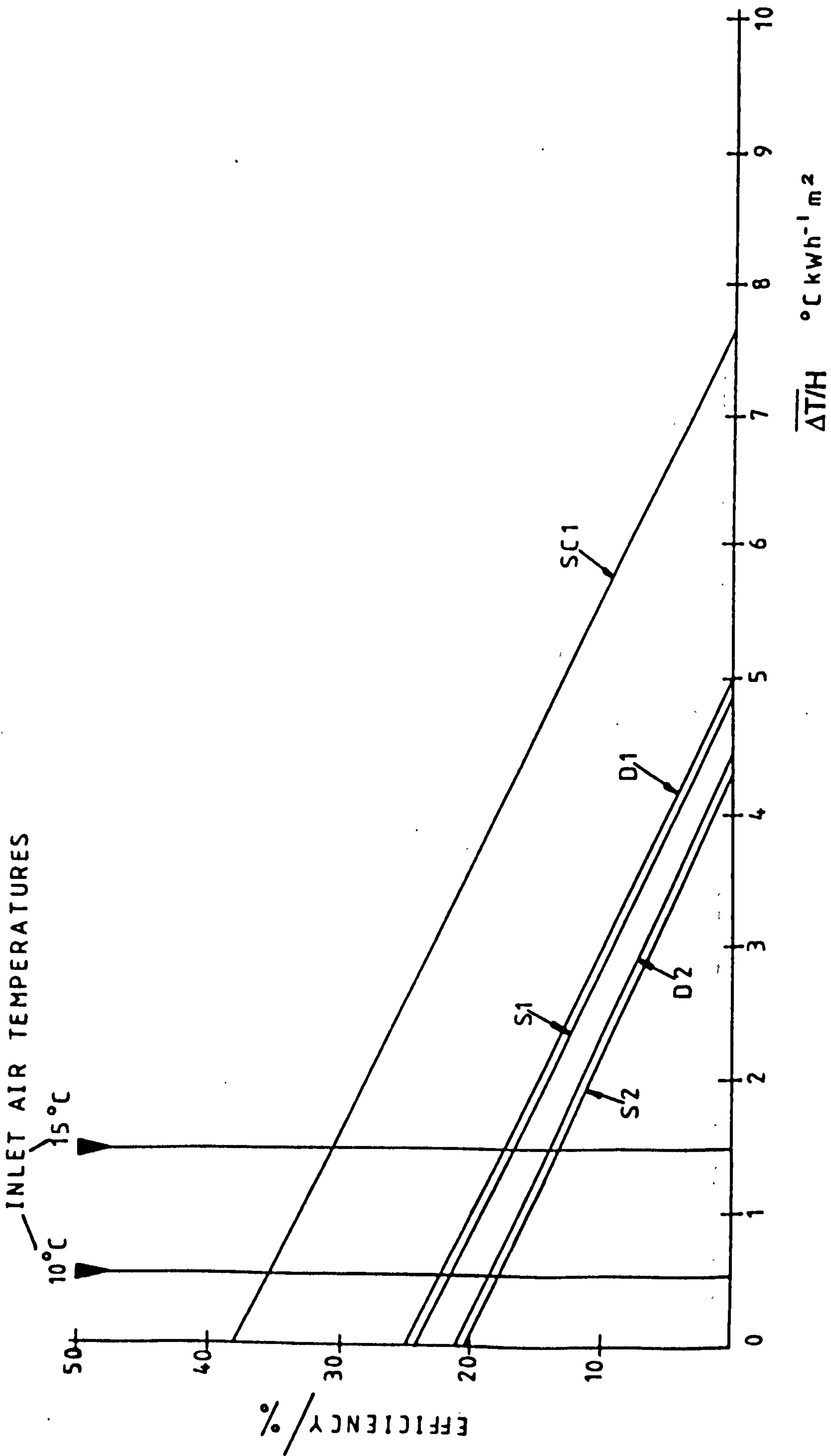


Fig. 5.9 Variation in efficiency of solar walls using March 1986 weather data.

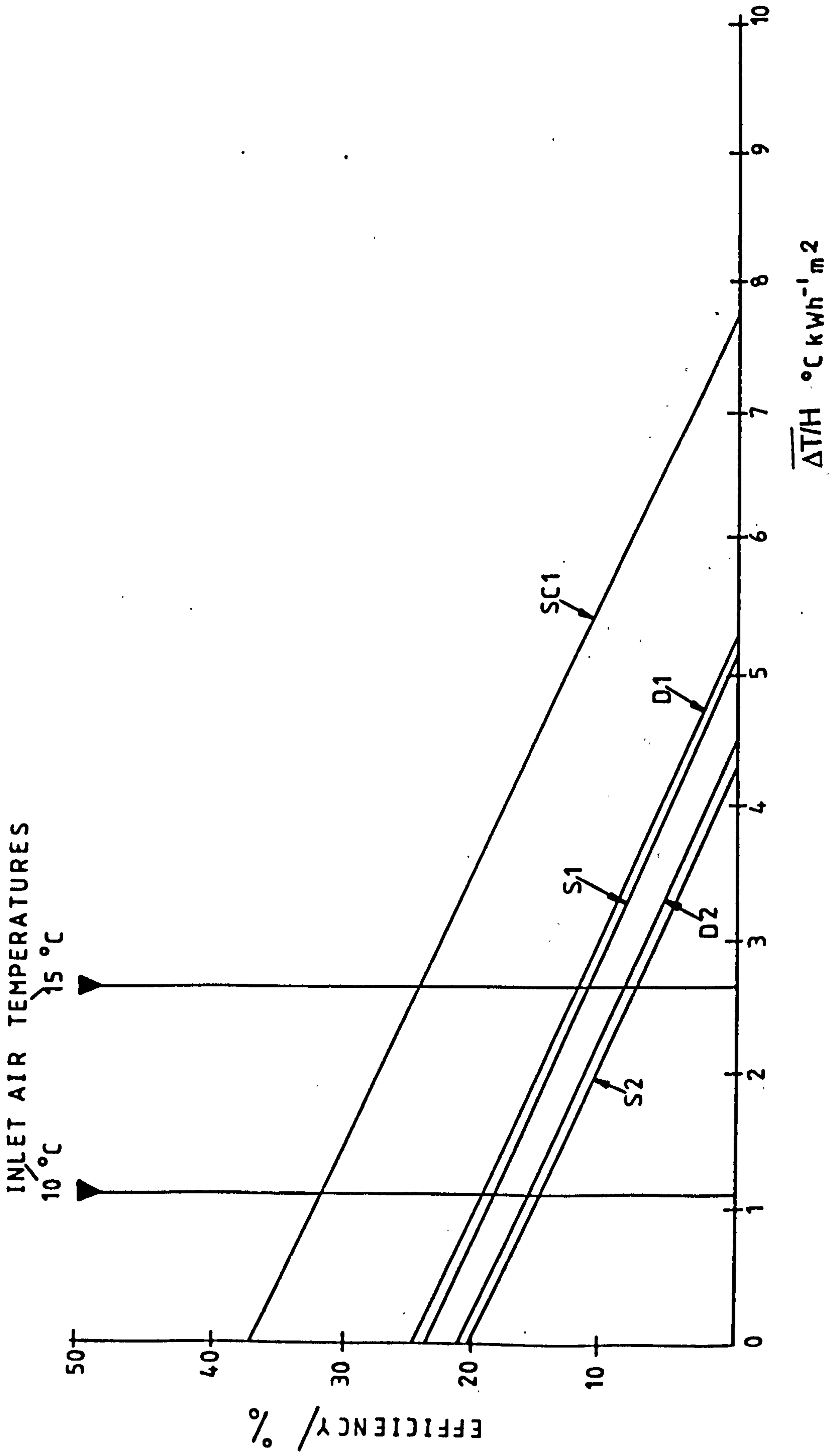


Fig. 5.10 Variation in efficiency of solar walls using April 1986 weather data.



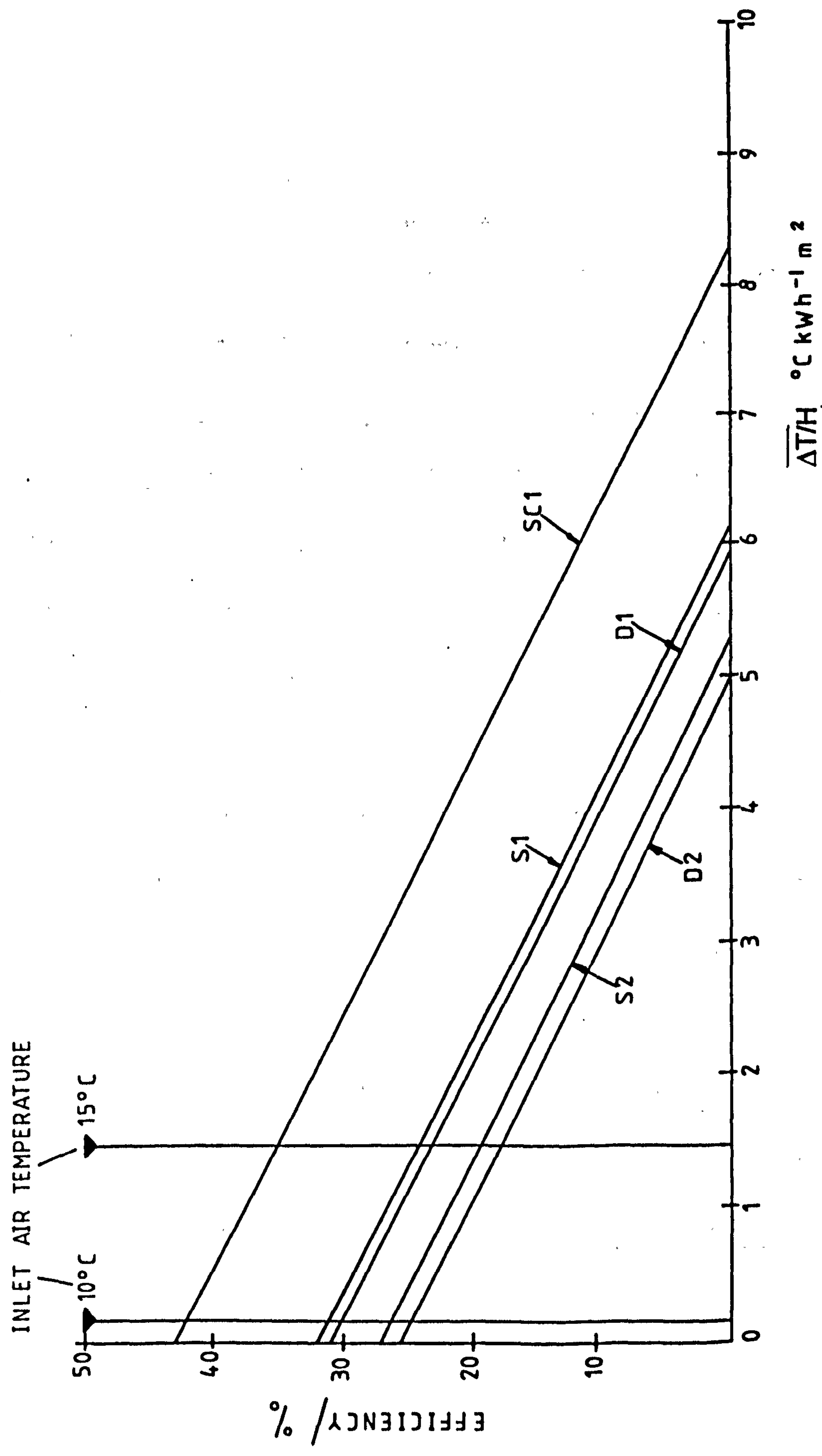


Fig. 5.11 Variation in efficiency of solar walls using May 1986 weather data.

**Table 5.2 Efficiencies computed for single glazed , black painted, single glazed selectively coated and low emissivity double glazed solar walls. Wall cavity air input temperatures are 10C, 15C and 18C**

Month	Per cent efficiencies produced at cavity air temperatures of 10C, 15C and 18C.											
	Solar wall S1			Solar wall S2			Selectively coated solar wall SC1			Low emissivity solar wall LED1		
	10 C	15 C	18 C	10 C	15 C	18 C	10 C	15 C	18 C	10 C	15 C	18 C
	September	30	21	16	27	18	13	42	35	30	51	44
October	29	21	16	26	18	13	42	36	32	50	41	38
November	21	11	5	18	8	2	35	25	19	40	29	22
December	17	3	0	13	0	0	32	13	2	27	5	0
January	10	0	0	8	0	0	28	17	10	26	4	0
February	14	7	3	12	5	1	29	22	18	35	23	19
March	20	16	13	18	14	11	35	28	19	39	31	22
April	17	10	6	15	8	4	32	24	20	39	30	24
May	42	36	31	26	19	16	40	35	30	39	32	25
Average Nov-Jan	16	5	2	13	3	1	32	18	10	31	13	7
Average Sep-May	22	14	10	18	10	7	35	26	20	38	26	20

Lancelyn type solar wall S2 which gives just 10% and 17% under the same air inlet temperature regime.

In addition to simulating solar wall performance on a typical sunny day for each month of the heating season, further simulations were performed using all the hourly solar and temperature data monitored during the 1985-1986 heating season. These results are presented in *Table 5.3*, and compare the simulated performance of a single glazed, 100 mm thick selectively coated wall SC1, with that of the Poulton Lancelyn type wall S2. The simulation results show that efficiency values obtained using sunny weather data at air inlet temperatures of 15°C (close to the overnight values in a well insulated building) correspond quite closely to the values obtained using monitored external solar, external temperature and internal temperature data throughout the year. This provides some justification for the proposition that the use of simplified computer simulation procedures should be quite acceptable for comparative purposes.

Simulations of the use of low emissivity double glazing as the transparent insulation fronting mass solar walls show that it will enhance their efficiency more than when selective coatings are used on single glazed mass walls. The greater thermal insulation provided by the low emissivity coatings which cut down the heat loss from solar walls, more than compensates for the reduced solar radiation transmission produced by the double glazing.

**Table 5.3 Computed efficiencies of solar walls using data monitored at Poulton Lancelyn. The table shows the reasonable approximation of the results of the simple simulation method to the more precise one. SC1=Selectively coated wall. S2=Poulton Lancelyn wall.**

Month	Percent efficiency at cavity air inlet temperature 15 C		Efficiency using monitored monthly weather data	
	SC1	S2	SC1	S2
September	35	18	34	18
October	36	15	33	17
November	25	8	30	14
December	13	0	16	7
January	15	0	7	1
February	22	5	17	4
March	30	14	25	10
April	24	8	20	7
May	36	19	28	15
Average Sep-May	26	10	23	10



## Conclusions

These results indicate that a solar wall composed of single glazing covering a 200 mm dark coloured brick surface, will operate with a very low efficiency during the winter in the North of England. Slightly higher efficiencies occur when ordinary double glazing is used, or the thickness of the external leaf reduced to 100 mm. The most significant improvement however, occurs when a glazed wall with an outer leaf of a material such as brick, has either its outer surface covered with a selective coating of high absorptance and low emittance. Alternatively, the single glazing can be replaced with low emissivity double glazing. It is predicted that such walls will operate with more than double the efficiency of ordinary double glazed mass solar walls without low emissivity coatings. Their performance improves at lower air temperatures, so they are well suited to heating intermittently occupied buildings, as indeed they were so used at Odeillo by Trombe.

## **5.2 VALIDATION BY MODELLING SOLAR WALLS**

### The establishment of a roof top solar wall exposure site <sup>68</sup>

The first phase in the use of the finite difference simulation program for this project has thus resulted in the identification of a superior type of solar wall: a selectively coated mass wall or a low emissivity double glazed mass solar wall; using a reduced wall thickness. Such walls will operate with greater efficiency in the heating season, the extra cost will be small, and they will be more economic.

It has been demonstrated that system specific finite difference simulation programs constitute a valuable tool for producing optimum designs for use in given climates.

In addition a south facing exposure site for solar walls would be invaluable for demonstrating in a practical manner, the validity of such predictions in a specific climate such as that of the North West of England. Insight into other problems connected with their construction, operation and durability would be extra benefits.

Such a site has been established at Clarence Street. Initially, two model solar walls were built on the roof of the School of the Built Environment building. Both were single glazed. One, simulating the solar wall at Poulton Lancelyn, had a black painted, 200 mm thick, front leaf of engineering brick. The other had a 100 mm thick, front leaf of the same brick, covered in a film of 'Maxorb'. 'Maxorb' is a black nickel foil providing a selective surface with high absorptance for solar radiation and low emittance for infra red radiation. It has a pressure sensitive, silicone based adhesive on its rear side, for ease of application<sup>69</sup>. A section through these model walls is shown in Fig 5.12. The rear leaves are well insulated with polystyrene. Instrumentation for the data logging of transducer output together with a computer for data transfer, data file handling and data interpretation were installed in a control room behind the exposure site.

In operation, air from the control room was drawn via well insulated ducting into slots at the bottom of the solar walls cavities. After solar heating, the warmed air was exhausted from the top of the cavities, using small fans. The control room could be heated, allowing the effect of changes in the air inlet temperatures to be studied. A differential temperature controller, designed specifically for the task of switching the fans on when the temperature of the air at the top of the cavity exceeded that of the room air, was an

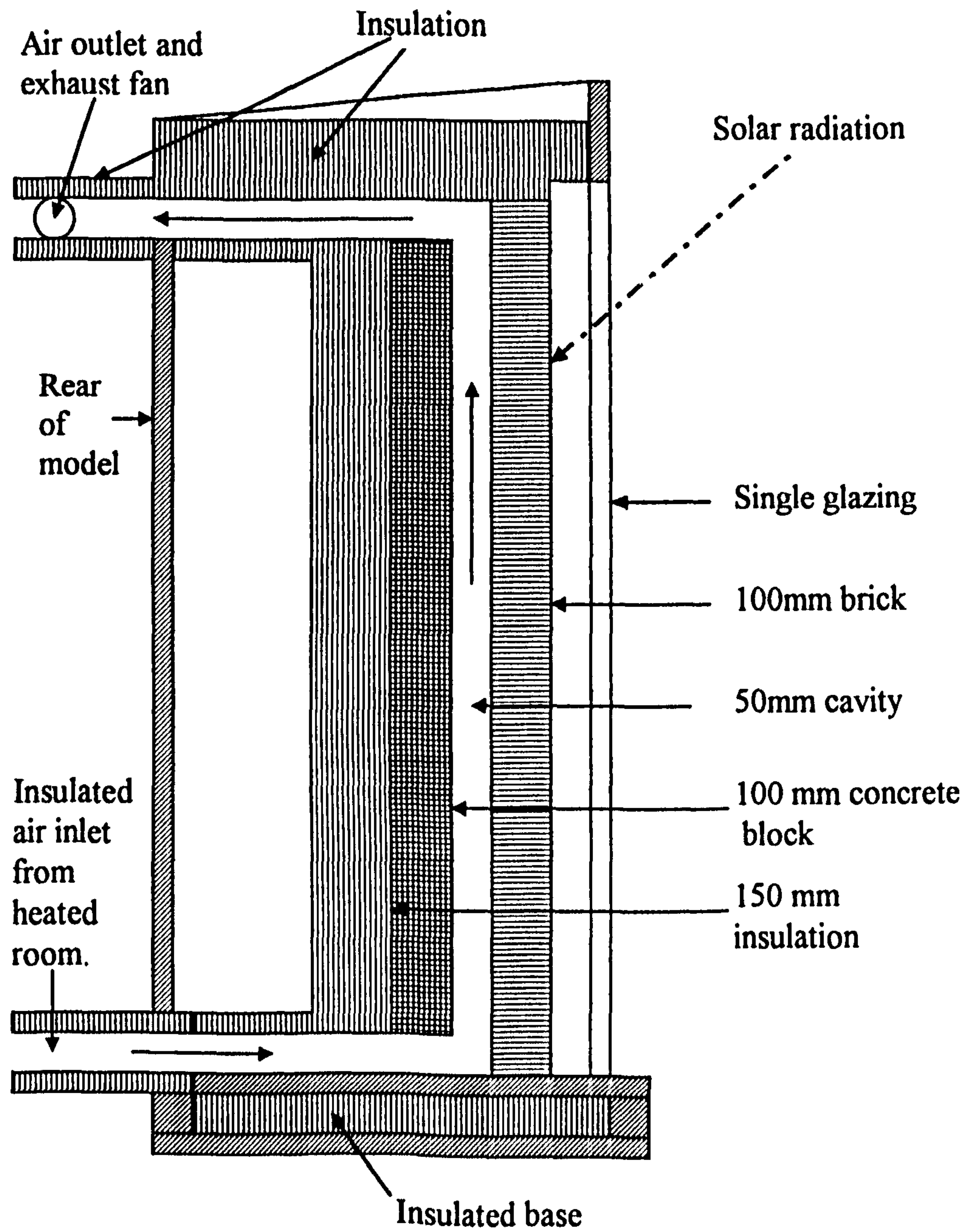


**Fig. 5.12** Section through a model solar wall. The area of the insulated mass wall surface is  $0.55 \text{ m}^2$ .

important feature of this installation (see *Appendix 2*). Differential temperatures between the two ducts, were measured using thermopiles of 6 thermocouples in series, which produced an accuracy to within  $\pm 0.1^\circ\text{C}$ . Other wall temperatures were measured with single thermocouples.

Tests were conducted in January 1987. Meteorological data from one of the test days was used as input to the computer simulation program to determine efficiencies for the two pertinent solar wall types, at various temperatures of the air entering the wall cavities. A graph was then drawn of computed efficiency versus  $\overline{\Delta T}/H$ , (see **Fig 5.13**). The outlet and inlet air temperature differences produced by solar heating and the average hourly irradiation values on the solar wall surface, were recorded throughout January. Air inlet temperatures were kept constant throughout each day.

Experimentally determined values of  $\overline{\Delta T}/H$  were then calculated for each days observations. Efficiencies were obtained from the ratio of daily energy production per unit area of collector to the daily solar irradiation  $H$ . The daily energy production was obtained by summing hourly energy values. The latter were obtained from the product of the specific heat of air, the air flow rate through the cavity, the temperature differential of inlet and outlet air and the fraction of time in an hour that the fan delivers energy.

Experimental values obtained for the efficiency of the model walls are also plotted in **Fig 5.13** for various values of  $\overline{\Delta T}/H$ . Scatter is evident, and expected, for monitoring took place over the whole of January, whereas the computer simulation uses the weather data for a single sunny day during that month. Nevertheless experimental and computed results agree quite well. For the selectively coated wall the results agree to within circa  $\pm 18\%$ , at air inlet temperature  $10^\circ\text{C}$ , to within  $12\%$  at  $15^\circ\text{C}$ . The use of simplified



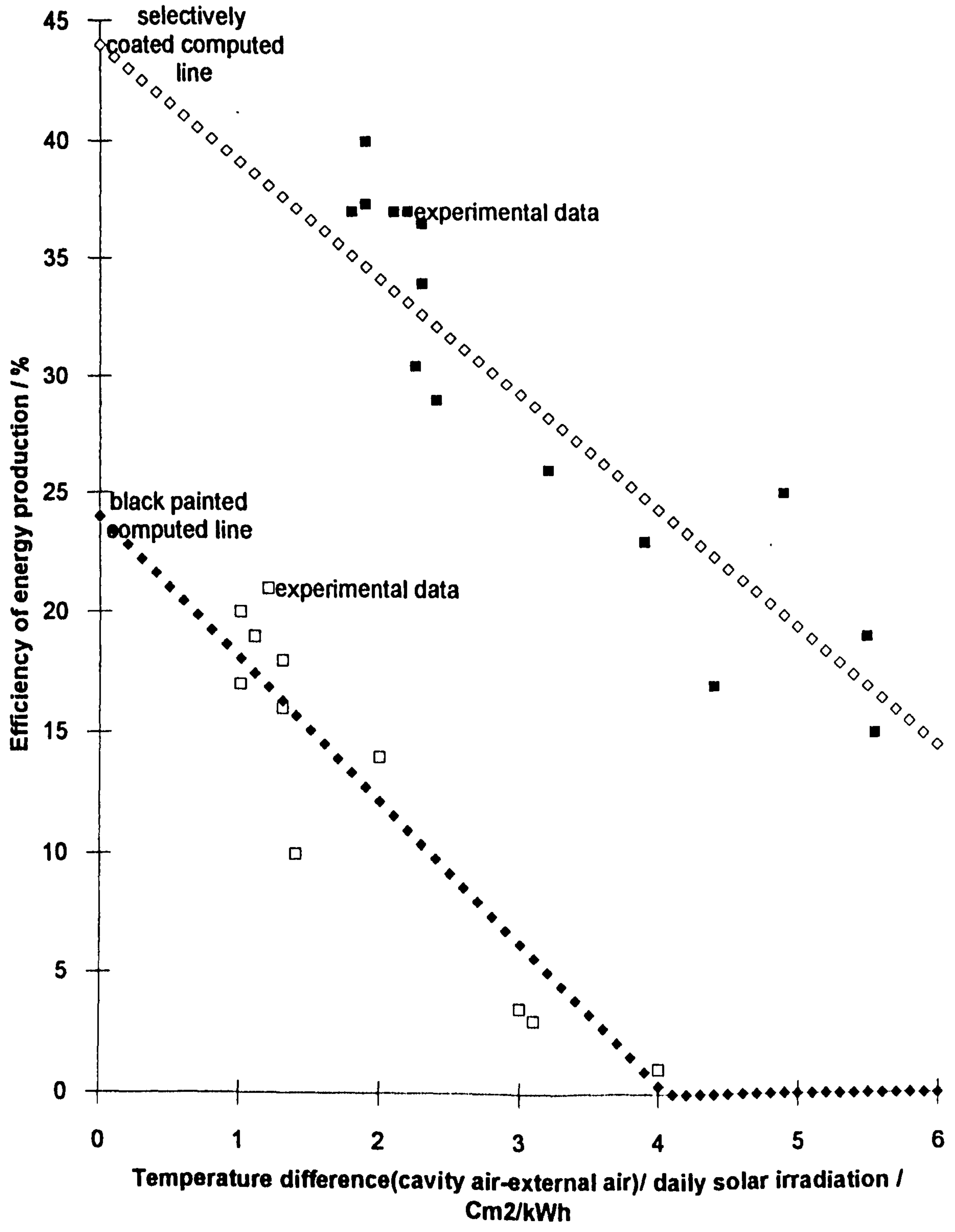


Fig. 5.13 Experimental and computed data for solar wall efficiency.

simulation procedures to predict the performance of solar walls has been convincingly supported. The same is true for the prediction that selective coatings or low emissivity double glazing in conjunction with thinner walls offers a promising approach to the production of efficient and therefore economically viable solar walls for use in northern latitudes.

### 5.3 ECONOMIC ASSESSMENT

Walls with low emissivity double glazing or selective coatings are more efficient than untreated glazed solar walls. If such walls have the potential to establish themselves as worthwhile passive solar components at high latitudes they should be able to payback their construction costs in a reasonable period of time. Accordingly an economic assessment has been performed with simple payback periods and NPV/K (net present value per unit capital cost) as the chosen indicators<sup>68</sup>.

#### **The energy produced by solar walls**

The amounts of seasonal energy produced by such walls is obtained by computer simulation, using weather data obtained during monitoring in the Wirral. Results of such simulation are shown in *Table 5.4*. The cost of the fuel saved, (as gas or electricity) is estimated assuming 100% utilisation and the fuel prices in *Table 6.7*.

**Table 5.4 Efficiencies of energy production, and the energy produced in kWh/m<sup>2</sup> from solar walls at various air inlet temperatures.**

<b>Cavity air inlet temperatures-&gt;</b>	10 C	10 C	15 C	15 C	18 C	18 C	<b>Using temperatures monitored at the low energy school</b>	
<b>Solar wall type--&gt;</b>	NSC	SC	NSC	SC	NSC	SC	NSC	SC
<b>% efficiency</b>	18	35	10	26	7	20	10	23
<b>Sept-May</b>								
<b>Energy produced</b>	100	182	57	136	45	110	57	123

SC=selectively coated wall      NSC= no selective coating

### The extra cost of a solar wall <sup>70</sup>

The extra costs of applying single glazing, selectively coated foils or low emissivity double glazing to 1 m<sup>2</sup> of a brick cavity wall are shown in *Table 5.5*.

### Economic assessments [see *Appendix 1*] <sup>71</sup>

#### Payback

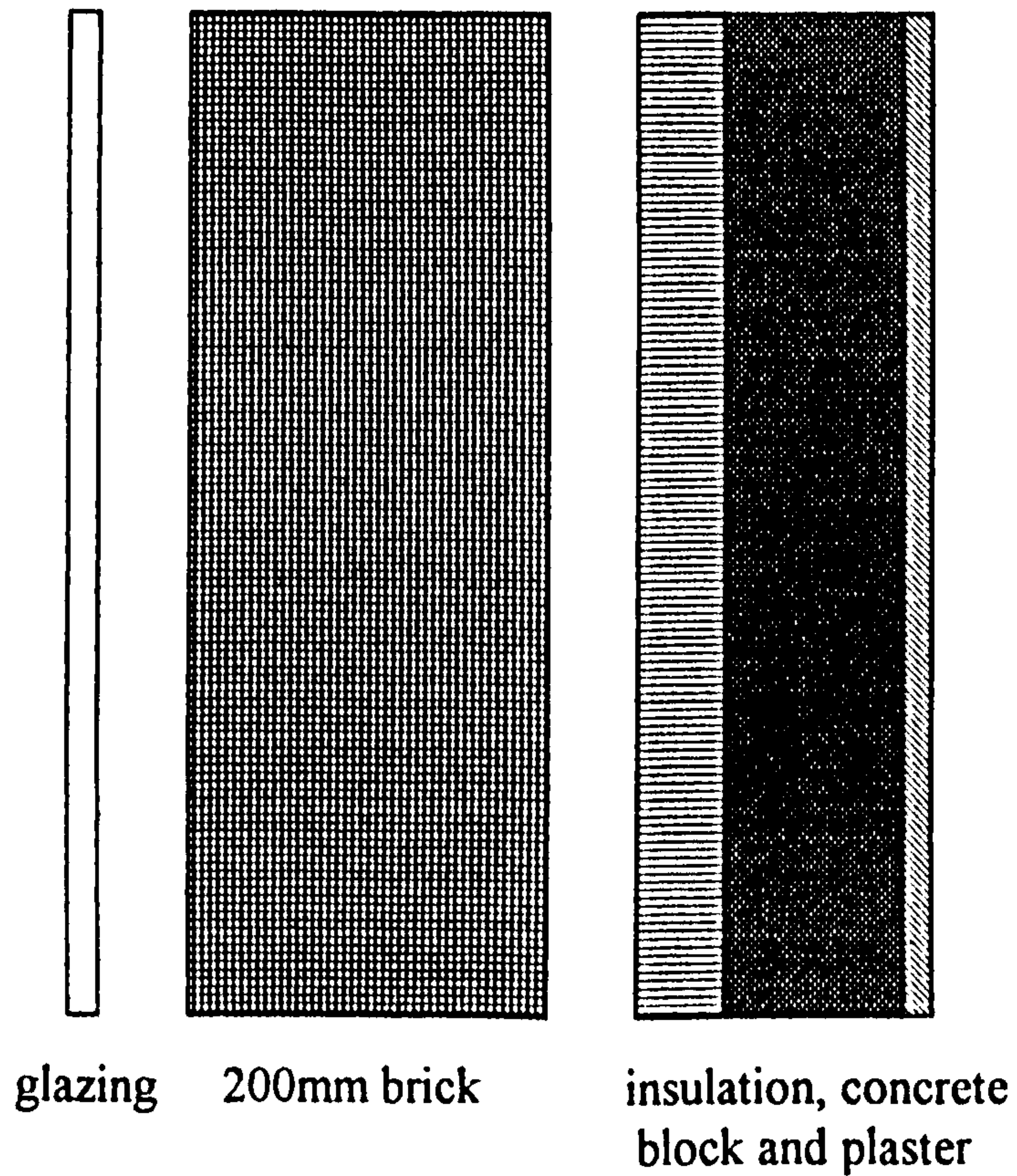
Simple payback times (the extra cost of a measure divided by the annual cost of energy saved by the use of that measure) were easily evaluated. They are shown in *Table 5.6* for two types of energy substitution (electricity or gas). Payback periods of 10 years are often used as a criteria of cost effectiveness for an energy conservation measure. On this basis, selective coatings and low emissivity double glazing produce cost effective solar walls, when used to supplant electricity but not when used to supplant natural gas, which is too cheap a fuel.

#### NPV/K

The net present value per unit of capital cost (NPV/K), takes into account all the costs and benefits of an energy project and gives a true measure of economic worth <sup>71</sup>. Results using this indicator are shown in *Table 5.7*, for different air inlet temperatures as before. In the evaluation of NPV/K, a 3% real rise in fuel costs per annum, a 5% annual discount rate, and a 30 year lifetime for the solar wall are assumed. NPV/K values greater than +1 represent good rates of return (greater than twice the invested capital regained). On



**Table 5.5(a) Extra costs incurred in solar wall construction in comparison to the cost of a well insulated reference cavity wall**

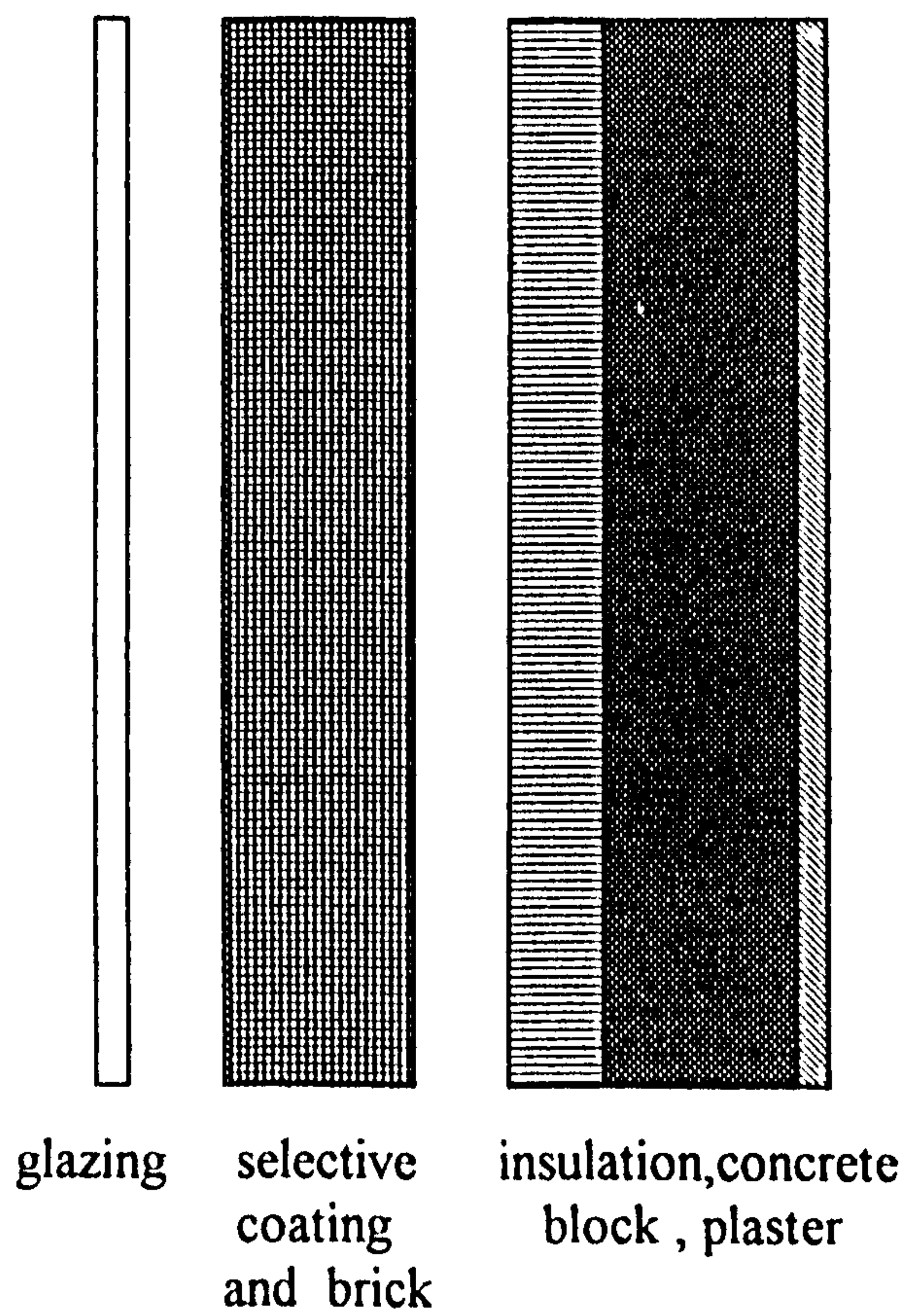


Poulton Lancelyn type uncoated solar wall based on 200mm brick outer leaf.

Extra cost

Single glazing	£13.17/m <sup>2</sup>
Frame	£34.00/m <sup>2</sup>
Extra brick	£27.61/m <sup>2</sup>
<b>Total</b>	<b>£74.78/m<sup>2</sup></b>

**Table 5.5(b) Extra costs incurred in solar wall construction in comparison to the cost of a well insulated reference cavity wall.**

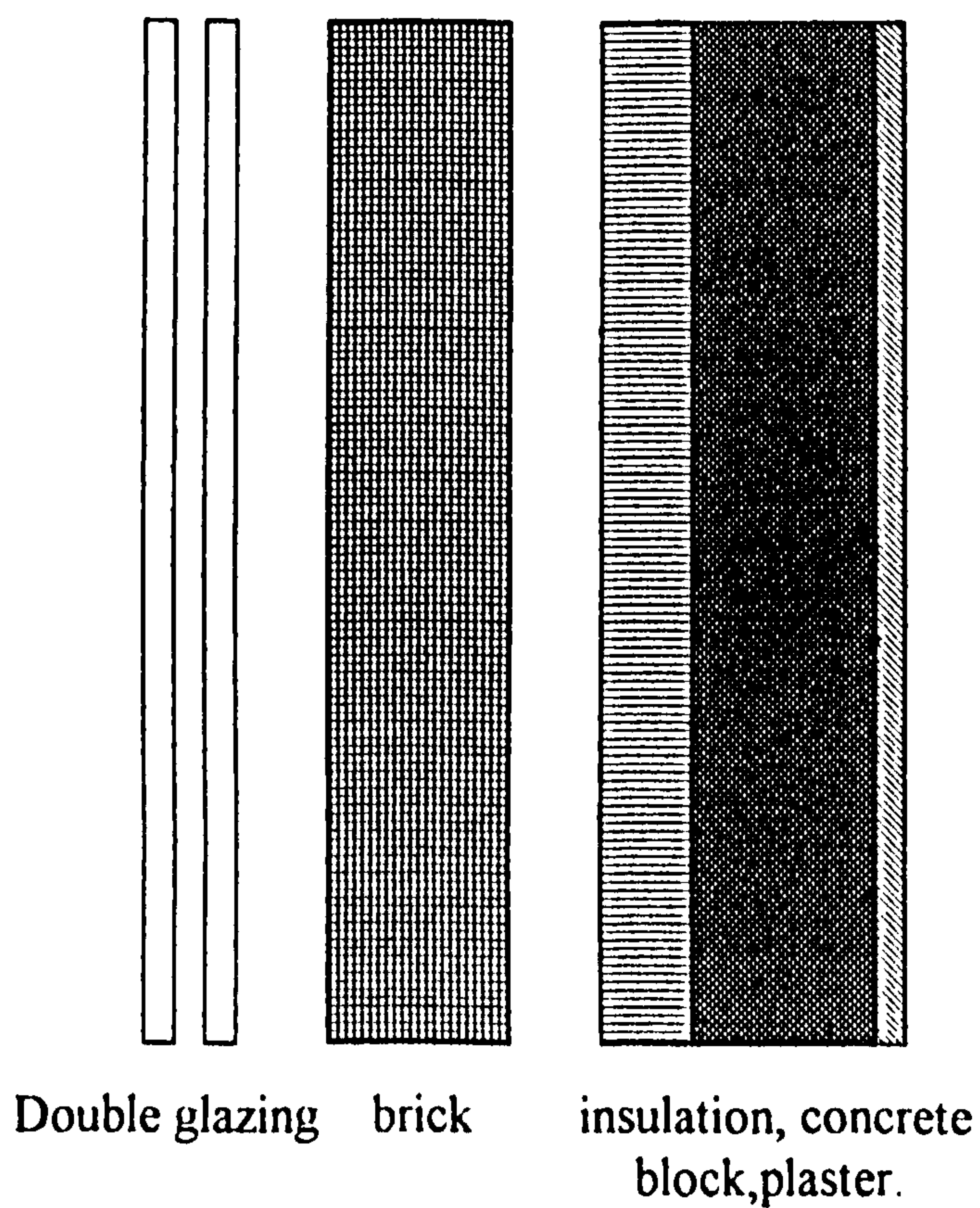


Selectively coated solar wall ( based on 100mm brick outer leaf).

Extra cost:

Single glazing and frame	£47.11/m <sup>2</sup>
Selective coating/foil/ adhesive	£14.8/m <sup>2</sup>
Total	£61.91/m <sup>2</sup>

**Table 5.5(c) Extra costs incurred in solar wall construction, versus a well insulated reference cavity wall.**



Low emissivity double glazed solar wall (based on 100mm brick outer leaf)

Extra cost:

Low emissivity double glazing and frame: £88.3/m<sup>2</sup>

Total: £88.3/m<sup>2</sup>

**Table 5.6 Payback periods (in years) for mass solar walls at different air inlet temperatures.**

Cavity air inlet temperatures->	10 C		15 C		18 C		Using temperatures monitored at the low energy school	
	Gas	Electricity	Gas	Electricity	Gas	Electricity	Gas	Electricity
NSC wall	36	14	60	23	67	29	60	23
SC wall	16	6	21	8	26	10	23	9
LEDG wall	23	8.5	30	11	37	14	33	13



**Table 5.7 NPV/K values for a three per cent rise in real fuel costs, a five per cent discount rate and a thirty year lifetime, at different air inlet temperatures.**

Cavity air inlet temperatures->	10 C		15 C		18 C		Using temperatures monitored at the low energy school	
	Gas	Electricity	Gas	Electricity	Gas	Electricity	Gas	Electricity
NSC wall	0	0.9	-0.4	0.6	-0.5	0.2	-0.4	0.6
SC wall	0.5	2.8	0	1.7	-0.2	1.3	0	1.6
LEDG wall	0.05	1.7	-0.3	0.9	-0.4	0.6	-0.3	0.8

this criterion, non selectively coated walls perform poorly, but selectively coated and low emissivity double glazed walls perform well when displacing electricity (but not gas).

When low values of NPV/K occur, the measure is hardly worthwhile with NPV/K=0 representing a break even situation. Non selectively coated walls for example never show a good rate of return under any circumstance.

## **5.4 CONCLUSIONS**

Selectively coated and low emissivity double glazed walls are cost effective (and produce more than double the energy of solar walls without such low emissivity coatings) when used to supplant electricity. They are not cost effective when used to replace natural gas. Natural gas, used for heating by 75% of households in the UK, is too cheap at present for these solar walls to be competitive in Northern latitudes.

# **CHAPTER SIX - TRANSPARENT INSULATION**

## 6.1 INTRODUCTION

In northern latitudes, daily irradiation on south facing surfaces is more than sufficient to compensate for the heat loss which occurs through them. As solar heat passes through a mass wall, heat loss from the front surface reduces the efficiency of the process.

Reduction of this heat loss by using single or double glazing to insulate the front surface produces a solar wall of moderate efficiency. The superior insulation provided by transparent honeycomb and capillary structures (see **Fig 6.1**) gives much better performance. These structures compartmentalise the low conductivity air or argon within them suppressing the convection heat losses that occur within the air gap of double glazing. A typical transparently insulated wall construction is shown in **Fig 6.2(a)**, and its functions illustrated in **Fig 6.3**. Jesch (1993) has produced a review of the field <sup>72</sup>.

To successfully produce solar walls of high efficiency a transparent insulation material should possess the following attributes:

- High optical transmission.
- Low thermal radiation transmission.
- Low thermal conductivity.
- Convection suppression.

Honeycomb or capillary structures made from thin wall polycarbonate, fronted by glazing fulfil these requirements.



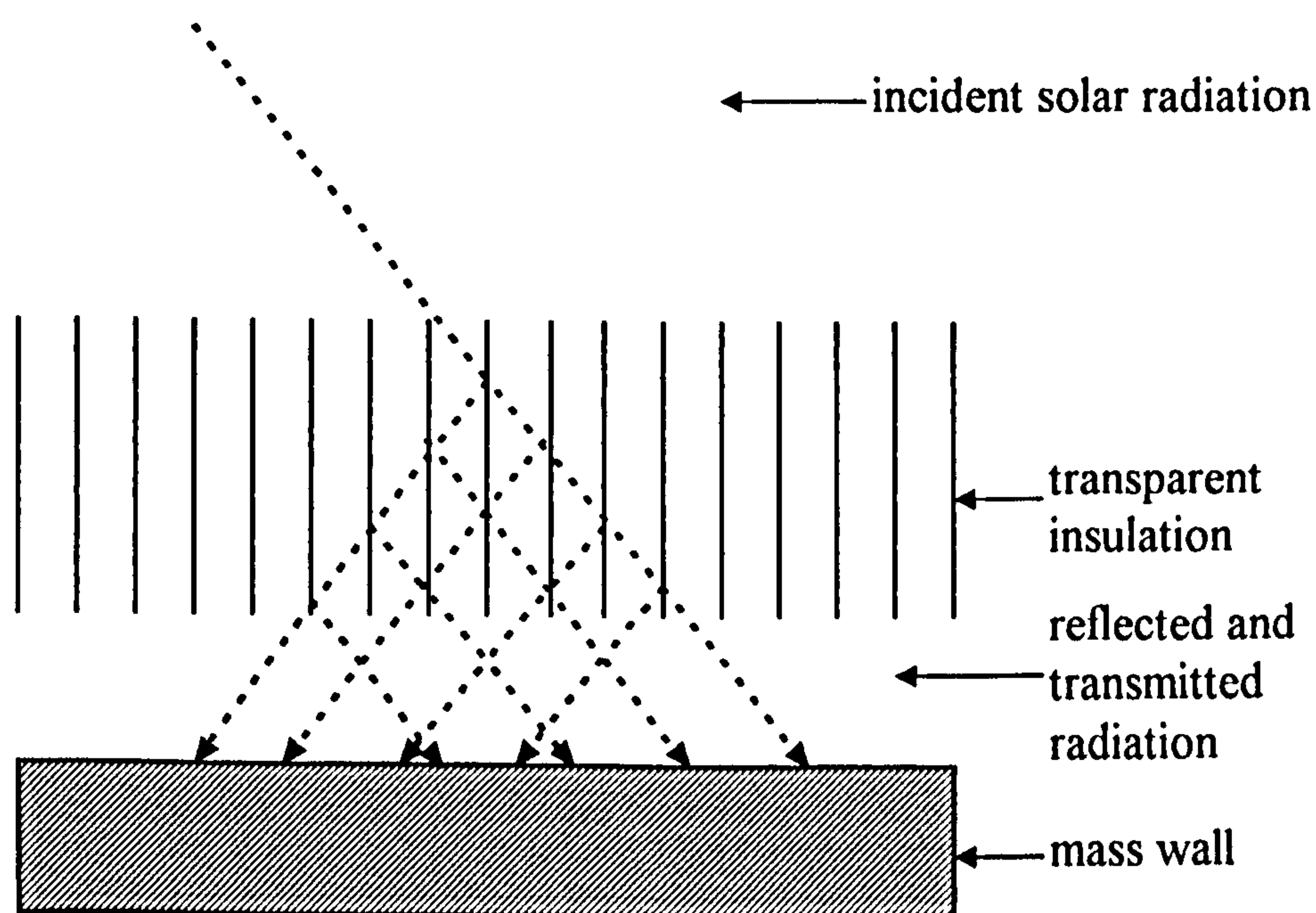


**Fig 6.1 Functioning of honeycombs or capillaries of transparent insulation material (TIM) with respect to solar radiation transmission.**

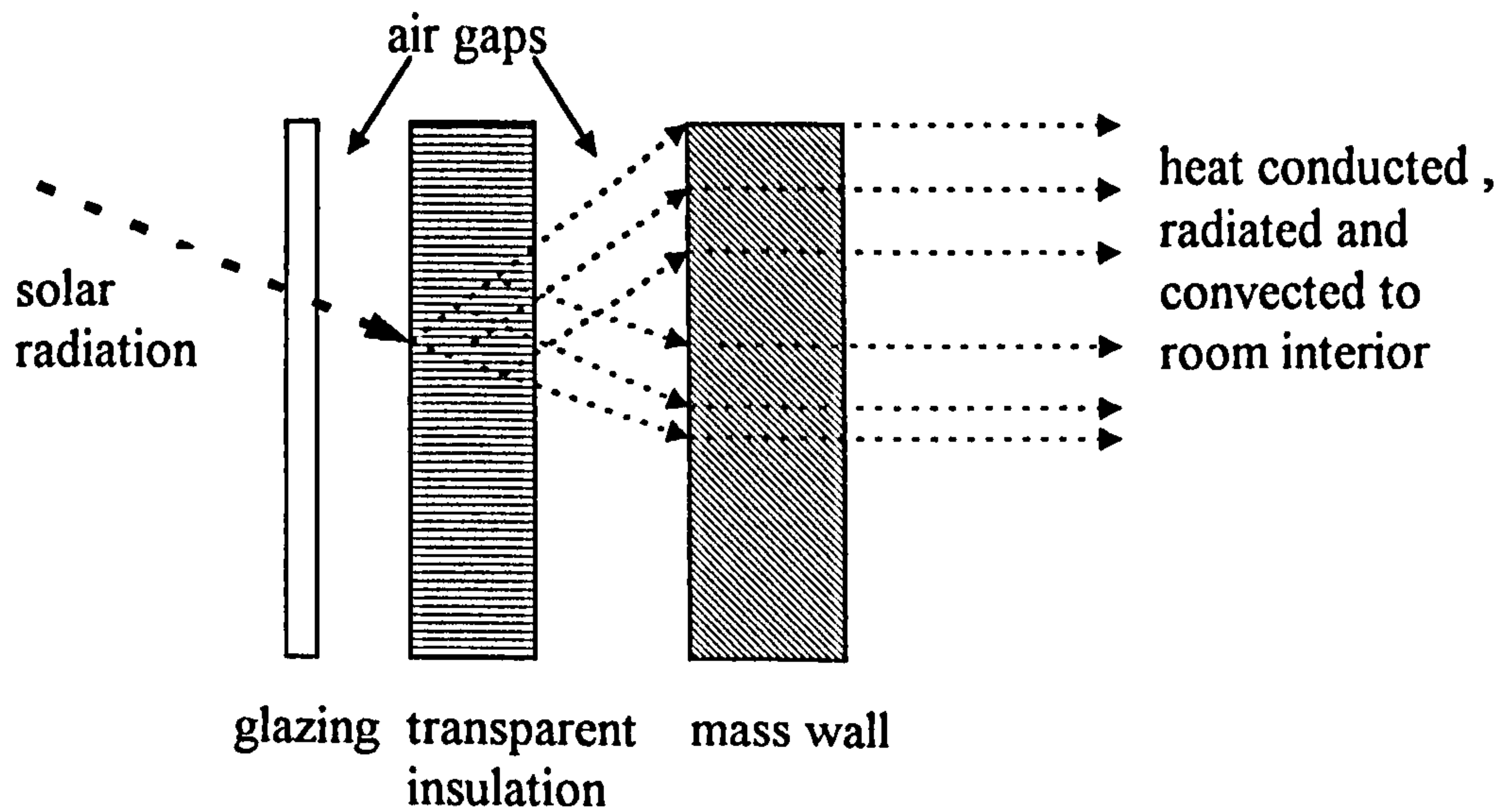


**Fig. 6.2(a) General principle underlying heat transmission in transparently insulated solar walls.**

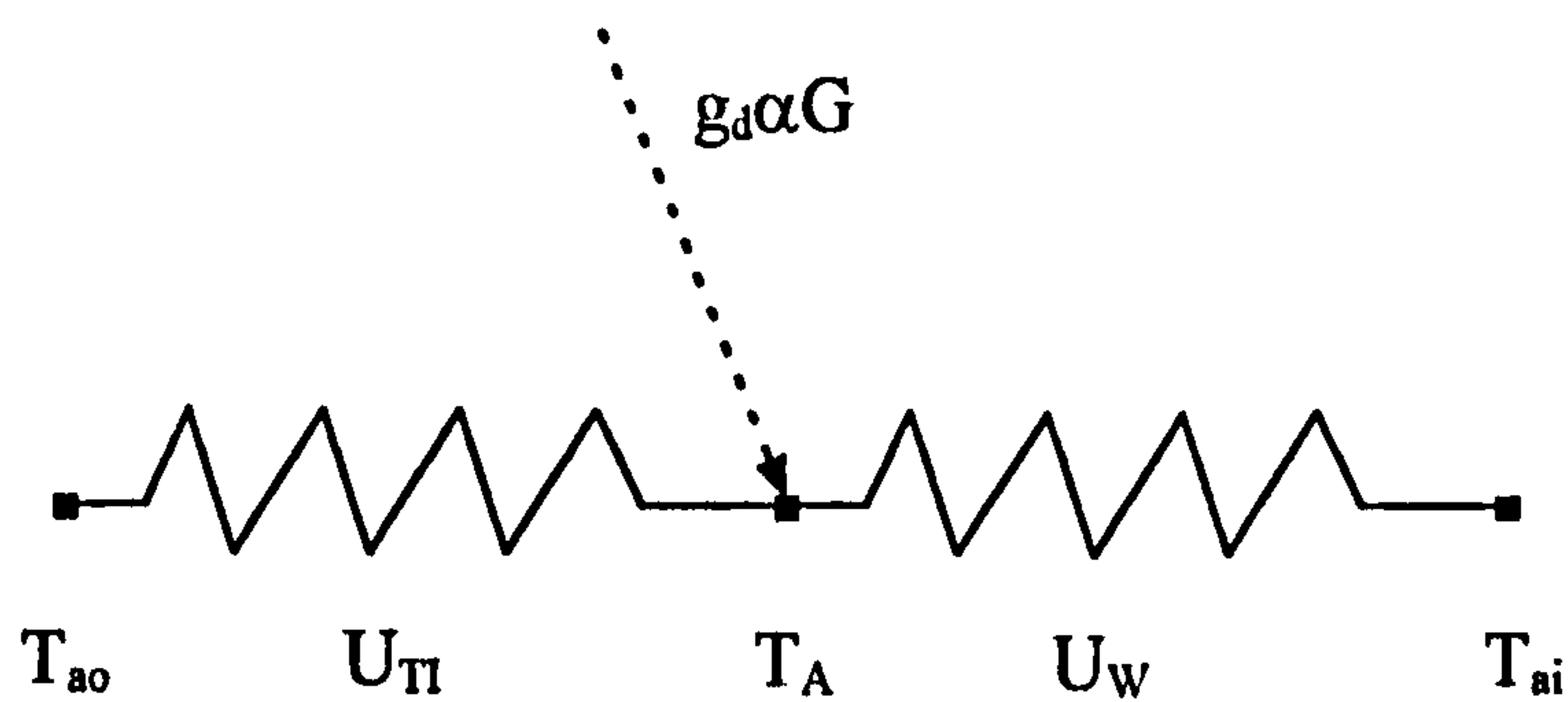
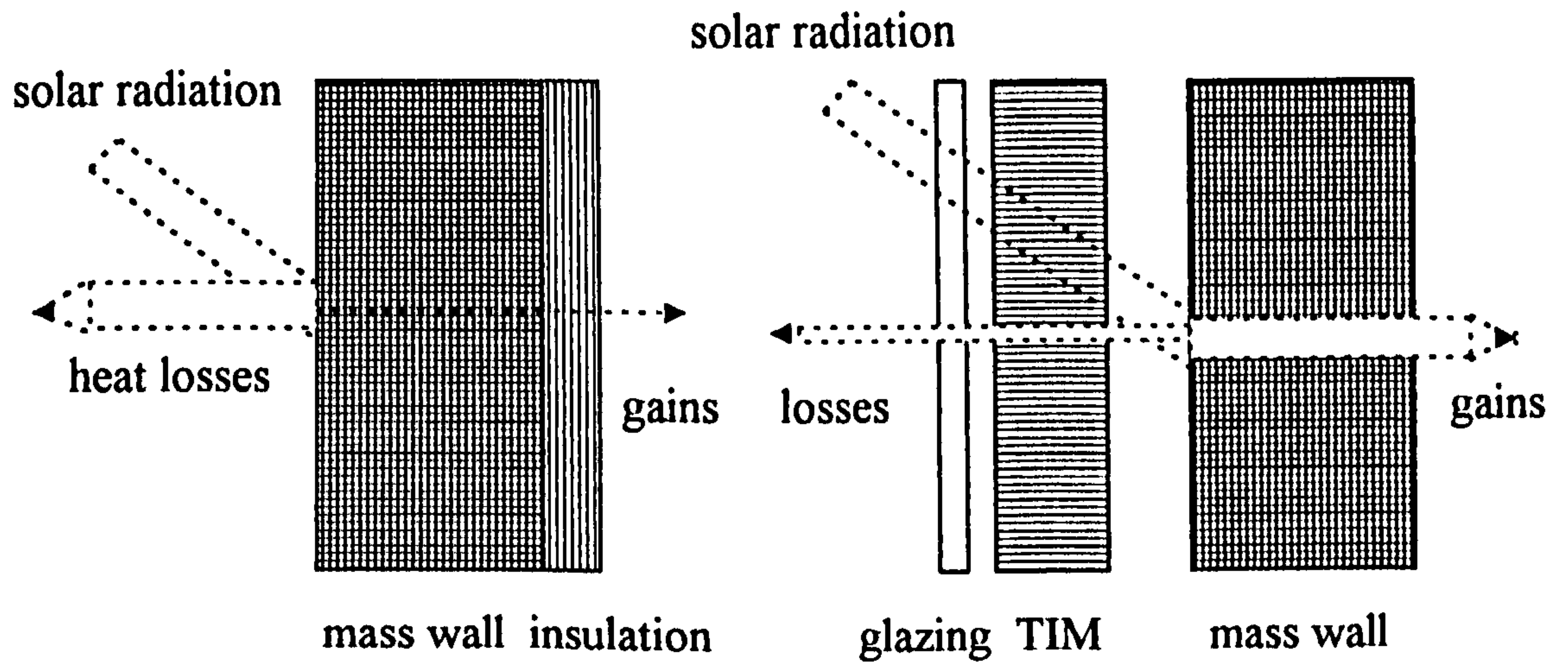
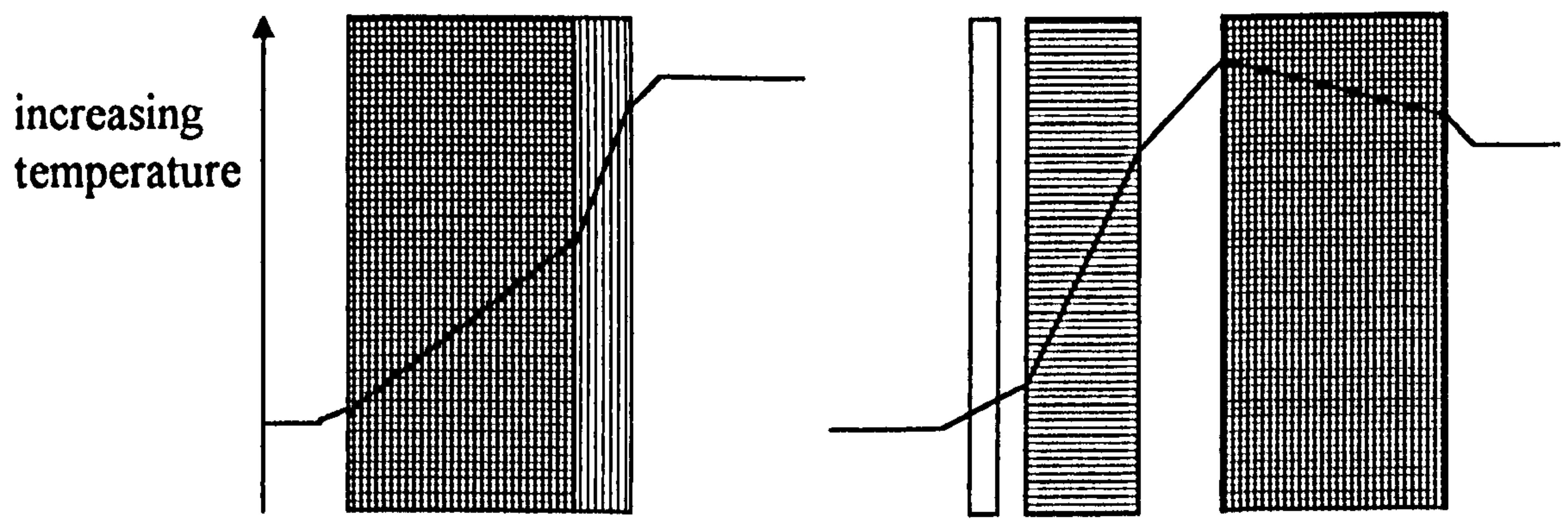


**Fig.6.2(b) The thermal equivalent circuit for a transparently insulated solar wall.**

- $U_{TI}$  = heat transfer coefficient of the TI element
- $U_W$  = heat transfer coefficient of the mass wall
- $T_{ai}$  = internal air temperature
- $T_{ao}$  = external air temperature
- $T_A$  = outer mass wall surface temperature
- $G$  = global radiation flux density on the outer glazing
- $g_d$  = total diffuse energy transmittance of the TI elements
- $\alpha$  = solar absorptivity of the mass wall
- $\eta_o$  = solar conversion efficiency of the TI element and associated construction



Heat fluxes passing through normal and TI walls



Temperature profiles through normal and TI walls in sunny weather

**Fig. 6.3 Comparative functioning of opaque and transparent insulated mass walls with respect to the heat fluxes and temperature distributions involved.**

## Basic principles

The first outdoor experiments with transparently insulated walls, were conducted in 1982, by the Fraunhofer Institute for Solar Systems, Freiburg, Germany<sup>73</sup>. **Fig 6.2(b)** shows the appropriate equivalent circuit for such a wall and defines the symbols used. Using this circuit it can be shown that the maximum solar conversion efficiency  $\eta_o$  of a transparently insulated wall under steady state conditions is:

$$\eta_o = g_d \alpha U_w / (U_{T1} + U_w) \quad (6.1)$$

where the solar conversion efficiency of the wall is defined as the ratio of heat flux density through the wall and global radiation flux density on the outer glazing of the TI element.

The rate of heat loss per square metre from this wall is then:

$$q_w = [U_{T1} U_w / (U_{T1} + U_w)] (T_{ai} - T_{ao}) - \eta_o G \quad (6.2)$$

The efficiency will increase if high values of the transmittance absorptance product ( $g_d \alpha$ ) and low values of the heat transfer coefficients of the transparently insulated element ( $U_{T1}$ ) are used. If values of the diffuse energy transmittance ( $g_d$ ) and the heat transfer coefficients of different glazing elements are inspected in **Fig 6.4**, it is seen that a system composed of 100 mm transparent insulation material plus glazing, possesses the best combination of these two criteria in comparison with other systems investigated. A system possessing such properties, should produce high efficiency when used in solar walls. **Fig 6.5** confirms this prediction. There, the transparently insulated wall is seen to produce higher efficiencies than any other available system investigated. Vacuum glazing has the potential to be even better, but at present is not commercially available.



**Fig. 6.4 Typical U values and total diffuse energy transmittance for glazings with or without TIM**

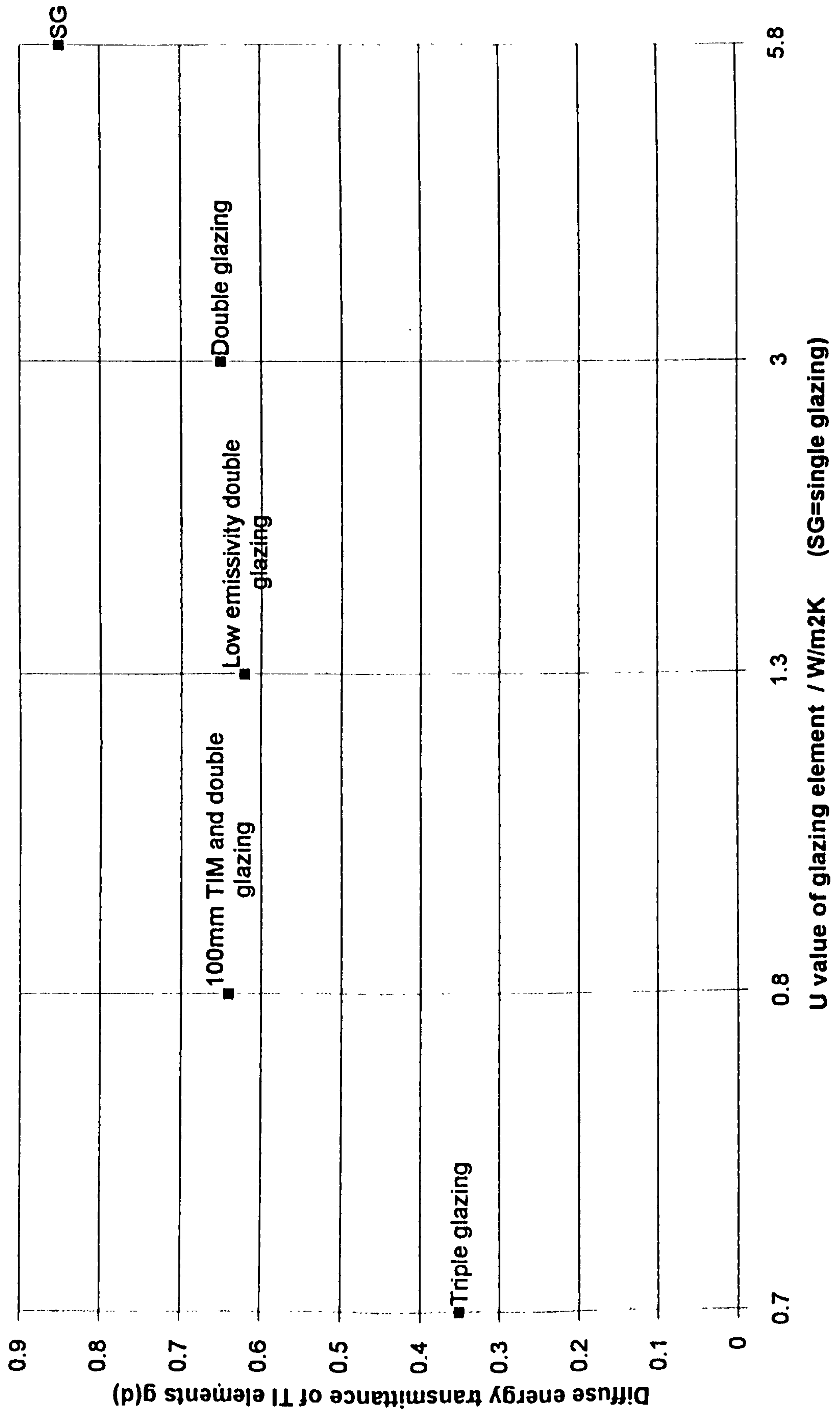
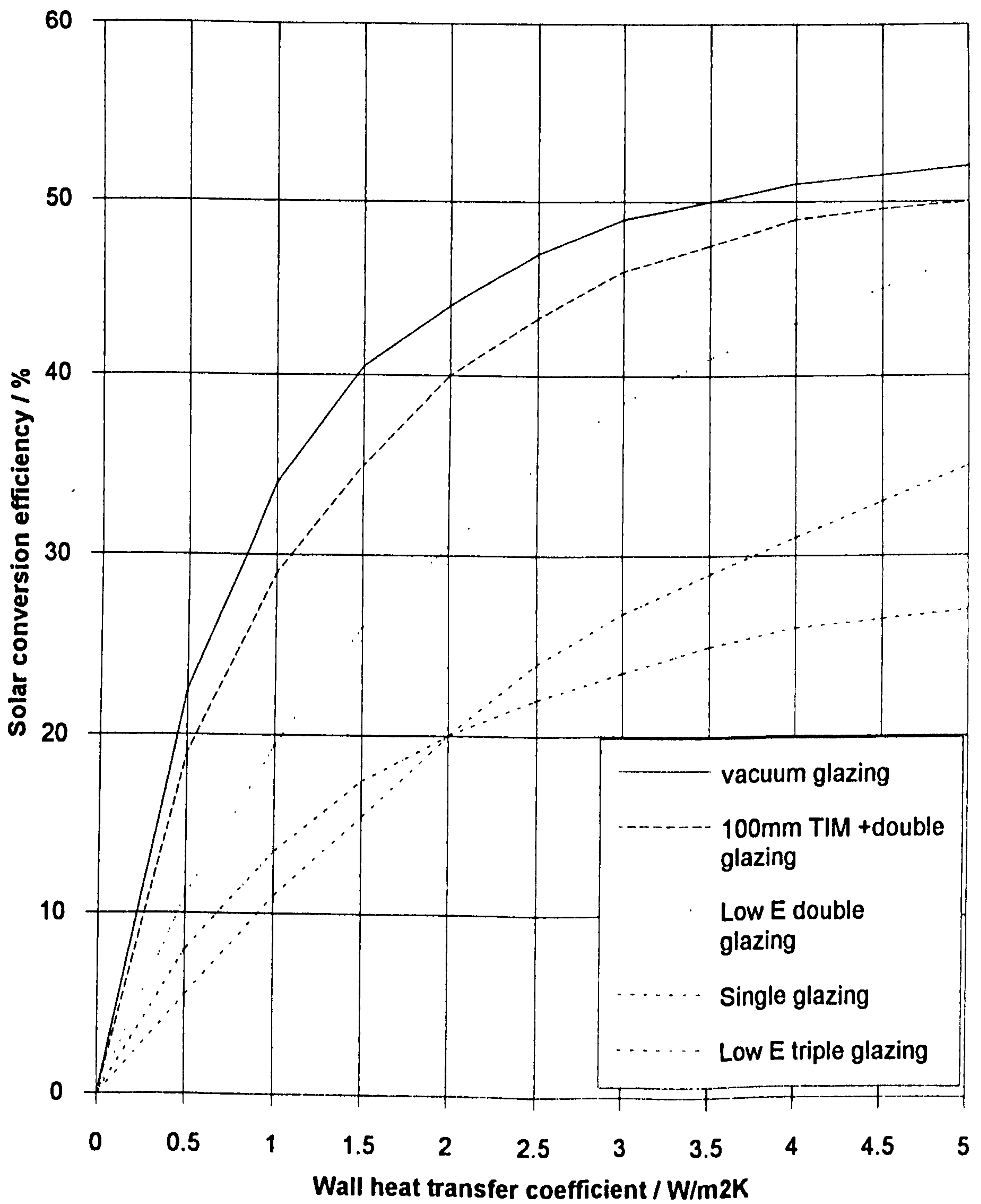


**Fig 6.5 Solar conversion efficiencies for different types of transparently insulated solar walls of absorptance 0.9**



When honeycomb or capillary transparent insulation is used, the efficiency of single glazed Trombe walls is raised from 10-15% to over 30%. Such high efficiency values have revived interest in the use of solar walls for space heating. Such transparently insulated walls achieve efficiencies surpassing those of any other solar space heating system. They satisfy the requirements of passivity in that they require no auxiliary energy for their operation.

Further quantification of transparently insulated wall performance is often made by defining an effective heat transfer coefficient  $U_{eff}$  for the wall. The value of  $U_{eff}$  is less than the normal value used for opaque walls because of the effects of solar heat transfer through the transparent material. Its value is calculated from:

$$U_{eff} = \frac{q_w}{(T_{ai} - T_{ao})} = \frac{U_{\pi}U_w}{(U_{\pi} + U_w)} - \frac{N\eta_g G}{(T_{ai} - T_{ao})} \quad (6.3)$$

where  $N$  is a utilisation factor, used if solar gain exceeds requirements.

From the above equation, energy flows in transparently insulated walls can be found, using appropriate temperature differences and integration over time to yield

$$Q_{eff} = Q_w - NQ_{solar} \quad (6.4)$$

where:

$Q_{eff}$  = energy balance of the T1 wall.

$Q_w$  = energy loss of the T1 wall.

$Q_{solar}$  = maximum possible solar energy gained by T1 wall.

$N$  = solar energy utilisation factor.

As a temperature wave passes through a solar wall, it is attenuated according to the equation:

$$T(x,t) = \exp(-x/\delta)\cos(\omega t - x/\delta) \quad (6.5)$$

where:

$$\delta = \sqrt{2\lambda / \omega C_v}$$

$\lambda$  = thermal conductivity

$\omega$  = angular frequency

$C_v$  = specific heat per unit volume of mass wall

$x$  = space coordinate perpendicular to the wall surface

$t$  = time

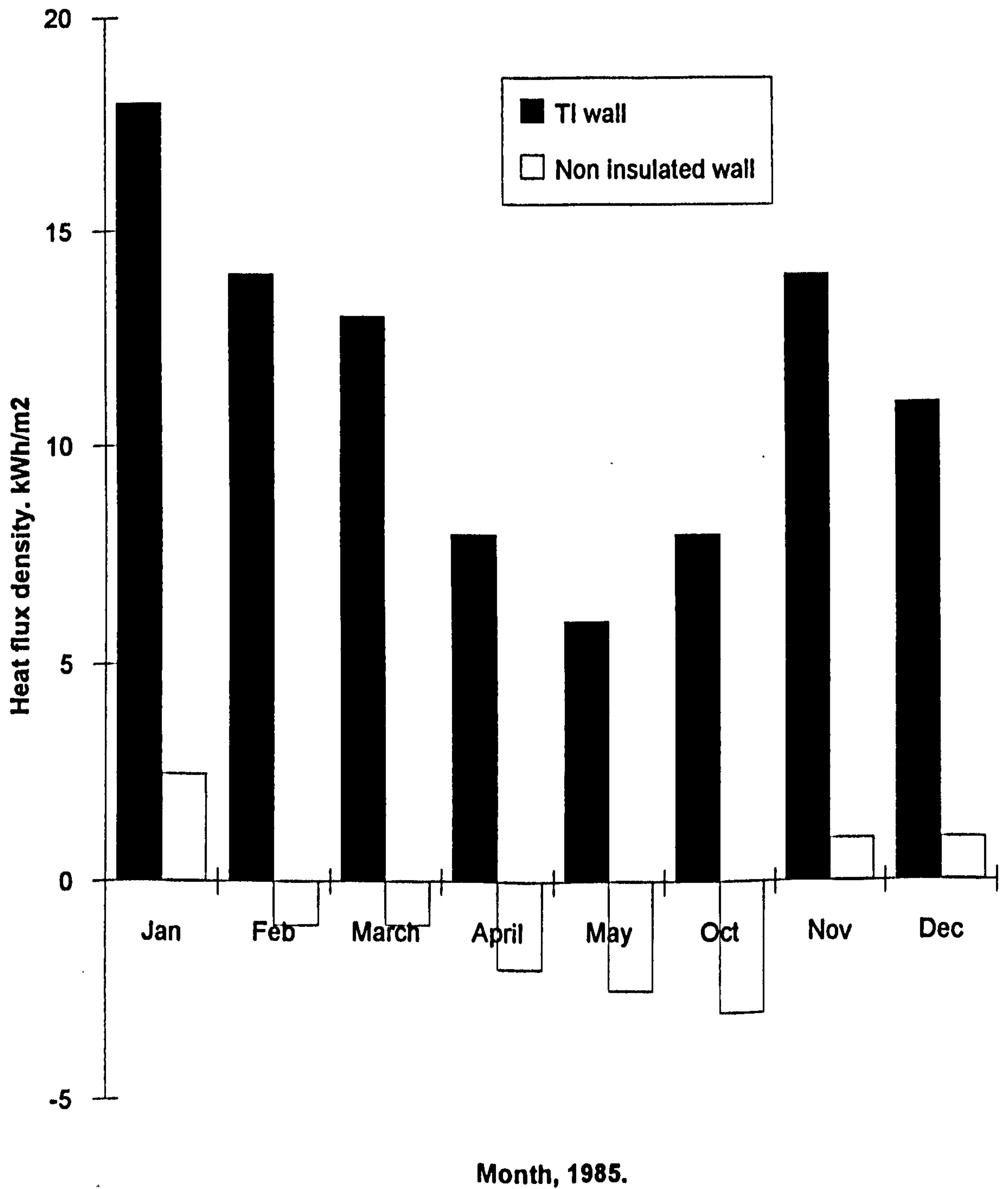
Use of this equation shows that the temperature of a 150 mm thick mass wall is attenuated by 40%, and time delayed by 3.6 hours as the temperature wave passes to the interior. Transparently insulated walls with their high efficiency should thus be well suited for use with direct gain windows in passive solar systems. The instant daytime gains from the windows are complimented by the delayed evening gains from the transparently insulated walls.

## 6.2 TRANSPARENT INSULATION IN PRACTICE

As stated the first experiments with transparently insulated walls were made by the Fraunhofer Institute for Solar Energy Systems<sup>73</sup>. In Fig 6.6 the monthly integrated values obtained from a heat flux meter placed on a transparently insulated wall are compared with the monthly heat losses from an uninsulated wall. Without transparent



**Fig. 6.6 Comparison of monthly integrated values of the heat flux density through the west oriented TI wall, compared to a non insulated wall in Freiburg, Germany.**



insulation there is continual heat loss. With transparent insulation the energy balance becomes negative and the wall gains energy from solar radiation throughout the year.

In 1983, the German Ministry for Research and Technology, started a transparent insulation research program, funding 19 transparent insulation material demonstration projects. One of the most interesting commenced in 1989<sup>74</sup>. This was the Self Sufficient House Project, which aimed to show the high potential of transparent insulation elements (see Fig 6.7) to meet space heating demand. The building was completed in 1992.

Without any fossil fuel input, without electricity grid connection, all energy needs in this house are supplied from the solar radiation falling upon it. Photovoltaic modules supply electricity for lighting and appliances. This electricity also generates a mixture of hydrogen and oxygen from water to produce a source of auxiliary heat. When opaque insulation is used, the best shape for a building to have in order to minimize heat loss is cubic. With transparent insulation material the best shape is one to maximize solar gain. Such a shape should be elongated along the southern facade in the northern hemisphere. The shape chosen for the Self Sufficient House was that of a sector of a circle, facing south. *Table 6.1* indicates the calculated heating demand for several different shapes. A semi circular shape combined with transparent insulation material has a heating demand which is only a small percentage of the demand of a normal building (*Table 6.2*). The house has proved very successful in operation. Its single glazed transparently insulated solar walls work with an overall solar conversion efficiency of 50%. A glance at *Table 6.3* indicates the incredibly low amounts of energy actually consumed in the house for space heating. *Fig 6.8* shows the indoor temperatures experienced throughout the heating season. Roller blinds are positioned between the glazing and the transparent insulation in this installation, to prevent overheating, for Freiburg at 48°N is further south than the UK.

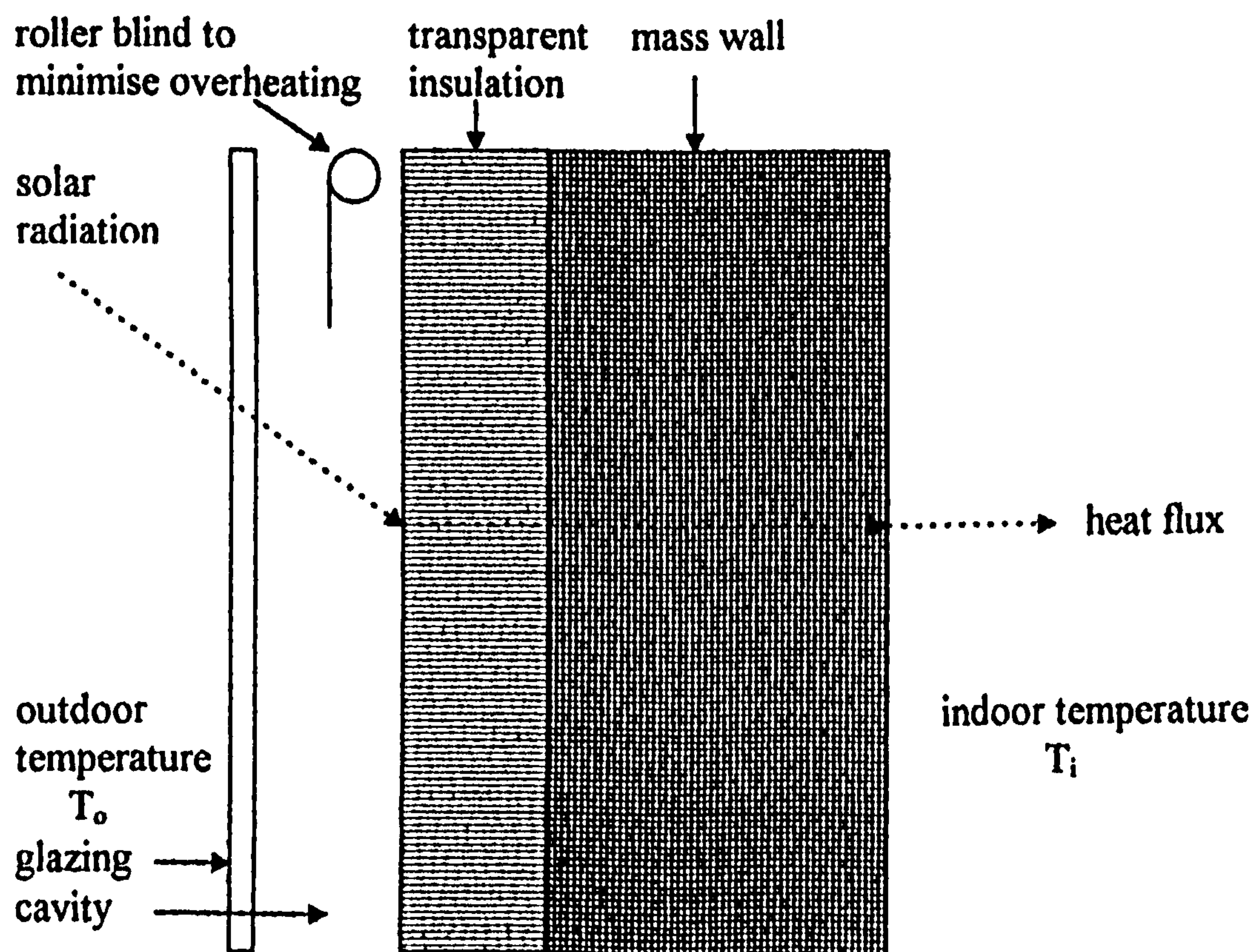


Fig. 6.7 TI principle as used in the self sufficient solar house in Freiburg, Germany.

**Table 6.1 Space heating demand of buildings having various ground plans with TI insulation applied to east, south and west orientations**

Plan	Insulation type	Location of insulation	Space heating demand kWh/yr	Space heating demand as % of opaque situation
10mx10m	opaque	all surfaces	3500	100
10mx10m	TI	E,S,W	440	13
16m(S)x6.25m	TI	E,S,W	290	8
Semi-circular	TI	E,S,W	250	7

**Table 6.2 Irradiation and wall heat loss data for  
Manchester (53.21 N)**

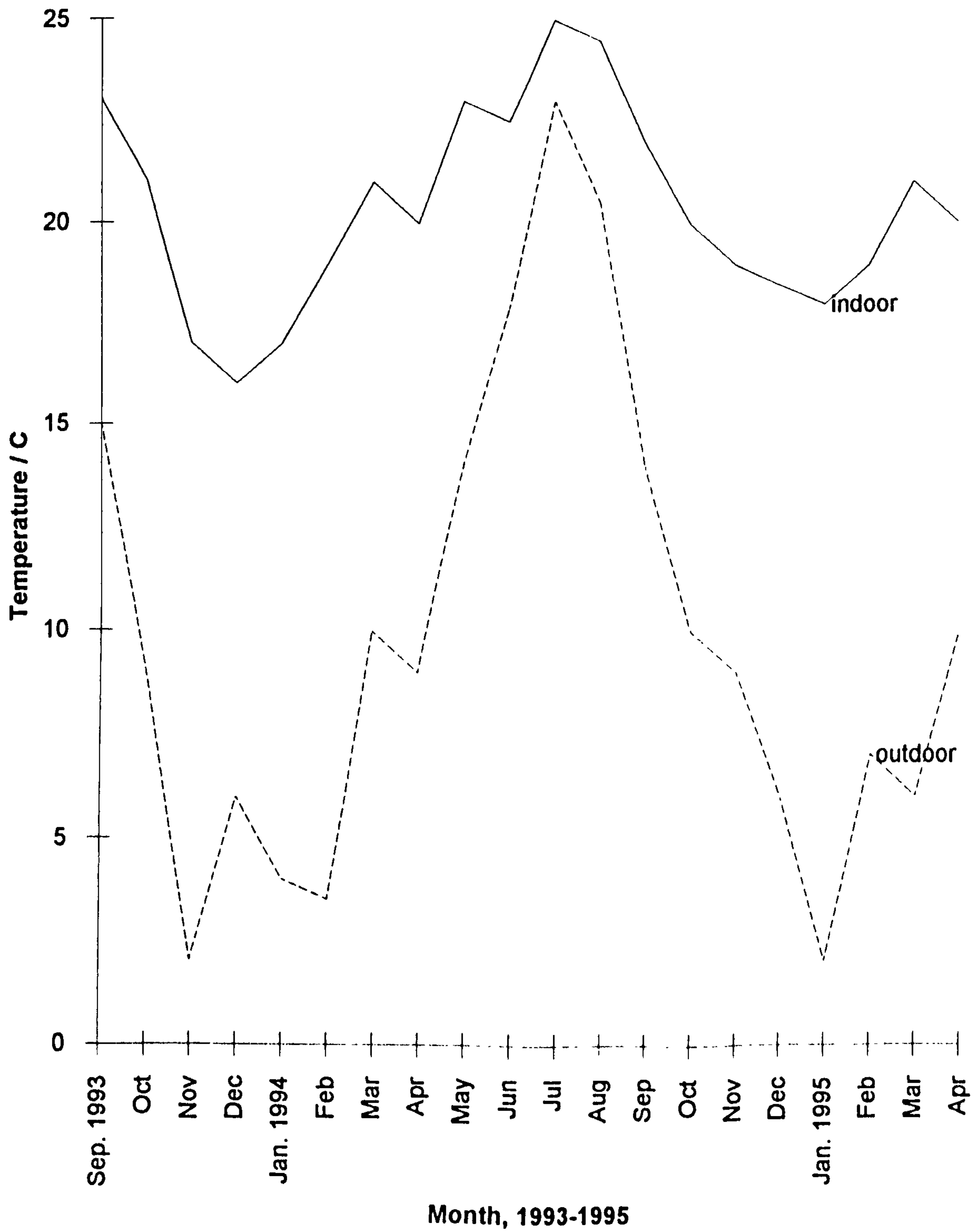
Month of heating season	Daily irradiation on a south facing vertical plane kWh/m <sup>2</sup>	Average internal to external air temperature difference		Daily heat loss through building walls with U=0.6 W/m <sup>2</sup> C kWh/m <sup>2</sup>
		0-7hours	8-24 hours	
January	0.9	17	16	0.23
February	1.47	17	15.5	0.21
March	2.21	16	13.5	0.17
April	2.6	14	11	0.13
May	2.81	11.5	7.5	0.1
September	2.39	8.5	4.5	0.085
October	1.96	12	10	0.15
November	1.18	14.5	13	0.2
December	0.86	16	15.5	0.22



**Table 6.3 Yearly energy consumption for space heating in the self sufficient solar house, Freiburg.**

Consumption of standard German house / kWh/m <sup>2</sup>	Consumption of Freiburg house / kWh/m <sup>2</sup>		
	1993	1994	1995
100	2.5	0.5	0.2

**Fig. 6.8 Monthly mean values of the indoor and outdoor temperatures experienced at the Self-Sufficient Solar House, Freiburg.**



The above project shows that it is possible to use transparent insulation material to construct an energy efficient building, with a very low energy consumption and virtually no heat demand in Central Europe. This was an exceptional, and expensive demonstration. Even so, large reductions in energy use still accrue in less costly applications. This is illustrated by the application of transparent insulation material to the facades of flats in Freiburg. Before renovation the heating energy demand was 225 kWh/m<sup>2</sup>, after renovation with transparent insulation material the demand fell to just 43 kWh/m<sup>2</sup> <sup>72</sup>.

There has been one major application of transparent insulation material in the United Kingdom: to the walls of the solar residences at Strathclyde University <sup>75</sup>. Such large reductions in energy usage were not obtained. The building is well insulated and uses triple glazing. The south facing walls of 150 mm thick concrete blocks are covered with 100mm thick polycarbonate honeycomb transparent insulation material. Solar control blinds are incorporated to reduce the risk of summer overheating.

The actual average energy consumption of the building during a year was 205 kWh/m<sup>2</sup>. On average, nationally, a building of this nature will consume 270 kWh/m<sup>2</sup> (the UK median of the building energy performance indicator). In contrast the average consumption of energy by city centre residences at the University of Strathclyde is much greater at 455 kWh/m<sup>2</sup>. The considerable reductions in energy use attained at more southerly locations have thus not been attained and the building would be placed in the 'better than good' category for its energy consumption.

### 6.3 PERFORMANCE OF MODEL SOLAR WALLS

#### Physical modelling

The use of exposed models provides a middle path between the artificiality of a laboratory test, and the uncertainties associated with measurements in real buildings. They allow tests to be performed under real conditions in real climates. Accordingly two south facing models were constructed on the roof of the School of the Built Environment (see **Fig 6.9a** and **Fig 6.9b**). Both were single glazed and had 100 mm of transparent insulation material in front of either a 100 mm engineering brick mass wall or a thin black painted aluminium absorber. Heat was extracted from the insulated cavities behind the mass walls to a stream of air fed from a control room. Pertinent physical parameters were monitored from January to June, 1993, and heat outputs plus efficiencies were evaluated. The results obtained and recorded in *Table 6.4* show the excellent performance produced by both types, a transparently insulated mass brick solar wall and a transparently insulated aluminium metal absorber plate air heater.

Norton cites the benefits of the short thermal response time of metal plated air heating collectors which makes them suitable for the solar heating of schools, without the risk of overheating were direct gain solar heating to be used. Norton<sup>76</sup> designed thermosyphoning air panels for the Nazeing Primary School, Essex, (they were single glazed and had a black painted aluminium absorber, see **Fig 6.10**). 140 kWh/m<sup>2</sup> of solar energy was produced by the solar collectors at 28 per cent efficiency. The payback time of 24 years when used to supplant electricity as a fuel is unattractive. This application could be ideal for similar air heaters provided with transparent insulation material. As

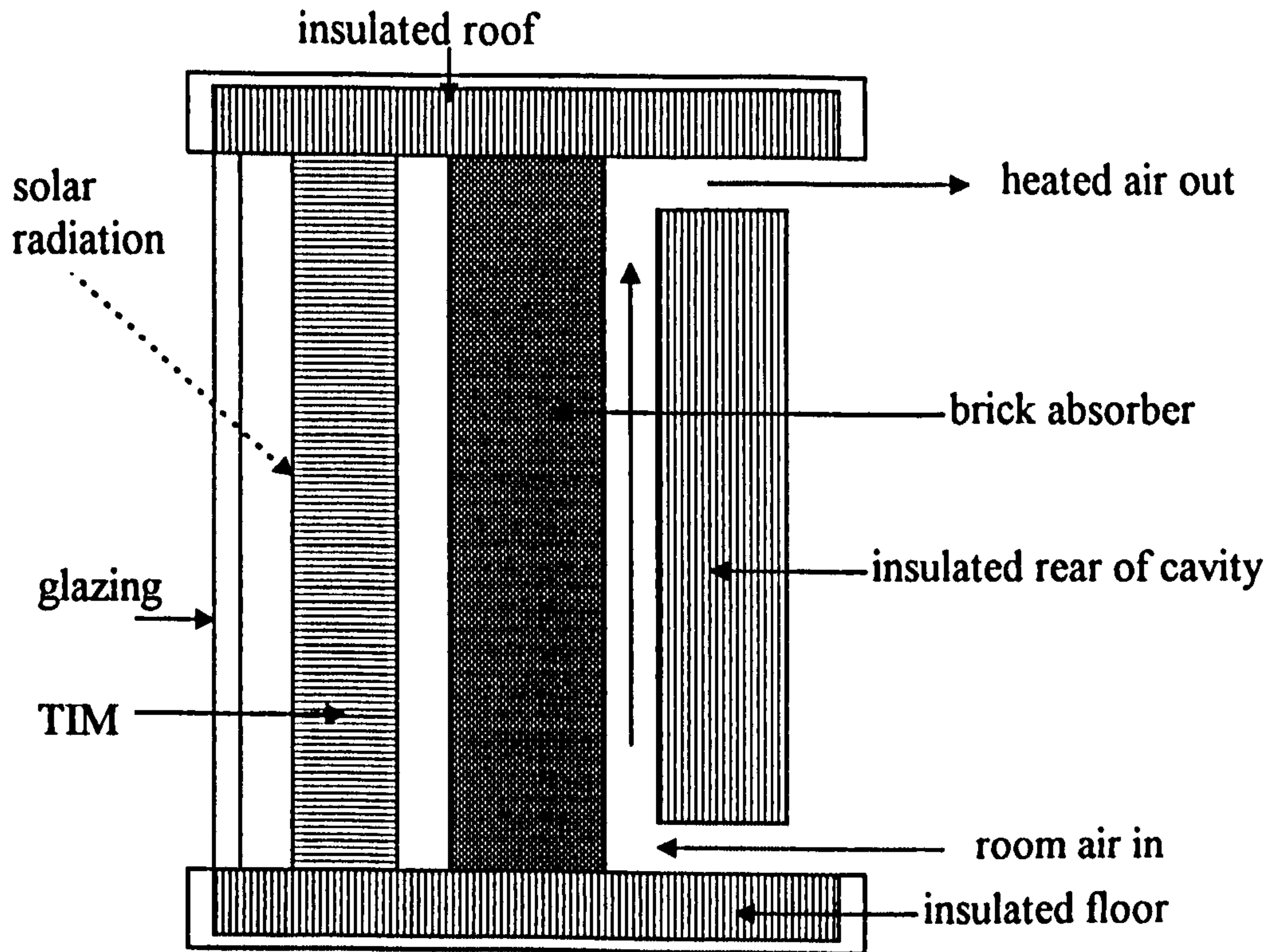


**Fig. 6.9(a) TIM clad model solar wall constructed with brick absorber.**

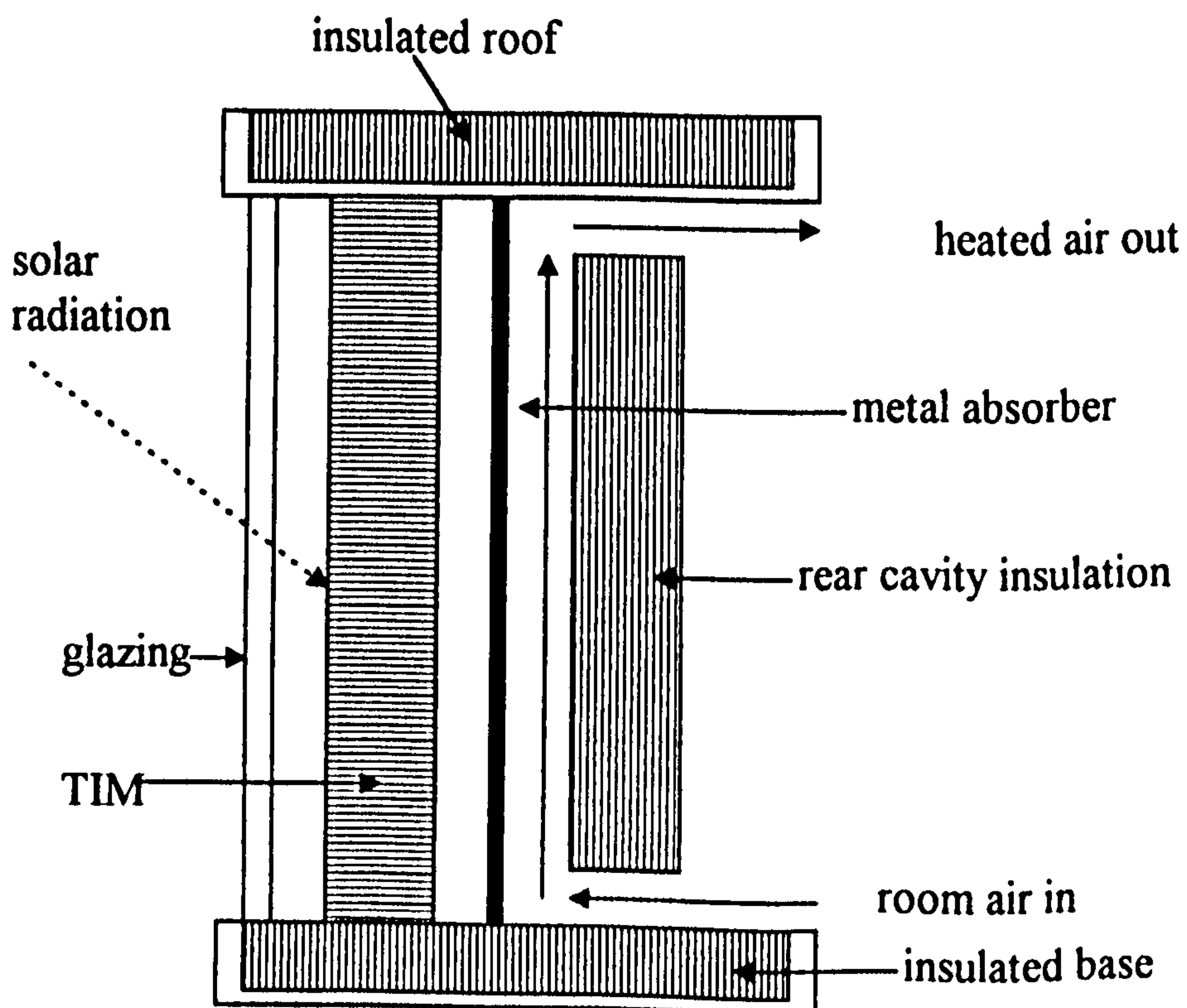
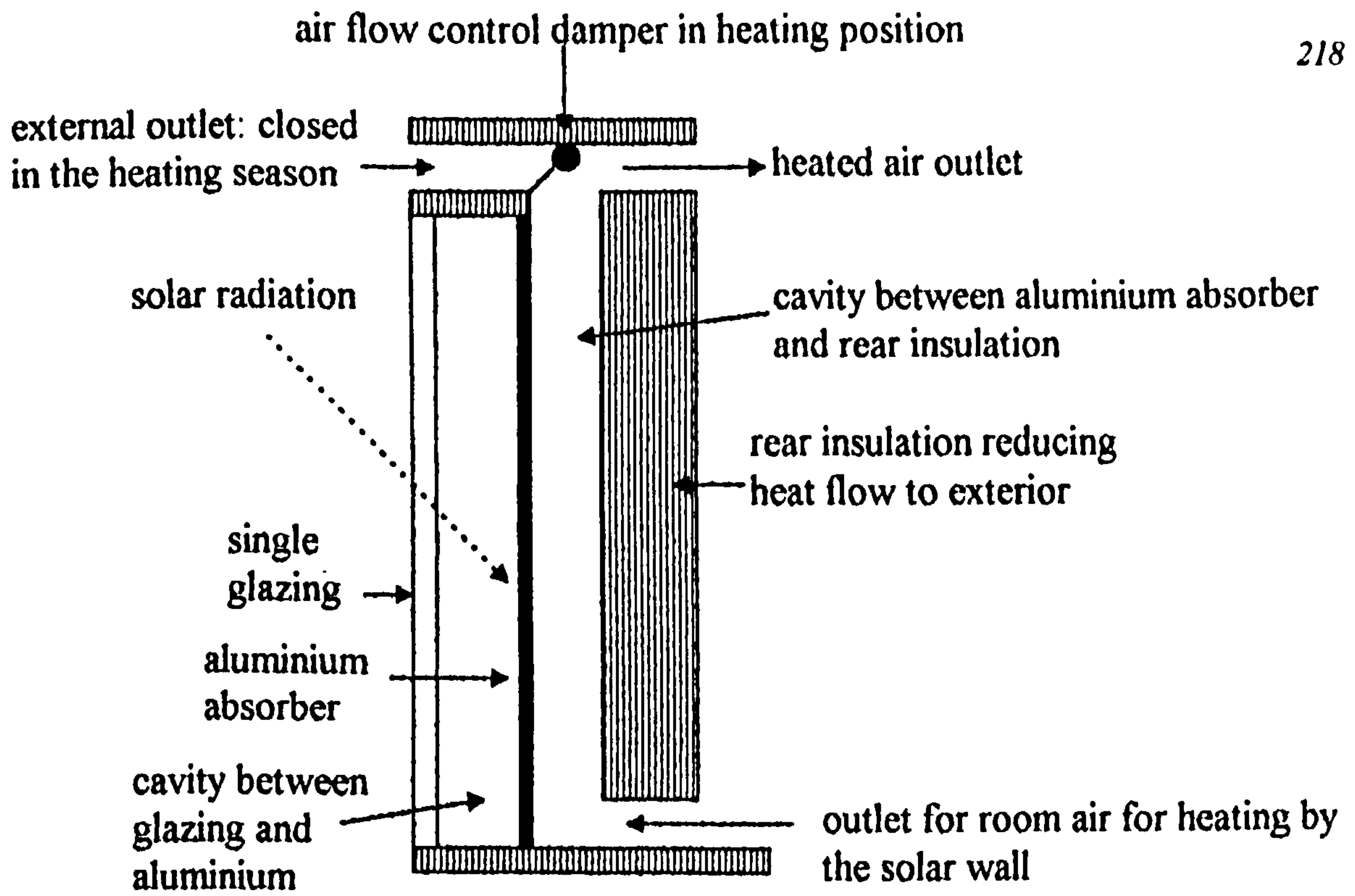


**Fig. 6.9(b) TIM clad model solar wall constructed with metal absorber.**

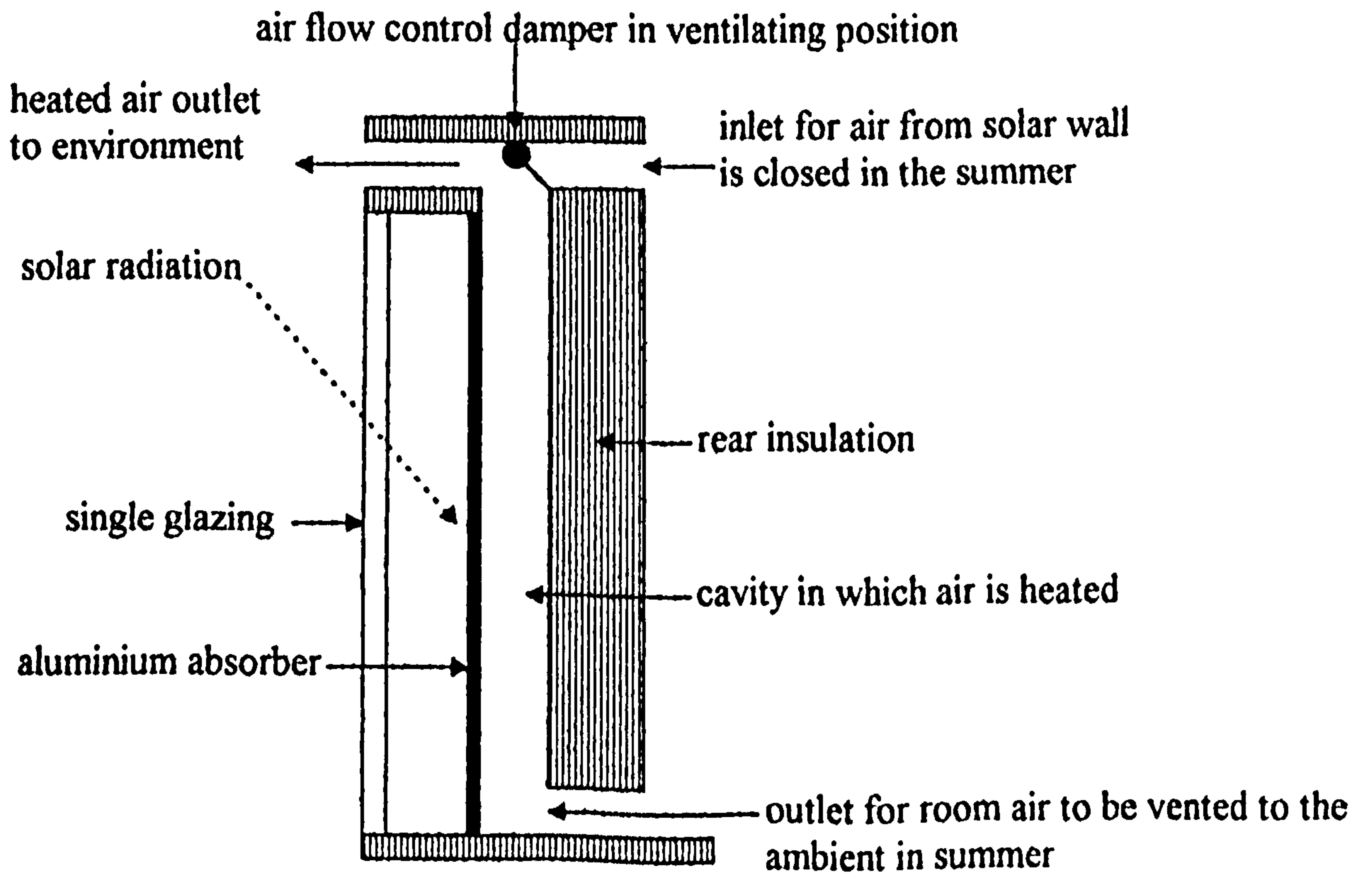


**Table 6.4 Monitored output and efficiencies of heat production from transparently insulated walls, Liverpool, 1993.**

Month	Incident solar radiation	Solar heat collected		Solar wall efficiency		Days readings taken
		brick absorber	metal absorber	brick absorber	metal absorber	
	MJ/m <sup>2</sup> day	MJ/m <sup>2</sup> day	MJ/m <sup>2</sup> day	%	%	
January	3.05	1.2	1.5	39	49	31
February	4.33	1.7	2.2	40	52	28
March	7.79	3.2	4.1	41	52	8
April	7.53	3.1	4	42	53	20
May	11.43	5.1	6.4	45	55	17
June	10.7	4.9	5.8	46	54	18



Norton air collector in heating mode.



Norton air collector in ventilating mode

Fig. 6.10 Norton solar thermosyphoning air heating panels.

indicated later, such air collectors operate at close to 50 per cent efficiency, with more acceptable payback times.

### Computer modelling

It is clear that comprehensive analysis of a transparent insulation system would be assisted by simulation modelling when assessing its performance at different localities. The previously cited simulation model (see Chapter 4) has proved a useful tool when investigating the effects of parameter change upon solar wall performance. It has been modified to allow it to be used for transparent insulation material applications (transmission data measured by Platzer as been used <sup>86</sup>).

The model is three dimensional, has 84 nodes, and uses finite difference techniques. It is written in Fortran, to use on any IBM compatible personal computer. Hourly values of direct and diffuse solar radiation, together with external and internal temperatures were used as the input variables. Moderate accuracy was expected. The program allowed pertinent parameters to be rapidly input so that the effect of changes in their values on solar wall performance could be quickly perceived (see *Appendix 3*).

The initial simulation used data monitored in Liverpool, obtained when measuring the exposed model transparently insulated wall performance. Calculated efficiencies, are plotted with previously measured values in **Fig 6.11**, and good agreement was found between the computed and measured data <sup>81</sup>. A transparently insulated brick solar wall was computed to have an average efficiency of about 41 per cent from January to June. This is in good agreement with 40 per cent measured in Liverpool and 40 per cent

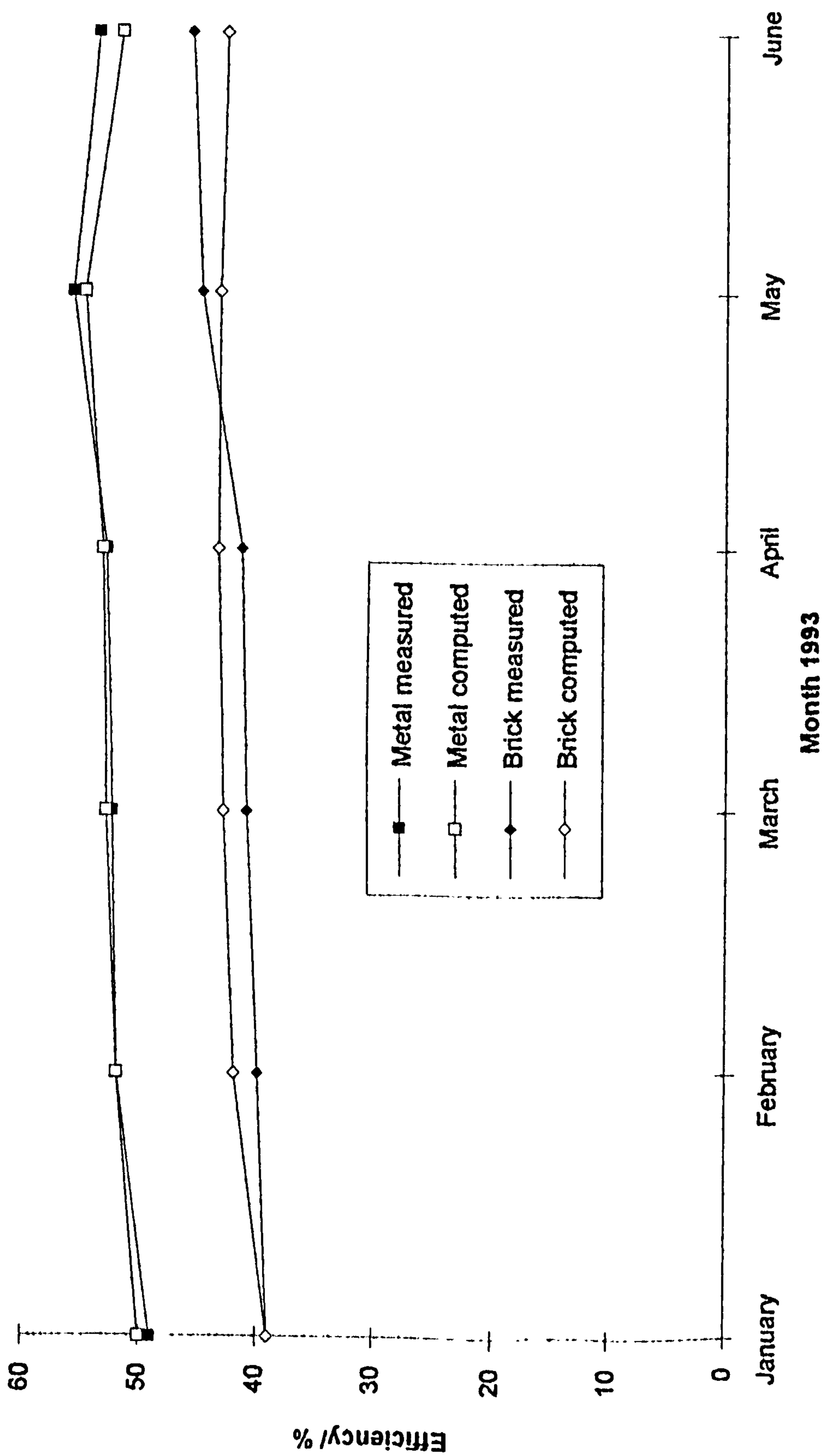


**Fig. 6.11 Monthly efficiencies of the heat production from transparently insulated solar walls in Liverpool, 1993.**

measured by Dolley<sup>77</sup> in Milton Keynes, both using single glazed 100 mm transparently insulated walls. A transparently insulated air collector, with metal plate absorber has, as expected, a higher efficiency of more than 50 per cent, due to its rapid response time, and reduced damping of the passage of heat.

Since there is good agreement between the measured and computed efficiencies, one must conclude that simplified system specific programs are suitable for predicting the potential of transparently insulated wall applications. What they will not measure is the effect of utilisation. Dolley<sup>79</sup> modified the modular dynamic building simulation program SERI-RES, to allow the simulation of transparently insulated walls. He analyzed the performance of a single family dwelling equipped with such walls, over a range of insulation and occupancy levels for a continuously occupied house in the London area. Utilisation of solar heat supplied was predicted to be 60 per cent, for houses built to 1990 UK Building Regulation Standards with a U-value of 0.45 W/m<sup>2</sup>K.

### Overheating problems

At the end of June 1993, the transparently insulated solar wall and air collector models were allowed to stagnate, their air flow fans were switched off. The temperatures reached by the front surfaces of the solar wall and the metal absorber were measured (see **Fig 6.12**). A maximum temperature of 56°C was recorded at midday for the brick absorber, and 80°C for the metal absorber over a three day period of constantly sunny weather. There seems little to fear from immediate degradation of the polycarbonate honeycomb material, for the plastics' glass transition temperature is 149°C, and its recommended service temperature is 110°C. Over a long period at these temperatures,



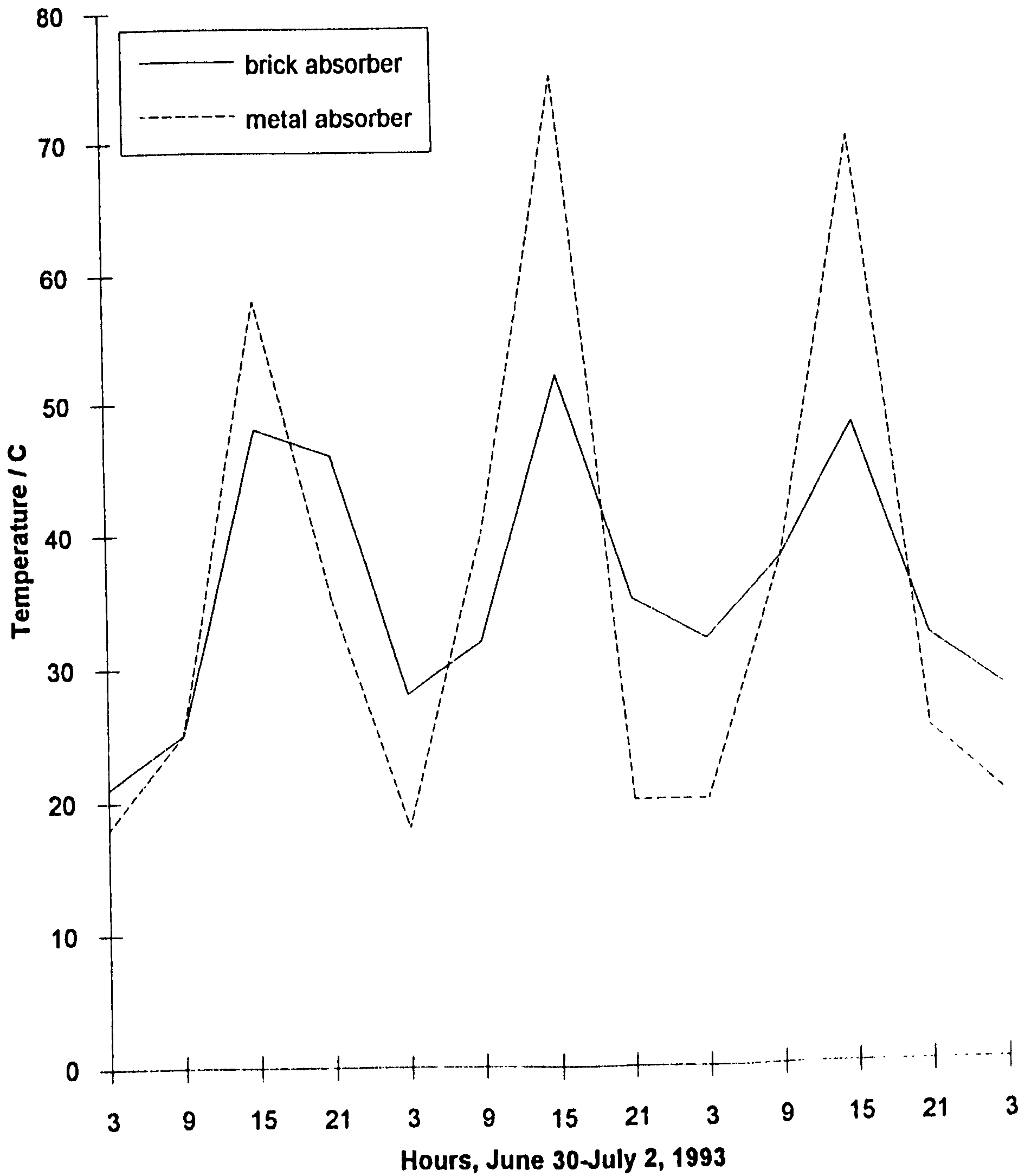


**Fig. 6.12** Temperatures of the transparent insulation material as measured in the model solar walls constructed in Liverpool.

photooxidation reactions producing carbonyl groups (C=O) which induce yellowing of the plastic are to be expected <sup>78</sup>.

The main concern will be that such high summer temperatures will produce room overheating. Overheating is defined as: the achievement of more than 175 occupied hours above 27°C, per year. Dolley <sup>79</sup> again provides encouraging results. He showed that, if a substantial amount of ventilation is available, none of the houses, simulated with Kew weather data, overheated significantly. This applied even if solar control blinds are not used in front of the transparent insulation material. His results suggest that the ventilation rate must be adequate and greater than five air changes per hour. If this is so, overheating will not occur in the summer, in transparently insulated buildings.

Dolley concludes that it is possible to discard the use of roller blinds when transparent insulation is used in the United Kingdom, provided that sufficient provision is made for summer time ventilation. *Table 6.5* presents some of his results on the overheating performance of buildings with transparently insulated walls. It is interesting to note that Jesch <sup>80</sup> at Bournville in Birmingham, has clad the east and south facing walls of his house with transparent insulation without solar control blinds. This application has been highly successful and well publicised. There have been no overheating problems.

#### Efficiency of operation of transparently insulated walls in the North West

The performance of transparently insulated solar walls and air collectors was simulated for a heating season in the North West using local weather data for walls with 50 mm and 100 mm thick transparent insulation. The results are presented in *Table 6.6*. They

**Table 6.5 The hours of overheating produced by TIM clad solar walls without protective blind systems and without summer ventilation. Over heating is stated to occur when the internal temperature exceeds 27C for more than 175 hours per annum. None of the constructions considered will overheat if adequate summer ventilation is used.**

House wall construction before installation of TIM	Area of TIM clad wall installed on a south facade m <sup>2</sup>			
	0	8	16	24
	Hours of overheating			
solid wall	4	31	82	162
cavity wall	20	70	153	280
1976/1982 UK building regulation standard	27	111	258	454
1990 UK building regulation standard	101	310	597	909
Super-insulated	320	784	1190	1431
				1674

overheating will occur in conditions under the line

**Table 6.6 Efficiencies of heat production from transparently insulated solar walls in North West of England.**

Month	Average monthly efficiencies of heat production from transparently insulated solar walls %			
	100 mm TIM		50 mm TIM	
	brick absorber	metal absorber	brick absorber	metal absorber
January	35	45	27	35
February	40	50	38	45
March	42	52	40	46
April	44	52	41	46
May	45	53	42	47
September	46	54	43	52
October	46	54	42	51
November	41	50	35	41
December	35	44	25	31
Seasonal average	42	50	37	44
Heat delivery potential from October -May	170 kWh/m <sup>2</sup>	200 kWh/m <sup>2</sup>	135 kWh/m <sup>2</sup>	175 kWh/m <sup>2</sup>

confirm the expectation that such walls and collectors operate at high efficiencies throughout the season. The best performance is produced by the 100 mm transparent insulation material. Almost uniformly high efficiencies are produced throughout the season<sup>81</sup>.

### Economic performance

An analysis was made to see how well such constructions perform in economic terms. Unless solar construction is affordable, it will not be used by the bulk of the population. Simple payback periods for transparently insulated walls were estimated for the Manchester climate using 1993 cost data. The costs are listed in *Table 6.7* and simple payback times and energy savings in *Table 6.8* and **Figs 6.13a** and **6.13b**. The preferred choice of construction uses 100 mm thick transparent insulation. Walls and air collectors using this thickness have superior insulation and deliver larger amounts of energy. Such walls and air collectors will be quasi economic when supplanting electricity using the conventional 10 year payback criterion as a measurement of acceptability. Occupancy reduces utilisation by up to 40% however, and increases payback times. When supplanting gas, payback times are larger, from 30 to 35 years. Thus transparently insulated walls, are not universally competitive and are applicable only in niche situations.



**Table 6.7 Estimated construction costs.**

Materials and fuel used.	Estimated cost.
100 mm TIM, timber frame, labour	£205/m <sup>2</sup>
50 mm TIM, timber frame, labour	£150 /m <sup>2</sup>
Electricity	£0.078 /kWh
Gas at 60% conversion efficiency	£0.025 / kWh

**Table 6.8 Energy savings and payback periods for a heating season extending from September to May in Manchester.**

Item	100 mm TIM		50 mm TIM	
	Brick absorber	Metal absorber	Brick absorber	Metal absorber
Fuel saving kWh/m <sup>2</sup>	220	270	200	240
Payback against electricity (years)	12	10	9.7	8
Payback against gas (years)	35	30	30	25

**Table 6 9 Diffuse solar transmission for 100mm TIM.**

Material	Thickness	Solar transmission
Okalux Transparent Insulation Material (TIM)	100 mm	72 %

**Fig. 6.13(a) Payback periods for delivered energy from solar walls in Manchester**

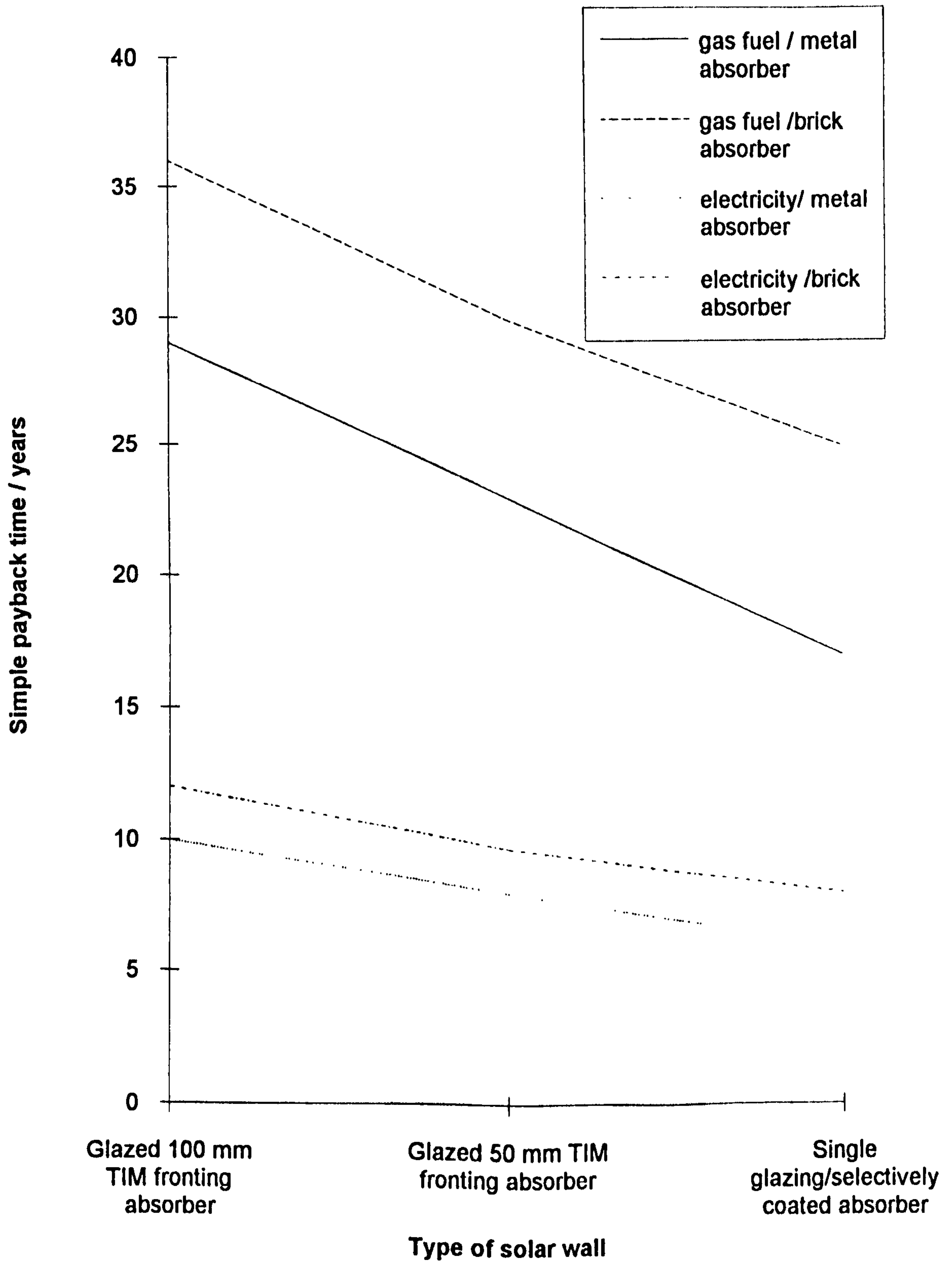
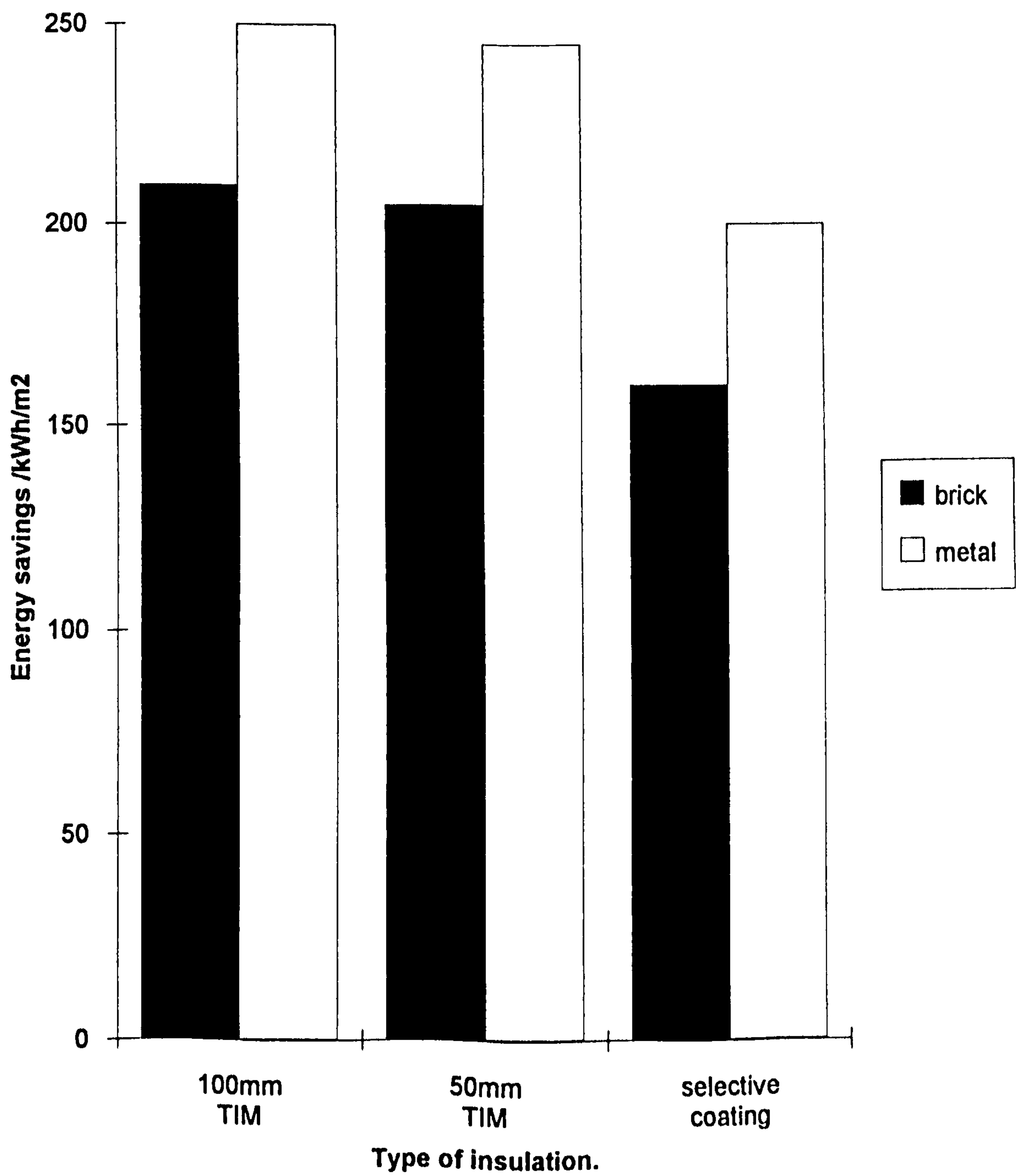


**Fig. 6.13(b) Potential energy delivery from September to May for solar walls in Manchester.**



## 6.4 THE POTENTIAL FOR SOLAR WALLS IN PROVIDING LOW TEMPERATURE HEAT IN EUROPE

### Introduction to the comparative performance of solar walls<sup>83</sup>

In the short term resource depletion is not a problem. In the long term, this epoch of massive fuel consumption and rabid consumerism, must be regarded as abnormal, transitory, and unsustainable. Renewable energy technologies, in conjunction with energy conservation, could therefore offer one way of combatting the systemic shocks that must occur when fuel prices inevitably rise. In such a context, the use of transparent insulation to produce solar walls for inclusion in environmentally benign buildings seems a promising approach. The potential for transparent insulation systems in Europe is therefore analysed below. A comparative analysis of solar heating systems has already been performed by Peuportier and Michel (1995)<sup>82</sup>. They have found that the use of transparent insulation doubles the gain of Trombe walls in France. The simulations presented here confirm this result. They also show that although poorly insulated Trombe walls produce little energy at high latitudes, the performance of a transparently insulated solar wall is largely unaffected by its location.

#### The overall heat balance

A solar wall (see Fig 6.14a), not only introduces useful heat into a building, it also saves the energy that would be lost by the outward flow of heat through the wall it replaces<sup>83</sup>. The thermal benefits resulting from its use, should therefore take into account the energy flows in a reference wall, often a well insulated cavity wall with a front leaf of brick (see

**Fig 6.15).** The energy saved by the use of a solar wall, is thus the sum of the heat it supplies, and the heat lost from a reference wall.

The concept of sol-air temperature<sup>84</sup> has proved helpful when developing equations to describe the steady state overall heat balance of a solar wall. Its application is described in *Appendix 4*, and the following relationships produced:

The monthly mean daily heat gain from a solar wall ( $Q_{sw}$ , kWhm<sup>-2</sup>)

$$Q_{sw} = U_{sw}(\tau\alpha) R_o H_m - 24 U_{sw} (T_{ai} - T_{ao}) \quad (6.6)$$

The monthly mean daily heat gain from a reference wall ( $Q_{rw}$ , kWhm<sup>-2</sup>)

$$Q_{rw} = U_{rw} \alpha R_{so} H_m - 24 U_{rw} (T_{ai} - T_{ao}) \quad (6.7)$$

The monthly mean daily heat savings from a solar wall ( $Q_t$ , kWhm<sup>-2</sup>)

$$Q_t = Q_{sw} - Q_{rw} = (U_{sw}(\tau\alpha)R_o - U_{rw} \alpha R_{so})H_m - 24(U_{sw} - U_{rw})(T_{ai} - T_{ao}) \quad (6.8)$$

Equation 6.8 will be used in the following analysis to compare the performance of Trombe and transparently insulated solar walls.

### Single glazed Trombe walls

As previously described, such walls were extensively studied by Trombe in 1979. They work by allowing solar radiation to pass through glazing to be absorbed by the darkened surface of the dense wall of brick or concrete behind. This energy is then transferred to a room by conduction through the wall, with subsequent radiation and convection from its inner surface. In the original design thermocirculating air currents carry heat from the front absorbing surface to the rear, via air vents placed at the top and bottom. The use



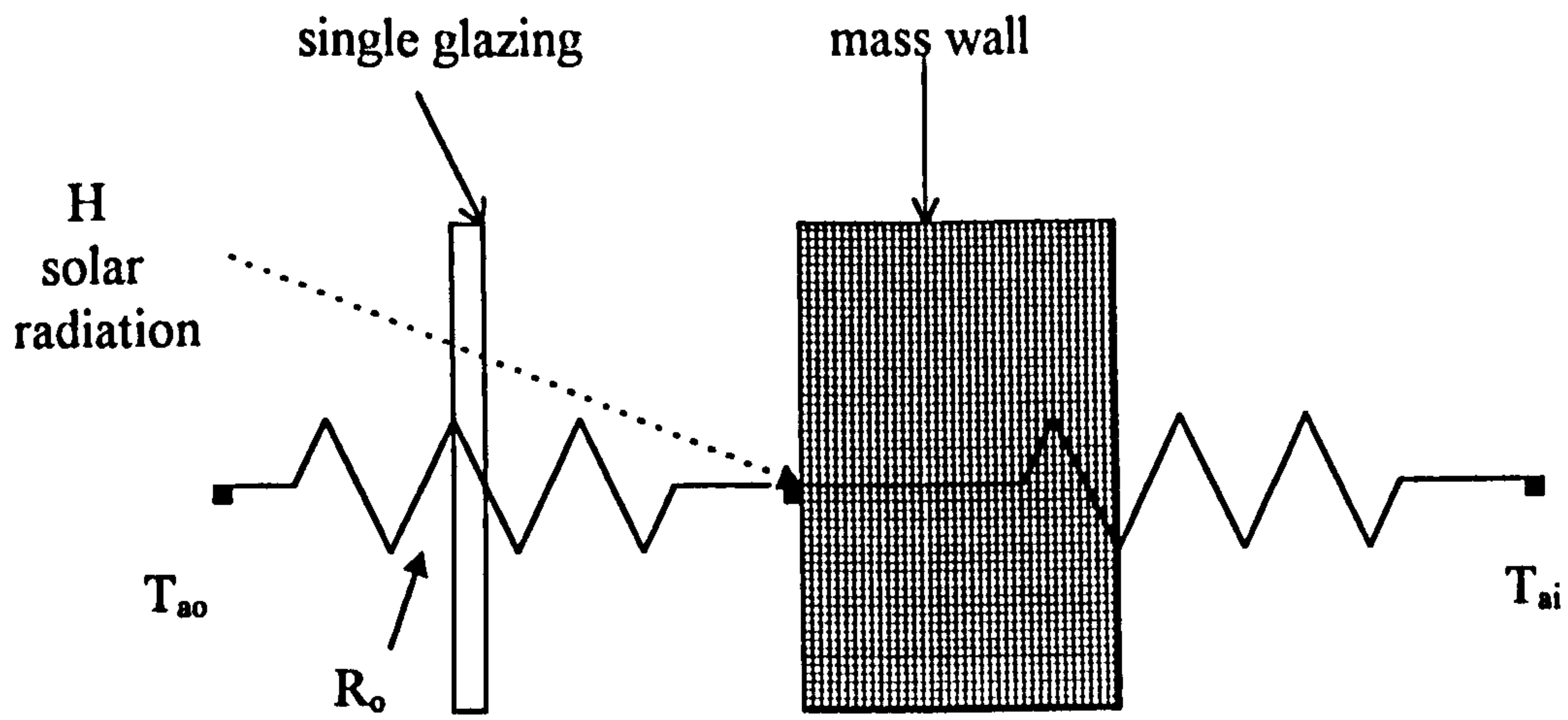


**Fig.6.14(a) Unvented single glazed Trombe wall**

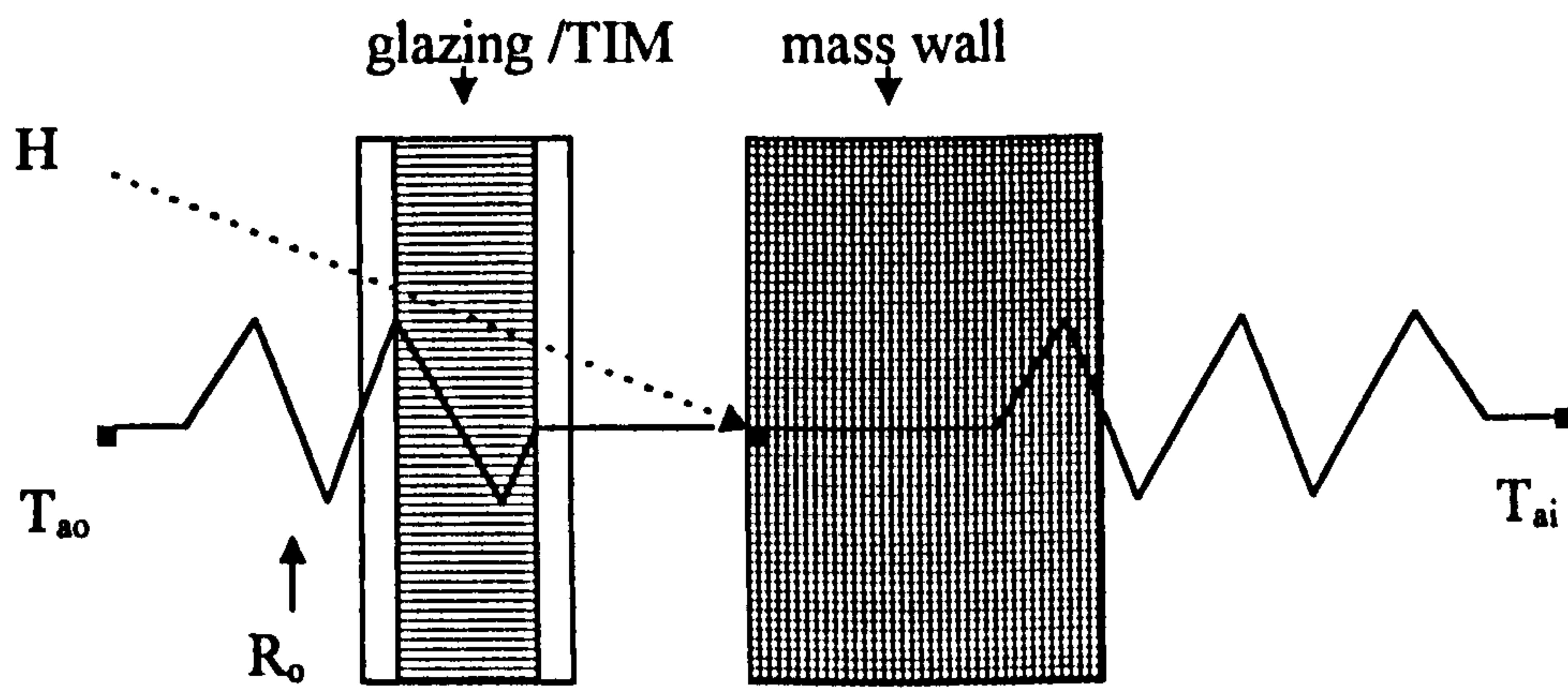


**Fig.6.14(b) Transparently insulated wall**

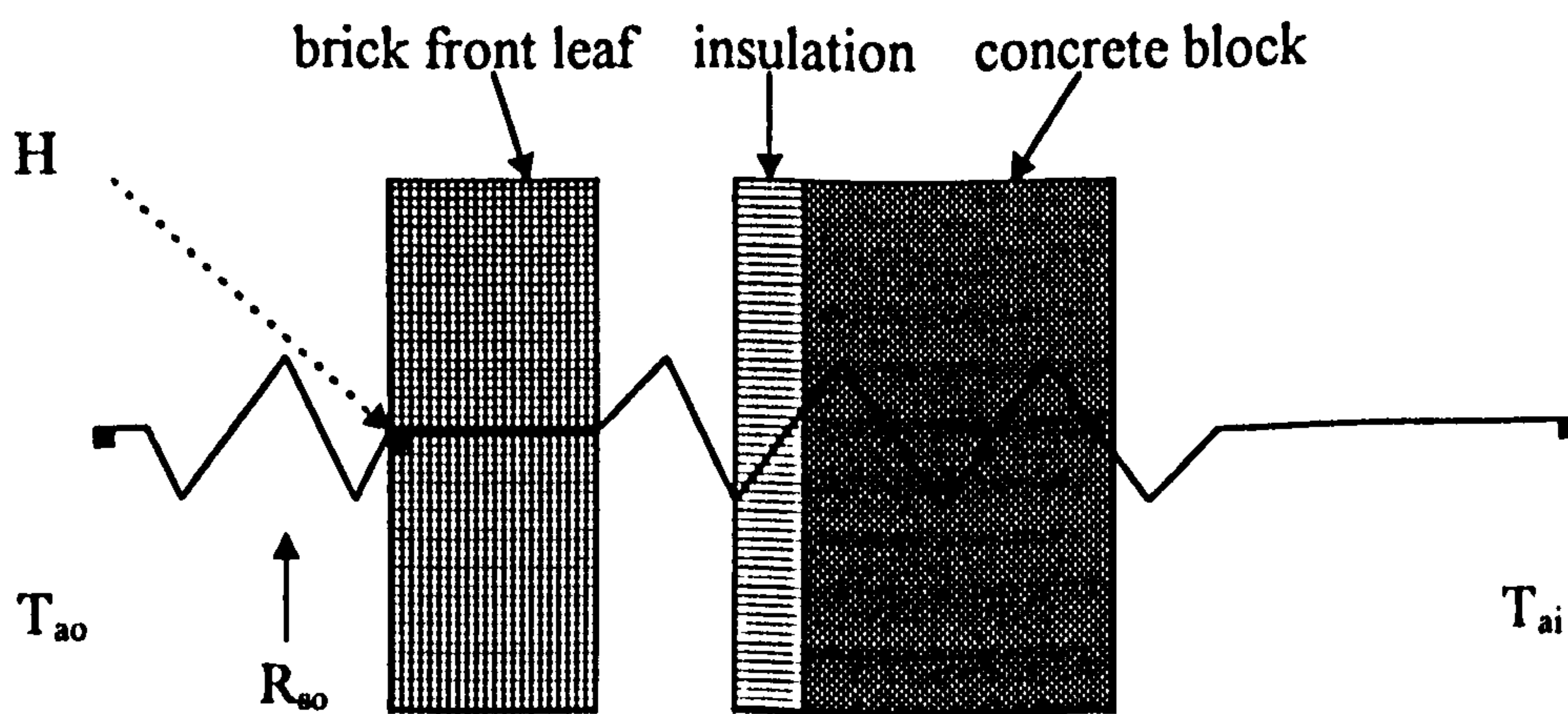


**Fig.6.15 Reference cavity wall**

of unvented walls which dispense with thermocirculation is often preferred in order to avoid the deposition of condensation and dirt on the glazing. The performance of such unvented solar walls is simulated here.

The rear of such a solar wall is usually left uninsulated allowing heat to pass unimpeded into the adjoining room. In the case of such a single glazed Trombe wall, its thermal transmittance ( $U_{tw}$ ,  $\text{kWm}^{-2}\text{K}^{-1}$ ) will be much larger than the thermal transmittance of a well insulated cavity wall ( $U_{rw}$ ,  $\text{kWm}^{-2}\text{K}^{-1}$ ). Trombe walls consequently produce excessive heat loss in cold climates.

#### Relationships for Trombe walls (see Fig 6.14a)

The U value of a Trombe wall and its external resistance from the mass wall surface  $R_o$ , are of the order of  $1.8 \text{ W/m}^2\text{K}$  and  $0.22 \text{ m}^2\text{K/W}$  respectively. Both are much greater than the corresponding values for the reference wall. This means that the following relationships hold for single glazed Trombe walls without any extra internal insulation:

$$U_{tw} \gg U_{rw} \quad (6.9)$$

$$U_{tw}R_o \gg U_{rw}R_{so} \quad (6.10)$$

Also one may equate :

$$U_{tw} = U_{sw} \quad (6.11)$$

The monthly mean daily heat savings from a Trombe wall ( $Q_{tw}$ , kWhm<sup>-2</sup>) are:

$$Q_{tw} = Q_{sw} - Q_{rw} = (U_{tw}(\tau\alpha)R_o - U_{rw} \alpha R_{so})H_m - 24(U_{tw} - U_{rw})(T_{ai} - T_{ao}) \quad (6.12)$$

hence:

$$Q_{tw} = U_{tw}(\tau\alpha)R_o H_m - 24U_{tw}(T_{ai} - T_{ao}) \quad (6.13)$$

The monthly relative efficiency of heat savings from a Trombe wall ( $\eta_{tw}$ ) equal:

$$\eta_{tw} = \frac{Q_{tw}}{H_m} = \frac{U_{tw}(\tau\alpha)R_o - 24U_{tw}(T_{ai} - T_{ao})}{H_m} \quad (6.14)$$

By inspection of the above equations it may be predicted that, the heat savings and efficiency of heat production from single glazed Trombe walls will be strongly influenced by the level of solar radiation  $H_m$ , and the external air temperature  $T_{ao}$ . Locations with low levels of solar radiation, and low levels of air temperature will be unsuitable for their implementation.

### **Relationships for transparently insulated solar walls (see Fig 6.14b)**

Transparent insulation has great potential for reducing fuel consumption in buildings. A solar wall incorporating this material, interposes it between the glazing and a dense brick or concrete wall. Its thermal transmittance ( $U_{ti}$ , kWm<sup>-2</sup>K<sup>-1</sup>) is then of the same order as that of a well insulated reference wall ( $U_{rw}$ , kWm<sup>-2</sup>K<sup>-1</sup>). The thermal resistance ( $R_o$ , m<sup>2</sup>K kW<sup>-1</sup>) from the mass wall surface to the outside air, is again much greater than the external surface resistance  $R_{so}$ .

The following relationships can thus be written:

$$U_{ti} = U_{sw} \quad (6.15)$$

$$U_{ti} = U_{rw} \quad (6.16)$$

$$R_o \gg R_{so} \quad (6.17)$$

The following relationships may be deduced:

The monthly mean daily heat savings from a T1 wall ( $Q_{ti}, kWhm^{-2}$ )

$$Q_{ti} = Q_{sw} - Q_{rw} = (U_{ti}(\tau\alpha)R_o - U_{rw}\alpha R_{so})H_m - 24(U_{ti} - U_{rw})(T_{ai} - T_{ao}) \quad (6.18)$$

hence:

$$Q_{ti} = U_{ti}(\tau\alpha)R_oH_m \quad (6.19)$$

The monthly relative efficiency of heat savings from a T1 wall ( $\eta_{ti}$ )

$$\eta_{ti} = \frac{Q_{ti}}{H_m} = U_{ti}(\tau\alpha)R_o \quad (6.20)$$

By inspection it is predicted that the heat savings are strongly influenced by the level of solar radiation ( $H_m$ ) present, but independent of external air temperature ( $T_{ao}$ ). The efficiency of heat savings is independent of either radiation or temperature of the location, and thus essentially constant for a given transparently insulated wall. Such walls could therefore be sensibly deployed for heating wherever there are reasonable amounts of solar insolation during a heating season, whatever the external air temperature may be.

## Nomenclature

Symbols used in the above equations

$Q_{sw}$	=	monthly mean daily heat gain from a solar wall ( $\text{kWhm}^{-2}$ )
$H_m$	=	monthly mean daily global radiation on a south facing vertical plane ( $\text{kWhm}^{-2}$ )
$\tau\alpha$	=	monthly mean transmittance - absorptance product for solar radiation
$U$	=	heat transfer coefficient ( $\text{kWm}^{-2}\text{K}^{-1}$ )
$R_{so}$	=	external surface resistance ( $\text{m}^2\text{K kW}^{-1}$ )
$R_o$	=	resistance, mass wall to outside, through glazing ( $\text{m}^2\text{K kW}^{-1}$ )
$T_{ai}$	=	monthly mean internal air temperature ( $^{\circ}\text{C}$ )
$T_{ao}$	=	monthly mean external air temperature ( $^{\circ}\text{C}$ )
$tw$	=	Trombe wall $rw$ = reference wall $ti$ = T1 wall

## **6.5 THE SIMULATION OF SOLAR WALL BEHAVIOUR IN EUROPEAN LOCATIONS <sup>85</sup>**

### Introduction

When monthly mean daily values for solar radiation, air temperature and the transmittance-absorptance product are used, the hourly changes in the heat stored in the mass wall may be ignored, and the use of steady state equations will then suffice to produce values for the heat flow through solar walls that reflect those occurring in practice. Thus, in the simulation of the monthly mean behaviour of solar walls, the steady



state equation 6.8 has been used. The solar radiation input has been split into beam (b) and diffuse (d) components in the simulation, so that:

$$(\tau\alpha)H = (\tau\alpha)_b H_b + (\tau\alpha)_d H_d \quad (6.21) \quad \text{and}$$

$$H = H_b + H_d \quad (6.22)$$

Here ( $H_b$ , kWhm<sup>-2</sup>) and ( $H_d$ , kWhm<sup>-2</sup>) are the beam and diffuse components of the monthly mean daily global irradiation and  $(\tau\alpha)_b$  and  $(\tau\alpha)_d$  are the beam and diffuse components of the monthly mean transmittance-absorptance product.

To obtain values for the beam transmittance-absorptance product of glazing, information is required on: the monthly mean incidence angle for beam radiation (see Fig 6.16)<sup>103</sup>, the variation of the transmittance-absorptance product with beam angle (see Fig 6.17)<sup>103</sup>, the transmittance of a glass cover (see Fig 6.18) and the absorptance of matt black surfaces. Values for the diffuse transmittance-absorptance product assume that the effective incidence angle for isotropic diffuse radiation on vertical slopes is approximately 60° (see Fig 2.8). The preceding data was obtained from sources such as Klein (1979)<sup>103</sup> and Duffie and Beckman<sup>28</sup>. The monthly mean transmittance of 100 mm capillary transparent insulation material for diffuse and beam radiation can similarly be found from data shown in Fig 6.19, Table 6.9<sup>86</sup>.

## Simulation

The performance of solar walls in this section has been simulated using a steady state technique, the requisite computer program being written in Basic (see Appendix 3.17).

The results obtained were later compared to those obtained with the system specific



**Fig. 6.17 Typical curve for 1 cover of glazing showing the variation of the ratio of transmittance-absorptance product at a given angle of incidence to that at normal incidence. Adapted from Klein (1979).**

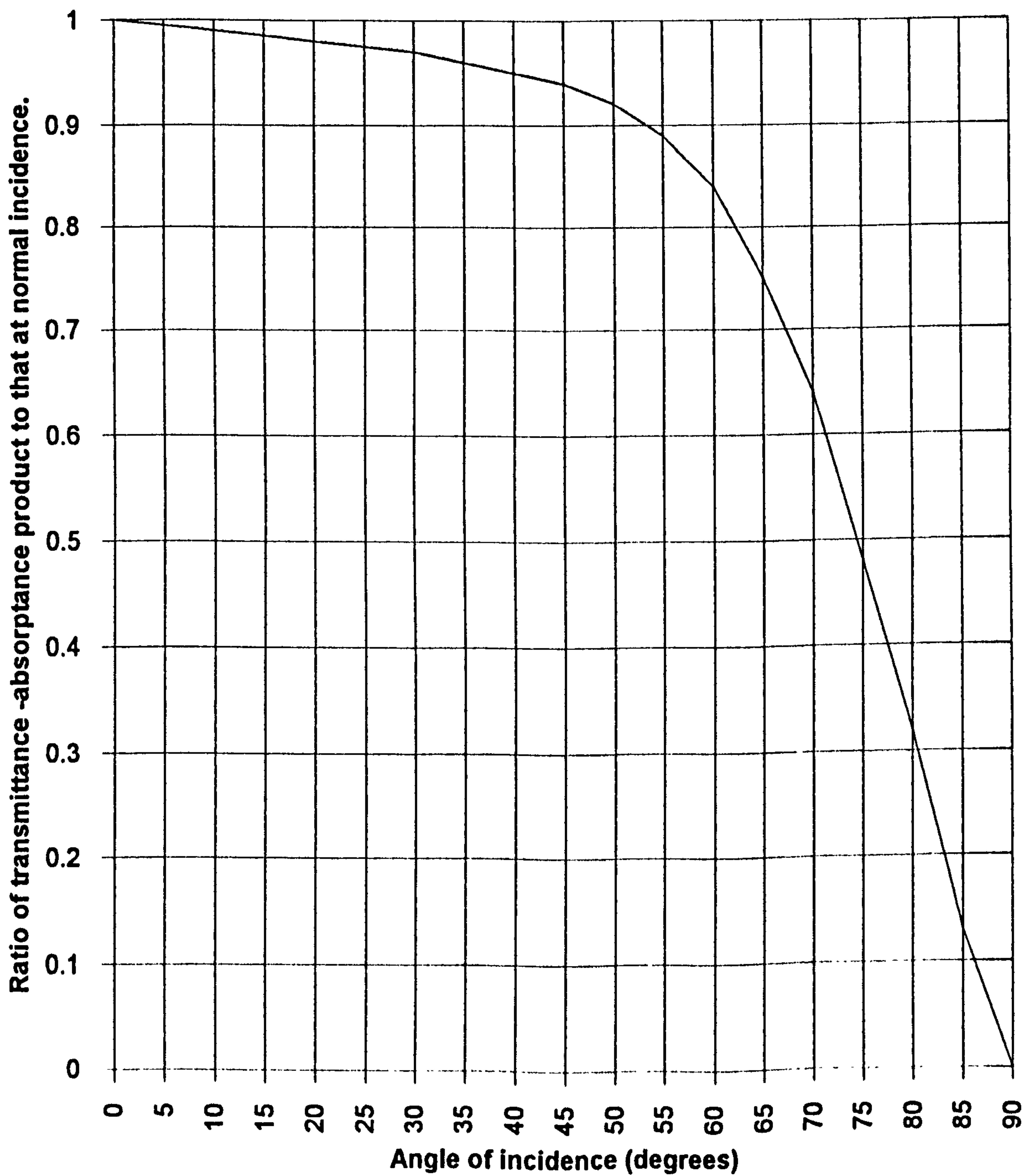


**Fig. 6.18 Transmittance of 1 cover of good quality glass  
( $KL=.025$ )**

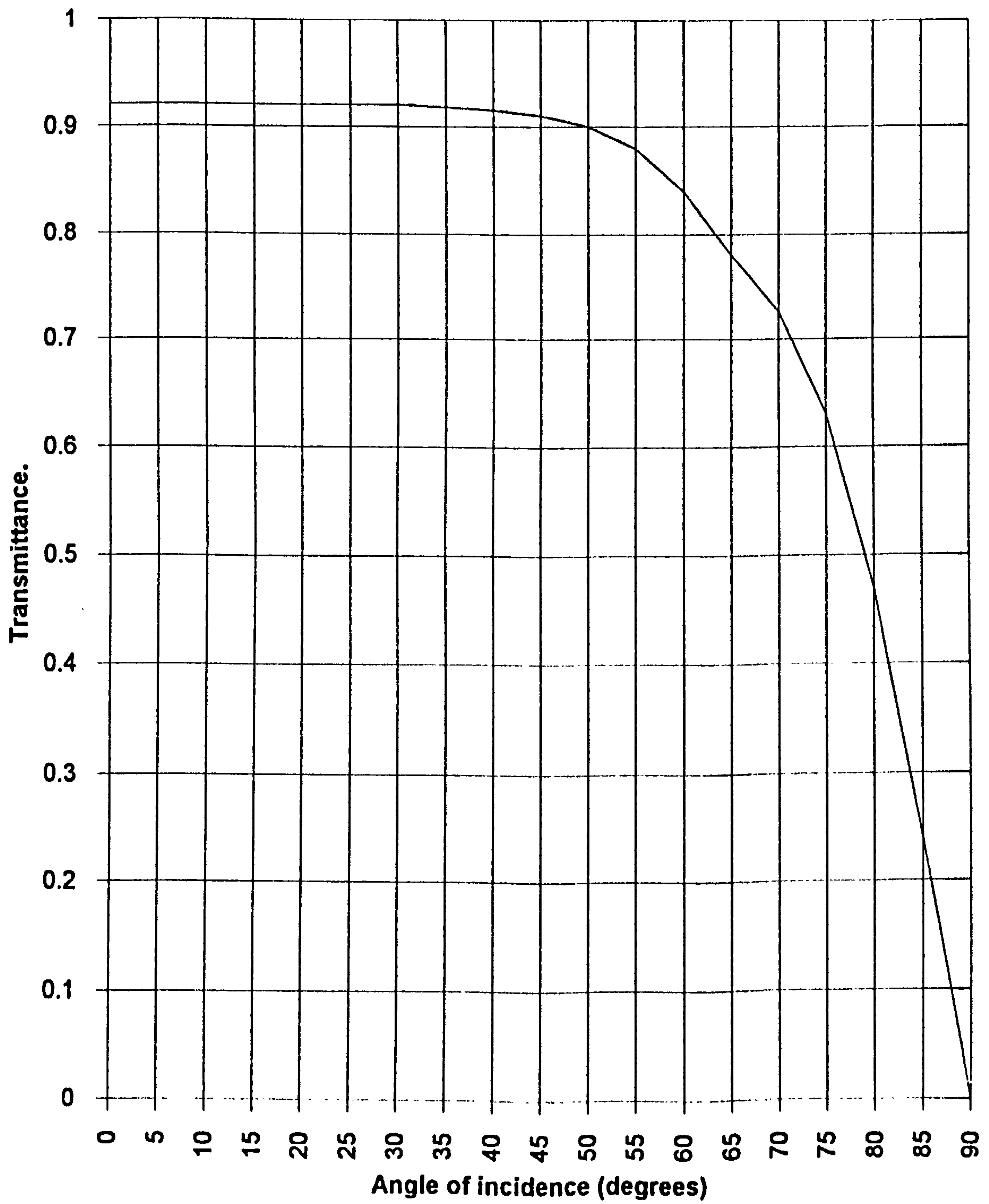
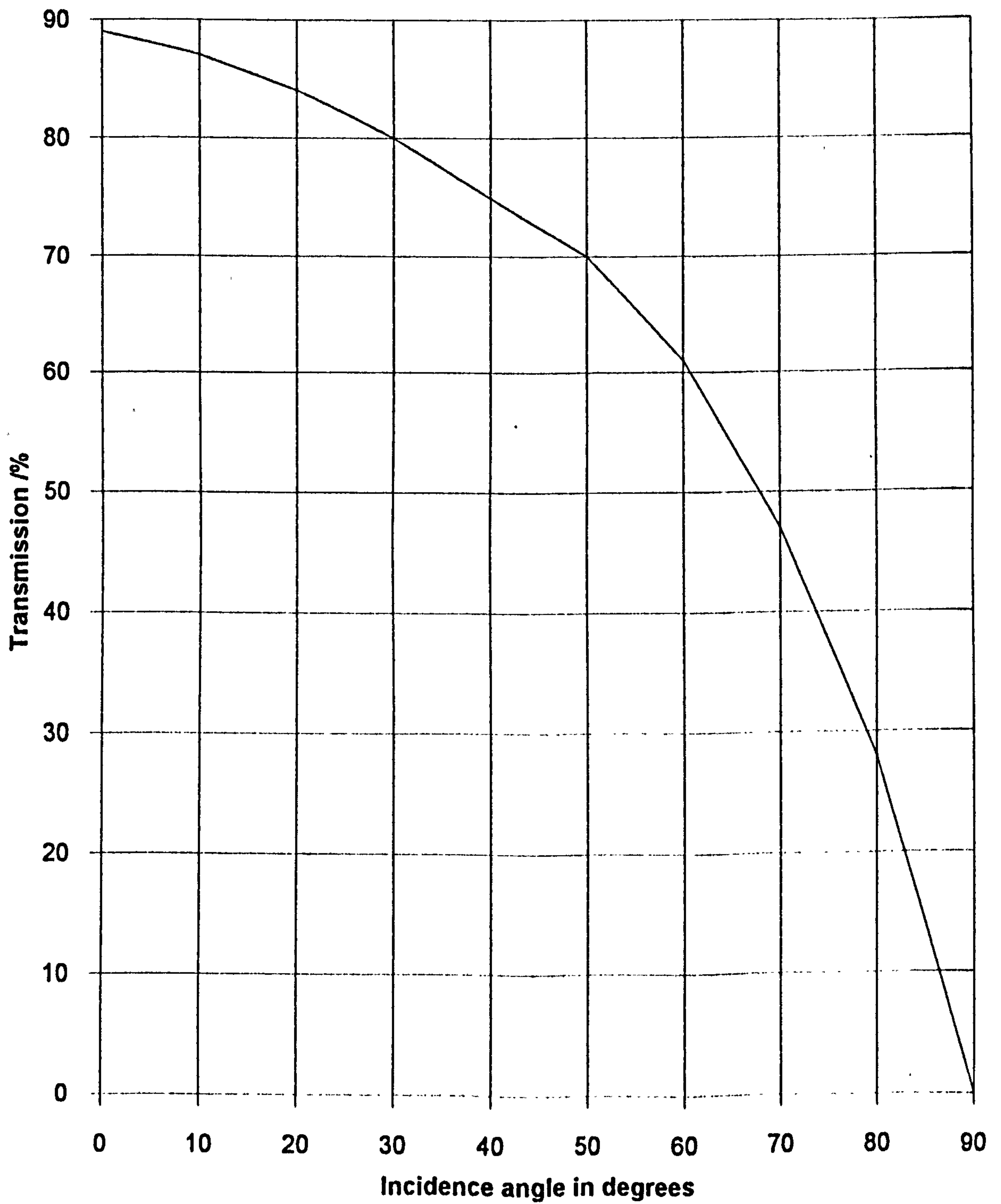


**Fig.6.19 Angular dependence of the solar transmission of Okalux capillary honeycomb material of 100mm thickness**





finite difference program, so that the validity of using such a method for the rapid assessment of solar wall performance could be made.

The steady state program was written using the monthly mean values of the required environmental parameters such as: beam and diffuse radiation, external air temperature, transmittance absorptance product. The program evaluates the monthly mean values of energy production, energy savings and the efficiency with which energy is saved. The effects of thermal capacity are ignored. The energy savings and efficiencies produced from the solar walls were evaluated for a whole heating season with reference to the heat balance of a well insulated cavity wall of  $U_{rw} = 0.45 \times 10^{-3} \text{ kWm}^{-2}\text{K}^{-1}$ .

Simple payback periods were computed. The cost of constructing a solar wall for the purpose of such estimation, was taken as the extra cost, in comparison with the cost of constructing a well insulated cavity reference wall. This extra cost (the solar overcost) includes the provision of glazing, transparent insulation material, and shutters. It was taken as  $\text{£}70\text{m}^{-2}$  for a single glazed Trombe wall, and  $\text{£}205\text{m}^{-2}$  for a double glazed, 100 mm transparently insulated wall. The cost of fuel used in such estimation was that prevailing in the United Kingdom.

#### Data sets used

Several sets of radiation and temperature data were obtained (for each month of a heating season) for several European sites<sup>87</sup> and the data placed within the steady state simulation program. The locations selected varied from Coimbra in the south, Lerwick in the north and Warsaw in the east. These locations are shown in Fig 6.20. Variations

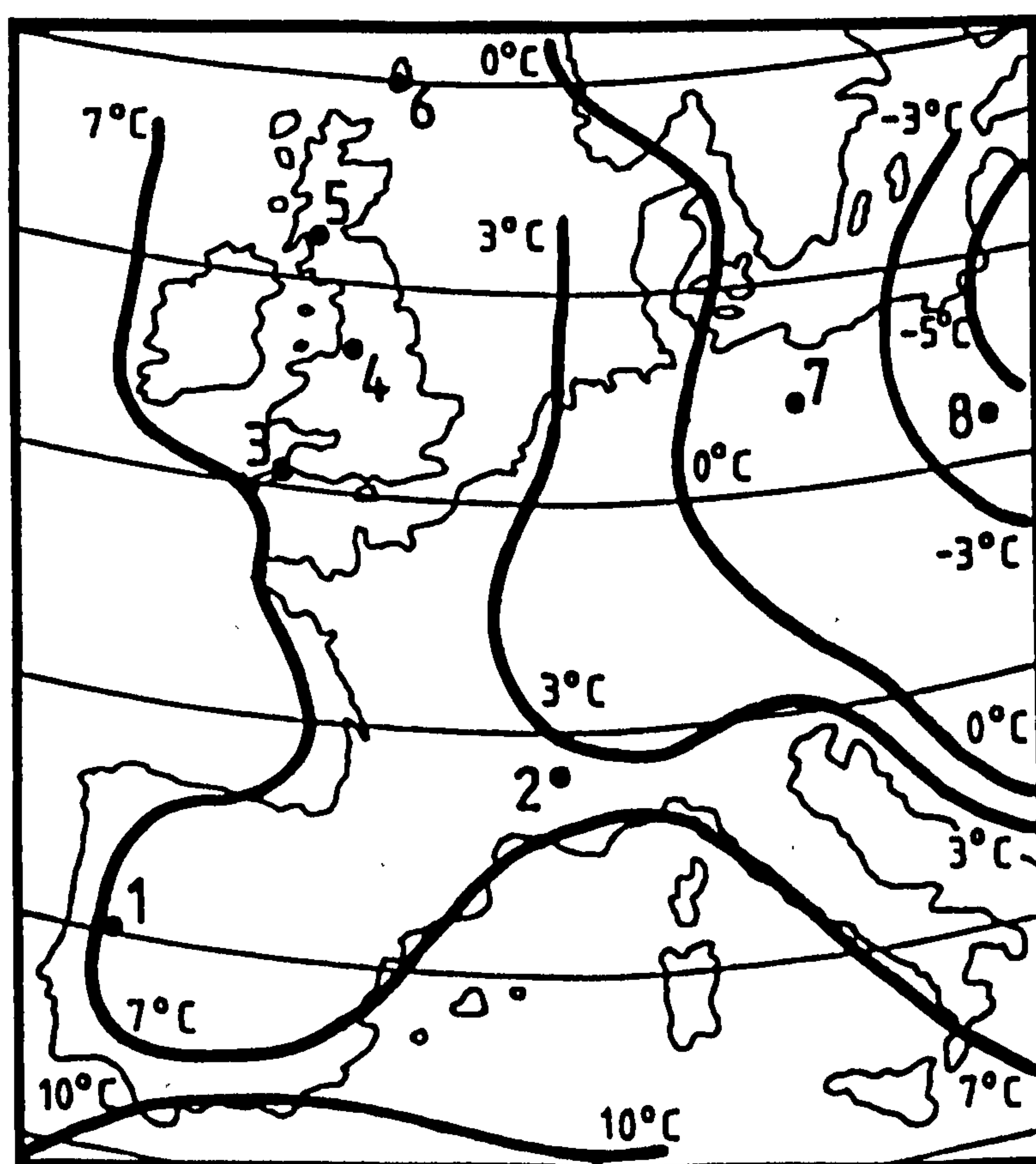


**Fig. 6.20 Locations used in simulations showing average January temperatures( $^{\circ}\text{C}$ ).**

**1= Coimbra 2= Carpentras 3=Plymouth 4= Manchester**  
**5= Glasgow 6= Lerwick 7= Berlin 8= Warsaw**

in winter temperature, and global insolation at these locations are displayed in *Table 6.10*.

## Results

The results of these simulations are shown in *Table 6.11*. There, the single glazed and poorly insulated Trombe walls are shown to be inefficient and completely inadequate in cold climates. That this is actually so, has been shown previously in this thesis, and reported in the literature<sup>81</sup>. Measurements of 5 per cent for the efficiency of heat delivery from a Trombe wall have been found at Poulton Lancelyn Wirral. F.Trombe<sup>39</sup> obtained 16 per cent for such efficiencies from a Trombe wall in Odeillo, Southern France. The rapid assessment program predicts 3 per cent and 15 per cent at such localities. The better efficiency of Odeillo is attributed to the higher levels of insolation found during the heating season, in Southern France. It is encouraging that predictions obtained by the rapid steady state program are close to those found in practice.

In contrast to the low values obtained for Trombe walls, transparently insulated walls produce constant and high efficiencies at every location. The rapid assessment program predicts circa 34-36 per cent heat production efficiency for double glazed, and 40-44 per cent for single glazed transparently insulated walls. Encouraging support for such predictions is given by the monitored results of Stahl in Freiburg<sup>74</sup> who measured 39 per cent and Jesch in Birmingham<sup>80</sup> who obtained 32 per cent for the efficiency of double glazed transparently insulated walls. Voss and Goetzberger in Freiburg<sup>88</sup> obtained 47 per cent and Dolley in Milton Keynes<sup>77</sup> 40 per cent for the efficiencies of single glazed transparently insulated solar walls.

**Table 6.10 Mean values of the air temperature and global irradiation during the heating season at different locations in Europe. The irradiation is measured on a south facing vertical plane.**

	Location	Latitude N	Length of heating season (months)	Mean air temperature (TS, C)	Seasonal total global irradiation (kWh/m <sup>2</sup> )	Mean daily global irradiation (HS.kWh/m <sup>2</sup> )
1	Coimbra	40	6	6.5	635	3.5
2	Carpentras	45	6	7.5	595	2.3
3	Plymouth	50	8	7.2	550	2
4	London	51.5	8		465	1.8
5	Manchester	53.5	9	7.5	500	1.7
6	Glasgow	55	9	7	450	1.6
7	Lerwick	60	10	6	500	
8	Hamburg	53.5	8		382	1.8
9	Berlin	52.5	8	5	430	1.6
10	Warsaw	52	8	3.5	380	0
11	Bergen	60.2	9	0	416	0
12	Stockholm	59.35	9	0	386	0

**Table 6.11 Comparison of the percentage efficiency predictions made by the rapid steady state assessment program with those made with the finite difference method. Some monitored results are also shown.**

FD=system specific finite difference program.

SS=rapid assessment steady state program.

MON= monitored results from : F=Freiburg B=Birmingham MK=Milton Keynes

LPL=Liverpool OD=Odeillo PI=Poulton Lancelyn

Location	Latitude	Single glazed Trombe wall			Double glazed TI wall			Single glazed TI wall		
	N	FD	SS	MON	FD	SS	MON	FD	SS	MON
Coimbra	40	13	12		36	36		42	44	
Carpentras	43	15	13	OD=16	39	36	F=39	45	44	F=47
Plymouth	50	7	8		38	36		45	43	
London	51	8	6		37	35		42	42	MK=40
Manchester	53.5	6	3	PI=5	36	34	B=32	41	41	LPL=42
Glasgow	55	4	2		36	34		41	41	S=43
Lerwick	60	-3	-2		36	34		41	40	



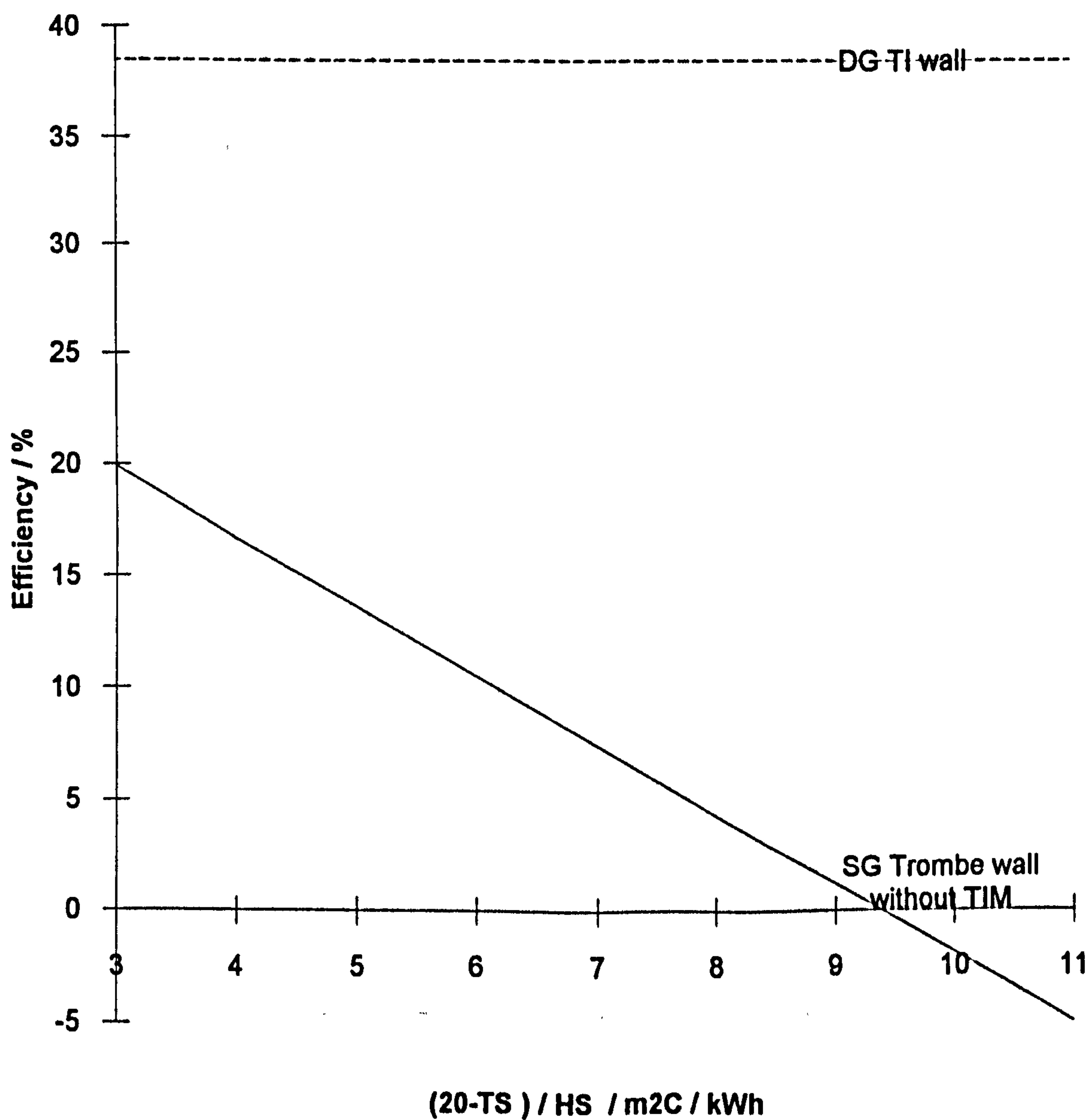
There is good agreement between the predictions produced using this rapid assessment steady state simulation, the system specific finite difference program, and monitored results. Such predictions and results are listed in *Table 6.11* and plotted in *Fig 6.21*. One can thus recommend the use of such approximate rapid assessment computational computer programs, for use in solar wall design as a rapid precursor to the eventual use of more sophisticated computer simulation techniques.

Trombe walls have been shown to be highly sensitive to the effects of external air temperature and global irradiation as deduced previously. The external air temperature has a great influence on their heat losses, the irradiation determines the quantity of heat available for passage through the solar wall. The factor  $(T_{ai}-T_{ao})/H_m$  has been shown to be important in determining the reduction in efficiency of Trombe walls (Equation 6.14), from their optimum value of  $U_{iw}(\tau\alpha)R_o$ . *Fig 6.22* plots this parameter against efficiency, for single glazed and double glazed 100 mm transparently insulated walls at various locations. The parameter is evaluated as  $(20-TS) / H_S$ , where  $20^\circ\text{C}$  is taken as the internal room air temperature,  $(TS,^\circ\text{C})$  is the mean external air temperature at a given location during the heating season, and  $(H_S, \text{kWhm}^{-2})$  represents the mean daily global irradiation on a south facing vertical plane during the heating season. These values are taken from *Table 6.10*. *Fig 6.22* shows the sharp decline in performance of poorly insulated Trombe walls in a heating season, as the temperature and irradiation intensity of a location decline.

Trombe walls work quite well where irradiation is high. They work less well in cold, poorly insulated regions. Trombe walls work well, for example, in Odeillo, Southern



**Fig.6.22 Variation of the efficiency of solar walls, at various European locations, with external temperature and insolation. 1=Coimbra 2=Carpentras 3=Plymouth 4=Manchester 5=Glasgow 6=Lerwick 7=Berlin 8=Warsaw**



France. In contrast, in *Table 6.12*, single glazed Trombe walls are seen to be totally uneconomic in Northern Europe.

Transparently insulated walls are much better. Their productive capacity and efficiency with which they operate was evaluated as  $U_{ii}R_o(\tau\alpha)$ . This equates to about 39 per cent for a double glazed and 47 per cent for a single glazed solar wall. These values for transparently insulated walls obtained by simulation, which are relatively constant, are shown in **Fig 6.21** and *Table 6.11*. These walls are almost economic when displacing electricity in Western Europe, but transparently insulated walls are not economic against gas.

Transparently insulated walls produce energy almost independently of the external temperature, because of their high insulation. Their efficiency of heat production and of energy savings is almost constant. Their energy savings are determined almost solely by the amount of radiation received. Transparently insulated walls work as successfully in the relatively benign climate of Freiburg, Southern Germany as in the colder climate of Glasgow. They only fail to produce worthwhile thermal benefits when the amount of winter sunshine received is too small as experience in Finland shows<sup>89</sup>.

## 6.6 ESTIMATION OF THE LENGTH OF A HEATING SEASON

A particular problem associated with solar wall simulation is the determination of the length of the heating season at a particular location. In the previous work, values used were based either on those used in UK practice or on estimations made by inspection of prevailing air temperatures. It would be preferable if the actual length of the heating

**Table 6.12 Energy savings, efficiencies and payback times for solar walls in the heating season.**

	Location	Energy savings		Efficiency of energy savings				Payback (years) when replacing:			
		kWh/m <sup>2</sup>		%				gas		electricity	
		TW	DGTI	TW	DGTI	SGTI	LOW E	TW	DGTI	TW	DGTI
1	Coimbra	90	240	14	38	46	32	35	33	11	10
2	Carpentras	90	230	15	39	46	33	35	34	1	11
3	Plymouth	60	210	11	38	45	32	50	37	16	12
4	London	60	180	8	39	46	32	78	44	25	12
5	Manchester	30	190	6	38	45	30	110	42	35	13
6	Glasgow	23	170	5	38	45	30	140	46	45	15
7	Lerwick	10	190	3	38	45	28	300	43	100	14
8	Hamburg	8	170	1	38	46	30	375	45	120	15
9	Berlin	5	165	1	38	46	27	370	48	120	15
10	Warsaw	-15	145	-4	39	46	29	infinite	53	infinite	17
11	Bergen	-6	150	-2	39	45	27	500	49	160	16
12	Stockholm	10	220	1	39	46	28	300	36	96	12

TW=single glazed Trombe wall

SGTI=single glazed transparently insulated solar wall.

DGTI=double glazed transparently insulated solar wall.



season at each chosen location could be calculated. A method is available and will be described. In this method one important parameter to specify, is the base temperature: the actual temperature to which the building needs to be heated, taking into account internal heat gains.

### The base temperature

The total heat loss from a building,  $Q$ , is given by the sum of the heat lost via the ventilation air ( $cpV$ ) and the fabric heat loss ( $\Sigma A_j U_j$ ):

$$Q = (cpV + \Sigma A_j U_j) (t_{ai} - t_{ao}) \quad (6.23)$$

where:

$V$  = Volume flow rate of air

$\rho$  = Density of air

$c$  = Specific heat of air

$U_j$  = Thermal transmittance of a building element (j)

$A_j$  = Surface area of a building element (j)

$t_{ai}$  = Internal air temperature

$t_{ao}$  = External air temperature

$$\text{If: } L = cpV + \Sigma A_j U_j \quad (6.24)$$

$$\text{Then the total heat loss is: } Q = L(t_{ai} - t_{ao}) \quad (6.25)$$

If the incidental heat gain from occupants, equipment and solar radiation is  $G$ , the heat to be supplied by the heating system ( $Q_h$ ) is the difference between the total heat loss,  $Q$ , and the incidental heat gains,  $G$  :

$$Q_h = Q - G \quad (6.26)$$

Although in real buildings there will be many departures from such basic conditions, such theory forms the basis of many simple modelling techniques. To conform to this pattern of heat loss, the building is heated by the heating system to a temperature lower than that needed by its occupants for their comfort. A base temperature ( $t_b$ ) is defined as the internal temperature level of a building that the heating system must be capable of reaching so that the difference between this base temperature and the higher internal temperature required for comfort can be provided for by internal heat gains. If

$$Q_h = 0,$$

$$Q = G,$$

$$t_{ao} = t_b,$$

$$G = L(t_{ai} - t_b)$$

hence the base temperature is given by:

$$t_b = t_{ai} - \frac{G}{L} \quad (6.27)$$

Above the base temperature no extra heating is required. A short while ago this temperature was taken in the UK as 15.5°C, but the use of higher levels of insulation have led to reduced base temperature values. 13°C seems appropriate for U values of 0.45W/m<sup>2</sup>K and air change rates of less than 1 per hour. The value of base temperature is of fundamental importance in determining the length of a heating season. 13°C has been used here as it is felt appropriate for the heating of the many low energy consuming buildings under construction which use U values of 0.4 W/m<sup>2</sup>K and air change rates of less than 1 per hour.

### Gustaffson's method <sup>90</sup>

In 1994 Evans <sup>91</sup> used this method to investigate the energy demand of solar heated buildings. Gustaffson's method is based on the use of the average monthly outside air temperature, a climatic parameter usually universally available. He arranged the temperature values ( $T, ^\circ\text{C}$ ) for each month of the year in ascending order. The cumulative number of days ( $D$ , days) corresponding to these temperatures was simultaneously calculated, as shown in *Table 6.13* for Manchester. A regression line was fitted to the data using the method of least squares with the form:  $T = a + b.D$  (see **Fig 6.23**). The intercept  $a$ , represents the lowest temperature (the design temperature) expected at the location. The slope  $b$ , is the daily rate of change of temperature. A line drawn from the chosen base temperature ( $t_b = 13^\circ\text{C}$ ) on the  $T$  axis, parallel to the  $D$  axis, will intercept the regression line at a value of  $D$  corresponding to the length of the heating season, (see **Fig 6.23**). In addition the area between the base temperature line and regression line represents the number of degree days in the heating season. This is a widely used parameter for estimating a buildings heating energy demand.

Gustaffson's method is rapid and precise. A computer program has been written to output regression line coefficients, length of heating season and number of degree days at several locations (see *Appendix 3.18*). Results are shown in *Table 6.14* and **Figs 6.24(a), 6.24(b), 6.24(c) and 6.24(d)** for locations from  $38^\circ\text{N}$  to  $60^\circ\text{N}$ . Gustaffson's method is eminently suitable for providing the length of heating season required by solar wall rapid assessment programs.

**Table 6.13 Monthly mean temperature in ascending order of magnitude, the cumulative number of days and the cumulative mean values of global solar radiation on a south facing vertical surface. Data for Manchester, UK.**

Month	Mean monthly temperature C	Days in the month	Cumulative days	Cumulative global solar radiation on a southern vertical plane kWh/m <sup>2</sup>
January	3.3	31	31	27.9
February	3.7	28	59	69.1
December	4.3	31	90	95.7
March	5.7	31	121	164.2
November	6.5	30	151	199.6
April	8.3	30	181	277.6
October	10.5	31	212	338.4
May	11.3	31	243	425.5
September	13.7	30	273	497
June	14.3	30	303	581
July	15.5	31	334	663
August	15.7	31	365	742

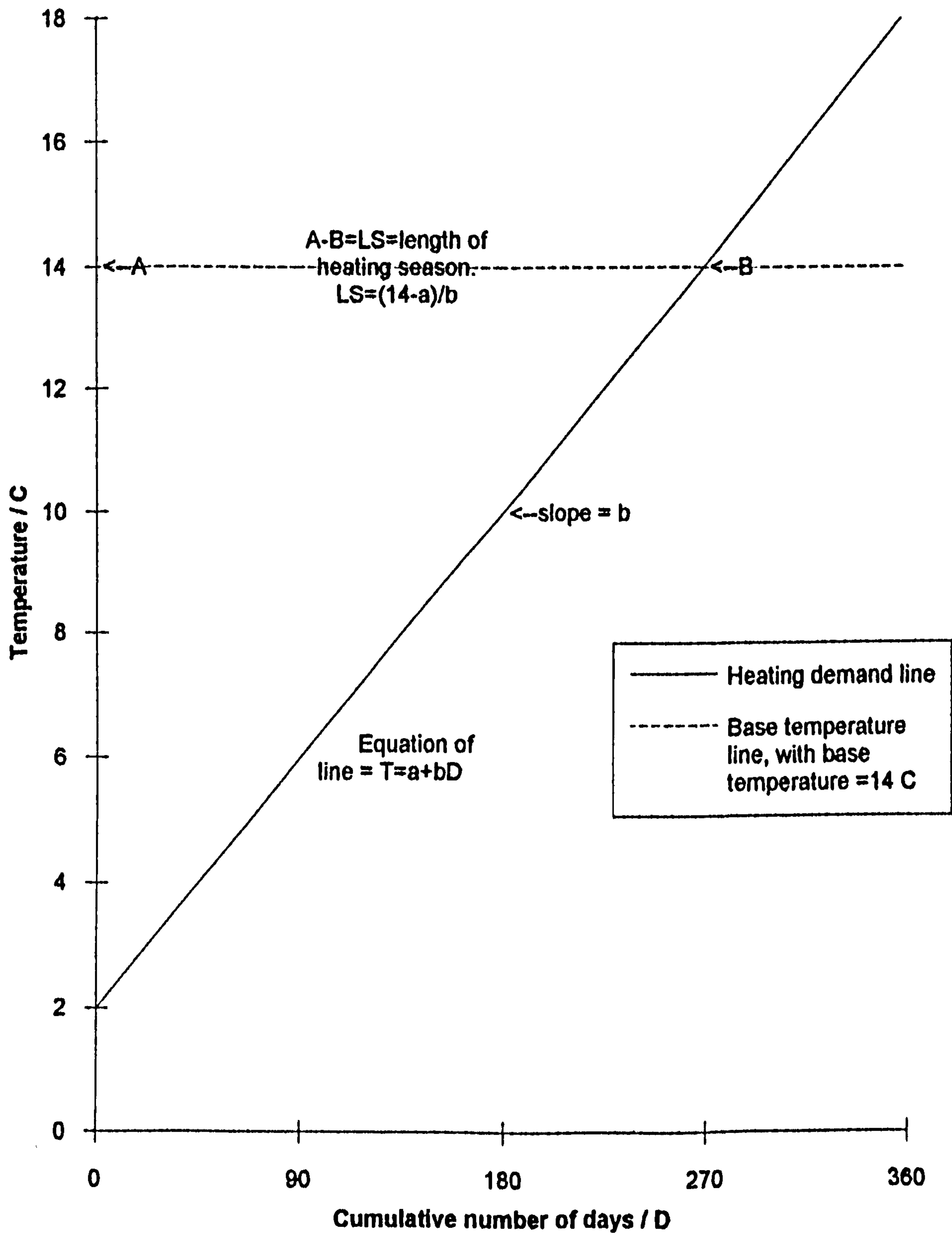


Fig. 6.23 Heating demand graph.



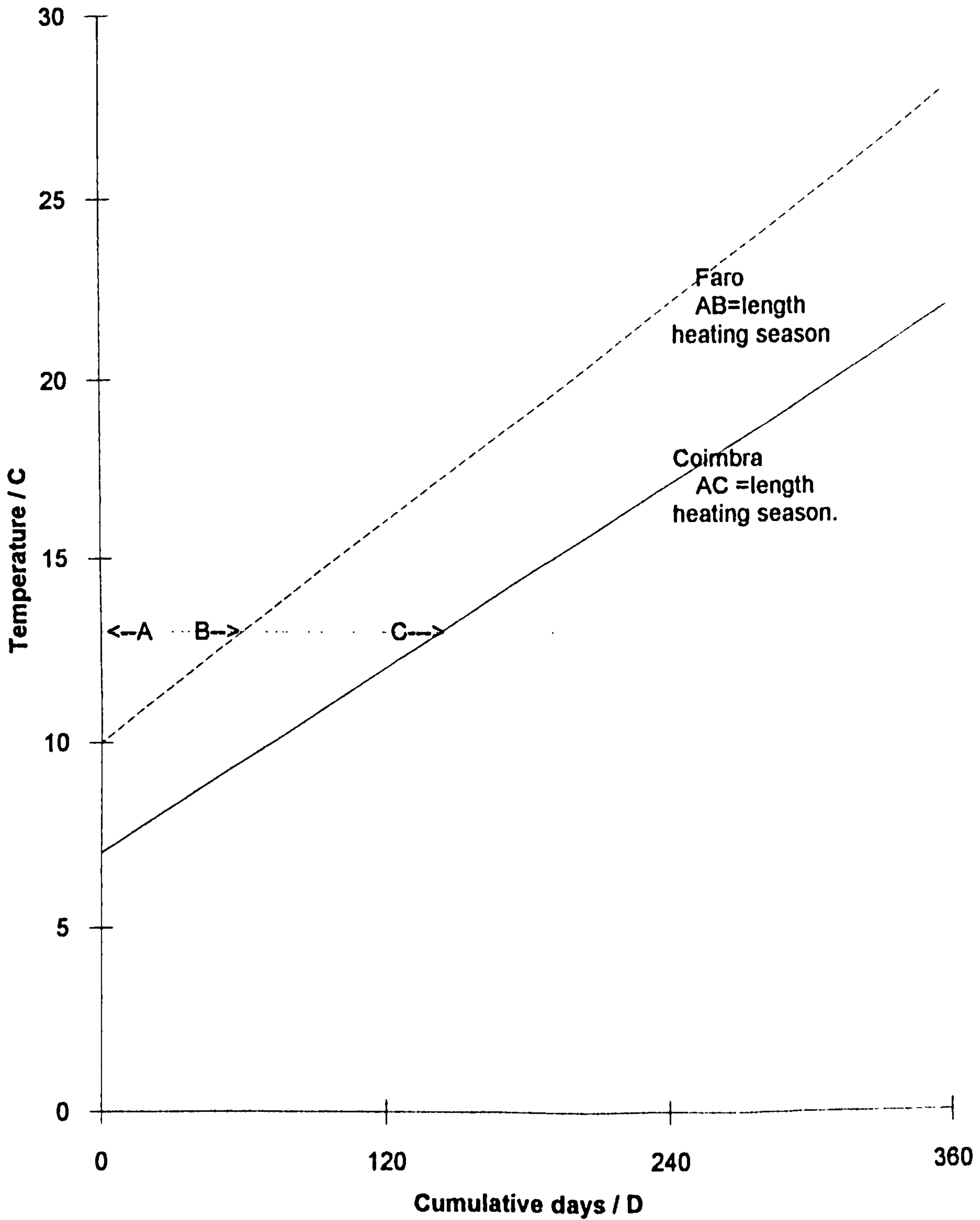


Fig. 6.24(a) Heating demand graph for the warmer winter climate of Southern Europe. A base temperature of 13C is used.

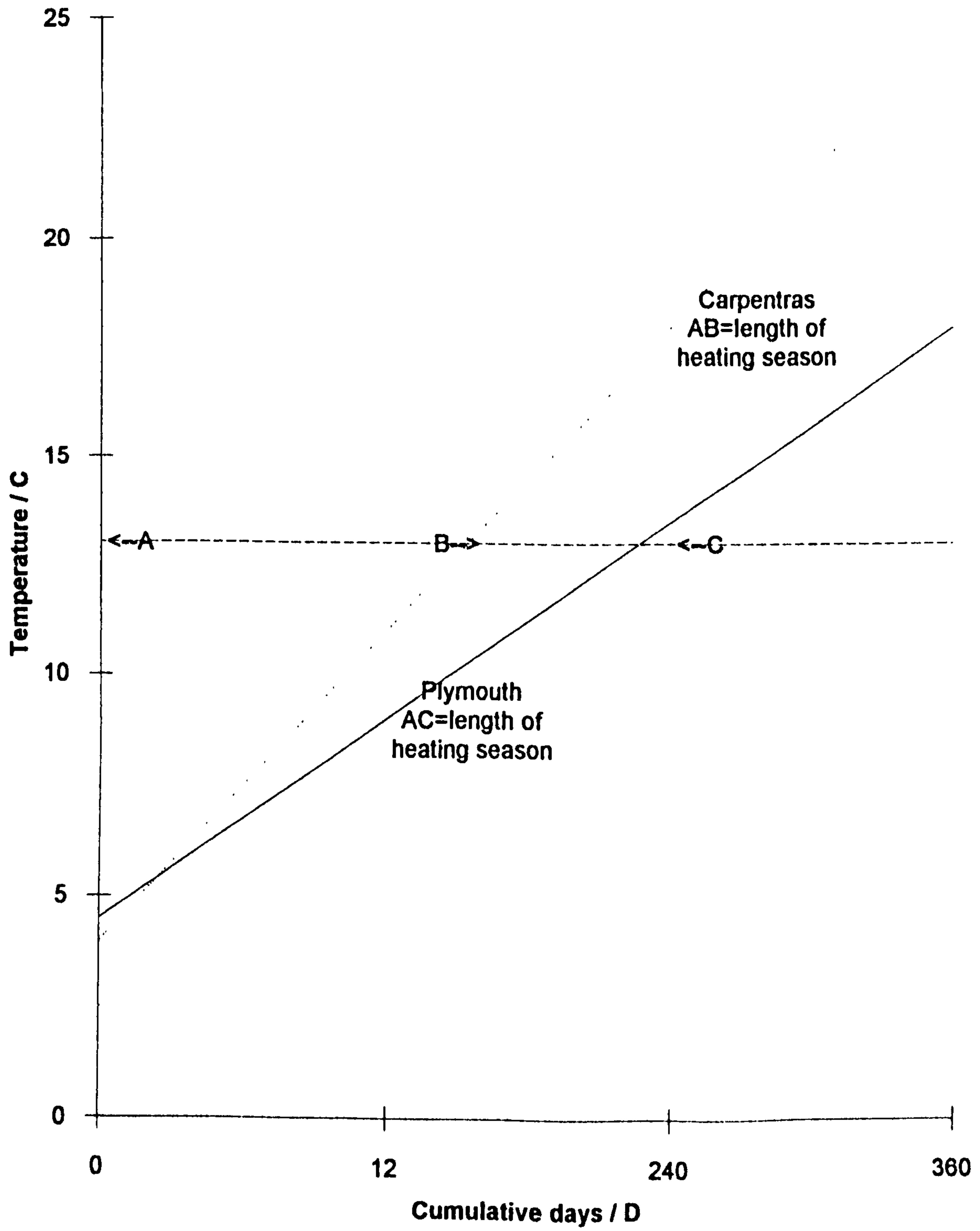


Fig. 6.24(b) Heating demand graphs for the mild winter climate of Carpentras and Plymouth. A 13C base temperature is used.

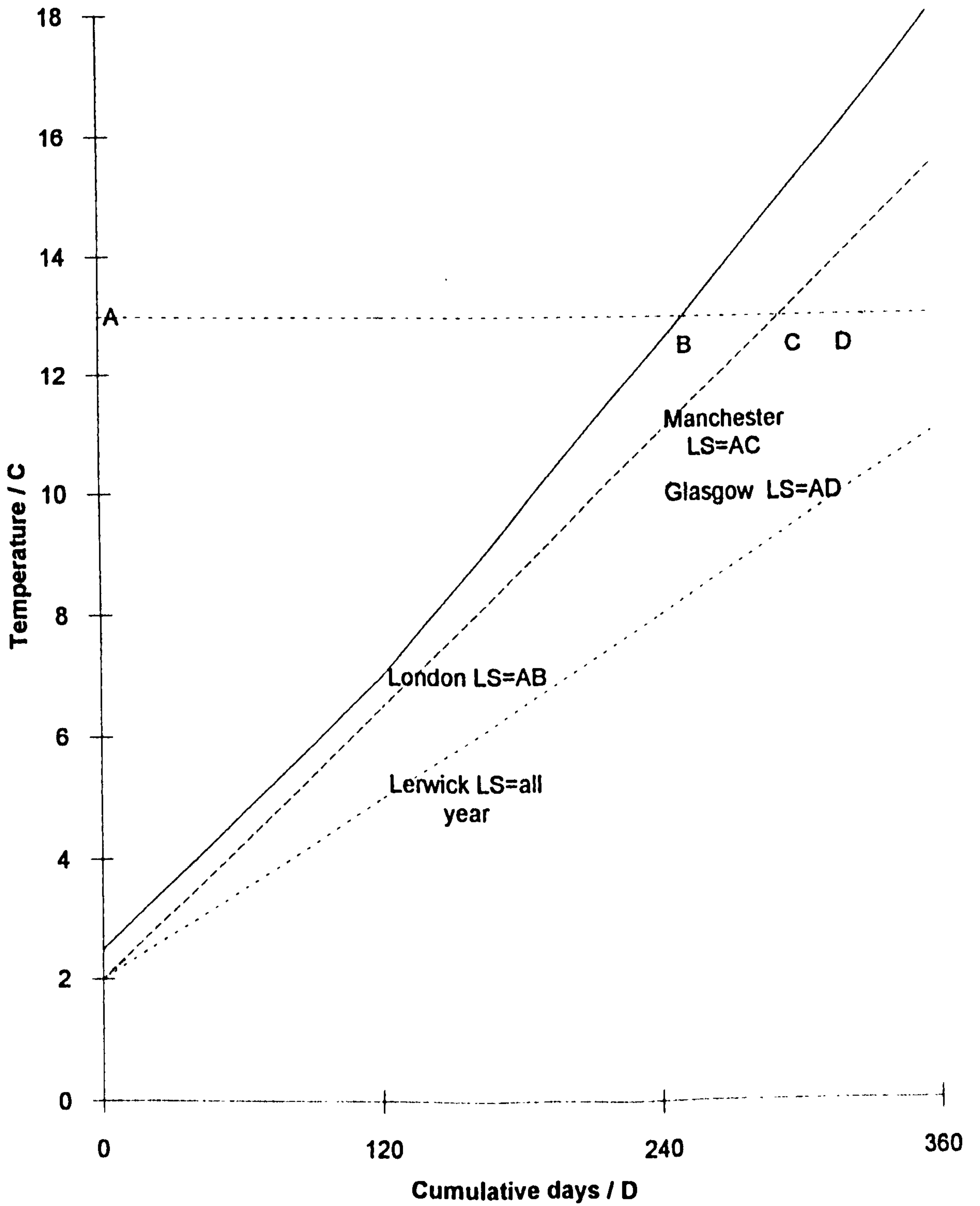
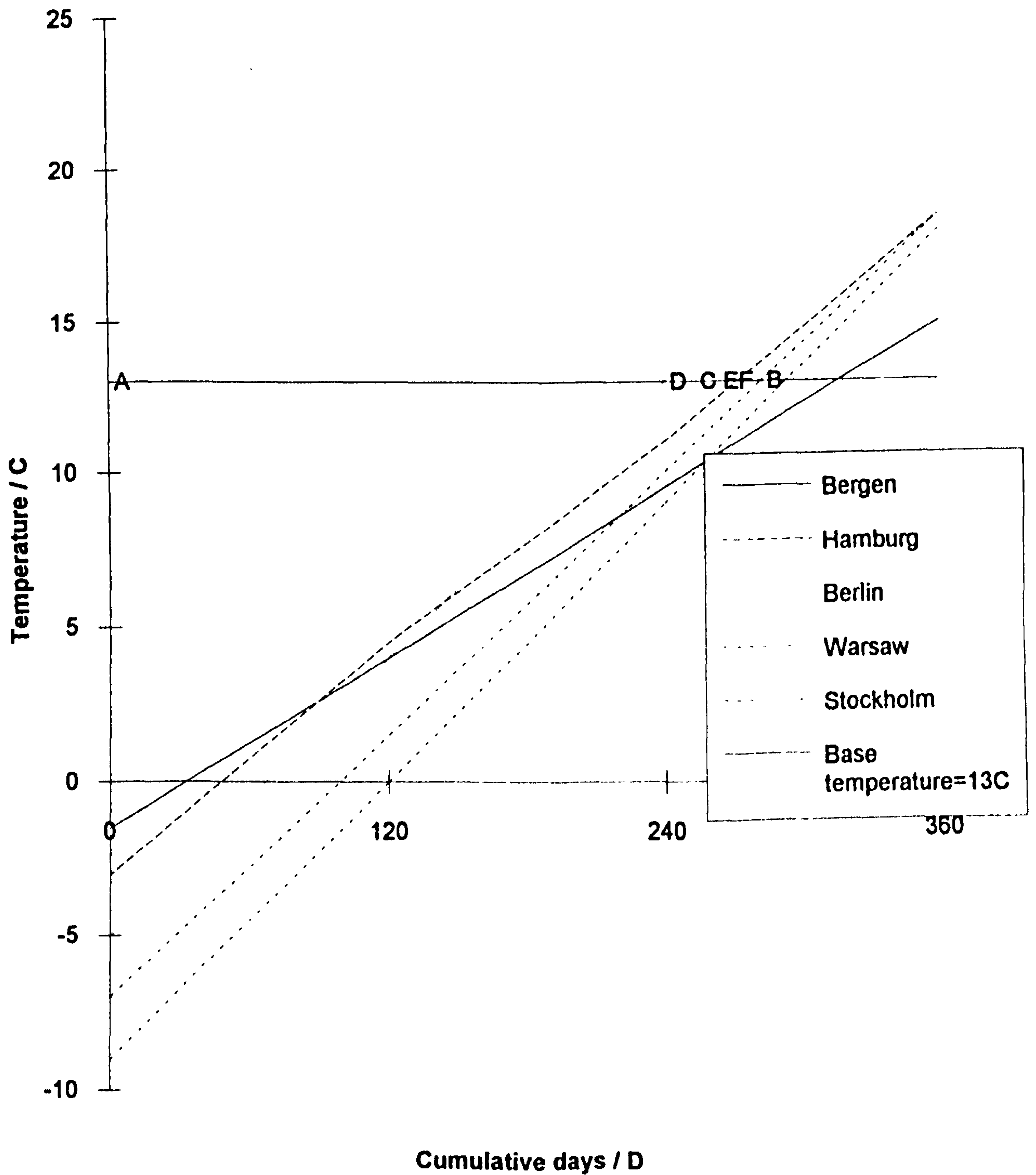


Fig. 6.24(c) Heating demand graph for other UK locations, (cool winters). A 13C base temperature is used. Lengths of heating season (LS) are indicated.



**Fig. 6.24(d) Heating demand graphs for northern, continental locations (cold winters). Length of heating season: Bergen=AB Hamburg=AC Berlin=AD Warsaw=AE Stockholm=AF.**

Gustaffson's method is extended to estimate the: "solar radiation resource" on an appropriate plane, in an appropriate direction, at a specified location. A regression equation of cumulative global solar radiation versus cumulative number of days in the heating season, arranged as before in ascending order of the prevailing average monthly external air temperature (*Table 6.14*), is computed. A graph of this equation (see **Fig 6.25**), for a south facing vertical plane, enables the total global solar radiation incident in the winter and heating season to be displayed for any location. Stockholm is more favoured than Bergen, for the implementation of transparently insulated walls by virtue of its superior solar resource in winter as well as autumn and spring. Such a graph could prove useful for quickly appraising the suitability of a site for the implementation of passive solar design.



**Table 6.14 Regression coefficients for temperature and global solar radiation at various European locations.**

Heating season length determined using a base temperature of 13C.

Location	Latitude	Regression equations		Design temperature	Length of heating season
		For temperature	For global solar radiation on a south vertical plane		
		C	kWh/m <sup>2</sup>		
	N	C	kWh/m <sup>2</sup>	C	months
Faro	38	$T=.039D+10$	$G=3.6D+14$	10.1	3.2
Coimbra	40	$T=.037D+7$	$G=3.5D-20$	7.3	5.9
Carpentras	45	$T=.056D+3$	$G=3.5D-30$	3.2	6.3
Plymouth	50	$T=.035D+3.8$	$G=2.45D-63$	3.2	9.4
London	51	$T=.045D-1.7$	$G=2.17D-83$	1.7	8.8
Manchester	53.5	$T=.042D+1.1$	$G=2.18D-90$	1.1	10
Glasgow	55	$T=.04D+1.07$	$G=1.97D-78$	1.1	10.7
Lerwick	59	$T=.03D+1.06$	$G=1.83D-67$	1.1	all year
Hamburg	53	$T=.06D-3$	$G=2.3D-102$	-3	9.3
Berlin	52	$T=.066D-4$	$G=2.3D-102$	-3.8	8.8
Warsaw	52	$T=.075D-7$	$G=2.18D-108$	-6.6	8.9
Bergen	60	$T=.049D-1.7$	$G=1.86D-99$	-1.7	10.5
Stockholm	59	$T=.069D-7$	$G=2.3D-102$	-7	9.9

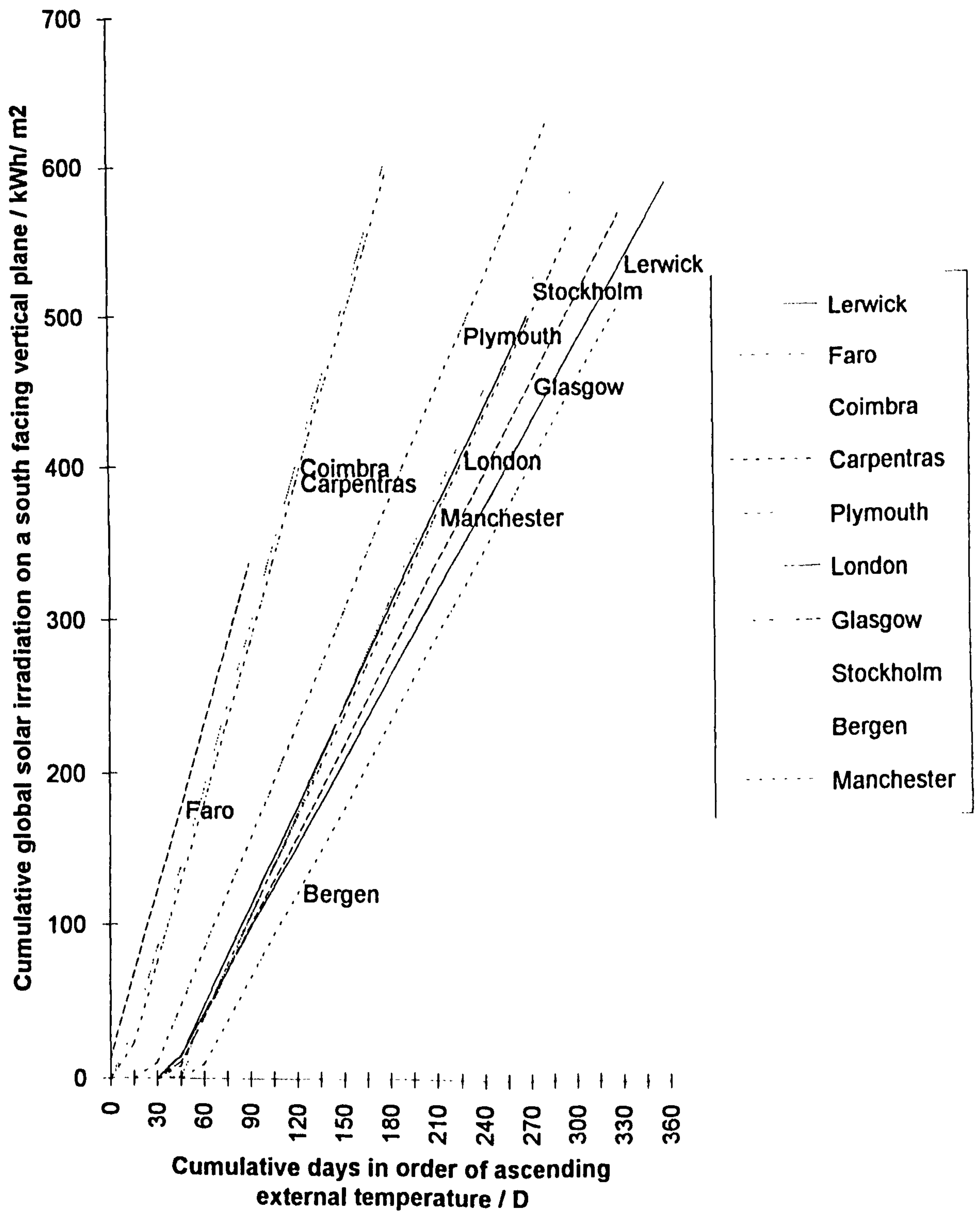


**Fig. 6.25 Modification of Gustaffson's method:  
The solar resource on a south facing vertical plane for  
European locations in the heating season.**

**CHAPTER 7 - CONCLUSION:  
FUTURE PROSPECTS FOR SOLAR  
ENERGY IN CONSTRUCTION**

## 7.1 FUTURE PROSPECTS

Some 20 years ago, new housing in Britain incorporated almost no thermal insulation. Since then the demand to reduce the energy used in buildings has become more imperative (see Fig 7.1) and thermal improvements have been made. The use of low energy passive solar designs can produce even more energy saving than has so far been achieved in conventional practice. Such designs can save at least 50% more energy than that obtained by building in conformity with the 1990 regulations.

To date such designs have not been widely adopted by mainstream builders<sup>92 & 93</sup> for reasons such as:

1. A lack of information on design principles.
2. A lack of credibility that solar designs can provide worthwhile energy contributions.
3. A lack of incentive due to low fuel prices, and thus the urgent need to save energy.
4. A lack of knowledge of the potential market for passive solar design by developers.

This thesis has addressed points 1 and 2. It has provided information on the design principles relating to solar walls. It has shown that technical innovation has enabled their construction to be so improved, that they can make valuable contributions to a buildings heating energy requirements in northern latitudes. To answer point 4 with respect to the more widespread use of TI walls, it is felt appropriate to study the market for renewable energies themselves.

The view of the Shell Petroleum Company<sup>18</sup> is that renewable energies must become competitive with existing fossil fuel based technologies before their widespread



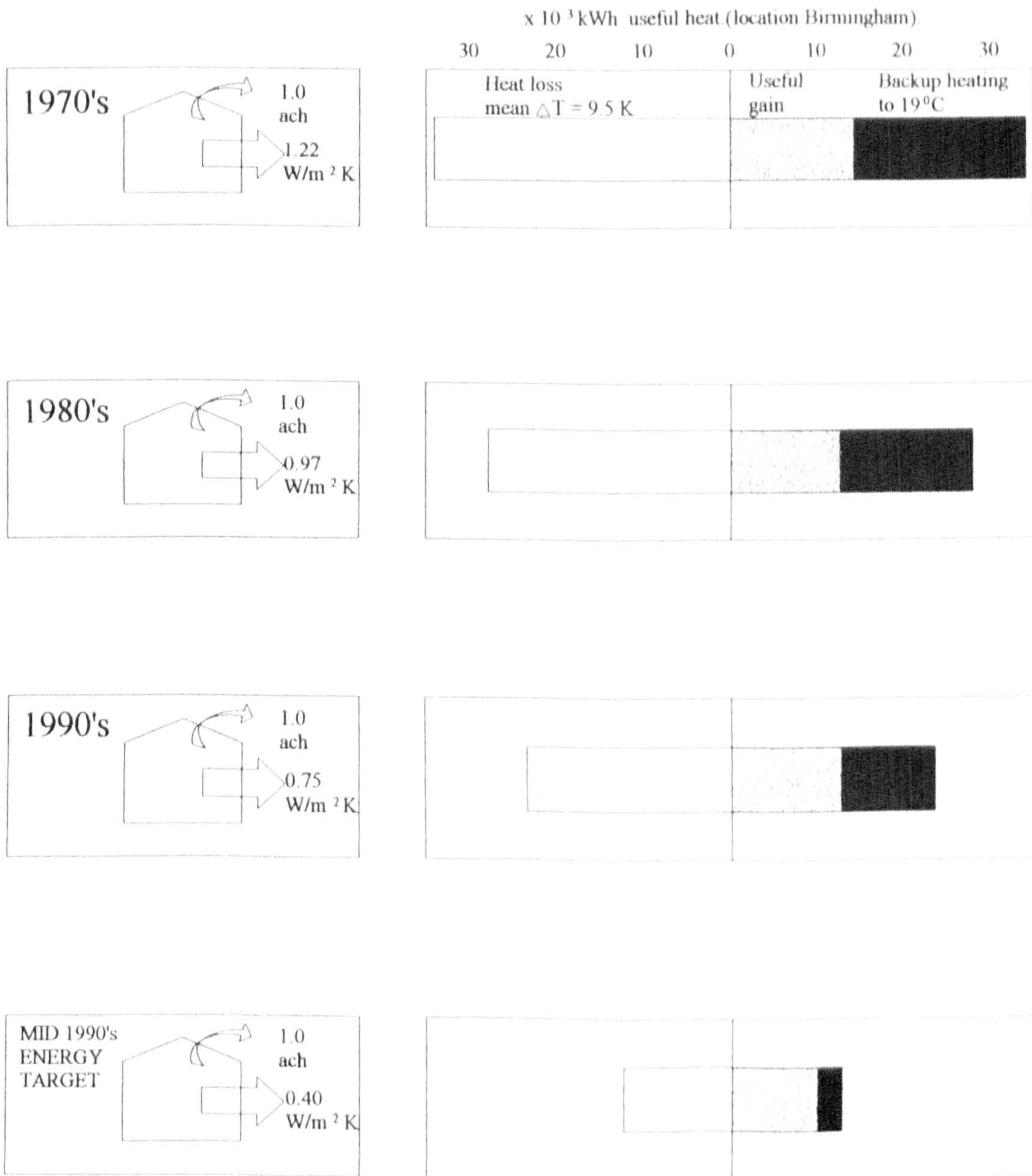


**Fig. 7.1 Building regulation mean U value (W/m<sup>2</sup>k) and mean air exchange (ach) together with the reduction in heat loss and backup heating as a result of thermal improvements in house design (whole house temperature=19°C).**



application can occur. A typical timescale for this might be deduced by the inspection of information relating to the future markets for the photovoltaic production of electricity.

Photovoltaic conversion of solar energy is a technically elegant and silent renewable solution for the replacement of fossil fuels used for electricity generation<sup>94 & 95</sup>. Modules can be sited on building facades and rooftops<sup>96 & 97</sup>, but at present the technology is only cost competitive in niche markets away from power distribution grids<sup>96</sup>. As can be seen from **Fig 7.2**, the cost of modules has fallen continuously from \$15/Wp in 1980 to \$5/Wp now. Cost competitiveness with fossil fuel generated electricity will occur when the modules cost less than \$2/Wp at present electricity prices.

At this point, one would expect more widespread use of photovoltaics, particularly in commercial buildings where the load-demand profile matches the photovoltaic electricity generation profile<sup>97</sup>. The emergence of PV roofing and cladding as a cost effective way of producing electricity would increase the credibility of solar designs as methods of making worthwhile and cost effective contributions to the energy demands of buildings<sup>98</sup>. TI walls and PV for example produce similar amounts of energy from the sun, although in different forms. A south facing roof or wall on a house in London, provides at 33000kWh per annum, more than its requirements for the whole year. Since symbiosis between PV and TI walls is implied, the date at which photovoltaic technology will reach cost effectiveness is clearly important.

## 7.2 THE WORLD PHOTOVOLTAIC MARKET<sup>99,100,101 & 102</sup>

The modern history of PV production is shown in **Fig 7.3** which represents annual shipments of PV modules. Rapid initial growth occurred through Government funded projects. This growth generated later slowed, but it is predicted to accelerate as the price

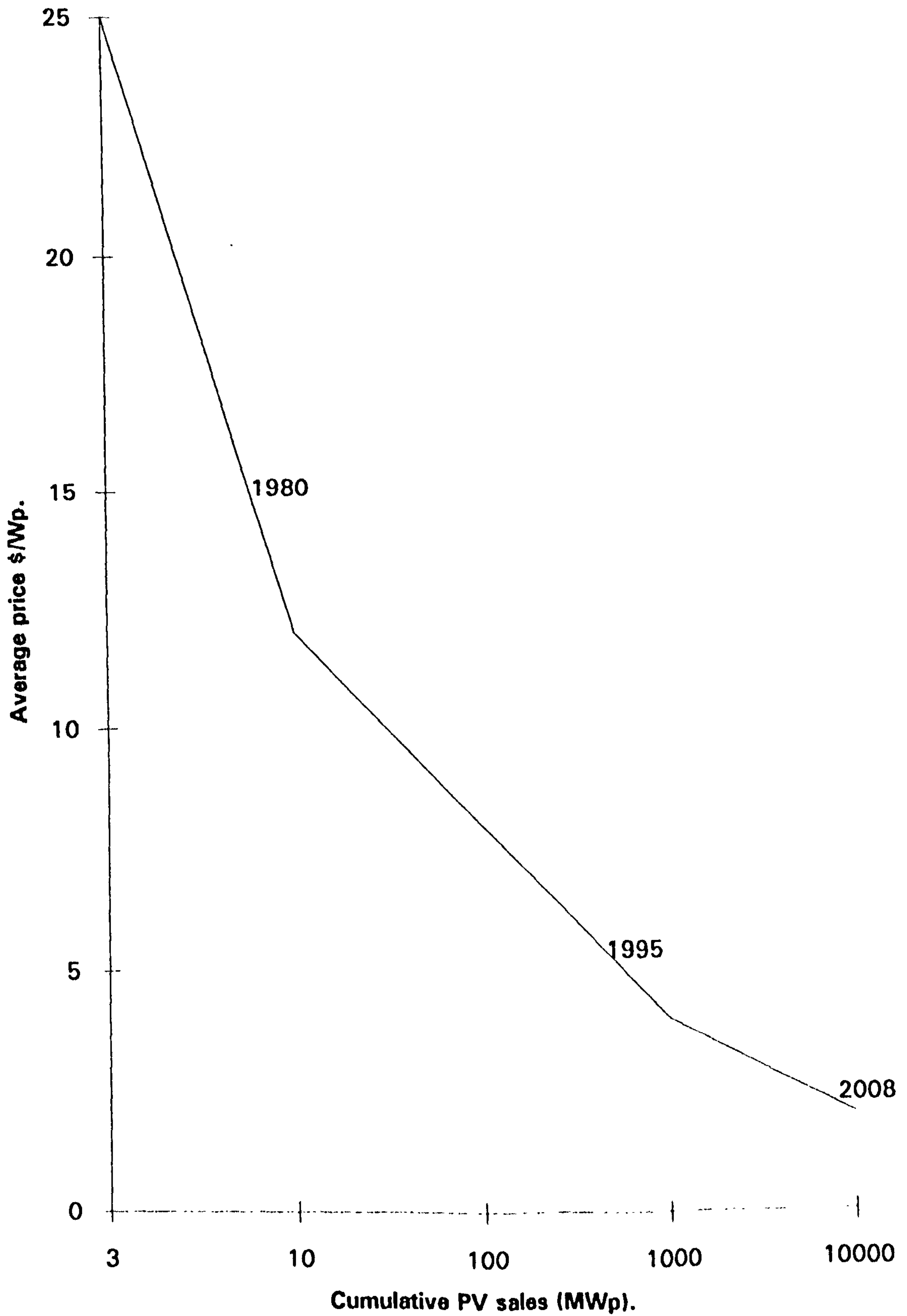
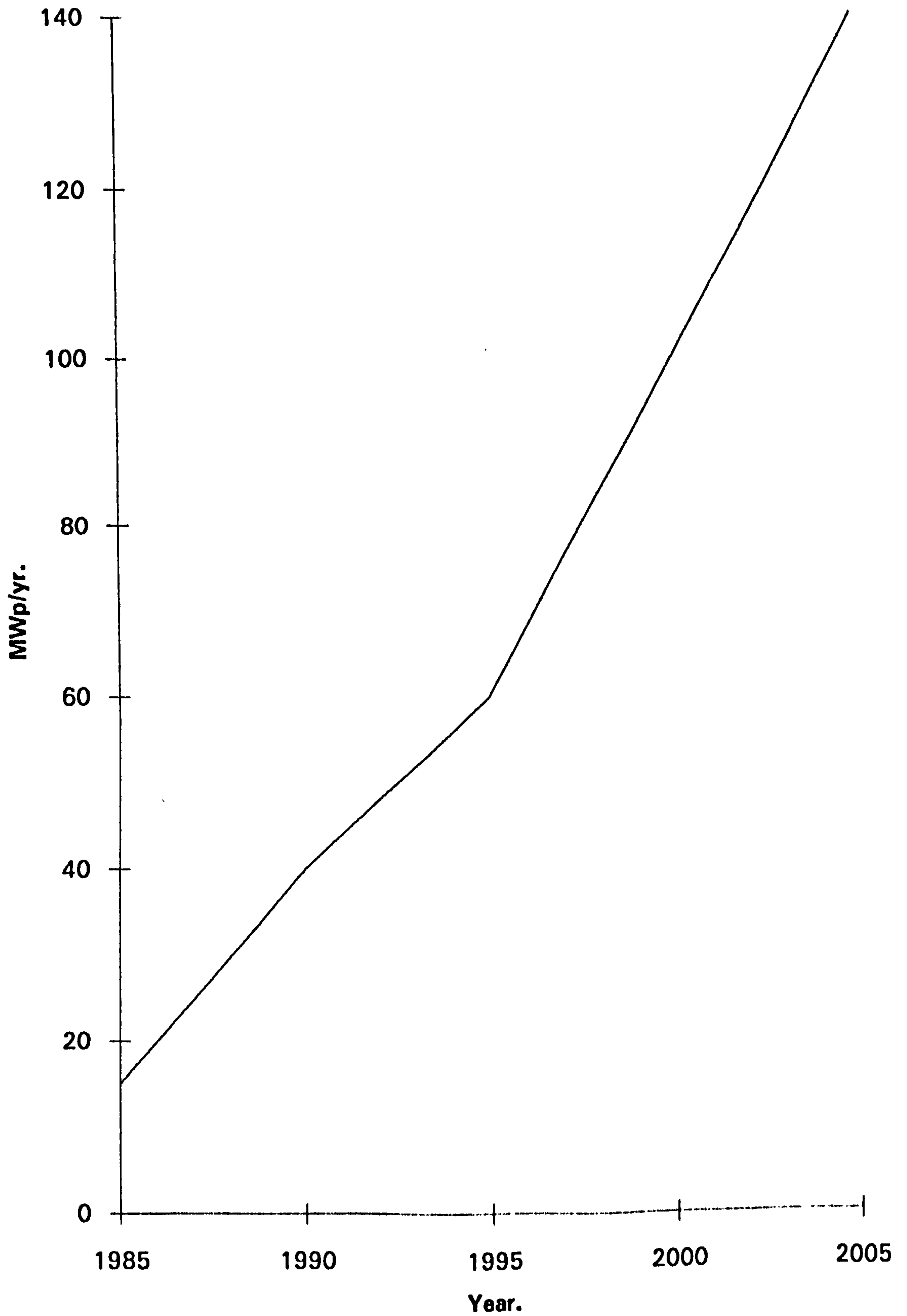


Fig. 7.2 PV market experience curve (with market forecast from 1995).



**Fig. 7.3 Annual shipments of PV modules from 1985 with a forecast from 1995.**

of crystalline silicon modules falls from a 5\$/Wp in 1993 to an expected 2.5\$/Wp in 2008.

BP Solar started production of cheaper, stabilised cadmium telluride thin film solar cells in 1996. Their price is expected to fall below 0.7\$/Wp. by the year 2010. The cost of electricity so produced could then be less than 10p/kWh which is commercially justifiable.<sup>93</sup>

If at this point the grid connected market for photovoltaic modules incorporated in the roofs and facades of buildings greatly increases, then the relevance of other applications of solar energy in those buildings will become plain, their use credible. The market for solar design in general and TI walls in particular would be stimulated by widespread expansion of such an attractive renewable technology.

That this may be so is indicated by the evidence presented above that photovoltaic technologies have rapidly matured, with prices decreasing to the point where they can be economically integrated into facades and roofs over the next decade in North West Europe. The cost effectiveness of electricity so generated should be reached by 2008. By 2010 it is predicted that grid connected schemes in buildings could be supplying up to 20% of the peak electric power demand.

The buildings in which such modules repose will have the ethos of producing electricity without greenhouse emissions, hopefully designed by the architectural fraternity to be both aesthetically pleasing and with the help of passive solar: environmentally benign.

### **7.3 THE MARKET FOR TRANSPARENTLY INSULATED WALLS**

Many people are convinced that renewable technologies, though scientifically interesting, are unlikely to make a significant contribution to the increasing demand for energy, except in the distant future. Yet hydro-electricity (a renewable energy source) meets 20% of the global electricity demand, and the earth intercepts 10,000 times more solar energy than the current primary energy demand. The potential is there, but widespread utilisation of renewable technologies will not occur, until they become cost competitive.

A growing world population will require continual increase in its supply of primary energy over the coming decades. The pressure of rising demand should eventually result in the cost of renewable energy converging to the market prices of fossil fuel based technologies themselves. For photovoltaic cladding modules and passive solar design this should occur from the year 2010. By the middle of the next century the so called new renewables could be providing half the global commercial demand, exceeding the total 1996 consumption of commercially traded energy. Renewables such as photovoltaics, and passive solar devices such as TI solar walls should then be able to play an important role in providing environmentally benign solutions to the energy demands of our buildings.

### **7.4 CONCLUSION**

Accurate dynamic and less accurate steady state system specific simulation programs have been written to simulate solar wall performance with a transparent insulation material covering and / or glazing in any climate. A rooftop exposure and data logging



site has been established for empirical validation of the dynamic model. The programs have been used:

1. To produce an optimum solar wall configuration, which using selective coatings produces three times as much energy as the earlier design.
2. To predict the usefulness of transparent insulation material for Western European buildings, in particular those at high latitudes, from the point of view of energy conservation and economy.

The in situ behaviour of a Trombe wall in a low energy school has been studied via long term monitoring and computer optimisation of solar wall performance. Such studies are rare, expensive, and time consuming, but each is unique. Lee <sup>43</sup> performed an analogous study. A model Trombe wall was exposed after computer optimisation and achieved 18% efficiency. The Poulton Lancelyn study extends Lee's work, highlights the effects of defective installation techniques on Trombe wall performance, shows that passive solar components must be simple for success and suggests design modifications to greatly improve solar utilisation efficiencies.

A claim for independent contribution to knowledge is hereby made on the following counts:

- (i) A unique study has been made of the performance of an in situ solar wall in a low energy school in North Western England.
- (ii) Two system specific simulation programs (one finite difference the other steady state) have been written to run on personal computers to predict the behaviour of solar walls at any location.

- (iii) The monitoring of model solar walls in Liverpool, and the use of a finite difference program to optimise their performance has shown that seasonal efficiencies can be dramatically improved.
- (iv) Use of the steady state simulation program to predict the heat generation and economic viability of solar walls in the northern latitudes of Western Europe.

Suggestions for further work and research include modification of the dynamic system specific simulation program to compute the mean radiant temperatures and internal air temperatures of well insulated rooms adjacent to south facing transparently insulated walls, in order to predict the improvement in comfort conditions produced by the solar energy influx. The new TIM module incorporated into TRNSYS could be used for program validation. Secondly TIM could be used to improve the thermal and optical performance of glass blocks. Finally true energy costs could be quantified in a comparative study of the environmental impact of passive solar energy versus the environmental impact of the use of fuels it will displace.

## REFERENCES

## REFERENCES

1. Ponting, C. (1991), A green history of the world, Sinclair-Stevenson, London.
2. Anon (1969), Resources and man, National Academy of Sciences-National Research Council, Freeman, San Francisco.
3. Scheer, H. (1994), A solar manifesto, James and James, London.
4. Anon (1993), Annual energy review, Directorate General for Energy (DG XVII), European Commission, Brussels.
5. Meadows, D.H. and Randers, J. (1992), Beyond the limits, Earthscan, London.
6. Malthus, T. R. (1798), An essay on the principle of population as it affects the future improvement of mankind, Facsimile reprint, Macmillan, London.
7. Roberts, N. (1994), The changing global environment, Blackwell, Oxford.
8. Leggett, J. (1990), Global warming, the Greenpeace report, Oxford University Press, Oxford.
9. Landsberg, P. T. (1979). Mathematical aspects of solar energy, British Association for the Advancement of Science, London, A49.
10. Twidell, J. and Weir, T. (1986), Renewable energy resources, Chapman and Hall, London, 78
11. Chapman, P. F. (1976), Principles of energy analysis, in Blair, Jones and Van Horn (eds), Aspects of energy conversion, Pergamon Press, Oxford, 723-724.
12. Barnola, J. M. et al (1987), Vostok ice core provides 160,000 year record of atmospheric CO<sub>2</sub>, Nature, 329, 408-414
13. Croll, J. (1867), Climate and time, Appleton and Co., New York.
14. Milankovitch, M. (1930), Mathematische klimaschrankungen, in W. Kloppen and R.Geiger (eds), Handbuch der klimatologie, Berlin, 1A.

15. Nisbett, E. G. (1989), Some northern sources of atmospheric methane: production history and future implications, *Canadian Journal of Earth Sciences*, 26, 1603-1611
16. Houghton, J. T. et al (eds) (1990), *Climate change, the IPCC scientific assessment*, Cambridge University Press, Cambridge.
17. Vaughan, D.G. and Doake, C. S. (1996), Recent atmospheric warming and retreat of ice shelves in the Antarctic Peninsula, *Nature*, 379, 328-331.
18. Booth, R. (1995), *Renewable energy, dream or reality?*, Solar Energy Society, Conference C63, Franklin Road, Birmingham.
19. World Energy Council (1994), *New renewable energy sources, a guide to the future*, Kogan-Page, London.
20. Grieff, J. (1995), *The EU support for renewable energies*, Solar Energy Society, conference C63, Franklin Road, Birmingham.
21. Hickey, J. R. et al (1982), Extraterrestrial solar irradiance variability: two and one half years measurements from Nimbus 7, *Solar Energy*, 28, 443.
22. Duncan, C. H. et al (1982), Latest rocket measurements of the solar constant, *Solar Energy*, 28, 385.
23. Waters, J. R., (1977), *The derivation and experimental verification of a computer aided thermal design method for buildings*, PhD Thesis, University of Coventry.
24. Fischenden, M. W. and Saunders, O. A., (1960), *Introduction to heat transfer*.
25. Danter, E. (1973), *Heat exchangers in a room*, IHVE symposium, June.
26. *CIBS Guide* (1970), Chartered Institute of Building Services, London.
27. Chapman, A.J. (1963), *Heat transfer*, Macmillan, New York.



28. Duffie, J. A. and Beckman, W. A. (1991), Solar engineering thermal processes, 2nd ed, John Wiley, New York.
29. Page, J. and Lebens, R. (1986), Climate in the United Kingdom, HMSO, London.
30. Beckman, W.A, Klein S.A. and Duffie, J.A. (1977) Solar heating design, Wiley, New York.
31. Wijesundara, N. E. (1978), Comparison of transient heat transfer models for flat plate collectors, Solar Energy, 21, 513
32. Hottel, H. C. and Woertz, B. B. (1942), Performance of flat-plate solar heat collectors, Trans. ASME, 64, 91.
33. Klein, S. A. et al (1990). TRNSYS users manual, version 1.3, Report 38, Solar Energy Laboratory, University of Wisconsin.
- 34 ASHRAE standard 93-77, (1977), Methods of testing to determine the thermal performance of solar collectors, American Society of Heating, Refrigeration and Air Conditioning Engineers, East 47th Street, New York.
35. Hobday, R. A. (1991), The heliotherapists, ISES conference report, Denver, vol 3, 1, 3039-3064
36. RIBA (1933). The orientation of buildings, Royal Institute of British Architects, London.
37. Sykes, J. M. (1989), Sick building syndrome, Building Services Engineering Research and Technology, 10, 1, 1-9.
38. Norton, B. and Hobday, R. A. (1990), Passive solar schools in the UK, International Journal of Ambient Energy, 11, 2
39. Trombe, F. et al (1979), Some performance characteristics of the CRNS solar house collectors. Solar Energy Society. Conference C19, London.

40. Utzinger, D. H. and Klein, S. A. (1980). Effect of air flow rate in collector-storage walls, *Solar Energy*, 25, 511.
41. Balcomb, J. D. Jones, G. and Yamaguchi, K. (1984), Natural convection air flow measurements and theory, 9th Passive solar conference, American Solar Energy Society, Boulder, CO.
42. Ohanessian, P. and Charters, W. (1978), Thermal simulation of a passive solar house using a Trombe-wall structure, *Solar Energy*, 20, 275-281.
43. Lee, J. B. G.(1978), Development and optimisation of Trombe's solar wall, Ph.D. Thesis, University of Leeds.
44. Balcomb J. D., Barley, R. et al (1980). Passive solar design handbook, U.S. Department of Energy, Washington DC.
45. Morse, L. S. (1881), US Patent 246626.
46. Norton, B. and Lo. S. (1989), Nazeing School thermosyphoning air panels, Report EVR 12110, CEC. Brussels.
47. Francheshi, L. (1985), A review of solar thermosyphoning air panels in the USA, Contract number E/5A/Con/1137/897. Wimpey Laboratories, Hayes, Middlesex.
48. Johnson, P. (1989), A passive solar heating facility for existing houses, Report EVR 12110, CEC, Brussels.
49. Penman, J. and Wingrave-Newall, P. (1984), The St. Cleer primary school, Cornwall: a design in passive solar techniques, Report 20, South West Energy Group, Exeter.
50. Johnson, D. (1982), Passive solar heating and a Trombe wall in a primary school, Solar Energy Society, Conference C29, Franklin Road, Birmingham.

51. Greenwood, P. and Ward, H. (1979), Solar houses for the elderly, Solar Energy Society, Conference C29, Franklin Road, Birmingham.
52. Morgan, E.A. (1966), Improvements in solar heated buildings, Patent Specification 1 022411, Patent Office, London.
53. Sweeney, M. E. and Wormald. R. (1987), The thermal performance of a fan assisted Trombe wall in a low energy school, SERC report GR/C/35400.
54. BS 4937: Part 5:1974 International thermocouple reference tables.
55. Latimer, J. R. (1978), Radiation measurement, International Field Year for the Great Lakes, National Research Council, Canada.
56. Solartron Instruments, (1982), 3530A Orion data logger operating manual, Solartron Instruments, Farnborough, UK
57. Hay, J. E. (1982), An assessment of the uncertainty in measurements of solar radiation, Solar Energy, 29, 4, 271-278.
58. Open University, (1970), The handling of experimental data, Science Foundation Course, Open University Press, Milton Keynes.
59. University of Wisconsin, (1993), TRNSYS, TRNSED, PRESIM users manual, version 2.0, Madison, Wisconsin, USA.
60. SERI-RES (1984), Solar energy research institute, Golden, Colorado, USA.
61. Clarke, J. A., (1980), ESP system users manual, Abacus, University of Strathclyde.
62. Myers, G. E. (1971), Analytical methods in construction heat transfer, McGraw Hill, New York.
63. Bhattacharya, A. (1986), A new explicit, stable, finite difference equation for heat conduction, internal report, Liverpool University.
64. Chapman, A. J. (1974), Heat transfer, Macmillan, London.

65. Waters, J. R. (1981), An investigation of some errors due to the use of finite difference techniques for building heat transfer calculations, *BSERT*, 2(1), 51-59.
66. Sweeney, M. E. and Wormald, R. (1987), Monitoring and improvement of the Poulton Lancelyn solar wall, *ISES congress proceedings, Hamburg*, 3642-3646.
67. Van Wieringen, J. S. (1981), Application of a simple model to the passive solar heating of houses, *Energy and Buildings*, 3, 335-337.
68. Wormald, R. and Sweeney, M. E. (1989), Performance of selectively coated walls in England, *ISES congress report, Kobe*.
69. International Nickel Company, (1987), Maxorb solar foil, *INCO selective surfaces, Birmingham*.
70. Davis Langdon and Everest (eds) (1992), *Spon's Architects' and Builders' Price Book*, E & FN Spon, London.
71. Pezzey, P. (1984), An economic assessment of some energy conservation measures in housing and other buildings, *Building Research Establishment Report, Department of the Environment, London*.
72. Jesch, L. F. (1993), *Transparent Insulation Technology*, ETSU, Harwell.
73. Braun, P. O. et al (1992), Transparent insulation of building facades, *Solar Energy*, 49, 5, 413-427.
74. Stahl, W., Voss, K. and Goetzberger, A. (1994), The self sufficient house in Freiburg, *Solar Energy*, 51, 1, 111-125
75. Twidell, J. W. et al (1994), Strathclyde's passive solar residences, *Solar Energy*, 52, 1, 85-109.
76. Norton, B. and Probert, S. D. (1984), Solar energy stimulated open loop thermosyphonic air heaters, *Applied Energy*, 217-234.



77. Dolley, P. R., Martin, C. J. and Watson D. M. J. (1993), The use of test rooms to determine the thermal performance of a transparently insulated opaque wall, *Building and Environment*, 28, 2, 139-143.
78. Pinner, S. H. (1966), *Weathering and degradation of plastics*, Columbine Press, London.
79. Dolley, P., Martin, C. and Watson, M. (1994), Performance of walls clad with transparent insulation material, *Building and Environment*, 29, 1, 83-88.
80. Fulop, L. and Jesch. L. F. (1993), Two years thermal monitoring of the Birmingham solar house equipped with transparent insulation, TI6 meeting on transparent insulation technology, 150-152.
81. Wormald, R. and Sweeney. M. E. (1993), The use of transparently insulated solar walls in Britain, ISES congress report, Budapest, 6, 237-242.
82. Peuportier, B. and Michel, J. (1995), Comparative analysis of active and passive solar heating systems with transparent insulation, *Solar Energy*, 54, 1, 13-18.
83. Wormald, R. and Sweeney, M. E. (1994), The prospects for solar walls in providing low temperature heat in Europe, *North Sun 94*, James and James, London, 271-276.
84. Markus, T. A. and Morris, E. N. (1980), *Buildings, climate and energy*, Pitman, London.
85. Wormald, R. and Sweeney, M. E. (1995), The potential for solar walls providing low temperature heat in Europe, ISES conference, Harare.
86. Oliver, F., Platzer, W. and Chevalier, J. L. (1993), Franco-German experimental programme for the optical characterisation of transparent insulation materials, TI6 meeting on transparent insulation technology, Birmingham, 82-85.



87. Page, J. K. and Flynn, D. J. (1986), European Solar Radiation Atlas, Vol 11, Global and diffuse radiation on vertical surfaces, TUV, Rheinland, Cologne.
88. Voss, K., et al (1995). The self-sufficient solar house Freiburg-results of three years of operation, ISES conference, Harare.
89. Kouhia, I. and Nieminen, J. (1993), Cold region applications in walls, TI6 meeting on transparent insulation technology, Birmingham, 50-53.
90. Gustafsson, S. et al (1988), Bivalent heating systems, retrofits and minimised life cycle costs, Royal Institute of Technology Bulletin, 153, Stockholm, 64-74.
91. Evans, J. and de Schiller, S. (1994), Energy demand for solar heated buildings: climatic characteristics and appropriate solar systems, North Sun 94, James and James, 4 165-170.
92. Yannas, S. (1994), Solar energy and housing design, Volume1: Principles, Objectives, Guidelines, Architectural Association, London.
93. Yannas S. (1994), Solar energy and housing design, Vol 2: Examples, Architectural Association, London.
94. Markvart, T. (1995), Solar Electricity, John Wiley, Chichester.
95. Roberts, S. (1991), Solar Electricity, Prentice Hall, London.
- 96 Lord, B. et al, (1993), A study of the feasibility of photovoltaic modules as a commercial buildings cladding component, ETSU report S /P2/ 00131/ REP, Department of Trade and Industry, London.
- 97 Pearsall, N. M. and Hill, R. (1994), Calculation of potential resource from building integrated PV systems in urban centres, First world conference on photovoltaic energy conversion, Hawaii.

- 98 Crick, F. et al (1994), The use of PV cladding for commercial buildings in the UK: costs and conclusions, 12th European Photovoltaic Solar Energy Conference, Amsterdam.
- 99 Barlow, R., Derrick, A. and Gregory, J. A. (1994), The world PV market:1993, status report and future prospects, 12th European Photovoltaic Solar Energy Conference, Amsterdam, 901-904.
100. Ricaud, A. (1994), Photovoltaic commercial modules: which product for what market?, 12th European Photovoltaic Solar Energy Conference, Amsterdam, 7-14.
101. Hohmeyer, O. (1994), The future of photovoltaics and the probable costs of climate change in the context of a sustainable world, 12th European photovoltaic solar energy conference, Amsterdam, 1155-1158.
102. Wormald, R. and Sweeney. M. E. (1995), The world photovoltaic market and Siberian Solar Silicon Incorporated, Irkutsk, Internal Report, Liverpool John Moore's University.
103. Klein, S. A. (1979), Calculation of monthly average transmittance - absorptance product, Solar Energy, 23, 6, 547-551.

## **APPENDICES**

## APPENDIX 1 - ECONOMIC ASSESSMENT METHODS

### Payback period and net present value

When an energy conservation project is undertaken, capital is substituted for energy, and the value of the energy subsequently saved can be regarded as the financial return on the capital invested. In this assessment, two methods of appraising the utility of the initial investment have been used: payback period and net present value per unit of capital cost (NPV/K).

Payback period is the time over which the value of the energy savings add up to cover the initial capital outlay. If the value of the annual savings is assumed constant then:

$P = C_0 / S$ , where  $C_0$  is the initial cost, and  $S$  is the value of the annual savings produced by the energy conservation measure.

A better method, taking into account all the costs and benefits accruing during the lifetime of the measure, is the use of the net present value per unit of capital cost. This measure, designated NPV, is the sum of the present values of all costs and benefits in the project using a standard rate of value:  $r$ .

NPV may be evaluated from the equation:

$$NPV = -C_0 + \sum_{t=1}^N (S_t / (1 + r)^t)$$

where:

$C_0$  = initial cost.

$S$  = savings in year  $t$ .

$N$  = lifetime of the measure in years.

$100r\%$  = annual rate of return on invested capital.

## APPENDIX 2 - THE TEMPERATURE CONTROLLER UNIT

### Introduction

This versatile temperature controller (see fig A1) was originally designed to control inductive loads, such as mains operated fans, over a temperature range of 0-40 degrees Celsius.

It can be used to switch either inductive or non-inductive loads of 5 amperes at 240 volts AC. Such loads include fans, heating elements, and lamps used for heating purposes. With modifications, the unit could be used to control lower voltage devices.

The temperature sensors are thermistors that are arranged in a bridge circuit. The bridge is balanced by a 10-turn potentiometer (R1) attached to a 10-turn dial. This potentiometer arrangement is accurate and easy to use.

A controlled device can be switched on or off at a pre-set temperature. Heating devices can be switched off or cooling devices switched on, depending on the position of the thermistor in the bridge circuit. A solar wall fan can be turned on or turned off when a difference in temperature exists between two thermistors placed in different arms of the bridge. The fan is switched on when the temperature of the solar wall outlet air exceeds that of the inlet air. It is switched off when the reverse situation occurs.

Terminals are provided on the front panel of the controller. They connect across a relay coil that, when closed, actuates the fan. Twelve volts will then appear across the terminals. This voltage can be used for event recording and enables the exact amount of time the fan operates to be determined. In conjunction with a knowledge of the solar



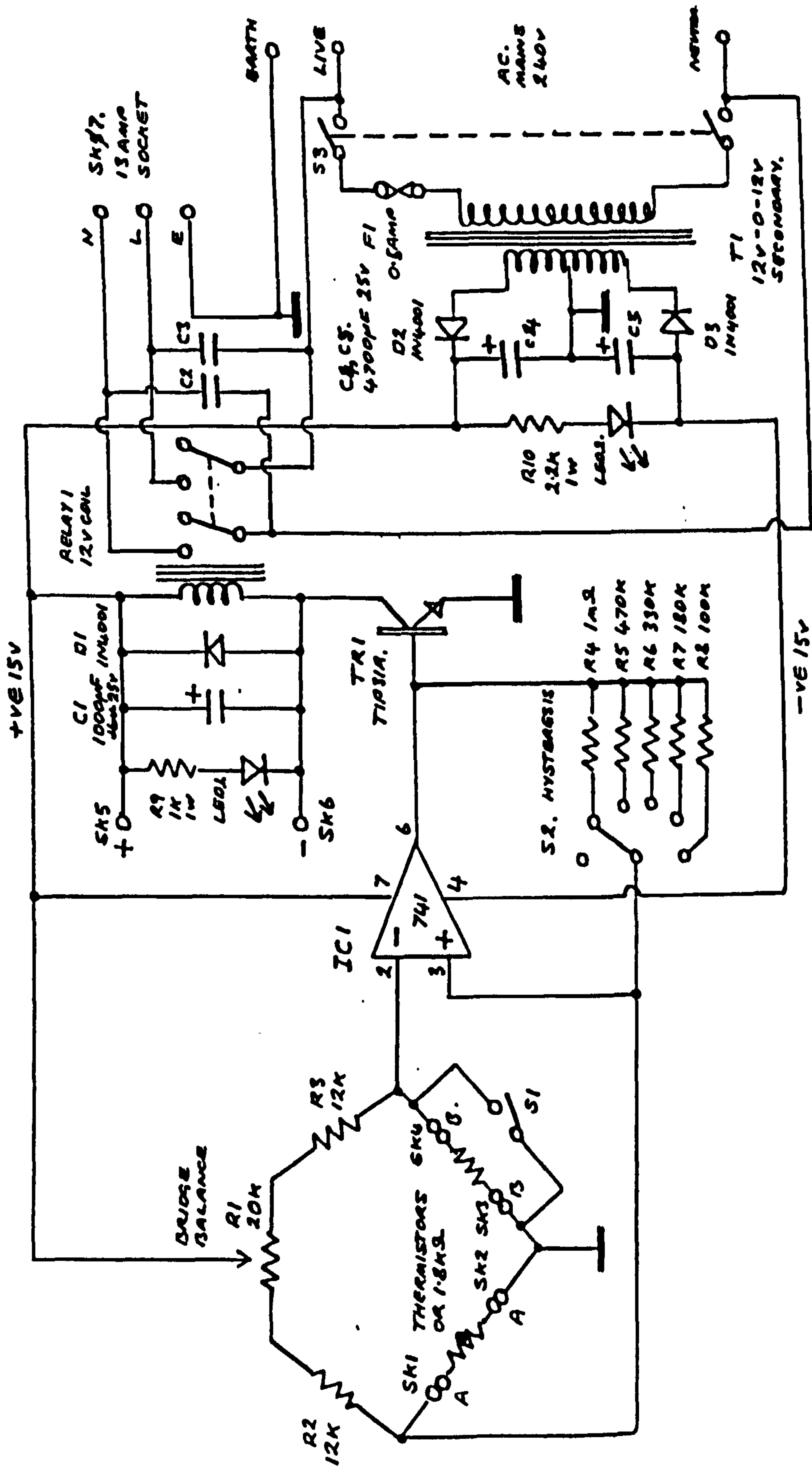


Fig. A1 Circuit diagram for temperature control unit.

wall input and output temperatures and the air flow rate, the energy produced from a solar wall may then be determined.

The relay may be actuated by switch S1 on the control panel without altering the setting of the bridge balance control, enabling the fan to be switched on and off manually if necessary. The fan may also be switched off without switching the unit off, by using a switch that is located on the 13 amp output socket.

Capacitors C2 and C3 are included to dampen arcing across the relay contacts. Such arcing can be troublesome when inductive loads are switched on and off.

A multi position switch on the front panel provides a means of varying the hold-on period of the relay after actuation or the hold-off period after turning off.

Resistances 1 and 2 are included to reduce the current in the thermistors which minimises self heating effects.

## **Construction**

The unit is incorporated into a plastic case with a sloping aluminium front panel. The panel supports the components fitted to the outside of the case, such as the controlling potentiometer, the switches, thermistor connections and 13 amp socket. The thermistors are soldered onto wires long enough to reach from the control unit to the inlet and outlet ducts of the fan. The soldered joints at the ends of the thermistors are surrounded by Araldite and covered with heat shrink sleeving. This arrangement makes the assembly waterproof.

## Calibration

The thermistors used have a negative temperature coefficient and a resistance at room temperature of about 2 kohms. Variation of resistances R2 and R3 in the other arms of the bridge circuit, alters the temperature range over which the unit operates.

To calibrate the unit, heated water is placed in a vacuum flask and its temperature checked with an accurate mercury in glass thermometer. A thermistor connected to the unit is immersed in the water and the potentiometer dial rotated to the position where the relay actuates. This is done for about 6 different temperatures and then a graph plotted of dial setting versus temperature. The unit will then be able to control temperature to about half a degree Celsius. Since two thermistors are used in the bridge, the unit will operate as a result of a difference in temperature between them for a wide range of ambient temperatures. The bridge was first balanced with the two thermistors at the same temperature. The unit will turn the relay on or off, depending on the initial setting of the bridge balance control and which thermistor is heated. For example, with both thermistors at the same temperature, if the bridge is balanced so that the relay is just turned off, heating the thermistor in arm B-B will turn the relay on. If the bridge is balanced so that the relay is just turned on, heating the thermistor in arm A-A will turn the relay off. Cooling the thermistors will produce the opposite effect.

## Mode of Operation

The circuit consists of a bridge containing thermistors as temperature sensing elements. The output from the bridge is fed into an operational amplifier to which a positive feedback has been applied. When either positive feedback or open circuit conditions exist

in the feedback loop, the amplifier is extremely sensitive to changes in the polarity of its input voltage. A change in input polarity will cause the amplifier output voltage to swing from full output at one polarity to full output at the other. When a thermistor is placed in arm A-A of the bridge in the circuit diagram, a rise in temperature will lower its resistance. In position A-A, a positive voltage will be produced at the input of the operational amplifier. This voltage is amplified, and arranged to present a negative voltage at the base of a power transistor. This transistor will stop conducting, and the relay that was previously actuated will now turn off the solar wall fan. Conversely, if a thermistor is placed in the arm B-B of the bridge circuit diagram, a rise in temperature will lower its resistance and present a negative voltage at the input of the operational amplifier. This voltage will be amplified and arranged to cause the power transistor to conduct, the relay to operate, the solar wall fan to actuate. The temperatures at which such events occur will depend on the setting of the bridge balance control. This control is a ten turn potentiometer (R1), fitted with a dial, so that the required temperature for relay actuation can be pre-set. In the event, lower dial settings represent lower temperatures at which the fan commences to operate.

There were some slight problems to overcome. Some hysteresis was shown by the circuit. Extra, selectable resistances (S2) were therefore included to provide compensation for this phenomenon. There can also be relay "chatter", this is prevented by placing a high value capacitor (C1) across the relay coil.



## APPENDIX 3 - COMPUTER PROGRAM CODES USED IN SOLAR WALL PERFORMANCE SIMULATION.

### A3.1 The Poulton Lancelyn solar wall program

Simulations of the performance of the Poulton Lancelyn Trombe wall were made using a computer program that modelled its construction with some accuracy. There were 175 nodal points used in total. These were arranged with 7 nodes along the length of the wall, 7 nodes along the height and 9 nodes along the width. Their positions have been shown in figs 4.4, 4.5 and 4.6 of the main text. The program code used is as follows:

```
C   A FORTRAN PROGRAM TO SIMULATE THE PERFORMANCE OF A FAN
C   ASSISTED TROMBE WALL.THIS SOLAR WALL IS TREATED THREE
C   DIMENSIONALLY. A FINITE DIFFERENCE METHOD IS USED TO
C   DETERMINE TRANSIENT STATE HEAT FLOWS. THE TEMPERATURE
C   DISTRIBUTIONS WITHIN AND THE HEAT OUTPUTS FROM SUCH
C   WALLS
C   ARE EVALUATED.
```

```
REAL KR1,KR2,K1,K2,K3,K4,LI,LJ,LK,KC,L1,L2,L3,L4,L5
```

```
REAL IP
```

```
COMMON TA,SR,TI,TR,DTR/HOT/D,ST,PL/TIME/MON,ND,FL
```

```
DIMENSION CA(10,10,),T(7,9,7),TI(31,0,:24),TA(31,0:24),
```

```
1F(7,9,7),FX(7,9,7),Q(7,9,7),CX(6),U(6),P(6),B(6),C(7,9,7),TV(24),
```

```
2SR(31:24),TH(24,5),Qh(24),LI(6),LJ(8),LK(6),TS(31,0:24),CI(6),
```

```
3ZD(7,9,7),X(7,9,7),Y(7,9,7),A(6,6),LINE(0:65),FLOW(7,9,7),
```

```
4TEMP(7,9,7),TCAV(24),AVTCAV(24),AB(12,0:23),TR(12,0:23),
```

```
5ST(31),CNS(6),CAX(6),DTR(12,0:23),UFL(7,9,7),DFL(7,9,7)CEL(7,9,7),
```

```
6QV(31)
```

```
INTEGER D,H,Z,G,PL,FG,HR,DY
```

```
DATA Z/2/
```

```
DATA C1,C2,C3,C4,C5/1600000,20000.,20000.,1000.,2040000./
```

```
DATA L1,L2,L3,L4/0.009,0.075,0.1,0.05/
```



```

DATA K1,K2,K3,K4/,16,.035,.035,1.0/
DATA KC,UW/0.2,0.27/
DATA TM,IDA/3600.,1/
DATA CINS/600000./
DATA TST,TDR/0,0/
DATA ITM,OTM/0,1/
DATA VR/98.2/
DATA PH,VN/2,1/
C ITM/0:TAI CONSTANT, ITM/1: TAI VARIABLE.
C OTM/0 TAO CONSTANT OTM/1 TAO VARIABLE.
C PH/0 HEAT 7-22 PH/1 HEAT 17-7 PH/2 HEAT ALL DAY.
C AREA OF WALL:13.4 M2. VOLUME OF CLASSROOM:7.2x6.22x22.2=98.2
M3.
C VENT RATE (OPH) 2 ACPH IE  $6.2 \times 0.05 \times V = 7.2 \times 6.2 \times 2.2 \times N / 3600$ 
C WHEN N=1 V=.09, N=2 V=.18 MS-1
C CAVITY CROSS SECTION AREA= $6.2 \times 0.05 = .31$  M2.
C VN/0 AIR INPUT AT TAI, VN/1 AIR INPUT AT TAO.
C TST/1 THERMOCIRCULATION OCCURS FROM FRONT CAVITY.
C TST/0 NO THERMOCIRCULATION FROM FRONT.
WRITE(5,12)
12 FORMAT(' NUMBER OF DAYS DATA TO BE INPUT.')
```

```

READ(5,19)TAO
IF(OTM.EQ.1)GO TO 4
WRITE(5,2)
2 FORMAT(' INPUT INITIAL EXTERNAL ROOM TEMPERATURE.')
```

```

READ(5,19)TAO
4 IF(ITM.EQ.1)GO TO 11
WRITE(5,18)
18 FORMAT(' INPUT INTERNAL ROOM TMPERATURE. ')
```

```

READ(5,19)RT
19 FORMAT (F)
11 WRITE(5,16)
16 FORMAT(' INPUT THICKNESS OF FRONT LEAF OF WALL.')
```

```

READ(5,3)L5
```

```
3   FORMAT(F)
   IF(OTM.EQ.1)GO TO 22
   DO 25 H=0,23
   DO 25 D=1,ND
   TA(D,H)=TAO
25  CONTINUE
22  IF(OTM.EQ.1)GOTO 15
   DO 14 D=1,ND
   DO 14 H=0,23
   TI(D,H,)=RT
14  CONTINUE
   GO TO 15
   WRITE(5,5)
5   FORMAT(' INPUT TOME INCREMENT IN SECONDS: EG 3600)
7   FORMAT(F7.0)
   WRITE(5,8)
8   FORMAT(' INPUT NUMBER OF MONTH : 1=JAN, 12 = DEC.')
```

6 READ(5,9)MON

9 FORMAT(I)

15 WRITE(5,10)

10 FORMAT(' ENTER 1=NO, 2=SINGLE,3=DOUBLE.4=SG+NIGHT  
1INSULATION,5=DG+NIGHT INSULSTION,6=SELECTIVE COATING+SG  
C SELECTIVE COATING IS MAXORB WHICH HAS EMISSIVITY=0.09 AND  
C ABSORPTIVITY OF 0.97.LP

READ(5,20)G

20 FORMAT( I1)

GOTO 165

WRITE(5,30)

30 FORMAT(' ENTER 1=SHELTERED, 2=NORMAL, 3=SEVERE  
EXPOSURE')

READ(5.40)Z

40 FORMAT(I1)

WRITE(5,50)

50 FORMAT(' ENTER FOLLOWING VALUES')

```
WRITE(5,60)
60  FORMAT('  PLASTER  INSULATION  INSIDE BRICK  CAVITY
        1OUTSIDE BRICK')
WRITE(5,70)
70  FORMAT(' THERMAL CAPACITY (J/M3)')
READ(5,80)C1,C2,C3,C4,C5
80  FORMAT(5F)
WRITE(5,90)
90  FORMAT(' THICKNESS (M)')
READ(5,100)L1,L2,L3,L4,L5
100 FORMAT(5F)
WRITE(5,105)
105 FORMAT(' PLASTER  INSULATION  INSIDE BRICK  OUTSIDE
        BRICK' )
WRITE(5,110)
110 FORMAT(' CONDUCTIVITY (W/MK)')
READ(5,120)K1,K2,K3,..K4
120 FORMAT(4F)
WRITE(5,130)
130 FORMAT(' ENTER U VALUE OF SIDE WALLS')
READ(5,140)UW
140 FORMAT(F)
WRITE(5,135)
135 FORMAT(' ENTER CONDUCTIVITY OF COCRTE IN SIDE WALL')
READ(5,138)KC
138 FORMAT(F)
PL=0
162 WRITE(5,150)
150 FORMAT(' NUMBER OF DAYS RESULTS BEING INPUT')
READ(5,160)ND
160 FORMAT(I)
WRITE(5,161)
READ(5,163)IBA
163 FORMAT(I)
```

```

165 DO 175 D=1,ND
    IF(IDA.EQ.1)GOTO 332
    WRITE(5,180)D
180 FORMAT(' DAY=',I2)
C    A FORMULA FOR THE ANNUAL VARIATION OF THE SOLI
    TEMPERATURE
C    IS TO BE INSERTED HERE, (SEE SHELL COMPUTER PROGRAM)
C    CAV=EXHR+HC,HC+5.8+4.1xFL THIS IS HALF THE CAVITY
    RESISTANCE.
332 DO 334 N=0,23
    TS(D,N)=10.
    TS(D,N+1)=10.
334 CONTINUE
175 CONTINUE
331 IF(G.EQ.1)AND.(Z.EQ.1)B=.08
2   IF(G.EQ.1)AND.(Z.EQ.2)B=.06
    IF(G.EQ.1)AND.(Z.EQ.3)B=.03
    IF(G.EQ.2)AND.(Z.EQ.1)B=.25
    IF(G.EQ.2)AND.(Z.EQ.2)B=.23
    IF(G.EQ.2)AND.(Z.EQ.3)B=.20
    IF(G.EQ.3)AND.(Z.EQ.1)B=.38
    IF(G.EQ.3)AND.(Z.EQ.2)B=.36
    IF(G.EQ.3)AND.(Z.EQ.3)B=.33
    IF(G.EQ.4)AND.(Z.EQ.1)BN=.95
    IF(G.EQ.4)AND.(Z.EQ.2)BN=.93
    IF(G.EQ.4)AND.(Z.EQ.3)BN=.90
    IF(G.EQ.5)AND.(Z.EQ.1)BN=1.08
    IF(G.EQ.5)AND.(Z.EQ.2)BN=1.06
    IF(G.EQ.5)AND.(Z.EQ.3)BN=1.03
    IF(G.EQ.4)AND.(Z.EQ.1)B=.25
    IF(G.EQ.4)AND.(Z.EQ.2)B=.23
    IF(G.EQ.4)AND.(Z.EQ.3)B=.20
    IF(G.EQ.5)AND.(Z.EQ.1)B=.38
    IF(G.EQ.5)AND.(Z.EQ.2)B=.36

```

```

IF(G.EQ.5)AND.(Z.EQ.3)B=.33
IF(G.EQ.6)AND.(Z.EQ.1)B=.45
IF(G.EQ.6)AND.(Z.EQ.2)B=.43
IF(G.EQ.6)AND.(Z.EQ.3)B=.40
WRITE(5,340)
340  FORMAT(' INPUT AIR FLOW RATE IN CAVITY')
      READ(5,350)FL
350  FORMAT(F4.1)
      AC=FLx6.04x.05x3600./VR
      IF(G.EQ.1)R9=.05
      IF(G.EQ.2)R9=.148
      IF(G.EQ.3)R9=.28
      DO 354 M=1,12
      DO 354 H=0,23
      IF(G.EQ.1)AB(M,H)=0.9
      IF(G.EQ.2)AB(M,H)=0.9xTR(M,H)
      IF(G.EQ.3)AB(M,H)=0.9xDTR(M,H)
      IF(G.EQ.4)AB(M,H)=0.9xTR(M,H)
      IF(G.EQ.5)AB(M,H)=0.9xDTR(M,H)
      IF(G.EQ.6)AB(M,H)=0.9xTR(M,H)
354  CONTINUE
      RCAV=1/(10.93+4.1xFL)
      2R1=.123
      R2=L1/K1
      R3=L2/K2
      R4=L3/K3
      R5=.09
      R6=.09
      R7=L5/K4
      R8=.09
      R=(R1+R2+R3+R4+R5+R6+R7+R8+R9)
      Q1=(TI(1,0)-TA(1,0))/R
      Q2=(TI(1,1)-TA(1,1))/R
      T1=TI(1,0)-Q1xR1

```



```
F1=TI(1,1)-Q2xR1
T2=T1-Q1xR2
F2=T2-Q2xR2
T3=T2-Q1xR3
F3=F2-Q2xR3
T4=T3-Q1xR4
F4=F3-Q2xR4
T5=T4-Q1xR5
F5=F4-Q2xR5
T6=T5-Q1xR6
F6=F5-Q2xR6
T7=T6-Q1xR7
F7=F6-Q2xR7
T8=T7-Q1xR8
F8=F7-Q2xR8
DO 440 K=2,6
DO 440 I=2,6
T(I,2,K)=T7
T(I,3,K)=T6
T(I,4,K)=T5
T(I,5,K)=T4
T(I,6,K)=T3
T(I,7,K)=T2
T(I,8,K)=T1
161  FORMAT(' IF DATA IS IN A COMMON BLOCK INPUT 1, ELSE 0')
F(I,2,K)=F7
F(I,3,K)=F6
F(I,4,K)=F5
F(I,5,K)=F4
F(I,6,K)=F3
F(I,7,K)=F2
F(I,8,K)=F1
440  CONTINUE
WRITE(5,360)
```

```

360  FORMAT(' COMPUTED INITIAL TEMPERATURES FOR ITERATIONS.')
```

WRITE(5,370)

```

370  FORMAT(' AIRIN AIR-PLASTER PLASTER INSULATION INSULATION-
1BRICK BRICK-CAVITY CAVITY CAVITY-BRICK BRICK-CAVITY
CAVITY
2AIROUT')
```

WRITE(5,380)TI(1,0),T1,T2,T3,T4,T5,T6,T7,T8,TA(1,0)

```

380  FORMAT(10F7.1)
335  CONTINUE
```

C ASSIGNMENT OF STARTING TEMPERATURES FOR THE GAUSS-  
SIEDE

C ITERATION PROCESS

DO 170 D=1,ND

WRITE(5,395)D

```

395  FORMAT(' DAY=', I2)
396  ST(D)=0
TI(D,284)=TI(D+1,0)
TA(D,24)=TA(D+1,0)
TS(D,24)=TS(D+1,0)
IF(D.EQ.ND)TI(D,24)=TI(D,23)
IF(D.EQ.ND)TA(D,24)=TA(D,23)
IF(D.EQ.24)TS(D,24)=TS(D,23)
DO 390 H=0,23
DO 400 I=2,6
DO 400 K=2,6
T(I,9,K)=TI(D,H)
F(I,9,K)=TI(D,H+1)
400  CONTINUE
DO 410 J=1,9
DO 410 K=2,7
T(I,J,K)=TA(D,H)
F(I,J,K)=TI(D,H+1)
T(7,J,K)=TA(D,H)
F(7,J,K)=TA(D,H+1)
```

```

410 CONTINUE
    DO 420 I=1,7
    DO 420 K=2,7
    T(I,1,K)=TA(D,H)
    F(I,1,K)=TA(D,H+1)

```

```

420 CONTINUE
    DO 430 J=1,9
    DO 430 I=1,7
    T(I,J,7)=TA(D,H)
    F(I,J,7)=TA(D,H+1)
    T(I,J,1)=TS(D,H)
    F(I,J,1)=TS(D,H+1)

```

```

430 CONTINUE
    TI(D,24)=TI(D+1,0)
    TA(D,24)=TA(D+1,0)
    TS(D,24)=TS(D+1,0)
    IF(D.EQ.ND)TI(D,24)=TI(D,23)
    IF(D.EQ.ND)TA(D,24)=TI(D,23)
    IF(D.EQ.ND)TS(D,24)=TS(D,23)

```

**C ASSIGNMENT OF LENGTHS ASSOCIATED WITH EACH MODE OF THE  
C ARRAY DESCRIBING THE RESISTANCE CAPACITANCE NETWORK.**

```

LI(2)=.825
LI(3)=.9
LI(4)=1.6
LI(5)=1.225
LI(6)=.9
LJ(2)=L5/2
LJ(3)=L5/2.
LJ(4)=L4
LJ(5)=L3/2.
LJ(6)=L3/2.+L2/2.
LJ(7)=L1/2.+L3/2.
L(8)=L1/2.
LK(2)=.98

```

$$LK(3)=.65$$

$$LK(4)=.8$$

$$LK(5)=.6$$

$$LK(6)=.2$$

$$V=0$$

**C ASSIGNMENT OF CAPACITANCES TO NODAL POINTS OF THE ARRAY.**

$$CX(2)=C5x.1x.98$$

$$CX(3)=C5x.1x.65$$

$$CX(4)=C5x.1x.8$$

$$CX(5)=C5x.1x.6$$

$$CX(6)=C5x.1x.2$$

$$CAX(2)=C3x.05x.98$$

$$CAX(3)=C3x.05x.65$$

$$CAX(4)=C3x.05x.8$$

$$CAX(5)=C3x.05x.6$$

$$CAX(6)=C3x.05x.2$$

$$BI=C2x.0375+C3x.05$$

$$IP=C2x.0375+C1x.0045$$

$$PS=C1x.0045$$

$$CNS(2)=CINSx.15x.98$$

$$CNS(3)=CINSx.15x.98$$

$$CNS(4)=CINSx.15x.8$$

$$CNS(5)=CINSx.15x.6$$

$$CNS(6)=CINSx.15x.2$$

$$U(2)=BIx.98$$

$$U(3)=BIx.65$$

$$U(4)=BIx.8$$

$$U(5)=BIx.6$$

$$U(6)=BIx .2$$

$$P(2)=IPx.15$$

$$P(3)=IPx.65$$

$$P(4)=IPx.88$$

$$P(5)=IPx.6$$

$$P(6)=IPx.2$$

$$S(2)=PSx.15$$

$$S(3)=PSx.65$$

$$S(4)=PSx.8$$

$$S(5)=PSx.6$$

$$S(6)=PSx.2$$

$$DO\ 460\ J=2,3$$

$$DO\ 460\ K=2,6$$

$$C(2,J,K)=CX(K)x.825$$

$$C(3,J,K)=CX(K)x.9$$

$$C(4,J,K)=CX(K)x1.6$$

$$C(5,J,K)=CX(K)x1.225$$

$$C(6,J,K)CX(K)x.9$$

$$C(2,5,K)=CAX(K)x.675+CNS(K)x.05$$

$$C(3,5,K)=CAX(K)x.9$$

$$C(4,5,K)=CAX(K)x1.6$$

$$C(5,5,K)=CAX(K)x1.225$$

$$C(6,5,K)=CAX(K)x.75+CNS(K)x.05$$

$$C(2,6,K)=U(K)x.825$$

$$C(3,6,K)=U(K)x.9$$

$$C(4,6,K)=U(K)x1.6$$

$$C(5,6,K)=U(K)x1.225$$

$$C(6,6,K)=U(K)x.75+CNS(K)x.0875$$

$$C(2,7,K)=P(K)x.675+CNS(K)x.042$$

$$C(3,7,K)=P(K)x.75+2CNS(K)x.042$$

$$C(4,7,K)=P(K)x1.6$$

$$C(5,7,K)=P(k)x1.225$$

$$C(6,7,K)=P(K)x.75+CNS(K)x.042$$

$$C(2,8,K)=S(K)x.675+CNS(K)x.0045$$

$$C(3,8,K)=S(K)x.9$$

$$C(4,8,K)=S(K)x1.6$$

$$C(5,8,K)=S(K)x1.225$$

$$C(6,8,K)=S(K)x.75+CNS(K)x.0045$$

$$C(5,J,2)=CX(2)x1.525$$



$C(6,J,2)=CX(2) \times 1.2$

$C(5,J,3)=CX(3) \times 1.375$

$C(6,J,3)=CX(3) \times 1.05$

$C(5,J,5)=CX(5) \times 1.375$

$C(6,J,5)=CX(5) \times 1.05$

$C(5,J,6)=CX(6) \times 1.525$

$C(6,J,6)=CX(6) \times 1.2$

460 CONTINUE

DO 470 j=2,3

$C(5,J,2)=CX(2) \times 1.525$

$C(6,J,6)=CX(6) \times 1.2$

$C(6,J,2)CX(2) \times 1.2$

$C(5,J,6)=CX(6) \times 1.525$

$C(5,J,3)=CX(3) \times 1.375$

$C(6,J,3)CX(3) \times 1.05$

$C(5,J,5)CX(5) \times 1.375$

$C(6,J,5)CX(6) \times 1.05$

470 CONTINUE

$C(5,5,6)=CAX(6) \times 1.525$

$C(5,5,2)=CAX(2) \times 1.525$

$C(6,5,2)=CAX(2) \times 1.2$

$C(6,5,6)=CAX(6) \times 1.2(U(2) \times 1.525$

$C(5,6,2)=U(2) \times 1.525$

$C(5,6,6)=U(6) \times 1.9$

$C(6,6,2)=U(2) \times 1.2$

$C(6,6,6)=U(6) \times 1.2$

$C(5,7,2)=P(2) \times 1.525$

$C(5,7,6)=P(6) \times 1.9$

$C(6,7,2)=P(2) \times 1.2$

$C(6,7,6)=P(6) \times 1.2$

$C(5,8,2)=S(2) \times 1.525$

$C(5,8,6)=S(6) \times 1.525$

$C(6,8,2)=S(2) \times 1.2$

$C(6,8,6)-S(6) \times 1.2$

```

DO 478 I=2,6
ZD(I,2,2)=(.73/K4+.73/1.7)/2.
ZD(I,3,2)=(.73/K4+.18)/2.
478 CONTINUE
C ASSIGNMENT OF RESISTANCES TO NODAL POINTS
DO 486 J=2,3
500 DO 481 I=5,6
ZD(I,J,3)=(.5/K4+.18)/2.
ZD(I,J,4)=(.8/K4+3*.18)/4.
ZD(I,J,5)=(.8/K4+.18)/2.
ZD(I,J,6)=(.4/K4+.18)/.2
ZD(I,J,7)=(.025/.035+.18)
486 CONTINUE
DO 481 J=2,3
DO 481 I=5,6
ZD(I,J,3)=(.5/K4+.18)/2.
ZD(I,J,4)=(.8/K4+.18)/4.
ZD(I,J,5)=(.8/K4+3x.18)/2.
ZD(I,J,6)=(.4/K4+.18/2.)
ZD(I,J,7)=(.125/.135+.18)
481 CONTINUE
J=5
504 DO 485 I=2,4
ZD(I,J,3)=(.5/K3+.18)/.2
ZD(I,J,4)=(.8/K3+3x.18)/2.
ZD(I,J,5)=(.8/K3+3x.18)/2.
ZD(I,J,6)=(.4/K3+.18)/2.
ZD(I,J,7)=(.025/.035+.18)
485 CONTINUE
DO 480 I=5,6
ZD(I,J,3)=(.5/K3+.18)/2.
ZD(I,J,4)=(.8/K3+3x.18)/4.
ZD(I,J,5)=(.8/K3+3x.18)/4.
ZD(I,J,6)=(.4/K3+.18/2.)

```

```

      ZD(I,J,7)=(.025/.035+.18)
480  CONTINUE
      DO 510 I=5,6
      ZD(I,6,2)= (.7/K3+.2/K2+1./1.7)2.
      ZD(I,6,3)=(.5/K3+.45/K2+.18)/2.
      ZD(I,6,4)=(.8/K3+.8/K2)/2.
      ZD(I,6,5)=(.8/K3+.8/K2)/2.
      ZD(I,6,6)=(.4/K3+.4/K2)/2.
      ZD(I,6,7)=(.125/.035+.18)
510  CONTINUE
      DO 520 I=5,6
      ZD(I,6,2)-(.7/K3+.2/K2+1./1.7)/2.
      ZD(I,6,3)=(.5/K3+.3/K2+.18)/2.
      ZD(I,6,4)=(.8/K3+.8/K2+.18)/2.
      ZD(I,6,5)=(.8/K3+.8/K2+.36)/4.
      ZD(I,6,6)=(.4/K3+.4/K2)/2.
      ZD(I,6,7)=(.125/.355+.18)
520  CONTINUE
      DO 530 K=2,6
      DO 530 I=2,6
      ZD(I,4,K)=2xRCAV
      ZD(I,4,7)=.18+.025/.035
530  CONTINUE
      DO 540 I=2,6
      ZD(I,7,2)=.15/KC+.05/.035+1./1.7
      ZD(I,7,3)=(.5/K2+.4/K1+.18)/2.
      ZD(I,7,4)=(.8/K2+.8/K1)/2.
      ZD(I,7,5)=(.8/K2+.8/K1)//2.
      ZD(I,7,6)=(.4/K2+.4/K1)/2.
      ZD(I,7,7)=(.125/.035+.18)
540  CONTINUE
      DO 560 I=2,4
      ZD(I,8,2)=(.15/KC+.05/.035+1./1.7)
      ZD(I,8,3)=(.5/K2+.4/K1+.18)/2.

```

```

2ZD(I,8,4)=(.8/K1+.18)/.2
ZD(I,8,5)=(.8/K1+.18)/2.
ZD(I,8,6)=(.4/K1+.18)/2.
ZD(I,8,7)=(.125/.135+.18)
560  CONTINUE
      DO 570 I=5,6
ZD(I,8,2)=(.15/KC+.05/.035+1./1.7)
ZD(I,8,3)=(.4/K1+..18)/2.+18
ZD(I,8,4)=(.8/K1+..18)/2.
ZD(I,8,5)=(.8/K1+.18)/2
ZD(I,8,6)=(.4/K1+.18)/2
ZD(I,8,7)=(.125/.035+.18)
570  CONTINUE
C     BN IS THE RESISTANCE IF NIGHT INSULATION IS USED.(SEE
      BALCOMB
C     ET AL. (1977), 'SIMULATION ANALYSIS OF PASSIVE SOLAR
      HEATED
C     BUILDINGS', SOLAR ENERGY 3, 19, P277.
      DO 580 K=3,5
      DO 580 I=2,6
X(I,2,K)=B
IF((SR(D,H+1).EQ.0).AND.(G.EQ.4))X(I,2,K)=BN
IF((SR(D,H+1).EQ.0).AND.(G.EQ.5))X(I,2,K)=BN
X(I,4,K)=.09
X(I,5,K)=.09
X(I,9,K)=.123
X(2,3,K)=L5/K4
X(3,3,K)=L5/K4
X(4,3,K)=L5/K4
X(2,6,K)=L3/K3
X(3,6,K)=L3/K3
X(4,6,K)=L3/K3
X(2,7,K)=L2.K2
X(3,7,K)=L2/K2

```

$X(4,7,K)=L2/K2$   
 $X(2,8,K)=L1/K1$   
 $X(3,8,K)=L1/K1$   
 $X(4,8,K)=L1/K1$   
 $X(5,3,K)=(3xL5/K4+.123)/2.$   
 $X(6,3,K)=(3xL5/K4+.123)/2.$   
 $X(5,6,K)=(3xL3/K3+.123)/2.$   
 $X(6,6,K)=(3xL3/K3+.123)/K2$   
 $X(5,7,K)=(3xL2/K2+.123)/2.$   
 $X(6,7,K)=(3xL2/K2+.123)/2.$   
 $X(5,8,K)=(3xL1/K1+.123)/2.$   
 $X(6,8,K)=(3xL1/K1+.123)/2.$

580

CONTINUE  
DO 590 I=2,6  
 $X(I,2,2)=B$   
 $X(I,3,2)=L5/K4$   
 $X(I,4,2)=RCAV$   
 $X(I,5,2)=L3/K3$   
 $X(I,6,2)=.19$   
 $X(I,7,2)=.19$   
 $X(I,8,2)=.06$   
 $X(I,9,2)=.06$   
 $X(I,2,6)=.01/.035+.18$   
 $X(I,3,6)=(L5/K4+.025/.035)/2.$   
 $X(I,4,6)=.09$   
 $X(I,5,6).09$   
 $X(I,6,6)=(L3/K3+.1/.035)/2.$   
 $X(I,7,6)=(L2/K2)$   
 $X(I,8,6)=L1/K1$   
 $X(I,9,6)=.123$

590

CONTINUE

C CR IS THE CONDUCTANCE OF A VERTICAL AIRSPACE WITH  
C HORIZONTAL HEAT FLOW. (SEE ANDERSON (1981), BUILDING AND  
C ENVIRONMENT, 16, 1, P35. )



$$\text{DELT}=\text{T}(2,5,4)-\text{T}(2,3,4)$$

$$\text{CON}=\text{AMAX1}(.025/\text{L4},.73\times(\text{DELT}^{**}(1/3)))$$

$$\text{CR}=\text{CON}+4.63$$

$$\text{DO } 600 \text{ K}=3,5$$

$$\text{Y}(2,2,\text{K})=1/\text{UW}+(\.3/\text{K}4-.123)/2.$$

$$\text{Y}(2,3,\text{K})=1/\text{UW}(\.3/\text{K}4-.123)/2.$$

$$\text{Y}(2,4,\text{K})=1/\text{UW}+.1/\text{K}4$$

$$\text{Y}(2,5,\text{K})=1/\text{UW}+(\.15/\text{K}C+1/\text{K}4)/2.+(\.15/\text{K}3-.123)/2.$$

$$\text{Y}(2,6,\text{K})=1/\text{UW}-.123+(\.15/\text{K}2+.15/\text{K}3)/2.+15/\text{K}C$$

$$\text{Y}(2,7,\text{K})=1/\text{UW}+.15/\text{K}C+(\.15/\text{K}1+.15/\text{K}2)/2.-.123$$

$$\text{Y}(2,8,\text{K})=1/\text{UW}+.15/\text{K}C+(\.15/\text{K}1-.123)/2.$$

$$\text{Y}(2,9,\text{K})=1/\text{UW}+.15/\text{K}C$$

$$\text{Y}(3,2,\text{K})=(.123+1.05/\text{K}4)/2.$$

$$\text{Y}(3,3,\text{K})=(.123+1.05/\text{K}4)/2$$

$$\text{Y}(3,4,\text{K})=\text{RCAV}\times 2.$$

$$\text{Y}(4,4,\text{K})=\text{RCAV}\times 2.$$

$$\text{Y}(5,4,\text{K})=\text{RCAV}\times 2.$$

$$\text{Y}(6,4,\text{K})=\text{RCAV}\times 2.$$

$$\text{Y}(3,5,\text{K})=(.123+1.05/\text{K}3)/2.$$

$$\text{Y}(3,6,\text{K})=(1.05/\text{K}3+1.05/\text{K}2)/2.$$

$$\text{Y}(3,7,\text{K})=(1.05/\text{K}2+1.05/\text{K}1)/2.$$

$$\text{Y}(3,8,\text{K})=(1.05/\text{K}1+.123)/2.$$

$$\text{Y}(4,2,\text{K})=(.123+.75/\text{K}4)/2.$$

$$\text{Y}(4,3,\text{K})=(.123+.75/\text{K}4)/2.$$

$$\text{Y}(4,5,\text{K})=(.123+.75/\text{K}3)/2.$$

$$\text{Y}(4,6,\text{K})=(.75/\text{K}3+.75/\text{K}2)/2.$$

$$\text{Y}(4,7,\text{K})=(.75/\text{K}2+.75/\text{K}1)/2.$$

$$\text{Y}(4,8,\text{K})=(.75/\text{K}1+.123)/2.$$

$$\text{Y}(5,2,\text{K})=(.123+2.45/\text{K}4)/2.$$

$$\text{Y}(5,3,\text{K})=(.123+2.45/\text{K}4)/2.$$

$$\text{Y}(5,5,\text{K})=(.123+2.45/\text{K}3)/2.$$

$$\text{Y}(5,6,\text{K})=(2.45/\text{K}2+2.45/\text{K}2)/2.$$

$$\text{Y}(5,7,\text{K})=(2.45/\text{K}2+2.45/\text{K}1)/2.$$

$$\text{Y}(5,8,\text{K})=(2.45/\text{K}1+.123)/2.$$

$$Y(6,2,K)=.18$$

$$Y(6,3,K)=.18$$

$$Y(6,5,K)=.18$$

$$Y(6,6,K)=.18$$

$$Y(6,7,K)=.18$$

$$Y(6,8,K)=.18$$

$$Y(6,8,2)=.18$$

$$Y(7,2,K)=1/UW+(.9/K4-.123)/2.$$

$$Y(7,3,K)=1/UW+(.9/K4-.123)/2.$$

$$Y(7,4,K)=1/UW$$

$$Y(7,5,K)=1/UW+(.75/K3-.123+.15/KC+.1/K4)/2.$$

$$Y(7,6,K)=1/UW+.15/KC-.123+(.75/K3+.75/K2)/2.$$

$$Y(7,7,K)=1/UW+.15/KC-.123+(.75/K2+.75/K1)/2.$$

$$Y(7,8,K)=1/UW+(.75/K1-.123)/2.$$

$$Y(7,9,K)=1/UW+.15/KC$$

600 CONTINUE

DO 610 J=2,9

$$Y(3,2,2)=Y(2,J,3)$$

$$Y(3,3,2)=Y(3,2,3)$$

$$Y(3,4,2)=1/.1$$

$$Y(4,4,2)=1/.1$$

$$Y(5,4,2)=1/.1$$

$$Y(6,4,2)=1/.1$$

$$Y(3,5,2)=Y(3,5,3)$$

$$Y(3,6,2)=(1.05/K3+.123)/2.$$

$$Y(3,7,2)=1/.1$$

$$Y(3,8,2)=1/.1$$

$$Y(4,7,2)=1/.1$$

$$Y(4,8,2)=1/.1$$

$$Y(4,6,2)=(.75/K3+.123)/2.$$

$$Y(5,6,2)=(2.45/K3+.123)/2.$$

$$Y(5,5,2)=(2.45/K3+.123)/2.$$

$$Y(5,2,2)=Y(5,2,3)$$

$$Y(5,3,2)=Y(5,2,3)$$

$$Y(5,7,2)=1/.1$$

$$Y(5,8,2)=1/.1$$

$$Y(6,2,2)=(.6/K4+.123)/2.$$

$$Y(6,3,2)=(.6/K4+.123)/2.$$

$$Y(6,5,2)=(.6/K3+.123)/2.$$

$$Y(6,6,2)=(.6/K3+.123)/2.$$

$$Y(6,7,2)=1/.1$$

$$KR1=.05/.035$$

$$KR2=.125/.035$$

$$Y(2,2,6)=(1/UW+(.3/K4-.123)/2.+KR1)/2.$$

$$Y(2,3,6)=(1/UW+(.3/K4-.123)/2.+KR1/2.)$$

$$Y(2,4,6)=(1/UW+.05/.035)/2.$$

$$Y(2,5,6)=(Y(2,5,5)+KR1)/2.$$

$$Y(2,6,6)=(Y(2,6,5)+KR2)/2.$$

$$Y(2,7,6)=(Y(2,7,5)+KR2)/2.$$

$$Y(2,8,6)=(Y(2,8,5)+KR2)/2.$$

DO 620 I=3,5

$$Y(I,2,6)=(Y(I,2,5)+KR1)/2.$$

$$Y(I,3,6)=(Y(I,3,5)+KR1)/2.$$

$$Y(I,4,6)=(Y(I,4,5)+KR1)/2,$$

$$Y(I,5,6)=(Y(I,5,5)+KR1)/2.$$

$$Y(I,6,6)=(Y(I,6,5)+KR2)/2.$$

$$Y(I,7,6)=(Y(I,7,5)+KR2)/2.$$

$$Y(I,8,6)=(Y(I,8,5)+KR2)/2.$$

620 CONTINUE

$$Y(6,2,6)=(.6/K4+.123+2.xKR1)/4.$$

$$Y(6,3,6)=(.6/K4+.123+2.xKR1)/4.$$

$$Y(6,4,6)=1/.1$$

$$Y(6,5,6)=(.6/K3+.123+2.xKR1)/4.$$

$$Y(6,7,6)=(.6.K2+.6/K1+2.xKR2)/4.$$

$$Y(6,6,6)=(.6/K3+.6/.K2+2.xKR2)/4$$

$$Y(6,8,6)=(.6/K1+.123+2.xKR2)/4.$$

$$Y(7,2,6)=(1./UW++(.9/K4-.123)/2.+KR1)/2.$$

$$Y(7,4,6)=1./UW$$

$$Y(7,3,6)=(1./UW+(.9.K4-.123)/2.+KR1)/2.$$

$$Y(7,5,6)=(1./UW+.15/KC+(.75/K3-.123)/2.+KR2)/2.$$

$$Y(7,7,6)=(1./UW+.15/KC-.123+(.75/K3+.75/K2)/2.+KR2)/2.$$

$$Y(7,8,6)=(1/UW +(.75/K1-.123)/2.+KR2)/2.$$

### C ASSIGNMENT OF NODAL AREAS FOR INCIDENT SOLAR RADIATION

$$A(2,2)=.25x.825$$

$$A(3,2)=.25x.9$$

$$A(4,2)=.25x1.6$$

$$A(5,2)=.25x1.525$$

$$A(6,2)=.25x1.2$$

$$A(2,4)=.8x.825$$

$$A(3,4)=.8x.9$$

$$A(4,4)=.8x1.6$$

$$A(5,4)=.8x1.525$$

$$A(6,4)=.8x.9$$

$$A(2,3)=.65x.825$$

$$A(3,3)=.65x.9$$

$$A(4,3)=.65x1.6$$

$$A(5,3)=.65x1.225+.25x.3$$

$$A(6,3)=.25x.3+.65x.9$$

$$A(2,5)=.6x.825$$

$$A(3,5)=.6x.9$$

$$A(4,5)=.6x1.9$$

$$A(5,5)=.6x1.225+.25x.3$$

$$(6,5)=.2x.3+.6x.9$$

$$A(2,6)=.05x.825$$

$$A(3,6)=.05x.9$$

$$A(4,6)=.05x1.6$$

$$A(5,6)=.05x1.525$$

$$A(6,6)=.05x.1.2$$

$$AT=0$$

$$DO 452 I=2,6$$

$$DO 452 J=2,6$$

$$AT=AT+A(I,J)$$

```

452 CONTINUE
   ST(D)=ST(D)+SR(D,H+1)*AT
   DY=D
   TCAV(H)=0
   DO 450 I=2,6
   TCAV(H)=T(I,4,6)+TCAV(H)
450 CONTINUEC
   AVTCAV(H)=TCAV(H)/5.
C   AVTCAV IS THE AVERAGE TOP OF CAVITY TEMPERATURE.
   HOUR=H.
   DO 630 K=2,6
   DO 630 I=2,6
   TEMP(I,4,K)=F(I,4,K)
   TEMP(I,4,1)=TI(D,H+1)
   TEMP(I,4,7)=TI(D,H+1)
630 CONTINUE
   DO 695 L=1,IFIX(3600./TM)
   IT=0
   Q(I,J,K)=0.
   FLOW(I,J,K)=0.
700 FG=0.
   DO 690 K=2,6
   DO 690 J=2,8
   DO 690 I=2,6
   Q(I,J,K)=0.
   FLOW(I,J,K)=0.
   UFL(I,J,K)=0.
   DFL(I,J,K)=0.
   CEL(I,2,K)=0
   CEL(I,2,1)=0.
   DEL(I,2,1)=0.
   VD=FL
   IF((H.LE.7).OR.(H.GE.17))VD=0.
   IF(F(I,4,6).GT.F(I,2,6))VD=0.

```



```

IF(TST.EQ.1)UFL(I,2,K)=1200.xVDx..05xLI(I)
IF(TST.EQ.1)DFL(I,4,K)=1200.xVDxL4xLI(I)
TEMP(I,4,K-1)=F(I,4,K-1)
IF(VN.EQ.1)TEMP(I,4,1)=TA(D,H+1)
IF(VN.EQ.0)TEMP(I,4,1)=TI(D,H+1)
V=0.
TI(D,24)=TI(D+1,0)
IF(VN.EQ.0)GOTO 693
IF(AVTCAV(H).GT.TA(D,H))V=FL
GOTO 696
693 IF(AVTCAV(H).GT.TI(D,H))V=FL
C PH/0 HEAT FLOW 7-22 PH/1 HEAT FLOW 17-7 PH/2 FLOW ALL DAY.
IF(PH.EQ.0)GOTO 690
IF(PH.EQ.1)GOTO 697
IF(PH.EQ.2)GOTO 707
690 IF(H.LT.7)OR.(H.GT.22)V=0.
697 IF(H.GT.7).AND.(H.LT.17))V=0.
C PRE-HEATING WITH OUTSIDE AIR WILL USE TA(D,H).
HEATING WITH RECYCLED AIR WILL USE TI(D,H).
707 FLOW(I,4,K)=1200.xVxL4xL(I)
701 Q(I,2,K)=AB(M,H)xSR(D,H)xA(I,K)x.95
702 FX(I,J,K) = F(I-1),J,K) x LJ(J) x LK(K) / Y(I,J,K) + F(I+1,J,K) x LJ(J) x
LK(K) /
1Y(I+1,J,K) + F(I,J-1,K) x LI(I) x LK(K) / X(I,J,K) + F(I,J+1,K) x LI(I) x
LK(K) /
2X(I,J+1,K) + F(I,J,K-1) x LI(I) x LJ(J) x / ZD(I,J,K) + F(I,J,K+1) x LI(I) x
LJ(J) /
3ZD(I,J,K+1) + C(I,J,K) x T(I,J,K) / TM + Q(I,J,K) + FLOW(I,J,K) x
TEMP(I,4,1) +
4 UFL(I,J,K) x CEL(I,2,K) DFL(I,J,K) x CEL(I,4,K+1) ) / ( LI(I)xLK(K) /
X(I,J,K)
5 + LI(I) x LK(K) / X(I,J+1,K) + LJ(J) x LK(K) / Y(I,J,K) + LJ(J) x LK(K) /
6Y(I+1,J,K) + LI(I) x LJ(J) / ZD(I,J,K) + LI(I) x LJ(J) / ZD(I,J,K+1) + C(I,J,K)
/ TM 7 + FLOW(I,J,K) UFL(I,J,K) + DFL(I,J,K) )

```

```

705  IF(ABS(FX(I,J,K)-F(I,J,K).GT.0.001)FG=1
      F(I,J,K) = FX(I,J,K)
690  CONTINUE
      IF (FG.EQ.1)GOTO 700
      IT=IT+1
695  CONTINUE
      TCAV(H+1)=0
      DO 691 I=2,6
      TCAV(H+1)=F(I,4,6)+TCAV(H+1)
691  CONTINUE
      AVTCAV(H+1)=TCAV(H+1)/5
      IF((H+1).EQ.24)TI(D,H+1)=TI(D+1,0)
      IF((H+1).EQ.24)TA(D,H+1)=TA(D+1,0)
      IF(VN.EQ.0)GOTO 708
C    IF USING THE TROMBE WALL FOR PRE-HEATING THEN INLET AIR
C    TEMPERATURE IS AT TA(D,H) AND VN = 1.
      IF( AVTCAV(H).GT.TI(D,H))AVTCAV(H)=TI(D,H)
      QH(H+1)= 1200. x V x L4 x 6.04 x (AVTCAV(H) - TA(D,H) )
      IF(QH(H+1).LT.0.)QH(H+1)=0.
      QV(H+1)= 1200.xVRxACx(TI(D,H)-TA(D,H)) / 3600.
      IF(TA(D,H).GT.TI(D,H))QV(H+1)=0.
      GOTO 709
C    USING THE TROMBE WALL FOR HEATING RECYCLED AIR
C    MEANS THAT INLET AIR IS AT TI(D,H) AND VN=0.
700  QH(H+1)= 1200. x V x L4 x 6.04 x (AVTCAV(H) - (TI(D,H) + TI(D,H+1) )/2.

```

**A3.2 Subroutine to print hourly values of solar wall temperatures**

```
SUBROUTINE HPRINT(T)
DIMENSION T(7,9,7),A(8)
INTEGER A
WRITE(5,10)
10  FORMAT(' INPUT 1,2,3,4,5,6,7 FOR REQUIRED HPRINT
POSITIONS.
ITERMINATE WITH 0. (POSITION 2=BOTTOM, 6=TOP OF
TROMBE WALL.)')
30  FORMAT(8I)
    IF(A(I).EQ.0.)GOTO 40
20  CONTINUE
    ENTRY HPT(T)
40  DO 90 J=1,7
    K=A(J)
    IF(A(J).EQ.0.)GOTO 60
    WRITE(5,100)I,T(I,1,K),T(I,2,K),T(I,3,K),T(I,4,K),T(I,5,K),
    1T(I,6,K),T(I,7,K),T(I,8,K),T(I,9,K)
100 FORMAT(7X,'I=',I1,9F5.1)
90  CONTINUE
60  RETURN
    STOP
    END
```

**A3.3 Subroutine to plot hourly values of solar wall temperatures**

```

SUBROUTINE HRPLOT (T,HR,DY)
DIMENSION A(8),T(7,9,7),LINE(0:65),C(0:65),X(2,9,6),Y(2,9,6)
DIMENSION AT(9),AX(9)
INTEGER A,HR,DY
WRITE(5,10)
10  FORMAT(' INPUT 1,2,3,4,5,6,7 FOR HPLOT POSITIONS,TERMINATE
        WITH 0.
        1(2=BOTTOM,6 = TOP OF TROMBE WALL.)')
DO 20 1,8
READ(5,30)A(I)
30  FORMAT(8I)
IF(A(I).EQ.0)GOTO 40.
20  CONTINUE
ENTRY PLOT(Y,HR,DY)
40  DO 50 L=1,7
K=A(L)
IF A(L).EQ.0)GOTO 60
WRITE(5,70)A(L)
70  FORMAT(' K=',I1)
WRITE(5,80)
80  FORMAT(' TEMPERATURE DISTRIBUTION THROUGH TROMBE WALL
        AT 1I=2')
IF(IND.EQ.1)GOTO 125
DO 90 N=0,65
CN='*'
LINE(N)=N
90  CONTINUE
WRITE(5,100)(LINE(M),M=0,65)
100  FORMAT(5X,14I5)
WRITE(5,110)(C(I),I=0,65)
110  FORMAT(9X,66A1)
DO 120 J=1,9

```



```
DO 130 P=1,64  
LINE(0)='*'  
LINE(65)='*'  
LINE(65)='*'  
LINE(P)=' '  
IF(P.EQ.INT(T(2,J,K)))LINE(P)='*'  
130 CONTINUE  
WRITE(5,140)J,(LINE(M),M=0,65)  
140 FORMAT(5X,I2,2X,66A1)  
120 CONTINUE  
RETURN
```



### A3.4 Subroutine to plot the daily change in temperatures of the inside and outside surfaces and internal cavity of the Poulton Lancelyn solar wall

```

SUBROUTINE DY PLOT (TH,DY)
DIMENSION TH(24,5),LINE(0:65),AX(24),AY(24),BY(24),CY(24)
INTEGER DY
WRITE(5,10)
10  FORMAT(' TEMPERATURE OF THE INTERNAL CAVITY AND THE
INSIDE 1 AND OUTSIDE SURFACES OF THE POULTON LANCELYN
SOLAR WALL, 2 VERSUS TIME IN HOURS AT I=2 AND K=5')
WRITE(5,20)
20  FORMAT(' 0 5 10 15 20 25 30 35 40 45 50 55 60 65 ')
WRITE(5,30)
30  FORMAT(' *****')
LINE(0)='*'
DO 40 M=1,24
DO 40 I=1,65
LINE(I)=' '
C  POSITION: J=2 IS THE OUTSIDE SOLAR WALL SURFACE. J=3 IS THE
INSIDE
C  SOLAR WALL SURFACE. J=4 IS THE INTERNAL SOLAR WALL CAVITY
.  IF(I.EQ.INT(TH(M,2)+0.5))LINE(I)='*'
IF(I.EQ.INT(TH(M,4)+0.5))LINE(I)='.'
IF(I.EQ.INT(TH(M,3)+0.5))LINE(I)='+'
50  CONTINUE
80  RETURN

```

### A3.5 Subroutine to determine the daily heat output from the Poulton Lancelyn Trombe wall

```

SUBROUTINE HEAT(QH)
COMMON /HOT/D,ST,PL/ENG/QME,EFF
DIMENSION H(24),QA(24),QH(24),QAJ(24),ST(31),TM(31), TE(0:31),
1QME(31),EFF(31)
INTEGER E,D,PL
SOL=ST(D)
IF(PL.EQ.6)GOTO 22
IF(PL.EQ.5)GOTO 22
8  WRITE(5,10)
10  FORMAT(' INPUT 1 IF ENERGY OUTPUT IS REQUIRED,ELSE 0')
    READ(5,20)E
20  FORM AT(I1)
    IF(E.EQ.0.)GOTO 100
22  QT=0.
    QTV=0.
    DO 30 J=1,24
        QA(J)=QH(J)/1000.
        QAJ(J)=QH(J)*3.6/1000.
        QT=QT+QA(J)
        QTV=QTV+QAJ(J)
30  CONTINUE
    TM(D)=0.
    DO 33 J=1,8
        TM(D)=QAJ(J)+TM(D)
33  CONTINUE
    TE(D)=0.
    DO 37 J=16,24
        TE(D)=QAJ(J)+TE(0.)
37  CONTINUE
    IF(PL.EQ.6)GOTO 124
    WRITE(5,140)
140  FORMAT(' ENERGY OUTPUT OF FAN ASSISTED TROMBE WALL IN

```

```

1KILOWATT HOURS')
WRITE (5,150)
150  FORMAT(' HOUR 1 2 3 4 5 6 7 8 9 10 11 12')
      WRITE (5,160)(QA(J),J=1,12)
160  FORMAT(' ENERGY',12F4.1)
      WRITE(5,170)
170  FORMAT(' HOUR 13 14 15 16 17 18 19 20 21 22 23 24')
      WRITE(5,180)(QA(J),J=13,24)
180  FORMAT(' ENERGY', 12 F4.1)
      WRITE(5,190)QT
190  FORMAT(' DAILY TOTAL=', F6.1,' KWH')
      WRITE(5,40)
40   FORMAT(' ENERGY OUTPUT OF FAN ASSISTED TROMBE WALL IN
          1MEGAJOULES')
      WRITE(5,50)
50   FORMAT(' HOUR 1 2 3 4 5 6 7 8 9 10 11 12')
      WRITE(5,60)(QAJ(J),J=1,12)
60   FORMAT(' ENERGY',12F4.1)
      WRITE 5,70)
70   FORMAT(' HOUR 13 14 15 16 17 18 19 20 21 22 23 24 ')
      WRITE(5,80)(QAJ(J),J=13,24)
80   FORMAT(' ENERGY',12F4.1)
      WRITE(5,90)QTV
90   FORMAT(' DAILY TOTAL=', F6.1,' MJ' )
      WRITE(5,110)TM(D)
110  FORMAT(' MORNING ENERGY=',F6.1, MJ')
      WRITE(5,120)TE(D)
120  FORMAT(' EVENING ENERGY=',F6.1,' MJ')
124  TE(0)=0.
      IF(D.EQ.1)GOTO 144
      QME(D-1)=TM(D)+TE(D-1)
      IF(PL.EQ.6)GOTO 141
      WRITE(5,130)QME(D-1)

```

```
130  FORMAT(' TOTAL ENERGY FROM PREVIOUS DAYS SOLAR=' ,F6.1,  
        MJ' )  
141  EFF(D-1)=QME(D-1)*100000./ (ST(D-1)*3.6)  
        IPD=D-1  
        IF(PL.EQ.6)GOTO 100  
        WRITE(5,142)IPD,EFF(D-1)  
142  FORMAT(' PREVIOUS DAYS EFFICIENCY OF POULTON LANCELYN  
        1TROMBE WALL. ',I2,'=' ,F4.1,' %' )  
        QME(D-1)=TM(D)+TE(D-1)  
144  SDE=ST(D-1)*3.6 / 1000.  
        WRITE(5,152)SDE  
152  FORMAT( ' PREVIOUS DAYS SOLAR ENERGY =,F5.1, ' MJ ' )  
100  RETURN  
        STOP  
        END
```



### A3.6 Subroutine to determine the energy output for the total number of days data input for a given month of the year.

```

SUBROUTINE ENERGY
COMMON /HOT/D,ST,PL/ENG/QME,EFF/TIME/MON,ND,FL
DIMENSION QME(31),ST(31),EFF(31)

INTEGER D

WRITE(5,16)ND,MON
16  FORMAT(' ND=', I2 , 'MON = ', I2 )
    FSUN=0.
    TOTEN=0.
    TEFF=0.
    IF(ND.EQ.1.)GOTO 11
    DO 10 D-1,ND-1
    TOTEN=TOTEN+QME(D)
    FSUN=FSUN+ST(D)
    TEFF=TEFF / FLOAT(ND-1)
10  CONTINUE
    AVEFF=TEFF / FLOAT(ND-1)
    GOTO 12
11  D=1
    TOTEN=TOTEN +QME(D)
    FSUN=ST(1)
    AVEFF=EFF(1)
    IF(ND.EQ.1)GOTO 14
12  AVSOL=FSUN*3.6 / (FLOAT(ND-1)*1000.)
14  SOL=FSUN*3.6/1000.
    IF(MON.EQ.1)TIM=' JAN'
    IF(MON.EQ.2)TIM=' FEB'
    IF(MON.EQ.3)TIM=' MAR'
    IF(MON.EQ.4)TIM=' APR'
    IF(MON.EQ.5)TIM=' MAY'
    IF(MON.EQ.6)TIM=' JUN'
    IF(MON.EQ.7)TIM=' JUL'

```



```
IF(MON.EQ.8)TIM=' AUG'  
IF(MON.EQ.9)TIM=' SEP'  
IF(MON.EQ.10)TIM=' OCT'  
IF(MON.EQ.11)TIM=' NOV'  
IF(MON.EQ.12)TIM=' DEC'  
WRITE(5,17)FL  
17  FORMAT(' FAN SPEEDS=', F4.1, ' M/S)  
    WRITE(5,15)TIM  
15  FORMAT(' RESULTS FOR ', A4/ )  
    WRITE (5,20)KD,AVEFF  
20  FORMAT(' AVERAGE EFFICIENCY OVER', I2, ' DAYS = ', F4.1, ' % ' )  
    WRITE(5,30)SOL  
30  FORMAT(' TOTAL SOLAR MEASURED = ',F7.1, ' MJ ' )  
    WRITE(5,35)AVSOL  
35  FORMAT(' AVERAGE SOLAR MEASURED = ', F6.1, ' MJ PER DAY ' )  
    WRITE(5,40)TOTEN  
40  FORMAT( ' TOTAL ENERGY FROM THE TROMBE WALL OVER THE  
    I MEASURED PERIOD = ', F6.1 , 'MJ ' )  
    RETURN  
    STOP
```

**A3.7 Block data input for the Poulton Lancelyn solar wall program. Hourly values are given for the glazing transmission occurring at the middle of each month, for a year at the latitude of the Poulton Lancelyn school. TR values are for the single glazing used and DTR for a double glazing alternative.**

```

DATA(TR(1,N)N=8,15)/.81,.81,815,815,825,815,81,81/
DATA(TR(2,N)N=7,17)/.7,.74,.79,.805,.815,.815,.815,.805,.79,.74,.7/
DATA(TR(3,N)N=6,18)/.3,.52,.69,.72,.81,.805,.805,.805,.81,.72,.69,.52,.3/
DATA(TR(4,N)N=6,18)/.2,.36,.58,.705,.75,.79,.79,.79,.77,.705,.58,.36,.2/
DATA(TR(5,N)N=7,17)/.2,.47,.65,.727,.75,.76,.75,.725,.65,.47,.2/
DATA(TR(6,N)N=7,17)/.2,.42,.6,.682,.725,.742,.725,.682,.6,.42,.2/
DATA(TR(7,N)N=7,17)/.2,.47,.65,.725,.75,.76,.75,.725,.65,.47,.2/
DATA(TR(8,N)N=6,18)/.2,.36,.58,.705,.77,.79,.79,.79,.77,.77,.705,.58,.36,.2/
DATA(TR(9,N)N=6,18)/.3,.52,.69,.72,.81,.805,.805,.805,.81,.72,.69,.52,.3/
DATA(TR(10,N)N=7,17)/.7,.74,.79,.805,.8115,.815,.815,.805,.79,.74,.7/
DATA(TR(11,N)N=8,16)/.81,.81,.815,.815,.825,.815,.815,.81,.81/
DATA(TR(12,N)N=8,16)/.8,.805,.815,.815,.816,.815,.815,.805,.8/
DATA(DTR(1,N)N=9,15)/.7,.71,.71,.73,.71,.71,.7/
DATA(DTR(2,N)N=8,16)/.61,66,.71,.72,75,72,.71,.66,.61/
DATA(DTR(3,N)N=7,17)/.36,.55,.65,.7,.7,.7,.7,.7,.65,.55,.36/
DATA(DTR(4,N)N=7,17)/.29,.41,.59,.65,.66,.67,.66,.65,.56,.41,.29/
DATA(DTR(5,N)N=8,16)/.25,.47,.58,.62,.63,.62,.58,.47,.25/
DATA(DTR(6,N)N=8,16)/.3,.45,.52,59,.61,.59,.52,.45,.3/
DATA(DTR(7,N)N=8,16)/.25,.47,.58,.62,.63,.62,.58,.47,.25/
DATA(DTR(8,N)N=7,17)/.29,.41,.58,.65,.66,.67,.66,.65,.56,.41,.29/
DATA(DTR(9,N)N=7,17)/.29,.41,.59,.65,.66,.67,.66,.65,.56,.41,.29/
DATA(DTR(10,N)N=8,16)/.61,.66,.71,.72,.72,.72,.71,.66,.61/
DATA(DTR(11,N)N=9,15)/.70,.71,.71,.73,.71,.71,.70
DATA(DTR(12,N)N=9,15)/.70,.71,.71,.73,.71,.71,.70/
END

```

**A3.8 Simplified solar wall program, written for IBM compatible PC's. with fewer internal nodes than the Poulton Lancelyn school program (45 only). This program will simulate the performance of solar walls with low thermal conductivity, high thermal capacity ceramic absorbers (brick, concrete etc.) as well as the performance of solar walls with high thermal conductivity, low thermal capacity (metals such as aluminium ). It will evaluate the output of such walls fronted by: no glazing, single glazing, double glazing, selective coatings and single glazing, low emissivity double glazing, and transparent insulation material of various thickness.**

**C THE TR (TRANSMISSION DATA) IS FOR DIRECT TRANSMISSION OF SOLAR THROUGH GLASS**

**C AIR COLLECTOR TPAN**

**REAL LI(4),LJ(6),LK(4)**

**REAL W,HT,RIN**

**REAL L1,L2,TM,K1,K2,L4,LIN,CABA,CABB,CBK,CAR,KAL,KBK,KPS**

**DIMENSION T(5,7,5),TI(31,0:24),TA(31,0:24),FX(5,7,5)**

**DIMENSION F(5,7,5),Q(5,7,5),C(5,7,5),SR(0:24),TH(24,4)**

**DIMENSION ALI(4),ALJ(6),ALK(4),TS(31,0:24),ZD(5,7,5)**

**DIMENSION X(5,7,5),Y(5,7,5),A (4,4),FLOW(5,7,5),QN(72)**

**DIMENSION TCAV(0:24),AVTCAV(0:24),AB(12,0:23),TEMP(5,7,5)**

**DIMENSION TR(12,0:23),DTR(12,0:23),ST(31),TMA(12,0:23)**

**DIMENSION SMR(12,0:23),FL(0:24),QH(0:24),TMI(12,0:23)**

**DIMENSION TX(5,7,5)**

**COMMON/CBA/TMA,SMR,TMI**

**COMMON/CBB/TR,DTR**

**COMMON/HOT/D,ST,PL,/TIME/MON,ND,FL**

**INTEGER D,H,Z,G,PL,FG,HR,DY**

**C Z.EQ.1 ETC SHELTER,NORMAL SEVERE**

**DATA Z,CABA,CAB,CBK,CAR/1,2460000,2000000,1000,1000/**

**C CABA AL CABB BRICK CBK PS CAR AIR**

**DATA L1,L2,L4/.1,.05,.05/**

**C L1 ABSORBER L2 BACK CAVITY L4 CAVITY**

```

DATA KAL,KBK,KPS,KAR/160,.84,.035,.025/
DATA TM,RIN,RAV,RAH/50.,1.,1.,14/
C   PANEL SURROUND RINS 3 M2K/W
DATA AR/1/
C   AR IS AREA CAV/AREA VENTS
PRINT*,'
PRINT*,' TIME INTERVAL SECS'
PRINT*,'
READ*,TM
PRINT*,' MONTH'
PRINT*,'
READ*,MON
PRINT*,'DAYS'
PRINT*,'
READ*,ND
PRINT*,'FAN OFF 0,FAN ON 1'
PRINT*,'
READ*,FAN
PRINT*,'ROOM T CONST 0 VAR 1'
PRINT*,'
READ*,MTI
M=MON
PRINT*,'TMIM0 ',TMI(M,0),' TMAM0 ',TMA(M,0)
PRINT*,'
IF(MTI.EQ.0)GOTO 21
DO 23 D=1,ND
DO 23 H=0,23
8   TI(D,H)=TMI(M,H)
23  CONTINUE
PRINT*,' TI(1,0)',TI(1,0),' TMI(M,0) ',TMI(M,0)
PRINT*,'
21  IF(MTI.EQ.1)GOTO 20
PRINT*,'INTERNAL TEMPERATURE'
PRINT*,'

```



```
      READ*,RT
8     DO 30 D=1,ND
      DO 30 H=0,24
      TI(D,H)=RT
30    CONTINUE
20    PRINT*,'EXTERNAL TEMPERATURE CONST 0 VAR 1'
      PRINT*,'
      READ*,MTO
      IF(MTO.EQ.1)GOTO 40
      PRINT*,'EXTERNAL TEMPERATURE'
      PRINT*,'
      READ*,TAO
      DO 50 D=1,ND
      DO 50 H=0,24
      TA(D,H)=TAO
50    CONTINUE
40    IF(MTO.EQ.0)GOTO 45
      DO 47 D=1,ND
      DO 47 H=0,23
      TA(D,H)=TMA(M,H)
47    CONTINUE
      PRINT*,' TA(1,0) ',TA(1,0),' TMA(M,0) ',TMA(M,0)
      PRINT*,'
45    IF(FAN.EQ.0)GOTO 60
      PRINT*,'AIR SPEED WITH FAN'
      PRINT*,'
      READ*,FLC
60    PRINT*,'ABSORBER THICKNESS'
      PRINT*,'
      READ*,L1
      PRINT*,'K OF ABSORBER: BK=.84,AL=160 '
      PRINT*,'
      READ*,K1
```



PRINT\*,'CAP ABSORBER AL=2000000 BK=2400000'

PRINT\*,''

PRINT\*,CAB

PRINT\*,'NG SG DG SC LEDG 0 1 2 3 10'

PRINT\*,'TW100 TW80 TW64 TW48 TW32 TW16 4 5 6 7 8 9'

PRINT\*,''

READ\*,G

C MAXORB A=.97 E=.09

DO 100 D=1,ND

DO 100 H=0,24

TS(D,H)=10

100 CONTINUE

IF((G.EQ.0).AND.(Z.EQ.1))B=.07

IF((G.EQ.0).AND.(Z.EQ.2))B=.06

IF((G.EQ.0).AND.(Z.EQ.3))B=.02

IF((G.EQ.1).AND.(Z.EQ.1))B=.25

IF((G.EQ.1).AND.(Z.EQ.2))B=.24

IF((G.EQ.1).AND.(Z.EQ.3))B=.20

IF((G.EQ.2).AND.(Z.EQ.1))B=.37

IF((G.EQ.2).AND.(Z.EQ.2))B=.36

IF((G.EQ.2).AND.(Z.EQ.3))B=.32

IF((G.EQ.3).AND.(Z.EQ.1))B=.41

IF((G.EQ.3).AND.(Z.EQ.2))B=.39

IF((G.EQ.3).AND.(Z.EQ.3))B=.35

IF((G.EQ.4).AND.(Z.EQ.1))B=1.34

IF((G.EQ.4).AND.(Z.EQ.2))B=1.33

IF((G.EQ.4).AND.(Z.EQ.3))B=1.30

IF((G.EQ.5).AND.(Z.EQ.1))B=1.16

IF((G.EQ.5).AND.(Z.EQ.2))B=1.14

IF((G.EQ.5).AND.(Z.EQ.3))B=1.11

IF((G.EQ.6).AND.(Z.EQ.1))B=.98

IF((G.EQ.6).AND.(Z.EQ.2))B=.96

IF((G.EQ.6).AND.(Z.EQ.3))B=.93

IF((G.EQ.7).AND.(Z.EQ.1))B=.79

```

IF((G.EQ.7).AND.(Z.EQ.2))B=.77
IF((G.EQ.7).AND.(Z.EQ.3))B=.74
IF((G.EQ.8).AND.(Z.EQ.1))B=.64
IF((G.EQ.8).AND.(Z.EQ.2))B=.62
IF((G.EQ.8).AND.(Z.EQ.3))B=.60

IF((G.EQ.9).AND.(Z.EQ.1))B=.44
IF((G.EQ.9).AND.(Z.EQ.2))B=.42
IF((G.EQ.92).AND.(Z.EQ.3))B=.40
IF((G.EQ.10).AND.(Z.EQ.1))B=.59
110 IF(G.EQ.0)R9=.05
IF(G.EQ.1)R9=.15
IF(G.EQ.2)R9=.28
IF(G.EQ.3)R9=.36
IF(G.EQ.4)R9=1.36
IF(G.EQ.5)R9=1.2
IF(G.EQ.6)R9=1.0
IF(G.EQ.7)R9=.8
IF(G.EQ.8)R9=.65

IF(G.EQ.9)R9=.45
IF(G.EQ.10)R9=.5
PRINT*,'INDOOR TEST 1,OUTDOOR 2 '
READ*,XP
DO 200 M=1,12
DO 200 H=0,23
IF(XP.EQ.2)GOTO 196
IF(G.EQ.0)AB(M,H)=.95
IF(G.EQ.1)AB(M,H)=.95*.85
IF(G.EQ.2)AB(M,H)=.95*.74
IF(G.EQ.3)AB(M,H)=.97*.85
IF(G.EQ.4)AB(M,H)=.95*.85*.82
IF(G.EQ.5)AB(M,H)=.95*.85*.83
IF(G.EQ.6)AB(M,H)=.95*.85*.84
IF(G.EQ.7)AB(M,H)=.95*.85*.85

```

```

IF(G.EQ.8)AB(M,H)=.95*.85*.87
IF(G.EQ.9)AB(M,H)=.95*.85*.89
IF(G.EQ.10)AB(M,H)=.95*.74
IF(XP.EQ.1)GOTO 200
196 IF(G.EQ.0)AB(M,H)=.95
IF(G.EQ.1)AB(M,H)=.95*TR(M,H)*1.03
IF(G.EQ.2)AB(M,H)=.95*DTR(M,H)*1.1
IF(G.EQ.3)AB(M,H)=.97*TR(M,H)*1.03
IF(G.EQ.4)AB(M,H)=.95*TR(M,H)*.82*1.03
IF(G.EQ.5)AB(M,H)=.95*TR(M,H)*.84*1.03
IF(G.EQ.7)AB(M,H)=.95*TR(M,H)*.84*1.03
IF(G.EQ.6)AB(M,H)=.95*TR(M,H)*.86*1.03
IF(G.EQ.8)AB(M,H)=.95*TR(M,H)*.86*1.03
IF(G.EQ.9)AB(M,H)=.95*TR(M,H)*.89*1.03
IF(G.EQ.10)AB(M,H)=.95*TR(M,H)*1.1
200 CONTINUE
C RESISTANCES L2/KPS BACK L1/KAL AL L1/KBK BRICK ABSORBER
R1=.12
R2=L2/KPS
R3=.09
R4=.09
K2=KPS
R5=L1/K1
PRINT*,'L1/K1 ',R5
R6=.09
R=R1+R2+R3+R4+R5+R6+R9
Q1=(TI(1,0)-TA(1,0))/R
Q2=(TI(1,1)-TA(1,1))/R
T1=TI(1,0)-Q1*R1
T2=T1-Q1*R2
T3=T2-Q1*R3
T4=T3-Q1*R4
T5=T4-Q1*R5
T6=T5-Q1*R6

```

```

F1=TI(1,1)-Q2*R1
F2=T1-Q2*R2
F3=T2-Q2*R3
F4=F3-Q2*R4
F5=F4-Q2*R5
F6=F5-Q2*R6
DO 250 K=2,4
DO 250 I=2,4
T(I,2,K)=T5
T(I,3,K)=T4
T(I,4,K)=T3
T(I,5,K)=T2
T(I,6,K)=T1
F(I,2,K)=T5
F(I,3,K)=T4
F(I,4,K)=T3
F(I,5,K)=T2
F(I,6,K)=T1
250 CONTINUE
PRINT*,'INITIAL TEMPERATURES'
C T1 INS T2 INS T3 CAV T4 ABS T5 ABS(F) T6 OUTER CAV
WRITE(6,305)
305 FORMAT(' TAI T1 T2 T3 T4 T5 T6 TAO')
WRITE(6,300)TI(1,0),T1,T2,T3,T4,T5,T6,TA(1,0)
300 FORMAT(8F5.1)
C LENGTHS L1/ABS L2/INS L4/CAV LIN/INS(COVER) W/WIDTH H/HT
PRINT*,'ABSORBER WIDTH'
PRINT*,' '
READ*,W
PRINT*,'ABSORBER HEIGHT'
PRINT*,' '
READ*,HT
PRINT*,'CAVITY THICKNESS'
PRINT*,' '

```

```

READ*,L4
C   I 2/WALL 3/CENTRE 4/WALL K 2/FLOOR 3/CENTRE 4/CEILING
LI(2)=W/4.
LI(3)=W/2.
LI(4)=W/4.
LJ(2)=L1/2.
LJ(3)=L1/2.
LJ(4)=L4
LJ(5)=L2/2.
LJ(6)=L2/2
LK(2)=HT/4
LK(3)=HT/2
LK(4)=HT/4
A(2,2)=W*HT/16
A(2,3)=W*HT/8
A(2,4)=W*HT/16
A(3,2)=W*HT/8
A(3,3)=W*HT/4
A(3,4)=W*HT/8
A(4,2)=W*HT/16
A(4,3)=W*HT/8
A(4,4)=W*HT/16
AT=0
DO 340 I=2,4
DO 340 K=2,4
AT=AT+A(I,K)
340 CONTINUE
C   CAPACITIES A(I,K)*NODE LENGTH*THRMAL CAPACITY
DO 350 I=2,4
DO 350 K=2,4
C(I,2,K)=A(I,K)*L1*CAB/2
C(I,3,K)=A(I,K)*L1*CAB/2
C(I,4,K)=A(I,K)*L4*CAR/2
C(I,5,K)=A(I,K)*L2*CBK/2

```



```

C(I,6,K)=A(I,K)*L2*CBK/2
350 CONTINUE
PRINT*,'C(3,3,3) ',C(3,3,3)
C RESISTANCES:INSULATION (RIN), RAV, RAH, RAV.
C CONDUCTIVITIES : ABSORBER: K1 (KAL, KBK), INSULATION: K2
DO 370 K=2,4
DO 370 J=2,6
Y(2,J,K)=RIN
Y(5,J,K)=RIN
Y(5,J,K)=RIN
370 CONTINUE
DO 380 I=3,4
DO 380 J=2,3
Y(I,J,2)=(W/(2*K1)+RAH+2*RIN)/4
Y(I,J,3)=(W/(2*K1)+RAH)/2
Y(I,J,4)=(W/(2*K1)+RAH+2*RIN)/4
380 CONTINUE
DO 390 I=3,4
DO 390 K=2,4
Y(I,4,K)=RAH
390 CONTINUE
DO 400 I=3,4
DO 400 J=5,6
Y(I,J,2)=(W/(2*K2)+RAH+2*RIN)/4
Y(I,J,3)=(W/(2*K2)+RAH)/2
Y(I,J,4)=(W/(2*K2)+RAH+2*RIN)/4
400 CONTINUE
C J RESISTANCES
DO 410 K=2,4
DO 410 I=2,4
X(I,2,K)=B
X(I,3,K)=L1/K1
X(I,4,K)=.09
X(I,5,K)=.09

```

```

X(I,6,K)=L2/K2
X(I,7,K)=.12
410 CONTINUE
PRINT*,' X3 ',X(3,3,3)
C K RESISITANCES
DO 420 I=2,4
DO 420 K=2,4
ZD(I,2,K)=(HT/(2*K1)+RAV)/2
ZD(I,3,K)=(HT/(2*K1)+RAV)/2
ZD(I,4,K)=RAV
ZD(I,5,K)=(HT/(2*K2)+RAV)/2
ZD(I,6,K)=(HT/(2*K2)+RAV)/2
420 CONTINUE
DO 430 I=2,4
DO 430 J=2,6
ZD(I,J,2)=RIN
ZD(I,J,5)=RIN
430 CONTINUE
M=MON
WRITE(6,460)M
460 FORMAT(' M',\I2)
PRINT*,' '
C FINITE DIFFERENCE EQUATIONS
DO 510 D=1,ND
WRITE(6,515)D
515 FORMAT(' DAY',\I2)
PRINT*,' '
ST(D)=0
DO 520 H=0,23
WRITE(6,530)H
530 FORMAT(' ',\I2)
IF(MTO.EQ.0)GOTO 540
TA(D,H)=TMA(M,H)
TA(D,24)=TMA(M,0)

```

```
540  IF(MTI.EQ.0)GOTO 550
      TI(D,H)=TMI(M,H)
      TI(D,24)=TMI(M,0)
550  DO 560 I=2,4
      DO 560 K=2,4
      T(I,7,K)=TI(D,H)
      F(I,7,K)=TI(D,H+1)
560  CONTINUE
      DO 570 J=2,6
      DO 570 K=2,4
      T(1,J,K)=TA(D,H)
      T(5,J,K)=TA(D,H)
      F(1,J,K)=TA(D,H+1)
      F(5,J,K)=TA(D,H+1)
570  CONTINUE
      DO 580 I=2,4
      DO 580 K=2,4
      T(I,1,K)=TA(D,H)
      F2(I,1,K)=TA(D,H+1)
580  CONTINUE
      DO 590 J=2,6
      DO 590 I=2,4
      T(I,J,5)=TA(D,H)
      F(I,J,5)=TA(D,H+1)
      T(I,J,1)=TA(D,H)
      F(I,J,1)=TA(D,H+1)
590  CONTINUE
      DO 600 I=2,4
      T(I,4,1)=TI(D,H)
      F(I,4,1)=TI(D,H+1)
600  CONTINUE
      DO 604 I=2,4
      DO 604 K=2,4
      TEMP(I,2,K)=F(I,4,K)
```

```

604  CONTINUE
      DO 605 I=2,4
      TEMP(I,4,1)=TI(D,H+1)
605  CONTINUE
      SR(H)=SMR(M,H)
      ST(D)=ST(D)+SR(H)*AT
      QH(H)=0
      N=0
606  AVTCAV(H)=0
      TCAV(H)=0
      DO 610 I=2,4
      TCAV(H)=TCAV(H)+F(I,4,4)
610  CONTINUE
      AVTCAV(H)=TCAV(H)/3.
      FLA=2.*9.81*HT*(T(3,4,4)-TI(D,H))
      IF(T(3,4,4).LE.TI(D,H))FLA=0
      FLB=(8.*AR**2+2.)*T(3,4,4)
      FL(H)=SQRT(FLA/FLB)
710  FG=0
      DO 700 K=2,4
      DO 700 I=2,4
      DO 700 J=2,6
      Q(I,J,K)=0
      FLOW(I,J,K)=0
      V=0
      TX(I,J,K)=F(I,J,K)
      TEMP(I,4,K)=F(I,4,K)
      TEMP(I,4,1)=TI(D,H)
      IF(FAN.EQ.1)V=FLC
      IF(FAN.EQ.0)V=FL(H)
      IF(T(3,4,4).LE.TI(D,H))V=0
      FLOW(I,4,K)=1200*V*L4*LI(I)
      Q(I,2,K)=AB(M,H)*SR(H)*A(I,K)
C    Q(I,2,K)=.85*SR(H)*A(I,K)*.98

```

```

FX(I,J,K)=(F(I-1,J,K)*LJ(J)*LK(K)/Y(I,J,K)+F(I+1,J,K)*LJ(J)*
1 LK(K)/Y(I+1,J,K)+F(I,J-1,K)*LI(I)*LK(K)/X(I,J,K)+F(I,J+1,K)
2 *LI(I)*LK(K)/X(I,J+1,K)+F(I,J,K-1)*LI(I)*LJ(J)/ZD(I,J,K)+
3 F(I,J,K+1)*LI(I)*LJ(J)/ZD(I,J,K+1)+C(I,J,K)*T(I,J,K)/TM+
4 Q(I,J,K)+FLOW(I,J,K)*TEMP(I,4,K-1))/(LJ(J)*LK(K)/Y(I,J,K)+
5 LI(I)*LK(K)/X(I,J,K)+LI(I)*LJ(J)/ZD(I,J,K)+C(I,J,K)/TM+FLOW
6 (I,J,K)+LJ(J)*LK(K)/Y(I+1,J,K)+LI(I)*LK(K)/X(I,J+1,K)+LI(I)
7 *LJ(J)/ZD(I,J,K+1))
VAL=FX(I,J,K)-F(I,J,K)
IF(ABSVAL.GT.0.01)FG=1
F(I,J,K)=FX(I,J,K)
700 CONTINUE
IF(FG.EQ.1)GOTO 710
N=N+1
XT=3600./TM
QN(N)=1200*V*L4*W*(T(3,4,4)-TI(D,H))
QH(H)=QH(H)+QN(N)/XT
DO 720 K=2,4
DO 720 J=2,6
DO 720 I=2,4
T(I,J,K)=TX(I,J,K)
720 CONTINUE
IF(N.LT.XT)GOTO 606
PRINT*,'B',T(3,3,4),'C4',T(3,4,4),'F',T(3,2,4),'TI',TI(D,H)
TH(H+1,2)=T(3,2,3)
TH(H+1,3)=T(3,3,4)
TH(H+1,4)=T(3,4,4)
HR=H+1
IF(PL.GT.0)GOTO 520
PRINT*,'DAYPLOT 1 DAYHEAT 2 MONTH ENERGY 3'
PRINT*,' '
READ*,PL
520 CONTINUE
C BACK TO HOUR

```



```

IF(PL.EQ.2)GOTO 750
IF(PL.EQ.3)GOTO 510
CALL DAYPLOT(TH,DY)
750 SOL=ST(D)/1000
    SJ=SOL*3.6
    IF(FAN.EQ.1)FR=FLC
    IF(FAN.EQ.0)FR=FL(H)
    PRINT*,'DAILY SOLAR',SJ,' KJ ',SOL,' KWH'
    PRINT*,'FLOW RATE MIDDAY',FR
    PRINT*,'HEAT 16HRS ',QH(16)/1000.,' KJ'
    CALL HEAT(QH)
510 CONTINUE
C BACK TO DAY (D=1,ND)
    IF(PL.EQ.2)GOTO 760
760 CALL ENERGY
    PRINT*,'END'
    END
    BLOCK DATA
    DIMENSION TR(12,0:23),DTR(12,0:23)
    COMMON /CBB/TR,DTR
    DATA (TR(1,N),N=8,16)/.81,.81,.815,.815,.825,.815,.815,.81,
1 .81/
    DATA(TR(2,N),N=7,17)/.7,.74,.79,.805,.815,.815,.815,.805,
1 .798,.74,.7/
    DATA(TR(3,N),N=6,18)/.3,.52,.69,.72,.81,.805,.805,.805,.81,
1 .72,.69,.52,.3/
    DATA(TR(4,N),N=6,18)/.2,.36,.58,.705,.77,.79,.79,.77,.70
1.5,.58,.36,.2/
    DATA(TR(5,N),N=7,17)/.2,.47,.65,.725,.75,.76,.75,.725,.65,.4
1 7,.2/
    DATA(TR(6,N),N=7,17)/.2,.42,.6,.682,.725,.742,.725,.682,.6,.
1 2,.2/
    DATA(TR(7,N),N=7,17)/.2,.47,.65,.725,.75,.76,.75,.725,.65,.4
1 7,.2/

```

DATA(TR(8,N),N=6,18)/.2,.36,.58,.705,.77,.79,.79,.79,.77,.70  
 1 5,.58,.36,.2/  
 DATA(TR(9,N),N=6,18)/.3,.52,.69,.72,.81,.805,.805,.805,.81,  
 1 .72,.69,.52,.3/  
 DATA(TR(10,N),N=7,17)/.7,.74,.79,.805,.815,.815,.815,.805,.7  
 1 9,.74,.7/  
 DATA(TR(11,N),N=8,16)/.81,.81,.815,.815,.825,.815,.815,.81,.  
 1 81/  
 DATA(TR(12,N),N=8,16)/.8,.805,.815,.815,.816,.815,.815,.805,  
 1 .8/  
 DATA(DTR(1,N),N=9,15)/.7,.71,.71,.73,.71,.71,.7/  
 DATA(DTR(2,N),N=8,16)/.61,.66,.71,.72,.72,.72,.71,.66,.61/  
 DATA(DTR(3,N),N=7,17)/.35,.55,.65,.7,.7,.7,.7,.65,.55,.36  
 1 /  
 DATA(DTR(4,N),N=7,17)/.29,.41,.59,.65,.66,.67,.66,.65,.56,.4  
 1 1,.29/  
 DATA(DTR(5,N),N=8,16)/.25,.47,.58,.62,.63,.62,.58,.47,.25/  
 DATA(DTR(6,N),N=8,16)/.3,.45,.52,.59,.61,.59,.52,.45,.3/  
 DATA(DTR(7,N),N=8,16)/.25,.47,.58,.62,.63,.62,.58,.47,.25/  
 DATA(DTR(8,N),N=7,17)/.29,.41,.59,.65,.66,.67,.66,.65,.56,.4  
 1 1,.29/  
 DATA(DTR(9,N),N=7,17)/.35,.55,.65,.7,.7,.7,.7,.65,.55,.36  
 1 /  
 DATA(DTR(10,N),N=8,16)/.61,.66,.71,.72,.72,.72,.71,.66,.61/  
 DATA(DTR(11,N),N=9,15)/.7,.71,.71,.73,.71,.71,.7/  
 DATA(DTR(12,N),N=9,15)/.7,.71,.71,.73,.71,.71,.7/  
 END

**A3.9 Subroutine that determines the energy produced by various types of solar wall over a period of several days using an IBM compatible PC.**

```

SUBROUTINE ENERGY
DIMENSION QME(31),ST(31),EFF(31)
COMMON /HOT/D,ST,PL,/ENG/QME,EFF/TIME/MON,ND,FL
CHARACTER TIM
INTEGER D
WRITE(6,10)ND,MON
10 FORMAT(' ND=',I2,'MON=',I3)
FSUN=0
TOTEN=0
TEFF=0
IF(ND.EQ.1)GOTO 30
DO 20 D=1,ND-1
    TOTEN=TOTEN+QME(D)
    FSUN=FSUN+ST(D)
    TEFF=TEFF+EFF(D)
20 CONTINUE
    AVEFF=TEFF/FLOAT(ND-1)
    GOTO 40
30 D=1
    TOTEN=QME(1)
    FSUN=ST(1)
    AVEFF=EFF(1)
    IF(ND.EQ.1)GOTO 50
40 AVSOL=FSUN*3.6/(FLOAT(ND-1)*1000.)
50 SOL=FSUN*3.6/1000.
    IF(MON.EQ.1)TIM='JAN'
    IF(MON.EQ.2)TIM='FEB'
    IF(MON.EQ.3)TIM='MAR'
    IF(MON.EQ.4)TIM='APRIL'
    IF(MON.EQ.5)TIM='MAY'
    IF(MON.EQ.6)TIM='JUN'

```

```
IF(MON.EQ.7)TIM='JUL'  
IF(MON.EQ.8)TIM='AUG'  
IF(MON.EQ.9)TIM='SEP'  
IF(MON.EQ.10)TIM='OCT'  
IF(MON.EQ.11)TIM='NOV'  
IF(MON.EQ.12)TIM='DEC'  
WRITE(6,60)TIM  
60 FORMAT(' RESULTS FOR ',A5)  
WRITE(6,70)FL  
70 FORMAT(' FAN SPEED=',F4.1,'M/S')  
WRITE(6,80)ND,AVEFF  
80 FORMAT(' AVERAGE EFFICIENCY OVER',I2,'-1 DAYS=',F4.1,'%')  
WRITE(6,90)SOL  
90 FORMAT(' TOTAL SOLAR=',F6.1,' MJ')  
WRITE(6,100)AVSOL  
100 FORMAT(' AVERAGE SOLAR=',F6.1,' MJ PER DAY')  
WRITE(6,110)TOTEN  
110 FORMAT(' TOTAL ENERGY FROM SOLAR WALL=',F6.1,' MJ')  
RETURN  
END
```

### A3.10 Subroutine which determines the daily heat produced by various solar wall types on an IBM compatible PC

```

SUBROUTINE HEAT(QH)
DIMENSION H(24),QA(24),QH(24),QAJ(24),ST(31),TM(31),TE(0:31)
1,QME(31),EFF(31),TEW(0:31),TMW(0:31)
COMMON/HOT/D,ST,PL,/ENG/QME,EFF
INTEGER E,D,PL
SOL=ST(D)
IF(PL.EQ.2)GOTO 22
IF(PL.EQ.3)GOTO 22
WRITE(6,10)
10 FORMAT(' 1 FOR ENERGY ELSE 0.')
```

    READ(5,20)E

```
20 FORMAT(I1)
    IF(E.EQ.0)GOTO 300
22 QT=0.
    QTV=0.
    DO 30 J=1,24
C QH/1000=KWH, QH*3.6/1000=MJ.
    QA(J)=QH(J)/1000.
    QAJ(J)=QH(J)*3.6/1000
    QT=QT+QA(J)
    QTV=QTV+QAJ(J)
30 CONTINUE
    TM(D)=0.
    TMW(D)=0.
    DO 33 J=1,12
    TM(D)=QAJ(J)+TM(D)
    TMW(D)=QA(J)+TMW(D)
33 CONTINUE
    TE(D)=0
    TEW(D)=0
    DO 37 J=13,24
```



```

TE(D)=QAJ(J)+TE(D)
TEW(D)=QA(J)+TEW(D)
37 CONTINUE
  IF(PL.EQ.3)GOTO 124
  WRITE(6,140)
140 FORMAT(/,' ENERGY OUTPUT:TROMBE WALL KWH')
  WRITE(6,150)
150 FORMAT(' HOUR    1  2  3  4  5  6  7  8  9 10 11 12')
  1 ')
  WRITE(6,160)(QA(J),J=1,12)
160 FORMAT(' ENERGY  ',12F4.1)
  WRITE(6,170)
170 FORMAT(' HOUR    13 14 15 16 17 18 19 20 21 22 23 24
  1')
  WRITE(6,180)(QA(J),J=13,24)
180 FORMAT(' ENERGY  ',12F4.1)
  WRITE(6,190)QTV,QT
190 FORMAT(' DAILY ENERGY= ',F6.1,' MJ',F6.1,' KWH')
  WRITE(6,196)TM(D),TMW(D)
196 FORMAT(' MORNING ENERGY= ',F6.1,' MJ',F6.1,' KWH')
  WRITE(6,200)TE(D),TEW(D)
200 FORMAT(' EVENING ENERGY= ',F6.1,' MJ',F6.1,' KWH')
124 TE(0)=0
  IF(D.EQ.1)GOTO 250
  QME(D-1)=TM(D)+TE(D-1)
  EN=QME(D-1)/3.6
  WRITE(6,215)QME(D-1),EN
215 FORMAT(' ENERGY PREVIOUS DAY SOLAR=',F5.1,' MJ',F5.1,' KWH')
220 EFF(D-1)=QME(D-1)*100000./(ST(D-1)*3.6)
  IPD=D-1
  IF(PL.EQ.3)GOTO 300
  WRITE(6,230)IPD,EFF(D-1)
230 FORMAT(' EFFICIENCY OF WALL (PREVIOUS DAY)',I2,'=',F4.1,'%')
250 SDE=ST(D-1)*3.6/1000.

```

SPK=ST(D-1)/1000

SJ=ST(D)\*3.6/1000.

SK=ST(D)/1000.

WRITE(6,243)SJ,SK

WRITE(6,245)SDE,SPK

243 FORMAT(' THIS DAYS SOLAR= ',F5.1,' MJ',F6.1,' KWH')

245 FORMAT(' SOLAR DAY BEFORE=',F5.1,' MJ',F6.1,' KWH')

300 RETURN

END

**A3.11 Subroutine which plots the solar wall surface and internal cavity temperatures for various solar wall types over 24 hour periods.**

```

SUBROUTINE DAYPLOT (TH,DY)
DIMENSION TH(24,5),AX(24),AY(24),BY(24),CY(24)
CHARACTER*66 LINE(65)
INTEGER DY
WRITE(6,10)
10 FORMAT(' WALL TEMPERATURES
1 INPUT 1 TO EXIT.')
WRITE(6,15)
15 FORMAT('    0  5 10 15 20 25 30 35 40 45
1 50 55 60 65 DEG C')
LINE(0)='*'
DO 30 M=1,23
DO 40 I=1,65
LINE(I)=' '
IF(I.EQ.INT(TH(M,2)+0.5))LINE(I)='*'
IF(I.EQ.INT(TH(M,4)+0.5))LINE(I)='.'
IF(I.EQ.INT(TH(M,3)+0.5))LINE(I)='+'
40 CONTINUE
IF(M.EQ.1)WRITE(6,45)'HR',M,(LINE(I),I=0,65)
IF(M.GT.1)WRITE(6,50)M,(LINE(I),I=0,65)
45 FORMAT(TR1,A2,TR1,I2,TR1,66A1)
50 FORMAT(TR4,I2,TR1,66A1)
30 CONTINUE
READ*,N
IF(N.EQ.1)GOTO 60
60 RETURN
END

```

**3.12 Block data for PC solar wall program. Mid monthly average hourly values of Manchester (UK) solar radiation on a south facing vertical plane plus external and internal temperature data for Manchester are listed in Fortran format**

C MONTHLY DAT FOR SOLWALL EX MANCHESTER.(J.K.PAGE DATA)

C DATA CONTAINS SOME CLEAR DAYS.CHECK BEFORE USE.2

BLOCK DATA SUNMAN

DIMENSION TMA(12,0:23),SMR(12,0:23),TMI(12,0:23)

COMMON /CBA/TMA,SMR,TMI

DATA(SMR(1,N),N=0,23)/0.,0.,0.,0.,0.,0.,0.,0.,0.,71,123,161,

1 175,161,123,71,0.,0.,0.,0.,0.,0.,0.,0./

DATA(SMR(3,N),N=0,23)/0.,0.,0.,0.,0.,0.,48,124,200,264,304

1 ,319,304,264,200,124,48,0.,0.,0.,0.,0./

DATA(SMR(4,N),N=0,23)/0.,0.,0.,0.,0.,0.,30,81,158,231,290,

1 329,344,329,290,231,158,81,30,0.,0.,0.,0.,0./

DATA(SMR(5,N),N=0,23)/0.,0.,0.,0.,0.,24,56,93,170,242,198,

1 340,354,340,298,242,170,93,56,24,0.,0.,0.,0./

DATA(SMR(6,N),N=0,23)/0.,0.,0.,0.,8,35,66,132,206,270,313,

1 338,336,306,289,233,165,98,66,35,8,0.,0.,0./

DATA(SMR(7,N),N=0,23)/0.,0.,0.,0.,3,27,57,89,154,216,267,302,

1 317,302,267,216,154,89,57,27,3,0.,0.,0./

DATA(SMR(8,N),N=0,23)/0.,0.,0.,0.,0.,8,41,85,162,232,287,328,

1 342,328,287,232,162,85,41,8,0.,0.,0.,0./

DATA(SMR(9,N),N=0,23)/0.,0.,0.,0.,0.,0.,10,65,141,217,277,

1 317,331,317,277,217,141,65,10,0.,0.,0.,0.,0./

DATA(SMR(10,N),N=0,23)/0.,0.,0.,0.,0.,0.,0.,25,99,175,242,283

1 ,298,283,242,175,99,25,0.,0.,0.,0.,0./

DATA(SMR(11,N),N=0,23)/0.,0.,0.,0.,0.,0.,0.,0.,32,95,156,197,

1 213,197,166,95,32,0.,0.,0.,0.,0.,0./

DATA(SMR(12,N),N=0,23)/0.,0.,0.,0.,0.,0.,0.,0.,0.,64,120,158,

1 171,158,120,64,0.,0.,0.,0.,0.,0.,0./

DATA(SMR(2,N),N=0,23)/0.,0.,0.,0.,0.,0.,0.,0.,59,128,190,230,

1 245,230,190,128,59,0.,0.,0.,0.,0.,0./

DATA(TMA(1,N),N=0,23)/3.5,3.4,3.3,3.3,3.2,3.1,3.1,3.1,3.1,



1 3.2,3.6,4.1,4.6,4.9,5.1,5.0,4.8,4.4,4.2,4.0,3.8,3.8,3.7,3.6/  
 DATA(TMA(2,N),N=0,23)/3.4,3.3,3.1,3.1,3.,2.9,2.9,2.9,3.,3.3,  
 1 4.,4.6,5.2,5.6,5.8,5.8,5.6,5.2,4.7,4.3,4.,3.9,3.7,3.5/  
 DATA(TMA(3,N),N=0,23)/4.6,4.5,4.3,4.2,4.,3.9,3.8,3.9,4.3,5.2,  
 1 6.,6.8,7.5,7.8,8.1,8.1,8.,7.6,7.,6.3,5.8,5.5,5.2,4.9/  
 DATA(TMA(4,N),N=0,23)/6.4,6.1,5.8,5.6,5.5,5.3,5.4,5.9,6.8,7.8  
 1 ,8.6,9.4,10.,10.4,10.7,10.7,10.6,10.3,9.8,9.,8.2,7.6,7.2,6.8/  
 DATA(TMA(5,N),N=0,23)/9.3,8.9,8.6,8.3,8.1,8.1,8.5,9.4,10.4,  
 1 11.4,12.3,13.,13.5,14.,14.2,14.4,14.3,14.,13.5,12.8,11.8,11.,  
 1 10.3,9.8/  
 DATA(TMA(6,N),N=0,23)/12.2,11.8,11.4,11.1,10.8,10.9,11.6,12.5  
 1 ,13.6,14.5,15.4,16.1,16.6,17.1,17.4,17.4,17.3,17.1,16.6,16.,  
 1 15.1,14.2,13.4,12.8/  
 DATA(TMA(7,N),N=0,23)/13.7,13.4,13.,12.8,12.6,12.6,12.9,13.7,  
 1 14.6,15.4.,16.2,16.8,17.4,17.8,18.1,18.3,18.2,18.0,17.6,17.,  
 1 16.2,15.4,14.7,14.2/  
 DATA(TMA(8,N),N=0,23)/13.7,13.4,13.1,12.9,12.7,12.5,12.7,13.4  
 1 ,14.4,15.4,16.3,17.,17.6,18.,18.3,18.4,18.3,18.,17.5,16.7,  
 1 15.8,15.1,14.5,14.1/  
 DATA(TMA(9,N),N=0,23)/12.,11.7,11.5,11.3,11.2,11.,11.,11.3,  
 1 12.1,13.2,14.2,15.,15.6,16.,16.2,16.3,16.1,15.6,14.9,14.1  
 1 ,13.5,13.,12.6,12.2/  
 DATA(TMA(10,N),N=0,23)/9.6,9.4,9.2,9.1,9.,8.9,8.9,8.9,9.3,10.  
 1 2,11.1,11.9,12.4,12.8,12.9,12.8,12.5,11.9,11.2,10.7,10.4,10.1  
 1 ,9.9,9.7/  
 DATA(TMA(11,N),N=0,23)/5.9,5.8,5.7,5.6,5.6,5.5,5.4,5.4,5.5,  
 1 5.8,6.4,7.1,7.7,8.,8.1,8.,7.6,7.1,6.8,6.5,6.3,6.2,6.,5.9/  
 DATA(TMA(12,N),N=0,23)/4.2,4.1,4.,4.,3.9,3.9,3.8,3.8,3.8,  
 1 3.8,4.2,4.7,5.2,5.6,5.6,5.5,5.2,4.9,4.7,4.6,4.5,4.4,4.3,4.2/  
 DATA(TMI(1,N),N=0,23)/10.,10.,10.,10.,10.,10.,10.,10.,18.,  
 1 18.,18.,18.,18.,18.,18.,18.,18.,17.,16.,15.,14.,13.,12.,11./  
 DATA(TMI(2,N),N=0,23)/10.,10.,10.,10.,10.,10.,10.,10.,18.,18.  
 1 ,18.,18.,18.,18.,18.,18.,18.,17.,16.,15.,14.,13.,12.,11./  
 DATA(TMI(3,N),N=0,23)/12.5,12.5,12.5,12.5,12.5,12.5,12.5,





**A3.13 Block data for PC solar wall program. Mid monthly average hourly values of Plymouth (UK) solar radiation falling on a south facing vertical plane and external and internal temperature data for Plymouth are listed in Fortran format**

**C MONTHLY DAT FOR SOLWALL EX PLYMOUTH(J.K.PAGE DATA)**

BLOCK DATA SUNPLYM

DIMENSION TMA(12,0:23),SMR(12,0:23),TMI(12,0:23)

COMMON /CBA/TMA,SMR,TMI

DATA(SMR(1,N),N=0,23)/0.,0.,0.,0.,0.,0.,0.,0.,0.,47.,117.,178.,

1 217.,232.,217.,178.,117.,47.,0.,0.,0.,0.,0.,0.,0./

DATA(SMR(2,N),N=0,23)/0.,0.,0.,0.,0.,0.,0.,0.,0.,99.,183.,252.,

1 298.,313.,298.,252.,183.,99.,0.,0.,0.,0.,0.,0.,0./

DATA(SMR(3,N),N=0,23)/0.,0.,0.,0.,0.,0.,0.,0.,69.,162.,248.,317.

1 ,360.,377.,360.,317.,248.,162.,99.,0.,0.,0.,0.,0.,0./

DATA(SMR(4,N),N=0,23)/0.,0.,0.,0.,0.,0.,33.,92.,185.,270.,

1 381.,399.,381.,336.,270.,185.,92.,33.,0.,0.,0.,0.,0.,0./

DATA(SMR(5,N),N=0,23)/0.,0.,0.,0.,0.,23.,59.,95.,179.,261.,

1 325.,371.,388.,371.,325.,261.,179.,95.,59.,23.,0.,0.,0.,0./

DATA(SMR(6,N),N=0,23)/0.,0.,0.,0.,2.,33.,65.,100.,163.,239.,

1 300.,344.,359.,344.,300.,239.,166.,100.,65.,33.,2.,0.,0.,0./

DATA(SMR(7,N),N=0,23)/0.,0.,0.,0.,0.,26.,60.,95.,166.,236.,29

1 4.,334.,351.,344.,294.,236.,166.,95.,60.,26.,0.,0.,0.,0./

DATA(SMR(8,N),N=0,23)/0.,0.,0.,0.,0.,6.,44.,90.,177.,255.,317

1 ,363.,379.,363.,317.,255.,177.,90.,44.,6.,0.,0.,0.,0./

DATA(SMR(9,N),N=0,23)/0.,0.,0.,0.,0.,0.,11.,78.,170.,255.,

1 319.,363.,379.,363.,319.,255.,170.,78.,11.,0.,0.,0.,0./

DATA(SMR(10,N),N=0,23)/0.,0.,0.,0.,0.,0.,0.,37.,129.,216.

1 ,287.,333.,346.,333.,287.,216.,129.,37.,0.,0.,0.,0.,0.,0./

DATA(SMR(11,N),N=0,23)/0.,0.,0.,0.,0.,0.,0.,0.,62.,143.,213.,

1 258.,273.,258.,213.,143.,72.,0.,0.,0.,0.,0.,0.,0./

DATA(SMR(12,N),N=0,23)/0.,0.,0.,0.,0.,0.,0.,0.,0.,117.,183.,

1 229.,244.,229.,283.,117.,0.,0.,0.,0.,0.,0.,0.,0./

DATA(TMA(1,N),N=0,23)/5.8,5.7,5.7,5.6,5.6,5.6,5.6,5.5,5.6,5.6

1 ,6.0,6.6,7.0,7.3,7.4,7.4,7.1,6.8,6.6,6.4,6.2,6.1,6.0,5.9/

DATA(TMA(2,N),N=0,23)/5.6,5.5,5.4,5.3,5.2,5.2,5.1,5.1,5.1,  
1 5.4,6.1,6.7,7.2,7.4,7.6,7.6,7.4,7.0,6.5,6.3,6.1,5.9,5.8,5.7/  
DATA(TMA(3,N),N=0,23)/6.2,6.1,6.,5.9,5.8,5.7,5.6,5.6,6.,6.8,  
1 7.6,8.2,8.6,8.9,9.,8.9,8.7,8.4,7.9,7.4,7.,6.8,6.6,6.4/  
DATA(TMA(4,N),N=0,23)/7.7,7.4,7.2,7.1,6.9,6.8,6.8,7.3,8.1,9.,  
1 .8,10.3,10.7,10.9,11.,11.,10.8,10.5,10.1,9.5,8.9,8.5,8.2,7.9/  
DATA(TMA(5,N),N=0,23)/9.9,9.6,9.4,9.3,9.1,9.,9.4,10.2,11.2,12  
1 ,12.6,13.,13.3,13.5,13.5,13.4,13.3,13.,12.6,12.2,11.5,11.,10.  
1 ,10.2/  
DATA(TMA(6,N),N=0,23)/12.7,12.4,12.2,12.,11.8,11.8,12.4,13.2,  
1 14.1,14.8,15.4,15.8,16.1,16.3,16.4,16.4,16.2,16.,15.7,15.2,14  
1 5,13.9,13.4,13.1/  
DATA(TMA(7,N),N=0,23)/14.3,14.,13.8,13.6,13.4,13.4,13.8,14.6,  
1 15.5,16.2,16.8,17.2,17.6,17.8,17.9,17.9,17.7,17.5,17.2,16.7,  
1 16.1,15.4,15.,14.6/  
DATA(TMA(8,N),N=0,23)/14.5,14.2,14.,13.8,13.7,13.6,13.7,14.3,  
1 15.3,16.2,17.,17.5,17.9,18.1,18.1,18.1,17.9,17.6,17.2,16.5,  
1 15.8,15.4,15.0,14.7/  
DATA(TMA(9,N),N=0,23)/13.1,12.9,12.7,12.6,12.5,12.4,12.3,12.6  
1 ,13.5,14.5,15.5,16.1,16.4,16.7,16.7,16.6,16.4,15.9,15.3,14.6,  
1 14.1,13.8,13.5,13.3/  
DATA(TMA(10,N),N=0,23)/11.3,11.1,11.,10.9,10.8,10.7,10.7,10.  
1 7,11.,11.8,12.7,13.4,13.8,14.,14.,13.9,13.6,13.1,12.6,12.2,1  
1 9,11.7,11.5,11.3/  
DATA(TMA(11,N),N=0,23)/8.3,8.2,8.2,8.1,8.,8.,7.9,7.8,7.9,8.2,  
1 8.9,9.6,10.,10.3,10.3,10.2,9.8,9.4,9.1,8.8,8.7,8.5,8.4,8.3/  
DATA(TMA(12,N),N=0,23)/6.7,6.6,6.6,6.6,6.5,6.5,6.4,6.4,6.4,6.  
1 5,6.8,7.4,7.9,8.2,8.3,8.1,7.8,7.5,7.3,7.1,7.,6.9,6.8,6.7/  
DATA(TMI(1,N),N=0,23)/11.5,12.,12.,12.,12.,12.,12.,12.,18.,  
1 18.,18.,18.,18.,18.,18.,18.,18.,17.,16.,15.,14.,13.,12.,12./  
DATA(TMI(2,N),N=0,23)/10.5,11.,11.,11.,11.,11.,11.,11.,18.,18  
1 ,18.,18.,18.,18.,18.,18.,18.,17.,16.,15.,14.,13.,12.,10.5/  
DATA(TMI(3,N),N=0,23)/11.5,12.,12.,12.,12.,12.,12.,12.,18.,  
1 18.,18.,18.,18.,18.,18.,18.,18.,17.,16.,15.,14.,13.,12.,12./

```

DATA(TMI(4,N),N=0,23)/13.,13.,13.,13.,13.,13.,13.,13.,18.,18.
1 ,18.,18.,18.,18.,18.,18.,18.,17.,16.,15.,14.,13.,13.,13./
DATA(TMI(5,N),N=0,23)/14.5,15.,15.,15.,15.,15.,15.,15.,18.,
1 18.,18.,18.,18.,18.,18.,18.,18.,17.,15.,15.,15.,15.,15.,15./
DATA(TMI(6,N),N=0,23)/16.5,17.,17.,17.,17.,17.,17.,17.,18.,
1 18.,18.,18.,18.,18.,18.,18.,18.,17.,16.5,16.5,16.5,16.5,16.5,
1 16.5/
DATA(TMI(7,N),N=0,23)/17.5,17.5,17.5,17.5,17.5,17.5,17.5,17.5
1 ,18.,18.,18.,18.,18.,18.,18.,18.,18.,17.5,17.5,17.5,17.5,17.5
1 ,17.5,17.5/
DATA(TMI(8,N),N=0,23)/18.,18.,18.,18.,18.,18.,18.,18.,18.,18.
1 ,18.,18.,18.,18.,18.,18.,18.,18.,18.,18.,18.,18.,18.,18./
DATA(TMI(9,N),N=0,23)/16.5,17.,17.,17.,17.,17.,17.,17.,18.,
1 18.,18.,18.,18.,18.,18.,18.,18.,17.,16.5,16.5,16.5,16.5,16.5,
1 16.5/
DATA(TMI(10,N),N=0,23)/15.,15.,15.,15.,15.,15.,15.,15.,18.,18
1 .,18.,18.,18.,18.,18.,18.,18.,17.,16.,15.,15.,15.,15.,15./
DATA(TMI(11,N),N=0,23)/13.5,14.,14.,14.,14.,14.,14.,14.,18.,
1 18.,18.,18.,18.,18.,18.,18.,18.,17.,16.,15.,14.,13.5,13.5,
1 13.5/
DATA(TMI(12,N),N=0,23)/12.,12.,12.,12.,12.,12.,12.,12.,18.,
1 18.,18.,18.,18.,18.,18.,18.,18.,17.,16.,15.,14.,13.,12.,12./
END

```



**A3.14 Block data for PC solar wall program. Mid monthly average hourly values of London (UK) solar radiation falling on a south facing vertical plane plus external and internal temperature data for London, are listed in Fortran format**

C MONTHLY AVERAGE SOLAR DATA EX LONDON(J.K.PAGE DATA)

BLOCK DATA SUNLON

DIMENSION TMA(12,0:23),SMR(12,0:23),TMI(12,0:23)

COMMON /CBA/TMA,SMR,TMI

DATA(SMR(1,N),N=0,23)/0.,0.,0.,0.,0.,0.,0.,0.,17,66,117,154,

1 166,154,117,66,17,0.,0.,0.,0.,0.,0./

DATA(SMR(2,N),N=0,23)/0.,0.,0.,0.,0.,0.,0.,0.,65,136,201,251,

1 255,251,201,135,65,0.,0.,0.,0.,0.,0./

DATA(SMR(3,N),N=0,23)/0.,0.,0.,0.,0.,0.,0.,0.,48,125,201,264,304

1 ,318,304,264,201,125,48,0.,0.,0.,0.,0.,0./

DATA(SMR(4,N),N=0,23)/0.,0.,0.,0.,0.,0.,26,72,143,211,265,301

1 ,315,301,265,211,143,72,26,0.,0.,0.,0.,0./

DATA(SMR(5,N),N=0,23)/0.,0.,0.,0.,0.,19,50,84,154,222,275,315

1 ,330,315,275,222,154,84,50,19,0.,0.,0.,0./

DATA(SMR(6,N),N=0,23)/0.,0.,0.,0.,4,31,62,95,157,228,285,326

1 ,342,326,285,228,157,95,62,31,4,0.,0.,0./

DATA(SMR(7,N),N=0,23)/0.,0.,0.,0.,24,54,88,153,218,271,310

1 ,324,310,271,218,153,88,54,24,0.,0.,0.,0./

DATA(SMR(8,N),N=0,23)/0.,0.,0.,0.,6,38,83,159,231,286,329,

1 344,329,286,231,159,83,38,6,0.,0.,0.,0./

DATA(SMR(9,N),N=0,23)/0.,0.,0.,0.,10,70,156,236,301,345

1 ,360,345,301,336,156,70,10,0.,0.,0.,0.,0./

DATA(SMR(10,N),N=0,23)/0.,0.,0.,0.,0.,0.,29,104,186,252,

1 294,310,294,252,186,104,29,0.,0.,0.,0.,0./

DATA(SMR(11,N),N=0,23)/0.,0.,0.,0.,0.,0.,0.,44,121,188,23

1 3,249,233,288,121,44,0.,0.,0.,0.,0.,0./

DATA(SMR(12,N),N=0,23)/0.,0.,0.,0.,0.,0.,0.,69,124,161

1 ,175,161,124,69,0.,0.,0.,0.,0.,0./

DATA(TMA(1,N),N=0,23)/4.2,4.1,4.,4.,3.9,3.9,3.8,3.8,3.8,4.1,

1 4.6,5.1,5.6,5.9,6.1,6.,5.7,5.4,5.1,4.9,4.7,4.6,4.5,4.4/



DATA(TMA(2,N),N=0,23)/4.3,4.2,4.1,4.,3.9,3.8,3.8,3.7,3.9,4.4,  
1 5.,5.7,6.2,6.7,6.9,6.9,6.7,6.3,5.9,5.5,5.2,5.,4.7,4.5/

DATA(TMA(3,N),N=0,23)/5.4,5.1,4.9,4.7,4.5,4.4,4.3,4.4,5.1,6.,  
1 6.9,7.7,8.4,8.9,9.1,9.1,9.,8.6,8.,7.3,6.8,6.4,6.,5.7/

DATA(TMA(4,N),N=0,23)/7.3,6.9,6.7,6.4,6.2,6.1,6.2,6.9,7.8,8.8  
1 ,9.6,10.4,11.,11.5,11.8,11.9,11.8,11.5,10.9,10.,9.2,8.7,8.1,7  
1 .7/

DATA(TMA(5,N),N=0,23)/10.1,9.7,9.3,9.,8.8,8.9,9.7,10.6,11.6,  
1 12.6,13.4,14.2,14.8,15.3,15.6,15.7,15.6,15.4,14.9,14.,12.9,12  
1 .,11.3,10.7/

DATA(TMA(6,N),N=0,23)/13.2,12.7,12.3,11.9,11.7,12.2,13.,13.8,  
1 14.8,15.9,16.8,17.5,18.1,18.7,19.,19.2,19.2,19.,18.6,17.8,16.  
1 7,15.6,14.7,14./

DATA(TMA(7,N),N=0,23)/15.1,14.7,14.3,14.,13.7,13.9,14.6,15.4,  
1 16.3,17.2,18.1,18.8,19.5,20.1,20.4,20.6,20.7,20.4,19.9,19.2,  
1 18.,17.,16.3,15.6/

DATA(TMA(8,N),N=0,23)/14.8,14.4,14.1,13.8,13.5,13.4,13.8,14.6  
1 ,15.6,16.7,17.5,18.4,19.1,19.6,20.,20.2,20.1,19.8,19.2,18.2,  
1 17.1,16.4,15.7,15.2/

DATA(TMA(9,N),N=0,23)/12.8,12.4,12.2,12.0,11.8,11.6,11.7,12.2  
1 ,13.3,14.4,15.5,16.4,17.1,17.6,17.9,17.9,17.7,17.2,16.3,15.2,  
1 14.5,14.0,13.5,13.1/

DATA(TMA(10,N),N=0,23)/10.4,10.2,10.,9.8,9.7,9.6,9.6,9.7,10.3  
1 ,11.3,12.2,13.1,13.7,14.2,14.4,14.4,14.0,13.2,12.5,11.9,11.4,  
1 11.1,10.7,10.5/

DATA(TMA(11,N),N=0,23)/6.9,6.7,6.6,6.6,6.5,6.4,6.4,6.3,6.5,7.  
1 ,7.7,8.4,8.9,9.2,9.4,9.2,8.8,8.3,8.,7.7,7.5,7.3,7.1,6.9/

DATA(TMA(12,N),N=0,23)/5.1,5.,5.,4.9,4.9,4.8,4.8,4.7,4.7,5.  
1 ,5.4,6.,6.4,6.7,6.8,6.7,6.3,6.,5.8,5.6,5.5,5.4,5.3,5.2/

DATA(TMI(1,N),N=0,23)/11.,11.,11.,11.,11.,11.,11.,11.,18.,  
1 18.,18.,18.,18.,18.,18.,18.,18.,17.,16.,15.,14.,13.,12.,11./

2 DATA(TMI(2,N),N=0,23)/11.,11.,11.,11.,11.,11.,11.,11.,18.,  
1 18.,18.,18.,18.,18.,18.,18.,18.,17.,16.,15.,14.,13.,12.,11./

DATA(TMI(3,N),N=0,23)/11.,11.,11.,11.,11.,11.,11.,11.,18.,

```

1 18.,18.,18.,18.,18.,18.,18.,18.,17.,16.,15.,14.,13.,12.,11./
  DATA(TMI(4,N),N=0,23)/12.,12.,12.,12.,12.,12.,12.,12.,18.,
1 18.,18.,18.,18.,18.,18.,18.,18.,17.,16.,15.,14.,13.,12.,12./
  DATA(TMI(5,N),N=0,23)/14.5,14.5,14.5,14.5,14.5,14.5,14.5,14.5
1 ,14.5,18.,18.,18.,18.,18.,18.,18.,18.,17.,16.,15.,14.5,14.5,
1 14.5,14.5/
  DATA(TMI(6,N),N=0,23)/17.,17.,17.,17.,17.,17.,17.,17.,18.,
1 18.,18.,18.,18.,18.,18.,18.,18.,17.,17.,17.,17.,17.,17.,17./
  DATA(TMI(7,N),N=0,23)/18.,18.,18.,18.,18.,18.,18.,18.,18.,
1 18.,18.,18.,18.,18.,18.,18.,18.,18.,18.,18.,18.,18.,18./
  DATA(TMI(8,N),N=0,23)/18.,18.,18.,18.,18.,18.,18.,18.,18.,
1 18.,18.,18.,18.,18.,18.,18.,18.,18.,18.,18.,18.,18.,18./
  DATA(TMI(9,N),N=0,23)/17.,17.,17.,17.,17.,17.,17.,17.,18.,
1 18.,18.,18.,18.,18.,18.,18.,18.,17.,17.,17.,17.,17.,17.,17./
  DATA(TMI(10,N),N=0,23)/15.,15.,15.,15.,15.,15.,15.,15.,18.,
1 18.,18.,18.,18.,18.,18.,18.,18.,15.,15.,15.,15.,15.,15.,15./
  DATA(TMI(11,N),N=0,23)/12.5,12.5,12.5,12.5,12.5,12.5,12.5,
1 12.5,18.,18.,18.,18.,18.,18.,18.,18.,18.,17.,16.,15.,14.,13.
1 ,12.5,12.5/
  DATA(TMI(12,N),N=0,23)/11.,11.,11.,11.,11.,11.,11.,11.,18.,
1 18.,18.,18.,18.,18.,18.,18.,18.,17.,16.,15.,14.,13.,12.,11/
  END

```

**A3.15 Block data for PC solar wall program. Mid monthly average hourly values of Lerwick (UK) solar radiation falling on a south facing vertical plane plus external and internal temperature for Lerwick. are listed in Fortran format**

C MONTHLY DAT FOR SOLWALL EX LERWICK(J.K.PAGE DATA)

C CLEAR DAY DATA

BLOCK DATA SUNLER

DIMENSION TMA(12,0:23),SMR(12,0:23),TMI(12,0:23)

COMMON /CBA/TMA,SMR,TMI

DATA(TMA(1,N),N=0,23)/3.4,3.4,3.4,3.4,3.4,3.3,3.3,3.3,3.3,3.4

1 ,3.4,3.6,3.8,3.9,3.8,3.6,3.5,3.4,3.5,3.5,3.4,3.4,3.4,3.4/

DATA(SMR(1,N),N=0,23)/0.,0.,0.,0.,0.,0.,0.,0.,0.,146,273,358,

1 389,358,273,146,0.,0.,0.,0.,0.,0.,0./

DATA(TMA(2,N),N=0,23)/2.8,2.8,2.8,2.8,2.8,2.7,2.7,2.7,2.7,3.

1 0,3.3,3.6,3.8,4.0,3.9,3.8,3.5,3.2,3.1,3.,2.9,3.,2.9,2.9/

DATA(SMR(2,N),N=0,23)/0.,0.,0.,0.,0.,0.,0.,0.,0.,213,399,558,660

1 ,696,660,558,399,213,0.,0.,0.,0.,0.,0.,0./

DATA(SMR(3,N),N=0,23)/0.,0.,0.,0.,0.,0.,31,128,233,333,412,46

1 3,480,463,412,333,233,128,31,0.,0.,0.,0.,0./

DATA(SMR(4,N),N=0,23)/0.,0.,0.,0.,0.,0.,30,81,158,231,290,

1 329,344,329,290,231,158,81,30,0.,0.,0.,0.,0./

DATA(SMR(5,N),N=0,23)/0.,0.,0.,0.,0.,24,56,93,225,362,476,

1 550,577,550,476,362,225,93,56,24,0.,0.,0.,0./

DATA(SMR(6,N),N=0,23)/0.,0.,0.,0.,8,35,66,132,206,270,313,

1 338,336,306,289,233,165,98,66,35,8,0.,0.,0./

DATA(SMR(7,N),N=0,23)/0.,0.,0.,0.,3,27,57,89,154,216,267,302,

1 317,302,267,216,154,89,57,27,3,0.,0.,0./

DATA(SMR(8,N),N=0,23)/0.,0.,0.,0.,0.,8,41,85,162,232,287,328,

1 342,328,287,232,162,85,41,8,0.,0.,0.,0./

DATA(SMR(9,N),N=0,23)/0.,0.,0.,0.,0.,10,65,141,217,277,

1 317,331,317,277,217,141,65,10,0.,0.,0.,0.,0./

DATA(SMR(10,N),N=0,23)/0.,0.,0.,0.,0.,0.,25,99,175,242,283

1 ,298,283,242,175,99,25,0.,0.,0.,0.,0.,0./

DATA(SMR(11,N),N=0,23)/0.,0.,0.,0.,0.,0.,0.,32,95,156,197,



1 213,197,166,95,32,0.,0.,0.,0.,0.,0./

DATA(SMR(12,N),N=0,23)/0.,0.,0.,0.,0.,0.,0.,0.,64,120,158,

1 171,158,120,64,0.,0.,0.,0.,0.,0./

DATA(TMA(3,N),N=0,23)/3.3,3.2,3.2,3.2,3.2,3.1,3.1,3.2,3.5,3.

1 9,4.3,4.6,4.8,4.9,4.8,4.7,4.4,4.1,3.8,3.5,3.3,3.3,3.2,3.2/

DATA(TMA(4,N),N=0,23)/4.0,4.,3.9,3.9,3.8,3.8,4.1,4.6,5.1,5.5

1 ,5.9,6.2,6.4,6.5,6.5,6.3,6.1,5.8,5.3,4.8,4.5,4.3,4.2,4.2/

DATA(TMA(5,N),N=0,23)/9.3,8.9,8.6,8.3,8.1,8.1,8.5,9.4,10.4,

1 11.4,12.3,13.,13.5,14.,14.2,14.4,14.3,14.,13.5,12.8,11.8,11.,

1 10.3,9.8/

DATA(TMA(6,N),N=0,23)/12.2,11.8,11.4,11.1,10.8,10.9,11.6,12.5

1 ,13.6,14.5,15.4,16.1,16.6,17.1,17.4,17.4,17.3,17.1,16.6,16.,

1 15.1,14.2,13.4,12.8/

DATA(TMA(7,N),N=0,23)/13.7,13.4,13.,12.8,12.6,12.6,12.9,13.7,

1 14.6,15.4.,16.2,16.8,17.4,17.8,18.1,18.3,18.2,18.0,17.6,17.,

1 16.2,15.4,14.7,14.2/

DATA(TMA(8,N),N=0,23)/13.7,13.4,13.1,12.9,12.7,12.5,12.7,13.4

1 ,14.4,15.4,16.3,17.,17.6,18.,18.3,18.4,18.3,18.,17.5,16.7,

1 15.8,15.1,14.5,14.1/

DATA(TMA(9,N),N=0,23)/12.,11.7,11.5,11.3,11.2,11.,11.,11.3,

1 12.1,13.2,14.2,15.,15.6,16.,16.2,16.3,16.1,15.6,14.9,14.1

1 ,13.5,13.,12.6,12.2/

DATA(TMA(10,N),N=0,23)/9.6,9.4,9.2,9.1,9.,8.9,8.9,8.9,9.3,10.

1 2,11.1,11.9,12.4,12.8,12.9,12.8,12.5,11.9,11.2,10.7,10.4,10.1

1 ,9.9,9.7/

DATA(TMA(11,N),N=0,23)/5.9,5.8,5.7,5.6,5.6,5.5,5.4,5.4,5.5,

1 5.8,6.4,7.1,7.7,8.,8.1,8.,7.6,7.1,6.8,6.5,6.3,6.2,6.,5.9/

DATA(TMA(12,N),N=0,23)/4.2,4.1,4.,4.,3.9,3.9,3.8,3.8,3.8,

1 3.8,4.2,4.7,5.2,5.6,5.6,5.5,5.2,4.9,4.7,4.6,4.5,4.4,4.3,4.2/

DATA(TMI(1,N),N=0,23)/10.,10.,10.,10.,10.,10.,11.,11.,11.,

1 18.,20.,20.,20.,20.,20.,20.,20.,20.,19.,19.,18.,18.,17.,16./

DATA(TMI(3,N),N=0,23)/10.,10.,10.,10.,10.,10.,11.,11.,11.,

1 18.,20.,20.,20.,20.,20.,20.,20.,20.,19.,19.,18.,18.,17.,16./

DATA(TMI(2,N),N=0,23)/10.,10.,10.,10.,10.,10.,11.,11.,11.,

```

1 18.,20.,20.,20.,20.,20.,20.,20.,20.,19.,19.,18.,18.,17.,16./
  DATA(TMI(4,N),N=0,23)/10.,10.,10.,10.,10.,10.,11.,11.,11.,
1 18.,20.,20.,20.,20.,20.,20.,20.,20.,19.,19.,18.,18.,17.,16./
  DATA(TMI(5,N),N=0,23)/10.,10.,10.,10.,10.,10.,11.,11.,11.,
1 18.,20.,20.,20.,20.,20.,20.,20.,20.,19.,19.,18.,18.,17.,16./
  DATA(TMI(6,N),N=0,23)/10.,10.,10.,10.,10.,10.,11.,11.,11.,
1 18.,20.,20.,20.,20.,20.,20.,20.,20.,19.,19.,18.,18.,17.,16./
  DATA(TMI(7,N),N=0,23)/10.,10.,10.,10.,10.,10.,11.,11.,11.,
1 18.,20.,20.,20.,20.,20.,20.,20.,20.,19.,19.,18.,18.,17.,16./
  DATA(TMI(8,N),N=0,23)/10.,10.,10.,10.,10.,10.,11.,11.,11.,
1 18.,20.,20.,20.,20.,20.,20.,20.,20.,19.,19.,18.,18.,17.,16./
  DATA(TMI(9,N),N=0,23)/10.,10.,10.,10.,10.,10.,11.,11.,11.,
1 18.,20.,20.,20.,20.,20.,20.,20.,20.,19.,19.,18.,18.,17.,16./
  DATA(TMI(10,N),N=0,23)/10.,10.,10.,10.,10.,10.,11.,11.,11.,
1 18.,20.,20.,20.,20.,20.,20.,20.,20.,19.,19.,18.,18.,17.,16./
  DATA(TMI(11,N),N=0,23)/10.,10.,10.,10.,10.,10.,11.,11.,11.,
1 18.,20.,20.,20.,20.,20.,20.,20.,20.,19.,19.,18.,18.,17.,16./
  DATA(TMI(12,N),N=0,23)/10.,10.,10.,10.,10.,10.,11.,11.,11.,
1 18.,20.,20.,20.,20.,20.,20.,20.,20.,19.,19.,18.,18.,17.,16./
  END

```



**A3.16 Block data for PC solar wall program. Mid month average hourly values of Aberdeen (UK) solar radiation falling on a south facing vertical plane, plus external and internal temperature for Aberdeen, are listed in Fortran format.**

```

C  MONTHLY DATA FOR ABERDEEN FOR USE BY SOLAR WALL
C  PROGRAM.(J.K.PAGE DATA)
C  MID MONTH AVERAGE HOURLY VALUES OF WEATHER DATA
BLOCK DATA SUNABER
DIMENSION TMA(12,0:23),SMR(12,0:23),TMI(12,0:23),SMD(12,0:23)
COMMON /CBA/TMA,SMR,TMI,SMD
DATA(SMR(1,N),N=0,23)/0.,0.,0.,0.,0.,0.,0.,0.,0.,0.,65,108,135,
1 146,135,108,65,0.,0.,0.,0.,0.,0.,0.,0./
DATA(SMR(2,N),N=0,23)/0.,0.,0.,0.,0.,0.,0.,0.,0.,56,113,162,193,
1 205,193,162,113,56,0.,0.,0.,0.,0.,0.,0./
DATA(SMR(3,N),N=0,23)/0.,0.,0.,0.,0.,0.,0.,0.,24,68,118,160,186,
1 195,186,160,118,68,24,0.,0.,0.,0.,0.,0./
DATA(SMR(4,N),N=0,23)/0.,0.,0.,0.,0.,0.,0.,0.,22,70,119,159,
1 185,193,185,159,119,70,22,0.,0.,0.,0.,0.,0./
DATA(SMR(5,N),N=0,23)/0.,0.,0.,0.,0.,0.,0.,0.,5.,46.,85.,118.,
1 141,149,141,118,85,46,5,0.,0.,0.,0.,0.,0./
DATA(SMR(6,N),N=0,23)/0.,0.,0.,0.,0.,0.,0.,0.,40,81,115,138,
1 146,138,115,81,40,0.,0.,0.,0.,0.,0.,0./
DATA(SMR(7,N),N=0,23)/0.,0.,0.,0.,0.,0.,0.,0.,36,72,101,120,
1 127,120,101,72,36,0.,0.,0.,0.,0.,0.,0./
DATA(SMR(8,N),N=0,23)/0.,0.,0.,0.,0.,0.,0.,0.,12,52,93,127,148,
1 155,148,127,93,52,12,0.,0.,0.,0.,0.,0./
DATA(SMR(9,N),N=0,23)/0.,0.,0.,0.,0.,0.,0.,0.,22,65,110,148,172,
1 181,172,148,110,65,22,0.,0.,0.,0.,0.,0./
DATA(SMR(10,N),N=0,23)/0.,0.,0.,0.,0.,0.,0.,0.,18,64,114,156,184
1 ,193,184,156,114,64,18,0.,0.,0.,0.,0.,0./
DATA(SMR(11,N),N=0,23)/0.,0.,0.,0.,0.,0.,0.,0.,0.,0.,81,126,
1 158,169,158,126,81,0.,0.,0.,0.,0.,0.,0./

```

DATA(SMR(12,N),N=0,23)/0.,0.,0.,0.,0.,0.,0.,0.,0.,0.,67,115,146,  
1 156,146,115,67,0.,0.,0.,0.,0.,0.,0.,0./

DATA(SMD(1,N),N=0,23)/0.,0.,0.,0.,0.,0.,0.,0.,0.,0.,16,31,42,45,  
1 42,31,16,0.,0.,0.,0.,0.,0.,0.,0./

DATA(SMD(2,N),N=0,23)/0.,0.,0.,0.,0.,0.,0.,0.,0.,0.,22,46,68,82,86,  
1 82,68,46,22,0.,0.,0.,0.,0.,0.,0.,0./

DATA(SMD(3,N),N=0,23)/0.,0.,0.,0.,0.,0.,0.,0.,0.,0.,26,55,81,102,116,  
1 121,116,102,81,55,26,0.,0.,0.,0.,0.,0./

DATA(SMD(4,N),N=0,23)/0.,0.,0.,0.,0.,2,33,66,98,124,145,160,  
1 165,160,145,124,98,66,33,2,0.,0.,0.,0./

DATA(SMD(5,N),N=0,23)/0.,0.,0.,0.,2,27,55,85,115,140,157,171,  
1 177,171,157,140,115,85,55,27,2,0.,0.,0./

DATA(SMD(6,N),N=0,23)/0.,0.,0.,0.,15,40,68,98,128,153,169,185  
1 ,190,185,169,153,128,98,68,40,15,0.,0.,0./

DATA(SMD(7,N),N=0,23)/0.,0.,0.,0.,8,30,57,85,113,136,152,167,  
1 172,167,152,136,113,85,57,30,8,0.,0.,0./

DATA(SMD(8,N),N=0,23)/0.,0.,0.,0.,0.,12,41,73,105,131,151,166  
1 ,171,166,151,131,105,73,41,12,0.,0.,0.,0./

DATA(SMD(9,N),N=0,23)/0.,0.,0.,0.,0.,0.,9,39,69,94,114,127,  
1 132,127,114,94,69,39,9,0.,0.,0.,0./

DATA(SMD(10,N),N=0,23)/0.,0.,0.,0.,0.,0.,0.,7,31,54,74,87,92,  
1 87,74,54,31,7,0.,0.,0.,0.,0.,0./

DATA(SMD(11,N),N=0,23)/0.,0.,0.,0.,0.,0.,0.,0.,0.,0.,25,43,55,59  
1 ,55,43,25,0.,0.,0.,0.,0.,0.,0.,0./

DATA(SMD(12,N),N=0,23)/0.,0.,0.,0.,0.,0.,0.,0.,0.,0.,11,,23,33,  
1 36,33,23,11,0.,0.,0.,0.,0.,0.,0.,0./

DATA(TMA(1,N),N=0,23)/2.8,2.8,2.8,2.7,2.8,2.7,2.7,2.7,2.8,2.9  
1 ,3.2,3.6,4.1,4.4,4.4,4.2,3.8,3.4,3.2,3.,2.9,2.8,2.7,2.7/

DATA(TMA(2,N),N=0,23)/2.6,2.5,2.4,2.3,2.2,2.1,2.1,2.1,2.3,2.7  
1 ,3.5,4.3,4.8,5.2,5.3,5.2,4.9,4.3,3.8,3.4,3.2,3.,2.9,2.8/

DATA(TMA(3,N),N=0,23)/3.2,3.1,3.,2.9,2.8,2.7,2.6,2.8,3.4,4.3,  
1 5.2,5.9,6.4,6.7,6.8,6.7,6.4,6.,5.2,4.4,4.,3.8,3.6,3.4/

DATA(TMA(4,N),N=0,23)/4.6,4.4,4.2,4.1,4.,3.9,4.,4.7,5.7,6.7,  
1 7.5,8.2,8.6,8.8,8.9,8.8,8.5,8.1,7.5,6.7,5.9,5.4,5.,4.8/

DATA(TMA(5,N),N=0,23)/7.,6.7,6.4,6.2,6.,6.2,7.,8.1,9.2,10,  
 1 10.8,11.2,11.6,11.8,11.7,11.7,11.4,11.,10.4,9.7,9.,8.3,10.7,  
 1 10.2/  
 DATA(TMA(6,N),N=0,23)/9.8,9.5,9.2,9.,8.9,9.4,10.2,11.2,12.1,  
 1 12.9,13.6,14.2,14.5,14.7,14.8,14.7,14.4,14,13.5,12.8,12.1,  
 1 11.4,10.7,10.2/  
 DATA(TMA(7,N),N=0,23)/11.6,11.3,11,10.7,10.5,10.9,11.8,12.8,  
 1 13.8,14.6,15.3,15.9,16.3,16.5,16.5,16.4,16.2,15.8,125.3,14.6,  
 1 13.8,13.1,12.4,12./  
 DATA(TMA(8,N),N=0,23)/11.7,11.4,11.1,10.9,10.7,10.6,10.9,12.,  
 1 13.2,14.3,15.3,15.9,16.4,16.7,16.7,16.6,16.2,15.8,15.1,14.3,  
 1 13.5,12.9,12.3,11.3/  
 DATA(TMA(9,N),N=0,23)/9.8,9.6,9.4,9.3,9.2,9.1,9.1,9.7,10.8,  
 1 11.8,12.7,13.3,13.8,14.,14.2,14.,13.7,13.2,12.4,11.5,10.9,  
 1 10.6,10.1,9.9/  
 DATA(TMA(10,N),N=0,23)/8.2,8.,7.9,7.8,7.8,7.8,7.7,7.7,8.2,9.,  
 1 10.,10.7,11.2,11.4,11.5,11.3,10.8,10.,9.3,8.9,8.7,8.5,8.3,8.2  
 1 /  
 DATA(TMA(11,N),N=0,23)/4.7,4.6,4.5,4.5,4.4,4.3,4.3,4.3,4.5,  
 1 4.8,5.6,6.3,6.9,7.2,7.2,6.8,6.1,5.6,5.3,5.1,4.9,4.7,4.7,4.6/  
 DATA(TMA(12,N),N=0,23)/4.,3.9,3.9,3.9,4.,4.,4.,4.,4.1,4.1,  
 1 4.5,4.9,5.4,5.6,5.5,5.2,4.8,4.5,4.5,4.3,4.2,4.1,4.1,4./  
 DATA(TMI(1,N),N=0,23)/10.,10.,10.,10.,10.,10.,11.,11.,11.,  
 1 18.,20.,20.,20.,20.,20.,20.,20.,20.,19.,19.,18.,18.,17.,16./  
 DATA(TMI(3,N),N=0,23)/10.,10.,10.,10.,10.,10.,11.,11.,11.,  
 1 18.,20.,20.,20.,20.,20.,20.,20.,20.,19.,19.,18.,18.,17.,16./  
 DATA(TMI(2,N),N=0,23)/10.,10.,10.,10.,10.,10.,11.,11.,11.,  
 1 18.,20.,20.,20.,20.,20.,20.,20.,20.,19.,19.,18.,18.,17.,16./  
 DATA(TMI(4,N),N=0,23)/10.,10.,10.,10.,10.,10.,11.,11.,11.,  
 1 18.,20.,20.,20.,20.,20.,20.,20.,20.,19.,19.,18.,18.,17.,16./  
 DATA(TMI(5,N),N=0,23)/10.,10.,10.,10.,10.,10.,11.,11.,11.,  
 1 18.,20.,20.,20.,20.,20.,20.,20.,20.,19.,19.,18.,18.,17.,16./  
 DATA(TMI(6,N),N=0,23)/10.,10.,10.,10.,10.,10.,11.,11.,11.,  
 1 18.,20.,20.,20.,20.,20.,20.,20.,20.,19.,19.,18.,18.,17.,16./

```
DATA(TMI(7,N),N=0,23)/10.,10.,10.,10.,10.,10.,11.,11.,11.,  
1 18.,20.,20.,20.,20.,20.,20.,20.,20.,19.,19.,18.,18.,17.,16./  
DATA(TMI(8,N),N=0,23)/10.,10.,10.,10.,10.,10.,11.,11.,11.,  
1 18.,20.,20.,20.,20.,20.,20.,20.,20.,19.,19.,18.,18.,17.,16./  
DATA(TMI(9,N),N=0,23)/10.,10.,10.,10.,10.,10.,11.,11.,11.,  
1 18.,20.,20.,20.,20.,20.,20.,20.,20.,19.,19.,18.,18.,17.,16./  
DATA(TMI(10,N),N=0,23)/10.,10.,10.,10.,10.,10.,11.,11.,11.,  
1 18.,20.,20.,20.,20.,20.,20.,20.,20.,19.,19.,18.,18.,17.,16./  
DATA(TMI(11,N),N=0,23)/10.,10.,10.,10.,10.,10.,11.,11.,11.,  
1 18.,20.,20.,20.,20.,20.,20.,20.,20.,19.,19.,18.,18.,17.,16./  
DATA(TMI(12,N),N=0,23)/10.,10.,10.,10.,10.,10.,11.,11.,11.,  
1 18.,20.,20.,20.,20.,20.,20.,20.,20.,19.,19.,18.,18.,17.,16./  
END
```



**A3.17 Simplified and easy to use, steady state solar wall program to simulate the performance of single glazed, single glazed and selectively coated, and transparently insulated solar walls at European locations from Lerwick to Coimbra and Warsaw. The program is written in Basic. It calculates energy savings and payback periods from solar walls,**

10 REM BASIC PROGRAM TO MEASURE THE HEAT OUTPUT OF WALLS AT  
VARIOUS LATITUDES

20 DIM Q(6,12,13)QA(6,13),TAS(6,12,13),U(6),TA(12,13),TRT(5,12,13),  
TQDF(6),D(12)

30 DIM TIN(12,13),TP2(6,12,13),RO(6),Q2(6,12,13),QW(6,12,13),QT(6,12,13),  
QTA(6,1,3), ST(13),EFF(6,13)

40 DIM MCW(5,13,2,2,),SCW(6),SCE(2),P(6,13,2),CE(5,13,2),SP(2),F(12,13),  
QTA(6,13)

41 INPUT "ARE PLATE TEMPERATURES AND MONTHLY HEAT OUTPUTS  
REQUIRED? N=1, Y=2 ";PT

42 CLS

43 PRINT " "

47 RESTORE 100

48 PRINT TAB(15); " SOLAR WLL OUTPUT FROM LERWICK TO FARO AND  
MANCHESTER TO WARSAW"

49 PRINT " "

50 FOR L=1 TO 13

60 FOR M=1 TO 12

70 READ H(M,L)

80 NEXT M

90 NEXT L

100 DATA .34,.38,2.03,2.71,2.5,2.79,2.49,2.43,2.01,1.46,.73,.24,

110 DATA .59,1.72,2.09,2.47,2.36,2.58,2.33,2.34,2.05,1.64,1.2,.71

120 DATA .83,1.48,2.05,2.42,2.66,2.77,2.48,2.48,2.33,1.92,1.56,1.23

130 DATA 1.36,1.99,2.7,3.01,3.02,2.86,2.78,2.9,2.36,2.3,1.6,1.3

140 2.9,3.52,3.62,2.58,2.19,3.07,3.48,3.83,3.96,4.12,3.14,3.

150 DATA 2.64,3.2,3.89,3.56,3.07,2.92,3.2,3.65,3.7,3.89,3.58,4.1

160 DATA 3.48,3.6,3.6,3.38,3.02,2.66,2.89,3.49,4.1,4.32,3.96,4.37



```

165 DATA .96,1.52,2.55,2.58,2.85,2.92,2.99,3.22,2.85,1.89,1.13,.74
167 DATA .81,1.16,2.36,2.46,2.74,2.89,2.85,3.27,2.68,1.75,.85,.59
169 DATA .83,1.56,2.33,2.72,2.87,3.01,2.81,3.12,2.6,1.9,1.08,.77
170 REM L:1-LERWICK 2-GLASGOW 3=LONDON 4=PLYMOUTH 5=SOUTH
FRANCE 6=COIMBRA 7=BERLIN 8=WARSAW 10=HAMBURG 11= BERGEN 12=
STOCKHOLM 3A=MANCHESTER
172 DATA .27,1.08,2.3,2.82,2.73,2.88,2.53,2.66,1.4,1.32,.48,.16
174 DATA .76,1.78,2.85,3.19,3.63,4.05,3.61,3.68,2.77,1.78,1.04,.82
178 DATA .9,1.47,2.21,2.6,2.81,2.8,2.55,2.64,2.39,1.96,1.18,.86
180 C=750000
190 REM C IS THERMAL CAPACITY
200 RESTORE 100
210 FOR L=1 TO 13
220 FOR M=1 TO 12
230 READ HDF(M,L)
240 NEXT M
250 NEXT L2
260 DATA .12,.38,.73,1.32,1.47,1.76,1.61,1.36,.86,.47,.2,.08
270 DATA .2,.51,.86,1.32,1.53,1.76,1.61,1.42,.98,.57,.32,.18
280 DATA .3,.6,1.,1.4,1.8,1.89,1.73,1.55,1.15,.7,.43,.24
290 DATA .36,.68,1.14,1.57,1.92,1.95,1.91,1.73,1.32,.87,.51,.32
300 DATA .77,1.08,1.39,1.7,1.93,1.92,1.94,1.83,1.52,1.2,.89,.66
310 DATA .69,1.06,1.41,1.74,2.01,2.05,2.04,1.93,1.62,1.22,.91,.7
320 DATA .85,1.18,1.48,1.7,1.92,1.86,1.86,1.79,1.68,1.38,1.06,.82
325 DATA .32,.53,1.09,1.45,1.82,1.95,2.01,1.87,1.3,.82,.39,.25
327 DATA .31M,52,1.,1.38,1.78,1.91,1.85,1.76,1.22,.67,.33,.22
329 DATA .29,.54,1.,1.46,1.8,1.97,1.91,1.85,1.76,1.22,.67,.33,.22
332 DATA .11,.41,.77,1.37,1.63,1.8,1.57,1.47,.8,.47,.19,.07
334 DATA .17,.44,.96,1.47,1.94,2.09,2.07,1.77,1.22,.63,.27,.14
336 DATA .28,.56,1.01,1.5,1.88,1.94,1.81,1.64,1.19,.75,.4,.23
338 RESTORE
360 READ TAS(1,M,L)
370 NEXT M
380 NEXT L

```

```
390 DATA .975,.96,.95,.91,.84,.77,.77,.88,.92,.96,.96,.97
400 DATA .975,.96,.94,.85,.79,.78,.78,.85,.91,.95,.96,.97
410 DATA .965,.96,.92,.84,.7,.62,.65,.77,.905,.95,.96,.97
420 DATA .96,.93,.9,.84,.7,.62,.65,.77,.9,.95,.96,.97
430 DATA .96,.95,.9,.77,.55,.4,.5,.7,.85,.92,.95,.96
440 DATA .96,.94,.85,.67,.45,.3,.4,.62,.84,.91,.95,.95
450 DATA .96,.93,.88,.65,.4,.28,.35,.62,.83,.91,.95,.95
455 DATA .96,.94,.91,.84,.7,.62,.65,.77,.9,.96,.96,.97
457 DATA .96,.94,.91,.84,.75,.7,.71,.8,.9,.96,.96,.97
459 DATA .97,.96,.93,.84,.75,.7,.71,.8,.9,.93,.96,.97
461 DATA .975,.96,.95,.91,.84,.77,.77,.88,.92,.96,.96,.97
463 DATA .975,.96,.95,.91,.84,.77,.77,.88,.92,.96,.96,.97
465 DATA .97,.96,.93,.845,.75,.7,.71,.81,.91,.95,.96,.97
468 RESTORE 520
470 FOR L=1 TO 13
2480 FOR M=1 TO 12
490 READ TA(M,L)
500 NEXT M
510 NEXT L
520 DATA 3,3,4,6,8,10,11,12,7,6,3
530 DATA 3.5,3.5,5,7.5,10,13,14.5,14.5,12.5,9.5,6.5,4.5
540 DATA 4,.4.5,6.5,8.5,12.5,16,18,17,15,11,7.5,5.5
550 DATA 5.9,5.5,7,9.2,12.5,14.5,15.9,24.5,12,8.5,7,7
560 DATA 3.5,5,8.5,13.5,17.5,21,23,22.5,20,15,9.5,5.5
570 DATA 2,5.5,6.5,10,12.5,15.5,21,23.5,19.5,19.5,9.5,5.5
580 DATA 12,13,14.5,16.5,18,21.5,24,24,22.5,19,16,13
585 DATA 5.9,5.5,7.1,9.2,12.5,14.5,15.9,14.5,12.1,8.7,7.1,7
590 RESTORE 630
600 FOR N=1 TO 4
610 READ U(N)
620 NEXT N
630 DATA .006,.0025,.00063,.00036
640 RESTORE 680
650 FOR N=1 TO 4
```

```
660 READ RO(N)
670 NEXT N
680 DATA .17,.4,1.62,2.8
690 RI=.3
700 REM RO/U=RESISTANCE AND U VALUE OUTSIDE WALL
710 REM RI=RESISTEANCE THROUGH .2M BRICK WALL TO THE INTERIOR
720 RESTORE 780
730 FOR L=1 TO 8
740 FOR M=1 TO 12
750 READ TRT(3,M,L)
760 NEXT M
770 NEXT L
2780 DATA 64,62,60,55,57,42,42,52,58,62,63,64
790 DATA 64,62,59,50,40,40,40,50,55,61,63,64
800 DATA 84,61,59,48,40,38,38,42,55,60,64,64
810 DATA 64,61,59,48,40,38,38,32,55,60,64,64
820 DATA 63,60,54,40,25,26,26,40,50,61,64
830 DATA 61,59,52,35,25,20,20,35,47,55,61,64
840 DATA 61,59,50,35,25,20,20,35,47,55,61,64
845 DATA 64,61,59,48,40,38,38,42,55,60,64,64
850 FOR L=1 TO 8
860 FOR M=1 TO 12
870 TAS(1,M,L)=TAS(1,M,L)*.85
880 REM TA PRODUCT AT NORMAL INCIDENCE IS .85 FOR SINGLE COVERS.
890 TAS(3,M,L)=TRT(3,M,L)*.9/100
900 TAS(4,M,L)=TAS(3,M,L)-.04
910 TAS(2,M,L)=TAS(1,M,L)*.97/.9
920 NEXT M
930 NEXT L
940 D(1)=31
950 D(2)=28
960 D(3)=31
970 D(4)=30
980 D(5)=31
```

```
990 D(6)=30
1000 D(7)=31
1010 D(8)=30
1020 D(9)=30
1030 D(10)=81
1040 D(11)=30
1050 D(12)=31
1060 RESTORE 1100
1070 FOR N=1 TO 4
1080 READ TADF(N)
1090 NEXT N
1100 DATA .85,.85,.55,.50
1110 FOR N=1 TO 4
1120 TADF(N)=TADF(N)*.85
1130 NEXT N
1140 GOSUB 1450
1150 FOR N=1 TO 4
1160 FOR L=1 TO 8
1170 FOR M=1 TO 12
1180 Q(N,M,L)=(H(M,L)-HDF(M,L))*TAS(N,M,L)+HDF(M,L)*TADF(N)-
U(N)*24*(TP2(N,M,L)-TA(M,L))
1182 Q2(N,M,L)=(TP2(N,M,L)-TIN(M,L))*24/RI*1000)
1184 Q2(N,M,L)=Q2(N,M,L)*D(M)
1186 Q2(N,M,L)=INT(Q2(N,M,L))
1190 REM Q IS :DAILY MEAN *DAYS = MONTHLY MEAN
1200 Q(N,M,L)=Q(N,M,L)*D(M)
!"!) q(N,M,L)=INT(Q(N,M,L))
1220 NEXT M
1230 NEXTL
1240 NEXT N
1245 ,IF PT=1 GOTO 1420
1250 PRINT " "
1260 PRINT " "
```



```

1270 PRINT TAB(13);"TABLE 2:HEAT OUTPUT FROM SOLAR WALLSIN
KWH/M2"
1280 FOR N=1 TP 4
1290 PRINT "N=";N
1300 FOR L=1 TO 8
1310 PRINT TAB(6);
1320 FOR M=1 TO 11
1330 PRINT M;TAB(6*M+6);
1340 NEXT M
1350 PRINT 12
1352 PRINT"L=";L;TAB(6);
1360 FOR M=1 TO 11
1360 PRINT Q(M,N,L);TAB(6*M+6);
1380 NEXT M
1490 PRINT Q(N,12,L)
1400 NEXT L
1410 NEXT N
1420GOSUB 1940
1440 END
1450 REM PLATE TEMPERATURES ESTIMATED
1460 RESTORE 1520
1470 FRO L=1 TO 8
1480 FOR M=1 TO 12
1490 READTIN(M,L
1500 NEXT M
1510 NEXT L
1520 DATA 14,14,14,14,14,14,16,16,14,14,14,14
1530 DATA 14,14,14,14,14,16,20,20,14,14,14,14
1540 DATA 14,14,14,14,14,20,20,20,14,14,14,14
1550 DATA 14,14,14,14,15,20,20,20,20,15,15,15
1560 DATA 14,14,14,15,20,20,20,20,20,20,14,14
1570 DATA 14,14,14,15,15,20,20,20,20,20,14,14
1580 DATA 15,16,18,20,20,20,20,20,20,20,15
1585 DATA 14,14,14,14,14,20,20,20,14,14,14,14

```



```

1590 FOR N=1 TO 4
1600 FRO L= 1 TO 8
1610 FOR M=1 TO 1
1620 TP1(N,M,L)=(TIN(M,L)*RO(N)+TA(M,L)*RI)/(RO(N)+RI
1625 REM GOTO 163
1630 TP2(N,M,L)=(1000*H(M,L)*TAS(N,M,L) +24*TA(M,L)/RO(N)
+C*TP1(N,M,L)/(3600))/(24/RO(N) +24/RI+C/(36060))
1640 TP2(N,M,L)=CINT(TP2(N,M,L))
1660 NEXT M
1665 NEXT L
1670 NEXTN
1680 PRINT " "
1690 PRINT TAB(3);"TABLE 1:BRICK PLATE AND OUTSIDE AIR
TEMPERATURES :7 LOCATIONS IN EUROPE."
1700 GOT 1710
1702 FOR M=1 TO 1
1703 FOR L=1 TO 8
1704 TA(M,L)=CINT(TA(M,L)*10/10)
1705 NEXT L
1706 NEXT M
1710 FOR N=1 TO 4
1720 PRINT "N= ";N
1750 PRINT "AREA";TAB(10);
1760 FOR M= 1 TO 1
1770 PRINT M;TAB(6*M+10)
1780 NEXT M
1790 PRINT 12
1800 FOR L=1 TO
18105 PRINT "L=";L;TAB(6);
1810 PRINT "TA";TAB(10);
1820 FOR M= 1 TO 11
1830PRINT TA(M,L);TAB(6*M+10);
1840 NEXT M
1850 PRINT TA(12,L)

```

```
1855 PRINT TAB(6);
1860 PRITN "TP";TAB(10);
1870 FOR M=1 TO 11
1880 PRINT TP2(N,M,L);TAB(6*M+10);
1890 NEXT M
1900 PRINT TP2(N,12,L)
1910 NEXT L
1920 NEXT N
1930 RETURN
1935 STOP
1940 REM: CALCULATION OF WALL COSTS, ENERGY COST AND PAYBACK.
1950 FOR M=1 TO 12
1960 FPR L=1 TO 8
1970 F(M,L)=1
1980 NEXT L
1990 NEXT M
1994 F(9,3)=0
1995 F(9,8)=0
1997 F(9,4)=0
2000 FOR M=6 TO 8
2010 FOR L=3 TO 8
2020 F(M,L)=0
2030 NEXT L
2040 NEXT M
2050 FRO M=9 TO 10
2060 FOR L=5 TO 7
2070 F(M,L)=0
2080 NEXT L
2090 NEXT M
2095 INPUT"LERWICK HEATING SEASON:9M=1;10M=2;11M=3";LS
2096 IF LS= 1 THEN GO TO 2100
2097 IF LS=2 THEN GOTO 2105
2098 IF LS=3 THEN GOTO 2106
```

2099 REM: LEGTH OF HEATING SEASON CAN BE DETERMINED USING THE HEATING SEASON LENGTH PROGRAM BASED ON GUSTAFFSONS METHOD GIVEN LATER. THE LENGTHS FOR VARIOUS LOCATIONS CAN THEN BE INSERTED INTO THE APPROPRIATE PART OF THIS PROGRAM.

2100 F(9,1)=0

2105 F(7,1)=0

2106 F(8,1)=0

2107 INPUT " LENGTH OF GLASGOW HEATING SEASON 9M=1 10 M=2 ";GS

2108 IF GS=1 THEN GOTO 2110

2109 IF GS=2 THEN GOTO 2120

2110 F(9,2)=0

2120 F(8,2)=0

2126 F(7,2)=0

2130 F(5,5)=0

2132 F(9,5)=0

2134 F(10,5)=0

2170 F(11,7)=0

2171 F(5,6)=0

2174 F(9,6)=0

2175 F(10,6)=0

2178 F(5,7)=0

2180 F(9,7)=0

2182 F(10,7)=0

2183 F(11,7)=0

2185 FOR N=1 TO 4

2190 FOR L=1 TO 8

2200 FOR M=1 TO 12

2210 REM QA IS THE ANNUAL ENERGY OUTPUT FROM A SOLAR WALL AT ALL LOCATIONS.

2220 QA(N,L)=QA(N,L)+Q(N,M,L)\*F(M,L)

2225 Q2A(N,L)=Q2A(N,L)+Q2(N,M,L)\*F(M,L)

2230 NEXT M

2240 NEXT L

2250 NEXT N

2260 REM MCW IS THE MAXIMUM COST OF A SOLAR WALL.  
 2262 REM CE IS THE COST OF ENERGY PRODUCED FROM THE WALL.  
 2264 REM P IS THE PAYBACK TIME.  
 2270 REM SP =WALL COST TO ACHIEVE A 5 OR 10 YEAR PAYBACK.  
 2275 REM SCE = COST IF UK ENERGY. SCW = SOLAR WALL COST.  
 2280 SP(10)=10  
 2290 SP(2)=5  
 2300 REM SCE(1)=ELECTRICITY COST SCE(2)=GAS COST.  
 2310 SCE(1)=.078  
 2320 SCE(2)=.025  
 2330 SCW(1)=.75  
 2340 SCW(2)=100  
 2350 SCW(3)=150  
 2360 SCW(4)=200  
 2370 REM FOR SCW: 1=TROMBE 2=SELECTIVE+SINGLE GLAZING  
 2375 REM 3=50 MM TIM+DOUBLE GLAZING 4=100MM TIM +DG.  
 2380FOR N=1 TO 4  
 2390 FOR L=1 TO 8  
 2400 FOR J=1 TO 2  
 2410 FOR K=1 TO 2  
 2420 NCW(N,L,J,K)=SCE(K)\*SP(J)\*QA(N,L)  
 2430 CE(N,L,J)=( SCW(N) / (QA(N,L)\*SP(J) ) )  
 2440 P(N,L,K)=SCW(N) / (QA(N,L)\*SCE(K))  
 2445 IF P(N,L,2)<0 THEN P(N,L,2)=200  
 2446 IF P(N,L,10)<0 THEN P(N,L,1)=100  
 2450 MCW(N,L,J,K)=CINT(MCW(N,L,J,K))  
 2460 CE(N,L,J)=CE(N,L,J)\*/01  
 2463 CE(N,L,J)=CINT(CE(N,L,J)\*100) / 100  
 2470 P(N.L.K)=CINT(P(N,L,K))  
 2480 NEXT K  
 2490 NEXT J  
 2500 NEXT L  
 2510 NEXT N  
 2520 FG=1

```
2540 PRINT TAB(26);" SOLAR WALL TYPE."  
2550 FOR N= 1 TO 4  
2570 PRINT N;TAB(6*N+22);  
2580 NEXT N  
2620 FOR L= 1 TO 8  
2630 PRINT TAB(16);L;TAB(22);  
2640 FOR N= 1 TO 3  
2650 PRINT QA(N,L0;TAB(6*N+22);  
2660 NEXT N  
2670 PRINT QA(4,L)  
2680 NEXT L  
2690 PRINT " "  
2700 PRINT TAB(4);" TABLE 1 :ENERGY SAVINGS FROM SOLAR WALLS IN  
THE HEATING SEASON (KWH/M2)"  
2710 PRINT " "  
2720 INPUT CH  
2730 PRINT TAB(22);  
2760 FOR N=1 TO 4  
2770 PRINT N;TAB(6*N+22);  
2780NEXT N  
2790 FOR L= 1 TO 8  
2830 PRINT TAB(16);L;TAB(22);  
2840 FOR N= 1 TO 3  
2850 PRINT Q2A(N,L);TAB(6*N+22);  
2860 NEXT N  
2870 PRINT Q2A(4,L)  
2880 NEXT L  
2890 PRINT " "  
2900 PRINT TAB(4);" TABLE 2: ENERGY FROM SOLAR WALLS (KWH/M2)  
FROM CONDUCTED HEAT ONLY."  
3540 PRINT TAB(28);" SOLAR WALL TYPE"  
3550 PRINT TAB(16);"AREA";TAB(22);  
3560 FOR N= 1 TO 4  
3570 PRINT N;TAB(8*N+20);
```



```
3580 NEXT N
3590 IF FG=2 GOTO 3740
3600 IF FDG=3 GOTO 3860
3610 IF FG=4 GOTO 3860
3620 FOR L= 1 TO 8
3630 PRINT TAB(16);L;TAB(22);
3640 FOR N= 1 TO 3
3650 PRINT CE(N,L,1);TAB(8*N+22);
3660 NEXT N
3670 PRINT CE(4,L,1)
3680 NEXT L
3690 PRINT " "
3700 PRINT TAB(4);" TABLE 3:COST OF ENERGY IN £/KWH FROM SOLAR
WALLS WITH A 10 YEAR PAYBACK"
3710 PRINT " "
3720 FG=2
3730 GOTO 3540
3740 FOR L= 1 TO 8
3750 PRINT TAB(16);L;TAB(22);
3760 FOR N= 1 TO 3
3770 PRINT MCW(N,L,1,1);TAB(6*N+22);
3780 NEXT N
3790 PRINT MCW(4,L,1,1)
3800 NEXT L
3810 PRINT " "
3820 PRINT " TABLE 4:COST (£) OF SOLAR WALLS :WITH 10 YEAR PAYBACK
AND uk ELECTRICITY COSTS."
3830 PRINT " "
3840 FG=3
3850 GOT 3540
3860 FOR L= 1 TO 8
3870 PRINT TAB(16);L;TAB(23);
3880 FOR N= 1 TO 3
3890 IF FG=3 GOTO 3920
```

```
3900 PRINT P(N,L,1);TAB(6*N+23);
3910 GOTO 3940
3920 PRINT P(N,L,2);TAB(6*N+23)
3930 GOTO 3940
3940 NEXT N
3950 IF FG=3 GOTO 3980
3960 PRINT P(4,L,1)
3970 GOTO 3990
3980 PRINT P(4,L,2)
3990 NEXT L
4000 PRINT " "
4010 IF FG=4 GOTO 4060
4020 PRINT TAB(2);" TABLE 5: PAYBACK PERIODS (YEARS): FOR UK GAS
COST AND UK WALL COSTS."
4030 PRINT " "
4040 FG=4
4050 GOTO 3540
4060 PRINT TAB(2);" TABLE 6: PAYBACK PERIODS (YEARS): FOR UK
ELECTRICITY COST AND UK WALL COSTS."
4070 PRINT " "
4080 RETURN
4090 END
```

### A3.18 Basic program to evaluate the length of the heating season at various locations in Europe

1 CLS

2 PRINT TAB(20);" A PROGRAM FOR THE RAPID DETERMINATION OF THE LENGTH OF A HEATING SEASON IN EUROPE."

3 REM LOCATIONS CHOSEN ARE:

4 REM PLYMOUTH(PL), LONDON(LN), MANCHESTER(MN),

5 REM GLASGOW(GL), LERWICK(LK),

6 REM CARPENTRAS(CARP), COIMBRA(CMB), FARO(FR), BERLIN(BR),

7 REM WARSAW(WS), BERGEN(BER),

8 REM STOCKHOLM(STCK), HAMBURG(HAM).

9 PRINT " "

10 DATA 6,5.5,7.5,9.1,11.5,14.5,16,16.1,15,12,9,7

20 DATA 4,4.5,6.5,9.5,12.5,16,18,17,15,11,7.5,6

30 DATA 3.3,3.7,5.7,8.3,11.3,14.3,15.7,15.5,13.7,10.5,6.5,4.3

40 DATA 3.1,3.5,5.5,7.9,10.7,13.6,14.7,14.5,12.7,9.9,6,4.2

50 DATA 3,2.8,3.8,5.4,7.6,10.1,11.7,11.9,10.6,8.5,5.6,4

60 DATA 6,7,10,13,16.5,20.5,23,22.5,20,15,10.5,7.1

70 DATA 9,9.5,12,13.5,15.5,18,20.1,20,19, 16,13,9.6

80 DATA 12,13,14.5,16.5,18,21.5,24.1,24,22.5,19,16,13.1

90 DATA -.5,0,4,8,5,13.5,17,19,18,15,9.5,4.5,1

100 DATA -3,-2.9,2,7.5,14.8,16,19.5,18.5,14.3,9,3.5,-.5

110 DATA 1,1.1,3,6,10.5,13,15.6,15.5,12.5,8.5,5.5,3.1

114 DATA -3.1,-3,-.5,4.5,10,15,18,16.6,12,7,3,0

116 DATA 0,.5,3,8,12.5,16,17.5,17,14.5,9.5,5,2

120 DIM TPL(12),TLN(12),TMN(12),TGL(12),TLK(12),TCR(12),TCM(12),  
TFR(12),TBR(12)

130 DIM TWS(12),TA(14),TX(14),DM(14),ZD(14),D(12),N(12),MN(12),DC(12)

140 DIM G(12,14),GD(12,13),GS(12),TBER(12),TST(12),TH(12), GX(12),  
GC(12),GDC(12)

145 DIM TAG(5),TAD(5)

150 FOR N=1 TO 12

160 READ TPL(N)

165 NEXT N

```
167 FOR N=1 TO 12
170 READ TLN(N)
175 NRXT N
177 FOR N= 1 TO 12
180 READ TMN(N)
185 NEXT N
187 FOR N= 1 TO 12
190 READ TGL(N)
195 NEXT N
197 FOR N= 1 TO 12
200 READ TLK(N)
205 NEXT N
207 FOR N= 1 TO 12
210 READ TCR(N)
215 NEXT N
217 FOR N= 1 TO 12
220 READ TCM(N)
225 NEXT N
227 FOR N= 1 TO 12
230 READ TFR(N)
235 NEDXT N
237 FOR N= 1 TO 12
240 READ TBR(N)
245 NEXT N
247 FOR N= 1 TO 12
250 READTWS(N)
260 NEXT N
265 FOR N= 1 TO 12
167 READ TBER(N)
268 NEXT N
270 FOR N= 1 TO 12
272 READTST(N)
274 NEXT N
276 FOR N= 1 TO 12
```

```
278 READ TH(N)
280 NEXT N
282 RESTORE 3000
284 FOR L= 1 TO 13
285 FOR M= 1 TO 12
286 READ G(M,L)
287 NEXT M
288 NEXT L
289 PRINT " "
290 PRINT ;"INPUT LOCATION NUMBER: PL=1 LN=2 MN=3 GL=4 LK=5
CARP=6 CMB=7 FR=8 BR=9 WS=10 BER=11 STCK=12 HAM=13"
291 RESTORE
292 FOR L= 1 TO 13
294 FOR M= 1 TO 12
296 READ GD(M,L)
297 NEXT M
298 NEXT L
299 PRINT " "
300 INPUT ;" LOCATION NUMBER";X
302 PRINT " "
303 INPUT ;" THE BASE TEMPERATURE TO BE USED FOR THE
BUILDING.";BDT
304 PRINT " "
306 IF X=1 THEN PRINT TAB(34); "PLYMOUTH."
308 IF X=2 THEN PRINT TAB(34);" LONDON."
310 IF X=3 THEN PRINT TAB(34);" MANCHESTER."
312 IF X=4 THEN PRINT TAB(34); " GLASGOW."
314 IF X=5 THEN PRINT TAB(34); " LERWICK."
316 IF X=6 THEN PRINT TAB(34); " CARPENTRAS."
318 IF X=7 THEN PRINT TAB(34); " COIMBRA."
320 IF X=8 THEN PRINT TAB(34); " FARO."
322 IF X= 9 THEN PRINT TAB(34); "BERLIN."
324 IF X=10 THEN PRINT TAB(34); " WARSAW."
325 IF X=11 THEN PRINT TAB(34); " BERGEN."
```



```
326 IF X= 12 THEN PRINT TAB(34);" STOCKHOLM."  
327 IF X=13 THEN PRINT TAB(34); " HAMBURG."  
328 FOR N= 1 TO 12  
329 IF X= 1 THEN TA(N)=TPL(N)  
330 IF X=2 THEN TA(N)=TLN(N)  
340 IF X=3 THEN TA(N)=TMN(N)  
350 IF X=4 THEN TA(N)=TGJ(N)  
360 IF X=5 THEN TA(N)=TLK(N)  
370 IF X=6 THEN TA(N)=TCR(N)  
380 IF X=7 THEN TA(N)=TCM(N)  
390 IF X=8 THEN TA(N)=TFR(N)  
400 IF X=9 THEN TA(N)=TBR(N)  
410 IF X=10 THEN TA(N)=TWS(N)  
412 IF X=11 THEN TA(N)=TBER(N)  
414 IF X=12 THEN TA(N)=TST(N)  
416 IF X=13 THEN TA(N)=TH(N)  
420 NEXT N  
422 PRINT " "  
425 FOR N= 1 TO 12  
427 D(N)=N  
430 NEXT N  
434 M(1)=31  
436 M(2)=28  
438 M(3)=31  
440 M(4)=30  
442 M(5)=31  
444 M(6)=30  
446 M(7)=31  
448 M(8)=31  
450 M(9)=30  
452 M(10)=31  
454 M(11)=30  
456 M(12)=31  
460 FOR Y=1 TO 12
```

```
465 TX(Y)=80
470 FOR N= 1 TO 12
490 IF TA(N)<TX(Y) THEN GOTO 495 ELSE GOTO 500
495 TX(Y)=TA(N)
496 DM(Y)=M(N)
498 GX(Y)=G(N,X)
500 NEXT N
510 FOR N= 1 TO 1
520 IF TA(N)=TX(Y) THEN TA(N)=100
530 NEXT N
540 NEXT Y
550 REM PRODUCTION OF REGRESSION EQUATION: T=A*ZD +B
560 REM WHERE ZD IS THE SUM OF THE DAYS OF THE MONTH IN
565 REM ORDER OF RISING TEMPERATURE. (AFTER GUSTAFFSON)
567 REM A AND B ARE CONSTANTS.
570 ZD=0
580 ZT=0
590 ZDZ=0
600 ZDT=0
602 ZG=0
604 ZGT=0
606 ZGG=0
608 GDC(0)=0
610 DC(1)=DM(1)
612 DC(2)=DC(1)+DM(2)
613 DC(3)=DC(2)+DM(3)
614 DC(4)=DC(3)+DM(4)
615 DC(5)=DC(4)+DM(5)
616 DC(6)=DC(5)+DM(6)
617 DC(7)=DC(6)+DM(7)
618 DC(8)=DC(7)+DM(8)
619 DC(9)=DC(8)+DM(9)
620 DC(10)=DC(9)+DM(10)
621 DC(11)=DC(10)+DM(11)
```

```

622 DC(12)=DC(11)+DM(12)
623 GC(0)=0
624 FOR N= 1 TO 12
625 GC(N)=GC(N-1)+GX(N)+DM(N)
626 GDC(N)=GDC(N-1)+GD(N,X)*DM(N)
629 NEXT N
630 PRINT TAB(10);"TEMP.";TAB(20);"DAYS.";TAB(30);"CUM. DAYS.";
TAB(40);" SOLAR.";TAB(50);"CUM. GLOBAL.";TAB(65);"CUM.DIFFUSE."
631 REM CUM=CUMULATIVE. SOLAR, GLOBAL, DIFFUSE REFER TO THE
632 REM MONTHLY MEAN AND CUMULATIVE VALUES OF RADIATION.
633 FOR Y= 1 TO 12
634 PRINT TAB(10);TX(Y); TAB(20);DM(Y); TAB(30),DC(Y); TAB(40);GX(Y);
TAB(50);GC(Y); TAB(65);GDC(Y)
636 NEXT Y
637 ZG=0
638 INPUT CH$
639 CLS
640 FOR N= 1 TO 12
642 ZG=ZG+GC(N)
645 ZDG=ZDG+DC(N)*GC(N)
650 ZD=DC(N)+ZD
660 ZT=DC(N)+ZD
670 ZDT=DC(N)*TX(N)+ZDT
680 ZDZ=DC(N)*DC(N)+ZDZ
684 ZDDF=ZDDF+GDC(N)*GDC(N)
690 ZDF=ZDF+GDC(N)
692 NEXT N
694 PRINT " 2
700 AT=(12*ZDT-ZD*ZT) / (12*ZDZ-ZD*ZD)
710 BT=(ZT*ZDZ-ZD*ZT) / (12*ZDZ-ZD*ZD)
720 D=(BDT-BT) / AT
723 DY=INT(D)
725 DM=INT(D*10 / 30.5) / 10
726 PRINT " "

```

```

730 PRINT ;"HEAT SEASON LENGTH:";DY;"DAYS:";DM;"MONTHS"
740 DD=D*(BDT-BT) /2
800 AG=(12*ZDG-ZG*ZD) / (12*ZDZ-ZD*ZD)
820 BG=(ZG*ZDZ-ZD*ZDG) / (12*ZDZ-ZD*ZD)
840 ADF=(12*ZDDF-ZD*ZDF) / (12*ZDZ-ZD*ZD)
860 BDF=(ZDF*ZDZ-ZDZDDF( / (12*ZDZ-ZD*ZD)
920 PRINT ; "REGRESSION EQUATION FOR TEMPERATURE VERSUS
CUMULATIVE DAYS"
950 PRINT ;L"TX=";AT;"DAYS+";BT
960 PRINT "EQUATION: CUMULATIVE GLOBAL RADIATION VERSUS
CUMULATIVE DAYS."
970 PRINT "GD=";AG;"DAYS+";BDF
1000 U(1)=.0065
1010 U(2)=.0025
1020 U(3)=.00063
1030 U(4)=.00036
1040 U(5)=.00172
1050 UW=3.1
1060 TA(1)=.76
1070 TA(2)=.8
1080 TA(3)=.54
1090 TA(4)=.5
1100 TA(5)=.55
3000 DATA 1.36,1.99,2.7,3.01,3.02,2.86,2.78,2.9,2.36,2.3,1.6,1.3
3010 DATA .83,1.48,2.02,2.42,2.66,2.77,2.48,2.49,2.33,1.92,1.56,1.23
3020 DATA .9,1.47,2.21,2.6,2.81,2.55,2.64,2.39,1.96,1.56,1.23
3030 DATA .59,1.72,2.09,2.47,2.36,2.58,2.33,2.34,2.05,1.64,1.2,.71
3040 DATA .34,1.38,.2.03,2.71,2.5,2.79,2.49,2.43,2.1/46./73./24
3050 DATA 2.9,3.52,3.62,3.58,3.19,3.07,3.48,3.83,3.96,4.12,3.14,3
3060 DATA 2.64,3.2,3.89,3.56,3.07,2.92,3.2,3.65,3.7,3.89,3.58,4.1
3070 DATA 3.48,3.6,3.61,3.38,3.02,2.66,2.89,3.49,4.1,4.32,3.96,4.37
3080 DATA .96,1.52,2.55,2.58,2.85,2.92,2.99,3.22,2.85,1.89,1.13,.74
3090 DATA .81,1.16,2.36,2.46,2.74,2.89,2.85,3.27,2.68,1.75,.85,.59
3100 DATA .27,1.08,2.03,2.82,2.73,2.88,2.53,2.66,1.84,1.32,.48,.16

```



```
3110 DATA .76,1.78,2.85,3.19,3.63,4.05,3.61,2.68,2.77,1.78,1.04,.82
3120 DATA .83,1.56,2.33,2.72,2.87,3.01,2.81,3.12,2.6,1.9,1.08,.77
3160 HG=AG*D+BG
3170 HDF=ADF*D+BDF
3270 FOR N= 1 TO 5
3280 Q(N)=((HG-HDF)*TAG(N)+HDF*(TAD(N)-24*D*U(N))*(BDT-BT) / 2)*UW /
(UW+U(N))
3285 PRINT "Q(N)";N;SPC(2);Q(N)
3290 NEXT N
4000 DATA .36,.68,1.14,1.57,1.92,1.91,1.73,1.32,.87,.51,.32
4010 DATA .3,.6,1,1.4,1.8,1.89,1.73,1.55,1.15,.7,.43,.24
4020 DATA .28,.56,1.01,1.5,1.88,1.94,1.81,1.64,1.19,.75,.4,.2
4030 DATA .2,.51,.86,1.32,1.53,1.76,1.61,1.42,.98,.57,.32,.18
4040 DATA .12,.38,.73,1.32,1.47,1.76,1.61,1.36,.86,.47,.2,.08
4050 DATA .77,1.08,1.39,1.7,1.93,1.94,1.83,1.52,1.2,.89,.66
4060 DATA .69,1.06,1.41,1.74,2.01,2.0,2.04,1.93,1.62,1.22,.91,.7
4070 DATA .89,1.18,1.46,1.7,1.92,1.86,1.86,1.79,1.68,1.38,1.06,.82
4080 DATA .32,.53,1.09,1.45,1.82,1.95,2.01,1.87,1.3,.82,.39,.25
4090 DATA .31,.52,1.,1.38,1.78,1.91,1.85,1.76,1.22,.67,.33,.22
4100 DATA .11,.41,.77,1.37,1.63,1.8,1.57,1.47,.8,.47,.19,.07
4110 DATA .17,.44,.96,1.47,1.94,2.09,2.07,1.77,1.22,.63,.27,.14
4120 DATA .29,.54,1.,1.46,1.8,1.97,1.91,1.77,1.22,.69,.33,.22
4130 END
```



**A3.19 Program to determine the angles of incidence of solar radiation on a vertical south facing solar wall throughout the year, the algorithms used are based on those presented in Page J. and Lebens R.(1986), Climate in the United Kingdom , HMSO. The angles so determined are used as input for the solar wall programs described previously.**

```

INTEGER L
REAL LO,JD(12),HA(0:23),ET(12),ANGL(12,0:23),D(12),LON
REAL J(12),DEG(12),LA,LAT,EA,AZI
C J(N) GIVES THE MID MONTH DAY NUMBER
DATA(J(N),N=1,12)/17.,46.,75.,105.,135.,162.,198.,228.,259.
1 ,289.,319.,345./
C RAD CONVERTS DEGREES TO RADIANS
RAD=3.1415927/180.0
DO 10 M=1,12
JD(M)=360.0*J(M)*RAD / 365.25
C ET EVALUATES THE EQUATION OF TIME (USED TO COMPUTE
C SOLAR TIME)
ET(M)=-.128*SIN(JD(M)-2.8*RAD)-.165*SIN(2*JD(M)+19.7*RAD)
PRINT*,'M ',M,'ET ',ET(M)
C D(M) EVALUATES THE SOLAR DECLINATION(NEEDED FOR THE
C ALTITUDE CALCULATION
D(M)=ASIN(.3978*SIN(JD(M)-80.2*RAD+1.92*RAD*SIN(JD(M)-2.8
1 *RAD)))
C DEG(M) CONVERTS BACK FROM RADIANS TO DEGREES.
DEG(M)=D(M) / RAD
10 CONTINUE
C THE LOCATIONS FOR WHICH ALTITUDES ARE COMPUTED ARE :
C P=PLYMOUTH L=LONDON M=MANCHESTER G=GLASGOW
C LK=LERWICK CR=CARPENTRAS CM=COIMBRA F=FARO
C H=HAMBURG B=BERLIN W=WARSAW
PRINT*,'INPUT P=1 L=2 M=3 G=4 LK=5 CR=6 CM=7 F=8 H=9 B=10 W=11
B=12 S=13'
PRINT*,' '

```

READ\*,L

C THE FOLLOWING ENTRIES GIVE THE LATITUDE (LA) AND  
C LONGITUDE (LO) FOR THE ABOVE LOCATIONS.

IF(L.EQ.1)LA=50.36

IF(L.EQ.2)LA=51.46

IF(L.EQ.3)LA=53.35

IF(L.EQ.4)LA=55.85

IF(L.EQ.8)LA=37

IF(L.EQ.9)LA=53.6

IF(L.EQ.7)LA=40

IF(L.EQ.11)LA=52.2

IF(L.EQ.5)LA=60.01

IF(L.EQ.6)LA=43

IF(L.EQ.10)LA=52.45

IF(L.EQ.11)LA=52.2

IF(L.EQ.12)LA=60.4

IF(L.EQ.13)LA=59.35

IF(L.EQ.1)LO=-4.0

IF(L.EQ.2)LO=-.31

IF(L.EQ.3)LO=-2.26

IF(L.EQ.4)LO=-4.4

IF(L.EQ.5)LO=-1.2

IF(L.EQ.6)LO=5

IF(L.EQ.7)LO=-8.6

IF(L.EQ.8)LO=-7.9

IF(L.EQ.10)LO=9

IF(L.EQ.11)LO=21

IF(L.EQ.12)LO=5

IF(L.EQ.13)LO=18

DO 25 M=1,12

C LAT GIVES THE RADIAN VALUE OF LATITUDE.

LAT=LA\*RAD

C BA AND CA ARE NEEDED IN THE CALCULATION OF SOLAR

C ALTITUDE

```

BA=SIN(LAT)*SIN(D(M))
CA=COS(LAT)*COS(D(M))
PRINT*,'MONTH NUMBER', M
DO 20 H=0,23
LT=REAL(H)
C ST CALCULATES SOLAR TIME FROM LOCAL TIME (LT)
ST=LT+L4 / 15.0+ET(M)
C HA EVALUATES THE SOLAR HOUR ANGLE IN DEGREES
HA(H)=15.0*(ST-12.0)
DA=HA(H)*RAD
C GA EVALUATES THE SINE OF THE SOLAR ALTITUDE
GA=BA+CA*COS(DA)
C AL IS THE SOLAR ALTITUDE
AL=ASIN(GA)
EA=AL / RAD
AL=EA*RAD
C THE FORMULA USED TO DETERMINE THE ANGLE OF INCIDENCE
C ON A VERTICAL SURFACE IS:
C  $\text{COS}(\text{ANGLE OF INCIDENCE}) = \text{COS}(\text{ALTITUDE}) * \text{COS}(\text{WALL SOLAR}$ 
C  $\text{AZIMUTH})$ 
C  $=\text{COS}(\text{ALTITUDE}) * \text{COS}(\text{SOLAR AZIMUTH})$  FOR SOUTH FACING
C WALLS
C THE FORMULA FOR THE COSINE OF THE WALL SOLAR AZIMUTH IS:
C  $\text{COS}(\text{AZIMUTH}) = (\text{SIN}(\text{LAT}) * \text{SIN}(\text{ALT}) - \text{SIN}(\text{DEC})) / (\text{COS}(\text{LAT})$ 
C  $* \text{COS}(\text{ALT}))$ . AZI REFERS TO THIS COSINE.
AZI=(SIN(LAT)*SIN(AL)-SIN(D(M))) / (COS(LAT)*COS(AL))
C CANG IS THE COSINE OF THE ANGLE OF INCIDENCE OF SOLAR
C RADIATION ON A SOUTH FACING VERTICAL WALL.
CANG=COS(AL)*AZI
C ANGL(M,H) GIVES THE ANGLE OF INCIDENCE IN DEGREES FOR
C HOUR H
ANGL(M,H)=ACOS(CANG) / RAD
IF(ANGL(M,H).GT.90.0) ANGL(M,H)=90.0
PRINT*,'HR',H,' INCIDENCE',ANGL(M,H),' ALT ',AL

```

20 CONTINUE

C THE FOLLOWING LINES OF CODE ENABLE THE PROGRAM TO PRINT  
 C OUT THE ANGLES OF INCIDENCE OF SOLAR RADIATION ON A  
 C SOUTH FACING VERTICAL WALL. THE ANGLES ARE FOR 7-17  
 C HOURS AT THE MIDDLE OF EACH MONTH, FROM JANUARY TO  
 C DECEMBER.  
 C ANG(21,4) FOR EXAMPLE, REFERS TO THE ANGLE OF INCIDENCE  
 C FOR DAY NUMBER 21.

PRINT \*, 'ANGLES OF INCIDENCE OF SOLAR RADIATION ON A  
 VERTICAL SOUTH FACING WALL FOR MID MONTH DAY NUMBERS. '

PRINT \*,

HOUR'

PRINT \*, 'DAY NUMBER            7    8    9    10   11   12   13   14

15   16   17 '

DO 30 M=1,12

DO 30 H=7,17

PRINT \*, J(M), ' ,ANGL(M,H), ' ,

30 CONTINUE

READ\*,CH

IF(CH.EQ.1)GOTO 25

25 CONTINUE

END



## APPENDIX 4: SOL-AIR TEMPERATURE

When solar energy falls upon a wall, its heat losses will be reduced, or reversed by the absorbed radiation. Neglecting heat loss due to long wave radiation from the wall surface, the heat gain through a reference wall (see Fig 6.15) ( $Q_{rw}$ , kWhm<sup>-2</sup>) will be:

$$Q_{rw} = 24 (T_{ao} - T_{so}) / R_{so} + \alpha H_m \quad (A1)$$

where  $T_{so}$  refers to the outside surface temperature of the front leaf.

Sol-air temperature ( $T_{eo}$ , °C) may be defined as: that external temperature which alone, would produce the same heat flow through a building fabric as the actual external air temperature and solar radiation combined. The heat gain through a reference wall using this concept will be:

$$Q_{rw} = 24 U_{rw} (T_{eo} - T_{ai}) = 24 (T_{eo} - T_{so}) / R_{so} \quad (A2)$$

From (A1) and (A2):

$$T_{eo} = T_{ao} + \alpha R_{so} H_m / 24 \quad (A3)$$

$$Q_{rw} = U_{rw} \alpha R_{so} H_m - 24 U_{rw} (T_{ai} - T_{ao}) \quad (A4)$$

The heat gain through a solar wall, (Fig 6.14a) ( $Q_{sw}$ , kWhm<sup>-2</sup>) may be similarly found:

$$Q_{sw} = 24 (T_{ao} - T_{so}) / R_o + (\tau\alpha) H_m \quad (A5)$$

where  $T_{so}$  refers to the outside surface temperature of the mass wall.

$$Q_{sw} = 24 U_{sw} (T_{eo} - T_{ai}) = 24 (T_{eo} - T_{so}) / R_o \quad (A6)$$

$$T_{eo} = T_{ao} + (\tau\alpha) R_o H_m / 24 \quad (A7)$$

$$Q_{sw} = U_{sw} (\tau\alpha) R_o H_m - 24 U_{sw} (T_{ai} - T_{ao}) \quad (A8)$$

When simulating heat flow in glazed solar walls, the beam and diffuse components of the monthly mean daily global irradiation on a south facing vertical plane ( $H_{bm}$ , kWhm<sup>-2</sup>) and ( $H_{dm}$ , kWhm<sup>-2</sup>) and the monthly mean transmittance - absorptance products  $(\tau\alpha)_b$  and  $(\tau\alpha)_d$  should be and have been used. For ease of comprehension, equation (A8) has been kept in simple format with the implication that:

$$(\tau\alpha) H_m = (\tau\alpha)_b H_{bm} + (\tau\alpha)_d H_{dm} \quad (A9)$$